Reprints of

Gas Exchange Studies at Pasoh

Vol. 1

Edited by

Yoshiko Kosugi

CONTENTS

ASIAFLUX WORKSHOP 2011 PRESENTATIONS

CANOPY GAS EXCHANGES

BOWEN RATIO H_2O AND ENERGY FLUXES

EDDY COVARIANCE CO_2, H_2O, AND ENERGY FLUXES (-2002)

EDDY COVARIANCE CO_2, H_2O, AND ENERGY FLUXES (2003-2005)

EDDY COVARIANCE CO_2, H_2O, AND ENERGY FLUXES (2003-2009)

BVOC FLUXES

COMPARISON OVER ASIAFLUX TOWER SITES

LEAF GAS EXCHANGES

SOIL GAS EXCHANGES

SPECIAL AND/OR TEMPORAL VARIABILITY OF ENVIRONMENT

Gas Exchange Studies at Pasoh

by Kyoto Univ./FFPRI/FRIM team in NIES/FRIM/UPM project

Pasoh Forest Reserve in Peninsula Malaysia is a famous IBP pioneer site on the carbon budget of the tropical rain forest (Kira, 1987), and also one of the oldest tower sites in South-east Asia. The aluminum tower canopy walkway system was established in 1992, and the microclimate observation at the 52m-tower started in 1995. Continuous eddy covariance flux observation has been carried out since September 2002, accompanied with environmental biophysical, ecophysiological, biogeochemical, and hydrological researches, to clarify gas exchange of South-east Asian tropical rain forests.

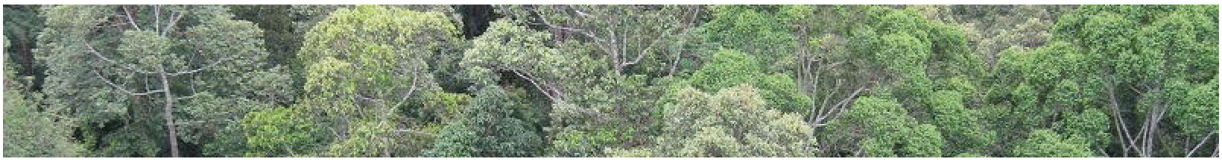

SITE INFORMATION

AsiaFlux site code : PSO
Management : FRIM, NIES/FRIM/UPM project
Position : 2°58' N, 102°18' E, 75-150m a.s.l.
Vegetation : lowland dipterocarp forest (>814 species)
LAI : approximately 6.5
Canopy Height : 30-40m (with emergent trees～45m)
Air temp : 25.3C
Precipitation : 1865mm (2003-2009)

PSO is roughly classified as the tropical rain forest. Though the average annual precipitation is about 1800 mm and not so many. Obvious dry season is not observed, but modulate dry and wet periods exist, depending on years. Most rainfall occurs after late afternoon. It can be defined as a border type of South-east Asian tropical rain forests. Therefore, PSO is a suitable site to evaluate how tropical rain forests change their functions under the future possible climate change, such as the change of rainfall pattern, temperature, air and soil humidity, radiation, and so on.

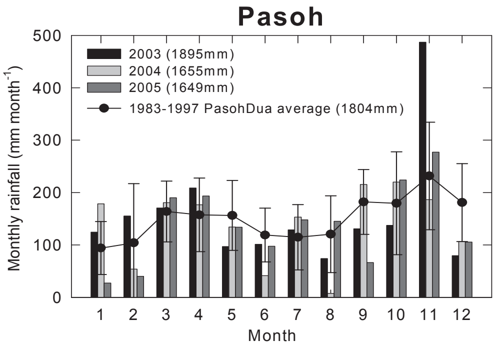

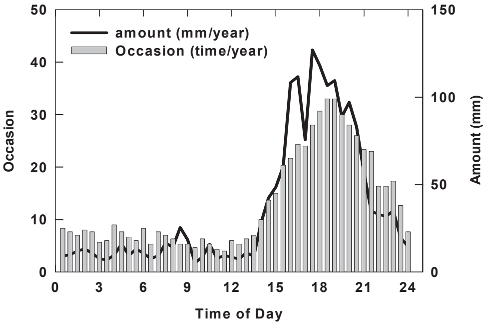

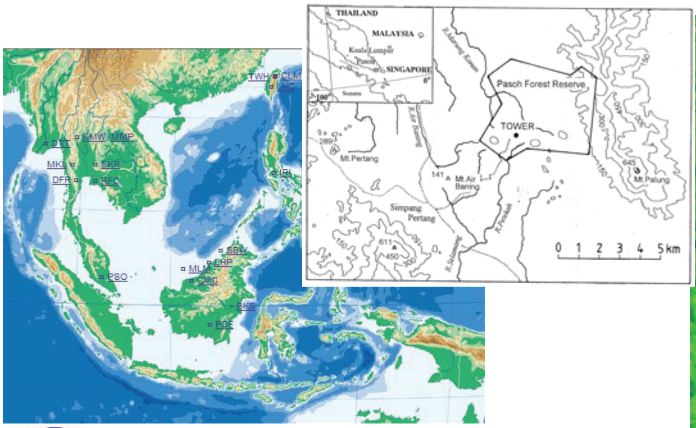

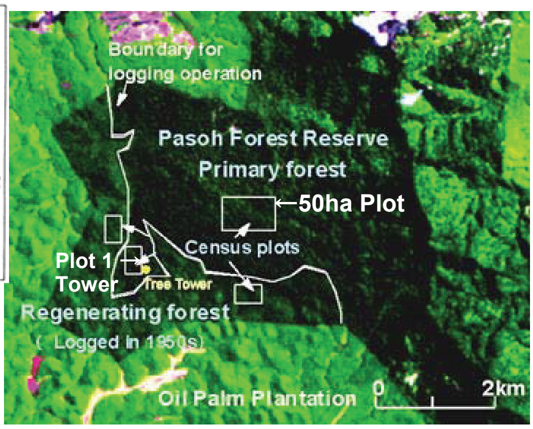

Contact : Kosugi, Y. (ykosugi@kais.kyoto-u.ac.jp)
http://www.bluemoon.kais.kyoto-u.ac.jp/pasoh

Gas Exchange Studies at Pasoh

by Kyoto Univ./FFPRI/FRIM team in NIES/FRIM/UPM project

At 52m Flux Tower

Flux and micrometeorological monitoring (2002-now)

Canopy CO_2/H_2O/Heat fluxes
(open-path Eddy Covariance)
Micrometeorology
radiations, CO_2, wind, Tair, RH
(tower top, profile, and forest floor)
rainfall, soil moisture

Ask details to Kosugi, Y. and Takanashi, S. (tnsatoru@ffpri.affrc.go.jp)

Studies on
7-year variation of CO_2/H_2O fluxes 22)
CO_2 exchange (03-05) 14)
Evapotranspiration (03-05) 20)
Storage fluxes (03-05) 17)
Comparison over AsiaFlux sites 15) 16)
Short report of 2003 flux 9)
Methyl chloride and isoprene flux 18)
Bowen ratio H_2O flux 3)6)7)8)
Rainfall pattern 5)
Pioneer works on EC fluxes for several days 1)2)

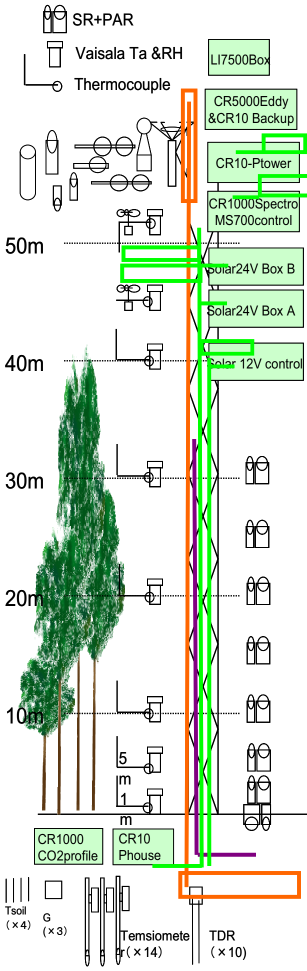

Pasoh Tower Equipments

Lightning conductor and network 🟧
a lightning rod at tower top
sheet line from tower top to the ground and their network under the ground to induce the electricity

Commercial electricity lines 🟪
100V line to the 30m corridor from the House.

Solar Panels and their systems 🟩
Main Solar 24V system (6 big panels, lines to and from the House, 2 control boxes at tower top)
Old 12V Solar system (2 panels, lines to and from House, one control box at tower top)
CR10-12V (a panel, line to CR10-Ptower、battery)
Spectrometer-12V (2 panels, line to CR1000-Specrto, 2 batteries)

Data Loggers and Boxes 🟩
4 data loggers and 7 boxes at the top of tower
2 data loggers at the House
Earth lines from data loggers to the ground

Equipments (line to the tower top loggers)
CR5000Eddy
SAT550, LI7500 Probe and Box
CR10-Ptower
Ta & RH Vaisala (53m, 45m, 40m, 30m, 20m)
Pair, Wind (53m, 45m) and wind direction(53m)
Rainfall gauge
SR (53m, upper & lower), LR (53m, upper & lower)
PAR (53m, upper & lower)
SR & PAR (30m, 25m, 20m, 15m)
Thermocouple (45-53, 53m, 40m, 30m, 20m, 10m, 5m, 1m)
CR10-Pbackup
SR(53m, upper & lower), LR(53m, upper & lower), PARdiffusive (53m), PAR (backup), Wind(53m)
CO_2-Vaisala (30m, 53m)
CR1000-Spectro
MS-700 Spectrometers (53m, upper & lower)
Phenology auto cameras

Equipments (line to the House loggers)
CR10-Phouse
Ta & RH Vaisala (10m, 5m, 1m)
SR & PAR (10m, 5m),
SR (1m, upper & lower), PAR (1m, upper & lower)
Soiltemp (A2cm, 10cm, B2cm, C2cm)
G (A1cm, B1cm, C1cm), TDR(10), Tensiometer (14)
CO_2-Vaisala(10m, 1m)
CR1000-CO_2pro
CO_2 sampling tube and filter (53m, 45m, 40m, 30m, 20m, 10m, 5m, 2m, 1m, 0.2m)

Vegetation Index monitoring (2009-now)

up- down- spectrometers
phenology cameras
Nakaji, T. (nakaji@fsc.hokudai.ac.jp)

At Plot 1 (6ha-Plot)

Spatial and temporal variabilities of

Thoughfall 10)
CO_2 flux from soil (×) 13)
CO_2/CH_4/N_2O fluxes from sol (×)
Itoh, M. (itoma@ecology.kyoto-u.ac.jp)
Soil water content and soil physics
Noguchi, S. (noguchi@affrc.go.jp)
Soil characteristics 4)

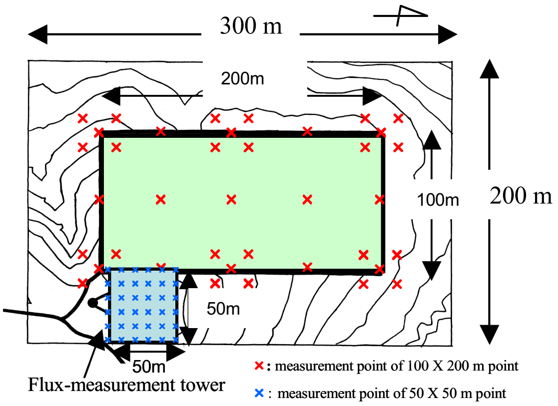

Gas Exchange Studies at Pasoh

by Kyoto Univ./FFPRI/FRIM team in NIES/FRIM/UPM project

At Aluminum Canopy Walkway

Leaf scale gas exchanges

Patchy stomatal closure and its effect on leaf photosynthesis 11), 19), 21)

Impact of patchy stomatal closure to canopy photosynthesis

Kamakura, M. (mkamakura@cc.nara-wu.ac.jp)

CH_4 fluxes from leaves 23)

BVOC fluxes from leaves

Okumura, M. (okumura.motonori.6v@kyoto-u.ac.jp)

Water use 12)

Vertical distribution of leaf properties

Multi-layer Model Analysis

Takanashi, S., Kosugi, Y.

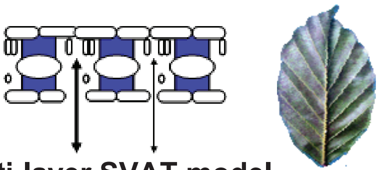

Multi-layer SVAT model

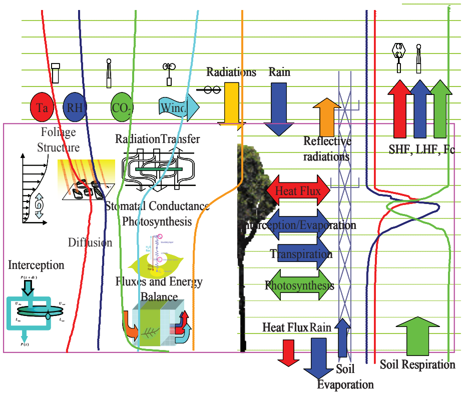

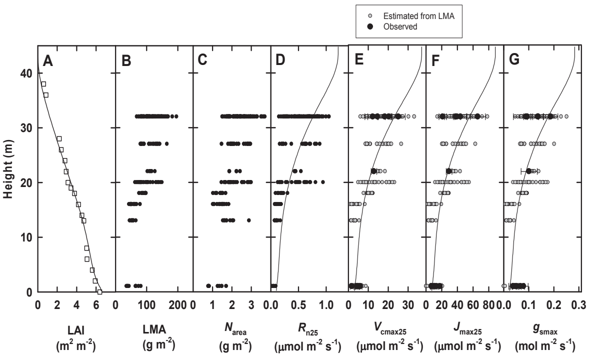

At Station Plot

Rainfall monitoring (1995-now)

Intensive observation campaign of

Leaf, stem, branch, coarse root, & fine root respiration 24)

Makita, N. (macky@kais.kyoto-u.ac.jp)

Dannoura, M. (dannoura@kais.kyoto-u.ac.jp)

Takanashi, S., Kosugi, Y.

Root distribution

Niiyama, K. (niiya@ffpri.affrc.go.jp)

Yamashita, T. (tamonyam@life.shimane-u.ac.jp)

Soil physics distribution Noguchi, S.

Depth of water uptake using 13C and 18O

Haruta, T., Matsuo, N. (naoko@bio.mie-u.ac.jp)

CWD decomposition and CO_2 emission

Majima, K. (majimako@kais.kyoto-u.ac.jp)

CWD monitoring with auto camera Nakaji, T.

Gas Exchange Studies at Pasoh

by Kyoto Univ./FFPRI/FRIM team in NIES/FRIM/UPM project

Topic 1 : Variations in micrometeorology

During 2003 and 2009, annual rainfall ranged between 1,451 and 2,235mm. The year 2009 was the driest year with ENSO. At Pasoh, rainfall pattern mainly governs the variations in micrometeorology.

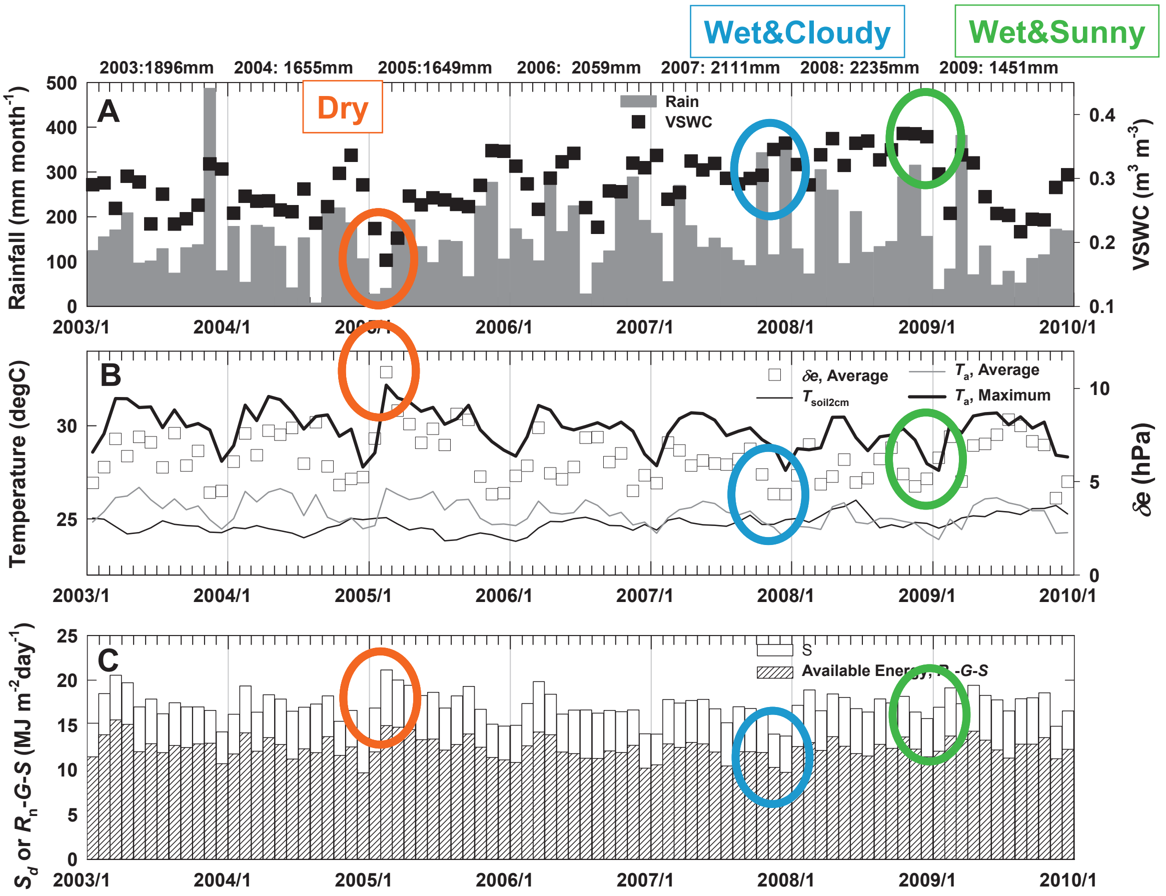

（Kosugi et al, 2011)

Large storage flux and dynamic diurnal variation in concentration of CO2

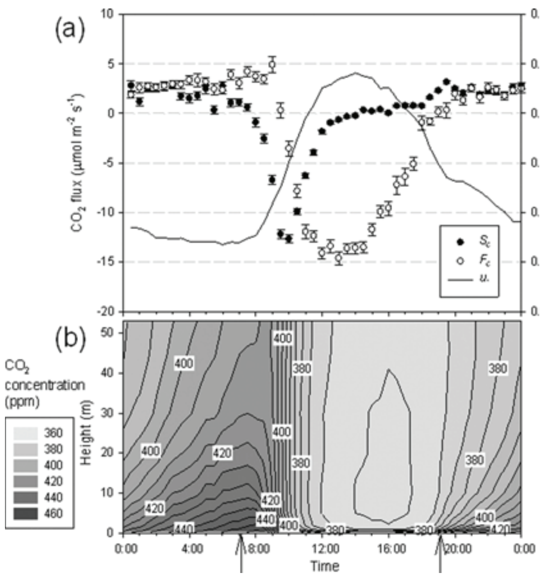

(a) Low nighttime u_*

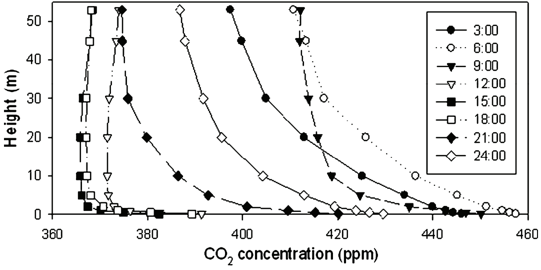

(b) High nighttime u_*

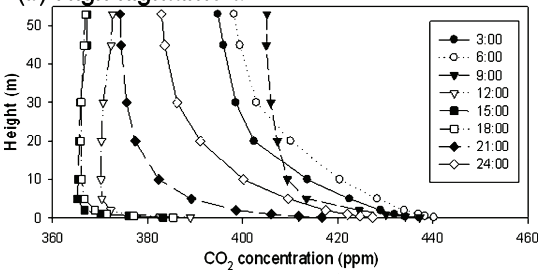

（Ohkubo et al, 2008)

Gas Exchange Studies at Pasoh

by Kyoto Univ./FFPRI/FRIM team in NIES/FRIM/UPM project

Topic 2 : Evapotranspiration and Water budget

Stomatal regulation occurred to maintain stable annual evapotranspiration (~1,300 mm /yr). At Pasoh, trees usually used the surface water around 0-50cm depth, while absorbed the water from deeper layer at the dry period.

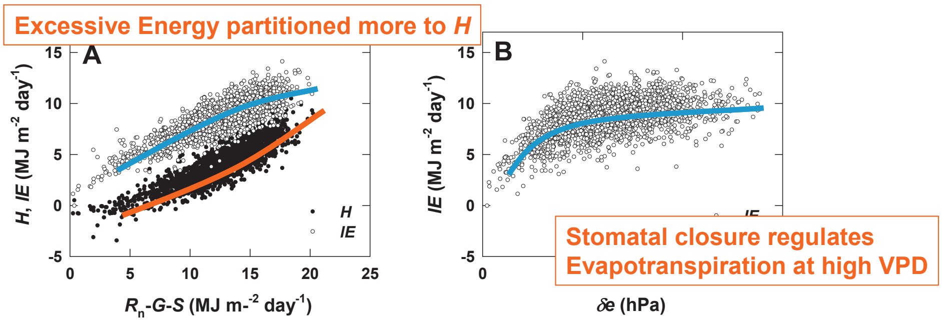

Excessive Energy partitioned more to *H*

Stomatal closure regulates Evapotranspiration at high VPD

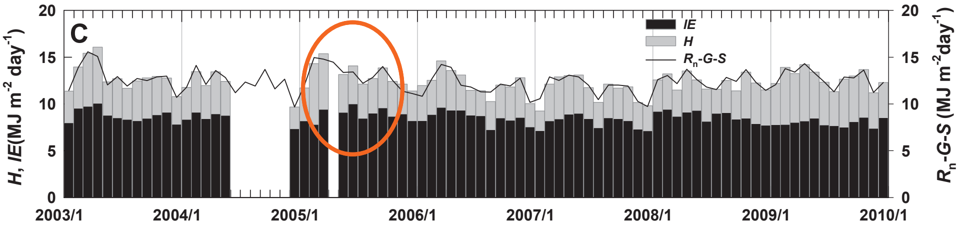

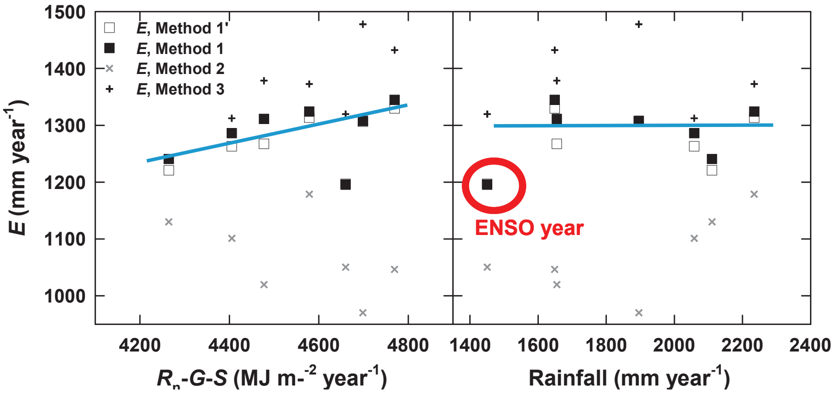

ENSO year

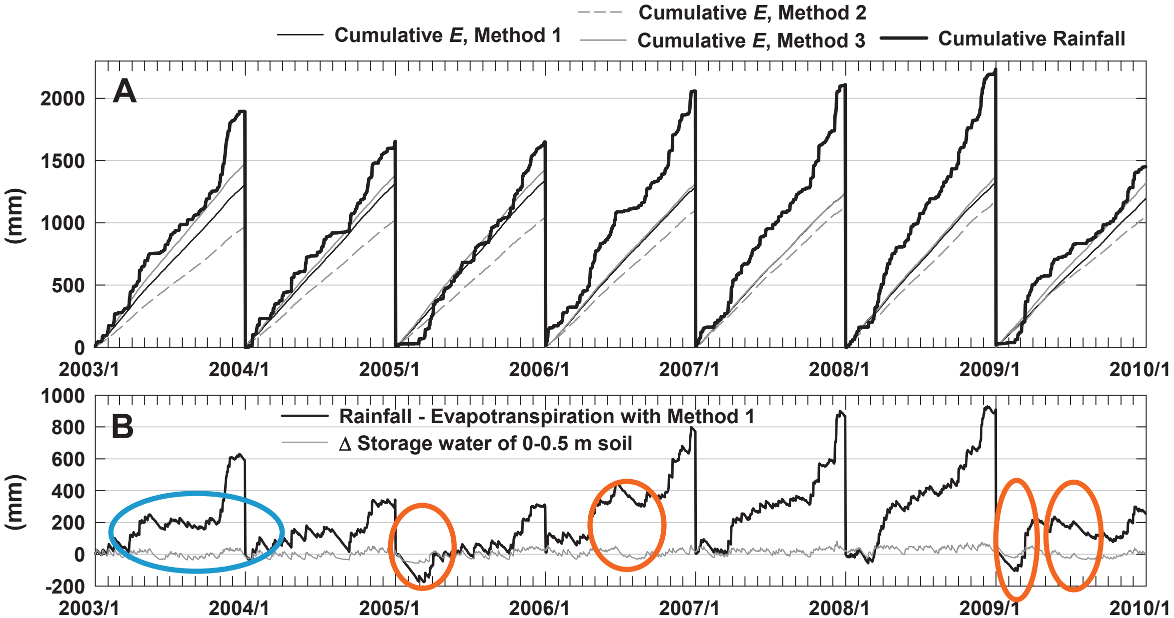

Water supply from 0-50cm layer at most periods, but from deeper layer under drought

（Takanashi et al, 2010; Kosugi et al, 2011)

Gas Exchange Studies at Pasoh

by Kyoto Univ./FFPRI/FRIM team in NIES/FRIM/UPM project

Topic 3 : Dynamic equilibrium of carbon budget

At Pasoh, ecosystem respiration (RE) increased with soil water content. GPP did not increase with solar radiation, while showed moderate increase with soil water content. Daytime NEE had an circadian rhythm independent of solar radiation, and with clear decline in the afternoon. Both GPP and RE increased a little with soil water content, resulted in very stable NEE.

GPP:30~36tC ha^{-1} yr^{-1} RE:30~36tC ha^{-1} yr^{-1} NEE:-2~2tC ha^{-1} yr^{-1}

Chamber Soil Respiration

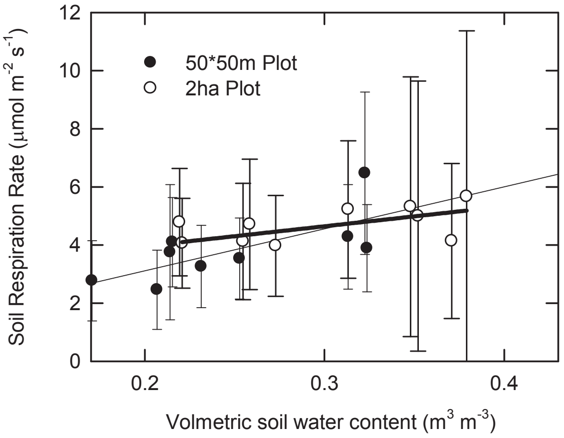

Coinsided with the soil respiration related with soil water content (base on 8-year chamber observations)

Nighttime NEE (=RE) versus Soil water content

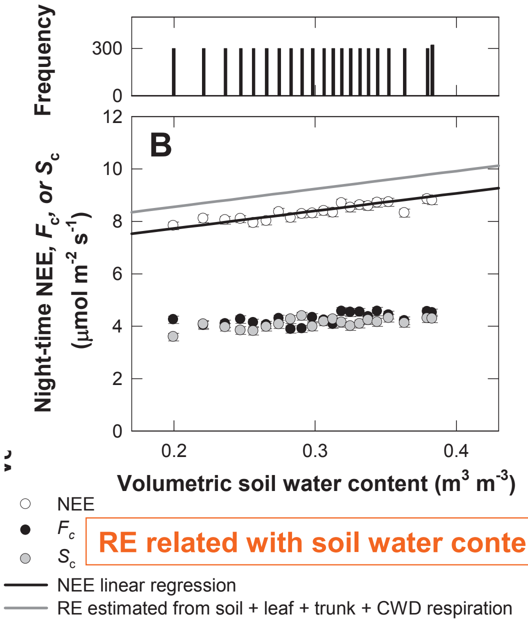

RE related with soil water content

No increase of daily GPP with solar radiation

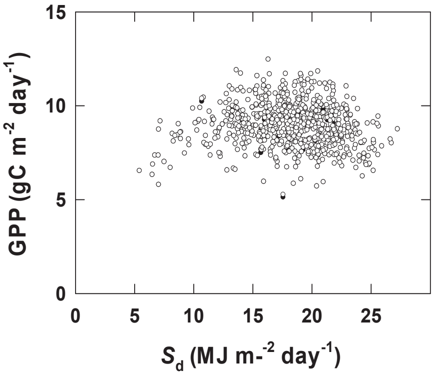

Moderate decline of GPP at the dry period

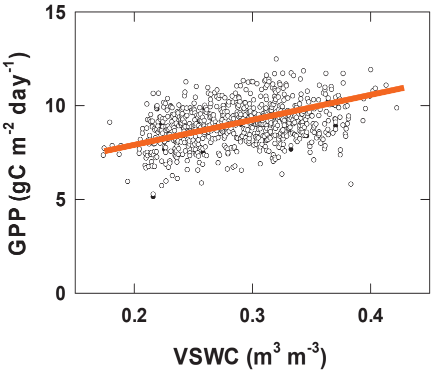

Daytime NEE had an circadian rhythm independent of PPFD, and with clear decline in the afternoon.

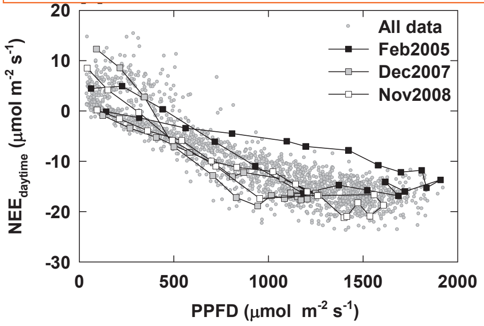

No dependence of daytime-mean NEE on solar radiation and soil water content

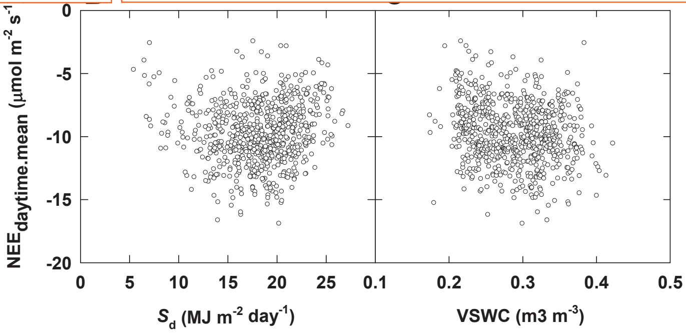

(Kosugi et al, 2011)

Gas Exchange Studies at Pasoh

by Kyoto Univ./FFPRI/FRIM team in NIES/FRIM/UPM project

Topic 3 : Dynamic equilibrium of carbon budget

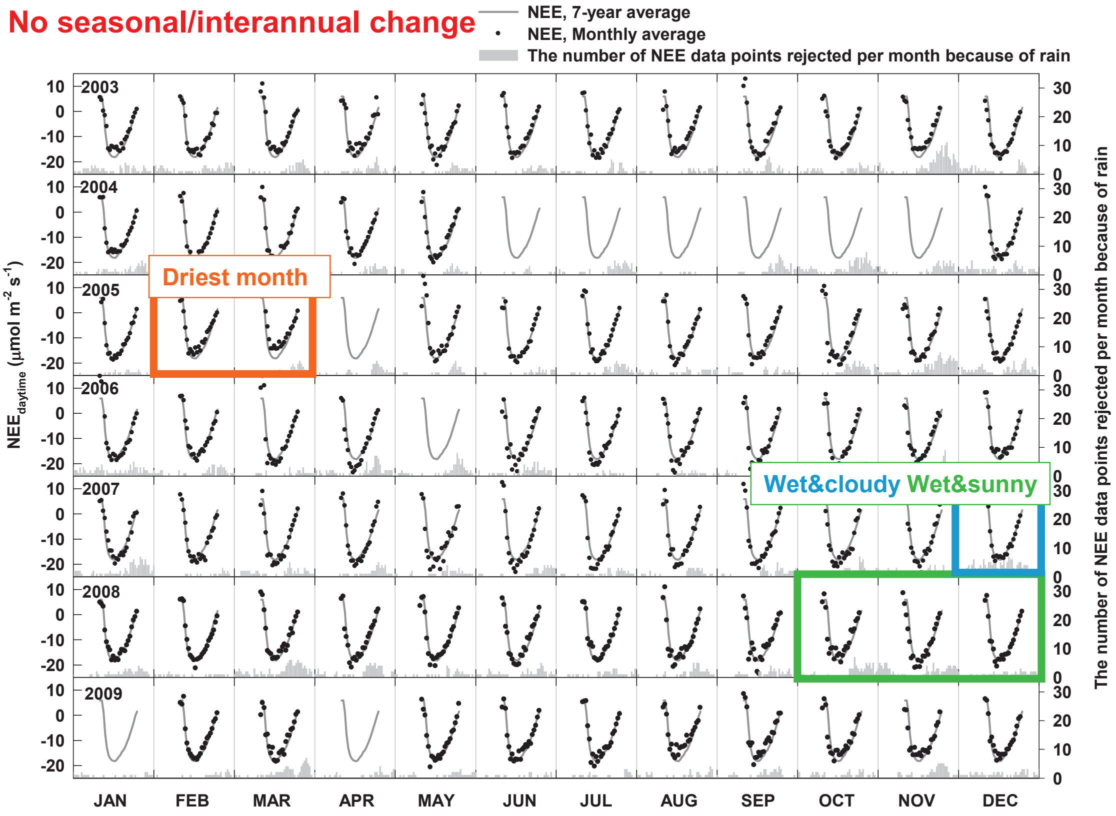
No seasonal/interannual change

Driest month

Wet&cloudy Wet&sunny

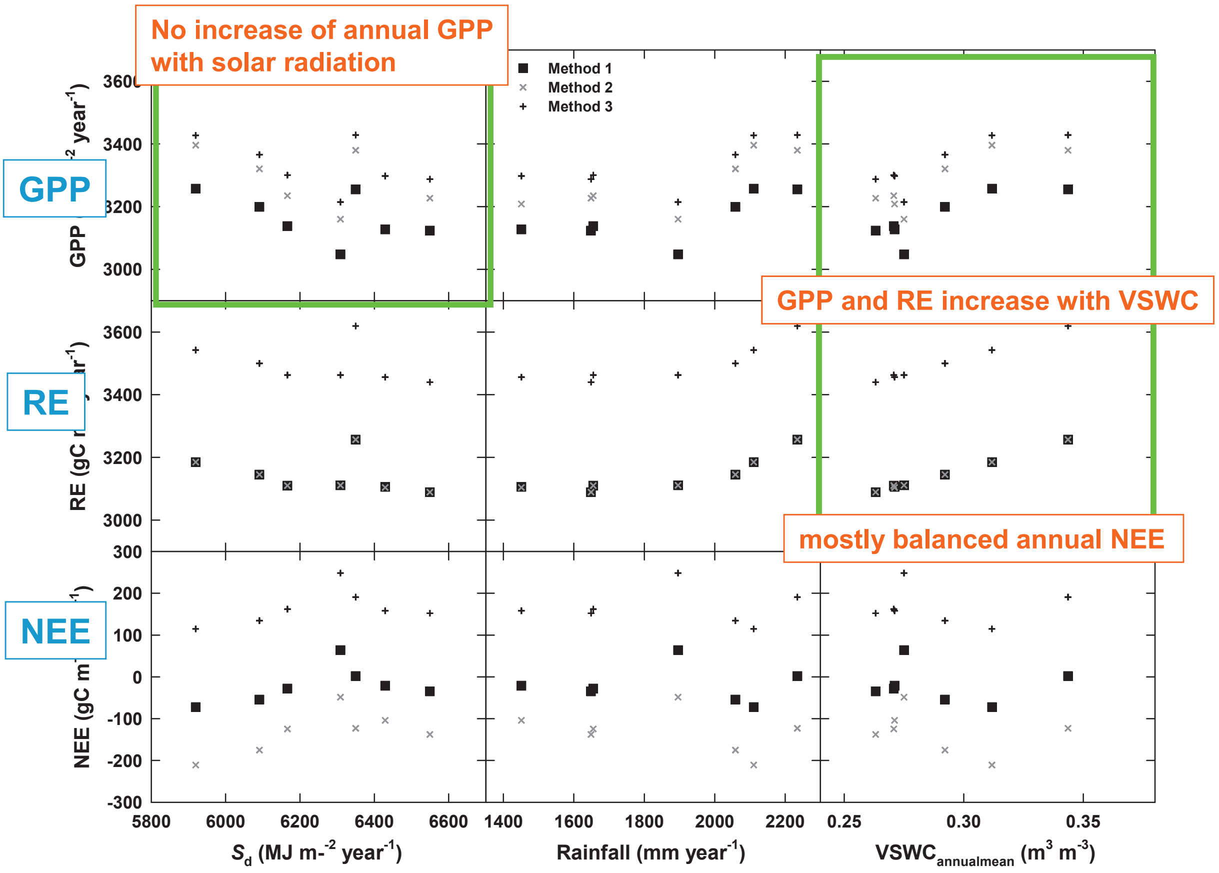
No increase of annual GPP with solar radiation

GPP and RE increase with VSWC

mostly balanced annual NEE

（Kosugi et al, 2011）

Gas Exchange Studies at Pasoh

by Kyoto Univ./FFPRI/FRIM team in NIES/FRIM/UPM project

Topic 4 : Soil water and soil fluxes

At Pasoh, soil CO2 flux was temporally increased with the increase of soil water content, while spatially decreased with the increae of soil water content. This paradox is important to understand the soil flux at this site. CH4 flux also closely related with soil water content.

(a) Temporally averaged VSWC ($m^3\ m^{-3}$)

(d) Temporally averaged CO_2 flux

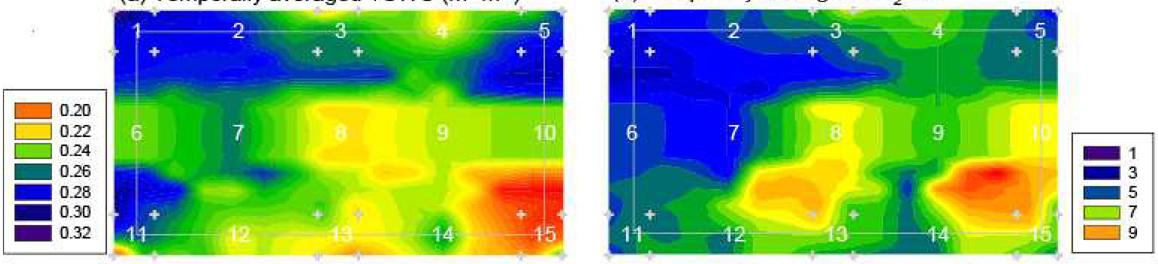

(b) Temporally averaged C concentration (%)

(e) Temporally averaged CH_4 flux

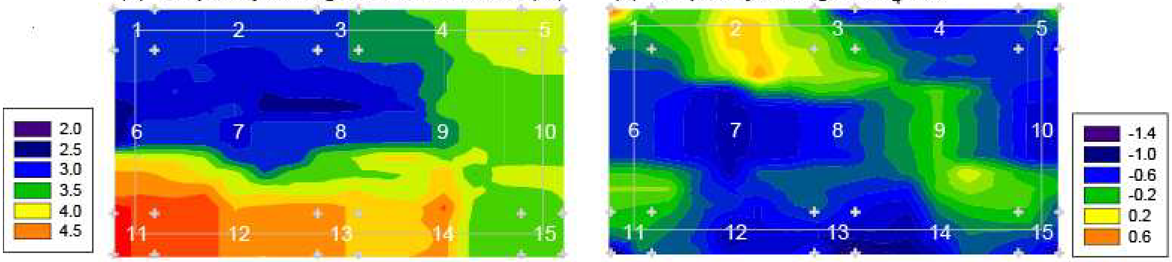

(c) Temporally averaged N concentration (%)

(f) Temporally averaged N_2O flux

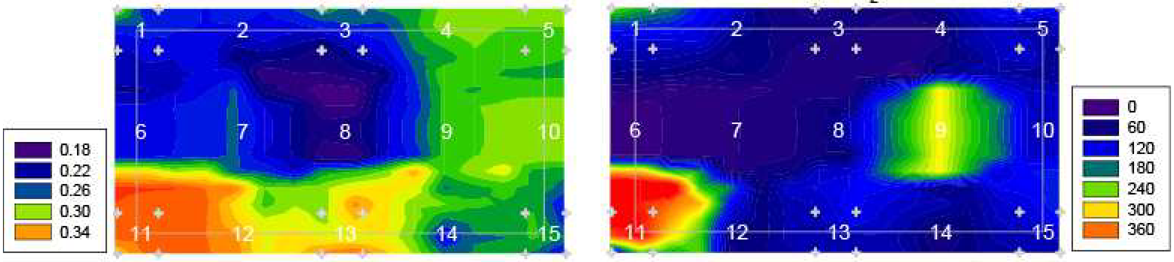

(Itoh et al, unpublished data)

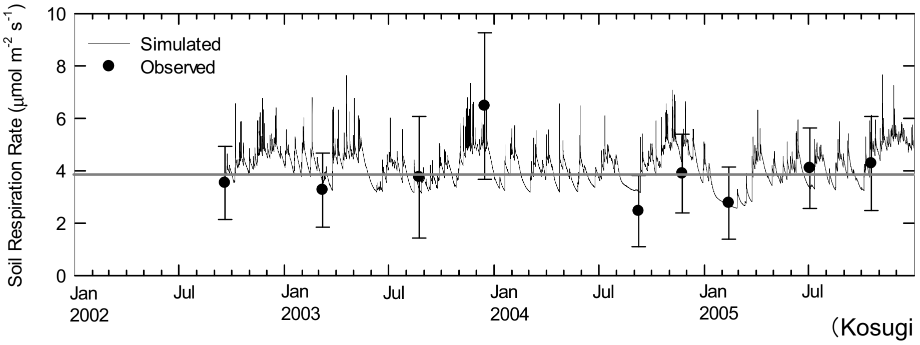

(Kosugi et al, 2008)

Annual estimation of soil respiration (excluding CWD flux ~0.8 tC ?) :
2003 : 15.9 tC ha^{-1} year^{-1} 2004 : 15.7 tC ha^{-1} year^{-1} 2005 : 15.3 tC ha^{-1} year^{-1}

Gas Exchange Studies at Pasoh

by Kyoto Univ./FFPRI/FRIM team in NIES/FRIM/UPM project

Topic 5 : Patchy stomatal closure of canopy leaves

At Pasoh, severe decline of canopy photosynthesis in the afternoon was occurred accompanied with the patchy stomatal closure of canopy leaves.

A: *Xanthophyllum stipitatum*

B: *Dipterocarpus sublamellatus*

B, D :
Emergent trees
Dipterocarpaceae
A, C :
Medium trees

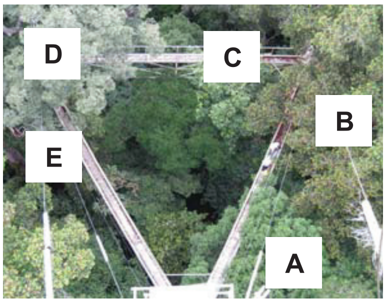

C: *Ptychopyxis caput-medusae*

D: *Neobalanocarpus heimii*

E: *D. sublamellatus* shaded

Sunlit leaves of every touchable trees (A to D) from aluminum walkway showed severe decline of photosynthesis coupled with patchy stomatal closure.

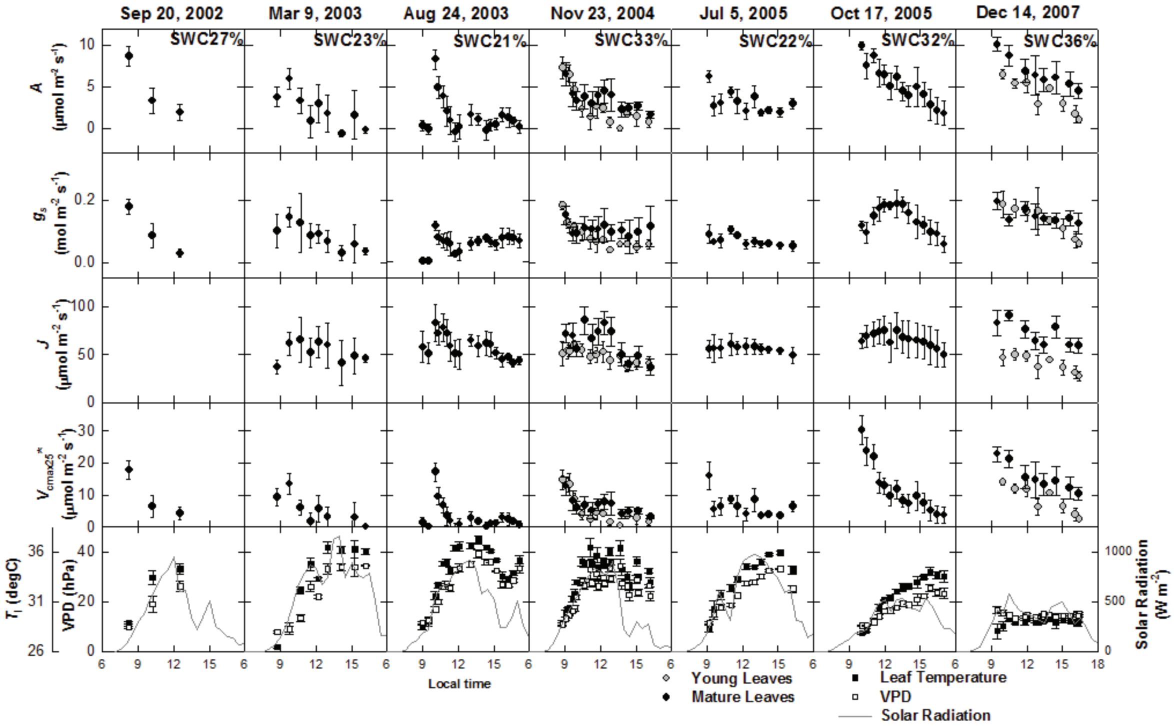

Dipterocarpus sublamellatus

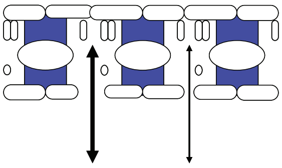

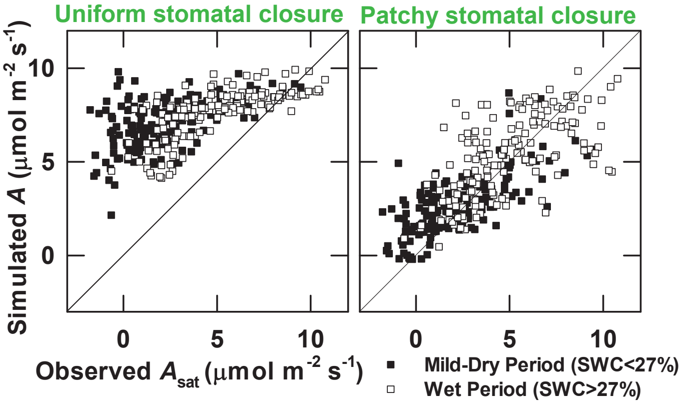

(Takanashi et al, 2006, Kosugi et al, 2009, Kamakura et al, 2011)

Gas Exchange Studies at Pasoh

by Kyoto Univ./FFPRI/FRIM team in NIES/FRIM/UPM project

List of Publications

24) Makita, N., Kosugi, Y., Dannoura, M., Takanashi, S., Niiyama, K., Abdul Rahman, K., Abdul Rahim, N.: Patterns of root respiration rates and morphological traits in 13 tree species in a tropical forest, Tree Physiology, in press

23) Kamakura, M., Kosugi, Y., Nakagawa, R., Itoh, M.: Methane flux of leaves in a tropical rainforest and a temperate conifer forest, Journal of Agricultural Meteorology, in press

22) Kosugi, Y., Takanashi, S., Tani, M., Ohkubo, S., Matsuo, N., Itoh, M., Noguchi, S., Abdul Rahim N.: Influence of inter-annual climate variability on evapotranspiration and canopy CO_2 exchange of a tropical rainforest in Peninsular Malaysia. Journal of Forest Research, DOI 10.1007/s10310-010-0235-4, 2011

21) Kamakura, M., Kosugi, Y., Takanashi, S., Matsumoto, K., Okumura, M., Philip, E.: Patchy stomatal behavior during midday depression of leaf CO_2 exchange in tropical trees. Tree Physiology, 31, 160-168, 2011

20) Takanashi, S., Kosugi, Y., Ohkubo, S., Matsuo, N., Tani, M., Abdul Rahim, N: Water and heat fluxes above a lowland dipterocarp forest in Peninsular Malaysia, Hydrological Processes, 24, 472-480, 2010

19) Kosugi, Y., Takanashi, S., Matsuo, N., Abdul Rahim, N: Midday depression of leaf CO_2 exchange within the crown of *Dipterocarpus sublamellatus* in a lowland dipterocarp forest in Peninsular Malaysia, Tree Physiology, 29, 505-515, 2009

18) Saito, T., Yokouchi, Y., Kosugi, Y., Tani, M., E. Philip, and T. Okuda, Methyl chloride and isoprene emissions from tropical rain forest in Southeast Asia, Geophys. Res. Lett., 35, L19812, doi:10.1029/2008GL035241, 2008

17) Ohkubo, S., Kosugi, Y., Takanashi. S., Matsuo, N., Tani, M.,Abdul Rahim, N.: Vertical profiles and storage fluxes of CO_2, heat, and water in a tropical rainforest at Pasoh, Peninsular Malaysia, Tellus, 60B, 569-582, 2008

16) Saigusa, N., Yamamoto, S., Hirata, R., Ohtani, Y, Ide, R., Asanuma, J., Gamo, M., Hirano, T., Kondo, H., Kosugi, Y., Li, S.G., Nakai, Y., Takagi, K., Tani. M., Wang, H.: Temporal and spatial variations in the seasonal patterns of CO_2 flux in boreal, temperate, and tropical forests in East Asia. Agricultural and Forest Meteorology, 148, 700-713, 2008

15) Hirata, R., Saigusa, N., Yamamoto, S., Ohtani, Y., Ide, R., Asanuma, J., Gamo, M., Hirano, T., Kondo, H., Kosugi, Y., Li, S.G., Nakai, Y., Takagi, K., Tani, M., Wang, H.: Spatial distribution of carbon balance in forest ecosystems across East Asia. Agricultural and Forest Meteorology, 148, 761-775, 2008

14) Kosugi, Y., Takanashi, S., Ohkubo, S., Matsuo, N., Tani, M., Mitani, T., Tsutsumi, D, Abdul Rahim, N: CO_2 exchange of a tropical rainforest at Pasoh in Peninsular Malaysia. Agricultural and Forest Meteorology, 148, 439-452, 2008

13) Kosugi, Y., Mitani, T., Itoh, M., Noguchi, S., Tani, M., Matsuo, N., Takanashi, S., Ohkubo, S., Abdul Rahim, N.: Spatial and temporal variation in soil respiration in a Southeast Asian tropical rainforest. Agricultural and Forest Meteorology 147, 35-47, 2007

12) Fukui, Y., Kosugi, Y., Matsuo, N., Takanashi, S., Tani, M.: Comparison of wate use of various trees grown in several different habitats. J. Japan Soc. Hydrol. & Water Resour 20, 265-277, 2007 (Japanese)

11) Takanashi, S., Kosugi, Y., Matsuo, N., Tani, M., and Ohte, N.: Patchy stomatal behavior in broad-leaved trees grown in different habitats. Tree Physiology 26, 1565-1578, 2006

10) Konishi, S., Tani, M., Kosugi, Y., Takanashi, S., Sahat, M.M., Abdul Rahim, N., Niiyama, K., Okuda, T.: Characteristics of spatial distribution of throughfall in a lowland tropical rainforest, Peninsular Malaysia. Forest Ecology and Management 224, 19-25, 2006

9) Takanashi, S., Kosugi, Y., Tani, M., Matsuo, N., Mitani, T., Abdul Rahim N., Characteristics of the gas exchange of a tropical rain forest in Peninsular Malaysia. Phyton 45, 61-66, 2005

8) Roberts, J.M., Tani, M. et al.: Controls on evaporation in lowland tropical rainforest. Bonell et al. (eds.) Forest, water and People in the Humid Tropics, Cambridge Press, 287-313, 2005

7) Tani, M., Abdul Rahim, N., Yasuda, Y., Noguchi, S., Siti Aisah, S., Mohd Md, S., Takanashi, S.: Long-term estimation of evapotranspiration from a tropical rain forest in Peninsular Malaysia, IAHS Publication No. 280 (Water Resources Systems - Water Availability and Global Change), 2003.

6) Tani, M., Abdul Rahim N, Noguchi, S..et al: Characteristics of energy exchange and surface conductance of a tropical rain forest in Peninsular Malaysia. In: Okuda, T. et al (Eds.), Pasoh : Ecology of a lowland rain forest in southeast Asia, Springer, Tokyo, 73-88, 2003

5) Noguchi, S., Abdul Rahim N., Tani, M.: Rainfall characteristics of tropical rainforest at Pasoh Forest Reserve, Negeri Sembilan, Peninsular Malaysia. In: Okuda, T. et al (Eds.), Pasoh : Ecology of a lowland rain forest in southeast Asia, Springer, Tokyo, 51-58, 2003

4) Yamashita, T., Kasuya, N., Wan Rashidah, K., Suhaimi, W.C., Quah, E.S., Okuda, T.: Soil and belowground characteristics of Pasoh forest reserve. In: Okuda, T. et al (Eds.), Pasoh : Ecology of a lowland rain forest in southeast Asia, Springer, Tokyo, 89–109, 2003

3) Takanashi, S., Tani, M., Abdul Rahim, N., Characteristics of transpiration over a tropical rainforest in Peninsula Malaysia. J. Jpn. Soc. Reveget. Tech. 29, 51-55, 2003 (Japanese)

2) Yasuda, Y., Ohtani, Y., Watanabe, T., Okano, M., Yokota, T., Liang, N., Tang, Y., Abdul Rahim N., Tani, M., Okuda, T.: Measurement of CO_2 flux above a tropical rain forest at Pasoh in Peninsular Malaysia. Agricultural and Forest Meteorology 114, 235-244, 2003

1) Ohtani, Y., Okano, M., Tani, M., Yamanoi, T., Watanabe, T., Yasuda, Y., Abdul Rahim N.: Energy and CO_2 fluxes above a tropical rain forest in Peninsular Malaysia. J Agric Meteorol 52, 453-456, 1997

IMPACT OF CLIMATE CHANGE ON CANOPY CO_2 AND H_2O EXCHANGE OF A TROPICAL RAINFOREST IN PENINSULAR MALAYSIA, PASOH

Yoshiko Kosugi[1], Satoru Takanashi[2], Makoto Tani[1], Shinjiro Ohkubo[3], Naoko Matsuo[4], Masayuki Itoh[5], Shoji Noguchi[6], Abdul Rahim Nik[7]

[1] Graduate School of Agriculture, Kyoto University, Kyoto, Japan
[2] Forestry, Forest Products Research Institute, Tsukuba, Japan
[3] National Agrcultural Research Center for Hokkaido Region, Sapporo, Japan
[4] Faculty of Bioresources, Mie University, Tsu, Mie, Japan
[5] Center for Ecological Research, Kyoto University, Shiga, Japan
[6] Tohoku Research Center, Forestry, Forest Products Research Institute, Morioka, Japan
[7] Ministry of Natural Resources and Environment, Putrajaya, Malaysia

Evaluating the impact of climate change on canopy CO_2 and H_2O exchange of tropical rainforests, and identifying the factors controlling these exchanges at different timescales are of primary importance to understanding the role of gas exchange in the global climate. To clarify the impact of the environmental factors and their future changes on gas exchange processes of tropical forests, we should first evaluate the actual range of their fluctuations as influenced by inter-annual climate variability. Long-term heat, H_2O, and CO_2 flux monitoring based on eddy covariance measurements allows the evaluation of inter-annual range of fluctuation in gas exchange, as well as a detailed analysis of the factors controlling gas exchanges. We investigated inter-annual variation of canopy CO_2 exchange (NEE) and evapotranspiration during a 7-year period over a lowland Dipterocarp forest in Pasoh, Peninsular Malaysia, using the eddy covariance method.

At the study site, annual rainfall fluctuated between 1,451 and 2,235 mm during the 7-year period. Despite of inter-annual variation in rainfall, annual evapotranspiration was stable (1,287 ± 52 mm), except for a slight decrease in at the driest year (2009). Evapotranspiration was roughly related to the amount of available energy, but regulated by stomatal closure to prevent excessive water loss at high vapour pressure deficit. Even during dry periods, no significant decrease in evapotranspiration occurred, as water was supplied from soil layers deeper than 0.5 m. Ecosystem respiration (RE) increased with soil water content. Daytime NEE was also stable during the 7 years despite climate variability. Afternoon inhibition of canopy photosynthesis was seen every month. Daytime NEE did not become more negative with increasing solar radiation, or with increasing soil water content. During dry periods, gross primary production (GPP) and thus canopy gross photosynthesis decreased slightly, coupling with decreased daytime RE. Our results strongly suggest values of GPP and RE of approximately 3,000–3,600 g C m^{-2} $year^{-1}$, and NEE of 0 ± 200 gC m^{-2} $year^{-1}$, with no clear dependence on annual solar radiation or air temperature, and some dependence on rainfall pattern and soil water content.

In this forest, variability in rainfall pattern resulted in seasonal and inter-annual variability in micrometeorology; evapotranspiration, photosynthesis, and ecosystem respiration responded to these changes, and compensated for each other and/or other components of micrometeorology, resulting in rather stable annual evapotranspiration and NEE, even during a considerably dry year associated with an ENSO event. Neither net nor gross canopy CO_2 uptake showed dependence on radiation. However canopy gross photosynthesis and ecosystem respiration showed dependence on soil water content. These results strongly suggest that the reduction in radiation caused by factors such as haze events does not cause a significant change in canopy CO_2 exchange. A decrease in rainfall and soil drought would however cause a decrease in both GPP and RE, resulting in no significant change in NEE, or shift in the direction of CO_2 uptake. We also detected a stomatal regulation of evapotranspiration at high vapour pressure deficit to mitigate excessive evapotranspiration under conditions of high energy, regardless of soil water content. Our results for 2009, an ENSO year, suggest that if more severely dry and hot years occur, the decline in evapotranspiration and GPP caused by the stomatal closure under conditions of higher vapour pressure deficit would increase significantly, to cause the break down of the 'homeostasis'.

RELATIONSHIP BETWEEN LUE AND TOWER-OBSERVED SPECTRAL VEGETATION INDICES IN A TROPICAL RAINFOREST AT PASOH, PENINSULAR MALAYSIA

Tatsuro Nakaji [1], Yoshiko Kosugi [2], Satoru Takanashi [3], Hiroyuki Oguma [4] and Abdul Rahim Nik [5]

[1] Hokkaido University, Tomakomai, Japan, [2] Kyoto University, Kyoto, Japan, [3] Forestry and Forest Products Research Institute, Tsukuba, Japan, [4] National Institute for Environmental Studies, Tsukuba, Japan, [5] Ministry of natural Resources and Environment, Putrajaya, Malaysia

The light use efficiency (LUE) is important parameters for the model estimation of productivity of vegetation cover. The LUE is calculated generally as the productivity divided by the absorbed PAR (LUE = GPP/APAR). In the field of forest remote sensing, many researchers has tried to estimate the LUE of forest canopy by using the spectral reflectance, and the Photochemical Reflectance Index (PRI) (1) is one of the useful vegetation indices (VIs) for the remote estimation of LUE (2, 3, 4). According to the recent review by Garbulsky *et al.* (2011) (4), the positive correlation between the PRI and LUE has been observed in many forest ecosystems. However, the slope of PRI-LUE regression line/curve tends to be varied with varying vegetation types. Grace *et al.* (2007) (5) have reported that the slope of the relationship was quite different between the Boreal forests and tropical woodland.

The aims of this study are (1) to confirm the sensitivity of PRI and other broadband/hyperspectral VIs in tropical rainforest and (2) to discuss the site-difference of PRI-LUE relationship. We have investigated the seasonal variations of canopy spectral reflectance and CO_2 flux in tropical rainforest at Pasoh Forest Reserve. Eddy CO_2 flux (3) and hyperspectral reflectance of forest canopy (6) were monitored by using tower-mounted devises since 2002 and 2008, respectively. In this study, we analyzed the field data between Oct 2008 and Dec 2009.

Firstly, we compared the variation in the LUE and six VIs (NDVI, EVI, GRVI, PRI, CCI and CI). Although the LUE did not show clear seasonal variation, peaky reduction/increment in LUE (min. 0.007 ~ max 0.020 mol mol^{-1}) was observed at about a monthly interval (data not shown). As for the VIs, similar peaky variation was found in CCI and PRI. The highest correlation coefficient was observed between the LUE and PRI (r = 0.46, p < 0.001). By comparing the LUE-PRI relationship in Pasoh tropical rain forest and other forest types in Siberia, Canada, Japan and Botswana, we found that the slope of regression line tend to be increased with elevating the latitude and/or air temperature (Fig. 1). Although further studies are necessary, these results indicate that the PRI is better index for LUE estimation even in the Pasoh tropical rain forest and the variation in the sensitivity of PRI might be estimated by using meteorological/geological parameter(s).

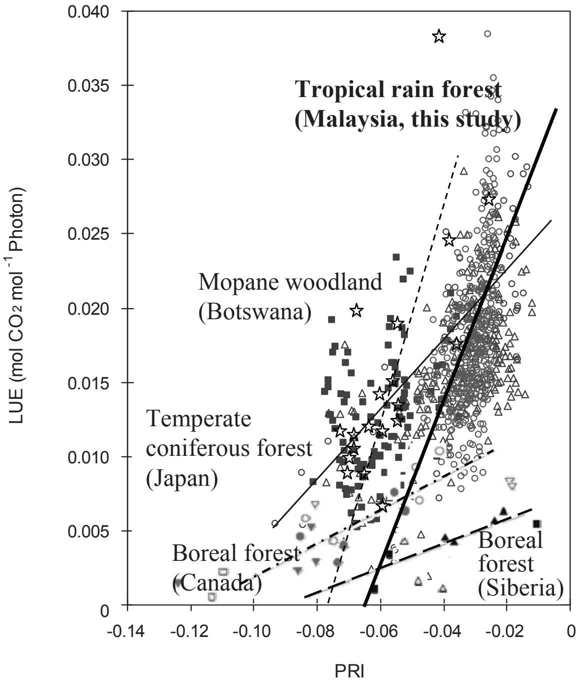

Figure 1. Relationships between photosynthetic LUE and PRI for Boreal forests (2, 5), Temperate forest (3) and Tropical forest. (5, this study)

(1) Gamon, J.A., Peñuelas, J., & Field, C.B. (1992). *Remote Sens. Environ.* 41, 35–44. (2) Nichol, C.J., Huemmrich, K.F., Black, T.A., *et al.* (2000). *Agr. For. Meteorol.*, 101, 131−142. (3) Nakaji, T., Ide, R., Takagi, K., *et al.* (2008). *Agr. For. Meteorol.*, 148, 776−787. (4) Garbulsky, M.F., Peñuelas, J., Gamon, J., *et al.* (2011). *Remote Sens. Environ.* 115, 281-297. (5) Grace, J., Nichol, C., Disney, M., *et al.* (2007). *Global Change Biol.*, 13, 1484−1497. (6) Yasuda, Y., Ohtani, Y., Watanabe, T. *et al.* (2003). *Agr. For. Meteorol.* 114, 235-244. (7) Motohka, T., Nasahara, K., Oguma, H., & Tsuchida, S. (2010). *Remote Sens.*, 2, 2369-2387.

Relationship between LUE and tower-observed spectral vegetation indices in a tropical rainforest at Pasoh, Peninsular Malaysia

Tatsuro Nakaji [a*], Yoshiko Kosugi [b], Satoru Takanashi [c], Hiroyuki Oguma [d] and Abdul Rahim Nik [e]

[a] Hokkaido University, Tomakomai, Japan, [b] Kyoto University, Kyoto, Japan, [c] Forestry and Forest Products Research Institute, Tsukuba, Japan, [d] National Institute for Environmental Studies, Tsukuba, Japan, [e] Ministry of natural Resources and Environment, Putrajaya, Malaysia (e-mail: nakaji@fsc.hokudai.ac.jp)*

Background and Objectives

- The **light use efficiency** (**LUE = GPP/APAR**) is one of the essential parameters for the vegetation productivity models.
- Although the remote-sensed spectral vegetation indices (VIs), such as **Photochemical Reflectance Index** (**PRI = [R_{531}-R_{570}]/[R_{531}+R_{570}]**) would be useful indicators for the estimation of spatial/temporal variations in LUE(1-4), we should confirm **whether site specific differences of VI's sensitivity exist or not**.
- In this study, we carried out tower monitoring of canopy spectral reflectance and eddy CO_2 flux (Fig.1) in **Pasoh Forest Reserve** to check the sensitivity of PRI and other broadband/hyperspectral VIs at the Asian tropical region.

Main results and conclusion

- **PRI is better index** for LUE estimation even in the Pasoh tropical rain forest. (Highest *r* value of PRI-LUE relationship, Table 1).
- **The sensitivity of PRI in Pasoh is quite different compared to the temperate forests and boreal forests.** Slope of regression line is higher in the tropical forests, supporting the similar result in another tropical forest in Botswana (5) (Comparison of tower/airborne RS studies, Fig. 2).
- When we use the PRI on a global scale, this sensitivity difference should be considered carefully.
- This difference may be estimated by other meteorological/geological parameter(s), such as mean air temperature (Positive correlation between mean *T* and slope, Fig. 3).

Materials & Methods

- **Pasoh Forest Reserve,** Lowland dipterocarp forest (LAI ≈ 6.5, 30-40mH)
- **Open pass** eddy CO_2 flux system on 52m tower (6)
- **Canopy spectral reflectance** (*R*) derived from tower-mounted 2 spectral radiometers (400~1100nm)

  R = downward / upward energy ratio)
- **Four broad-band VIs** (NDVI, EVI, GRVI & CI) and **two hyperspectral VIs** (PRI and CCI) (3, 7).
- **Oct 2008 ~ Dec 2009** culmination (13:00) and sunny sky condition.

NDVI = Normalized Difference Vegetation Index, EVI = Enhanced Vegetation Index, GRVI = Green Red Vegetation Index, PRI = Photochemical Vegetation Index, CCI = Canopy Chlorophyll Index, CI = Chlorophyll Index.

Monitoring data

- No clear seasonal variations in GPP and LUE were observed in Pasoh tropical forest.
- Short term depression of LUE was well linked with PRI partially (Fig. 4).

Fig. 4 Time course of parameters.

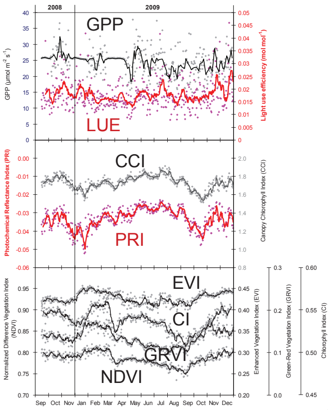

Fig. 1

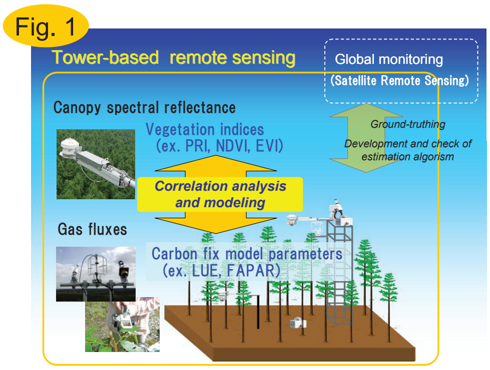

Outline of tower monitoring study

Table 1. Correlation coefficient between the productivity and VIs (*n* = 421)

	Spectral vegetation index (VI)					
	NDVI	EVI	GRVI	PRI	CCI	CI
GPP	0.16	0.09	0.09	0.12 **	0.11 ***	0.22
LUE	-0.19 ***	0.32 ***	-0.20 ***	**0.46** ***	0.39 ***	-0.08 ***

Significance: ** $p < 0.01$, *** $p < 0.001$ (Pearson's correlation test)

Fig. 2

Relationship between PRI and LUE in 13 forests. Data source: references (2), (3) and (5)

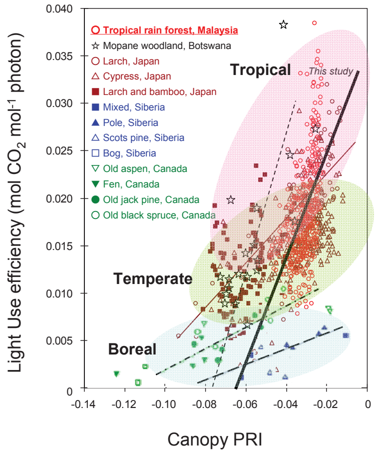

Fig. 3

Relationship between air temperature and slope of PRI-LUE regression line.

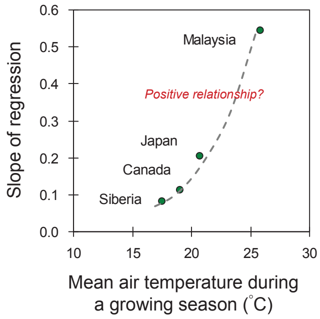

References

(1) Gamon J.A. *et al*. (1992). *Remote Sens. Environ*. 41, 35–44. (2) Nichol, C.J. *et al*. (2000). *Agr. For. Meteorol*., 101, 131–142. (3) Nakaji, T. *et al*. (2008). *Agr. For. Meteorol*., 148, 776–787. (4) Garbulsky, M.F. *et al*. (2011). *Remote Sens. Environ*. 115, 281-297. (5) Grace, J. *et al*. (2007). *Global Change Biol*., 13, 1484–1497. (6) Yasuda, Y. *et al*. (2003). *Agr. For. Meteorol*. 114, 235-244. (7) Motohka, T. *et al*. (2010). *Remote Sens*., 2, 2369-2387.

The effect of patchy stomatal behavior on leaf- and canopy-scale CO_2 flux of a tropical rainforest in Peninsular Malaysia, Pasoh

Mai Kamakura[1], Yoshiko Kosugi[2], Satoru Takanashi[3], Elizabeth Philip[4]

[1]Nara Women's University, Nara, Japan
[2]Kyoto University, Kyoto, Japan
[3]Forestry and Forest Products Research Institute, Tsukuba, Japan
[4]Forest Research Institute Malaysia, Kuala Lumpur, Malaysia

The canopy leaves of many tropical trees show midday depression of photosynthesis which is caused by high light occurring with high leaf temperature or water deficit (Ishida et al. Tree Physiol. 1999). In a primary tropical rainforest at Pasoh Forest Reserve in Peninsular Malaysia, the leaf-scale net assmilation rate (A), stomatal conductance (g_s), and the 'apparent' maximum carboxylation rate (V_{cmax}*) in leaves of dipterocarp trees were depressed in the afternoon (Takanashi et al. Tree Physiol. 2006). The apparent maximum carboxylation rate (V_{cmax}*) was estimated from the leaf gas exchange data in the field using one-point method, which is an inverse method based on the Farquhar-von Caemmerer-Berry model. The leaf CO_2 exchange calculations based on the Farquhar-von Caemmerer-Berry model under assumption of uniform stomatal behavior could not explain depressed values of A during midday. Numerical analysis of leaf CO_2 exchange calculated under assumption of patchy stomatal behavior showed that main factor in the inhibition of A during midday was patchy stomatal closure with a bimodal manner (Kosugi et al. Tree Physiol. 2009, Kamakura et al. Tree Physiol. 2011). Direct observation of stomatal aperture distribution in leaves of some canopy tree species consisting tropical dipterocarp forests also demonstrated midday patchy stomatal closure that fits a bimodal pattern.

The objective of this study is to determine whether midday depression of photosynthesis induced by patchy stomatal closure seen in leaves of many canopy trees consisting tropical dipterocarp forests affects canopy photosynthesis. At Pasoh, one of the flux tower sites in Southeast Asia, canopy CO_2 exchange has been measured with eddy covariance method (EC). The core area is covered with a primary lowland mixed dipterocarp forest (tropical evergreen broadleaf forest), consisting of various species of *Shorea* and *Dipterocarpus*. In this site, the diurnal pattern of CO_2 exchange at the canopy-scale also showed a clear restriction of canopy photosynthesis in the afternoon (Kosugi et al. Agric. Forest Meteorol. 2008). Canopy-scale photosynthesis is mainly determined by gas exchange of leaves at the top of the canopy. We investigated the diurnal change of gas exchange parameters at the canopy-scale such as canopy conductance (g_c) and the 'apparent' maximum carboxylation rate of canopy (V_{CMAX}*) using inverse Big-Leaf model analysis of EC fluxes (Kosugi et al. Agric. Forest Meteorol. 2005). Canopy conductance (g_c) and V_{CMAX}* decreased with a reduction of canopy photosynthesis in the afternoon. These results suggest that patchy stomatal behavior affects canopy-scale CO_2 exchange as well as leaf CO_2 exchange.

The effect of patchy stomatal behavior on leaf- and canopy-scale CO_2 flux of a tropical rainforest in Peninsular Malaysia, Pasoh

M. Kamakura[1], Y. Kosugi[2], S. Takanashi[3], E. Philip[4]
[1] Nara Women's University, Nara, Japan
[2] Kyoto University, Kyoto, Japan
[3] Forestry and Forest Products Research Institute, Tsukuba, Japan
[4] Forest Research Institute Malaysia, Kuala Lumpur, Malaysia
✉ mkamakura@cc.nara-wu.ac.jp

Introduction

The canopy leaves of many tropical trees show midday depression of photosynthesis which is caused by high irradiance occurring with high leaf temperature or vapor pressure deficit. In a primary tropical rainforest at Pasoh Forest Reserve in Peninsular Malaysia, patchy (non-uniform) stomatal closure occurs during midday depression **(Fig. 1)**.

When patchy stomatal closure with a bimodal manner occurs — The 'apparent' maximum carboxylation rate of the leaf (V_{cmax}*) decreases **(Fig. 2)**. Actually, however, the lack of CO_2 caused by stomatal closure leads to severe depression of leaf photosynthesis.

Numerical analysis of leaf CO_2 exchange calculated under assumption of patchy stomatal behavior and direct observation of stomatal aperture in leaves of some upper-canopy layers of tropical rainforest trees showed that main factor in the midday depression was patchy stomatal closure with a bimodal manner **(Takanashi et al. 2006, Kosugi et al. 2009, Kamakura et al. 2011, Fig. 3)**.

Canopy-scale photosynthesis is mainly determined by gas exchange of leaves at the top of the canopy. Thus, **the objective of this study is to determine whether midday depression of photosynthesis induced by patchy stomatal closure seen in leaves of many canopy trees consisting tropical dipterocarp forests affects canopy photosynthesis.**

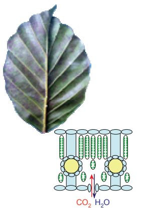

Fig. 1 Patchy stomatal behavior of *Dipterocarpus sublamellatus* (Takanashi et al. 2006).

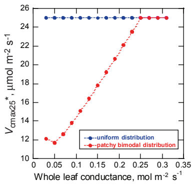

Fig. 2 Relationship between whole leaf conductance and normalized apparent maximum carboxylation rate of *D. sublamellatus* (V_{cmax25}*, Takanashi et al. 2006).

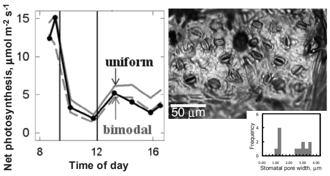

Fig. 3 Simulation and direct observation of bimodal stomatal closure of *Shorea leprosula* at midday (Kamakura et al. 2011).

Site Description

Mean annual air temperature: 25.5 °C
Mean annual rainfall: 1754 mm
Canopy height: 35 m
Vegetation: mixed dipterocarp forest

Tower flux observation: 2002.9 - now

Fig. 4 Pasoh Forest Reserve (PSO) in Peninsular Malaysia (2°58'N, 102°18'E).

Methods

Eddy covariance (EC) tower flux observation has been conducted since September 2002 until now (reported in an oral presentation by Y. Kosugi).
We investigated the diurnal change of gas exchange parameters at the canopy-scale such as canopy conductance (g_c) and the 'apparent' maximum carboxylation rate of the canopy (V_{CMAX}*) using inverse Big-Leaf model analysis of EC fluxes (Kosugi et al. 2005).

Inverse Big-Leaf model analysis of EC fluxes

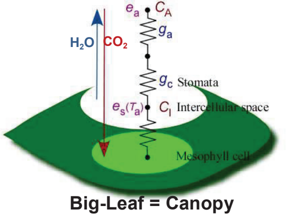

Big-Leaf = Canopy

Fig. 5 Extended Big-Leaf model (Kosugi et al. 2005).

·Canopy conductance (g_c, mm s^{-1})

$$\lambda E = \frac{\Delta(R_n - G) + \rho \cdot C_p \cdot g_a (e_s(T_a) - e_a)}{\Delta + \gamma(1 + g_a/g_c)}$$

(Penman-Monteith equation)

g_c: canopy conductance
V_{CMAX}*: apparent maximum carboxylation rate of the canopy
C_i: intercellular CO_2 conc. of the canopy
RE: ecosystem respiration

·Apparent maximum carboxylation rate of the canopy (V_{cMAX}*, μmol m^{-2} s^{-1}) derived from 30min fluxes

$$C_i = C_A - \frac{(GPP - RE_{leaf})(1/g_{aCO_2} + 1/g_{cCO_2})}{\rho_{mol}}$$

$$GPP = -NEE + RE = W_c \left[1 - \frac{\Gamma^*}{p(C_i)} \right]$$

$$W_c = \frac{V_{CMAX}{}^{*} \cdot p(C_i)}{p(C_i) + K_c(1 + p(O)/K_o)}$$

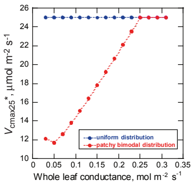

In the leaf-scale, V_{cmax}* decreases when patchy stomatal closure occurs.

Results and Discussion

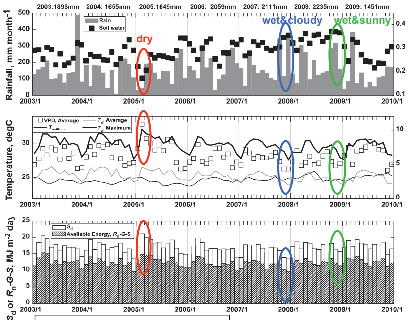

Dry : Feb, Mar 2005
Wet & cloudy : Nov, Dec 2007
Wet & sunny : Nov, Dec 2008

Fig. 6 Amount of rainfall, soil water content, air temperature, vapor pressure deficit, solar radiation, and available energy at Pasoh in 7 years between 2003and 2009.

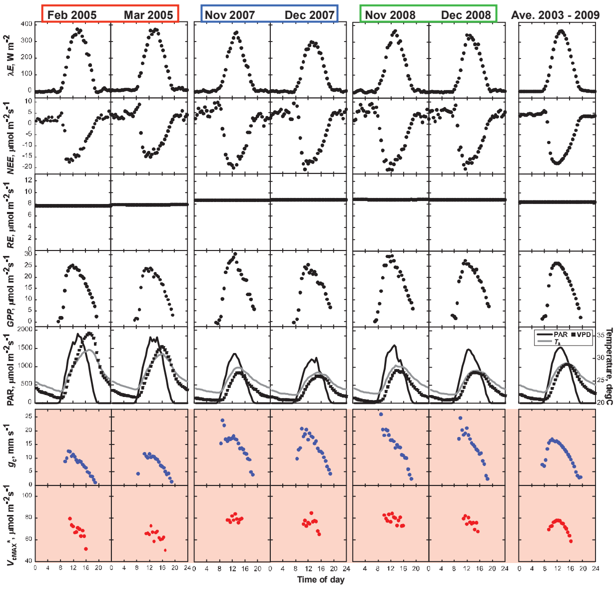

Fig. 7 Diurnal and seasonal fluctuations of Big-Leaf parameters, g_c and V_{cMAX}*, with evapotranspiration, NEE, RE, and GPP. Monthly averages are shown. NEE data during rain are rejected.

· Over the entire period, canopy conductance (g_c) decreased in the afternoon. The apparent maximum carboxylation rate of the canopy (canopy V_{cMAX}*) also decreased with decreasing g_c.

These results suggest that patchy stomatal behavior influenced the CO_2 flux at the canopy-scale as well as at the leaf-scale.

·During the drought period from Feb to Mar 2005, smaller g_c in related to higher VPD was observed. Moreover, decline in V_{cMAX}* in the afternoon was significant.

Conclusion

The apparent maximum carboxylation rate of the canopy (V_{cMAX}*) decreased with decreasing g_c in the afternoon. Thus, severe depression of photosynthesis caused by patchy stomatal closure in leaves of many canopy trees consisting tropical dipterocarp forests affects canopy-scale CO_2 flux.

BIOGENIC VOLATILE ORGANIC COMPOUND EMISSIONS FROM THIRTY EIGHT TROPICAL TREE SPECIES IN MALAYSIA

[1]Motonori Okumura, [2]Yoshiko Kosugi, [3]Satoru Takanashi, [4]Mai Kamakura,
[5]Kazuho Matsumoto, [1]Susumu Tohno, [6]Elizabeth Philip

[1]Graduate School of Energy Science, Kyoto University, Kyoto, Japan
[2]Graduate School of Agriculture, Kyoto University, Kyoto, Japan
[3]Forestry and Forest Products Research Institute, Ibaraki, Japan
[4]Kyousei Science Center for Life and Nature, Nara Women's University, Nara, Japan
[5]Faculty of Agriculture, University of the Ryukyus, Okinawa*, Japan*
[6]Forest Research Institute Malaysia, Kuala Lumpur, Malaysia

Biogenic volatile organic compounds (BVOCs) are emitted by many plant species and include terpenoids such as isoprene (C_5H_8), monoterpenes ($C_{10}H_{16}$), sesquiterpenes ($C_{15}H_{24}$) and alcohols. Terpenoids are highly reactive with ozone and hydroxyl radicals as compared with most anthropogenic volatile organic compounds and, therefore, contribute to the formation of ozone and other photochemical oxidants in the lower atmosphere.

We conducted measurements of BVOC emissions from leaves of 38 tropical tree species in a nursery at Forest Research Institute Malaysia (FRIM) from 29 January to 3 February 2010. The selected species were located at the middle and upper canopies as well as forest floor levels in Malaysia. The biogenic emission rate, together with the net assimilation rate and photosynthetic photon flux density, was measured using a leaf cuvette (LI6400, Li-cor). BVOC emission from the plant was identified and quantified using gas chromatography-mass spectrometry (GCMS QP2010plus, Shimadzu). The samples underwent thermal desorption by a TD-20 system (Shimadzu), and compound separation was achieved using an SLB-5ms capillary column (30 m × 0.25 mm, ID 1 µm, Supelco). Rate of isoprene emission (I, nmol m^{-2} s^{-1}) from the leaf was calculated according to the following equation.

$$I = \left\{ C_{out}\left(\frac{1-w_{in}}{1-w_{out}}\right) - C_{in} \right\} v_{in} / LA$$

where C_{in} and C_{out} are the isoprene concentrations (nmol mol^{-1}) in the inflow and outflow samples, respectively, and w_{in} and w_{out}, the water vapor concentrations (mol mol^{-1}) in the inflow and outflow samples, respectively. v_{in} is the flow rate (mol s^{-1}) in the cuvette and LA is the enclosed leaf area (m^2).

Screening of BVOC-emitting species showed that 12 tree species were isoprene emitters (Table 1). No isoprene emitter was found in dipterocarp trees.

Table 1. List of tree species measured in this study.

Family	Species		Family	Species
Dipterocarparpaceae	*Shorea singkawang*	*Hopea sublanceolata*	Sapindaceae	*Pometia pinnata*
	S. sumatrana	*H. glaucescens*		*Xerospermum noronhianum*
	S. leprosula	*H. subalata*	Thymelaeaceae	*Gonystylus affinis*
	S. macrantha	*H. auriculata*		*Aquilaria malaccensis*
	S. hemsleyana	*H. bilitonensis*	Lauraceae	*Cinnamomum iners*
	S. lepidota	*Vatica nitens*	Anacardiaceae	*Bouea oppositifolia*
	S. parvifolia	*V. pauciflora*	Meliaceae	*Azadirachta excelsa*
	Dipterocarpus gracilis	*V. flavida*	Moraceae	*Streblus elongatus*
	D. grandiflorus		Lecythidaceae	*Barringtonia fusiformis*
	D. rigidus		Flacourtiaceae	*Flacourtia rukam*
	D. tempehes			
	D. crinitus			
Fabaceae	*Cynometra malaccensis*	*Intsia palembanica*		
	Callerya atropurpurea	*Archidendron bubalinum*		
	Cassia nodosa			
Clusiaceae	*Garcinia hombroniana*	*Mesua ferrea*		
	G. nigrolineata			

BIOGENIC VOLATILE ORGANIC COMPOUND EMISSIONS FROM THIRTY EIGHT TROPICAL TREE SPECIES IN MALAYSIA

[1]Motonori Okumura, [2]Yoshiko Kosugi, [3]Satoru Takanashi, [4]Mai Kamakura, [5]Kazuho Matsumoto, [1]Susumu Tohno, [6]Elizabeth Philip
Graduate School of Energy Science, Kyoto University, Kyoto, Japan, [2]Graduate School of Agriculture, Kyoto University, Kyoto, Japan
[3]Forestry and Forest Products Research Institute, Ibaraki, Japan, [4]Kyousei Science Center for Life and Nature, Nara Women's University, Nara, Japan,
[5]Faculty of Agriculture, University of the Ryukyus, Okinawa, Japan, *[6]Forest Research Institute Malaysia, Kuala Lumpur, Malaysia*
E-mail: okumura.motonori.6v@kyoto-u.ac.jp

INTRODUCTION

Biogenic Volatile Organic Compounds (BVOCs) including isoprene (C_5H_8), monoterpene ($C_{10}H_{16}$), alcohols, organic acids and aldehydes are released from many plant species. BVOCs are highly reactive with ozone and hydroxyl radicals as compared with most anthropogenic volatile organic compounds and, therefore, contribute to the formation of ozone and other photochemical oxidants in the lower atmosphere. The estimation of annual global emission of all BVOCs has been conducted previously (e.g., Guenther *et al*., 1995, IPCC, 2001), according to which the estimated values greatly exceed the annual global emission of anthropogenic non-methane VOCs. Global emission of isoprene accounts for about 50 % of total BVOCs emission.

METHODS

Plant materials

We conducted measurements of BVOC emissions from leaves of tropical tree species in the Pasoh Forest Reservea, Malaysia (2° 58′N, 102° 18′E, Fig. 1) and in Forest Research Institute Malaysia (FRIM, Fig. 1). Field measurements were carried out in a primary lowland mixed dipterocarp forest in Pasoh in December 2007 and September 2009. A 30m walk-up tower provided access to the canopy top of trees (Fig. 1 & Fig. 2). Thirty eight tree species were screened for emissions of isoprene and other BVOCs in a nursery at FRIM from 29 January to 3 February 2010. The selected seedling species were located at the middle and upper canopies as well as forest floor levels in Malaysia (Table 1).

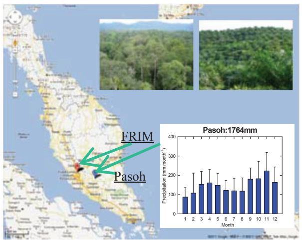

Fig. 1 Location of Pasoh and FRIM.

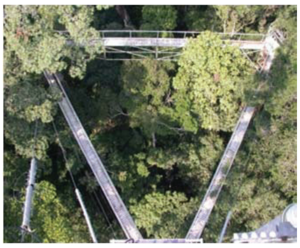

Photo 1 A view of canopy walk in Pasoh.

Xanthophyllum stipitatum *Dipterocarpus sublamellatus* *Ptychopyxis caput-medusae* *Neobalanocarpus heimii*

Alphonsea maingayi *Rinorea anguifera* *Macaranga lowii* Oil Palm (*Elaeis guineensis*)

Photo 2 Ttree species measured in the Pasoh Forest.

Table 1. List of tree species measured in this study (FRIM).

Family	Species		Family	Species
Dipterocarparpaceae	*Shorea singkawang*	*Hopea sublanceolata*	Sapindaceae	*Pometia pinnata*
	S. sumatrana	*H. glaucescens*		*Xerospermum noronhianum*
	S. leprosula	*H. subalata*	Thymelaeaceae	*Gonystylus affinis*
	S. macrantha	*H. auriculata*		*Aquilaria malaccensis*
	S. hemsleyana	*H. bilitonensis*	Lauraceae	*Cinnamomum iners*
	S. lepidota	*Vatica nitens*	Anacardiaceae	*Bouea oppositifolia*
	S. parvifolia	*V. pauciflora*	Meliaceae	*Azadirachta excelsa*
	Dipterocarpus gracilis	*V. flavida*	Moraceae	*Streblus elongatus*
	D. grandiflorus		Lecythidaceae	*Barringtonia fusiformis*
	D. rigidus		Flacourtiaceae	*Flacourtia rukam*
	D. tempehes			
	D. crinitus			
Fabaceae	*Cynometra malaccensis*	*Intsia palembanica*		
	Callerya atropurpurea	*Archidendron bubalinum*		
	Cassia nodosa			
Clusiaceae	*Garcinia hombroniana*	*Mesua ferrea*		
	G. nigrolineata			

Photo 3 The measurements of BVOC emissions from leaves of 38 tropical tree species in a nursery at Forest Research Institute Malaysia (FRIM).

Leaf cuvette method

The biogenic emission rate, together with the net assimilation rate and photosynthetic photon flux density, was measured using a leaf cuvette (LI6400, Li-cor). BVOC emission from the plant was identified and quantified using gas chromatography-mass spectrometry (GCMS QP2010plus, Shimadzu). The samples underwent thermal desorption by a TD-20 system (Shimadzu), and compound separation was achieved using an SLB-5ms capillary column (30 m × 0.25 mm, ID 1 μm, Supelco). Rate of isoprene emission (I, nmol m^{-2} s^{-1}) from the leaf was calculated according to the following equation.

$$I = \left\{ C_{out}\left(\frac{1-w_{in}}{1-w_{out}}\right) - C_{in} \right\} v_{in} / LA$$

where C_{in} and C_{out} are the isoprene concentrations (nmol mol^{-1}) in the inflow and outflow samples, respectively, and w_{in} and w_{out}, the water vapor concentrations (mol mol^{-1}) in the inflow and outflow samples, respectively. v_{in} is the flow rate (mol s^{-1}) in the cuvette and LA is the enclosed leaf area (m^2).

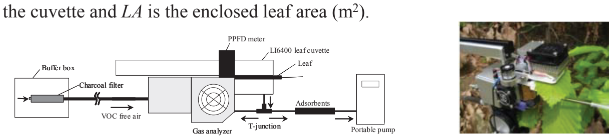

Fig. 2. A schematic diagram of BVOCs sampling using a portable photosynthesis system (LI6400). For measuring the isoprene emission, the outlet air flow from the leaf cuvette was divided into two streams by a Teflon T-junction.

RESULTS

One species was found to be monoterpene emitter (*Xanthophyllum stipitatum,* Fig. 4) in the Pasoh Forest. In a nursery at FRIM, Screening of BVOC-emitting species showed that 12 tree species were isoprene emitters (Table 2). No isoprene and monoterpene emitter was found in dipterocarp trees in this study. On the other hand, It has been found that Oil palms are very high isoprene emitters. This results indicate that increasing areas of oil palm plantations in the future could increase ozone and other photochemical oxidants in South East Asia.

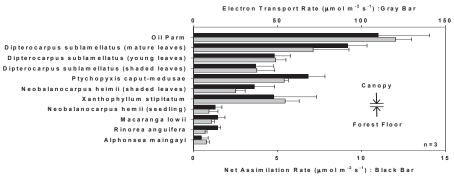

Fig. 3 Net assimilation rates and electron transport rates (Pasoh forest)

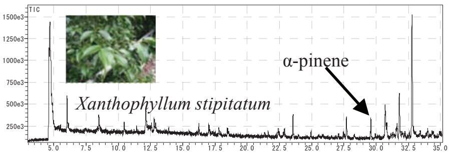

Fig. 4 Total ion chromatogram of emission gases from *X. stipitatum.*

Table 2. Isoprene emissions from leaves of tropical tree species. Screening of BVOC-emitting species showed that 12 tree species were isoprene emitters.

Spieces	Compound	Emission	Spieces	Compound	Emission
Bouea oppositifolia	isoprene	high	*Cynometra malaccensis*	isoprene	middle
Streblus elongatus	isoprene	low	*Callerya atropurpurea*	isoprene	high
Aquilaria malaccensis	isoprene	very high	*Cassia nodosa*	isoprene	middle
Garcinia nigrolineata	isoprene	high	*Garcinia hombroniana*	isoprene	middle
Flacourtia rukam	isoprene	low	*Mesua ferrea*	isoprene	high
Archidendron bubalinum	isoprene	low	*Cinnamomum iners*	isoprene	middle

ACKNOWLEDGMENT

We thanks Ms Lillian and Chua and Mr Qua Eng Seng for organizing our research in a nursery at FRIM. We also thanks Dr Makoto Tani, Dr Abdul Rahim Nik and Dr Toshinori Okuda and a joint research project between FRIM, UPM and NIES. This study was supported in part by funds from the Grant-in-Aid for Scientific Research on Priority Areas under Grant No. 2012005 from Japanese Ministry of Education, Culture, Sports, Science and Technology.

MEASUREMENT OF AUTOTROPHIC RESPIRATION OF TREE IN PASOH -FROM LEAVES TO ROOTS-

Masako Dannoura[1], Yoshiko Kosugi[1], Satoru Takanashi[2], Naoki Makita[1], Shuhei Kanemitsu[1], Katsunori Tanaka[3], Takehiko Haruta[4], Kaoru Niiyama[5] Abd Rahman Kassim [6] and Abdul Rahim Nik [7]

[1] Graduate School of Agriculture, Kyoto University, Kyoto, Japan
[2] Forestry, Forest Products Research Institute, Tsukuba, Japan
[3] Japan Agency for Marine-Earth Science and Technology, Yokohama, Japan
[4] Faculty of Bioresources, Mie University, Tsu, Mie, Japan
[5] Tohoku Research Center, Forestry, Forest Products Research Institute, Morioka, Japan
[6]Forest Research Institute Malaysia, Kepong, Malaysia
[7]Ministry of Natural Resources and Environment, Putrajaya, Malaysia

Introduction

Net Primary Production (NPP) of forest is calculated by subtraction of autotrophic respiration (R_a) taken from photosynthesis. R_a is from metabolic process of carbon which plant fixed. Mori et al.(2010) led size dependency of R_a by measuring whole tree's respiration. R_a accounts for 40-70 % of fixed carbon in temperate forest, (Ryan et al., 1995; Saxe et al., 2001), and 70% in tropic forest (Chambers et al., 2004). For accurate estimation of forest carbon cycle, it is needed to combine knowledge of whole ecosystem level and understanding of characteristic of each component. In this research, we measured R_a from each component to scale up to the whole tree.

Method

Measurements were conducted in Pasoh Forest Reserve (2°59'N, 102°19'E) in Peninsula Malaysia. This is one of AsiaFlux tower sites, which aimed to compare meteorological measurement with ecological research. The average annual temperature is 25.5°C, and annual precipitation is 1754 mm.

Fourteen trees of 0.9 – 29.1 m height were cut in Feb.2010. Sample trees were divided to leaves (n=234), branches (n=157), stems (n=119), coarse roots (n=150) and fine roots (d<2 mm; n=220). Aboveground samples were measured immediately after cutting and belowground parts were just after washing. Cutting sections were covered by silicone to avoid additional wound respiration. CO_2 efflux was measured by closing chamber system connected to IRGA (LI-840, Li-cor, USA). Surface temperature was measured by thermo couple. CO_2 efflux at 25°C was calculated assuming Q_{10}=2.0. Dry weight, diameter, surface area and volume of samples were measured. For leaves and fine roots, we analyzed scanned images for the measurement of surface area.

Results and Discussion

Average respiration rates per sample dry weight (nmol CO_2 g^{-1} s^{-1}; (sd)) from each compartment were 3.42 (1.73) in leaves, 0.85(1.12) in branches, 0.085(0.084) in stems, 0.31(0.29) in coarse roots, 8.16(6.22) in fine roots. Respiration rates per sample weight were higher in ticker leaves, especially well related to Leaf Mass Area (g m^{-2}) (see presentation of Takanashi *et al.*). The leaves, branches, stem which located at higher position had higher respiration rate, but there were some exceptions. Thinner branch and root samples had higher respiration rate per weight. However, root finer than 5 mm in the diameter had high respiration with wide variation.

Whole tree's respiration was estimated using the data of tree biomass. Stem respiration was calculated every meter height. Bottom part of stem which has large biomass per unit height has lower respiration than upper part of stem. Thus, it mitigates the height variation within stem. Leaf respiration takes large part in total respiration especially in smaller trees. The composition of respiration from each component changes according with the tree size.

MEASUREMENT OF AUTOTROPHIC RESPIRATION OF TREE IN PASOH -FROM LEAVES TO ROOTS-

Masako Dannoura[1], Yoshiko Kosugi[1], Satoru Takanashi[2], Naoki Makita[1], Shuhei Kanemitsu[1], Katsunori Tanaka[3], Takehiko Haruta[4], Kaoru Niiyama[5], Abd Rahman Kassim[6] and Abdul Rahim Nik[7]

[1] *Graduate School of Agriculture, Kyoto University, Kyoto, Japan.* [2] *Forestry, Forest Products Research Institute, Tsukuba, Japan.* [3] *Japan Agency for Marine-Earth Science and Technology, Yokohama, Japan.* [4] *Faculty of Bioresources, Mie University, Tsu, Mie, Japan.* [5] *Tohoku Research Center, Forestry, Forest Products Research Institute, Morioka, Japan.* [6] *Forest Research Institute Malaysia, Kepong, Malaysia.* [7] *Ministry of Natural Resources and Environment, Putrajaya, Malaysia*

AIM

Net Primary Production (NPP) of forest is calculated by subtraction of autotrophic respiration (Ra) from photosynthesis. Ra is from the metabolic process of carbon which plant fixed. Ra accounts for 40-70 % of fixed carbon in temperate forest, (Ryan et al., 1995; Saxe et al., 2001), and 70% in tropic forest (Chambers et al., 2004). For accurate estimation of the forest carbon cycle, it is needed to combine knowledge of whole ecosystem level and understanding of characteristic of each component. In this research, we measured Ra from each component to scale up to the whole tree.

METHODS

Site

Pasoh Forest Reserve in Peninsula Malaysia
(2° 58'N, 102° 18'E)
Tree height; 30-40 m
(with emergent tree ～45m)
Air temperature; 25.3 ℃
Precipitation; 1865 mm
(2003-2009)

Sample trees

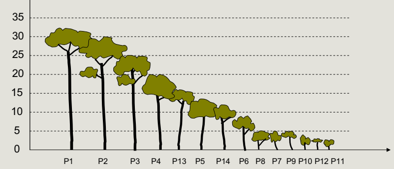

P1 *Shorea Leprosula*
P2 *Shorea Acuminata*
P3 *Hypobathrum racemosum (Roxb.) Kurz*
P4 *Shorea Multiflora*
P5 *Aporosa Bracteosa*
P6 *Anayagorea Javanica*
P7 *Galearia maingayi Hook.f.*
P8 *Aglaia Odoratissima*
P9 *Aglaia Exstipulata*
P10 *Shorea Multiflora*
P11 *Sterculia Macrophylla*
P12 *Dacryodes Rugosa*
P13 *Pentaspadon Motleyi*
P14 *Blumeodemdron Tokbrai*

CO_2 efflux measurement

Measurements were conducted 31/Jan.-5/Feb.in 2009. Sample trees were cut and separated into leaves, branches, stems (every one meter) , and coarse roots. Fine root samples were taken from trench 4m in depth.

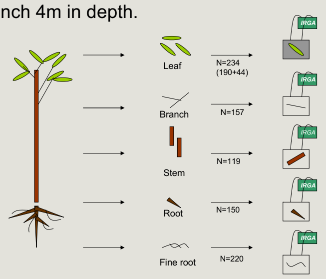

Samples were put into chambers connected with IRGA (LI 840, Li-cor, USA) to measure CO_2 efflux. Temperature, dry weight, diameter, length of samples were measured. Leaf Area, root surface area were also measured using image analysis with images taken by scanner.

CO_2 efflux (μ mol m^{-2} s^{-1}) were calculated as below; then normalized to that of at 25 ℃ assuming Q10=2.

$$CO_2 \text{ efflux} = \frac{[CO_2] \times P}{8.314 \times T \times Sc}$$

$[CO_2]$=increasing ratio of CO_2 concentration (mol s^{-1})
P=atmospheric pressure (Pa)
Sc=surface area (m^2)
T= temperature (K°)
8.314J mol^{-1} K^{-1}= ideal gas constant

RESULTS

Leaf

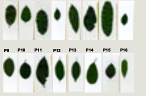

■Higher respiration in higher position
■Leaf respiration and LMA (Leaf Mass Area) has positive relation

(see Takanashi's poster)

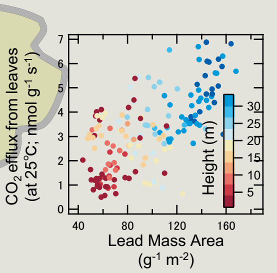

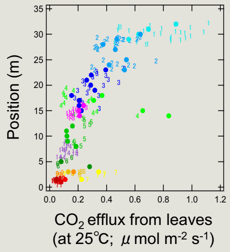

Branch

■Higher respiration in smaller branch
■Higher respiration in high position branch

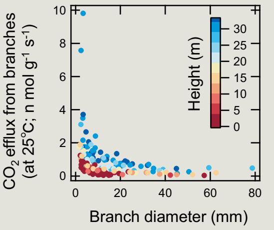

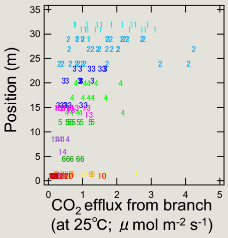

Stem

■Higher respiration in smaller stem
■Higher respiration in high position stem
■Different depends on tree

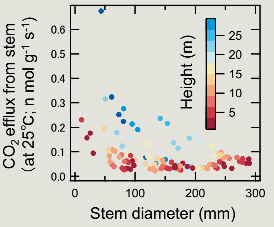

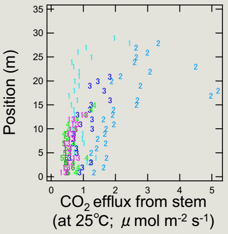

Coarse Root

■Higher respiration in smaller root
■No clear relation between depth

(see Makita's poster)

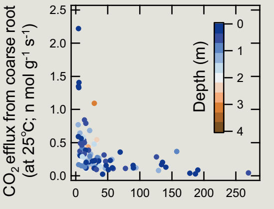

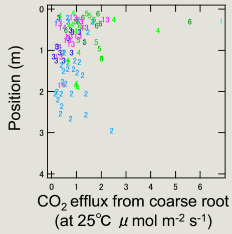

Fine Root

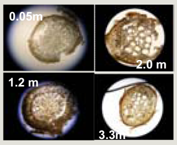

■Higher respiration in smaller root
■Higher respiration in upper position

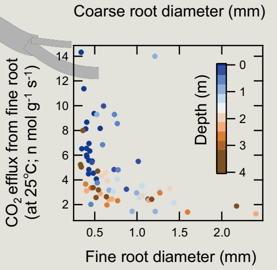

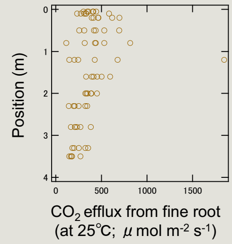

Biomass & respiration distribution

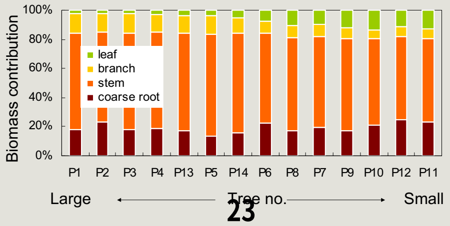

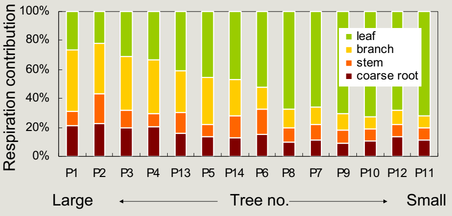

CONCLUSION

■In tropical rain forest, tree height was a quite important factor of Ra.
■There are relationships between Ra (branch, stem and coarse/fine root) and diameter, if same size, higher position had higher respiration rate.
■Leaf, branch, and stem respiration in higher position tended to be higher, but there were some exceptions.
■Woody part (stem& branch) was important in biomass contribution, leaf was important in respiration contribution.
■Fine roots might have an important role in total Ra.

VERTICAL PROFILE OF LEAF PHOTOSYNTHETIC CHARACTERISTICS IN A TROPICAL LOWLAND DIPTEROCARP FOREST AT PASOH, PENINSULAR MALAYSIA

Satoru Takanashi[1], Yoshiko Kosugi[2], Takehiko Haruta[3], Masako Dannoura[2], Naoki Makita[2], Katsunori Tanaka[4], Kaoru Niiyama[5], Abdul Rahman bin Kassim[6], Abdul Rahim Nik[7]

[1] *Forestry and Forest Products Research Institute, Tsukuba, Japan*
[2] *Graduate School of Agriculture, Kyoto University, Kyoto, Japan*
[3] *Faculty of Bioresources, Mie University, Tsu, Japan*
[4] *Japan Agency for Marine-Earth Science and Technology, Yokohama, Japan*
[5] *Tohoku Research Center, Forestry and Forest Products Research Institute, Morioka, Japan*
[6]*Forest Research Institute Malaysia, Kepong, Malaysia*
[7] *Ministry of Natural Resources and Environment, Putrajaya, Malaysia*

Introduction

Tropical rainforests are very important for evaluating the role of terrestrial ecosystems in climate change because of their huge biomass and their large gas-exchanges of water vapor or carbon dioxide. Tropical rainforests consist of many sizes of trees. A leaf photosynthetic capacity was mainly controlled by light environment, although trees have own strategies for an efficient photosynthesis conserving their water adapting the environments. To understand H_2O/CO_2 exchange processes of tropical rainforests, we need to know both canopy gas-exchange characteristics (captured by the eddy covariance method) and the distribution of leaf photosynthetic characteristics with their environments. In this study, the electron transport rate for PSII (ETR) and the leaf respiration of tree species in a primary lowland dipterocarp forest were investigated with the tree size, the leaf mass per area (LMA), the height of the leaf.

Methods

Measurements were conducted at Pasoh Forest Reserve (AsiaFlux site code:PSO, 2°58’ N, 102°18’ E), Peninsular Malaysia from 31st Jan. to 6th Feb. 2010.We are continuously observing meteorological factors including solar radiation, temperature, humidity, and wind speed and H_2O/CO_2/energy fluxes using the eddy covariance method at an observation tower. More than 800 tree species is present in this study forest. The continuous canopy height is approximately 35 m in height, although some emergent trees exceed 45 m in height. Average plant area index optically measured by a plant canopy analyzer (LAI-2000, Licor, USA) at the tower was about 6.5 m^2 m^{-2}. At 300 m south west from the tower, fourteen trees of 0.9 – 29.1 m height were cut down for the samplings. Leaves were sampled from the cut down tree recoding each height from the ground, and ETR in saturated photosynthetic photon flux density condition of 1000 µmol m^{-2} s^{-1} (ETR_{sat}) was immediately measured using a photosynthesis yield analyzer (Mini-PAM, Waltz, Germany). After measurement of ETR, we measure a leaf dark respiration using three closed dynamic chamber systems, each of which was consisted of a dark chamber, a pump and an infra-red gas analyzer (Li-840, Licor, USA). Additionally, leaves of two emergent tree species which can be sampled at the aluminum canopy walkway at the tower site were measured in the same way. Surface areas of leaves were calculated from the digitalized image taken by a digital scanner before dry weight and leaf thickness were measured. Leaf dark respiration per surface area at 25°C (R_{leaf25}) was calculated assuming Q^{10}=2.

Results and Discussion

Average and standard deviation of ETR_{sat} were 31.6 µmol m^{-2} s^{-1} and 19.0 µmol m^{-2} s^{-1} respectively. Average and standard deviation of R_{leaf25} were 0.37 µmol CO_2 m^{-2} s^{-1} and 0.27µmol CO_2 m^{-2} s^{-1} respectively. Averages of ETR_{sat} and R_{leaf25} grouped by each tree species tend to be high at higher layer and this tendency was found within some tree species. The values of LMA were increased with increase of their height, although scattered in some species. The values of R_{leaf25} were positively related to LMA, and the values of ETR_{sat} were also related to LMA. These results suggest that higher trees adapting their local environment have thicker leaves which are characterized by high photosynthetic capacity and high respiration rate.

Vertical profile of leaf photosynthesis characteristics in a tropical lowland dipterocarp forest at Pasoh, Peninsular Malaysia

S. Takanashi[1], Y. Kosugi[2], T. Haruta[3], M. Dannoura[2], N. Makita[2], K. Tanaka[4], K. Niiyama[5],
Abdul Rahman bin Kassim[6], Abdul Rahim Nik[7]

[1]Forestry and Forest Products Research Institute, Tsukuba, Japan
[2]Graduate School of Agriculture, Kyoto University, Kyoto, Japan
[3]Faculty of Bioresources, Mie University, Tsu, Japan
[4]Japan Agency for Marine-Earth Science and Technology, Yokohama, Japan
[5]Tohoku Research Center, Forestry and Forest Products Research Institute, Morioka, Japan
[6]Forest Research Institute Malaysia,Kepong, Malaysia
[7]Ministry of Natural Resources and Environment, Putrajaya, Malaysia

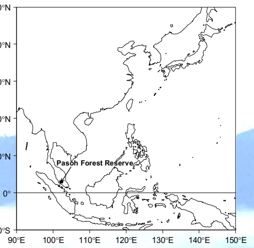

Introduction

Tropical rainforests are very important for evaluating the role of terrestrial ecosystems in climate change because of their huge biomass and their large gas-exchanges of water vapor or carbon dioxide. Tropical rainforests consist of many sizes of trees. A leaf photosynthetic capacity was mainly controlled by light environment, although trees have own strategies for an efficient photosynthesis conserving their water adapting the environments. To understand H_2O/CO_2 exchange processes of tropical rainforests, we need to know both canopy gas-exchange characteristics (captured by the eddy covariance method) and the distribution of leaf photosynthetic characteristics with their environments. In this study, the electron transport rate for PSII (ETR) and the leaf respiration of tree species in a primary lowland dipterocarp forest were investigated with the tree size, the leaf mass per area (LMA), the height of the leaf.

Site description

Measurements were conducted at Pasoh Forest Reserve (AsiaFlux site code:PSO, 2° 58' N, 102° 18' E), Peninsular Malaysia from 31st Jan. to 6th Feb. 2010.We are continuously observing meteorological factors including solar radiation, temperature, humidity, and wind speed and H_2O/CO_2/energy fluxes using the eddy covariance method at an observation tower. More than 800 tree species is present in this study forest. The continuous canopy height is approximately 35 m in height, although some emergent trees exceed 45 m in height. Average plant area index optically measured by a plant canopy analyzer (LAI-2000, Licor, USA) at the tower was about 6.5 m^2 m^{-2}.

Materials

At 300 m south west from the tower, fourteen trees of 0.9 – 29.1 m height were cut down for the samplings (sp. 1-14). Additionally, leaves of two emergent tree species which can be sampled at the aluminum canopy walkway at the tower site were measured in the same way (sp. 15 and 16).

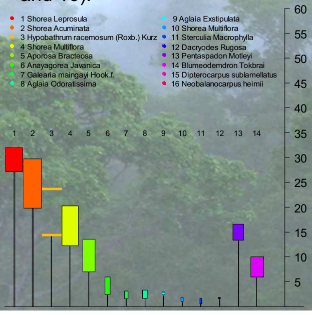

Methods

Leaves were sampled from the cut down tree recoding each height from the ground, and ETR in saturated photosynthetic photon flux density condition of 1000 μmol m^{-2} s^{-1} (ETR_{sat}) was immediately measured using a photosynthesis yield analyzer (Mini-PAM, Waltz, Germany). After measurement of ETR, we measure a leaf dark respiration using three closed dynamic chamber systems, each of which was consisted of a dark chamber, a pump and an infra-red gas analyzer (Li-840, Licor, USA). Surface areas of leaves were calculated from the digitalized image taken by a digital scanner before dry weight and leaf thickness were measured. Leaf dark respiration per surface area at 25° C (R_{leaf25}) was calculated assuming Q^{10}=2.

Results and Discussion

Average and standard deviation of ETR_{sat} were 31.6 μmol m^{-2} s^{-1} and 19.0 μmol m^{-2} s^{-1} respectively. Average and standard deviation of R_{leaf25} were 0.37 μmol CO_2 m^{-2} s^{-1} and 0.27μmol CO_2 m^{-2} s^{-1} respectively. Averages of ETR_{sat} and R_{leaf25} grouped by each tree species tend to be high at higher layer and this tendency was found within some tree species.

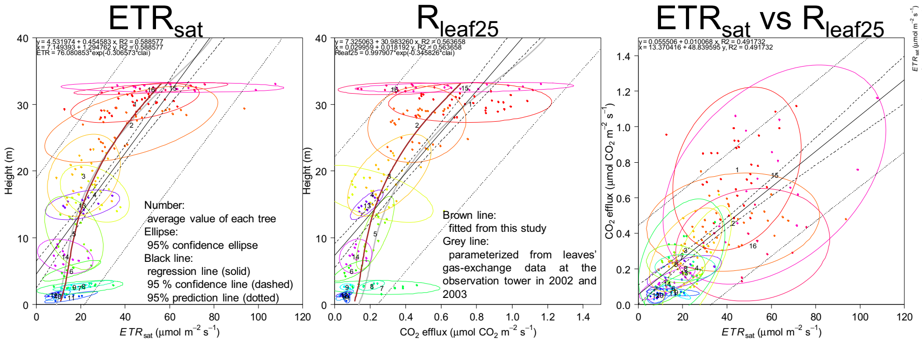
ETR_{sat}

R_{leaf25}

ETR_{sat} vs R_{leaf25}

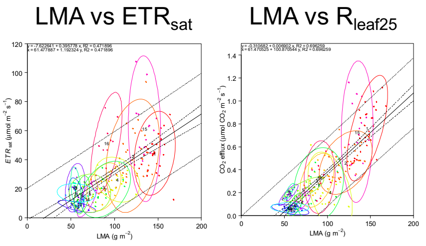
LMA vs ETR_{sat}

LMA vs R_{leaf25}

The values of LMA were increased with increase of their height, although scattered in some species. The values of R_{leaf25} were positively related to LMA, and the values of ETR_{sat} were also related to LMA. These results suggest that higher trees adapting their local environment have thicker leaves which are characterized by high photosynthetic capacity and high respiration rate.

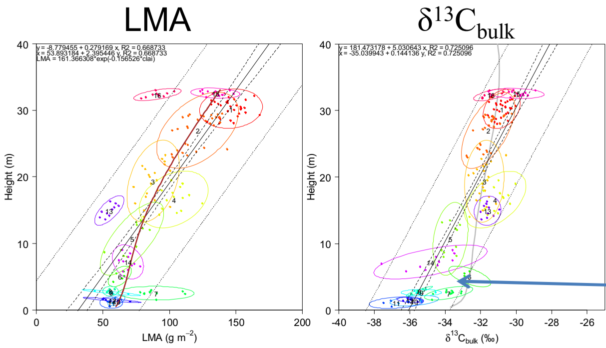
LMA

$\delta^{13}C_{bulk}$

ETR_{sat} and R_{leaf25} are related with cumulative Leaf Area Index (light environment)
$y = a*exp(-b*cumLAI)$

Carbon isotopic conposition of leaves ($\delta^{13}C_{bulk}$) increased with their height.

We need to re-analyze parameters of stomatal conductance and carbon isotope discrimination in the forest floor.

Multi-layered modeling at the observation tower

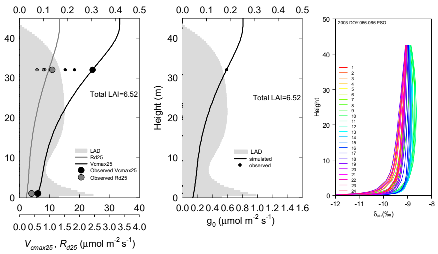

Acknowledgement

This work was supported by JSPS Grant-in-Aid for Scientific Research (KAKENHI: 20255010) and the joint research project between Forest Research Institute Malaysia (FRIM), Universiti Putra Malaysia (UPM) and National Institute of Environmental Studies (NIES).

AsiaFlux Workshop 2011, 10 November, Johor Bahru Malaysia WP039

PATTERN IN ROOT RESPIRATION RATES WITH THEIR MORPHOLOGICAL TRAITS IN 13 TREE SPECIES IN TROPICAL FOREST

Naoki Makita[1], Yoshiko Kosugi[1], Masako Dannoura[1], Satoru Takanashi[2], Kaoru Niiyama[3], Abd Rahman Kassim[4], Abdul Rahim Nik[4]

[1] *Graduate School of Agriculture, Kyoto University, Kyoto 606-8502, Japan*
[2] *Forestry and Forest Products Research Institute (FFPRI), Ibaraki 305-8687, Japan*
[3] *Tohoku Research Center, FFPRI, Morioka 020-0123, Japan*
[4] *Forest Research Institute Malaysia, Kepong, Kuala Lumpur 52109, Malaysia*

Tree roots constitute a large fraction of annual net primary production, resulting in a large flux of carbon (C) and nutrients into the belowground system. The root systems are composed of different diameters and heterogeneous physiological traits. There is now considerable evidence that difference in root diameter size influence the respiration. However, current understanding of the patterns and controls of root respiration from small fine roots to large coarse roots across species is limited, because previous studies focused on specific diameter sizes and specific species. Here, we attempted to clarify the species-specific respiration rates of fine roots (<2 mm diameter; n=125) and coarse roots (2–269 mm diameter; n=175) of 13 species in 14 trees differing in tree height and age in a primary tropical rainforest. The variability in respiration rates was examined in relation to mean root diameter (*D*; mm) of various diameter sizes and the root tissue density (RTD: g cm^{-3}),) and specific root length (SRL: m g^{-1}) of fine roots.

This study site was located in the Pasoh Forest Reserve (28590N, 1028180E) of the Forest Research Institute Malaysia in Peninsula Malaysia. Root sampling was conducted from 31 Jan. to 6 Feb. 2010. Each root segment was carefully isolated from the soil and then gently washed. The root respiration rate was measured using a closed dynamic chamber system equipped with an infrared gas analyzer (LI-840). The most suitable chamber was selected from nine size patterns (volume=0.12, 0.21, 0.34, 0.48, 0.94, 1.45, 2.17, 11.60, or 22.50 L). Following the respiration measurements, root samples were measured for morphological traits. The root length, volume, and mean root diameter of all samples <2 mm in diameter were determined using WinRHIZO Pro 2007a. Roots >2 mm in diameter were measured manually using a vernier scale and ruler. After measuring the morphological traits, all root segments were dried at 70°C for 48 h and weighed. These procedures were repeated for 300 samples from 14 trees.

Coarse root respiration rates increased with decreasing D, resulting in significant relationships between root respiration and diameter across species. A model based on a radial gradient of respiration rates of coarse roots simulated the exponential decrease in respiration with diameter. We found a high correlation between the estimated and measured respiration rates for coarse roots. Conversely, when the model was fitted to the data from coarse roots, the measured respiration rate of fine roots was higher than the estimated respiration rate of fine roots. This result suggests that fine roots, which appear to be analogous to leaves, have additional different functions than coarse roots. Fine root respiration rates were much higher and more variable than those of larger diameter roots. For fine roots, the mean respiration rates for each species increased with decreasing D. The respiration rates of fine roots declined markedly with increasing RTD and increased with increasing SRL, which explained a significant portion of the variation in the respiration among the 14 tree species examined.

These results indicate that coarse root respiration in tree species follows a basic relationship with D across species and that most of the variation in fine root respiration among species is explained by D, RTD, and SRL. Our findings provide evidence of the generality and specificity of root respiration from very fine roots to coarse roots in relation to their morphological traits across species. Examining root respiration is a time consuming and difficult endeavor because it requires excavating and identifying the roots of each species in mixed tropical forest. In practice, if it is possible to use physio-morphological traits beyond species, root respiration could be more easily and quickly scaled up to the forest stand level, such as by using the proportions of each root biomass distribution for fine and coarse roots in the field.

Patterns of root respiration rates and morphological traits in 13 tree species in a tropical forest

Naoki Makita*[1] (*macky@kais.kyoto-u.ac.jp*)
Kosugi Y.[1], Dannoura M.[1], Takanashi S.[2]
Niiyama K.[2], Kassim AR.[3], Nik AR.[3]

[1] Graduate School of Agriculture, Kyoto University, Kyoto, Japan
[2] Forestry and Forest Products Research Institute, Ibaraki, Japan
[3] Forest Research Institute Malaysia, Kepong, Kuala Lumpur, Malaysia

1. Introduction

Is there a strong relationship across species between root respiration rates and morphological traits?

Root respiration is a major source of CO_2 efflux from forest soils. The root systems are composed of different diameters and heterogeneous physiological traits. There is now considerable evidence that difference in root diameter size influence the respiration. However, the pattern of root respiration rates from finer and coarser roots across various tropical species remains unknown. Here, we evaluated specific root respiration and its relationships to mean root diameter (D) of various diameter sizes and root tissue density (RTD: g cm^{-3}) of the fine roots among 14 tropical trees of 13 species.

2. Methods

Pasoh Forest Reserve (2°58' N, 102°18' E)

1, Root sampling was conducted from 31th Jan. to 6th Feb. 2010.
2, Each root segment (0.22—264 mm, n=300) was gently washed.
3, The root respiration rate was measured using a closed dynamic chamber system equipped with an infrared gas analyzer (LI-840).
4, The volume and mean diameter of all samples were measured using WinRHIZO (< 2mm) or a vernier scale and ruler (>2mm).

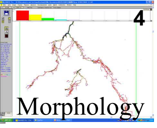

Root diameter	Physiological index of resource uptake and transport capacity
Root tissue density	Anatomical index of strength, water potential, construction cost

Species

We selected 14 trees of 13 species. The selected species represented a broad range of taxa of the common woody species in the Pasoh.

Species name	Abbreviation	DBH	Tree height	Number of root sample	
		cm	m	Fine root	Coarse root
Shorea acuminata	SA	29.1	29.7	27	33
Shorea leprosula	SL	25.6	32	23	27
Hypobathrum racemosum	HR	18.9	23.7	20	19
Shorea multiflora	SM1	16.7	20.2	9	21
Pentaspadon motleyi	PM	9.2	16.5	11	11
Aporosa bracteosa	AB	8.5	13.5	9	11
Blumeodendron tokbrai	BT	5.7	10	6	5
Anaxagorea javanica	AJ	3	5.9	5	6
Galearia maingayi	GM	1.6	3.1	3	7
Aglaia odoratissima	AO	1.4	3.3	4	6
Dacryodes rugosa	DR	1.2	1.8	3	6
Aglaia exstipulata	AE	1.1	2.8	3	7
Shorea multiflora	SM2	0.9	1.9	3	5
Sterculia macrophylla	StM	0.9	1.6	3	7

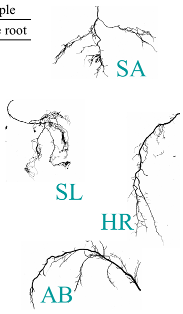

3. Results & Discussion

Marsden et al. (2008 *New Phytol.*) model

$$\bar{R}_v = R_{vm}\left(\frac{2}{k^2r^2}\left(e^{-kr}+kr-1\right)\right)^{\alpha}$$

Rvm : maximum respiration rate
k : exponential coefficient
α : empirical power coefficient

To simulate the decrease of root respiration with increasing diameter, Marsden model is based on the hypothesis that the CO_2 production of a certain tissue volume decreases exponentially from the root surface towards the center

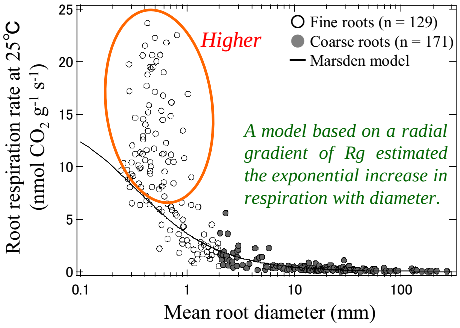

A model based on a radial gradient of Rg estimated the exponential increase in respiration with diameter.

※ All respiration rates measured in the field were normalized to mean soil temperature (25° C) with a fixed Q_{10} temperature coefficient.

Fig1. Root respiration at 25 ℃ and the diameter relationship

- When the model was fitted to the data from the coarse roots, the measured respiration of the coarse roots agreed with the estimated respiration and reflected an exponential decrease in the proportion of living tissues with increasing distance from the root surface. .
- Conversely, the measured respiration rate of fine roots was higher than the estimated respiration rate of fine roots

Differences in the respiration between fine roots and coarse roots could appear the variation in root functions (e.g., nutrient and water uptake, or transport to other tissues).

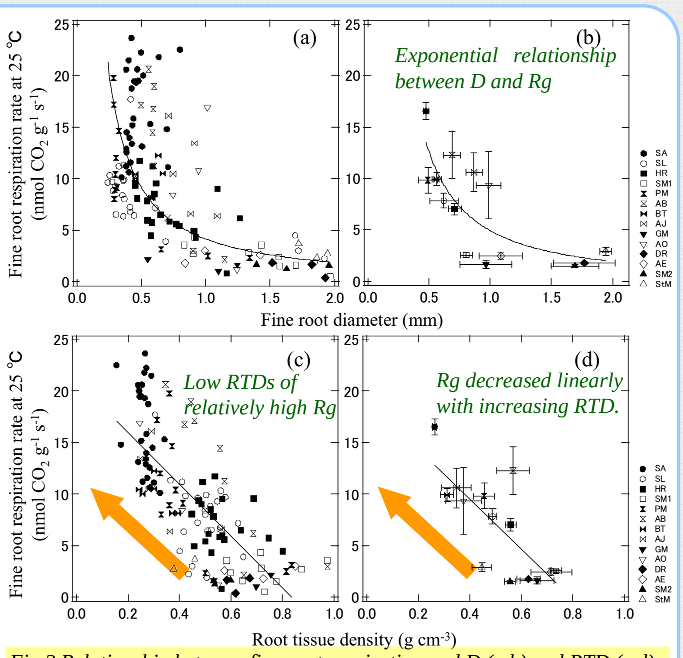

Exponential relationship between D and Rg

Low RTDs of relatively high Rg

Rg decreased linearly with increasing RTD.

Fig.2 Relationship between fine root respiration and D (a,b) and RTD (c,d). (a,c) Data for every fine root sample. (b,d) Mean value (±SE) within a tree.

Fine root respiration rates among species were dependent on root diameter even within 2.0 mm. RTD could have consequences for the hydraulic and physiological performance and explain root anatomical development strongly alters root respiration beyond species.

4. Conclusion

Beyond species,
Coarse root respiration follows a basic relationship with D.
Fine root respiration is explained by D and RTD!!

We propose to combine the respiration and morphological traits of roots separated into detailed diameter size classes. In practice, if it is possible to use physio-morphological traits beyond species, root respiration could be more easily and quickly scaled up to the forest stand level, such as by using the proportions of each biomass distribution for fine and coarse roots in the field. Knowledge of the relationships between the respiration and morphological traits of roots in a wide variety of tropical forest species is necessary to further improve our understanding of belowground C cycling.

We gratefully acknowledge Dr. Tanaka, Mr. Kanemitsu, Mr. Haruta, Dr. Yamashita, Dr. Noguchi and staffs of FRIM for their valuable help in the field.

6 Characteristics of Energy Exchange and Surface Conductance of a Tropical Rain Forest in Peninsular Malaysia

Makoto Tani[1], Abdul Rahim Nik[2], Yoshikazu Ohtani[3], YukioYasuda[3], Mohd Md. Sahat[2], Baharuddin Kasran[2], Satoru Takanashi[1], Shoji Noguchi[4], Zulkifli Yusop[5] & Tsutomu Watanabe[3]

Abstract: Energy exchange above tropical rain forest was studied using micrometeorological monitoring from a 52 m tower established in the Pasoh Forest Reserve (Pasoh FR) in Peninsular Malaysia. The meteorological conditions were comparatively drier during the first half of the year and wetter toward the end of the year due to the seasonal variation of rainfall. The five-year observational period from 1995 to 1999 included a low rainfall duration due to the El Niño from 1997 to 1998. The latent heat flux estimated by the Bowen ratio method occupied a dominant portion of the energy exchange even in the driest condition in early 1998. Although evapotranspiration from the dry canopy tended to be smaller in this period than in a wet period during the end of 1998, the surface conductance estimated using the Penman Monteith Equation was consistently controlled by the same function of solar radiation and specific humidity deficit. This suggests the evaporation did not suffer from severe stress of soil water even in the driest condition.

Key words: energy flux, evapotranspiration, meteorology, surface conductance, tropical rainforest.

1. INTRODUCTION

Understanding the effects of tropical rain forest on climate and water resources at both local and global scales is one of the most important current environmental issues (Nobre et al. 1991). Intensive observational studies for estimating energy exchange including heat and vapor fluxes between tropical forest and the atmosphere are critical to develop such an understanding. Although forest hydrology has provided annual evapotranspiration estimates from annual water budgets in small experimental catchments (Bruijnzeel 1990), it is difficult to understand flux responses to many variables such as meteorology, physiology and soil moisture. Micrometeorological observations are necessary to understand such flux responses. However, such data have been obtained from limited regions such as the Amazonian rain forest in South America (Shuttleworth 1988). This study demonstrated that a large percentage of incoming net radiation was used as latent heat by evapotranspiration and that actual evapotranspiration in each month was nearly equal to its potential value.

In South East Asia, only a few findings have been obtained from

---

[1] Kyoto University, Kyoto 606-8502, Japan. E-mail: tani@kais.kyoto-u.ac.jp
[2] Forest Research Institute Malaysia (FRIM), Malaysia.
[3] Forestry and Forest Products Research Institute (FFPRI), Japan.
[4] Japan International Research Center for Agricultural Sciences.
[5] Universiti Teknologi Malaysia (UTM), Malaysia.

observational studies estimating fluxes from tropical forests. For a tropical savannah with a long dry season (November–March), Pinker et al. (1980) presented a large difference in the radiative energy into sensible and latent heats between dry and wet seasons. For a tropical rain forest in Java, Indonesia, Calder et al. (1986) reported a slightly larger annual evapotranspiration amount than that of the Amazonian forest. However, evapotranspiration from dry canopy was estimated indirectly from soil moisture measurements over a short duration because no meteorological variables were monitored above the canopy.

A study estimating energy exchange above forest has been conducted under NIES-FRIM-UPM Joint Research Project using an observation tower established at Pasoh Forest Reserve (Pasoh FR) in Peninsular Malaysia. This paper reports meteorological observation results during the recent five years and analyzes the characteristics of energy exchange above the forest and the characteristics of surface conductance of the forest using the meteorological data sets.

2. SITE DESCRIPTION

This study was conducted in the Pasoh FR, which is located near Simpang Pertang in Negeri Sembilan about 140 km south east of Kuala Lumpur in Peninsular Malaysia (2°59' N, 102°18' E). An intensive research project by the International Biological Programme (IBP) was concentrated in this forest reserve from 1970 to 1974 (e.g. Soepadmo 1978). Micro-meteorological measurements for a short duration were reported as one of the findings from the project (Aoki et al. 1975) though the energy exchange was not estimated.

The core area (600 ha) of the reserve is covered with a primary lowland mixed dipterocarp forest, which consists of various species of *Shorea* and *Dipterocarpus*. The continuous canopy height is about 35 m, although some emergent trees exceed 45 m. Based on the empirical equations obtained for the Pasoh FR by Kato et al. (1978), the leaf area index (LAI) estimated from tree diameter observations (Niiyama, unpublished) was 6.52. The core area is surrounded by a buffer zone (650 ha) of regenerating logged over forest and primary hill dipterocarp forest (1,000 ha) (Manokaran & Kochummen 1994; Soepadmo 1978). The area has a gently undulating topographical feature. The altitude of the core area ranges from 75 to 150 m a.s.l. Soils belong to Durian Series characterized by the presence of a band of laterite and compact structure derived from shales within the area. The A horizon is thin (0–2 cm) and deeper soils are bright yellowish or reddish brown and light to heavy clay. Lateritic boulders are abundant below 30 cm depth and increasing with depth (Yoda 1978).

3. OBSERVATION DESIGN

A 52 m tower (Chaps. 1, 2) established near the IBP Plot 1 in the core area was used for our observation. The tower is located at the top of gentle hill. Meteorological factors were monitored by sensors installed at the 52 m height. They consisted of downward and upward solar radiations (albedometer EKO MR-22), net radiation (EKO MF-40), air temperature and humidity (Visala HMP-35C), wind direction and wind velocity (Campbell 03001, the threshold of wind speed is 0.5 m s^{-1}) and rainfall (Yokogawa Weathac B-011-00). Except for rainfall, the above factors were measured every 15-second and their 30-minute averages were recorded in a data logger (Campbell CR10X), which also recorded the maximum wind velocity and 30-minute rainfall totals. Accurate vertical profiles of air temperature, vapor pressure and wind velocity necessary for an energy flux estimation were measured by two ventilated psychrometers (EKO MH-020S) with platinum resistance temperature devices at 43.6 and 52.6 m, and four three-cup anemometers (Ikeda WM-30P, the threshold is 0.3 m s^{-1}) at 43.6, 46.6, 49.1 and 52.6 m. The 30-minute averages of the ventilated psychrometers were recorded using the same CR10 data logger. The 30-minute cumulated pulses from the four anemometers (1 pulse for 1 m run-of-wind) were counted by two additional loggers (Kona Sapporo DS-64K).

The net radiometer was calibrated in Tsukuba, Japan by comparing its values with the accurate values authorized by Japan Meteorological Agency. The values obtained from the two ventilated psychrometers and the four anemometers were sometimes compared to each other by installing them at the same height.

The vertical profiles of air temperature, vapor pressure and wind velocity at 6 heights (1.0, 17.0, 33.0, 41.5, 49.1 and 52.6 m) measured on the 4th and 5th of March 1995 was also used to understand the heat storage within canopy (Ohtani et al. 1997). The heat flux into the soil was neglected in the routine of energy flux estimation since its magnitude was smaller than these three storage terms.

4. DATA ANALYSIS

4.1 Energy budget

The Bowen ratio method was used for estimating sensible and latent heat fluxes from the forest canopy. The energy budget above the canopy is described as:

$$R_n = H + lE + Q_s + A \tag{1}$$

where R_n(kW m^{-2}) is the net radiation, H and lE are the sensible and latent heat fluxes, Q_s is the stored energy increase within a forest canopy, and A is the net rate of energy absorption by photosynthesis and other biochemical processes. Q_s consists of:

$$Q_s = Q_a + Q_w + Q_b + Q_g \tag{2}$$

where Q_a and Q_w are the sensible and latent heat storage increases in the canopy air (kW m^{-2}), and Q_b and Q_g are the heat storage increases within the biomass of the canopy and the soil, respectively.

Since A is assumed to be around 3% of R_n (Jarvis et al. 1976), this term was neglected. R_n and Q_g were obtained from the routine monitoring. Q_a, Q_w and Q_b were estimated from the air temperature and vapor pressure monitored at the reference height of 52.6 m (Ohtani et al. 1997). The empirical equations used here were developed based on the measurement of vertical profiles of air temperature and vapor pressure within the canopy carried out in March 1995 as described earlier:

$$Q_a = 0.0172(dT/dt) \tag{3}$$

$$Q_w = 0.0253(dV/dt) \tag{4}$$

$$Q_b = 0.0180(dT/dt) \tag{5}$$

where T and V are the air temperature (°C) and vapor pressure (hPa), and dT/dt and dV/dt are their increases in an hour, respectively. Thus, the available energy Q distributed to sensible and latent was calculated as:

$$Q = R_n - Q_s \tag{6}$$

4.2 Bowen ratio method

Sensible and latent heat fluxes are estimated from the available energy using Bowen ratio method as:

$$H = \frac{B}{1+B}Q \tag{7}$$

$$lE = \frac{1}{1+B}Q \tag{8}$$

Bowen ratio, B, is calculated from differences in potential temperature and vapor pressure between the two heights:

$$B = \frac{c_p}{l}\frac{\theta_1 - \theta_2}{q_1 - q_2} \tag{9}$$

where θ is the potential temperature (°C), q is the specific humidity (kg kg^{-1}), c_p is the specific heat of air (kJ kg^{-1} K^{-1}) and l is the latent heat of vaporization (kJ kg^{-1}). The two heights indicated by suffixes 1 and 2 were assigned to 43.6 and 52.6 m in our site.

4.3 Estimation of surface conductance

Effects of environmental variables on transpiration are represented by the control of the surface conductance, which means the integrated behavior of stomatal conductance at an individual leaf scale. The surface conductance (g_c m s^{-1}) is calculated by Penman Monteith Equation (Monteith 1965) as:

$$g_c = \left\{\left[(\Delta l / c_p)B - 1\right]r_a + \left[(\rho l / lE)(q_{SAT}(T) - q)\right]\right\}^{-1} \tag{10}$$

where Δ is the slope of saturated specific humidity curve against temperature (kg kg^{-1} K^{-1}), ρ is the density of air (kg m^{-3}), r_a is the aerodynamic resistance (m^{-1} s), and q and $q_{SAT}(T)$ are the specific humidity at the reference height (52.6 m) and the saturated specific humidity (kg kg^{-1}) for the air temperature (T) at the reference height. The value of g_c can be calculated from the r_a value since Bowen ratio (B) and lE are calculated in Eqs. 8 and 9. Considering that sensitivity of the aerodynamic resistance (r_a) to the evapotranspiration was estimated small for Amazonian rain forest (Shuttleworth 1988), r_a was assumed to be equal to the aerodynamic resistance for the momentum transfer (r_m) as:

$$r_a = r_m = \frac{u_r}{u_*^2} \tag{11}$$

where u_r is the wind velocity at the reference height (m s^{-1}) and u_* is the friction velocity (m s^{-1}).

The friction velocity was calculated from the profile of wind velocity measured at the four heights above the canopy in terms of the correction of atmospheric stability.

$$u_* = ku_r\left[\int_{\varsigma_0}^{\varsigma_r}\frac{\phi_m}{\varsigma}d\varsigma\right]^{-1} \tag{12}$$

where

$$\varsigma = (z - d) / L \tag{13}$$

$$L = \frac{-u_*^{\,3}\rho}{k\,g\,(\dfrac{H}{T_k\,c_p} + 0.61E\,)} \tag{14}$$

ϕ_m is the non-dimensional universal function for momentum, k is Karman's constant (= 0.4), $\zeta_0 = z_0/L$, z_0 is the roughness length, $\zeta_r = (z_r - d)/L$, z_r is the reference height (52.6 m) , d is the zero plane displacement, L is the Obukov's stability length, T_k is the air temperature at the reference height in absolute temperature (K) and E is the vapor flux (kg $m^{-2}\,s^{-1}$). In the calculation process, a constant value of the zero plane displacement (d) was given first as 33.0 m considering the canopy height of 43.0 m.

Estimating u_* through the above equations requires an iterative calculation process using universal functions. Although the universal functions have not been established for tall vegetation such as forest (Viswanadham et al. 1987), simple non-dimensional universal functions for short vegetation were employed here to produce our estimation of g_c. The functions for unstable conditions (Dyer & Hicks 1970) are:

$$\phi_m = (1 - 16\varsigma)^{-1/4} \tag{15}$$

For stable conditions, the following equation is used here (Kondo et al. 1978).

$$\phi_m = 1 + \frac{7\varsigma + 70\varsigma^3}{1 + 3\varsigma + 10\varsigma^2} \tag{16}$$

4.4 Periods for flux analyses

Analyses of energy fluxes were applied to the records in the daytime from DOY (Day of the year) 65 (March 6) to 95 of 1998 for the dry period and from DOY 338 (December 4) to 356 of 1998 for the wet period. Days with rainfall and days with rainfall on their previous days were both removed from the analyses to avoid influences of evaporation from the wet canopy. Twenty and eleven days were screened for the analyses in the dry and wet periods, respectively.

5. RESULTS AND DISCUSSION

5.1 Meteorological characteristics

Monthly mean values of meteorological variables monitored at the tower from March 1995 to December 1999 are shown in Fig. 1. Table 1 summarizes the annual mean values. In addition to the tower data, rainfall records monitored at the nearest meteorological observatory, Federal Land Development Authorities (FELDA) Pasoh Dua, located at the 3 km south of our tower site were employed in Fig. 1 to know the seasonal variations of rainfall in the normal year. The monthly rainfall values averaged from 1983 to 1997 were illustrated with those monitored at the tower. Fluctuations of Southern Oscillation Index (SOI) are also plotted to survey El Niño and La Niña conditions (Data were obtained from the web page of Long Paddock Historical SOI Data, http:// www.dnr.qld.gov.au/longpdk).

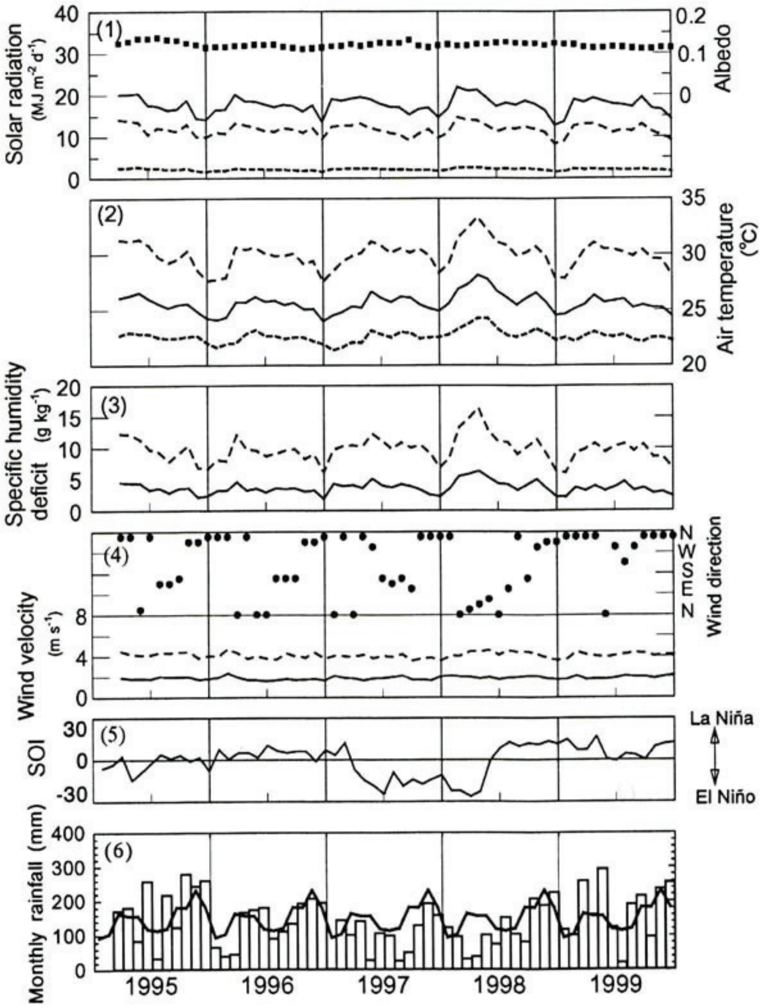

Fig. 1 Seasonal variations in monthly averages of meteorological variables at Pasoh Tower.

(1) ——— Daily total of downward solar radiation; -------- Daily total of upward solar radiation; ·············· Daily total of net radiation; ■ Daily average of albedo

(2) ——— Daily average of air temperature; -------- Daily maximum of air temperature; ·············· Daily minimum of air temperature

(3) ——— Daily average of specific humidity deficit; -------- Daily maximum of specific humidity deficit

(4) ● Daily vector average of wind direction; ——— Daily average of wind velocity; -------- Daily maximum of wind velocity

(5) ——— Southern Oscillation Index (SOI)

(6) Bar: Monthly rainfall; ——— Monthly rainfall in the normal year at FELDA Pasoh Dua

Table 1 Annual mean or total values of meteorological factors.

Year	Rainfall	Solar rad.	Albedo	Net rad.	Air temperature			Spec. humid. deficit		Wind velocity	
		MJ $m^{-2}d^{-1}$		MJ $m^{-2}d^{-1}$	Mean	Max	Min	Mean	Max	Mean	Max
	(mm y^{-1})	(mm y^{-1})		(mm y^{-1})	(deg C)			(g kg^{-1})		(m s^{-1})	
1995(Mar.-)	1855	17.26 (2585)	0.130	11.77 (1764)	25.5	29.8	22.6	3.35	9.26	1.90	4.22
1996	1610	17.30 (2590)	0.117	11.61 (1738)	25.2	29.4	22.4	3.29	9.03	1.81	4.04
1997	1182	17.59 (2634)	0.121	11.43 (1712)	25.5	29.9	23.2	3.74	10.10	1.87	3.90
1998	1426	18.21 (2729)	0.115	12.07 (1809)	26.4	30.7	22.5	4.40	11.09	1.93	4.22
1999	2065	17.36 (2600)	0.119	11.48 (1719)	25.4	29.7	22.6	3.26	9.13	1.93	4.07
1996-99	1571	17.62 (2638)	0.118	11.65 (1744)	25.6	29.9	22.6	3.67	9.84	1.89	4.07

'Mean', 'Max'and 'Min' indicate annual averages of daily mean, maximum and minimum values, respectively. Max' in wind velocity indicates annual averages of daily maximum values in 30-minute average wind velocity. Number in parentheses indicate energy flux value converted to mm y^{-1} of water equivalent using latent heat of vaporization.

Although seasonal variations of meteorological variables in Pasoh FR were small under the climate of tropical rain forest, radiative energy was comparatively high at the first half of the year and decreased toward the end of the year (Fig. 1). A similar trend was detected in the seasonal fluctuations of air temperature and specific humidity deficit. These characteristics may be due to the seasonal variations of rainfall in this region: a major rainy season is produced by the northeast monsoon from October to December while the generally weak southwest monsoon yields only a small peak of rainfall from March to May. Thus, the maximum and minimum monthly rainfall values in the normal year were recorded in November and in January (Fig. 1), and the annual amount was only 1,804 mm, lower than that in other regions of Peninsular Malaysia. It can be summarized that climate in Pasoh FR is characterized by low rainfall due to the inland location and that it was dry at the first half of a year, getting wetter toward the end of the year.

Four-year averages of meteorological variables in our tower observation period are also listed in Table 1. The annual rainfall average (1,571 mm) was much smaller than that of the normal year in FELDA Pasoh Dua (1,804 mm). The average net radiation 11.65 MJ m^{-2} d^{-1} coincides with the annual water vaporization energy of 1,744 mm y^{-1}, which is larger than the annual rainfall. This indicates the Budyko's radiation dryness was larger than unity, suggesting too dry condition for tropical rain forest. The rainfall was larger in 1995 and 1999 than in the normal year, similar to the normal year in 1996 but much smaller in 1997 and 1998. A tendency of high radiation, high air temperature and high specific humidity deficit was recorded in 1998 and was particularly remarkable from March to May in 1998 (Fig. 1). This was caused by unusual small rainfall in this duration, which clearly coincides to the El Niño from 1997 to early 1998 as shown in Fig. 1.

Details of radiative energy are described next. The averaged albedo was about 0.120, which is comparable to values observed in other tropical rain forests such as 0.1225 in Ducke, Amazon (Shuttleworth et al. 1984) and 0.12 – 0.13 in Nigeria (Oguntoyinbo 1970). Relationships of net radiation to solar radiation calculated from their hourly values in the daytime were expressed in the following regression equation ($R^2 = 0.996$):

$$R_n = 0.820 S_d - 0.0342 \qquad (17)$$

where S_d is the downward solar radiation (kW m^{-2}). The relationship for the Amazonian forest was expressed by Shuttleworth et al. (1984) as:

$$R_n = 0.858 S_d - 0.035 \qquad (18)$$

Both of the forests had very similar relationships. However, the annual total of net radiation 4,255 MJ m^{-2} in our site was larger than that in other tropical rain forests, that is about 3,600 MJ m^{-2} in Ducke, Amazon (Shuttleworth 1988) or 3,730 MJ m^{-2} in Java (Calder et al. 1986), probably because the annual rainfall amount during the observation period at Pasoh FR was very small compared to that in the normal year and was much smaller than the other forests (2,650 mm in Amazon and 2,850 mm in Java).

The wind velocity (Fig. 1) did not have a remarkable seasonal variation, and the monthly mean values of the daily average and the maximum were about 2 m s^{-1} and 4 m s^{-1}, generally weak under the tropical climate (Table 1). The predominant wind direction was north in general although the southern wind was dominant only from June to September.

5.2 Typical diurnal variations in fluxes

Figure 2 shows typical diurnal variations in heat fluxes with meteorological variables on rainless days, from DOY of 92 (April 2) to 94 in 1998, while Fig. 3 shows those on DOY of 345 (December 11), 355 and 356 in 1998. The atmospheric condition was very dry in the former period and wet in the latter. In the dry condition as shown in Fig. 2, the specific humidity deficit increased up to over 16 g kg^{-1} in the afternoon especially on fine days of DOY 92 and 94 caused by the increase of air temperature and the decrease of specific humidity. In spite of a dry condition, the latent heat flux was dominant throughout the three days (Fig. 2). The averaged fractions of latent heat to the net radiation in the daytime on DOY of 92, 93 and 94 were 0.65, 0.68 and 0.65, respectively. The value averaged over 20 days without influences of rainfall from DOY 65 to 95 was 0.68. In the wet period, the fractions on DOY of 345, 355 and 356 were 0.71, 0.73 and 0.75, and the value averaged over 11 days from DOY 338 to 356 was 0.73, which means higher fractions of the radiative energy were used by evapotranspiration in this wet period than in the dry period. However, it is important that the fraction did not drastically decrease due to the dry condition. This fraction value was similar to the value of 0.698 obtained from an Amazonian forest in Ducke (Shuttleworth et al. 1984). These data demonstrates that most of radiative energy is used by evapotranspiration in tropical rain forests even in dry seasons.

Daily variations of the surface conductance are also plotted in Figs. 2 and 3, showing that it reached a peak after a sharp increase in the morning and gradually decreased in the afternoon. This diurnal pattern was the same as that of stomatal conductance of an individual leaf measured with a porometer in this forest (Furukawa et al. 1994, 2001). A similar pattern was widely reported from temperate and tropical forests (Shuttleworth 1989). For example, an averaged daily variation obtained from Ducke was expressed as:

$$g_c = 12.17 - 0.531\,(t_s - 12) - 0.233\,(t_s - 12)^2 \tag{19}$$

where t_s is the local time of day in hours. Curves calculated in Eq. 19 were also illustrated on each day in Fig. 3. Because the local time in Malaysia, t_m is one-hour later than the solar time there, $t_s = t_m - 1$ is substituted into Eq. 19 for the curves in Figs. 2 and 3. The patterns for our site and for Ducke are similar to each other, but it can be found that g_c for our site is larger than that for Ducke in the morning. This is caused by most of radiative energy is used for the latent heat flux in the rising limb of radiation in the morning (Figs. 2 and 3). One of the causes for the large g_c in the morning may be attributed to evaporation from free surface water due to the formation of dew in the previous night time (Kelliher et al. 1995) though we have no direct evidence for this phenomenon at Pasoh FR.

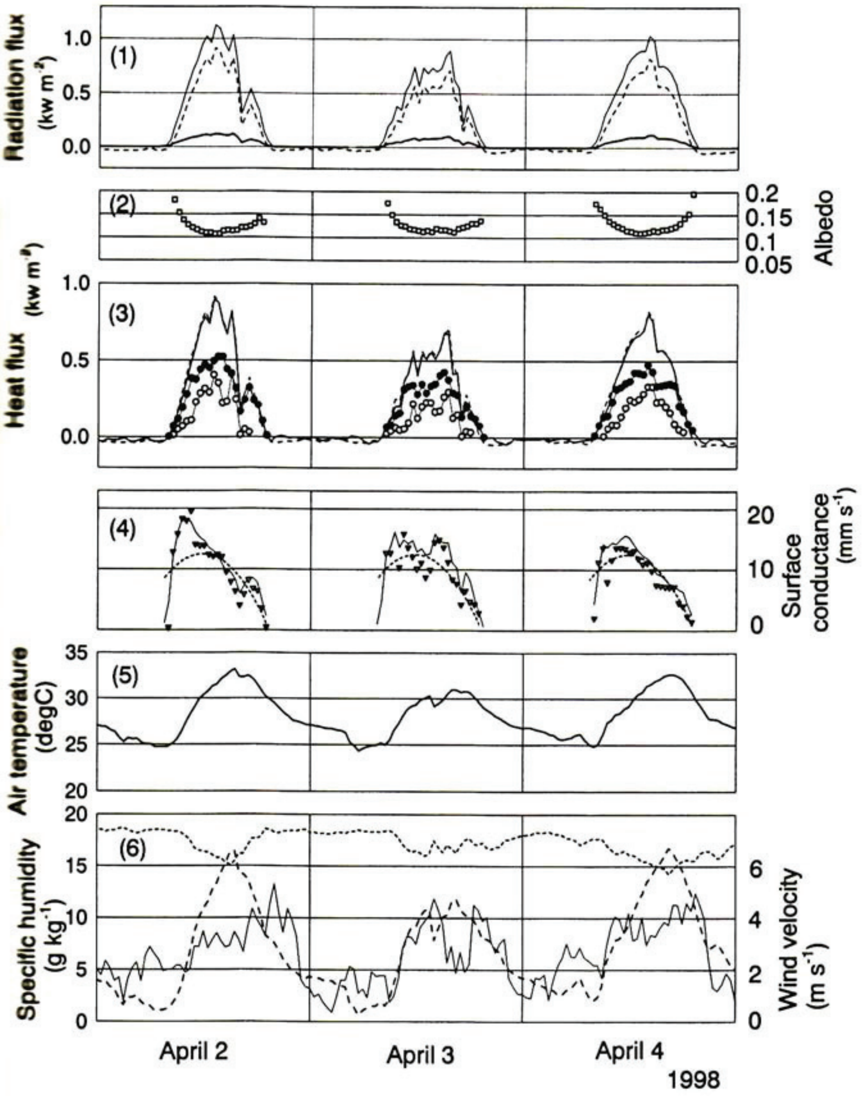

Fig. 2 Diurnal variations of energy fluxes with meteorological variables at Pasoh Tower in a dry period.

(1) ——— Downward solar radiation; ——— Upward solar radiation; ·············· Net radiation

(2) □ Albedo

(3) ·············· Net radiation; ——— Available energy; ○ Sensible heat flux; ● Latent heat flux

(4) ▽ Surface conductance estimated from the observation by Eq. 10; ——— Surface conductance calculated from environmental variables by Eq. 20; ·············· Averaged daily variation of surface conductance for Amazonian forest calculated by Eq. 19

(5) ——— Air temperature

(6) ·············· Specific humidity; - - - - Specific humidity deficit; ——— Wind velocity

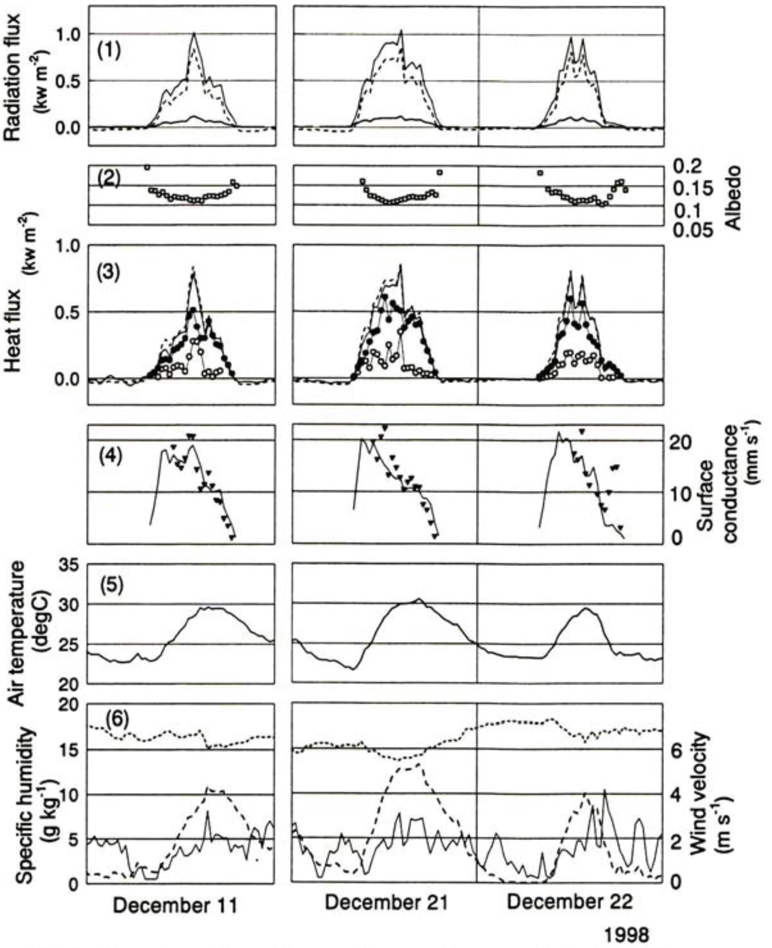

Fig. 3 Diurnal variations of energy fluxes with meteorological variables at Pasoh Tower in a wet period. Symbols are the same as Fig. 2.

5.3 Dependence of surface conductance on the environment

This section attempts to evaluate responses of surface conductance to the environmental variables in Pasoh FR. The surface conductance which represents the integrated behavior of the stomatal conductance at the canopy scale depends upon the environmental variables such as solar radiation, specific humidity deficit, temperature and soil moisture deficit (Jarvis 1976; Stewart 1988). For tropical forests, however, effects of some variables may be less critical for the responses. Previous results from Amazonian rain forests indicated that no substantial soil moisture deficits occurred (Dolman et al. 1991; Shuttleworth 1989). The annual variation range of air temperature was small only from 20 to 35℃ in our forest (Fig. 1). Hence, we omitted controls of soil moisture deficit and air temperature, and attempted to simply examine effects of solar radiation and specific humidity deficit on surface conductance.

Figs. 4 and 5 show responses of surface conductance to specific humidity deficit classified with the solar radiation range in the dry and wet periods, respectively. Plots of the surface conductance in Fig. 4 are distributed in a high range of specific humidity deficit due to a continuous dry condition since 1997 (see Fig. 1), while those in Figure 5 are in its low range. Curves in these figures indicate functional relationships of the responses (Jarvis 1976) expressed as:

$$g_c = g_0 g_r g_d \tag{20}$$

$$g_r = \frac{S_d / (S_d + a_1)}{1 / (1 + a_1)} \tag{21}$$

$$g_d = \exp(a_2 \delta q) \tag{22}$$

where g_r is the radiation stress function, g_d is the specific humidity deficit stress function, g_0 is a constant representing the maximum surface conductance, and a_1 and a_2 are empirical constants. The constants, g_0, a_1, and a_2, fitted to the observational results throughout both the dry and wet periods are 35 mm s^{-1}, 0.6 kW, and -0.08 g^{-1} kg , respectively. The curves agree consistently with the responses of surface conductance in Figs. 4 and 5. The daily variations of g_c calculated in Eq. 20 also show good agreements with those observed in Figs. 2 and 3. These results mean the surface conductance was sufficiently controlled by solar radiation and humidity deficit through a simple functional relationship though the driest conditions in 1998 in our 5-year observational period was included.

Functional relationships in Eq. 20 obtained from our forest and from an Amazonian rain forest in Ducke (Dolman et al. 1991) are illustrated in Fig. 6. The constants, g_0, a_1 and a_2, for Ducke were 20.8 mm s^{-1}, 0.25 kW, and -0.064 g kg^{-1}, respectively. Figs. 4 and 5 indicate the differences in surface conductance between our site and Ducke is large particularly at small specific humidity deficits. The large differences in g_c occurred in the morning may be attributed to evaporation from dew as mentioned before (Figs. 2 and 3). In addition to this, however, some differences in canopy structure and/or physiological processes between these forests may influence surface conductance. Gash et al. (1989) compared the surface conductance of temperate pine forests between two sites, and found large differences in g_0 values (e.g. 33 mm s^{-1} for one site and 23 mm s^{-1} for the other) although the responses to environmental variables were similar at each site. They suggested the differences might originate from physiological structure or behavior and the contribution of transpiration from the bracken understorey. More detailed physiological data as well as flux data may be necessary to determine mechanisms for differences in surface conductance characteristics between different tropical rain forests.

5.4 Discussion on high evapotranspiration in a dry period

Our analyses demonstrate that responses of the surface conductance to specific humidity deficit in a dry period were consistently expressed with the same simple functional relationship in Eq. 20 as those in a wet period (Figs. 4 and 5). It may be surprising that high evapotranspiration rates or large fractions of the latent heat flux to the radiative energy could be maintained (Fig. 2) considering very small amounts of rainfall in 1997 and 1998 in Pasoh FR. Trees there may tolerate droughts because of the climatic environment characterized by low rainfall (Fig. 1). Discussion will be made on a background of high evapotranspiration in the dry period.

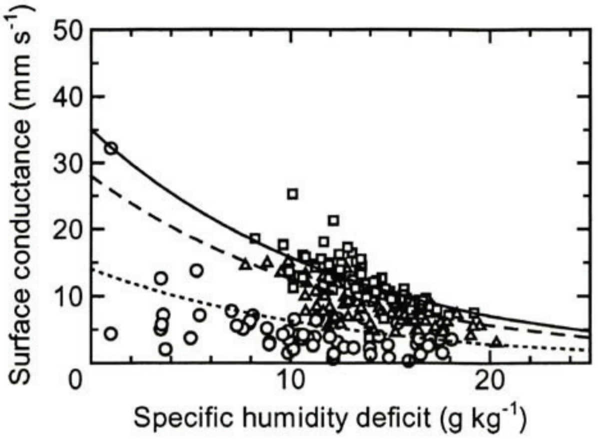

Fig. 4 Relationship of surface conductance to specific humidity deficit as a function of downward solar radiation S_d in a dry period.Symbols are estimated from the observation. □ $S_d \geqq 0.8$ kW s^{-1}; △ $0.8 > S_d \geqq 0.4$; ○ $0.4 > S_d$. Curves are calculated by from the environmental variables by Eq. 20.
——— $g_0 = 35$ mm s^{-1}, $a_1 = 0.6$ kW and $a_2 = -0.08$ g^{-1} kg and $S_d = 1$ kW s^{-1};
- - - - the same except for $S_d = 0.6$; ·············· the same except for $S_d = 0.2$.

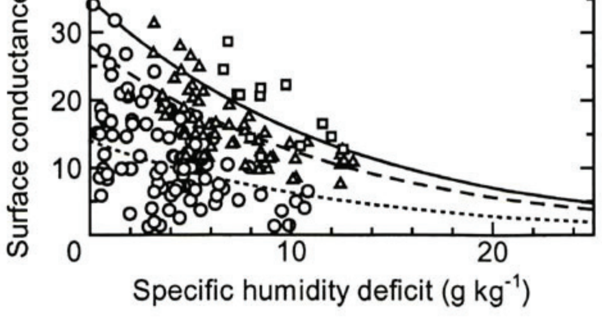

Fig. 5 Relationship of surface conductance to specific humidity deficit as a function of downward solar radiation S_d in a dry period. Symbols and curves are the same as Fig. 4.

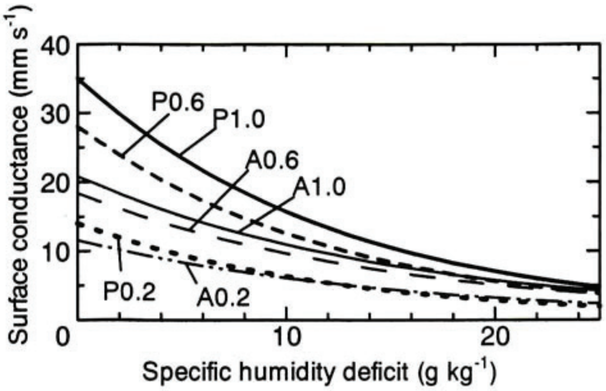

Fig. 6 Comparisons of functional relationship in Eq. 20 between Pasoh and Amazonian forests. P and A indicate Pasoh and Amazon respectively. Numbers are values of solar radiation S_d in kW s^{-1}. The other parameter values in Eq. 20 are the same as Fig. 4 for Pasoh FR, and those for Amazon are g_0 = 20.8 mm s^{-1}, a_1=0.25 kW and a_2 = -0.064 g^{-1} kg.

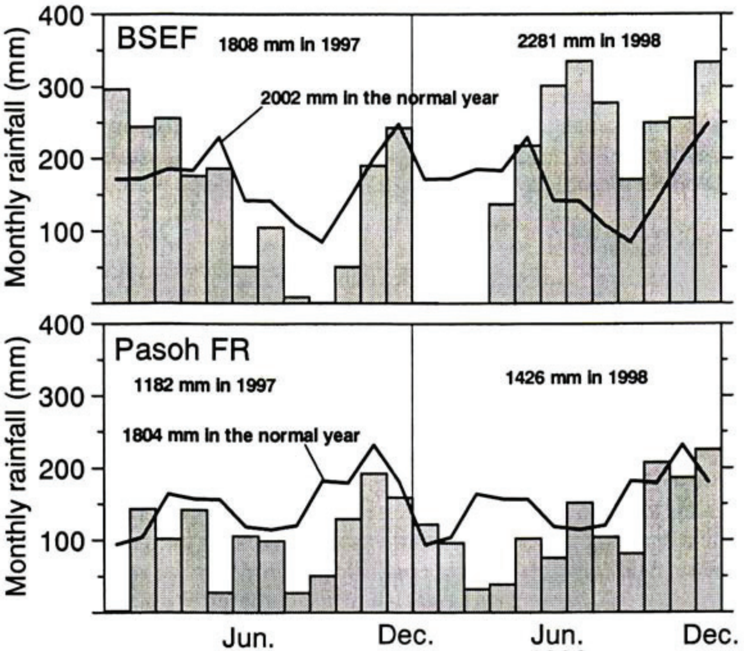

Fig. 7 Variations of monthly rainfall in Pasoh FR and Bukit Soeharto Education Forest (BSEF, East Kalimantan). Lines indicate monthly rainfall in the normal year. Numbers are the annual total. The values in normal year for Pasoh are calculated from the records in FELDA Pasoh Dua. Data of BSEF are after Toma et al. (2000a).

Some studies from Amazon suggested that maintenance of high transpiration from a tropical rain forest was supported by deep root system (Hodnet et al. 1996; Nepstad et al. 1994), which may partly cause our result. In addition to this, we should take it into consideration that rainless period was not long enough for a clear decreasing of evapotranspiration in Pasoh FR. From results on a physiological study in Bukit Soeharto Education Forest (BSEF, East Kalimantan), Indonesia, Ishida et al. (2000) reported that a severe drought occurred in 1997 and 1998 there due to El Niño and that stomatal conductance of the top canopy leaves of an evergreen pioneer tree, *Macaranga conifera,* did not decrease only with increasing specific humidity deficit but also with decreasing soil water potential in the dry period in early 1998. Although this result was not derived from a natural forest, many trees including dipterocarp trees besides *Macaranga* species partly shed their leaves (Toma et al. 2000b). Fig. 7 shows monthly rainfall amounts in Pasoh FR and BSEF (Toma et al. 2000a) in 1997 and 1998 with those in the normal year. Although the annual amounts of rainfall in the two years as well as those in the normal year were larger in BSEF than in Pasoh FR, rainfall condition during the El Niño in BSEF was characterized by two long rainless durations from August to October in 1997 and from January to March in 1998. The severe damage of trees in BSEF may strongly depend on these long rainless conditions. On the other hand, distributions of monthly rainfall were less fluctuant and rainless durations were shorter in Pasoh FR though the annual amounts in 1997 and 1998 there were much smaller than those in BSEF (Fig. 7). Therefore, the continuous supply of small rainfall amount during the driest periods may barely maintain the high evapotranspiration rate in Pasoh FR even though trees there tend to tolerate droughts due to the normal low rainfall climate. We should note that trees might suffer from severe water stress if a longer rainless duration visits Pasoh FR in the future. It will be particularly important for our coming research in Pasoh FR to detect effects of droughts on evapotranspiration using continuous long-term records on meteorology.

6. CONCLUSION

Findings obtained from meteorological observations in Pasoh FR are summarized below.

(1) Climate in Pasoh FR is characterized by low rainfall due to the inland location. Rainfall amount during observational period from 1995 to 1999 was generally small due to the El Niño event of 1997 and 1998.

(2) Seasonal variations in meteorological variables were not remarkable, but it was dry at the first half of a year, getting wetter toward the end of the year.

(3) Forest albedo and the relationship of net radiation and solar radiation were similar to those previously obtained from other tropical rain forests.

(4) Latent heat flux was dominant in the energy exchange even under dry conditions.

(5) The surface conductance was controlled mainly by solar radiation and specific humidity deficit and was consistently expressed with a simple functional relationship throughout dry and wet periods.

(6) A comparison of rainfall characteristics with another tropical rain forest in East Kalimantan suffering severe damage by a drought suggested that high evapotranspiration under dry conditions in Pasoh FR may barely be maintained by continuous supply of small rainfall amount.

ACKNOWLEDGEMENTS

We thank the Forestry Department of Negeri Sembilan and Director General of FRIM for giving us permission to work in the Pasoh FR, the Japanese Meteorological Agency for calibration of net radiometer and Dr. Kaoru Niiyama, FFPRI, for providing the tree diameter data. The staffs of Hydrology Unit and Pasoh Station of FRIM are greatly acknowledged for collecting the data and maintaining the meteorological observation system. They are Rajendran Pavadai, Ahmad Shahar Mohamad Yusof, Ibharim Hashim, Hashim Mohd, Abu Husin Harun, Hamidon Ahmad (Hydrology) and Ahmad Awang (Pasoh). This study is conducted as a part of joint research project between the NIES, FRIM and UPM (Global Environmental Research Programme granted by the Japanese Environment Agency, Grant No. E-3).

REFERENCES

Aoki, M., Yabuki, K. & Koyama, H. (1975) Micrometeorology and assessment of primary production of a tropical rain forest in West Malaysia. J. Agrc. Meteorol. 31: 115-124.

Bruijnzeel, L. A. (1990) Hydrology of moist tropical forest and effects of conversion: a state-of-knowledge review, UNESCO, Paris, 24pp.

Calder, I. R., Wright, I. R. & Murdiyarso, D. (1986) A study of evaporation from tropical rain forest -West Java. J. Hydrol. 89: 13-31.

Dolman, A. J., Gash, J. H. C., Roberts, J. & James, W. (1991) Stomatal and surface conductances of tropical rainforest. Agric. For. Meteorol. 54: 303-318.

Dyer, A. J. & Hicks, B. B. (1970) Flux-gradient relationships in the constant flux layer. Quart. J. R. Met. Soc. 96: 5715-5721.

Furukawa, A., Awang, M., Abdular, A. M., Yap, S. K., Toma, T., Matsumoto, Y., Maruyama, Y. & Uemura, A. (1994) Photosynthetic and stomatal characteristics of tropical tree species. In Research Report of the NIES/FRIM/UPM Joint Research Project 1993: National Reserch Institution Enviromental Studies, Tsukuba, pp.47-57.

Furukawa, A., Toma, T., Maruyama, Y., Matsumoto, Y., Uemura, A., Ahmad Makmam, A., Muhamad, Awang, M. (2001) Photosynthetic rates of four tree species in the upper canopy of a tropical rain forest at the Pasoh Forest Reserve in Peninsular Malaysia. Tropics. 10: 519-527.

Gash, J. H. C., Shuttleworth, W. J., Lloyd, C. R., Andre, J. C. & Goutorbe, J. P. (1989) Micrometeorological measurements in Les Landes Forest during HAPEX-MOBILITY, Agric. For. Meteorol. 46: 131-147.

Hodnet, M. G, Tomasella, J., Marques Filho, A. de O. & Oyama, M. D. (1996) Deep soil water uptake by forest and pasture in central Amazonia: predictions from long-term daily rainfall data using a simple water balance model. In Gash, J. H. C., Nobre, J. M., Roberts, J. M. & Victoria, R. L. (eds). Amazonian Deforestation and Climate, Institute of Wiley, Chichester, pp.79-99.

Ishida, A., Toma, T. & Marjenah (2000) Leaf gas exchange and canopy structure in wet and drought years in Macaranga conifera, a tropical pioneer tree. In Guhardja, E., Fatawi, M., Sutisna, M., Mori, T. & Ohta, S. (eds). Rainforest Ecosystems of East Kalimantan: El Niño, Drought, Fire and Human Impacts. Ecological Studies vol. 140. Springer-Verlag, Tokyo, pp.129-142.

Jarvis., P. G. (1976) The interpretation of variations in leaf water potential and stomatal conductances found in canopies in the field. Philos. Trans. R. Soc. London Ser. B 273: 593-610.

Jarvis, P. G, James, G B. & Landsberg, J. J. (1976) Coniferous forest. In Monteith, J. L. (ed). Vegetation and the atmosphere, vol. 2. Academic Press, New York, pp.171-236.

Kato, R., Tadaki, Y. & Ogawa, H. (1978) Plant biomass and growth increment studies in Pasoh Forest. Malay. Nat. J. 30: 211-245.

Kellihar, F. M., Leuning, R., Raupach, M. R. & Schulze, E. D. (1995) Maximum conductances for evaporation from global vegetation types. Agric. For. Meteorol. 73: 1-16.

Kondo, J., Kanechika, O. & Yasuda, N. (1978) Heat and momentum transfers under strong stability in the atmospheric surface layer. J. Atmos. Sci. 35: 1012-1021.

Manokaran, N. & Kochummen, K. M. (1994) Tree growth in primary lowland and hill dipterocarp forests, J. Tropic. For. Sci. 6: 332-345.

Monteith, J. L. (1965) Evaporation and environment. Symp. Soc. Exp. Biol. 19:206-234.

Nepstad, D. C., de Carvalho, C. R. Davidson, E. A., Jipp, P. H., Lefebvre, P. A., Negreiros, D. G H., da Silva, E. D. & Stone, T. A. (1994) The role of deep roots in the hydrological and carbon cycles of Amazonian forests and pastures. Nature 372: 666-669.

Nobre, C. A., Sellers, P. J. & Shukla, J. (1991) Amazonian deforestation and regional climate change. J. Clim. 4: 957-988.

Oguntoyinbo, J. S. (1970) reflection coefficient of natural vegetation, crops and urban surfaces in Nigeria. Quar. J. R. Met. Soc. 96: 430-441.

Ohtani, Y., Okano, M., Tani, M., Yamanoi, K., Watanabe, T., Yasuda, Y. & Abdul Rahim, N. (1997) Energy and CO_2 fluxes above a tropical rain forest in Peninsular Malaysia. - Under estimation of eddy correlation fluxes during low wind speed conditions. J. Agric. Meteorol. 52: 453-456.

Pinker, R. T., Thompson, O. E. & Eck, T. F. (1980) The energy balance of a tropical evergreen forest. J. Appl. Meteorol. 19: 1341-1350.

Shuttleworth, W. J. (1988) Evaporation from Amazonian rainforest. Proc. R. Soc. London Ser. B 233: 321-346.

Shuttleworth, W. J. (1989) Micrometeorology of temperate and tropical forest. Phils. Trans. R. Soc. London Ser. B 324: 299-334.

Shuttleworth, W. J. Gash, J. H. C., Lloyd, C. R., Moore, C. J., Roberts, J., Marques, A. de O., Fisch, G., Silva, V. de P., Ribeiro, M. N. G., Molion, L. C. B., de Sa, L. D. A., Nobre, J. C., Cabral, O. M. R., Patel, S. R. & Moraes, J. C. (1984) Observations of radiation exchange above and below Amazonian forest. Quart. J. R. Met. Soc. 110: 1163-1169.

Soepadmo, E. (1978) Introduction to the Malaysian I. B. P. Synthesis Meetings. Malay. Nat. J. 30: 119-124.

Stewart, J. B. (1988) Modelling surface conductance of pine forest. Agric. For. Meteorol. 43: 19-35.

Toma, T., Marjenah & Hastaniah (2000a) Climate in Bukit Soeharto, East Kalimantan, In Guhardja, E., Fatawi, M., Sutisna, M., Mori, T. & Ohta, S. (eds). Rainforest Ecosystems of East Kalimantan: El Niño, Drought, Fire and Human Impacts. Ecological Studies vol. 140. Springer-Verlag, Tokyo, pp.13-27.

Toma, T., Matius, P., Hastaniah, Kiyono, Y., Watanabe, R. & Okimori, Y. (2000b) Dynamics of burned lowland dipterocarp forest stands in Bukit Soeharto, East Kalimantan, In Guhardja, E., Fatawi, M., Sutisna, M., Mori, T. & Ohta, S. (eds). Rainforest Ecosystems of East Kalimantan: El Niño, Drought, Fire and Human Impacts. Ecological Studies vol. 140. Springer-Verlag, Tokyo, pp.107-119.

Viswanadham, Y., Sa, L. D. de A., Silva, V. de P. & Manzi, A. O. (1987) Ratios of eddy transfer coefficients over the Amazon forest. In Forest Hydrology and Watershed Management, IAHS Publ. No. 167. IAHS Press, Wallingford, pp.365-373.

Yoda, K. (1978) Organic carbon, nitrogen and mineral nutrient stock in the soils of Pasoh Forest. Malay. Nat. J. 30: 229-251.

Water Resources Systems—Water Availability and Global Change (Proceedings of symposium HS02a held during IUGG2003 at Sapporo, July 2003). IAHS Publ. no. 280, 2003.

Long-term estimation of evapotranspiration from a tropical rain forest in Peninsular Malaysia

MAKOTO TANI[1], ABDUL RAHIM NIK[2], YUKIO YASUDA[3], SHOJI NOGUCHI[4], SITI AISAH SHAMSUDDIN[2], MOHD MD SAHAT[2] & SATORU TAKANASHI[1]

1 *Graduate School of Agriculture, Kyoto University, Sakyo-ku, Kyoto, 606-8502, Japan*
tani@kais.kyoto-u.ac.jp

2 *Forest Research Institute Malaysia, Kepong 52109 Kuala Lumpur, Malaysia*

3 *Forestry and Forest Products Research Institute, Matsunosato 1, Tsukuba, Ibaraki 305-8687, Japan*

4 *Japan International Research Center for Agricultural Sciences, 1-1,Ohwashi, Tsukuba, Ibaraki 305-8686, Japan*

Abstract Field observations for estimating long-term evapotranspiration from a tropical rain forest were made in the Pasoh Forest Reserve, Peninsular Malaysia. The Penman-Monteith-Rutter model was applied to four-years of meteorological records to enable continuous estimation of evapotranspiration during dry and wet canopy conditions. The estimates show that the annual average total evapotranspiration, transpiration and interception loss for 1996–1999 were 1548 mm, 1218 mm and 331 mm, respectively, cf. annual rainfall of 1571 mm and net radiation of 1744 mm (water equivalent). Although a long dry period was included as a result of the strong El Niño in 1997 and 1998, evapotranspiration always accounted for a large portion of the net radiation.

Key words Evapotranspiration, tropical forest, Penman-Monteith-Rutter model, El Niño, Pasoh Forest Reserve

INTRODUCTION

Long-term estimation of evapotranspiration from tropical rain forest is important from aspects of both hydrological and climatic issues. In Southeast Asia, some estimation results, based on annual water budgets in small study catchments, have been documented (Bruijnzeel, 1990). However, such results give us only annual evapotranspiration amounts and very little information relating to long-term characteristics, including the responses to environmental variables. In the Pasoh Forest Reserve, meteorological observations above the tropical rain forest were made using a 52-m tower, and evapotranspiration estimated through the Bowen ratio method (Tani *et al.*, 2003). This study showed that most of radiant energy was used for latent heat of evapotranspiration even in dry seasons and that the surface conductance was controlled by the same functions of solar radiation and specific humidity deficit in both dry and rainy seasons. Attempts to estimate long-term continuous evapotranspiration throughout dry and wet canopy conditions using results from short-term flux measurements by an eddy covariance method, and from throughfall and stemflow measurements, are reported here.

STUDY SITE AND OBSERVATION DESIGN

This study was conducted in the Pasoh Forest Reserve of FRIM in Negeri Sembilan in

Peninsular Malaysia (2°58′N, 102°18′E). The climate is characterized by small seasonal variations, and the southwest and northeast monsoons yield only small rainfall peaks around April and November. The annual rainfall of the normal year observed from 1983 to 1999 at a meteorological station (Pasoh Dua) near our site was 1804 mm. The core area (650 ha) of the Pasoh Forest Reserve (2450 ha) is covered with a primary lowland mixed Dipterocarp forest, which consists of various species of *Shorea* and *Dipterocarpus*. The continuous canopy height is about 35 m, although some emergent trees exceed 45 m. The leaf area index (LAI) was 6.52.

Meteorological variables were monitored by sensors installed at 52.6 m height on a tower. Continuous records were obtained for downward and upward solar radiation, net radiation, air temperature, humidity, wind direction, wind velocity, and rainfall. Air temperature and vapour pressure for the estimation of evapotranspiration by Bowen ratio method were measured by two ventilated psychrometers at 43.6 and 52.6 m. One-week of observations of a closed-path eddy covariance system was conducted in March 1998 (Yasuda *et al*., 2003). Friction velocity, sensible heat, latent heat and CO_2 flux were estimated from these observations. Throughfall and stemflow were monitored near the tower. The throughfall was measured by 20 pots, each with an area of 366.4 cm^2, in a square plot of 20 × 15 m, and stemflow was measured from seven trees reaching the upper canopy layer in a square plot of 10 × 15 m within the throughfall plot. Interception loss was calculated from difference between gross rainfall above the canopy at the height of 52.6 m and the total of throughfall and stemflow.

A model system composed of a big-leaf parameterization and interception model is necessary for estimating long-term evapotranspiration from dry and wet canopies. The Penman-Monteith equation for the big-leaf parameterization and the Rutter model for the interception component has been widely used for the estimation (Shuttleworth, 1988). Hence, the Penman-Monteith-Rutter model was also employed for our estimation. For the application of this model, potential evaporation from the wet canopy is firstly calculated from the aerodynamic resistance, and the actual evaporation can be calculated from the potential value and current water storage on the canopy, where the saturation storage capacity maximum can be estimated from the throughfall and stemflow measurements. Calculating actual evapotranspiration from the dry canopy needs an additional parameter, that is, surface resistance representing the control by stomata. Characteristics of the surface resistance, the reciprocal of surface conductance, had already been analysed and its functional relationship to solar radiation and specific humidity deficit was fixed from the analysis (Tani *et al*., 2003). The evaluation of aerodynamic resistance and canopy storage capacity are discussed later in this paper.

MODEL DESCRIPTION

Long-term evapotranspiration was estimated using the Penman-Monteith-Rutter model, following its application to Amazonian rain forest by Shuttleworth (1988). Actual evapotranspiration is composed of evaporation from the wet canopy and evapotranspiration from the dry canopy and is calculated as their total when some portion of the canopy is wet and other parts are dry, during and after a rainfall event. The potential evapotranspiration values from the totally wet and dry canopies (E_c and

E_t) can be estimated by Penman-Monteith equation as:

$$lE = (\Delta Q + \rho c_p V_d / r_A) / \lfloor \Delta + c_p (1 + r_c / r_A) / l \rfloor \tag{1}$$

where E is the evapotranspiration, l is the latent heat of vaporization, Δ is the mean rate of change of specific humidity with temperature, Q is the available energy, V_d is the specific humidity deficit, ρ is the density of air, c_p is the specific heat at constant pressure, r_A is the aerodynamic resistance, and r_c is the surface conductance. E_c and E_t can be calculated if the values $r_c = 0$ and $r_c > 0$, respectively, are assumed.

The canopy storage characteristics have to be described by Rutter model as:

$$\mathrm{d}C / \mathrm{d}t = P(1 - p - p_t) - (C/S) E_c - D \tag{2}$$

$$D = D_0 \exp[b(C - S)] \tag{3}$$

where C is the actual stored water on the canopy, S is the saturation storage capacity, P is the gross rainfall, p is the rainfall fraction falling directly to the ground, p_t is the rainfall fraction diverted to the trunks, E_c is the evaporation from the completely wet canopy, D is the drainage from the canopy, D_0 is the drainage rate when the storage on the canopy is equal to S, and b is an empirical parameter. Hence, the equation for estimating actual evapotranspiration (E_a) is written:

$$E_a = (C/S) E_c + (1 - C/S) E_t \tag{4}$$

RESULTS AND DISCUSSION

Annual amounts of throughfall, stemflow and interception

The relationships of throughfall, stemflow and interception to gross rainfall in each measuring period of about two weeks are plotted in Figs 1(a)–(c), and show good linear correlations. The annual amounts of gross rainfall, throughfall, stemflow and interception from 1 July 1999 to 30 June 2000 were 2262.3, 1879.4, 6.8 and 381.3 mm, respectively. The ratios of the throughfall, stemflow and interception to gross rainfall were 83.1%, 0.3% and 16.9%. Another interception observation carried out in Pasoh Forest (Manokaran, 1979) showed the respective ratios to be 77.56%, 0.64% and 21.80%. The very small percentages of stemflow were remarkable in both studies as they were smaller than the values obtained from other tropical rain forests (e.g. Lloyd *et al.*, 1988; Jetten, 1996), that are usually even smaller than those obtained from temperate forests. Although our results on stemflow are not without doubt, due to forest heterogeneities, the contribution of its small absolute value to interception may be evaluated as insignificant in the overall evaporation estimation. The interception ratio of 16.9% in our estimate lies between 8.9% in Amazon (Lloyd *et al.*, 1988) and 21% in West Java (Calder *et al.*, 1986).

Penman-Monteith-Rutter model application

Application of the Penman-Monteith-Rutter model first requires a parameter estimation process. However, estimating parameters in the Rutter model from relationships between gross rainfall, throughfall and stemflow was not easy mainly because the relationships are widely scattered (Figs 1(a)–(c)). One strategy for optimizing

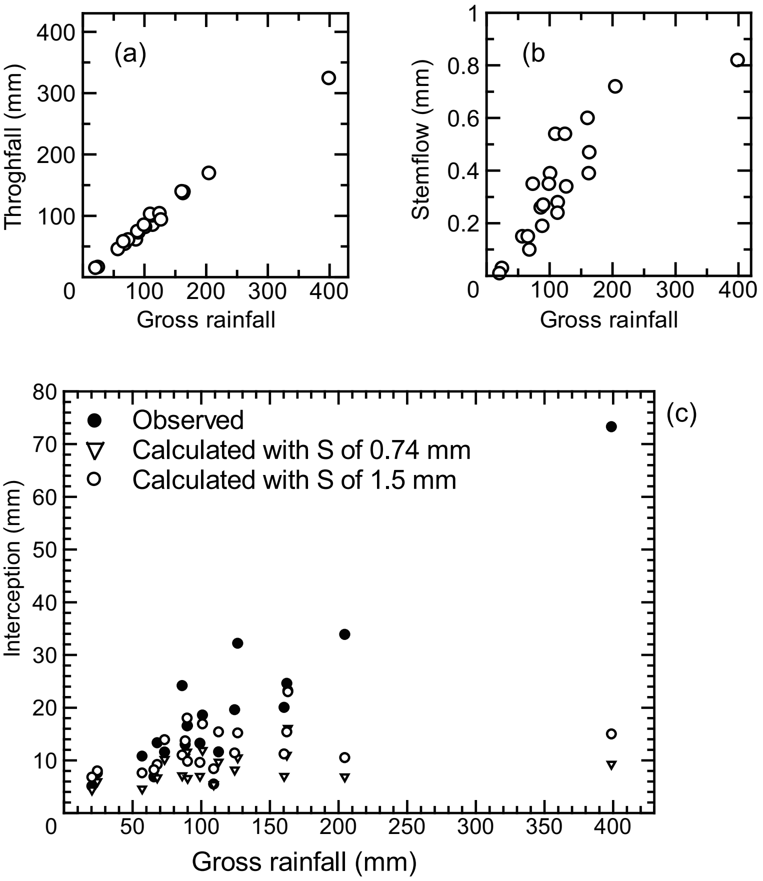

Fig. 1 (a) Relationships of throughfall to gross rainfall. (b) Relationships of stemflow to gross rainfall. (c) Relationships of interception to gross rainfall.

the parameter values is to first follow previous studies and to modify the values by comparisons between the tentative calculation results and the observations. A parameter value set was obtained for the Amazonian forest (Lloyd *et al.*, 1988). Thus, the assumed parameters were as $S = 0.74$ mm, $p = 0.08$, $D_0 = 0.0014$ mm min^{-1}, and $b = 5.25$. As the stem flow fraction was very small (Fig. 1(c)), p_t was assumed to be 0.

The Penman-Monteith equation requires values of aerodynamic resistance for the sensible and latent heat fluxes. We assumed that they are equal to the aerodynamic resistance for momentum, as used by similar estimations (e.g. Shuttleworth, 1988). Because the friction velocity was directly measured by the eddy covariance method, we calculated r_M from the relationship of $r_M = U/U^{*2}$, where U is the wind velocity and U^* is the friction velocity. In our estimates using this method, we derived simple relations between r_M and U for a long-term estimation because the observation by the eddy covariance method was carried out only for a week. Hence, we employ $r_A = 36.7/U$ for the daytime and $r_A = 123/U$ for thenighttime.

Another parameter in the Penman-Monteith equation for calculating evapotranspiration from a dry canopy is a surface resistance or its reciprocal, surface conductance (g_C). Our previous study (Tani *et al.*, 2003) demonstrated the following Jarvis type functional relationship of g_C ($= 1/r_C$) was applicable to dry and wet conditions including the driest condition in 1998 due to the El Niño event:

$$g_c = 35\left[1.6S_d/(S_d + 0.6)\right]\exp(-80V_d) \tag{5}$$

where S_d is the solar radiation. This relationship was used for our estimates.

Since parameter values in the Rutter model are tentatively given as similar values to those for Amazonian forest, the calculated results on interception were compared with the observations (Fig. 1(c)). The calculated values are much smaller than those observed, and the annual total of calculated interception was 182 mm compared with the observation of 381 mm, suggesting the saturation storage capacity (*S*) was too small. The LAI of 6.52 for Pasoh is slightly larger than that of 6.0 for Amazon, and this may be underestimated because another investigation in the Pasoh Forest Reserve determined a value of 7.99 (Kato, 1978). Therefore, we tried to use the maximum value based on a review on *S* of tropical forests (Jetten, 1996). As a result, the annual interception was calculated as 265 mm using a larger *S* value of 1.5 mm, but it is still smaller than the observation. A detailed comparison between the calculated and observed plots in Fig. 1(c) shows they are similar to each other within the range of small rainfall events. This may suggest that the parameters for storage capacity roughly represented the canopy storage capacity of Pasoh Forest, and these values were used for the present estimation of long-term evapotranspiration. Differences in the plots in Fig. 1(c) mainly appear in the range of large rainfall events. The calculations do not agree with a tendency in the observations that interception linearly increases with rainfall. Under applications of the Rutter model, since evaporation mainly occurs in a rainless period, interception tends to be large for rainfall events of weak intensity and long duration, including rainless periods. Therefore, the calculated interception is liable to be small under a tropical rain forest climate of characterized by heavy storms within short durations. Therefore, the disagreement in Fig. 1(c) may suggest more intense evaporation during and after a rainfall event though it is difficult to explain with our model framework. However, the observations may include some errors during a big storm with very intense rainfall. More careful and more detailed observation may be necessary to detect the cause of the disagreement.

Long-term evapotranspiration

Long-term evapotranspiration from the Pasoh Forest was estimated using the Penman-Monteith-Rutter model application. The meteorology, evapotranspiration and their annual amounts from 1995 to 1999 are shown in Figs 4 and 5, and Table 1. Figure 5 displays both the results of interception calculated using two values for the saturation storage capacity on the canopy (*S*), 0.74 mm and 1.5 mm, suggested from Amazonian forest and regarded as the maxima for tropical forests, respectively. The sensitivity of interception to the total evapotranspiration seems small in this figure. This is not only caused by the fact that a larger value of *S* produces a longer period of wet canopy for interception and a shorter period of dry canopy, but also due to the small ratios of interception to total evapotranspiration compared with those under a temperate climate. We therefore *S* = 1.5 mm was employed in the final estimation in Table 1, although some errors were still included in it.

Figure 5 also shows that the total evapotranspiration occupied a large portion of the net radiation, and that their high ratio did not decrease even in a remarkable dry

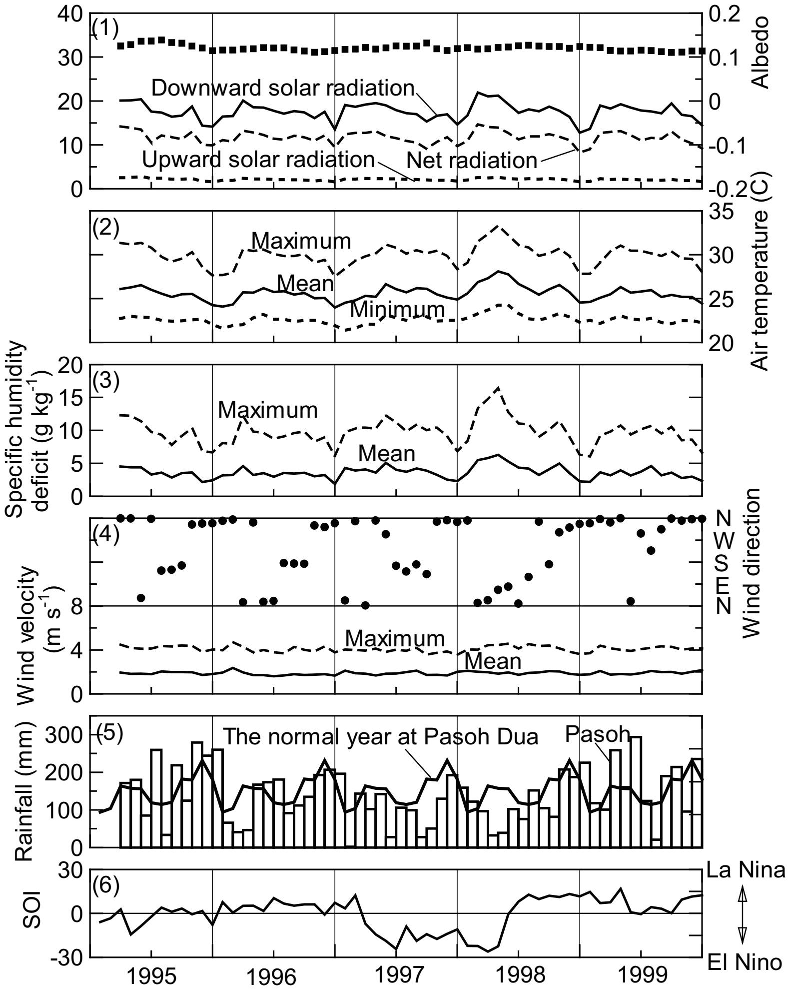

Fig. 4 Seasonal variations in monthly averages of meteorological variables. (1) Daily total of downward and upward solar radiations, net radiation and daily mean albedo. (2) Daily mean, maximum and minimum of air temperature. (3) Daily mean and maximum of specific humidity deficit. (4) Daily vector averaged wind direction and daily mean and maximum of wind velocity. (5) Monthly rainfall at Pasoh Tower and that of the normal year at Pasoh Dua. (6) Southern Oscillation Index (SOI).

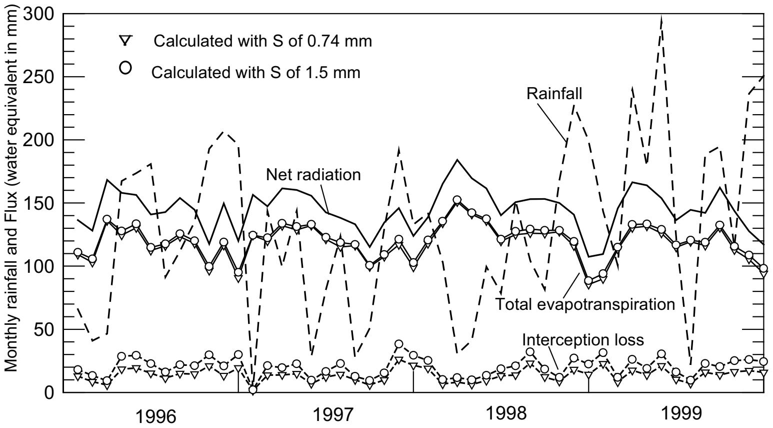

Fig. 5 Estimation results of monthly evapotranspiration with observed monthly rainfall and net radiation.

Table 1 Annual evapotranspiration in the Pasoh Forest (mm).

Year	Rainfall	Net radiation	Interception	Transpiration	Total evapotranspiration	ET/NR
1996	1610	1721	261	1146	1407	82%
1997	1182	1715	220	1218	1438	84%
1998	1426	1821	222	1309	1531	84%
1999	2065	1717	264	1152	1416	82%
Mean	1571	1744	242	1206	1448	83%

The values of energy flux are converted to those in water equivalent using latent heat for vaporization.

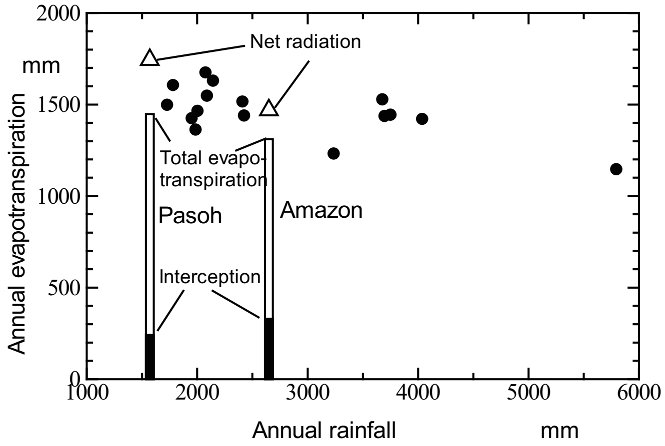

Fig. 6 Comparison of annual evapotranspiration estimated by micro-meteorological observation with that calculated from catchment water budget. Bar: micro-meteorological observation with net radiation (Δ), ●: Catchment water budget after Bruijnzeel (1990).

condition due to the El Niño in 1997 and 1998. The mean ratio of 0.83 (Table 1) was smaller than that of 0.90 for Amazonian rain forest (Shuttleworth, 1988) but the characteristics seems to be common to both forests considering small rainfall conditions during our observation period. Indeed, the mean annual total values (water equivalent using latent heat of vaporization) of net radiation and rainfall of 1744 and 1571 mm in Pasoh during our observation period indicate a fairly dry climate compared with the respective values of 1469 and 2599 mm for the Amazon (annual mean values averaged from October 1983 to September 1985 in Shuttleworth, 1988). Nevertheless, the annual evapotranspiration for Pasoh was 1448 mm, larger than the 1311 mm determined for the Amazon. Such a large evapotranspiration value may have been sustained by soil water storage supplied by rainfall in the wetter years previous to our observation period. A recent observation in a hill evergreen forest in Thailand with a long and severe dry season from December to March showed a large evapotranspiration value was estimated throughout year (Tanaka *et al.*, 2003). These observation results suggest that evergreen forests in humid tropics may maintain high evapotranspiration rates even in dry seasons and that seasonal variation follows the net radiation. This characteristic found first in the Amazonian forest may occur widely in tropical rain forests with smaller rainfall amounts.

Relationships of annual evapotranspiration to annual rainfall estimated from micro-meteorological observations in Pasoh and the Amazon are plotted with net radiation in Fig. 6, which demonstrates the relationships obtained from catchment water-budget observations in tropical lowland forests (Bruijnzeel, 1990). The two micro-meteorological results fall within a small range of evapotranspiration values given by many catchment studies with large variations of rainfall. In addition, both of them are plotted at the lower range of the water-budget values. This may be plausible because a catchment water budget is obliged to overestimate evapotranspiration in the case of runoff underestimation caused by deep percolation. Therefore, this comparison supports our result that evapotranspiration accounted for a large portion of the net radiation.

Acknowledgements We thank the Forestry Department of Negeri Sembilan and Director General of FRIM for giving us permission to work in the Pasoh Forest Reserve, and Prof. M. Suzuki of University of Tokyo and Dr H. Takizawa of Nihon University for their information. The staff of the Hydrology Unit and Pasoh Station of FRIM is acknowledged for collecting data. This study was conducted as a part of joint research project between the Forest Research Institute Malaysia, Universiti Putra Malaysia and National Institute for Environmental Studies (Global Environment Research Program granted by Ministry of the Environment, Japan).

REFERENCES

Bruijnzeel, L. A. (1990) Hydrology of Moist Tropical Forest and Effects of Conversion: A State-Of-Knowledge Review. UNESCO-IHP, Paris, France.

Calder, I. R., Wright, I. R. & Murdiyarso, D. (1986) A study of evaporation from tropical forest—West Java. J. Hydrol. **89**, 13–30.

Jetten, V. G. (1996) Interception of tropical rain forest: performance of a canopy water balance model. Hydrol. Processes **10**, 671–685.

Kato, R., Tadaki, Y. & Ogawa, F. (1978) Plant biomass and growth increment studies in Pasoh Forest. Malay. Nat. **30**(2), 211–224.

Lloyd, C. R., Gash, J. H. C., Shuttleworth, W. J., & Marques, F. A. de O. (2003) The measurement and modeling of rainfall interception by Amazonian rainforest. Agric. For. Met. **43**, 277–294.

Manokaran, N. (1979) Stemflow, throughfall and rainfall interception in a lowland tropical rain forest in Peninsular Malaysia. The Malaysian Forester **42**(3), 174–201.

Shuttleworth, W .J. (1988) Evaporation from Amazonian rainforest. Proc. Roy. Soc. **B 233**, 321–346.

Tanaka, K., Takizawa, H., Tanaka, N., Kosaka, I., Yoshifuji, N., Tantasirin, C., Piman, C. and Suzuki, M. (2003) Transpiration peak over a hill evergreen forest in northern Thailand in the late dry season: assessing the seasonal changes in evapotranspiration using a multi-layer model, J. Geophys. Res., (in press).

Tani, M., Abdul Rahim, N., Ohtani, Y., Yasuda, Y., Mohd, Md S., Baharuddin, K., Takanashi, S., Noguchi, S., Zulkifli, Y. & Watanabe, T. (2003) Characteristics of energy exchange and surface conductance of a tropical rain forest in Peninsular Malaysia. In: Pasoh: Ecology and Natural History of a Lowland Tropical Rain Forest in Southeast Asia (ed. by T. Okuda, K. Niiyama & S. C. Thomas). Springer, Tokyo, Japan (in press).

Yasuda, Y., Ohtani, Y., Watanabe, T., Okano, M., Yokota, T., Liang, N., Tang, Y., Abudl Rahim, N., Tani, M. & Okuda, T. (2003) Measurement of CO_2 flux above a tropical rain forest at Pasoh in Peninsular Malaysia. Agric. For. Met.. **114**, 235–244.

日緑工誌，J. Jpn. Soc. Reveget. Tech., 29(1), 51-55

論　文　*ORIGINAL ARTICLE*

半島マレーシア熱帯雨林の蒸散特性

高梨　聡1)・谷　誠1)・Abdul Rahim Nik2)

1) 京都大学農学研究科　Graduate School of Agric., Kyoto Univ.
takanash@kais.kyoto-u.ac.jp
2) マレーシア森林研究所　Forest Research Institute Malaysia

摘要：半島マレーシア熱帯雨林において行われた1998 年の気象観測データを用いて，群落コンダクタンスの解析を行った。群落コンダクタンスと日射量，大気飽差との関係には良い相関がみられた。飽差と日射量を説明変数とする群落コンダクタンスモデルを適用した結果，年間を通して良好な再現結果が得られた。熱帯雨林の中では，かなり大気や土壌が乾燥する当試験地において，土壌が乾燥しても群落コンダクタンスの特性に変化はなく，蒸散が低下することがなかった。

キーワード：群落コンダクタンス，蒸散，熱帯雨林

TAKANASHI, Satoru, TANI, Makoto, Abdul Rahim, Nik：**Characteristics of transpiration over a tropical rainforest in Peninsular Malaysia**

Abstract：Surface conductance was studied using micrometeorological data obtained at a tropical rain forest in Peninsular Malaysia in 1998. Surface conductance could be estimated through the year using the surface conductance model expressed as the function of solar radiation and specific humidity deficit. Soil drought did not affect the characteristic of the surface conductance and transpiration rate in the driest period at this study site where soil and the air tend to dry in a tropical rain forest.

Key words：surface conductance, transpiration, tropical rain forest

1. はじめに

地球温暖化などの環境変動に対する森林の役割を評価することに国際的な関心が持たれている現在，森林の蒸発散過程の評価は最も重要な課題として位置づけられる。なかでも太陽エネルギーの豊富な熱帯地域において，森林は蒸散作用によって熱環境を和らげていると考えられ，熱帯雨林の気候におよぼす影響解明にその蒸散特性を解析することは重要であると考えられる。アマゾン熱帯雨林において進められてきた長期観測によると，純放射エネルギーの蒸発散潜熱に配分される割合は大きく，年間を通じてペンマン式などで表される可能蒸発量に対する比はほとんど同じになる。熱帯雨林であるからには長期の無降雨期間は見られないが，雨季と乾季の交代がある。しかし乾季においても，土壌水分の乾燥による蒸発散の抑制はほとんど見られなかったということが結論となっている1)。そこで，東南アジア熱帯雨林の蒸発散・エネルギー交換の研究では，アマゾンと同じような傾向があるかどうか，エルニーニョなどの数年周期の気候変動に伴って生じるような，長期無降雨条件によって蒸発散にどのような影響が見られるのかが，ひとつの重要な着眼点になると考えられる。そこで本研究では，半島マレーシアの中でも特に降雨の少ないPasoh保護林において，環境条件に対して気孔調節によってどのように蒸散を制御しているかについて，そのモデルパラメータである群落コンダクタンスの日射量と大気飽差に対する関係を明らかにする。

2. 観測方法

2.1　観測地概要

気象観測は，半島マレーシアのPasoh森林保護区の低地フタバガキ林に設置された52.6 mのタワーを使用して実施された。Pasoh保護林はNegeri Sembilan州，北緯2度58分，東経102度18分にあり，年平均気温は24.8 ℃，平年の降雨量は1804 mmである10)。降雨量は，南西モンスーンの4-5月，北東モンスーンの10-11月に多いが，半島の内陸にあるため，半島マレーシアの中では比較的少雨の地域に位置づけられる。Pasoh保護林2450 haの中央650 haが多くのフタバガキ科樹種により構成される低地原生林であり，連続した樹冠の高さは約35 mであるが，突出したエマージェント木の高さは45 mに達する。葉面積指数LAIは6.52と見積もられる(新山ら，未公表)。地形は緩やかな起伏をもち，標高は75-150 mである。土壌は粘土質であり30 cm以深は礫に富む12)。

2.2　気象観測

タワー最上部52.6 mにおいて，下向き，上向きの短波放射

量をアルベドメーター(EKO MR-22)で，純放射量を放射収支計(EKO MF-40)で，気温湿度を温湿度計(Visala HMP-35C)で，風向きと風速を風向風速計(Campbell 03001)で，降雨量を雨量計(Yokogawa B-011-00)で測定した。サンプリングは15秒毎に行い，30分間の平均値をデータロガー(Campbell CR-10)に記録した。これに加え，ボーエン比法等による蒸発散とエネルギー交換量の推定のため，52.6 mと43.6 mの気温･湿度を，通風乾湿計(EKO MH-020S)で，52.6 m，49.1 m，46.6 m，43.6 mの風速を三杯式微風速計(Ikeda WM-30P)で測定した。森林群落内の空気の顕熱・潜熱貯熱，樹体貯熱を算出するため，1995年3月4-5日に，通風乾湿計，微風速計を52.6 m，49.1 m，41.5 m，33.0 m，17.0 m，1.0 mに設置して林内気象条件を測定した。なお，解析の対象とした期間は1998年の1年間である。

3. 解析方法

3.1　蒸散量

群落におけるエネルギー交換は，下記のエネルギー収支式によって表現される。

$$Rn = H + \lambda E + Q_s + A \tag{1}$$

ここで，R_nは純放射，Hは顕熱フラックス，λEは潜熱フラックス，Aは光合成などによるエネルギー吸収量である。Q_sは群落貯熱変化であって，群落内の顕熱および潜熱の増加(Q_a, Q_w)，樹体貯熱増加(Q_b)，地中貯熱(Q_g)によって構成され，下記のように表される。

$$Q_s = Q_a + Q_w + Q_b + Q_g \tag{2}$$

Q_a, Q_w, Q_b については，1995年3月に実施した気温・湿度の鉛直分布の集中観測結果を基に，これらの時間変化から求めたQ_a, Q_w, Q_bの値とタワー最上部52.6mの気温(T)と水蒸気圧(V)の関係を次の経験式7)で表して推定した。

$$Q_a = 0.0172(dT/dt) \tag{3}$$

$$Q_w = 0.0253(dV/dt) \tag{4}$$

$$Q_b = 0.0180(dT/dt) \tag{5}$$

このようにして，これらの貯熱変化量を継続観測の行われている後者の気温･湿度のデータから計算で推定した。なお，熱量，温度，水蒸気圧の単位はkW m-1，℃，hPaとし，dT/dt，dV/dt については1 時間の気温，水蒸気圧の変化量から計算した。Q_gの値は熱流板で測定したが1 %未満であったので無視可能であった。光合成，呼吸に関する(A)については3 %未満とされており3)，無視した。

以上の処理によって，エネルギー収支式は，純放射(R_n)から群落貯熱量(Q_s)を差し引いて求めた有効エネルギー(Q)を顕熱と潜熱に配分する形になる。

$$Q = H + E \tag{6}$$

顕熱および潜熱フラックスはボーエン比法を用いて有効エネルギーから以下のようにして求められる。

$$H = \frac{B}{1+B}Q \tag{7}$$

$$\lambda E = \frac{1}{1+B}Q \tag{8}$$

ボーエン比(B)は，43.6 mと52.6 mの通風乾湿計の気温･湿度から計算される温位･水蒸気圧の値，θ_1，θ_2，e_1，e_2から次式で計算される。

$$B = \gamma\frac{\theta_1 - \theta_2}{e_1 - e_2} \tag{9}$$

ここでγは乾湿計定数である。

3.2　群落コンダクタンス

森林群落におけるエネルギー交換に関与する条件は，放射エネルギー・気温・湿度などの与えられた気象環境条件と森林群落条件に大きく分けられる。これは，最も簡単には，いわゆるビッグリーフモデルにより表現できる。すなわち，群落上部の気象環境条件と向き合う一枚の葉（仮想葉）を考え，その空気力学的な特性と植物が蒸散を制御する特性を抵抗またはコンダクタンスで表現するモデルが用いられる。ビッグリーフモデルにおいて，潜熱フラックスは，仮想葉内部と大気との間の水蒸気圧差という濃度勾配と，抵抗，またはその逆数であるコンダクタンスという拡散の度合いによって決定される。このようなモデルにより，エネルギー交換量の推定プロセスから，エネルギー交換に関するその群落の特性を検討するプロセスに移行することができる。ここでは，ビッグリーフモデルの代表的な式として，Penman-Monteith式6)を用いて以下のように植物の生理的な活動による気孔開閉の度合いを示す群落コンダクタンス(g_c)を算出した。

$$g_c = \frac{1}{r_c} = \left[\left\{\left(\frac{\Delta Q + \rho C_p\left(e_s(T_a) - e_a\right)/r_a}{\lambda E} - \Delta\right)\frac{1}{\gamma} - 1\right\}r_a\right]^{-1} \tag{10}$$

ここで，Δは飽和水蒸気圧曲線の傾き (hPa K-1)，ρは空気密度(kg m-3)，C_pは空気の定圧比熱(kJ kg-1 K-1)，e_a，$e_s(T_a)$は測定高度(52.6m)における水蒸気圧および飽和水蒸気圧(hPa)である。群落コンダクタンス(g_c)はボーエン比法によって式(8) (9)から計算されたλEと空気力学的抵抗(r_a)から計算できる。森林群落の空気力学的抵抗は主に群落の粗度長と風速に支配され，風速以外の環境条件の変化による変動は少なく，蒸発散に対する影響は小さいため，大気の中立を仮定し，運動量に関する抵抗(r_m)と等しいとして以下のように計算した。

$$r_a = r_m = \frac{u_r}{u_*^2} \tag{11}$$

ここでu_rは52.6 mにおける風速，u_*は摩擦速度である。摩擦速度u_*は4高度での風速分布から対数則と呼ばれる以下の式に回帰し計算した。

$$u = \frac{u_*}{\kappa}\ln\frac{z-d}{z_0} \tag{12}$$

ここでuは各測定高度における風速(m s-1)，κはカルマン定数，zは測定高度(m)，dは地面修正量(m)，z_0は粗度長(m)である。ただし，地面修正量(d)は，複雑な多層構造をもつ熱帯雨林で定めるのは困難ではあるが，樹高を43 mとし，文献11)による式をもとに33 mと見積もった。

また，52.6 mにおける風速(u_r)と摩擦速度(u_*)との間には図-1のように相関があるので，

$$\frac{u_*}{u_r} = c \tag{13}$$

とおけ，

$$r_a = \frac{u_r}{u_*^2} = \frac{1}{c^2 u_r} \tag{14}$$

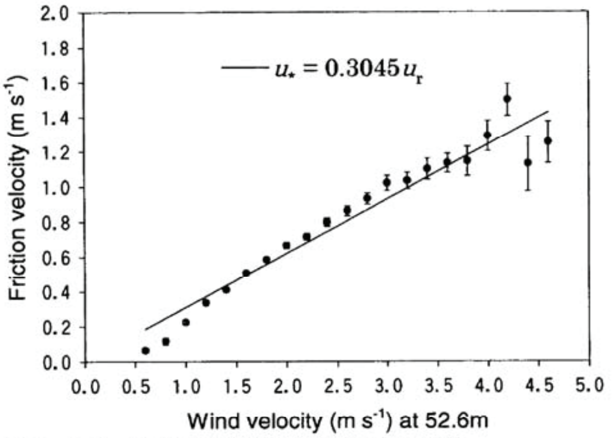

図-1　52.6 mにおける風速と摩擦速度との関係
Fig. 1　Relationship between wind velocity at 52.6 m and friction velocity.

となる。式(14)によって，1高度での風速から空気力学的抵抗(r_a)が計算できる。

4.　観測結果および解析

4.1　一般気象要素

1998年1月1日から12月31日までの日単位の気象観測結果を図-2に示す。時間単位は1月1日を1とした通し日数(Julian日)を用いた。図-2を見ると，日射量や気温は，北緯3度の条件から，季節変化が乏しい。ただし，3-5月に日射量が大きく，飽差が大きくなる傾向が認められる。この時期には，エルニーニョであった1997 年からの継続的な少雨傾向の中で最も大気と土壌が乾燥していたと考えられる。年末には日射量は小さくなり，飽差についても小さくなる傾向が見られる。1998 年の降雨量は1425.9 mm，平均気温は26.4 ℃であった。

4.2　群落コンダクタンスの特性

群落コンダクタンスの特性の季節変動を調べるため，期間A-Fを抽出し，遮断蒸発の影響がないと考えられる前日，当日に雨のない日を解析期間とした。気孔を介さない蒸発現象である遮断蒸発の影響を取り除くことにより，ボーエン比法により得られた潜熱フラックスは蒸散量と考えることができ，これにより算出された群落コンダクタンスは気孔の開閉の度合いを表していると言える。

各期間の気象諸要素を表-1に示す。年末に当たる期間Fで日射量が小さく，飽差が小さく，先行雨量の多い傾向が見られ，大気が比較的湿潤な期間といえ，土壌も湿潤であったと考えられる。群落コンダクタンスの値は，植物の気孔の開閉に依存して変化していると考えられ日射量や飽差と関係が深いので，各期間の群落コンダクタンスの値と，日射量，飽差との関係を図-3 に示す。各期間の群落コンダクタンスの傾向を比較するため，群落コンダクタンスの値を比湿による飽差で2 g kg^{-1}ごとに区切り，その間の平均値をプロットし，その標準誤差をエラーバーで表現したものである。図-3を見ると，飽差が大きくなるにつれてコンダクタンスが小さくなること，日射量が大きくなるとコンダクタンスが大きくなることが分かる。しかし，各期間において同じ日射量，飽差に対して群落コンダクタンスの値は同程度となっており，コンダクタンスの特性の明確な季節変化は見られない。特に大気や土壌が比較的湿潤だと考えられる期間Fにおいて植物の気孔は開きやすくなっていると考えられ，それに対応して同じ日射量，飽差に対して群落コンダクタンスの値は大きくなることが予想されたが，そのような傾向は見られなかった。なお，図中の曲線は群落コンダクタンスモデルの適用結果であり，次節に詳細を記す。

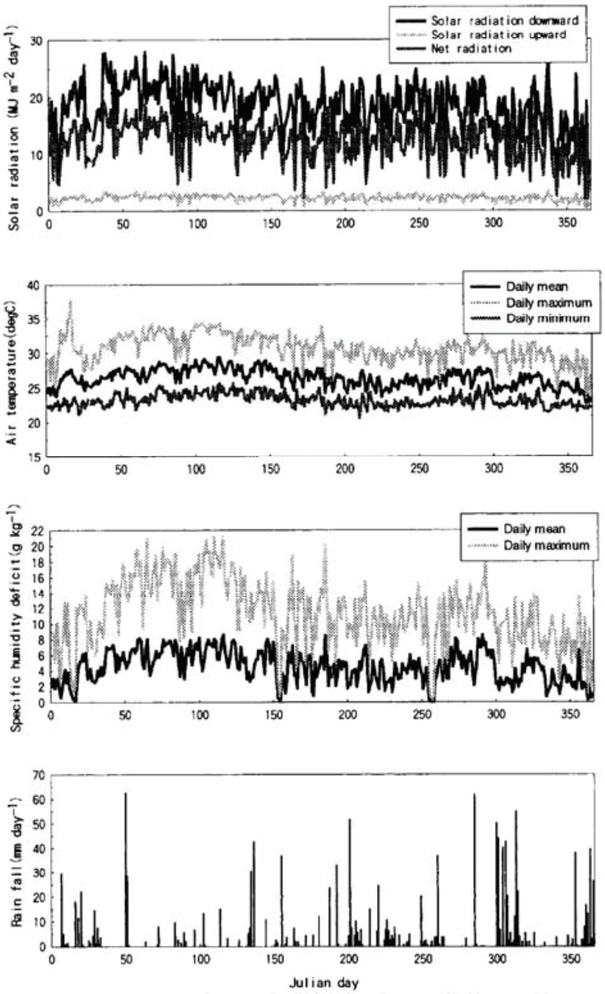

図-2　観測された日射量，純放射量，気温，飽差，雨量
Fig. 2　Seasonal change of solar radiation, net radiation air temperature, specific humidity deficit and daily rainfall.

4.3　群落コンダクタンスモデルの適用結果

森林群落からの蒸散量は，究極的には気孔にある孔辺細胞によって制御されている。しかし，これらの生理的な過程をそのままモデル化し，森林群落レベルの微気象特性の解析に用いるには現実的ではない。群落レベルでのコンダクタンスの環境変化に対する応答を記述するモデルが必要である。気孔レベルにおける代表的なモデルとして，気象環境条件に対する気孔の応答をそれぞれの独立変数として表現したJarvis型のモデル[2)]が存在する。このモデルは森林群落に拡張され，いろいろな森林での観測結果を基に改善され，現実

表-1 抽出された期間の気象諸要素

Table 1 Daily mean or total meteorological variables in each period.

期間		下向き日射日総量 (MJ m^{-2}d^{-1})	純放射日総量 (MJ m^{-2}d^{-1})	平均気温 (degC)	平均飽差 (g kg^{-1})	平均風速 (m s^{-1})	30日先行降雨量 (mm)
A	3/2-4/6	21.30	14.37	27.49	6.25	1.99	96.53
B	4/16-4/23	21.35	13.61	28.25	7.14	1.75	42.31
C	5/19-5/31	20.51	13.86	28.04	5.93	2.05	107.0
D	6/10-6/25	18.61	12.04	26.79	5.06	1.83	142.5
E	9/29-10/6	18.08	11.38	26.99	6.10	1.90	81.44
F	12/5-12/23	13.34	8.399	24.91	2.86	1.57	175.4

的に適用可能なモデルとして提案されている[4,8,9]。本研究では，Dolmanと同様のJarvis 型のモデル[1]を用いて，群落コンダクタンスの再現計算を試みた。

群落コンダクタンス(g_c)を，比湿による飽差(δq)，日射量(S_d)，気温(T)，土壌水分($\delta\theta$)の関数とし，次式で表す。

$$g_c = a_1 f(\delta q) f(S_d) f(T) f(\delta\theta) \tag{15}$$

このモデルは，比湿による飽差(δq)，日射量(S_d)，気温(T)，土壌水分($\delta\theta$)を説明変数とする関数で群落コンダクタンスを表現しているが，当地の気温の日変化は日射量に近く，季節変化も乏しいので，気温の関数は省略した。また，前節で見たように群落コンダクタンスの特性は日射量と飽差でおおむね説明でき，土壌の乾燥によるコンダクタンスの低下は見られなかったため土壌水分の影響はないものとした。比湿による飽差(δq)，日射量(S_d)の関数は以下の式を用いた。

$$f(\delta q) = \exp(-a_2 \delta q) \tag{16}$$

$$f(S_d) = [S_d/(a_3 + S_d)]/[1000/(1000 + a_3)] \tag{17}$$

ここでδqは比湿による飽差(g kg^{-1})，S_d は日射量(kW m^{-2})，またa_1，a_2，a_3，は群落ごとに固有のパラメータであり，それぞれ，最大群落コンダクタンス，飽差の増大に対する群落コンダクタンスの減少率，日射量の増加に対する群落コンダクタンスの初期増加率に関連した値である。

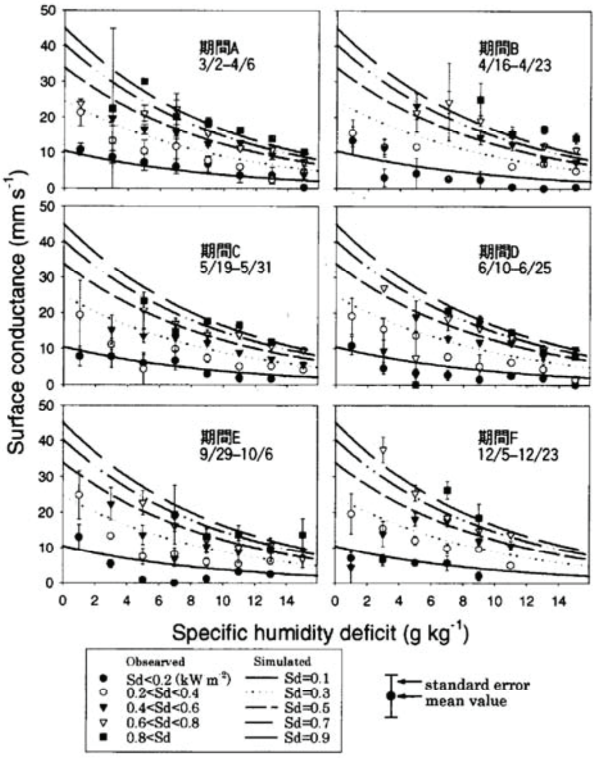

図-3 群落コンダクタンスと飽差，日射量との関係

Fig. 3 Relationship of surface conductance to specific humidity deficit as a function of downward solar radiation.

各期間において，計算される群落コンダクタンスと観測値との残差平方和が最小となるように非線形回帰分析[5]により，モデル中のパラメータを決定した。表-2に，決定されたモデルパラメータを示す。この中で，期間Aが最も解析期間が長く取れ，飽差の条件も広い範囲にわたっているため，期間Aにおいて見積もられたパラメータを最も信頼できるパラメータとして考え，これを用いて群落コンダクタンスモデルの再現性を検証した。

図-3の曲線は期間Aにおいて見積もられたパラメータにより再現された群落コンダクタンスのS_d=0.1, 0.3, 0.5, 0.7, 0.9 kW m^{-2}の場合を示したものである。期間Bなど外れる部分がある期間もあるがおおむね良好に再現できている。

期間Aは比較的大気と土壌が乾燥した期間であるが，この期間Aにおいて見積もられたパラメータにより湿潤な期間Fにおいても良好に再現できている。したがって，群落コンダクタンスの応答特性に季節変化は乏しいといえる。次に各期間での比較的よく晴れた3日間のモデルの再現結果と観測値の日変化を図-4に示す。図-5は群落コンダクタンスモデルを再びPenman-Monteith式に代入し，蒸散量を算出したものである。曲線がモデルによる再現値であり，パラメータは期間A において見積もられたものを使用したが，どの期間においても良好に再現された。

表-2 各期間で見積もられたパラメータ

Table 2 The optimized parameters in each period.

期間		a_1	a_2	a_3
A	3/2-4/6	47.0	0.10	632.3
B	4/16-4/23	33.8	0.07	161.1
C	5/19-5/31	35.2	0.08	599.4
D	6/10-6/25	47.9	0.13	233.6
E	9/29-10/6	50.3	0.13	597.0
F	12/5-12/23	59.5	0.17	265.3
Amazon (Dolman et al, 1991)		20.8	0.06	250.0

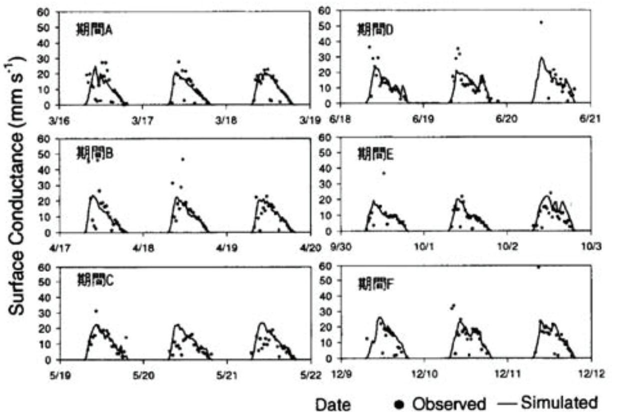

図-4 群落コンダクタンスの再現計算結果

Fig. 4 Comparison of observed and simulated surface conductance using optimized parameters in period A.

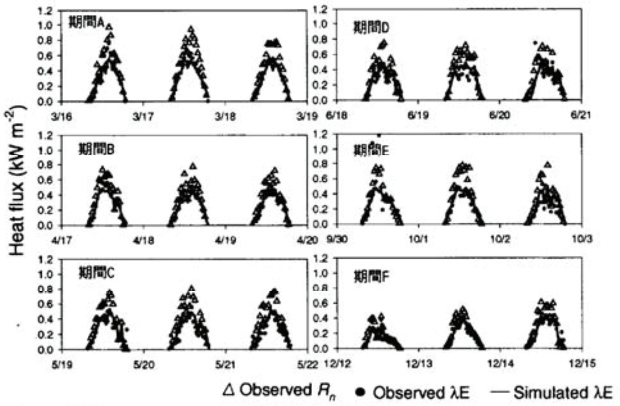

図-5 潜熱フラックスの再現計算結果

Fig. 5 Comparison of observed and simulated latent heat flux using optimized parameters in period A.

表-2の末尾にアマゾンで見積もられたパラメータ1)を示す。Pasohでは最大群落コンダクタンスは大きいが，飽差の増大に対して群落コンダクタンスが敏感に小さくなる傾向が見られた。これが測定などの誤差によるものだとすると，通風乾湿計につく露が影響し飽差の小さいところで大きなコンダクタンスが観測されてしまったことが原因として考えられる。しかしながら，森林群落の生理特性や構造に起因するものである可能性もあり，そうであるならば熱帯雨林のなかでは大気や土壌の乾燥が進むPasohにおいては飽差の増大に対して敏感に反応し，乾燥に適応しているのだと考えられる。この点について詳しく議論するためには，今後精度の高い乱流変動法を用いてフラックスを観測するなどの改善が必要だと考えられる。

5. 結論

半島マレーシア熱帯雨林において行われた気象観測データを用いて，群落コンダクタンスの解析を行った。熱帯雨林の中では，かなり大気や土壌が乾燥するPasohにおいて，土壌が乾燥しても群落コンダクタンスは日射量と大気飽差によって制御されており，蒸散が低下することがなかった。また，飽差と日射量を説明変数とする群落コンダクタンスモデルを適用した結果，土壌が乾燥した期間のパラメータを用いて，年間を通して良好な再現結果が得られた。したがって，気象環境条件の変化に乏しい半島マレーシア熱帯雨林において，蒸散特性は季節変化に乏しいと考えられた。

引用文献

1) Dolman, A. J., Gash, J. H. C., Roberts, J. and Shuttleworth, W. J. (1991) Stomatal and surface conductance of tropical rainforest. Agric. For. Meteorol., 54 : 303-318.

2) Jarvis, P. G. (1976) The interpretation of the variations in leaf water potential and stomatal conductance found in canopies in the field. Phil. Trans. R. Soc. Lond. B., 273 : 593-610.

3) Jarvis., P. G., James, G. B. and Landsberg, J. J. (1976) Coniferous forest. In Monteith, J. L. (ed). Vegetation and the atmosphere. vol. 2. Academic Press, New York, pp.171-236

4) Lindroth, A. (1985) Canopy conductance of coniferous forests related to climate. Water Resources Research, 21(3) : 297-304

5) Marquardt, D. W. (1963) An algorithm for least-squares estimation on nonlinear parameters. SIAM J. Appl. Math., 11 : 441-443

6) Monteith, J.L. (1965) Evaporation and environment. Symp. Soc. Exp. Biol., 19 : 206-234

7) Ohtani, Y., Okano, M., Tani, M., Yamanoi, K., Watanabe, T., Yasuda, Y. and Abdul Rahim, N. (1997) Energy and CO_2 fluxes above a tropical rain forest in Peninsular Malaysia. – Under estimation of eddy correlation fluxes during low wind speed conditions. J. Agric. Meteorol., 52 : 453-456

8) Stewart, J. B. (1988) Modelling surface conductance of pine forest. Agric. For. Meteorol., 43 : 19-35

9) Stewart, J. B. and Gay, L. W. (1989) Preliminary modeling of transpiration from the FIFE site in Kansas. Agric. For. Meteorol., 43 : 305-315

10) Tani, M., Abdul Rahim, N., Mohd Md, S., Noguchi, S. and Ohtani, Y. (2003) Five-year meteorological observation at Pasoh Forest Reserve, Negeri Sembilan, Peninsular Malaysia. Forest Research Institute Malaysia, Kuala Lumpur (in press)

11) Watanabe, T. (1994) Bulk parameterization for a vegetated surface and its application to a simulation of nocturnal drainage flow. Boundary-Layer Meteorol., 70 : 13-35

12) Yoda, K. (1978) Organic carbon, nitrogen and mineral nutrient stock in the soils of Pasoh Forest. Malay. Nat. J., 30 : 229-251

（2003.5.17受理）

J. Agric. Meteorol. 52 (5) 453−456, 1997

Energy and CO_2 fluxes above a tropical rain forest in Peninsular Malaysia
- Under estimation of eddy correlation fluxes during low wind speed conditions -

Y. Ohtani*, M. Okano*, M. Tani*, K. Yamanoi*, T. Watanabe*, Y. Yasuda** and A. R. Nik***
(*Forestry and Forest Products Research Institute, Ibaraki 305, Japan)
(**Chiba University, Chiba 271, Japan)
(***Forest Research Institute Malaysia, 52109 Kuala Lumpur, Malaysia)

Abstract

Eddy correlation observation of sensible, latent heat and carbon dioxide fluxes above a tropical rain forest were conducted in March 1995 in Peninsular Malaysia. The calculated total energy flux consisted of both sensible and latent heats ranged from 50% to 80% of the available energy. Under the low wind speed conditions, the sensible and latent heats were intermittently transported upward according to the plume events. Sum of the sensible and latent heat fluxes generally ranged from 1000 to 2000Wm^{-2} during individual plume events, though the time averaged flux was apparently insufficient. It was suggested that the occurrence of large plume events could be spatially localized.

Key words: CO_2 flux, eddy correlation method, latent heat, sensible heat, tropical rain forest

1. Introduction

Energy budget and CO_2 flux observations in the tropical rain forest have conducted primarily in Amazonean rain forests (Fan *et al.*, 1990; Fitzjarrald *et al.*, 1988; Shuttleworth *et al.*, 1984; Wofsky *et al.*, 1988). In Southeast Asia there is limited understanding of the micrometeorological processes in and above the forest. Eddy correlation fluxes were observed in this study. The results of the flux calculation and the micrometeorological characteristics above the tropical rain forest during the low wind speed conditions are the primary focus of this report.

2. Experimental site

A tropical rain forest for our study is in Pasoh Forest Reserve, Forest Research Institute Malaysia, located in the center of Peninsular Malaysia (2°58N 102°18E). The elevation of the gently undulated terrain is approximately 120m. The forest has a complex canopy. The general height is approximately 35m, although emergent trees exceed 45m. The biomass and leaf area of the forest are determined by the tree diameter observation (Niiyama, unpublished), adapting the empirical equations which were obtained in the same forest by Kato *et al.*(1978).

3. Method

3.1 Observation

A 52m tall tower constructed in the forest was used for the platform of the meteorological observations (Fig.1). A three dimensional ultrasonic anemometer-thermometer (DAT-600, Kaijo) and an infrared H_2O/CO_2 fluctuation meter(E-009A, Advanet) were installed on the tower at a height of 52.6m. Turbulent fluxes of sensible and latent heat, and CO_2 were measured from March 21-28, 1995. Data were recorded at the sampling frequency of 10 Hz (every 0.1 s) . At the same height, the average values of air temperature, humidity and CO_2 concentration were measured with a ventilated psychrometer and NDIR, respectively. Net radiation, global solar radiation and albedo also were observed at the top of the tower. Soil heat flux was observed at 2cm under the soil surface.

3.2 Energy budget

The energy budget above the forest canopy is written as

$$Rn = H + lE + Qs \qquad (1)$$

where *Rn* is the net radiation; *H* and *lE* are the sensible and the latent heat fluxes by the eddy correlation method; and *Qs* is the stored energy under the reference height within a forest canopy. The storage term, *Qs*, is defined further as

$$Qs = Qa + Qw + Qv + Qg + Qp \qquad (2)$$

where Qa and Qw are the sensible and latent heat storage in the canopy air, respectively; Qv and Qg are the sensible heat storage within the biomass and the soil, respectively; and Qp is the net photosynthetic energy. Based on the observation, Qg was less than 1% of Rn throughout the day, and since Qp is assumed to be around 3% of Rn (Jarvis et al., 1976), thus the storage terms Qg and Qp can be ignored. Qa, Qw and Qv were estimated by the empirical formulae obtained by the vertical distributions of temperature and vapor pressure observed in and above the forest. Following

$$Qa = 17.2\,(dT/dt) \qquad (3)$$

$$Qw = 25.3\,(de/dt) \qquad (4)$$

$$Qv = 18.0\,(dT/dt) \qquad (5)$$

where dT/dt and de/dt are the rate of air temperature and vapor pressure changes in one hour at the reference height.

3.3 Data processing

The eddy correlation method was used for the computation of sensible and latent heat and CO_2 fluxes. A correction for the thermal component (Kaimal and Gaynor, 1991) was applied to the data. The procedural coordinate's transformation for three dimensional components of wind velocity (Kaimal, 1988) was taken into account, but the transformation generated unexpected axis rotation in this case (Fig.2-3). Then the mean and the perturbation part of the data, both for the vertical wind speed component and scalars, were separated by the moving-average filter which has a Hamming data window. McMillen (1987) used a recursive digital filter for the separation. The filter we used is two-sided and

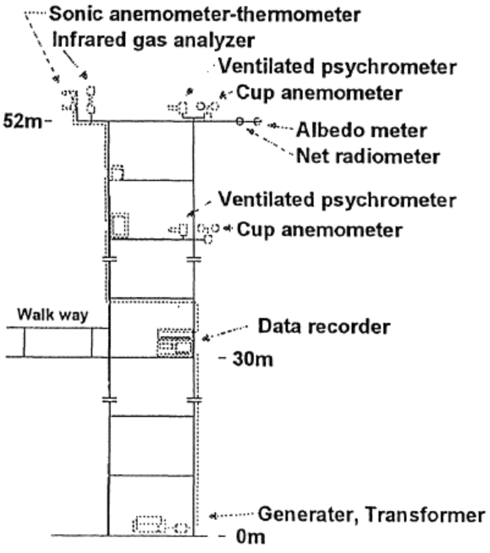

Fig.1 Arrangement of instruments.

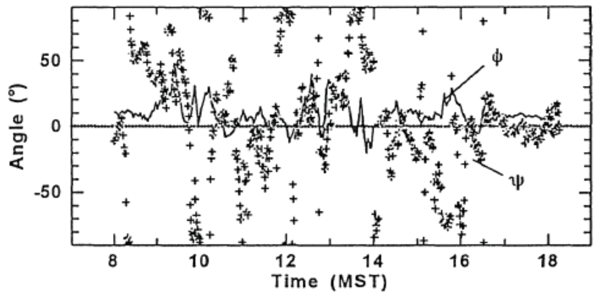

Fig.2 Changes of correction angles. The correction angle φ shows the elevation, and ψ is to satisfy $\overline{v'w'} = 0$ (Kaimal, 1988).

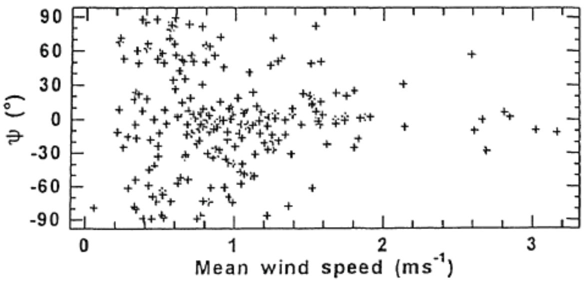

Fig.3 Relationship between the horizontal mean wind speed and the correction angle ψ.

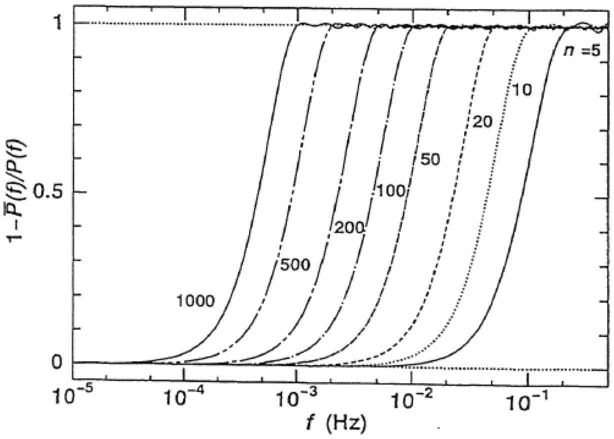

Fig.4 Cut-off frequency of the filter.

there is no time lag in the filtered data. The cut off frequency of the filter according to the various averaging runs is shown in Figure 4. The Webb's correction (Webb *et al.*, 1980) also was taken into account. In the present study, the upward vertical wind velocity treated as positive.

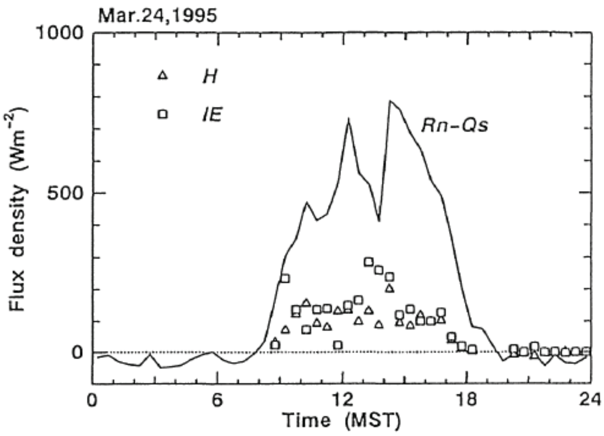

Fig.5 Energy budget.

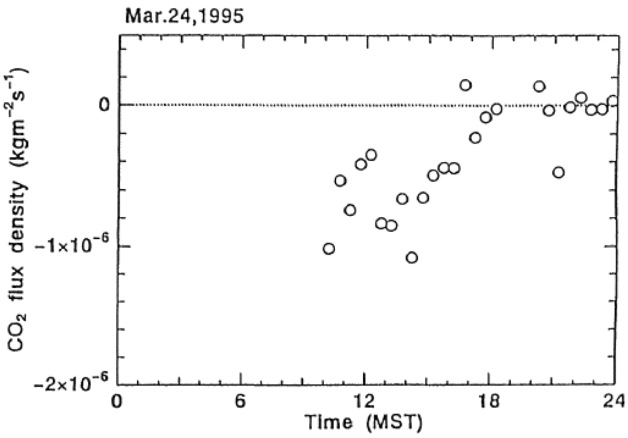

Fig.6 Diurnal change in CO_2 flux.

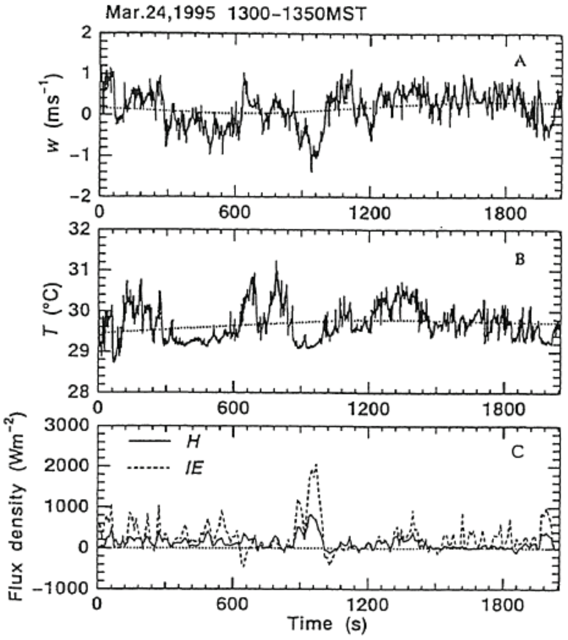

Fig.7 Instantaneous fluxes of *H* and *lE* (1300-1330MST).

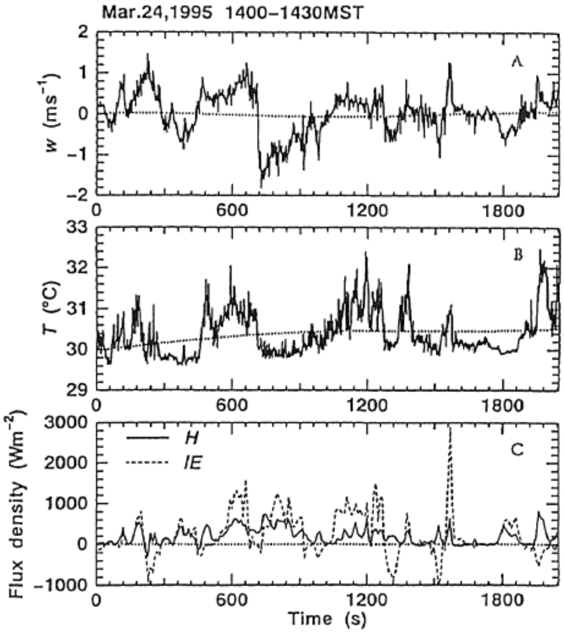

Fig.8 Instantaneous fluxes of *H* and *lE* (1400-1430MST).

4. Results and discussion

4.1 Calculated fluxes

The diurnal changes in the sensible and latent heat fluxes are shown in Figure 5. The maximum eddy correlation fluxes for the sensible and the latent heat are around $200Wm^{-2}$ and $300Wm^{-2}$, respectively. The approximate range of CO_2 flux was $-6x10^{-7}kgm^{-2}s^{-1}$ during mid day (Fig.6). The flux gradually increases up to approximately zero until the early evening. Percentages of the total flux consisting of both sensible and latent heat ranging from 50% to 80% of the available energy. The energy budget in the daytime is not closed. The following topics should be considered for the apparent insufficiency of fluxes: 1) mean horizontal wind velocity is low (i.e. $0.5ms^{-1}$ to $1.5ms^{-1}$) throughout the observation period except while the squall occurred, 2) the forest has a very complex canopy.

4.2 Cause of the calculated flux insufficiency

The instantaneous vertical wind speed component (A), air temperature (B), and sensible and latent heat fluxes (C) are shown in Figure 7 (1300-1330MST) and Figure 8 (1400-1430MST). The fluctuations of both air temperature and vertical wind velocity show the typical change of the unstable boundary layer, thus the existence of convective plumes is suggested. The largest plume event in the observation period occurs around 1410MST continues for 10 minutes. The sensible and latent heat are intermittently transported upward according to the events. The available energy fluxes for Figure 7 and Figure 8 are $525Wm^{-2}$ and $789Wm^{-2}$, respectively, though the calculated total fluxes (sum of sensible and latent heat fluxes) are $416Wm^{-2}$ and $441Wm^{-2}$, respectively. The time averaged flux is apparently insufficient. During individual plume events, the maximum total instantaneous flux was $3000Wm^{-2}$, but generally ranged from 1000 to $2000Wm^{-2}$. The Bowen ratio in the plume events ranged from 0.2 to 0.5, and roughly corresponds to that of from the gradient observation above the canopy. Energy budget should be closed if all the plume events are counted within the averaging runs of the eddy correlation method, but the insufficiency occurs in every calculation period during the daytime. The actual spatial and observed temporal distributions appear to be inconsistent, and the occurrence of large plume events could be spatially localized.

5. Conclusion

The observed fluxes of sensible and latent heat by the eddy correlation method were insufficient to the available energy. Throughout the observation, the mean wind velocity was very low. The convective plume was the main cause of the eddy fluxes, though the actual spatial and observed temporal distributions of the events appeared to be inconsistent. It was suggested that the occurrence of large plume could be spatially localized.

Acknowledgment

The research is part of a joint research project between Forest Research Institute Malaysia (FRIM), Universiti Pertanian Malaysia (UPM) and National Institute for Environmental Studies of Japan (NIES) (Global Environmental Research Program granted by Japan Environmental Agency, Grant No. E-3). We thank the Forestry Department of Negri Sembilan for permission to work in the Pasoh Forest Reserve. We also thank the stuffs of Forest Hydrology Laboratory of FRIM for their great contributions to the micrometeorological observation at the site. We are indebted to Dr. K. Niiyama for providing his tree diameter data observed in Pasoh Forest Reserve for us.

References

Aston, A.R., 1985: Heat storage in a young Eucalypt forest. *J. Agric. Forest Meteorol.*, **35**, 281-297.

Fan, S.M., Wofsy, S.C., Bakwin, P.S., Jacob, D.J. and Fitzjarrald, D.R., 1990: Atmosphere-biosphere exchange of CO_2 and O_3 in the central Amazon forest. *J. Geophys. Res.*, **95**, 16851-16864.

Fitzjarrald, D.R., Stormwind, B.L., Fisch, G. and Cabral, O.M.R., 1988: Turbulent transport observed just above the Amazonean forest. *J. Geophys. Res.*, **93**, 1551-1563.

Kaimal J.C., 1988: The atmospheric boundary layer: Structure and measurement. Gihoudou, Tokyo, pp.116.

Kaimal J.C. and Gaynor, J.E., 1991: Another look at sonic thermometry. *Boundary-Layer Meteorol.*, **56**, 401- 410.

Kato, R., Tadaki, Y. and Ogawa, H., 1978: Plant biomass and growth increment studies in Pasoh Forest. *Malayan Nat. J.*, **30(2)**, 211-224.

McMillen, R.T., 1987: An eddy correlation technique with extended applicability to non-simple terrain. *Boundary-Layer Meteorol.*, **43**, 231-245.

Niiyama, K., personal communication.

Shuttleworth *et al.*, 1984: Eddy correlation measurements of energy partition for Amazonian forest. *Quart. J. Roy. Meteorol. Soc.*, **110**, 1143-1162.

Webb, E. K., Pearman, G.T. and Leuning, R., 1980: Correction of flux measurements for density effects due to heat and water vapour transfer. *Quart. J. Roy. Meteorol. Soc.*, **106**, 85-100.

Wofsky, S.C., Harriss, R.C. and Kaplan, W.A., 1988: Carbon dioxide in the atomosphere over the Amazon basin. *J. Geophys. Res.*, **93**, 1377-1387.

ELSEVIER

Agricultural and Forest Meteorology 114 (2003) 235–244

AGRICULTURAL AND FOREST METEOROLOGY
www.elsevier.com/locate/agrformet

Measurement of CO_2 flux above a tropical rain forest at Pasoh in Peninsular Malaysia

Yukio Yasuda[a,*], Yoshikazu Ohtani[a], Tsutomu Watanabe[a], Michiaki Okano[a], Takeo Yokota[b], Naishen Liang[c], Yanhong Tang[c], Abdul Rahim Nik[d], Makoto Tani[e], Toshinori Okuda[c]

[a] *Department of Meteorological Environment, Forestry and Forest Products Research Institute, P.O. Box 16, Tsukuba-Norin, Ibaraki 305-8687, Japan*
[b] *Faculty of Science, Nara Women's University, Kita-Uoya Nishi, Nara-City, Nara 630-8506, Japan*
[c] *National Institute for Environmental Studies, 16-2 Onogawa, Tsukuba, Ibaraki 305-8506, Japan*
[d] *Forest Research Institute Malaysia, Kepong, 52109 Kuala Lumpur, Malaysia*
[e] *School of Agricultural Sciences, Kyoto University, Kitashirakawa Oiwake-Cho, Sakyo-Ku, Kyoto 606-8502, Japan*

Received 17 April 2002; accepted 23 August 2002

Abstract

This paper reports on the results of a short-term observation of CO_2 flux above a tropical forest at Pasoh in Peninsular Malaysia, using the eddy covariance method with a closed-path CO_2 analyzer, in March 1998. CO_2 concentration profiles above and in a canopy were also measured. In the daytime, the time series of fluctuations in CO_2 concentration above the forest drew the ramp pattern with a period of 2 min. This suggests that large-scale turbulent motions contribute to CO_2 flux in the daytime. We obtained data on the CO_2 flux for 6 days and CO_2 storage flux under the flux measurement level for 3 days in this observation. The values of the CO_2 flux fell within -1.0 to 0.5 mg CO_2 m^{-2} s^{-1}. Net ecosystem CO_2 exchange (NEE) was estimated as the sum of the CO_2 flux and the CO_2 storage flux. Compared with the CO_2 flux, the CO_2 storage flux was relatively large in the early morning and the nighttime, therefore, the storage flux became important to estimate the NEE in those periods. The daily values of the NEE ranged from -2.08 to -2.74 g C m^{-2} per day. The results suggest that this tropical forest was a CO_2 sink during the period. Although we tired to calculate the mass flow component proposed by Lee [Agric. For. Meteorol. 91 (1998) 39], the magnitudes of the mass flow obtained here were, from 5.20 to 12.55 g C m^{-2} per day, much larger than the magnitudes of the NEE.

Keywords: CO_2 flux; Eddy-covariance; Net ecosystem CO_2 exchange; Tropical rain forest; Southeast Asia

1. Introduction

Eddy covariance measurements of carbon dioxide (CO_2) flux between a forest ecosystem and the atmosphere is a sound way to evaluate CO_2 uptake by the forest. Continuous observations of CO_2 flux have been conducted for various types of forests, but the vast majority of these sites have been in boreal and temperate forests in Europe and North America. Observation sites in tropical rain forests conducting routine CO_2 flux measurements are probably only in Central and South America.

---

* Corresponding author. Fax: +81-298-74-3720.
E-mail address: yassan@ffpri.affrc.go.jp (Y. Yasuda).

PII: S0168-1923(02)00198-3

Direct measurements of CO_2 flux over Amazonian tropical rain forests clearly documented that these forests were a sink of CO_2 at least for a short term period (Fan et al., 1990), and possibly even for a whole year (Grace et al., 1995; Malhi et al., 1998). Tropical rain forests cover 12% of the vegetated surface of the earth (Whittaker and Likens, 1975; Malhi et al., 1998). They play a major role in the global uptake of CO_2 by the biosphere. To investigate this, many more measurements are required for tropical rain forests in different areas.

Aoki et al. (1975) took intermittent measurements of CO_2 flux above a tropical rain forest in Southeast Asia. This experiment was carried out at Pasoh in Peninsular Malaysia (Pasoh forest). Pasoh forest was a study area of the International Biological Program (IBP) in the 1970s. Aoki et al. (1975) estimated the CO_2 flux from vertical CO_2 profiles above the forest in November 1973, and they calculated that the net CO_2 uptake rate by the forest was 1.2 mg CO_2 $m^{-2}\,s^{-1}$ when the incoming solar radiation was 907 $W\,m^{-2}$.

In the present study, we conducted a short-term measurement of CO_2 flux above the Pasoh forest, adopting the eddy covariance method. Then net ecosystem CO_2 exchange (NEE) of the forest was estimated as the sum of CO_2 flux and the change rate of CO_2 concentration in the air layer below the flux measuring height (Wofsy et al., 1993; Greco and Baldocchi, 1996; Baldocchi et al., 1997). We collected the available data of CO_2 flux for 6 days and CO_2 storage for 3 days during the observation. This experiment was the first attempt to take direct measurements of CO_2 flux above the Pasoh forest, and was carried out to obtain basic knowledge on characteristics of CO_2 flux above a tropical forest in Southeast Asia.

2. Experiment

2.1. Site description

The observation was conducted in Pasoh Forest Reserve of Forest Research Institute Malaysia (FRIM) from 5 to 15 March in 1998. This forest reserve is located about 140 km southeast of Kuala Lumpur in Peninsular Malaysia, and is 2450 ha in area (see Fig. 1). The reserve is mostly covered with lowland mixed dipterocarp forest. The forest contains primary

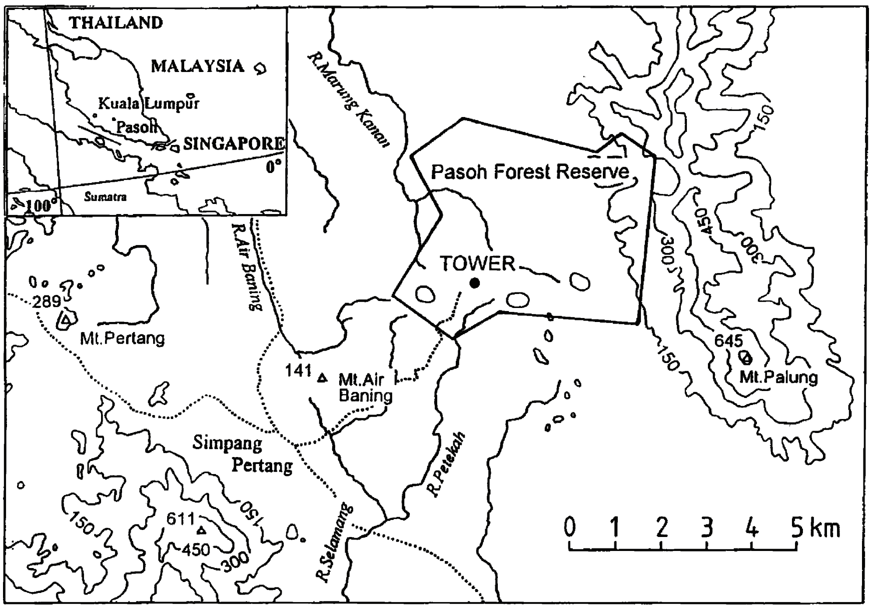

Fig. 1. Location map of the Pasoh Forest Reserve.

and secondary forests (about 1650 and 650 ha, respectively), consisting of various species of Shorea and Dipterocarpus (Soepadmo, 1978). The regenerating area was selectively logged between 1955 and 1960 (Manokaran and Kochummen, 1994). Although the continuous canopy height is about 35 m, there are some emergent trees that exceed 45 m. The dry biomass above the ground and the leaf area index (LAI) were estimated as 463.6 $\mathrm{t\,ha^{-1}}$ and 6.25 by tree diameter observation (Niiyama, unpublished), with empirical equations made for this forest (Kato et al., 1978). The topography in the forest is gently undulating. The soils are characterized by the presence of a band of laterite and a compact structure derived from shales within the area of Durian Series, are poor in cations (except for aluminum) and available phosphorous, and have a low pH of pH 3.5–4.8 (Soepadmo, 1978).

The climate of the forest is summarized by Soepadmo (1978). There is little seasonal variation in air temperature. The mean air temperature is 24.8 °C at 3 m above the ground at an open space in the forest. There are two rainy and dry seasons in this region. The rainy seasons are during April–May and October–November, responding the southwest and northeast monsoons, respectively. The mean annual rainfall is about 2050 mm.

The maximum fetch of the forest is about 3500 m to the north and the minimum one is about 800 m to the southeast, so that the ratios of the fetch to the height of the flux-measurement point (52 m) from the continuous canopy height are 206 and 47, respectively. Northerly winds dominated during the observation.

2.2. Measurements

CO_2 flux was measured at the top of a 52 m-tall scaffold tower. The closed-path technique was applied to the eddy covariance measurement. Wind speed and temperature were measured with a three-axis sonic anemometer (DA-600, Kaijo), and CO_2 concentration was monitored with a closed-path CO_2/H_2O analyzer (LI-6262, LICOR). The sonic anemometer and the inlet of a sampling tube were installed at 52 m. Sample air was drawn through a polyethylene tube (16 m long, 6 mm in diameter) with a diaphragm pump and was pushed by the pump to the CO_2 analyzer through a Teflon tube (3 m long, 4 mm in diameter). The flow rates before and after the pump were about 8.5 $\mathrm{l\,min^{-1}}$ and 2.0 $\mathrm{l\,min^{-1}}$. Residual air was exhausted from a vent. The signals from the eddy covariance sensors were sampled at 5 Hz, and directly recorded with a digital data recorder (DRM2a, TEAC).

Two CO_2 analyzers were used to measure the vertical profile of CO_2 concentrations at six levels above and within the canopy. One analyzer (LI-6252) measured CO_2 profile above the canopy (52, 48 and 40 m) at the flow rate of 2.0 $\mathrm{l\,min^{-1}}$ and another one (LI-6251) measured it within the canopy (30, 21 and 11 m) at the flow rate of 0.5 $\mathrm{l\,min^{-1}}$. Sampling heights were changed at 5 min intervals above the canopy and 10 min intervals within the canopy, allowing enough time to flush tubes containing residual air of last sampling.

Meteorological data were also collected at the top of the tower (solar radiation, temperature, humidity, wind velocity, rainfall, etc.). All instruments were powered using a generator put at the base of the tower. The CO_2 analyzers were calibrated once or twice a day using N_2 and CO_2 standard gases. For H_2O output, the LI-6262 was also calibrated using a dew point generator (LI-610, LICOR) as many as CO_2 calibrations.

CO_2 fluxes were calculated using the covariance of vertical wind velocity and the mixing ratio of CO_2 (Grelle and Lindroth, 1996) for every 30 min. The three-dimensional coordinate rotation of wind velocity components (McMillen, 1988) was applied to set mean vertical wind velocity on zero ($\bar{w} = 0$). The data of fluctuations in CO_2 concentration were detrended by linear least squares fittings to remove diurnal variation. The lag time caused by the air sampling through tubes was 4.8 s determined by the maximum correlation between fluctuations in temperature and those in CO_2 concentration.

Frequency correction for the damping of fluctuation at high frequencies was applied to flux calculations. Here, we used the procedure based on the spectral similarity of scalar fluxes (Aubinet et al., 2001). Although the frequency correction increased absolute values of CO_2 flux during the day and night, the typical increasing rates were only 1–2% in the daytime and <10% in the nighttime when the magnitudes of CO_2 flux were not extremely small. Malhi et al. (1998) mentioned that the frequency correction for the damping ranged from 10 to 25% in the daytime (mean = 16%) and from 10 to 30% in the nighttime (mean = 11%)

above an Amazonian tropical rain forest. Our correction rates were much smaller than their results.

3. Results and discussion

3.1. Fluctuations in CO_2

Fig. 2 shows typical fluctuations in the mixing ratios of CO_2 and H_2O (measured with LI-6262) and air temperature above the Pasoh forest. The data in the figure were collected under unstable conditions and are illustrated by time traces at intervals of 1 s. The mean wind velocity during the period was $1.9\,m\,s^{-1}$, and the Monin–Obkov length was -16.1 m. The amplitude of dominant fluctuation in CO_2 was about $7\,mg\,kg^{-1}$, and fluctuations with a period of about 2 min are apparent. The variations in CO_2 concentration frequently have gradual decreases followed by rapid increases (so-called the ramp pattern). The ramp patterns are also obvious in the time series of humidity and air temperature, although these ramps are inverted because the vertical gradients of humidity and air temperature are opposite to that of CO_2 concentration. We cannot see small fluctuations in humidity at high frequencies, since the damping of humidity fluctuations due to air sampling through a long tube is more serious than CO_2. The ramp patterns are de-

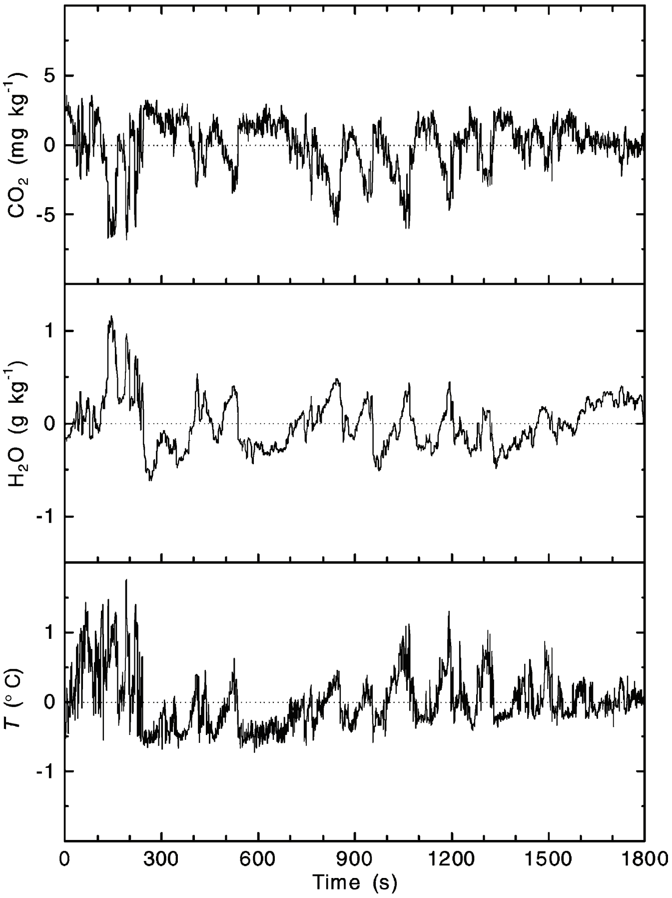

Fig. 2. Fluctuations in the mixing ratios of CO_2 and H_2O and in air temperature for 30 min above the Pasoh forest. The data were obtained under unstable conditions, from 12:00 to 12:30 h on 13 March.

tected above agricultural fields (short vegetation) and forests (Gao et al., 1989; Paw U et al., 1992), and organized turbulent motions that produce the ramp pattern greatly contribute to scalar fluxes (Gao et al., 1989). The fluctuations with a period of about 2 min would account for a large portion of scalar fluxes during the daytime.

3.2. Diurnal variations in CO_2 flux and NEE

Fig. 3 shows the diurnal variations in CO_2 flux, solar radiation, air temperature, water vapor pressure deficit (VPD) and wind speed measured at the top of the tower (52 m). All data are 30 min mean values. The sign convention of the CO_2 flux is that downward flux is negative and upward flux is positive. In the afternoon on 10 March (DOY 68), the CO_2 flux data could not be obtained because of instrument trouble. During the observation period, the maximum solar radiation was $1080\,W\,m^{-2}$ and mean air temperature was 26.9 °C. The maximum VPD was 30.2 h Pa, which is very dry for the region. However, it was very humid from midnight to early morning. We observed mist formation in the early morning of almost all days. Two rain events were observed on the nights of DOY 70 (0.73 mm) and DOY 71 (8.0 mm), and the total amount of rainfall was 8.73 mm. Wind speed was generally low, especially in the morning. The lowest wind speed was $0.2\,m\,s^{-1}$ measured in the morning of DOY 68, and the mean wind speed throughout the period was $1.6\,m\,s^{-1}$.

For reference, we also show CO_2 flux calculated without linear detrending of CO_2 data (block-average removal). The linear detrending of CO_2 data reduces extreme positive and negative values of flux, when the diurnal variation of CO_2 concentration is large. The simple-mean removal keeps low-frequency components arising from the diurnal variation, which are not related to eddy fluxes.

The diurnal variations in CO_2 flux clearly document the activity of the forest ecosystem. The values of the fluxes had a range of -1.0 to $0.5\,mg\,CO_2\,m^{-2}\,s^{-1}$ (-22.7 to $11.4\,\mu mol\,m^{-2}\,s^{-1}$). The peaks of the downward CO_2 flux appeared earlier than the peaks of the solar radiation on clear days (DOY 67, 69, 72). In such cases, the magnitude of the CO_2 flux increased rapidly in the morning, but decreased gradually in the afternoon. A similar variation in CO_2 flux was measured above a Brazilian rain forest (Grace et al., 1996).

We obtained data on stored CO_2 in the air layer under the flux-measurement height (CO_2 storage flux) for 3 days: 9, 11 and 12 March (DOY 67, 69 and 70, respectively). The units of the CO_2 storage flux were the same as those of CO_2 flux; positive and negative signs indicate the increase and the decrease of stored CO_2 in the air layer. Fig. 4 shows the diurnal variations of the CO_2 flux (F_c), the CO_2 storage flux ($F_{storage}$) on 9, 11 and 12 March. The diurnal variations in the net ecosystem exchange (NEE) evaluated as $F_c + F_{storage}$ are also shown in Fig. 4.

We can see $F_{storage}$ has the same order as F_c. In the morning, $F_{storage}$ started to decrease earlier than F_c. $F_{storage}$ then reached the negative peak in the early morning and increased before F_c reached its negative maximum. These variations mean that trees first consume CO_2 stored in the canopy air layer, and later, as the vertical gradient of CO_2 becomes large, CO_2 flux tends to be downward. After the canopy air layer is well mixed, the contribution of the storage becomes small, however, the low wind conditions in the morning raise the importance of the CO_2 stored in the canopy layer.

The NEE represents the net biotic CO_2 flux of the forest. The amount of the NEE was larger than that of the CO_2 flux during the low turbulence period from night to morning, especially in the morning when the storage flux dominated F_c. However, the NEE and F_c had almost the same values in the afternoon, because the changes of stored CO_2 in the underlying layer were small ($F_{storage}$ was small) in that period. We confirm that the measurements of CO_2 storage during the night and morning were particularly important, when we consider CO_2 uptake by a forest ecosystem.

Fig. 5 presents the response of NEE in the Pasoh forest to solar radiation obtained during the daytime on 9, 11 and 12 March. It is clearly shown that the amount of NEE increases as the incident solar radiation increases. However, when the solar radiation is $>800\,W\,m^{-2}$, the NEE seems to be saturated. All plots are distinguished according to the water vapor pressure deficit: VPD $\leq$ 16 h Pa or VPD $>$ 16 h Pa. Curves in the figure denote rectangular hyperbolas fitted to the plots. When the VPD was $\leq$16 h Pa, the magnitude of the NEE sharply increased under low light condition (about $<300\,W\,m^{-2}$) and saturated under high light condition. When the VPD was >16 h Pa, the magnitude

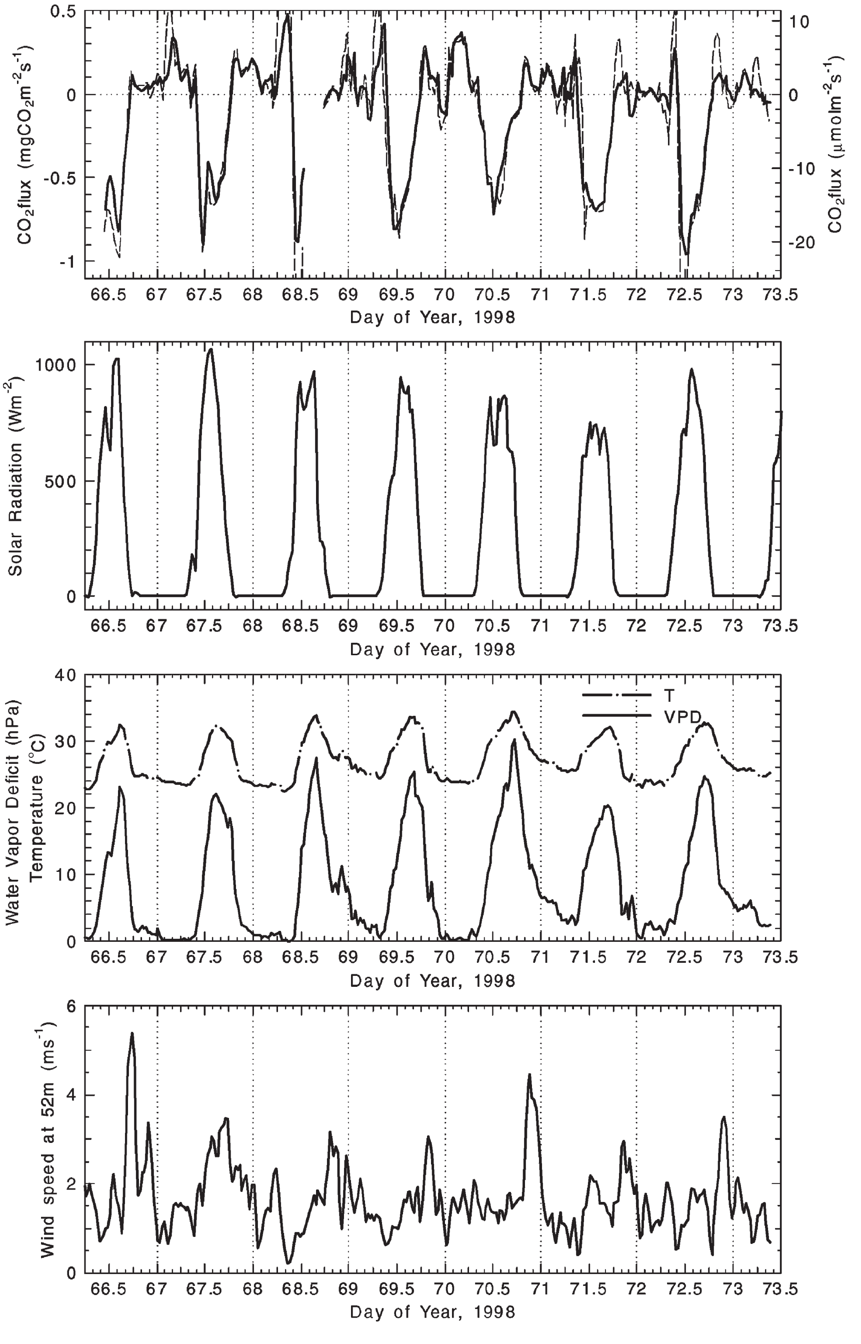

Fig. 3. Diurnal variations in CO_2 flux above the Pasoh forest, and half-hourly averaged meteorological data (solar radiation, air temperature, water vapor pressure deficit and wind speed) at 52 m height on 8–15 March (DOY 66–73). The broken line in the top figure indicates CO_2 flux calculated from the block-average removal (without linear detrending).

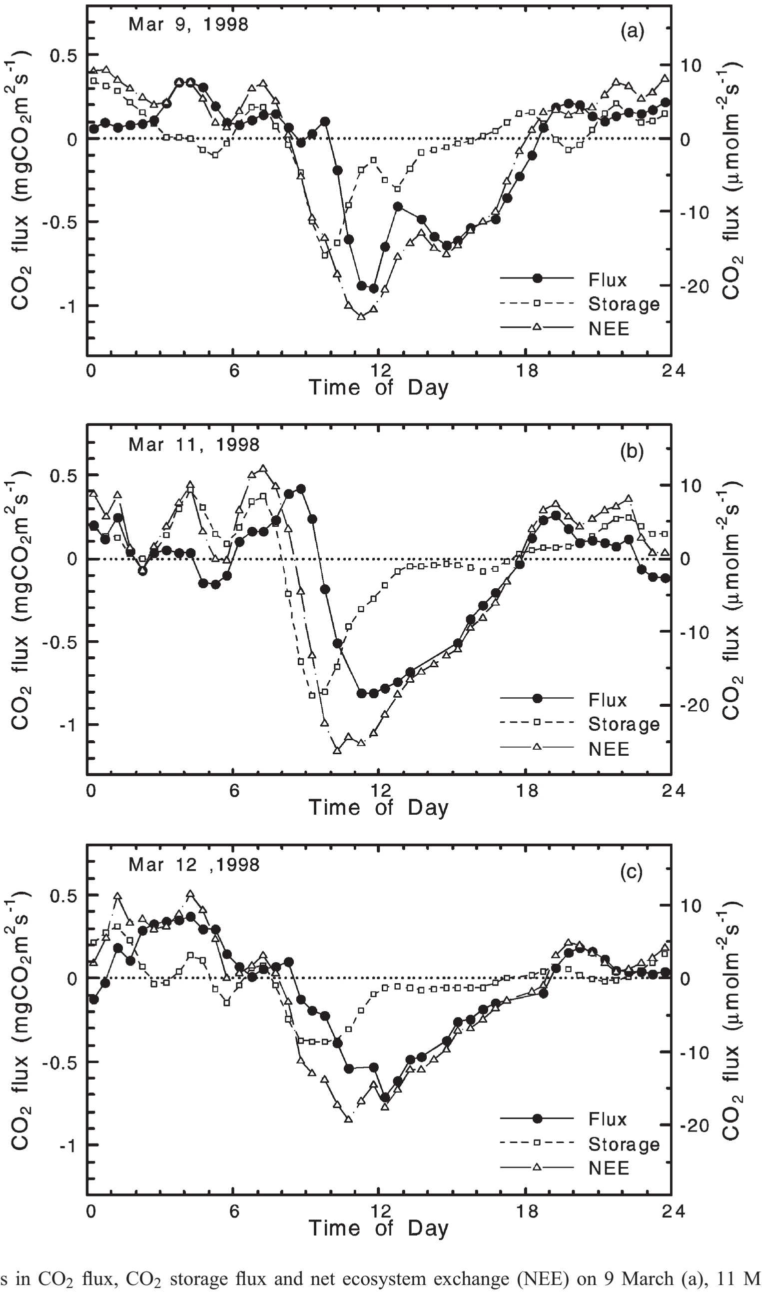

Fig. 4. Diurnal variations in CO_2 flux, CO_2 storage flux and net ecosystem exchange (NEE) on 9 March (a), 11 March (b), 12 March (c) in 1998.

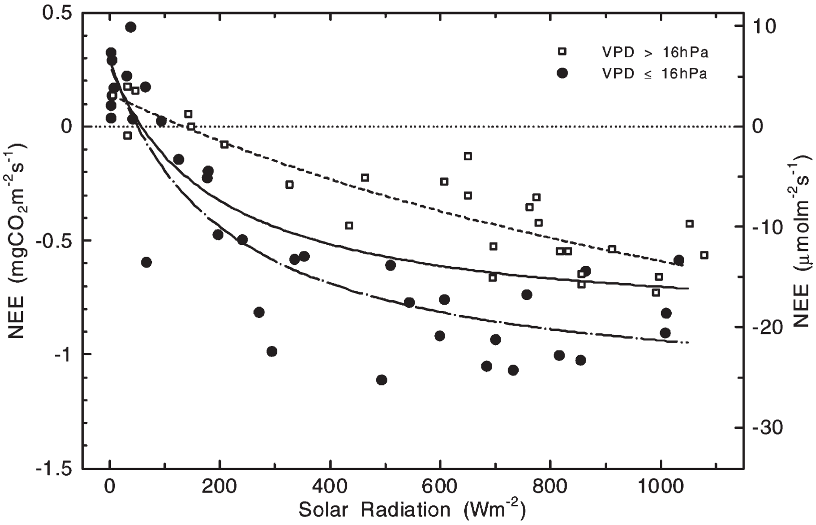

Fig. 5. Response of daytime NEE to solar radiation for 3 days (9, 11 and 12 March). The lines indicate the least squares fitting of rectangular hyperbolic function for different conditions of water vapor pressure deficit (VPD): broken line, VPD > 16 h Pa; dashed line, VPD ≤ 16 h Pa; solid line, total.

of the NEE was smaller than that for VPD ≤ 16 h Pa and was never saturated.

The mean daily value of NEE was $-2.44\,\mathrm{g\,C\,m^{-2}}$ per day. Fan et al. (1990) and Grace et al. (1996) evaluated the daily values of NEE in Amazonian tropical forests as about $-0.60\,\mathrm{g\,C\,m^{-2}}$ per day ($-0.05\,\mathrm{mol\,m^{-2}}$ per day) calculated from a short-term measurement and $-0.54\,\mathrm{g\,C\,m^{-2}}$ per day ($-0.045\,\mathrm{mol\,m^{-2}}$ per day) measured during a 44 day-observation. The daily NEE in the Pasoh forest is 4.1–4.5 times that in the Amazonian forest. Moreover, Grace et al. (1996) obtained daily NEE in the Amazonian forest in the dry season as $-1.08\,\mathrm{g\,C\,m^{-2}}$ per day ($-0.09\,\mathrm{mol\,m^{-2}}$ per day). Our measurements, which were taken on clear days in the dry season, were 2.3 times larger than the daily NEE in the Amazonian forest in the dry season. The daily NEE in this study were correspond to daily NEE of temperate deciduous forests in autumn (Greco and Baldocchi, 1996; Lee et al., 1999).

3.3. Discussion of the mass flow effect on daily NEE

Lee (1998) showed that NEE should be evaluated as the sum of CO_2 flux, CO_2 storage and vertical mass flow (vertical advective flow) arising from non-zero mean vertical wind velocity. Here, we try to calculate the mass flow component, following the procedure suggested by Lee (1998). In our calculation, the true mean vertical velocities were calculated with linear fitting of vertical wind velocity to horizontal wind velocity for every 1° interval in the wind direction. For the present short-term experiment, we made a linear fitting for each wind direction using the wind data in directions of ±20°, thereby increasing the number of data for each regression always larger than 20.

Table 1 shows daily values of CO_2 flux, CO_2 storage, NEE (flux + storage) and vertical mass flow for 3 days. The daily CO_2 flux values were negative for 3 days, while daily CO_2 storage values were negative for 2 days and slightly positive on 11 March. Therefore, the daily NEE values were negative for all days. The daily values of the mass flow component were positive for 3 days. The absolute values of the mass flow were 2.0–4.6 times larger than those of the NEE. Anthoni et al. (1999) and Baldocchi et al. (2000) showed that the amount of CO_2 released from an ecosystem was increased at night when the mass flow component was taken into account. However, according to their estimates, the daily value of mass flow component did not exceed that of the sum of daily CO_2 flux and daily

Table 1
Daily values of CO_2 flux, CO_2 storage, NEE and mass flow

Period	CO_2 flux	CO_2 storage	NEE	Mass flow
9 March	−2.14 (−0.178)	−0.36 (−0.030)	−2.50 (−0.208)	5.02 (0.418)
11 March	−2.73 (−0.228)	0.01 (8.3×10^{-4})	−2.74 (−0.228)	12.55 (1.046)
12 March	−1.51 (−0.126)	−0.57 (−0.048)	−2.08 (−0.173)	8.75 (0.729)
Three-day mean	−2.13 (−0.178)	−0.31 (−0.026)	−2.44 (−0.203)	8.77 (0.731)

Units are in $g\,C\,m^{-2}$ per day ($mol\,m^{-2}$ per day).

storage of CO_2. If the net ecosystem CO_2 uptake of the Pasoh forest is estimated as the total amount of three components (CO_2 flux, CO_2 storage and vertical mass flow), our results will indicate that this tropical forest functions as a CO_2 source.

There seems to be considerable errors in the estimation of the mass flow, since our values of the mass flow were too large, compared to other results. One of reasons for errors would be in the evaluation of the true vertical wind velocity from limited data set. Lee (1998) obtained the true mean vertical velocities from longer data sets (over 1.5 months). Our data set may be short for reliable estimations. Another error could arise from neglecting horizontal advection in Lee's method. Finnigan (1999) pointed out that horizontal advection cannot be neglected in most cases when we must bother with advective fluxes. Although the effect of horizontal advection might be large, we do not have a procedure for measuring it at a single-point observation. It is worth challenging to find how to evaluate effects of horizontal and vertical advections on NEE.

Acknowledgements

We thank the Forestry Department of Negeri Sembilan and the Director General of FRIM for granting us permission to work in the Pasoh Forest Reserve and Dr. K. Niiyama for providing his tree diameter data obtained in the forest reserve. The meteorological observations were carried out with the cooperation of the Hydorology Laboratory of FRIM. We would like to acknowledge the tremendous support received from Drs. Baharuddin Kasran, Zulkifli Yusop (present address: University of Technology Malaysia) and Azman Hassan, and the reseach assistants in the laboratory. This study was made as part of a joint research project between FRIM, UPM and NIES (Global Environmental Research Programme granted by the Japanese Environment Agency, Grant no. E-3).

References

Anthoni, P.M., Law, B.E., Unsworth, M.H., 1999. Carbon and water vapor exchange of an open-canopied ponderosa pine ecosystem. Agric. For. Meteorol. 95, 151–168.

Aoki, M., Yabuki, K., Koyama, H., 1975. Micrometeorology and assessment of primary production of a tropical rain forest in West Malaysia. J. Agric. Met. 31, 115–124.

Aubinet, M., Chermanne, B., Vandenhaute, M., Longdoz, B., Yernaux, M., Laitat, E., 2001. Long term carbon dioxide exchange above a mixed forest in the Belgian Ardennes. Agric. For. Meteorol. 108, 293–315.

Baldocchi, D.D., Vogel, C.A., Hall, B., 1997. Seasonal variation of carbon dioxide exchange rates above and below a boreal jack pine forest. Agric. For. Meteorol. 83, 147–170.

Baldocchi, D., Finnigan, J., Wilson, K., Paw U, K.T., Falge, E., 2000. On measuring net ecosystem carbon exchange over tall vegetation on complex terrain. Boundary-Layer Meteorol. 96, 257–291.

Fan, S.-M., Wofsy, S.C., Bakwin, P.S., Jacob, D.J., 1990. Atmosphere—biosphere exchange of CO_2 and O_3 in the Central Amazon forest. J. Geophys. Res. 95 (D10), 16851–16864.

Finnigan, J., 1999. A comment on the paper by Lee (1998): On micrometeorological observations of surface-air exchange over tall vegetation. Agric. For. Meteorol. 97, 55–64.

Gao, W., Shaw, R.H., Paw U, K.T., 1989. Observation of organized structure in turbulent flow within and above a forest canopy. Boundary-Layer Meteorol. 47, 349–377.

Grace, J., Lloyd, J., McIntyre, J., Miranda, A.C., Meir, P., Miranda, H.S., Nobre, C., Moncrieff, J., Massheder, J., Malhi, Y., Wright, I., Gash, J., 1995. Carbon dioxide uptake by an undisturbed tropical rain forest in southwest Amazonia, 1992–1993. Science 270, 778–780.

Grace, J., Malhi, Y., Lloyd, J., McIntyre, J., Miranda, A.C., Meir, P., Miranda, H.S., 1996. The use of eddy covariance to infer the net carbon dioxide uptake of Brazilian rain forest. Global Change Biol. 2, 209–218.

Greco, S., Baldocchi, D.D., 1996. Seasonal variations of CO_2 and water vapour exchange rates over a temperate deciduous forest. Global Change Biol. 2, 183–198.

Grelle, A., Lindroth, A., 1996. Eddy-correlation system for long-term monitoring of fluxes of heat, water vapour and CO_2. Global Change Biol. 2, 297–308.

Kato, R., Tadaki, Y., Ogawa, H., 1978. Plant biomass and growth increment studies in Pasoh forest. Malay. Nat. J. 30, 211–224.

Lee, X., 1998. On micrometeorological observations of surface-air exchange over tall vegetation. Agric. For. Meteorol. 91, 39–49.

Lee, X., Fuentes, J.D., Staebler, R.M., Neumann, H.H., 1999. Long-term observation of the atmospheric exchange of CO_2 with a temperate deciduous forest in southern Ontario, Canada. J. Geophys. Res. 104 (D13), 15975–15984.

Malhi, Y., Nobre, A.D., Grace, J., Kruijt, B., P, M.G., Culf, A., Scott, S., 1998. Carbon dioxide transfer over a Central Amazonian rain forest. J. Geophys. Res. 130 (D24), 31593–31612.

McMillen, R.T., 1988. An eddy correlation technique with extended applicability to non-simple terrain. Boundary-Layer Meteorol. 43, 231–245.

Manokaran, N., Kochummen, K.M., 1994. Tree growth in primary lowland and hill dipterocarp forests. J. Tropic. For. Sci. 6, 332–345.

Paw U, K.T., Brunet, Y., Collineau, S., Shaw, R.H., Maitani, T., Qiu, J., Hipps, L., 1992. On coherent structures in turbulence above and within agricultural plant canopies. Agric. For. Meteorol. 61, 55–68.

Soepadmo, E., 1978. Introduction to the Malaysian I.B.P. Synthesis Meetings. Malay. Nat. J. 30, 119–124.

Whittaker, R.H., Likens G.E., 1975. The biosphere and man. In: Lieth, H., Whittaker, R.H. (Eds.), Primary Productivity of the Biosphere. Springer, New York, pp. 305–328.

Wofsy, S.C., Goulden, M.L., Munger, J.W., Fan, S.M., Bakwin, P.S., Daube, B.C., Bassow, S.L., Bazzaz, F.A., 1993. Net exchange of CO_2 in a mid-latitude forest. Science 260, 1314–1317.

Phyton (Austria) Special issue: "APGC 2004"	**Vol. 45**	Fasc. 4	(61)-(6)	1.10.2005

Characteristics of the Gas Exchange of a Tropical Rain Forest in Peninsular Malaysia

By

S. TAKANASHI(1), Y. KOSUGI(1), M. TANI(1), N. MATSUO(1), T. MITANI(1) & A. R. NIK(2)

Key words: CO_2 flux, eddy covariance, tropical rain forest, Malaysia, energy budget.

Summary

TAKANASHI S., KOSUGI Y., TANI M., MATSUO N., MITANI T. & NIK A.R. 2004. Characteristics of the gas exchange of a tropical rain forest in Peninsular Malaysia. – Phyton 45 (4): (xx)-(xx).

Understanding the energy/H_2O/CO_2 exchange processes of tropical rain forests is very important for evaluating their roles in climate change. We measured sensible heat, latent heat, and CO_2 fluxes above a tropical rain forest in Peninsular Malaysia using the eddy covariance method for the year 2003. The average daily sensible and latent heat fluxes were 3.0 and 6.1 MJ, respectively. After considering the calculated heat storage terms, energy budget closure was estimated to be approximately 65%, even during the day. The average daily CO_2 flux was –2.1 g C m^{-2} in 2003. The average diurnal change of CO_2 flux ranged from –18.0 to 10.0 µmol m^{-2} s^{-1}, and no significant seasonal changes were observed. In the night time, CO_2 efflux measured using the eddy covariance method increased with friction velocity, suggesting an underestimation of ecosystem respiration under poor mixing conditions.

Introduction

Understanding the energy/H_2O/CO_2 exchange processes of tropical rain forests is very important for evaluating their roles in climate change. Ecosystems absorb carbon dioxide by photosynthesis and release it by autotrophic and heterotrophic respiration. The rates of photosynthesis and respiration constitute very large units in tropical rain forests; therefore, a high level of accuracy and a carefully thought out strategy at the experimental design stage are necessary in order to examine the balance of absorption and emission in terms of small differences in the

---

(1) Lab. of Forest Hydrology, Division of Environmental Science and Technology, Graduate School of Agriculture, Kyoto University. Kitashirakawa Oiwake-cho, Sakyo-ku, Kyoto 606-8502, Japan. Fax: +81-75-753-6088, e-mail: takanash@kais.kyoto-u.ac.jp

(2) Forest Research Institute Malaysia, Kepong, Kuala Lumpur 52109, Malaysia.

gross values of both. These rates vary diurnally and seasonally in response to interactions between the physical environment and physiological factors. A flux measurement above the forest canopy using a micro-meteorological method permits direct computation of gas exchange in the forest ecosystem and analysis of the characteristics at various time scales. Flux measurements using the eddy covariance method have been conducted for various vegetation types and ages (e.g., VALENTINI & al. 2000, BALDOCCHI & al. 2001). However, in Southeast Asia very few studies have been initiated for estimating net ecosystem exchange (NEE) from micro-meteorological observations, although net ecosystem production has been estimated from ecological studies at sites such as the Pasoh Forest Reserve (HOSHIZAKI & al. 1999, 2001). Only a short term observation of CO_2 flux was conducted in March 1998 at Pasoh (YASUDA & al. 2003). In order to describe and explain the temporal patterns of gas exchange in tropical rain forests there is a clear need for further data sets and analyses, especially with regard to long term CO_2 flux. In this paper, we present long term observations of sensible heat, latent heat, and CO_2 fluxes related to environmental factors, including solar radiation, air temperature, vapour pressure deficit, rainfall, and soil moisture, as well as their diurnal and seasonal changes for the year 2003.

Material and Methods

Site description

Observations were conducted at the Pasoh Forest Reserve near Simpang Pertang in Negeri Sembilan, about 140 km southeast of Kuala Lumpur, in Peninsular Malaysia (2°58'N, 102°18'E). The core area (600 ha) of the reserve is covered with a primary lowland mixed dipterocarp forest, which consists of various species of *Shorea* and *Dipterocarpus*. The continuous canopy height is approximately 35 m, although some emergent trees exceed 45 m. Based on empirical equations obtained for the Pasoh Forest Reserve by KATO & al. 1978, the leaf area index (LAI) estimated from tree diameter observations (Niiyama, unpublished) was 6.52.

Observations

Fluxes of sensible heat, water vapour, and carbon dioxide were measured at a height of 54 m on an observation tower. Wind velocity and temperature were observed with a three-axis sonic anemometer (SAT-550, Kaijo). Carbon dioxide concentration was monitored with an open path CO_2/H_2O analyzer (LI-7500, Licor). Data were sampled at 10 Hz and sent to a data logger (CR-5000, Campbell). Fluxes were calculated for the momentum, heat, H_2O, and CO_2 at an averaging time of 30 minutes. The wind field coordinates were rotated so that the mean vertical wind was zero. Spike and range over data were interpolated and counted. If the number of spikes or out-of-range data exceeded 1% of the total number of data points for each element, then the 30-minute flux data were considered to be invalid. The linear trends of temperature, water vapour, and CO_2 concentration were removed. We also corrected for the effect of air density fluctuation (WEBB & al. 1980).

Meteorological variables monitored at a height of 52 m on the tower included downward and upward ranges of short-wave radiation (MR22, Eko), ranges of long-wave radiation (PIR, Eppley), air temperature, humidity (HMP45A, Visala), wind velocity (AC750, Makino), and rainfall. Soil water content at depths of 10, 20, and 30 cm (CS515, Campbell), and soil heat flux at a depth of 2 cm (HFP01, HukuseFlux), were monitored at three points around the tower.

Results and Discussion

Daily mean values of meteorological variables and monthly mean diurnal changes in fluxes, air temperature, and vapour pressure deficit monitored at this site, for the year 2003, are shown in Fig. 1a. The mean air temperature (25.9 °C) and vapour pressure deficit (6.2 hPa) at 52 m showed little seasonal change. The absolute daily maximum air temperature was 33.9 °C on 5 March (day 64 day of the year 2003) and the absolute daily minimum air temperature was 20.8 °C on 25 October (day 298). Relatively cool air temperatures and low vapour pressure deficits in January-February and October-December coincided with a cloudy period. Annual rainfall in 2003 (1,896 mm) was larger than the four-year average (1,571 mm) from 1996 to 1999, including the El Niño event from 1997 to early 1998, but slightly larger than that of a normal year in FELDA Pasoh Dua (1,804 mm; TANI & al. 2003). Soil water content was comparatively constant throughout the year.

The average daily sensible and latent heat fluxes were 3.0 and 6.1 MJ m^{-2}, respectively. After considering the heat storage terms, calculated using an empirical equation for this study site (OHTANI & al. 1997), energy budget closure was estimated to be approximately 65%, even during the day. Non-closure of the energy budget is consistent with observations in many other forests, and the closure deficit of about 35% is larger than that of other tropical rain forest sites (e.g., KUMAGAI & al. 2004, DA ROCHA & al. 2004). Various causes may have influenced this result, but recent studies (LEE 1998, WATANABE & KANDA 2002) have shown that such an imbalance may inevitably occur owing to mass flow, even when the measurement includes the minimum errors, and the data represent the spatially averaged fluxes. Further analyses (e.g., mass flow rate, horizontal advection) are needed, therefore, to solve this problem. The evapotranspiration rate was directly calculated at 2.50 mm day^{-1} using an eddy covariance latent heat flux. If the Bowen ratio calculated by eddy covariance was correct, and the closure deficits were divided into sensible and latent heat fluxes by the Bowen ratio, then the evapotranspiration rate was recalculated as 3.04 mm day^{-1}. This value is similar to those reported in other tropical rain forests (3.45 mm day^{-1}, SHUTTLEWORTH & al. 1984; 3.45 mm day^{-1}, DA ROCHA & al. 2004; 2.86-3.48 mm day^{-1}, KUMAGAI & al. 2004).

The average diurnal changes in CO_2 flux ranged from –18.0 to 10.0 μmol m^{-2} s^{-1}, and did not show clear seasonal changes corresponding to soil moisture and air temperature conditions (Fig. 1b). Under relatively cool and wet conditions in January-February and October-December, no significant changes in CO_2 fluxes were observed. These diurnal changes are similar to those reported for other tropical forests (GRACE & al. 1996, GOULDEN & al. 2004). The average daily eddy covariance CO_2 flux was –2.1 g C m^{-2} in 2003. This value was larger than the value of NEE reported in other tropical forests (–0.60 g C m^{-2}, FAN & al. 1990; –0.95 g C m^{-2}, GRACE & al. 1996; –1.5 g C m^{-2}, GOULDEN & al. 2004), but similar to NEE obtained from short term observations at this forest (–2.4 g C m^{-2}, YASUDA & al. 2003). In the night time, CO_2 efflux measured using the eddy covariance method increased with friction velocity rise, suggesting an underestimation of ecosystem respiration under poor mixing conditions (Fig. 2). Uncertainties in CO_2 fluxes under poor mixing conditions influence the absolute accuracy. Taking energy imbalance into account, accuracy would be influenced by vertical mass flow rates and/or horizontal advection terms, even under good mixing conditions. Therefore, the absolute value of daily net CO_2 exchange should be precisely analyzed and corrected by cross-checking other techniques, including process-based models, chamber CO_2 flux observations of all components of the forest, and both biomass and necromass increment observations.

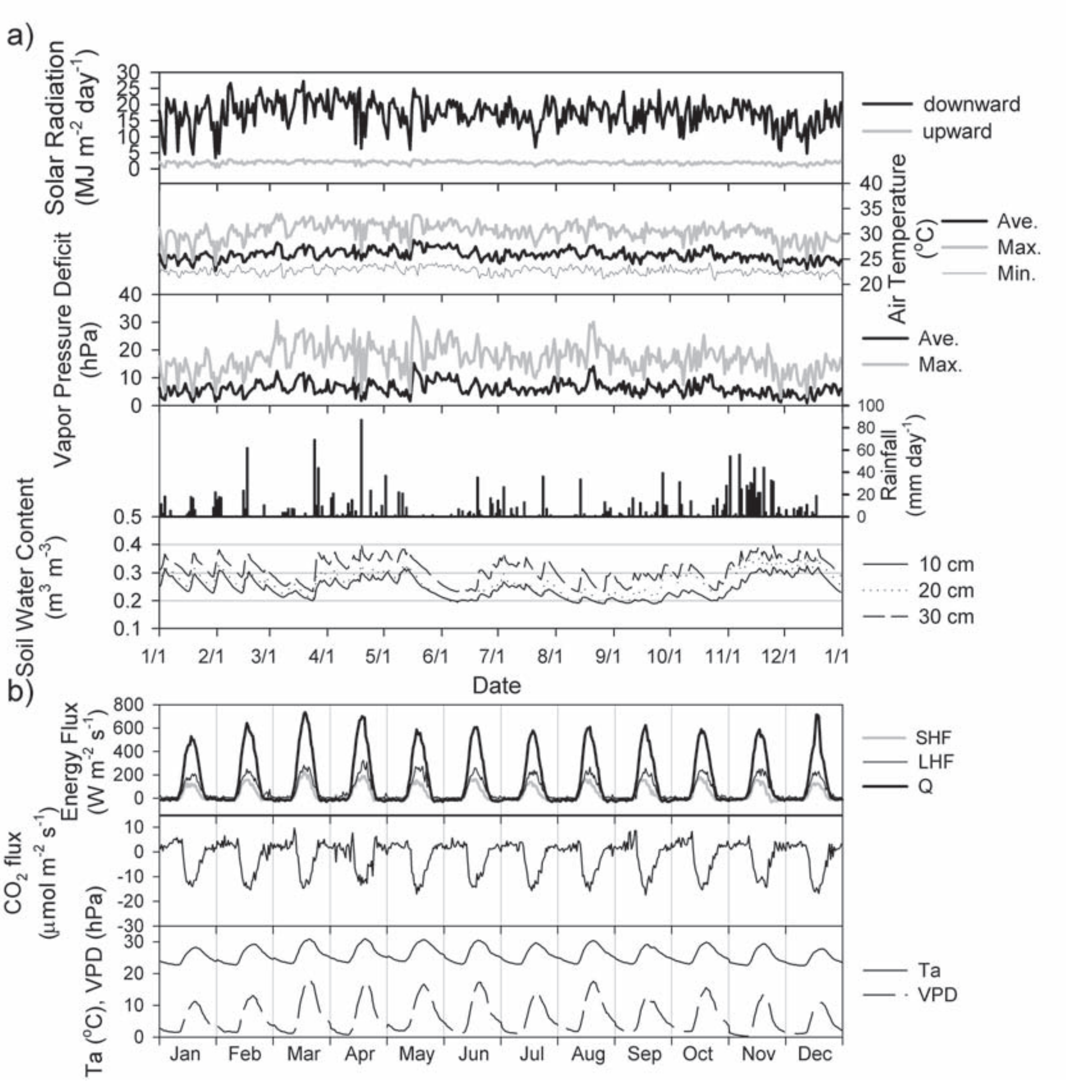

Fig. 1. Seasonal fluctuations in the daily total downward and upward solar radiation, daily average, maximum, and minimum air temperatures, daily average and maximum vapour pressure deficits, daily total rainfall, and volumetric soil water content at depth of 10, 20, and 30 cm (a). Seasonal changes in average diurnal course of the available energy (Q), sensible and latent heat fluxes (SHF, LHF), eddy covariance CO_2 flux, air temperature (Ta), and vapour pressure deficit (VPD) at 52 m (b).

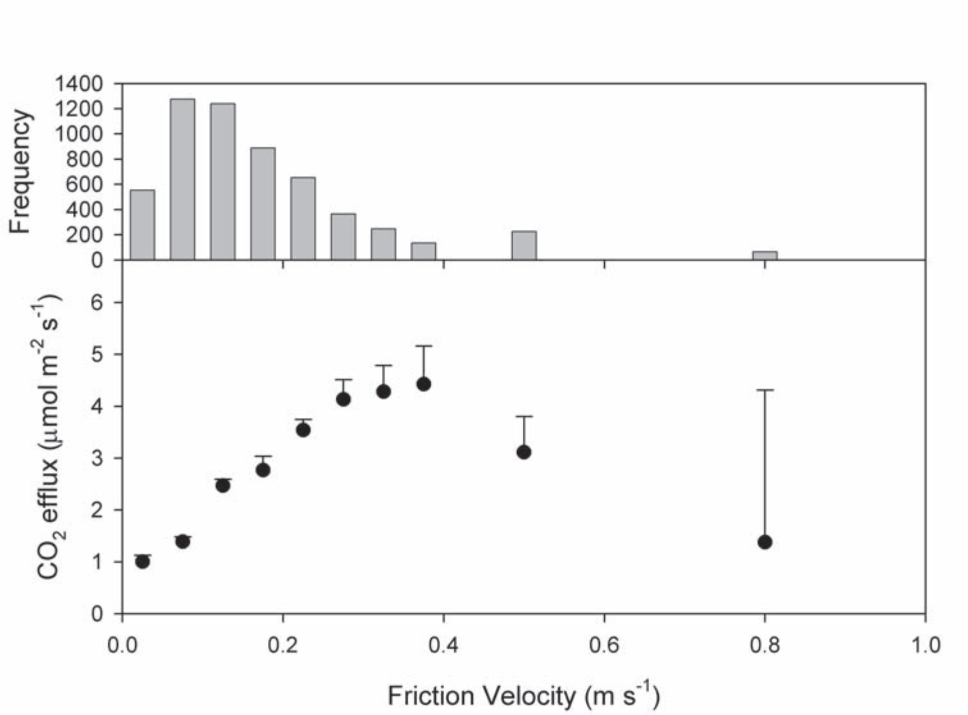

Fig. 2. Relationship between friction velocity and nighttime CO$_2$ efflux, with the frequency of each friction velocity (u_*) class (class 1-8, in the range of 0.05 m s^{-1} $u_*<0.4$ m s^{-1}; class 9, $0.4\leq u_*<0.6$ m s^{-1}; class 10, $0.6\leq u_*<1.0$ m s^{-1}). The circles represent the average eddy covariance data in each friction velocity class, and the error bars represent standard error.

Acknowledgements

We thank the Forestry Department of Negeri Sembilan and the Director General of FRIM for giving us permission to work in the Pasoh Forest Reserve. The staff of the Hydrology Unit and the Pasoh Station of FRIM are gratefully acknowledged for collecting data.

References

BALDOCCHI D., FALGE E., GU L., OLSON R., HOLLINGER D., RUNNING S., ANTHONI P., BERNHOFER C., DAVIS K., EVANS R., FUENTES J., GOLDSTEIN A., KATUL G., LAW B., LEE X., MALHI Y., MEYERS T., MUNGER W., OECHEL W., PAW U K. T., PILEGAARD K., SCHMID H. P., VALENTINI R., VERMA S., VESALA T., WILSON K. & WOFSY S. 2001. FLUXNET: A new tool to study the temporal and spatial variability of ecosystem-scale carbon dioxide, water vapor, and energy flux densities. - Bulletin of the American Meteorological Society 82: 2415-2434.

DA ROCHA H. R., GOULDEN M. L., MILLER S. D., MENTON M. C., PINTO L. D. V. O., DE FREITAS H. C. & E SILVA FIGUEIRA A. M. 2004. Seasonality of water and heat fluxes over a tropical forest in eastern Amazonia. - Ecological Applications 14: 22-32.

FAN S. -M., WOFSY S. C., BAKWIN P. S. & JACOB D. J. 1990. Atmosphere—biosphere exchange of CO$_2$ and O$_3$ in the Central Amazon forest. - Journal of Geophysical Research 95(D10): 16851-16864.

GOULDEN M. L., MILLER S. D., DA ROCHA H. R., MENTON M. C., DE FREITAS H. C., E SILVA FIGUEIRA A. M. & DIAS DE SOUSA C. A. 2004. Diel and seasonal patterns of tropical forest CO_2 exchange. - Ecological Applications 14: 42-54.

GRACE J., MALHI Y., LLOYD J., MCINTYRE J., MIRANDA A. C., MEIR P. & MIRANDA H. S. 1996. The use of eddy covariance to infer the net carbon dioxide uptake of Brazilian rain forest. - Global Change Biology 2: 209-217.

HOSHIZAKI K., ADACHI M., ADACHI N., BEKKU-SAKATA Y., KOIZUMI H., NIIYAMA K., OKUDA T., YAMASHITA T., NUR SUPARDI N. & QUAH E. S. 2001. Trials for construction of carbon-cycling compartment models in a tropical rainforest, Pasoh Forest Reserve. - Research report of the NIES/FRIM/UPM Joint Research Project 2001: 127-146.

— , NIIYAMA K., KIMURA K., YAMASHITA T., BEKKU Y., OKUDA T., TAKEDA H., TANG Y., NUR SUPARDI N., QUAH E. S. & ADACHI N. 1999. Recent biomass change in a tropical primary forest in Pasoh: current status for evaluating carbon-sequestering function. - Research report of the NIES/FRIM/UPM Joint Research Project 1999: 2-17.

KATO R., TADAKI Y. & HUSATO O. 1978. Plant biomass and growth increment studies in Pasoh Forest. - Malayan Nature Journal 30: 211-245.

KUMAGAI T., SAITOH T. M., SATO Y., MOROOKA T., MANFROI O. J., KURAJI K. & SUZUKI M. 2004. Transpiration, canopy conductance and the decoupling coefficient of a lowland mixed dipterocarp forest in Sarawak, Borneo: dry spell effects. - Journal of Hydrology 287: 237-251.

LEE X. 1998. On micrometeorological observations of surface-air exchange over tall vegetation. - Agricultural and Forest Meteorology 91: 39-49.

OHTANI Y., OKANO M., TANI M., YAMANOI K., WATANABE T., YASUDA Y. & NIK A. R. 1997. Energy and CO_2 fluxes above a tropical rain forest in Peninsular Malaysia. - Journal of Agricultural Meteorology 52: 453-456.

SHUTTLEWORTH W. J., GASH J. H. C., LLOYD C. R., MOORE C. J. & ROBERTS J. 1984. Eddy correlation measurements of energy partition for Amazonian forest. - Quart. J. R. Met. Soc. 110: 1143-1162.

TANI M., ABDUL RAHIM N., MOHD MD S., NOGUCHI S. & OHTANI Y. 2003. Five-year meteorological observation at Pasoh Forest Reserve, Negeri Sembilan, Peninsular Malaysia. - Forest Research Institute Malaysia Reports 78: .

VALENTINI R., MATTEUCCI G., DOLMAN A. J., SCHULZE E.-D., REBMANN C., MOORS E. J., GRANIER A., GROSS P., JENSEN N. O., PILEGAARD K., LINDROTH A., GRELLE A., BERNHOFER C., GRÜNWALD T., AUBINET M., CEULEMANS R., KOWALSKI A. S., VESALA T., RANNIK Ü., BERBIGIER P., LOUSTAU D., GUÐMUNDSSON J., THORGEIRSSON H., IBROM A., MORGENSTERN K., CLEMENT R., MONCRIEFF J., MONTAGNANI L., MINERBI S. & JARVIS P. G. 2000. Respiration as the main determinant of carbon balance in European forests. - Nature 404: 861-865.

WATANABE T. & KANDA M. 2002. LES study on the energy imbalance problem with eddy covariance fluxes. II: Analysis for a neutrally stratified surface boundary layer above and within a homogeneous plant canopy. – Journal of Japan Society of Hydrology & Water Resources 15: 253-263. (in Japanese with English abstract)

WEBB E. K., PEARMAN G. I. & LEUNING R. 1980. Correction of flux measurements for density effects due to heat and water vapour transfer. - Quarterly Journal of the Royal Meteorological Society 106: 85-100.

YASUDA Y., OHTANI Y., WATANABE T., OKANO M., YOKOTA T., LIANG N., TANG Y., ABDUL RAHIM N., TANI M. & OKUDA T. 2003. Measurement of CO_2 flux above a tropical rain forest at Pasoh in Peninsular Malaysia. - Agricultural and Forest Meteorology 114: 235-244.

AGRICULTURAL AND FOREST METEOROLOGY 148 (2008) 439–452

available at www.sciencedirect.com

ScienceDirect

journal homepage: www.elsevier.com/locate/agrformet

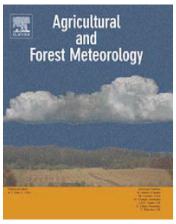

CO_2 exchange of a tropical rainforest at Pasoh in Peninsular Malaysia

Yoshiko Kosugi [a,*], *Satoru Takanashi* [b], *Shinjiro Ohkubo* [a], *Naoko Matsuo* [c], *Makoto Tani* [a], *Tomonori Mitani* [d], *Daizo Tsutsumi* [e], *Abdul Rahim Nik* [f]

[a] *Laboratory of Forest Hydrology, Division of Environmental Science and Technology, Graduate School of Agriculture, Kyoto University, Kyoto 606-8502, Japan*
[b] *Forestry and Forest Products Research Institute, Tsukuba, Ibaraki 305-8687, Japan*
[c] *Faculty of Bioresources, Mie University, Tsu, Mie 514-8507, Japan*
[d] *Forestry Agency Japan, Tokyo 100-8952, Japan*
[e] *Disaster Prevention Research Institute, Kyoto University, Kyoto 611-0011, Japan*
[f] *Forest Research Institute Malaysia, Kepong, Kuala Lumpur 52109, Malaysia*

ARTICLE INFO

Article history:
Received 14 February 2007
Received in revised form
3 October 2007
Accepted 5 October 2007

Keywords:
CO_2 exchange
Tropical rainforest
Southeast Asia
Eddy covariance
Soil respiration

ABSTRACT

The eddy covariance method was used to observe carbon dioxide flux (F_c) for 3 years over an old-growth tropical rainforest at Pasoh in Peninsular Malaysia. The average nighttime F_c and NEE were 3.6 and 4.7 μmol m^{-2} s^{-1}, respectively, when friction velocity (u_*) $\geq$ 0.2, while the average soil respiration rate measured occasionally with the chamber method was estimated to be 4.1 μmol m^{-2} s^{-1} if we used the relationship between volumetric soil water content, or 3.8 μmol m^{-2} s^{-1} if we used the pure average of nine observations. The comparison of F_c, NEE and soil respiration strongly suggests that nighttime CO_2 efflux was underestimated even when the CO_2 storage term is considered. The correction of F_c data for low u_* did not correct this underestimate, and it was strongly suggested that this forest was not a strong carbon sink, as raw F_c data, even with the u_* filtering, implied. Monthly average daytime diurnal changes in CO_2 exchange over the canopy were fairly constant from 2003 to 2005 despite fluctuations in soil moisture, solar radiation, air temperature and vapor pressure deficit between dry and wet periods. An obvious inhibition of canopy CO_2 exchange in the afternoon coupling with increases in VPD and air temperature was observed year-round. In the case of nighttime NEE, a slight increase in wet period was observed. Diurnal pattern of CO_2 exchange revealed that obvious restriction of canopy photosynthesis in the afternoon was occurred in this forest irrespective of soil moisture. Seasonal and annual patterns of CO_2 exchange reveal that one of the main causes which induce the difference in NEE pattern between Amazonian and Southeast Asian rainforests was not the difference in daytime photosynthesis but the difference in ecosystem respiration related with dry and rainy seasons. The decrease of CO_2 uptake (increase of NEE) at wet period was also observed at this site, but did not form an obvious seasonality such as in Amazonian forests.

---

[*] *Corresponding author*. Tel.: +81 75 753 6089; fax: +81 75 753 6088.
E-mail address: ykosugi@kais.kyoto-u.ac.jp (Y. Kosugi).

0168-1923/$ – see front matter © 2007 Elsevier B.V. All rights reserved.
doi:10.1016/j.agrformet.2007.10.007

1. Introduction

The tropical rainforest plays a major role in the global carbon budget because of absorption and emission of CO_2 through photosynthesis, respiration and decomposition associated with its large biomass (Malhi et al., 1999; Malhi and Grace, 2000). Clarification of the nature and magnitude of diurnal, seasonal and annual CO_2 exchanges in tropical rainforests and what controls the exchanges at different timescales is a primary issue for understanding the role of these exchanges on the global carbon budget. Unfortunately, flux measurements that use eddy covariance methods in the tropical rainforest are sparse compared to studies on other vegetation types (e.g. Valentini et al., 2000; Baldocchi et al., 2001). Recent studies have reported on long-term flux observations at several sites in the Amazonian rainforest (Malhi et al., 1998, 2002; Araujo et al., 2002; Saleska et al., 2003; Chambers et al., 2004; Goulden et al., 2004; Kruijt et al., 2004; Miller et al., 2004; da Rocha et al., 2004). Few studies, however, have estimated net ecosystem exchange (NEE) from tower observations in Southeast Asian tropical rainforest. Eddy covariance CO_2/H_2O gas exchange data covering up to 1 year has been reported only at two sites: Lambir on Borneo in Malaysia (Kumagai et al., 2004a,b,c, 2005, 2006) and Pasoh in Peninsular Malaysia (the site of the present study; Yasuda et al., 2003; Takanashi et al., 2005). Further data sets and analyses, especially with regard to long-term CO_2 flux, are clearly warranted to describe and explain gas exchange in tropical rainforests.

Eddy covariance measurements coupled with micrometeorological data allow a detailed analysis of the factors controlling gas exchanges. However, net ecosystem CO_2 exchange measurements are unreliable when turbulence is weak, for example, as at night (Goulden et al., 1996; Lavigne et al., 1997; Law et al., 1999; Baldocchi and Bowling, 2003). Uncertainties in the nighttime flux and thus in the annual carbon budget might be especially severe for tropical forests with large sinks and sources year-round and frequent calm atmospheric conditions. Measurements derived using the chamber method can describe nocturnal CO_2 exchange by using techniques to extrapolate the measurements to entire ecosystems (Anthoni et al., 1999). It is, however, very difficult to evaluate variations at larger temporal and spatial scales with enough accuracy to permit a comparison with data from spatially integrated eddy covariance techniques (Drewitt et al., 2002). Nevertheless, a comparison of ecosystem respiration using data from both methods will yield insights into uncertainties in nighttime flux measurements and the computed annual carbon budget in tropical rainforests (Chambers et al., 2004) and at other sites with other vegetation types (Goulden et al., 1996; Lavigne et al., 1997; Law et al., 1999, 2001; Bolstad et al., 2004; Ohkubo et al., 2007).

Major environmental differences exist between Amazonian and Southeast Asian rainforests with respect to factors determining the nature and magnitude of diurnal, seasonal and annual CO_2 exchanges. For example, the patterns of rainfall are different. Most sites in the Amazon rainforests have distinct dry and wet seasons during the year and the affect of drought stress on CO_2 exchange and the carbon budget is an important issue in this region (e.g. Asner et al., 2004). In contrast, Southeast Asian rainforests such as Lambir and Pasoh do not experience distinct dry and wet seasons during the year although dry and wet periods do exist as part of the seasonal fluctuation with considerable variability between years (Tani et al., 2003; Kumagai et al., 2005). Goulden et al. (2004) described results from their 1-year eddy covariance data set at Tapajós and showed that NEE decreased during the dry season because soil respiration decreased. They also showed no obvious influence of drought stress on daytime net canopy photosynthesis, probably because of deep rooting systems. It is unknown if these results are equally valid for Southeast Asian rainforests. Further study is warranted to investigate issues related to CO_2 exchange in tropical rainforests, especially for inter comparisons of the nature, magnitude and controls of diurnal, seasonal and annual CO_2 exchanges over Amazon and Southeast Asian rainforests.

This paper considers 3 years of eddy covariance CO_2 flux data coupled with occasional measurements of soil respiration derived using the chamber method at a primary tropical rainforest in the Pasoh Forest Reserve on Peninsular Malaysia, Southeast Asia. This paper will assess the uncertainty of nighttime fluxes and the annual carbon budget at this site by comparing nighttime CO_2 flux at the canopy, net CO_2 exchange of the forest including the CO_2 storage term and chamber measurements of soil respiration. The paper will describe the nature and magnitude of diurnal, seasonal and annual CO_2 exchanges and analyze factors, including drought stress, that determine the exchanges.

2. Methods

2.1. Site

Observations were conducted in the Pasoh Forest Reserve of the Forest Research Institute Malaysia (FRIM), located near Simpang Pertang in Negeri Sembilan, on Peninsular Malaysia (2°58′N, 102°18′E, 75–150 m a.s.l.). The core area (600 ha) of the reserve (2450 ha) is covered with primary lowland mixed dipterocarp forest (tropical evergreen broad-leaved forest) that includes various species of *Shorea* and *Dipterocarpus*. The continuous canopy height is approximately 35 m, but some emergent trees exceed 45 m. Empirical equations obtained for the Pasoh Forest Reserve by Kato et al. (1978) yielded leaf area index (LAI) estimates of 6.52 from tree diameter observations (Niiyama, unpublished data). The core area is buffered by a secondary forest (650 ha) and primary hill dipterocarp forest (1000 ha) (Soepadmo, 1978; Manokaran and Kochummern, 1992). Yamashita et al. (2003) described the soil characteristics of the area in detail. Soil type around the tower is Haplic Acrisol according to FAO classifications. The A horizon is thin (0–5 cm). Lateritic gravels are abundant below 30 cm (Soepadmo, 1978; Yamashita et al., 2003). The core area of the forest reserve includes plot 1, a 2-ha plot used extensively to study primary productivity of the tropical rainforest by the International Biological Programme (IBP) (Kato et al., 1978). Biometric observations have been carried out continuously also in a 6-ha plot that extends plot 1, and a 50-ha plot (e.g., Niiyama et al., 2003; Hoshizaki et al., 2004). The area has gently undulating topography. The flux observation tower sits in the 6-ha plot.

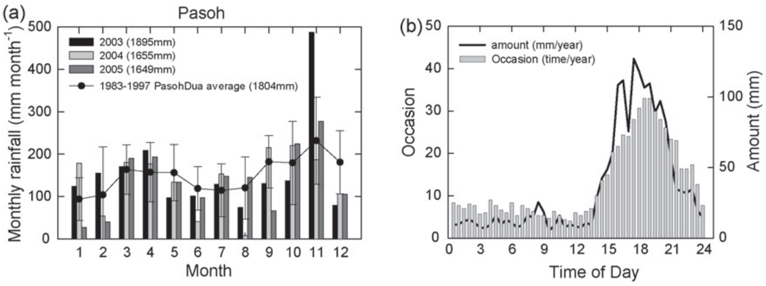

Fig. 1 – (a) Monthly rainfall at the site in 2003, 2004, 2005 and the average value between 1983 and 1997, and (b) diurnal pattern of rainfall at the site in 2003, 2004, and 2005.

Mean annual rainfall is 1804 mm (1983–1997; Tani et al., 2003), a total less than in other regions of Peninsular Malaysia (Noguchi et al., 2003). In comparison, the Lambir site on Borneo has an annual rainfall of 2734 mm (1968–2001) (Kumagai et al., 2005). Rainfall totals show peaks from March to May and from October to December (Fig. 1a). Rainfall is also characterized by its short duration (mean = 3.8 h) and relatively high intensity (mean storm intensity = 7.8 mm h^{-1}) (Noguchi et al., 2003). A distinct diurnal cycle exists in rainfall (Fig. 1b).

2.2. *Observations*

Meteorological variables monitored at a height of 52 m on the tower included downward and upward shortwave radiation (measured using MR22, Eko, Japan), longwave radiation (PIR, Eppley, USA), air temperature, humidity (HMP45A, HMP45C, Vaisala, Finland), wind velocity (AC750, Makino, Japan) and rainfall. Soil water content at depths of 0.1, 0.2 and 0.3 m (CS515, Campbell Scientific, USA), soil heat flux (HFP01, Hukseflux Thermal Sensors B.V., Netherlands) and soil temperature (thermocouple model 107, Campbell Scientific) at a depth of 0.02 m were monitored at three points around the tower. Rainfall was measured by tipping bucket rain gauges (Ota Keiki 34-T, Japan) at the top of the 52-m tower and at an observatory located 430 m away from the tower. These data were compared with the storage rain measured at the observatory and corrected. The Vaisala sensor was calibrated periodically using an Assmann psychrometer (SY-3D, Yoshino Keiki, Japan). In addition, vertical profiles of CO_2 concentration, air temperature and humidity were also derived from measurements at several heights on the same tower to assess fluxes of sensible and latent heat and CO_2 storage (S_c, μmol m^{-2} s^{-1}). Air samples for CO_2 measurement were drawn continuously at a flow rate of 2000 ml min^{-1} through a 4-mm internal diameter polyethylene tube at each inlet from ten levels (0.2, 0.5, 1, 2, 5, 10, 20, 30, 45, and 53 m) by an IRGA (LI-7000, Li-Cor, Inc., USA). The IRGA was located in an observation house on the forest floor. The profile system sampled cycling through the entire profile every 5 min. At each height, sufficient time was allowed to flush the tubing of residual air before sampling with the IRGA. The IRGA was automatically calibrated daily using zero concentration gas (N_2). The CO_2 profile was measured intermittently from September 2004 to November 2005. The profile data available for calculating the storage terms were limited by an occasional system breakdown or trouble with any of the sensors, mainly caused by lightning.

Fluxes of sensible heat, water vapor and carbon dioxide were measured at a height of 54 m on the observation tower. Wind velocity and temperature were observed with a three-axis sonic anemometer (SAT-550, Kaijo, Japan). We tested that this sonic anemometer showed an enough accuracy comparing *in situ* with a higher-class instrument (DAT660, Kaijyo, Japan). Carbon dioxide concentration was monitored with an open path CO_2/H_2O analyzer (LI-7500, Li-Cor, Inc., USA). The LI-7500 was mounted at an angle so that water drops could not sit on the sensor lens, and the radiation effect would be minimized. No smearing was used for the sensor lens. Data were sampled at 10 Hz and sent to a data logger (CR-5000, Campbell Scientific). A solar power system drove the flux and meteorological observation system. However, the profile measurement of CO_2 concentration was operated with a commercial power supply that was installed at this site in December 2003. Raw data recorded to the memory card were transferred every 10 days to the laboratory. Fluxes of momentum, heat (H, W m^{-2}), H_2O (λE, W m^{-2}) and CO_2 (F_c, μmol m^{-2} s^{-1}) were calculated with an averaging time of 30 min. The manufacturer's recommended correction for time lag in the LI-7500 was included in the open-path system. A three-dimensional coordinate rotation for the vertical wind velocity normal to the mean wind direction (double rotation; McMillen, 1988) was applied assuming a zero mean vertical wind. Spike and range over data were interpolated and counted. If the number of spikes or out-of-range data exceeded 1% of the total number of data points for each element, then the 30-min flux data samples were considered to be invalid. A Webb, Pearman and Leuning (WPL) correction for the effect of air density fluctuations (Webb et al., 1980) was applied. Linear trends in temperature, water vapor and CO_2 concentration were not removed. Linear detrending might cause underestimates of low-frequency flux, which is supposed to be large for tall tropical forests with low wind speeds, low turbulent intensity and thus large eddies that can transport flux. The influence of linear detrending can also be assessed by considering the annual integration of CO_2 exchange. The comparison of averaging time of 1 h and 30-min showed that the contribution of larger scale component was approximately 2.0% (n = 12,094, median, 1-h F_c data were compared with the average of 30-min F_c for an hour, data from 2002 to 2005). We did not install the closed path system at this site for the comparison with open path system, mainly because of the difficulty of introducing the closed path system at this site, although we intensively compared these two methods in our other domestic sites (Kosugi et al., 2005, 2007a).

Fluxes have been observed since September 2002 and this paper considers approximately 3 years of data through December 2005. In 2004 and 2005, severe instrument damage due to lightning strikes occurred, and all flux data were missing from 5 June to 20 November 2004 and from 24 March to 7 May 2005. Thresholds were set for CO_2 flux ($-50 < F_c < 50$, $\mu mol\ m^{-2}\ s^{-1}$), sensible head flux ($-400 < H < 1000$, $W\ m^{-2}$) and latent head flux ($-400 < \lambda E < 1000$, $W\ m^{-2}$). Data coverage for CO_2 flux was 22.4% (2002), 84.3% (2003), 48.7% (2004) and 76.4% (2005).

Soil respiration rates observed using the chamber method were applied to estimate the annual amount and seasonal trend of soil respiration with a scale that was comparable to eddy covariance measurements. A 50-m × 50-m plot was established north of the tower within the 6-ha plot established for long-term ecological research (Fig. 2). Within this plot, measurements were made at 36 points on a 10-m grid. Fine surface litter was included in the chamber. Measurements were conducted nine times including dry, transient and wet periods from September 2002 to October 2005. Soil respiration rate was measured using an infrared gas analyzer (LI-6262 or LI-820, Li-Cor, Inc., USA) equipped with a closed dynamic chamber made of PVC. Details of the soil respiration measurement and its spatial and temporal distribution were reported by Kosugi et al. (2007b).

2.3. *Gap filling policy*

The net CO_2 exchange of the forest (NEE) can be assessed by adding the CO_2 storage flux to F_c measured at the top of canopy. One of the most common gap filling method which is widely used is perhaps to fill the daytime gap with monthly light-curve and to fill the nighttime gap with temperature dependence curve with u_* filter, after adding the CO_2 storage flux to F_c. Although, periods of CO_2 storage flux data are limited compared to F_c data, mainly because of power supply limitation, though CO_2 storage flux contributed greatly to NEE in this forest (Yasuda et al., 2003). Besides, daytime CO_2 absorption in our site has severe decline in the afternoon (see Figs. 7 and 10) and light curve interpolation will induce serious errors. Nighttime CO_2 emission in our site did not depend on temperature but rather depended on soil water content (see Fig. 6). So we avoided this most common gap filling method, which would induce a serious bias in our data and also make our analysis on CO_2 exchange meaningless.

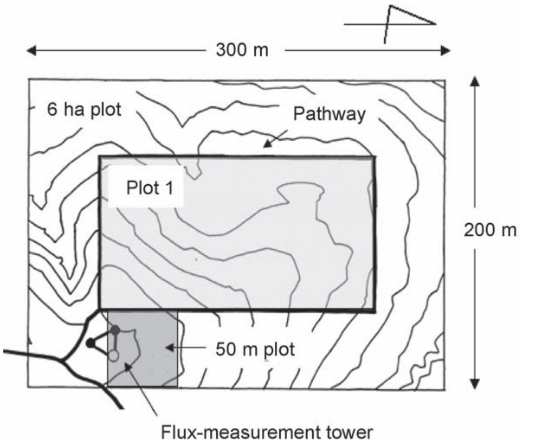

Fig. 2 – Map of the tower site, soil respiration plot and two biometric observation plots (plot 1 of the IBP, Kato et al., 1978; 6 ha-plot, Niiyama et al., 2003). The triangle is a tower-bridge system including a flux-measurement tower (white dot) and other two towers (black dots). The contour interval is 1 m.

The F_c shown in Fig. 3, F_c, S_c and NEE in Fig. 5, F_c and NEE in Fig. 6, and NEE shown with black dots in Fig. 7 are completely composed of observed data. The interpolation of missing data was done in the following two datasets in our study.

(1) Monthly averaged diurnal course (Figs. 9 and 10 use this data);
(2) cumulative NEE and annual estimation (Figs. 7 and 8 and Table 1 deal on this data).

In the case of (1), we averaged every available 30-min data for each month. So the gaps were filled with the average value of all available 30-min data at each time in a day for each month. For the preparation of monthly averaged diurnal course of NEE for each month (Fig. 9), we used the monthly averaged diurnal course of F_c and added the average diurnal course of storage flux using all available storage data. Our artifice is based on the result of storage flux, which revealed if we averaged the storage data for a month, diurnal change of storage flux became almost same as the average diurnal change using all available storage data. The monthly average diurnal course of F_c and NEE (adding whole-period average diurnal course of S_c to monthly average diurnal course of F_c) will be thus marginally competent for the monthly scale analyses of factors determining the nature and magnitude of diurnal, seasonal and annual CO_2 exchanges. No correction of nighttime data was done in this dataset.

In the case of (2), we tested the pure average and average diurnal course to fill the daytime and nighttime gap to evaluate line (2) in Fig. 8, and confirmed that the difference between these two gap-filling methods was quite small (27, 44 and 6 $gC\ m^{-2}\ yr^{-1}$ for the year of 2003, 2004 and 2005). So we just showed the data that was filled the gaps with the pure average of each dataset. For the treatment of S_c and correction of nighttime data, we discussed on the several methods in Section 3.

3. Results and discussion

3.1. *Meteorology and raw F_c*

Fig. 3 shows daily solar radiation, mean and maximum air temperature, daytime average and maximum vapor pressure deficit, daily rainfall, volumetric soil water content (the

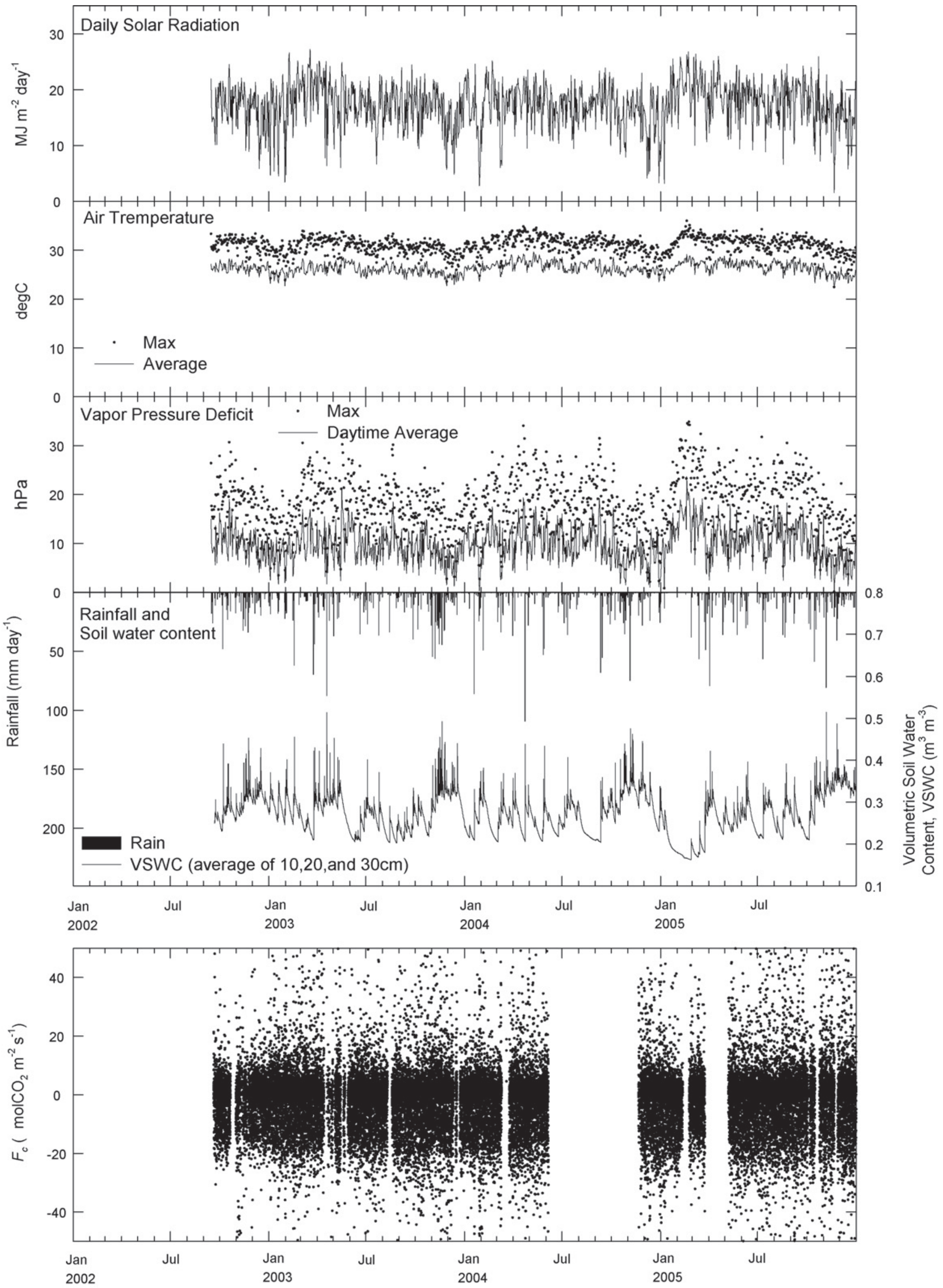

Fig. 3 – Daily solar radiation, mean and maximum air temperature, daytime average and maximum vapor pressure deficit, daily rainfall, volumetric soil water content as the average from observations at 0.1, 0.2 and 0.3 m taken with nine sensors, and canopy CO_2 flux measured between September 2002 and December 2005.

average value from nine total sensors at 0.1, 0.2 and 0.3 m depth) and canopy CO_2 flux from September 2002 to December 2005. The mean and standard deviation of daily solar radiation (17.3 ± 4.1 MJ m^{-2} day^{-1}), daily mean air temperature (26.3 ± 1.2 °C), daily maximum air temperature (31.0 ± 1.8 °C), daytime mean vapor pressure deficit (9.9 ± 3.7 hPa) and daytime maximum vapor pressure deficit (18.1 ± 5.6 hPa) at 52 m for the entire period show that these environmental variables

Table 1 – Annual amount of net ecosystem exchange (NEE), total ecosystem respiration (RE), soil respiration (REsoil) and gross ecosystem production (GPP) for 2003, 2004 and 2005, estimated with the assumption that nighttime soil respiration was 50% of total ecosystem respiration [line (5) in Fig. 8]

Year	NEE ($gC\ m^{-2}\ yr^{-1}$)	RE (REsoil) ($gC\ m^{-2}\ yr^{-1}$)	GPP ($gC\ m^{-2}\ yr^{-1}$)
2003	−79	3176 (1588)	3255
2004	−147	3130 (1565)	3277
2005	−146	3052 (1526)	3198
3-year average	−124	3119 (1560)	3243

experience small seasonal fluctuations compared to other types of forests (e.g. Fig. 2 of Kosugi et al., 2005). Relatively cool air temperatures and low vapor pressure deficits in January–February and October–December coincide with wet and cloudy periods. Annual rainfall in 2003 (1896 mm), 2004 (1655 mm) and 2005 (1649 mm) exceeded the 4-year average (1571 mm) from 1996 to 1999 that includes the El Niño event from 1997 to early 1998 (Tani et al., 2003), but was similar to totals in a normal year (see Fig. 1). Soil water content showed fluctuation between seasons. The driest period was in February 2005. Values of 30-min raw F_c data showed no clear seasonal changes corresponding to soil moisture and air temperature conditions (Fig. 3).

Diurnal and seasonal variations in soil temperature were very small and within 24.9 ± 0.5 °C (mean ± standard deviation). In contrast, seasonal variation in the soil water content fluctuated considerably between wet and dry periods (Fig. 3).

3.2. *Comparison of canopy eddy covariance CO$_2$ flux, NEE and soil respiration*

The influence of soil temperature and water content on soil respiration rate, and its spatio-temporal variation, were evaluated at this site by a companion paper (Kosugi et al., 2007b). Soil respiration rate, temperature and water content were measured in a 50-m × 50-m plot with a nested sampling design of varying grid size. Spatially, the soil respiration rate was low where soil water content was high. In contrast, temporally, the soil respiration rate was low when the soil was dry. During dry periods, the soil respiration rate was still lower in wetter areas. These results alerted us that we should not mix up the influences of soil water content on seasonal and spatial variation of soil respiration rate. Temporal variation in spatially averaged soil respiration rate over 36 points in the 50-m × 50-m plot was positively correlated with the soil water content computed as the average of the 0.1, 0.2 and 0.3 m depth measurements taken continuously at three points near the flux observation tower ($R = 0.71$, $p < 0.001$, $n = 9$, Kosugi et al., 2007b).

Various relationships between soil respiration rate and soil water content have been reported, including linear (Morén and Lindroth, 2000; Rey et al., 2002; Savage and Davidson, 2003; Scott-Denton et al., 2003; Hashimoto et al., 2004), quadratic (Qi and Xu, 2001; Kang et al., 2003; Sotta et al., 2004) and logarithmic (Irvine and Law, 2002). In tropical regions, Schwendenmann et al. (2003) reported the parabolic relationship between soil water content and seasonal variation of soil respiration rate in an old-growth neotropical rainforest in Costa Rica. Sotta et al. (2004, 2006) also reported the parabolic relationship in an old-growth eastern Amazonian rainforest, although they combined the seasonal and spatial variation of soil respiration rate in one dataset. On the other hand, Davidson et al. (2000) reported the temporal positive relationship between soil water content and respiration rate at a primary forest in eastern Amazonia. Our result in a Southeast Asian primary rainforest also showed a positive linear relationship. Further investigation of spatio-temporal variation of soil respiration is needed to determine the precise relationship, but the linear relationship was assumed for this study, as we did not detect the decline of soil respiration rate at the wettest periods in our site (Kosugi et al., 2007b). We also tested the average of nine observations as another reference for estimation of annual value of soil respiration. We did not use the relationship between temporal variation of soil respiration and temperature in our study, because seasonal variation in daily average soil temperature was low and no significant relationship was detected with soil respiration, although it should be noted that temperature sometimes strongly correlated with soil water content as Davidson et al. (1998) showed.

The annual amount of soil respiration estimated using the average soil water content of the continuous measurements at 0.1, 0.2 and 0.3 m near the flux observation tower was 15.9, 15.7 and 15.3 tC $ha^{-1}\ yr^{-1}$ for 2003, 2004 and 2005, respectively (values shown as a black line in Fig. 4), which was equivalent with 4.1 $\mu mol\ m^{-2}\ s^{-1}$ for 3-year average. As nine observation campaigns are not enough to parameterize the model for annual estimation, another estimation using the pure average of nine observations (3.8 ± 0.4 $\mu mol\ m^{-2}\ s^{-1}$, mean ± S.E.) was showed as a gray line in Fig. 4, which is corresponded to be 14.5 ± 1.5 tC $ha^{-1}\ yr^{-1}$. For the comparison, Raich and Schlesinger (1992) reported the average annual soil respiration rates (12.6 ± 0.6 tC $ha^{-1}\ yr^{-1}$, mean ± S.E.) in tropical and subtropical moist forests. In Amazonian tropical forests, Keller et al. (2005) reported the annual averaged values for Oxisol (3.6 ± 0.4 $\mu mol\ m^{-2}\ s^{-1}$, mean ± S.E.) and Ultisol (4.9 ± 1.1 $\mu mol\ m^{-2}\ s^{-1}$, mean ± S.E.). Davidson et al. (2004) reported the mean annual values of 10.0 ± 0.9 tC $ha^{-1}\ yr^{-1}$ (mean ± S.E.) based on 14 sampling dates during 3 years. Chambers et al. (2004) reported the average value of 3.2 $\mu mol\ m^{-2}\ s^{-1}$. While in the Southeast Asian tropical regions, the average soil respiration rate at 50 points at the same site of this study observed in March 2000 by Adachi et al. (2005) was equivalent to the soil respiration rate of 4.9 ± 2.1 $\mu mol\ m^{-2}\ s^{-1}$ (mean ± S.D.). Ishizuka et al. (2005a,b) reported 3.5 ± 1.3 $\mu mol\ m^{-2}\ s^{-1}$ as the value of 80 points for a tropical rainforest, 3.7 ± 0.5 $\mu mol\ m^{-2}\ s^{-1}$ for the average of nine forest sites, 3.5 ± 0.8 $\mu mol\ m^{-2}\ s^{-1}$ for the average of 27 sites with various land-use, in Indonesia (mean ± S.D.). Our results and annual estimation is close to these values.

Eddy covariance estimates of nocturnal CO$_2$ emission at this site showed an obvious underestimate for small friction velocities (u_*). The site in the present study is characterized by a small u_* (mean = 0.18) at night. During the night, CO$_2$ flux measured using the eddy covariance method increased as the friction velocity increased, suggesting an underestimate of

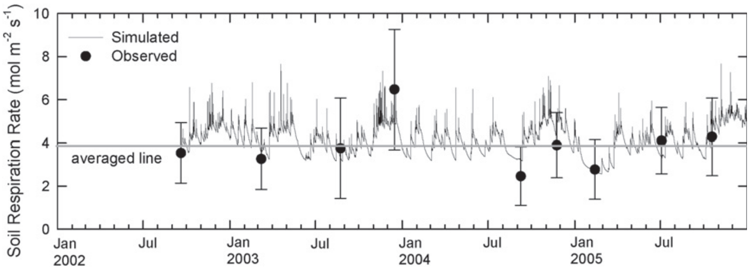

Fig. 4 – Seasonal variations in observed (dot) and simulated (black line) soil respiration rate. Observed soil respiration rate shown in this figure was the spatially averaged value of 36 points. Bars represent the S.D. ($n = 36$). The linear relationship between soil water content (θ, $m^3\ m^{-3}$) as the average from observations at 0.1, 0.2 and 0.3 m taken with nine sensors and the spatially averaged value of soil respiration rate (R_{soil}, mmol $m^{-2}\ s^{-1}$) ($R_{soil} = 14.442\ \theta + 0.2253$) was used to calculate the simulated values. Pure average of soil respiration at nine observations were shown with gray line.

ecosystem respiration under conditions of poor mixing (Fig. 5). The average and standard error of nighttime F_c were 3.6 ± 0.1 μmol $m^{-2}\ s^{-1}$ when $u_* \geq 0.2$. The average value decreased to 2.5 ± 0.1 μmol $m^{-2}\ s^{-1}$ without u_* filter for all available 30-min flux data from January 2003 to December 2005 ($n = 15{,}050$). S_c ($n = 2178$) decreased as u_* increased, so the underestimate at low friction velocities of actual nighttime CO_2 exchange denoted as NEE was moderated. The average value of observed NEE ($n = 2067$) was 4.7 ± 0.2 μmol $m^{-2}\ s^{-1}$ when $u_* \geq 0.2$, and 4.6 ± 0.1 μmol $m^{-2}\ s^{-1}$ without u_* filter. Considerable fluctuations of NEE at high u_* might be due to insufficient data for the instantaneous NEE as the sum of F_c and S_c.

F_c and NEE when $u_* \geq 0.2$ showed a similar dependence as the soil respiration rate with volumetric soil water content at depths of 0.1, 0.2 and 0.3 m (Fig. 6). The linear and positive relationship between soil respiration and volumetric soil water content at depths of 0.1, 0.2 and 0.3 m (Kosugi et al., 2007b) is shown as a gray bold line in Fig. 6. It can be said that soil respiration rate determined using the chamber method almost corresponded to the observed F_c or NEE. This means the nocturnal CO_2 flux measured with the eddy covariance method over the canopy corresponded only with the component of soil respiration estimated with the chamber method in this study, even at a moderate friction velocity ($u_* > 0.2$) and considering storage component.

While, total ecosystem respiration includes respirations from stem, foliage and coarse surface litter components other than soil respiration (root respiration, fine surface litter and soil organic matter decomposition) and will likely be much greater than soil respiration. Chambers et al. (2004) reported that soil respiration in a Central Amazon forest was 41% (12.1 tC $ha^{-1}\ yr^{-1}$) of the total ecosystem respiration (29.5 tC $ha^{-1}\ yr^{-1}$). Goulden et al. (1996) reported that the soil respiration for a cool–temperate deciduous forest was 67% of the total ecosystem respiration during the summer. Ohkubo et al. (2007) reported a soil respiration of 7.1 tC $ha^{-1}\ yr^{-1}$ for a temperate evergreen Japanese cypress forest, which was 49% of the ecosystem respiration. The comparison with the eddy covariance nocturnal F_c or NEE at a moderate friction velocity ($u_* > 0.2$) and the chamber measurements of soil respiration rate strongly suggests a severe underestimate for nocturnal ecosystem respiration when the eddy covariance method is used even for moderate friction velocities, even considering the differences may exist in the scales between the chamber measurements (50 m × 50 m) and the eddy covariance measurements. The situation may be site-dependent. For example, recent work on a temperate evergreen coniferous forest (Ohkubo et al., 2007) showed agreement between both methods when the friction velocity was large. Few studies have compared estimates of ecosystem respiration using data from the chamber method and the eddy covariance method. Further investigation is warranted and checking results with data from the chamber method is essential.

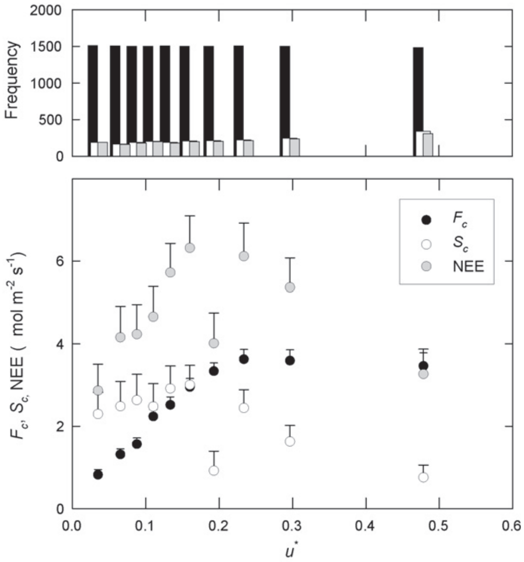

Fig. 5 – Nighttime F_c ($n = 15{,}540$), S_c ($n = 2178$) and NEE ($n = 2067$) vs. friction velocity. Data were classified into ten u_* groups; average values with a standard error for each class are shown by dots and error bars. Frequencies are shown as bar graphs at the top of the diagram. Black bar: number of F_c data. White bar: number of S_c data. Gray bar: number of NEE data. Black dot: average value of F_c at each u_* class. White dot: average value of S_c at each u_* class. Gray dot: average value of NEE at each u_* class.

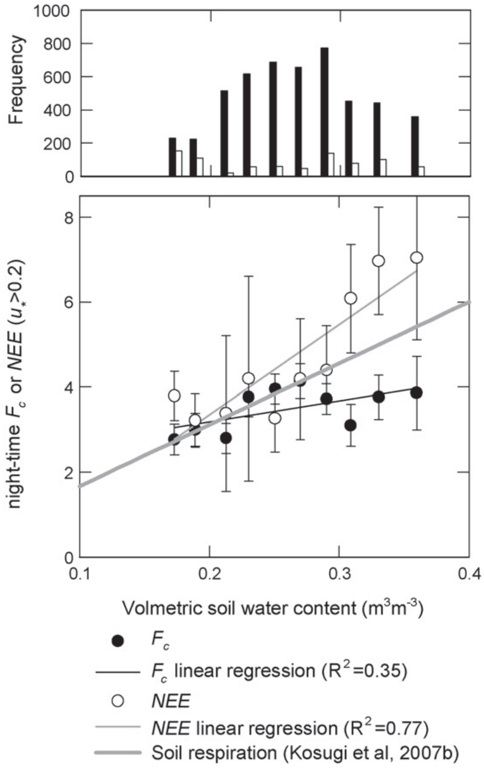

Fig. 6 – Relationship between the volumetric soil water content at the depth between 0.1 and 0.3 m and F_c (black dot) or NEE (white dot) when $u_* \geq 0.2$. Lines denote the linear regressions. Bold gray line indicates the linear regression for soil respiration with chamber observations (Kosugi et al., 2007b) as a reference. Data were classified into every 0.02 of volumetric soil water content. Average values with a standard deviation for each class are shown by dots and error bars in the figure. Frequencies are shown as bar graphs at the top of the diagram (black bar: F_c, white bar: NEE).

3.3. *Annual carbon budget*

Fig. 7 shows the average diurnal changes in F_c, S_c, NEE without u_* filter and soil respiration rate using all available data from January 2003 to December 2005. Comparison between observed diurnal changes in NEE (black dots in Fig. 7) as the sum of available observed data for F_c and S_c ($n = 2067$) and estimated diurnal changes in NEE using the average diurnal changes in F_c and S_c (line 3 in Fig. 7) allowed an interpolation of missing S_c data using average diurnal changes in S_c for the analysis of 3-year averaged diurnal change in NEE. Fig. 7 shows that NEE consisted primarily of S_c in the morning, and that NEE was about the same as F_c in the afternoon. NEE showed a distinct minimum in absorption in the afternoon compared to the morning. At night, NEE matched the soil respiration rate.

This average diurnal change in F_c without any corrections yielded an NEE of −2.26 gC m^{-2} day^{-1} (−8.5 tC ha^{-1} yr^{-1}) as the average value from January 2003 to December 2005, if the average daily sum of S_c was assumed to be nearly zero. Yearly values were −8.2, −9.5 and −8.4 tC ha^{-1} yr^{-1} for 2003, 2004 and 2005, respectively. Note that larger values for 2004 might be related to the large amount of missing data that followed the lightning strikes. A short-term observation of CO_2 exchange using the closed-path eddy covariance method was performed at this site in March 1998 (Yasuda et al., 2003). This study, which was conducted in a dry season, reported CO_2 absorption of approximately −2.24 to −2.58 gC m^{-2} day^{-1} in this forest. Values at this site were smaller than the values of NEE reported at Amazonian forests (−0.60 gC m^{-2} day^{-1}, Fan et al., 1990; −0.95 gC m^{-2} day^{-1}, Grace et al., 1996; −1.5 gC m^{-2} day^{-1}, Goulden et al., 2004), and especially comparing with large carbon loss reported at two old-growth Amazonian forest after natural disturbance (3-year average NEE:1.3 tC ha^{-1} yr^{-1}, Saleska et al., 2003).

Fig. 8 shows the sensitivity of the annual carbon balance to detrending, and different correction methods for nighttime flux. Periods with missing data were filled in this figure with values interpolated with pure average of each dataset. The linear detrending caused the NEE to decrease by −0.4 tC ha^{-1} yr^{-1} for 3-year average [compare lines (1) and (2) in Fig. 8]. The u_* filtering used two methods. One method replaced all nighttime F_c data when $u_* < 0.2$ with the value derived from the relationship between F_c when $u_* \geq 0.2$ and volumetric the soil water content shown by the black bold line in Fig. 6. With this correction, data at the scale of more than a day can be considered to represent NEE, assuming daily total S_c should be nearly zero. In the other method, all nighttime NEE at the 30-min scale was interpolated with the value derived from the relationship between NEE when $u_* \geq 0.2$ and the volumetric soil water content shown by the thin black line in Fig. 6, and daytime NEE was calculated adding the average

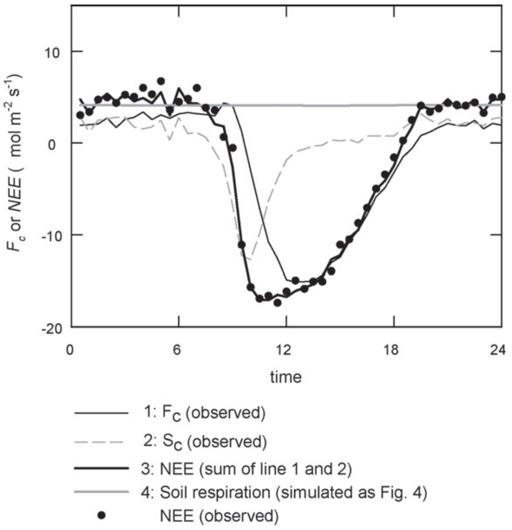

Fig. 7 – Average diurnal changes in F_c (narrow black line), S_c (narrow gray line), NEE (bold black line and black dot) and soil respiration rate (bold gray line) using all available data from January 2003 to December 2005. The correction with u_* filter did not apply to this dataset.

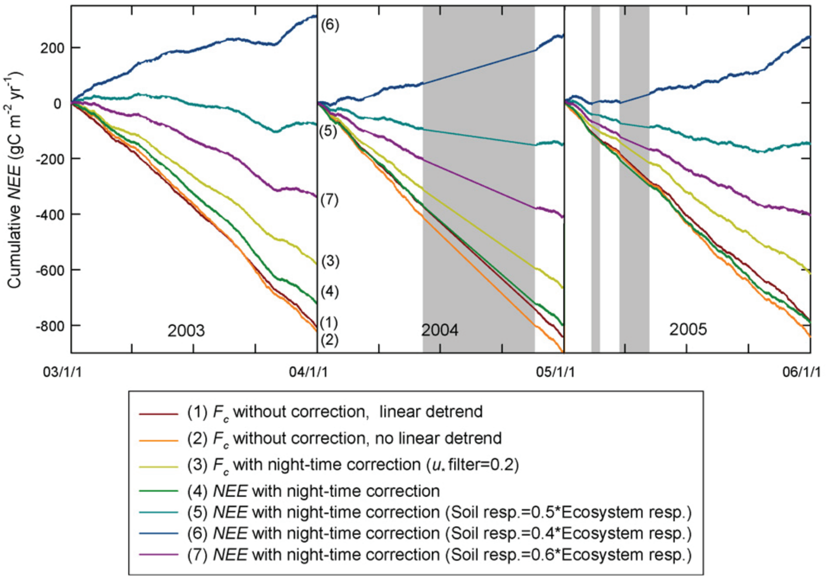

Fig. 8 – Cumulative NEE for each year from January 2003 to December 2005 at Pasoh. (1) Open-path F_c with linear detrending. (2) Open-path F_c without linear detrending. (3) Open-path F_c without linear detrending, with nighttime correction with u_* filter, replacing all nighttime (solar radiation <2.0 W s^{-1}) F_c data when $u_* < 0.2$ using the value derived from the relationship between F_c when $u_* \geq 0.2$ and the volumetric soil water content shown by the black bold line in Fig. 6. (4) NEE with nighttime correction, replacing all nighttime data to the value derived from the relationship between NEE when $u_* \geq 0.2$ and the volumetric soil water content shown by the black narrow line in Fig. 6, and adding average diurnal course of S_c to daytime F_c without linear detrending. (5)–(7) NEE with nighttime correction, replacing all nighttime data to the estimated ecosystem respiration based on chamber estimations of annual soil respiration subject to the assumption that soil respiration is (5) 50%, (6) 40% or (7) 60% of the ecosystem respiration, and adding average diurnal course of S_c to daytime F_c without linear detrending. In this figure, missing data were interpolated by pure average of each dataset. Shadows in the figure indicate missing data periods longer than 10 days.

diurnal course of S_c to F_c. With this correction, data at the scale of more than monthly can be considered to represent NEE, assuming monthly average diurnal change of S_c should be similar to the 3-year-average diurnal change of S_c. It should be noted that both treatments still showed considerable absorption, with values between −5.8 and −8.0 tC ha^{-1} yr^{-1}, with all that the relationships between raw F_c or NEE and volumetric soil water content shown with lines in Fig. 6 were not statistically significant because raw F_c and NEE data were usually highly scattered, and the uncertainty in estimating ecosystem respiration with OLS optimization (Richardson and Hollinger, 2005).

We also tested to replace all nighttime eddy covariance data to the estimated ecosystem respiration based on the chamber estimate of annual soil respiration of 15.9, 15.7 and 15.3 tC ha^{-1} yr^{-1} for 2003, 2004 and 2005, respectively, assuming that soil respiration comprised 50, 40 or 60% of the ecosystem respiration [lines (5), (6) and (7) in Fig. 8, respectively]. Results show average NEE values for 3 years of −1.2, 2.7, and −3.9 tC ha^{-1} yr^{-1} for the 50, 40 and 60% treatments, respectively.

There have been few reports in the literatures for the bottom up estimation of ecosystem respiration, though the ratio of soil to total ecosystem respiration ranges between 41% for a Central Amazon forest (Chambers et al., 2004) to 67% a cool–temperate deciduous forest (estimation for during summer, Goulden et al., 1996). Ohkubo et al. (2007) reported 49% for a temperate evergreen Japanese cypress forest. It is supposed that the respiration component other than soil almost matched soil respiration. From this, a more reliable value for the carbon budget probably lays somewhere between lines (5)–(7), rather than that of lines (1)–(4). Thus estimation of the components (other than soil) of ecosystem respiration is quite important for the carbon budget at this site and we need much more information. Table 1 shows a reference annual amount of net ecosystem exchange (NEE), total ecosystem respiration (RE), soil respiration (REsoil) and gross ecosystem production (GPP) for 2003, 2004 and 2005, if we assume that nighttime soil respiration was 50% of the total ecosystem respiration [line (5) in Fig. 8]. With this assumption, annual NEE for 2003, 2004 and 2005 was estimated to be −0.8, −1.5 and −1.5 tC ha^{-1} yr^{-1}, respectively. The 3-year average value was −1.2 tC ha^{-1} yr^{-1}. This value would be −2.2 tC ha^{-1} yr^{-1}, if we used the estimation of annual soil respiration of 14.5 tC ha^{-1} $yr^{-1}$and 50% treatment.

Biometric investigations at this site revealed a decrease (−3.4 tC ha^{-1} yr^{-1}, 1994–1998) of total aboveground biomass (TAGB) (Kato et al., 1978; Hoshizaki et al., 2004). Considerable tree death (6.2 tC ha^{-1} yr^{-1}, 1994–1998) was also reported by Hoshizaki et al. (2004). Similar large disturbance proceeded the initiation of the eddy flux observation in 2000s was also reported in Amazonian forests (Rice et al., 2004) and might be triggered by the El Niño events in 1990s as Rice et al. (2004) pointed out. Saleska et al. (2003) reported the carbon emission (NEE:1.3 tC ha^{-1} yr^{-1} for 3-year average) after disturbance at two Amazonian forests. It is also supposed that some parts of the coarse woody debris (CED) were considered to remain undecayed. Chambers et al. (2000) investigated the decomposition rate of dead trees in Amazonian forest and reported the mean residence time of coarse litter to be 5.9 years. The decrease of TAGB at this site was mitigated in more recent survey to be nearly balanced (Niiyama et al., unpublished data). If oscillations of NEE, growth and decay rates are considered, NEE values of −1.2, 2.7, and −3.9 tC ha^{-1} yr^{-1} for the 50, 40 and 60% treatments shown with lines (5)–(7) in Fig. 8 are also supposed to be more probable than raw F_c data or even with the u_* filtering shown with lines (1)–(4) in Fig. 8, despite of many uncertainties in the estimation of nighttime ecosystem respiration based on soil respiration with chamber method, such as possible errors in soil respiration rate measured with closed dynamic chamber method (e.g., Davidson et al., 2002; Bain et al., 2005), uncertainties in the spatial and temporal variations in the annual estimation, and scaling factor from soil to total ecosystem respiration. As Miller et al. (2004) pointed out, uncertainty in estimates of nighttime flux by the eddy covariance method makes the annual carbon budget less

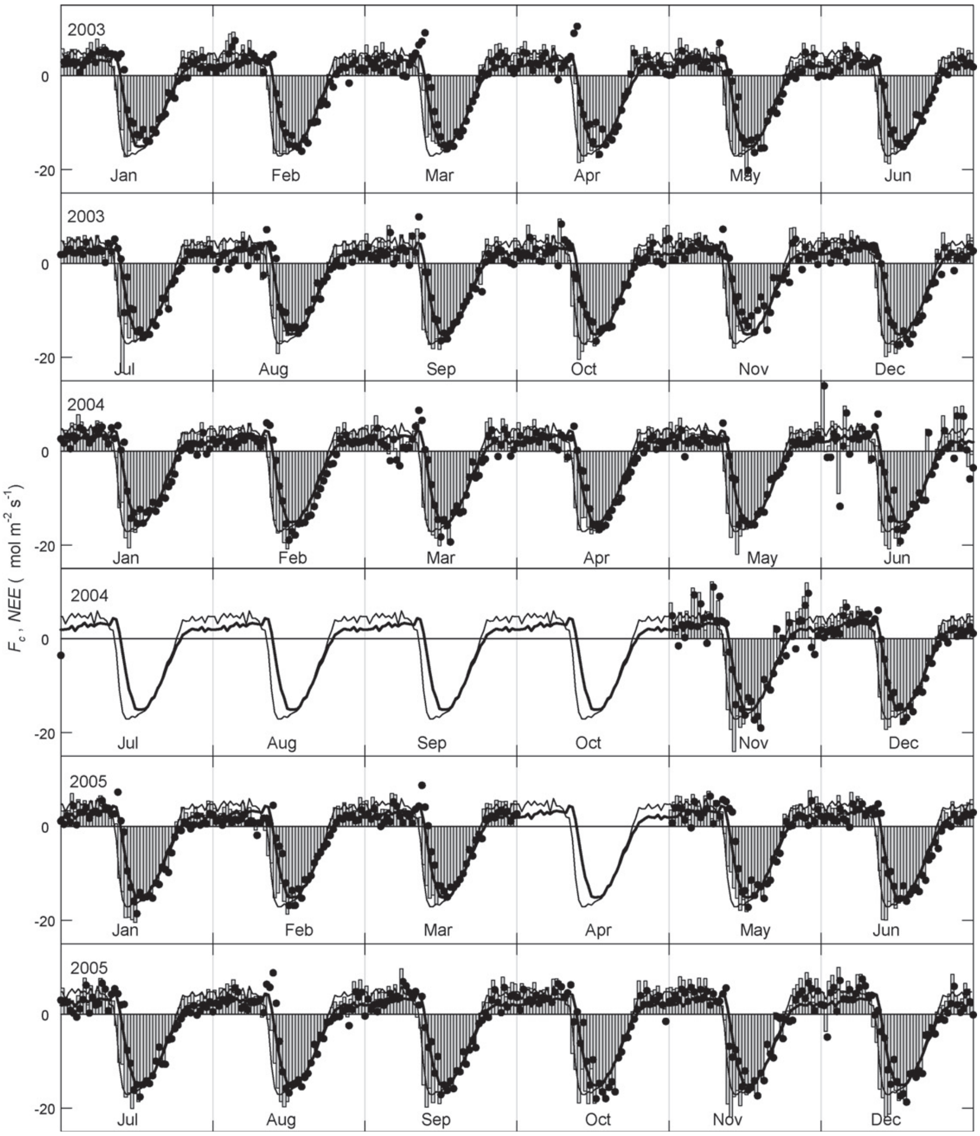

Fig. 9 – Monthly average diurnal changes in 30-min F_c and NEE. The average diurnal change in S_c for the whole period was added to the monthly average diurnal change in F_c to calculate the monthly average diurnal course of NEE. Black dots: monthly average diurnal change in F_c. Gray bar: monthly average diurnal change in NEE. Bold black line: 3-year average diurnal change in F_c. Narrow black line: 3-year average diurnal change in NEE.

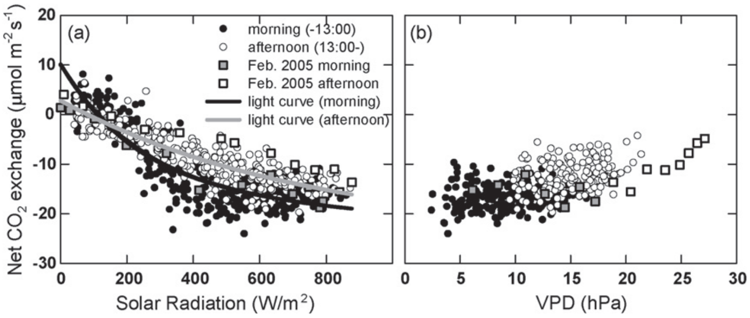

Fig. 10 – Relationship between CO_2 exchange and (a) solar radiation or (b) VPD. Monthly averaged diurnal changes in NEE as shown in Fig. 9 were used in this analysis. Black circles denote the data in the morning, and white circles represent the data in the afternoon of the usual months. Grey squares indicate the data in the morning and white squares show the data in the afternoon of the driest month (February 2005). (a) Monthly average 30-min data with solar radiation >40 W m^{-2} were plotted. (b) Monthly average 30-min data with solar radiation >400 W m^{-2} were plotted.

certain for tropical than temperate forests because of the large nighttime ecosystem respiration. Nevertheless, this analysis strongly suggests that the Southeast Asian tropical rainforest was not a strong carbon sink, as raw F_c data, even with the u_* filtering, suggested.

3.4. Diel and seasonal change patterns of CO_2 exchange

Fig. 9 shows the monthly average diurnal changes in 30-min CO_2 flux and NEE. The monthly average diurnal change in NEE was calculated by adding whole-period average diurnal changes in S_c to monthly average diurnal changes in F_c. No obvious changes in CO_2 fluxes were observed under the relatively cool and wet conditions during October–December. Nighttime flux was slightly smaller under the driest conditions of February 2005, but no obvious changes in daytime CO_2 absorption were observed in that month. Daytime CO_2 absorption was larger in the morning than in the afternoon for every month.

Fig. 10 shows the relationship between CO_2 exchange and solar radiation or VPD. Monthly averaged diurnal changes in NEE as shown in Fig. 9 were used in this analysis. Non-rectangular hyperbola light curves were fitted to the morning and afternoon data and the interceptions were 10.1 and 2.8 μmol m^{-2} s^{-1}, respectively. NEE at a given irradiance was larger in the morning than afternoon throughout the year, indicating the photosynthetic inhibition of canopy leaves in the afternoon, irrespective of soil moisture. The interception of light curve for morning data suggests a quite large ecosystem respiration at this site. NEE at high irradiance decreased as VPD decreased. Nevertheless, NEE at a given VPD was lower in the afternoon than in the morning. No obvious difference was observed in this diurnal pattern of NEE even in February 2005, the driest period during the study. Photosynthetic inhibition in the afternoon was probably caused by leaves responding not only to single environmental factors such as VPD or soil moisture, but perhaps also to an intrinsic rhythm, or some restrictions in the water supply that might occur in tall canopy trees in the tropical rainforest, irrespective of soil moisture conditions. Doughty et al. (2006) reported that circadian rhythms constrain leaf gas exchange of many tree species grown in Amazonian forest. Evidence exists that patch stomatal closure caused the severe photosynthetic inhibition in the afternoon for the canopy leaves in this forest (Takanashi et al., 2006).

The diurnal and seasonal pattern and amplitude in daytime CO_2 exchange were similar to those reported for the Amazon tropical rainforests (Grace et al., 1996; Araujo et al., 2002; Saleska et al., 2003; Goulden et al., 2004) despite differences in rain patterns. Goulden et al. (2004) and Saleska et al. (2003) investigated seasonal fluctuations in CO_2 exchange for Amazon tropical rainforests and showed that a reduction in respiration caused the increase in CO_2 sequestration by the forest during the dry season and that canopy photosynthesis was not significantly reduced even during the dry season. Results in this study were similar, but the difference in the pattern for dry and rainy seasons caused the difference in the pattern of cumulative NEE between our result (Fig. 8) and [Saleska et al. (2003), Fig. 3] or [Miller et al. (2004), Fig. 4)], which showed distinctly higher CO_2 sequestration in the dry season than in the rainy season. The present study also indicates an increase in soil respiration, F_c and NEE during wet periods and thus a decrease in CO_2 sequestration. Fig. 8 shows that NEE had larger values in November and December, the period that the soil water content was higher and thus soil respiration was larger than in other months. However, in the Southeast Asian tropical rainforest, wet and dry periods do not persist for as long as in the Amazon rainforest, and that creates the difference in the pattern of cumulative NEE.

4. Conclusions

Three years of eddy covariance CO_2 flux at a primary Southeast Asian tropical rainforest in the Pasoh Forest Reserve on Peninsular Malaysia, was investigated. The uncertainty of nighttime fluxes and the annual carbon budget at this site was assessed by comparing nighttime CO_2 flux at the canopy, net CO_2 exchange of the forest including the CO_2 storage term and chamber measurements of soil respiration. The analysis strongly suggested that raw F_c data, even with u_* filtering, underestimated the nighttime CO_2 efflux as the ecosystem respiration. Diurnal pattern of CO_2 exchange revealed that obvious restriction of canopy photosynthesis in the afternoon was occurred in this forest irrespective of soil moisture. Seasonal and annual patterns of CO_2 exchange reveals that one of the main causes which induce the difference in NEE pattern between Amazonian and Southeast Asian rainforests was not the difference in daytime photosynthesis but the difference in ecosystem respiration related with dry and rainy seasons. The decrease of CO_2 uptake (increase of NEE) at wet period was also observed at this site, but did not form an obvious seasonality such as in Amazonian forests. Much more dataset from worldwide flux sites should be accumulated in future to clarify the characteristics of CO_2 exchange in tropical regions with various environmental and vegetation types.

Acknowledgements

We thank the Forestry Department of Negeri Sembilan and the director general of FRIM for granting us permission to work in the Pasoh Forest Reserve. We gratefully acknowledge the staffs of the Hydrology Unit and the Pasoh Station of FRIM for collecting field data. Dr. Shoji Noguchi and Dr. Jyunjiro Negishi helped install the soil moisture sensors, Dr. Tamon Yamashita provided information on soil properties, Dr. Kaoru Niiyama provided biometric observations and LAI data obtained in this forest reserve, and Dr. Tsuyoshi Yoneda and Dr. Kazuhiro Hoshizaki provided valuable information on the relationship between our result and ecological observations. Mr. Tatsuya Katayama, Mr. Takumi Wada, Mr. Shinji Konishi, Mr. Yusuke Fukui, Ms. Rie Nakanishi, Dr. Masayuki Ito and Mr. Naoto Yokoyama assisted with the fieldwork. We also thank Dr. Toshinori Okuda, Dr. Naishen Liang and a joint research project between FRIM, UPM and NIES. This work was supported by the Global Environment Research Fund of the Japan Environment Agency, and by grants for scientific research from the Ministry of Education, Culture, Sports, Science and Technology, Japan.

REFERENCES

Adachi, M., Bekku, Y.S., Konuma, A., Kadir, W.R., Okuda, T., Koizumi, H., 2005. Required sample size for estimating soil respiration rates in large areas of two tropical forests and of two types of plantation in Malaysia. Forest Ecol. Manage. 210, 455–459.

Anthoni, P.M., Law, B.E., Unsworth, M.H., 1999. Carbon and water vapor exchange of an open-canopied ponderosa pine ecosystem. Agric. For. Meteorol. 95, 151–168.

Araujo, A.C., Nobre, A.D., Kruijt, B., Dallarosa, R., Stefani, P., von Randow, C., Manzi, A.O., Culf, A.D., Gash, J.H.C., Valentini, R., Kabat, P., 2002. Comparative measurements of carbon dioxide fluxes from two nearby towers in a central Amazonian rainforest: The Manaus LBA site. J. Geophys. Res. 107, 8090-.

Asner, G.P., Nepstad, D., Cardinot, G., David, R., 2004. Drought stress and carbon uptake in an Amazon forest measured with spaceborne imaging spectroscopy. In: Proceedings of the National Academy of Sciences of the United States of America 101. pp. 6039–6044.

Bain, W.G., Hutyra, L., Patterson, D.C., Bright, A.V., Daube, B.C., Munger, J.W., Wofsy, S.C., 2005. Wind-induced error in the measurement of soil respiration using closed dynamic chambers. Agric. For. Meteorol. 131, 225–232.

Baldocchi, D., Falge, E., Wilson, K., 2001. A spectral analysis of biosphere–atmosphere trace gas flux densities and meteorological variables across hour to multi-year time scales. Agric. For. Meteorol. 107, 1–27.

Baldocchi, D.D., Bowling, D.R., 2003. Modelling the discrimination of $^{13}CO_2$ above and within a temperate broad-leaved forest canopy on hourly to seasonal time scales. Plant Cell Environ. 26, 231–244.

Bolstad, P.V., Davis, K.J., Martin, J., Cook, B.D., Wang, W., 2004. Component and whole-system respiration fluxes in northern deciduous forests. Tree Physiol. 24, 493–504.

Chambers, J.Q., Higuchi, N., Schimel, J.P., Ferreira, L.V., Melack, J.M., 2000. Decomposition and carbon cycling of dead trees in tropical forests of the central Amazon. Oecologia 122, 380–388.

Chambers, J.Q., Tribuzy, E.S., Toledo, L.C., Crispim, B.F., Higuchi, N., Santos, J.D., Araújo, A.C., Kruijt, B., Nobre, A.D., Trumbore, S.E., 2004. Respiration from a tropical forest ecosystem: partitioning of sources and low carbon use efficiency. Ecol. Appl. 14, S72–S88.

da Rocha, H.R., Goulden, M.L., Miller, S.D., Menton, M.C., Pinto, L.D.V.O., de Freitas, H.C., e Silva Figueira, A.M., 2004. Seasonality of water and heat fluxes over a tropical forest in eastern amazonia. Ecol. Appl. 14, S22–S32.

Davidson, E.A., Belk, E., Boone, R.D., 1998. Soil water content and temperature as independent or confounded factors controlling soil respiration in a temperate mixed hardwood forest. Global Change Biol. 4, 217–227.

Davidson, E.A., Verchot, L.V., Cattânio, J.H., Ackerman, I., Carvalho, J.E.M., 2000. Effects of soil water content on soil respiration in forests and cattle pastures of eastern Amazonia. Biogeochemistry 48, 53–69.

Davidson, E.A., Savage, K., Verchot, L.V., Navarro, R., 2002. Minimizing artifacts and biases in chamber-based measurements of soil respiration. Agric. For. Meteorol. 113, 21–37.

Davidson, E.A., Ishida, F.Y., Nepstad, D.C., 2004. Effects of an experimental drought on soil emissions of carbon dioxide, methane, nitrous oxide, and nitric oxide in a moist tropical forest. Global Change Biol. 10, 718–730.

Doughty, C.E., Goulden, M.L., Miller, S.D., da Rocha, H.R., 2006. Circadian rhythms constrain leaf and canopy gas exchange in an Amazonian forest. Geophys. Res. Lett. 33, L15404.

Drewitt, G.B., Black, T.A., Nesic, Z., Humphreys, E.R., Jork, E.M., Swanson, R., Ethier, G.J., Griffis, T., Morgenstern, K., 2002. Measuring forest floor CO_2 fluxes in a Douglas-fir forest. Agric. For. Meteorol. 110, 299–317.

Fan, S.-M., Wofsy, S.C., Bakwin, P.S., Jacob, D.J., 1990. Atmosphere–biosphere exchange of CO_2 and O_3 in the central Amazon forest. J. Geophys. Res. 95 (D10), 16851–16864.

Goulden, M.L., Munger, J.W., Fan, S.-M., Daube, B.C., Wofsy, S.C., 1996. Measurements of carbon sequestration by long-term eddy covariance: methods and a critical evaluation of accuracy. Global Change Biol. 2, 169–182.

Goulden, M.L., Miller, S.D., da Rocha, H.R., Menton, M.C., de Freitas, H.C., e Silva Figueira, A.M., Dias de Sousa, C.A., 2004. Diel and seasonal patterns of tropical forest CO_2 exchange. Ecol. Appl. 14, S42–S54.

Grace, J., Malhi, Y., Lloyd, J., McIntyre, J., Miranda, A.C., Meir, P., Miranda, H.S., 1996. The use of eddy covariance to infer the net carbon dioxide uptake of Brazilian rain forest. Global Change Biol. 2, 209–217.

Hashimoto, S., Tanaka, N., Suzuki, M., Inoue, A., Takizawa, H., Kosaka, I., Tanaka, K., Tantarsirin, C., Tangtham, N., 2004. Seasonal and topographic patterns of forest floor CO_2 efflux from an upland oak forest. J. Forest Res. 9, 75–79.

Hoshizaki, K., Niiyama, K., Kimura, K., Yamashita, T., Bekku, Y., Okuda, T., Quah, E.S., Noor, N.S.M., 2004. Temporal and spatial variation of forest biomass in relation to stand dynamics in a mature, lowland tropical rainforest, Malaysia. Ecol. Res. 19, 357–363.

Irvine, J., Law, B.E., 2002. Contrasting soil respiration in young and old-growth ponderosa pine forests. Global Change Biol. 8, 1183–1194.

Ishizuka, S., Iswandi, A., Nakajima, Y., Yonemura, S., Sudo, S., Tsuruta, H., Muriyarso, D., 2005a. The variation of greenhouse gas emissions from soils of various land-use/cover types in Jambi province, Indonesia. Nutr. Cycl. Agroecosyst. 71, 17–32.

Ishizuka, S., Iswandi, A., Nakajima, Y., Yonemura, S., Sudo, S., Tsuruta, H., Muriyarso, D., 2005b. Spatial pattern of green house gas emission in a tropical rainforest in Indonesia. Nutr. Cycl. Agroecosyst. 71, 55–62.

Kang, S., Doh, S., Lee, D., Lee, D., Jin, V.L., Kimball, J.S., 2003. Topographic and climatic controls on soil respiration in six temperate mixed-hardwood forest slopes, Korea. Global Change Biol. 9, 1427–1437.

Kato, R., Tadaki, Y., Husato, O., 1978. Plant biomass and growth increment studies in Pasoh Forest. Malayan Nat. J. 30, 211–245.

Keller, M., Varner, R., Dias, J.D., Silva, H., Crill, P., de Oliveira, R.C., Asner, G.P., 2005. Soil-atmosphere exchange of nitrous oxide, nitric oxide, methane, and carbon dioxide in logged and undisturbed forest in the Tapajos National Forest. Brazil. Earth Interact. 9, 1–28.

Kosugi, Y., Tanaka, H., Takanashi, S., Matsuo, N., Ohte, N., Shibata, S., Tani, M., 2005. Three years of carbon and energy fluxes from Japanese evergreen broad-leaved forest. Agric. For. Meteorol. 132, 329–343.

Kosugi, Y., Takanashi, S., Tanaka, H., Ohkubo, S., Tani, M., Yano, M., Katayama, T., 2007a. Evapotranspiration over a Japanese cypress forest. I. Eddy covariance fluxes and surface conductance characteristics for three years. J. Hydrol. 337, 269–283.

Kosugi, Y., Mitani, T., Itoh, M., Noguchi, S., Tani, M., Matsuo, N., Takanashi, S., Ohkubo, S., Abdul Rahim, N., 2007b. Spatial and temporal variation in soil respiration in a Southeast Asian tropical rainforest. Agric. For. Meteorol. 147, 35–47.

Kruijt, B., Elbers, J.A., von Randow, C., Araújo, A.C., Oliveira, P.J., Culf, A., Manzi, A.O., Nobre, A.D., Kabat, P., Moors, E.J., 2004. The robustness of eddy correlation fluxes for Amazon rain forest conditions. Ecol. Appl. 14, S101–S113.

Kumagai, T., Katul, G.G., Porporato, A., Saitoh, T.M., Ohashi, M., Ichie, T., Suzuki, M., 2004a. Carbon and water cycling in a Bornean tropical rainforest under current and future climate scenarios. Adv. Water Resour. 27, 1135–1150.

Kumagai, T., Katul, G.G., Saitoh, T.M., Sato, Y., Manfroi, O.J., Morooka, T., Ichie, T., Kuraji, K., Suzuki, M., Porporato, A., 2004b. Water cycling in a Bornean tropical rain forest under current and projected precipitation scenarios. Water Resour. Res. 40, W01104.

Kumagai, T., Saitoh, T.M., Sato, Y., Morooka, T., Manfroi, O.J., Kuraji, K., Suzuki, M., 2004c. Transpiration, canopy conductance and the decoupling coefficient of a lowland mixed dipterocarp forest in Sarawak, Borneo: dry spell effects. J. Hydrol. 287, 237–251.

Kumagai, T., Saitoh, T.M., Sato, Y., Takahashi, H., Manfroi, O.J., Morooka, T., Kuraji, K., Suzuki, M., Yasunari, T., Komatsu, H., 2005. Annual water balance and seasonality of evapotranspiration in a Bornean tropical rainforest. Agric. For. Meteorol. 128, 81–92.

Kumagai, T., Ichie, T., Yoshimura, M., Yamashita, M., Kenzo, T., Saitoh, T.M., Ohashi, M., Suzuki, M., Koike, T., Komatsu, H., 2006. Modeling CO_2 exchange over a Bornean tropical rain forest using measured vertical and horizontal variations in leaf-level physiological parameters and leaf area densities. J. Geophys. Res. 111, D10107.

Lavigne, M.B., Ryan, M.G., Anderson, D.E., Baldocchi, D.D., Crill, P.M., Fitzjarrald, D.R., Goulden, M.L., Gower, S.T., Massheder, J.M., McCaughey, J.H., Rayment, M., Striegl, R.G., 1997. Comparing nocturnal eddy covariance measurements to estimates of ecosystem respiration made by scaling chamber measurements at six coniferous boreal sites. J. Geophys. Res. 102, 28977–28985.

Law, B.E., Ryan, M.G., Anthoni, P.M., 1999. Seasonal and annual respiration of a ponderosa pine ecosystem. Global Change Biol. 5, 169–182.

Law, B.E., Kelliher, F.M., Baldocchi, D.D., Anthoni, P.M., Irvine, J., Moore, D., Tuyl, S.V., 2001. Spatial and temporal variation in respiration in a young ponderosa pine forest during a summer drought. Agric. For. Meteorol. 110, 27–43.

Malhi, Y., Nobre, A.D., Grace, J., Kruijt, B., Pereira, M.G.P., Culf, A., Scott, S., 1998. Carbon dioxide transfer over a Central Amazonian rain forest. J. Geophys. Res. 103, 31593–31612.

Malhi, Y., Baldocchi, D.D., Jarvis, P.G., 1999. The carbon balance of tropical, temperate and boreal forests. Plant Cell Environ. 22, 715–740.

Malhi, Y., Grace, J., 2000. Tropical forests and atmospheric carbon dioxide. Trends Ecol. Evolut. 15, 332–337.

Malhi, Y., Pegoraro, E., Nobre, A.D., Pereira, M.G.P., Grace, J., Culf, A.D., Clement, R., 2002. Energy and water dynamics of a central Amazonian rain forest. J. Geophys. Res. 107, 8061.

Manokaran, N., Kochummern, K.M., 1992. Tree growth in primary lowland and hill dipterocarp forests. J. Tropical Forest Sci. 6, 332–345.

McMillen, R.T., 1988. An eddy correlation technique with extended applicability to non-simple terrain. Boundary Layer Meteorol. 43, 231–245.

Miller, S.D., Goulden, M.L., Menton, M.C., da Rocha, H.R., de Freitas, H.C., e Silva Figueira, A.M., Dias de Sousa, C.A., 2004. Biometric and micrometeorological measurements of tropical forest carbon balance. Ecol. Appl. 14, S114–S126.

Morén, A.-S., Lindroth, A., 2000. CO_2 exchange at the floor of a boreal forest. Agric. For. Meteorol. 101, 1–14.

Niiyama, K., Abdul Rahman, K., Iida, S., Kimura, K., Ripin, A., Appanah, S., 2003. Regeneration of a clear-cut plot in a lowland dipterocarp forest in Pasoh Forest Reserve, Peninsular Malaysia. In: Okuda, T., Manokaran, N., Matsumoto, Y., Niiyama, K., Thomas, S.C., Ashton, P.S. (Eds.), Pasoh: Ecology of a Lowland Rain Forest in Southeast Asia. Springer, Tokyo, pp. 559–568.

Noguchi, S., Abdul Rahim, N., Tani, M., 2003. Rainfall characteristics of tropical rainforest at Pasoh Forest Reserve, Negeri Sembilan, Peninsular Malaysia. In: Okuda, T., Manokaran, N., Matsumoto, Y., Niiyama, K., Thomas, S.C., Ashton, P.S. (Eds.), Pasoh: Ecology of a Lowland Rain Forest in Southeast Asia. Springer, Tokyo, pp. 51–58.

Ohkubo, S., Kosugi, Y., Takanashi, S., Mitani, T., Tani, M., 2007. Comparison of the eddy covariance and automated closed chamber methods for evaluating nocturnal CO_2 exchange in a Japanese cypress forest. Agric. For. Meteorol. 142, 50–65.

Qi, Y., Xu, M., 2001. Separating the effects of moisture and temperature on soil CO_2 efflux in a coniferous forest in the Sierra Nevada mountains. Plant Soil 237, 15–23.

Raich, B.J.W., Schlesinger, W.H., 1992. The global carbon dioxide flux in soil respiration and its relationship to vegetation and climate. Tellus B 44, 81–99.

Rey, A., Pegoraro, E., Tedeschi, V., De Parri, I., Jarvis, P.G., Valentini, R., 2002. Annual variation in soil respiration and its components in a coppice oak forest in Central Italy. Global Change Biol. 8, 851–866.

Rice, A.H., Hammond, E.P., Saleska, S.R., Hutyra, L., Palace, M., Keller, M., de Carmargo, P.B., Portilho, K., Marques, D., Wofsy, S.C., 2004. Carbon balance and vegetation dynamics in an old-growth Amazonian forest. Ecol. Appl. 14, 55–71.

Richardson, A.D., Hollinger, D.Y., 2005. Statistical modeling of ecosystem respiration using eddy covariance data: maximum likelihood parameter estimation, and Monte Carlo simulation of model and parameter uncertainty, applied to three simple models. Agric. For. Meteorol. 131, 191–208.

Saleska, S.R., Miller, S.D., Matross, D.M., Goulden, M.L., Wofsy, S.C., da Rocha, H.R., de Camargo, P.B., Crill, P., Daube, B.C., de Freitas, H.C., Hutyra, L., Keller, M., Kirchhoff, V., Menton, M., Munger, J.W., Pyle, E.H., Rice, A.H., Silva, H., 2003. Carbon in Amazonian forests: unexpected seasonal fluxes and disturbance-induced losses. Science 302, 1554–1557.

Savage, K.E., Davidson, E.A., 2003. A comparison of manual and automated systems for soil CO_2 flux measurements: trade-offs between spatial and temporal resolution. J. Exp. Bot. 54, 891–899.

Scott-Denton, L.E., Sparks, K.L., Monson, R.K., 2003. Spatial and temporal controls of soil respiration rate in a high-elevation, subalpine forest. Soil Biol. Biochem. 35, 525–534.

Schwendenmann, L., Veldkamp, E., Brenes, T., O'brien, J., Mackensen, J., 2003. Spatial and temporal variation in soil CO_2 efflux in an old-growth neotropical rain forest, La Salva, Costa Rica. Biogeochemistry 64, 111–128.

Soepadmo, E., 1978. Introduction to the Malaysian I.B.P. synthesis meetings. Malaysian Nat. J. 30, 119–124.

Sotta, E.D., Meir, P., Malhi, Y., Nobre, A.D., Hodnett, M., Grace, J., 2004. Soil CO_2 efflux in a tropical forest in the central Amazon. Global Change Biol. 10, 601–617.

Sotta, E.D., Valdkamp, E., Guimarães, B.R., Paixão, R.K., Ruivo, M.L.P., Almeida, S.S., 2006. Landscape and climatic controls on spatial and temporal variation in soil CO_2 efflux in an Eastern Amazonian Rainforest, Caxiuanã, Brazil. Forest Ecol. Manage. 237, 57–64.

Takanashi, S., Kosugi, Y., Tani, M., Matsuo, N., Mitani, T., Abdul Rahim, N., 2005. Characteristics of the gas exchange of a tropical rain forest in Peninsular Malaysia. Phyton 45, 61–66.

Takanashi, S., Kosugi, Y., Matsuo, N., Tani, M., Ohte, N., 2006. Patchy stomatal behavior in broad-leaved trees grown in different habitats. Tree Physiol. 26, 1565–1578.

Tani, M., Abdul Rahim, N., Ohtani, Y., Yasuda, Y., Mohd Md, S., Baharuddin, K., Takanashi, S., Noguchi, S., Zulkifli, Y., Watanabe, T., 2003. Characteristics of energy exchange and surface conductance of a tropical rain forest in Peninsular Malaysia. In: Okuda, T., Manokaran, N., Matsumoto, Y., Niiyama, K., Thomas, S.C., Ashton, P.S. (Eds.), Pasoh: Ecology of a Lowland Rain Forest in Southeast Asia. Springer, Tokyo, pp. 73–88.

Valentini, R., Matteucci, G., Dolman, A.J., Schulze, E.-D., Rebmann, C., Moors, E.J., Granier, A., Gross, P., Jensen, N.O., Pilegaard, K., Lindroth, A., Grelle, A., Bernhofer, C., Grünwald, T., Aubinet, M., Ceulemans, R., Kowalski, A.S., Vesala, T., Rannik, Ü., Berbigier, P., Loustau, D., Guðmundsson, J., Thorgeirsson, H., Ibrom, A., Morgenstern, K., Clement, R., Moncrieff, J., Montagnani, L., Minerbi, S., Jarvis, P.G., 2000. Respiration as the main determinant of carbon balance in European forests. Nature 404, 861–865.

Webb, E.K., Pearman, G.I., Leuning, R., 1980. Correction of flux measurements for density effects due to heat and water vapour transfer. Q. J. R. Meteorol. Soc. 106, 85–100.

Yamashita, T., Kasuya, N., Wan Rasidah, K., Sumaimi Wan, C., Quah, E.S., Okuda, T., 2003. Soil and belowground characteristics of Pasoh Forest Reserve. In: Okuda, T., Manokaran, N., Matsumoto, Y., Niiyama, K., Thomas, S.C., Ashton, P.S. (Eds.), Pasoh: Ecology of a Lowland Rain Forest in Southeast Asia. Springer, Tokyo, pp. 89–109.

Yasuda, Y., Ohtani, Y., Watanabe, T., Okano, M., Yokota, T., Liang, N., Tang, Y., Abdul Rahim, N., Tani, M., Okuda, T., 2003. Measurement of CO_2 flux above a tropical rain forest at Pasoh in Peninsular Malaysia. Agric. For. Meteorol. 114, 235–244.

Tellus (2008), 60B, 569–582
Printed in Singapore. All rights reserved

TELLUS

Vertical profiles and storage fluxes of CO_2, heat and water in a tropical rainforest at Pasoh, Peninsular Malaysia

By SHINJIRO OHKUBO[1]*, YOSHIKO KOSUGI[1], SATORU TAKANASHI[2], NAOKO MATSUO[3], MAKOTO TANI[1] and ABDUL RAHIM NIK[4], [1]*Graduate School of Agriculture, Kyoto University, Kyoto 606-8502, Japan;* [2]*Forestry and Forest Products Research Institute, Tsukuba, Ibaraki 305-8687, Japan;* [3]*Faculty of Bioresources, Mie University, Tsu, Mie 514-8507, Japan;* [4]*Forest Research Institute Malaysia, Kepong, Kuala Lumpur 52109, Malaysia*

(Manuscript received 8 November 2007; in final form 27 April 2008)

ABSTRACT

Ambient CO_2 concentration, air temperature and relative humidity were measured intermittently for a 3-year period from the floor to the canopy top of a tropical rainforest in Pasoh, Peninsular Malaysia. Mean diurnal CO_2 storage flux (S_c; μmol m^{-2} s^{-1}) and sensible and latent heat storage fluxes (Q_a and Q_w; W m^{-2}) ranged from −12.7 to 3.2 μmol m^{-2} s^{-1}, −15 to 27 W m^{-2} and −10 to 20 W m^{-2}, respectively. Small differences in diurnal changes were observed in S_c and Q_a between the driest and wettest periods. Compared with the ranges of mean diurnal CO_2 eddy flux (−14.7 to 4.9 μmol m^{-2} s^{-1}), sensible eddy flux (−12 to 169 W m^{-2}) and latent eddy flux (0 to 250 W m^{-2}), the contribution of CO_2 storage flux was especially large. Comparison with summertime data from a temperate Japanese cypress forest suggested a higher contribution of S_c in the tropical rainforest, probably mainly due to the difference in nighttime friction velocity at the sites. On the other hand, differences in Q_a and Q_w were smaller than the difference in S_c, probably because of the smaller nighttime sinks/sources of heat and water vapour.

1. Introduction

Globally, the most important interactions between terrestrial ecosystems and the atmosphere include energy, water and carbon transfers. The magnitudes of these exchange processes vary with climate and vegetation. Eddy covariance is one of the best meteorological methods for evaluating CO_2 and energy exchanges between forests and the atmosphere. However, this method has been widely reported as unreliable for estimating CO_2 exchange between forests and the atmosphere at night (e.g. Law et al., 1999; Baldocchi, 2003). Eddy covariance generally underestimates nighttime CO_2 emission from forests (i.e. ecosystem respiration). Energy exchange imbalance has also been reported at many forest sites (Wilson et al., 2002). To overcome these problems, we must clarify the processes of CO_2 and energy exchanges between forests and the atmosphere. Generally, CO_2 and energy exchanges between a forest and the atmosphere consist of three components: eddy flux; storage flux and mass flow—arising from horizontal flow convergence/divergence or a non-zero mean vertical velocity at the observation height (e.g. Lee, 1998). Recently, horizontal and vertical advective CO_2 fluxes have been estimated by observing wind speed and CO_2 concentration spatially at many points with numerous instruments (Sun et al., 2007; Feigenwinter et al., 2008). They showed the characteristics of the advective CO_2 fluxes and indicated that the contributions of advective fluxes to CO_2 exchange were not negligible, although detailed investigations are needed for more accurate estimation. Storage fluxes of CO_2, sensible heat and latent heat also cannot be ignored, especially for closed forests with a tall canopy. In the absence of advection, the daily net storage of CO_2, sensible heat and latent heat in the air column should be roughly zero. Over the course of a day or more, stored CO_2, sensible heat and latent heat change very little; however, under some conditions, large contributions of these storage fluxes may occur over shorter time scales and should be evaluated to assess their contributions to eddy fluxes. Within the air space of such a forest, the meteorological environment varies from the floor to

---

[*] Corresponding author.
e-mail: shinjiro@kais.kyoto-u.ac.jp

DOI: 10.1111/j.1600-0889.2008.00367.x

the canopy top, and vertical profiling is a very important method for evaluating storage fluxes and understanding the process of gas exchange.

By measuring the CO_2 concentration ([CO_2]) at several heights, vertical concentration (μmol m^{-3}) profiles and CO_2 storage flux (S_c; μmol m^{-2} s^{-1}) estimates have been made for a number of forest types (e.g. Brooks et al., 1997; Jarvis et al., 1997; Hollinger et al., 1998; Malhi et al., 1998; Dolman et al., 2002; Kondo et al., 2005; Ohkubo et al., 2007). Similarly, by measuring the air temperature and relative humidity at several heights, sensible and latent heat storage flux (Q_a and Q_w, respectively; W m^{-2}) estimates have been made in a several kinds of forests (e.g. McCaughey and Saxton, 1988; Vogt et al., 1996; Silberstein et al., 2001; Turnipseed et al., 2002; Oliphant et al., 2004).

A great deal of gas exchange is thought to occur in tropical rainforests. Despite the importance of such exchanges, however, few studies have continuously measured the stored CO_2, sensible heat and latent heat fluxes in tropical rainforests, coupled with eddy flux measurements above the canopy. Massive stores of CO_2, heat and water are thought to exist in tropical rainforests due to the warm temperature, generous year-round incoming radiation and large quantity of biomass. Moreover, tropical rainforests are structurally complex, with tall canopies, and their environmental factors vary from the forest floor to canopy top. Thus, much more information is needed to understand the exchange of CO_2, sensible heat and latent heat within the tropical region. Previous studies of storage fluxes in Southeast Asian tropical rainforests have mainly relied on short-term measurements collected at only two sites: Lambir Hills National Park in Sarawak, Malaysia (H_c, 50–60 m; leaf area index, LAI, 5.1) and the Pasoh Forest Reserve (PSO) in Peninsular Malaysia (H_c, 35–45 m; LAI, 6.52). Kumagai et al. (2001) described the micrometeorological conditions in a forest canopy at Lambir Hills National Park, using measurements of several environmental factors, including global solar radiation, wind speed, air temperature, humidity and [CO_2] above and within the canopy, which were collected for a week. Similarly, in PSO, Aoki et al. (1975) measured environmental factors over a several-day period to study the micrometeorology and primary production of the forest, whereas Yasuda et al. (2003) used data collected over a 3-d period to produce a six-level [CO_2] profile to estimate CO_2 storage flux and net ecosystem exchange (NEE). Clearly, long-term observation of these storage parameters is needed to understand the process of each element's formation under various conditions.

In this study, we profiled [CO_2], air temperature and relative humidity at 8 or 10 heights intermittently for 2 or 3 yr, concomitantly with eddy covariance measurements over the canopy to clarify the diurnal and seasonal patterns of vertical profiles and storage fluxes, changes in the storage fluxes under various meteorological conditions and the contribution of the storage fluxes to CO_2 and energy exchanges.

2. Materials and methods

2.1. Site description

The study site is located in the PSO near Simpang Pertang at Negri Sembilan in Peninsular Malaysia (2°58′N, 102°18′E). The core area (600 ha) of the reserve (2450 ha) is covered with a primary lowland mixed dipterocarp forest (tropical evergreen broadleaved forest) that includes various species of *Shorea* and *Dipterocarpus*. The continuous canopy height is approximately 35 m, although some emergent trees exceed 45 m. The LAI, estimated from tree-diameter measurements (Niiyama, unpublished), is 6.52. The topography in the forest is gently undulating. There are two rainy seasons in the region (March–May and October–December), brought by the southwestern and northeastern monsoons, respectively. Seasonal rainfall fluctuations have been described by Noguchi et al. (2003) and Kosugi et al. (2008). From 2003 to 2005, the average annual air temperature at 52 m was 26.2 °C and the mean annual precipitation was 1739 mm.

2.2. Measurements

Eddy fluxes of CO_2, sensible heat and latent heat were measured by the eddy covariance method at a height of 54 m from an observation tower. The wind speed and temperature were measured with a three-axis sonic anemometer (SAT-550, Kaijo, Tokyo, Japan), and the concentrations of CO_2 and H_2O were monitored with an open-path infrared gas analyzer (IRGA; LI-7500, LI-COR, Inc., Lincoln, NE, USA). The data were sampled at 10 Hz and sent to a data logger (CR-5000, Campbell Scientific, Logan, UT, USA). Detailed descriptions of the eddy covariance measurements have been provided by Kosugi et al. (2008). Downward short-wave radiation was monitored from the observation tower at a height of 52 m (MR22, EKO, Tokyo, Japan). Soil water contents at depths of 0.1, 0.2 and 0.3 m (CS515, Campbell Scientific) were monitored with nine sensors at three points around the tower. Vertical profiles of air temperature and relative humidity were made at eight levels (1, 5, 10, 20, 30, 40, 45 and 53 m) using ventilated temperature and relative humidity sensors (HMP45A and HMP45C, Vaisala, Boulder, CO, USA). The air temperature and relative humidity at the site have been under continuous observation since March 2003. Other meteorological observations, described by Kosugi et al. (2008), were logged every 10 min using three data loggers (CR-10X, Campbell Scientific).

We used an IRGA and an automated profiling system (HT-CT-P; Hydrotech, Shiga, Japan) to produce the [CO_2] profile. Air samples for [CO_2] measurement were drawn continuously at a flow rate of 2000 ml min^{-1} through a 4-mm internal diameter polyethylene tube at each inlet from ten levels (0.2, 0.5, 1, 2, 5, 10, 20, 30, 45 and 53 m) by a closed-path IRGA (LI-7000, LI-COR, Inc.). The IRGA was located in an observation house on the forest floor. The profile system sampled an entire profile every 5 min. Depending on the measuring height, 12 to 35 s were allowed to flush the tubing of residual air before sampling with the IRGA. We selected the purging time based on a pulse test of high-concentration CO_2 through a tube. The IRGA was automatically calibrated daily, using zero concentration gas (N_2). We conducted continuous short-term [CO_2] profile measurements several times a year for terms of several weeks to 1 month. We replaced the IRGA after every observation term and checked the zero and span of CO_2 at the beginning and end of each observation term. Data collected when a serious gap in zero was observed were excluded. In every case, the span was quite stable. Switching between the canopy heights was controlled by a control port module (SDM-CD16AC, Campbell Scientific) and a series of solenoid valves (FAG31-6-4-12C, CKD, Rolling Meadows, IL, USA). The [CO_2] was recorded by a data logger (CR-23X, Campbell Scientific). The basic principles of the profiling system for CO_2 and its accuracy are described in detail in Xu et al. (1999) and Mölder et al. (2000), although some minor parts of their measurement systems are different from ours. The CO_2 profile was measured intermittently from September 2004 to November 2005, a period that included rainy and dry seasons. Occasional system breakdown or trouble with the sensors, mainly caused by thunder, limited the completeness of the profile data available for calculating the storage terms.

2.3. Calculations

Eddy fluxes of CO_2 (F_c, μmol m^{-2} s^{-1}), sensible heat ($\boldsymbol{H}$, W m^{-2}) and latent heat ($\lambda \boldsymbol{E}$, W m^{-2}) over the canopy were calculated with an averaging time of 30 min. The F_c, $\boldsymbol{H}$ and $\lambda \boldsymbol{E}$ in this study showed the eddy covariance fluxes measured over the canopy, not including the storage fluxes. A Webb, Penman and Leuning (WPL) correction for the effect of air density fluctuations (Webb et al., 1980) was applied. Linear trends in temperature, water vapour and CO_2 concentration were not removed, as linear de-trending might cause underestimates of low-frequency flux, which is thought to be large for tall tropical forests with low wind speeds, low turbulent intensity, and thus, large eddies that can transport flux. The influence of linear de-trending can also be assessed by considering the annual integration of CO_2 exchange (Kosugi et al., 2008). Comparison of averaging times of 1 h and 30 min showed that the contribution of the larger scale component was approximately 2.0% (n = 12 094, median; 1-h F_c data were compared with the average of 30-min F_c for 1 h, for data from 2002 to 2005). Although this difference should be accounted for, we used 30 min for the averaging time, because with a 1-h averaging time, a stationarity check showed too many data of poor quality (Kosugi et al., 2008).

The storage fluxes (S_c, Q_a and Q_w) were calculated from the following equations:

$$S_c = \int_0^{Z_r} \left(\frac{\delta c}{\delta t}\right) dz \tag{1}$$

where Z_r, c, t and z represent the height of the eddy flux measurement (m), the [CO_2], the time (s) and the height from the ground (m), respectively. Considering the time from each inlet to the IRGA, we used data from the last 11 s of each cycle. We collected data six times and calculated the average at each height every 30 min:

$$Q_a = \int_0^{Z_r} \rho C_p \left(\frac{\delta T_a}{\delta t}\right) dz \tag{2}$$

where ρ, C_p and T_a are the air density (kg m^{-3}), specific heat (J kg^{-1} K^{-1}) and air temperature (K), respectively. We calculated the average T_a every 30 min. The storage flux Q_w was given by

$$Q_w = \int_0^{Z_r} \left(\frac{\rho C_p}{\Gamma}\right)\left(\frac{\delta e}{\delta t}\right) dz \tag{3}$$

where Γ and e are the psychrometric constant (hPa K^{-1}) and water vapour pressure (hPa), respectively. The values of $\delta c/\delta t$, $\delta T_a/\delta t$ and $\delta e/\delta t$ were calculated by dividing 30 min into the difference in 30-min mean c, T_a and e between the beginning and end of each 30-min run. We assumed that c, T_a and e varied linearly between the measurement points. Finally, we determined each storage flux by calculating $\delta c/\delta t$, $\delta T_a/\delta t$ and $\delta e/\delta t$ from the differences between the averaged values for c, T_a and e, respectively, every 30 min. A previous study estimated that the biomass heat storage in the study forest ranges from -10 to 15 W m^{-2} based on short-term stem temperature and heat-plate measurements. Lamaud et al. (2001) reported that the energy fixed by photosynthesis represents only 1–3% of the incident net radiation at the canopy scale. Although these terms can sometimes be significant, we did not deal with them in this study.

Recently, Finnigan (2006) showed that for accuracy, the storage flux should be calculated using the difference between the volume mean scalar at the beginning and end of each run. To assess the difference between the two methods, we also calculated CO_2 concentration at each height every 5 and 15 min and calculated CO_2 storage fluxes (S_{c5} and S_{c15}, μmol m^{-2} s^{-1}) every 30 min by averaging the results of six and two runs, respectively. We also compared these storage fluxes (S_{c5} and S_{c15}) with S_c (Fig. 1). The data were divided by u_*. The relationships between S_c and S_{c5} and S_{c15} seem to be approximately 1:1, although some dispersion was observed. In addition, open circles representing high u_* seemed to be concentrated near the 1:1 lines. Large differences between S_c and S_{c5} and S_{c15} were seen when S_c was large and u_* was small during nighttime (data not shown). The indices of dispersion $\frac{\sum (S_c - S_{c5})^2}{N}$ and $\frac{\sum (S_c - S_{c15})^2}{N}$ (N is the number of data) were 45.2 and 28.4 with small u_* (<0.4 m s^{-1}) and 9.7 and 4.8 with large u_* ($\geq$0.4 m s^{-1}), respectively. These values indicate that data averaged over a short time might be influenced by horizontal heterogeneity in the CO_2 concentration; strong air mixing decreases the heterogeneity. In this study, we adopted a 30-min averaging time because short-time-averaged data might be biased by a single gust. For the period from 0:00 to 0:30, we averaged the [CO_2] data from 0:05 to 0:30, because the IRGA

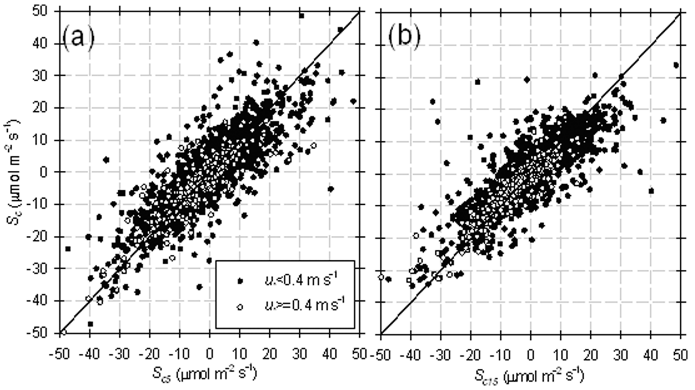

Fig. 1. Relationship between S_c and S_{c5} (a) and S_{c15} (b). We classified the data as small u_* (<0.4 m s^{-1}; solid circles) and large u_* ($\geq$0.4 m s^{-1}; open circles). The lines indicate a 1:1 relationship.

Table 1. The ratio of the number of available 30-min data to the whole period for each month for S_c and Q_a and Q_w (%)

		Jan	Feb	Mar	Apr	May	Jun	Jul	Aug	Sep	Oct	Nov	Dec
2003	S_c	–	–	–	–	–	–	–	–	–	–	–	–
	Q_a, Q_w	–	–	–	–	–	–	–	30	100	61	–	48
2004	S_c	–	–	–	–	–	–	–	–	21	90	28	100
	Q_a, Q_w	100	100	40	34	100	79	–	–	–	–	–	–
2005	S_c	40	48	72	–	–	21	8	–	–	42	25	–
	Q_a, Q_w	–	–	–	–	–	–	98	100	98	62	73	–

was calibrated from 0:00 to 0:05 every day. Table 1 shows the ratio of the number of available 30-min data points to the whole period for each month.

We compared the data from this study with results from the Kiryu Experimental Watershed in a temperate Japanese cypress forest in Shiga Prefecture, Japan (34°58′N, 136°00′E). From 2004 to 2006, the Kiryu site had an average annual air temperature of 13.3 °C and mean annual precipitation of 1599 mm. The canopy height was 19 m and the LAI ranged from 4.5 to 5.5, with little fluctuation. The area around the observation tower tended to mildly incline at approximately 9.2°. The CO_2 concentration was measured at five heights (0.3, 1, 4, 14 and 20 m), and air temperature and relative humidity were measured at six heights (1, 4, 10, 14, 20 and 28 m). The measurement system and calculation method were almost the same as in this study. Reports by Ohkubo et al. (2007) and Ohkubo and Kosugi (2008) provide further details.

3. Results and discussion

3.1. Seasonal changes in storage fluxes

We calculated the mean diurnal changes in S_c, Q_a and Q_w by averaging all acquired data in every 30-min period for each month. During rain, we could obtain storage-flux data but not eddy-flux data because drops of water became attached to the lens of the IRGA probe (Li-7500). Figures 2–4 show the monthly mean diurnal changes in S_c, Q_a and Q_w, respectively. The plots show some scattering, which could be due to the small number of data (Table 1). As indicated in these figures, none of the storage fluxes showed large seasonal fluctuation. To investigate the seasonality of storage fluxes in detail, we compared the mean diurnal variations of storage fluxes with meteorological factors in the driest and wettest periods.

Figure 5 shows the mean diurnal variations of rainfall (a), solar radiation (b), air temperature at 53 m (c), vapour pressure deficit at 53 m (d), S_c (e), Q_a (f) and Q_w (g) in the driest and wettest periods during the observation. We selected the driest period data from days with the small volumetric soil water content (the daily average value from nine total sensors at 0.1, 0.2 and 0.3 m depths, <0.22 m^3 m^{-3}) during the dry season and the wettest period data from days with large volumetric soil water content ($\geq$0.33 m^3 m^{-3}) during the rainy season. During the rainy season, it usually rained from afternoon until midnight. Rain and low solar radiation seldom occurred continuously all day long. Mean daily rainfall in the driest and wettest period were 0.9 and 12.7 (mm d^{-1}), respectively. Solar radiation values were similar in the early morning in the driest and wettest periods, but daily solar radiation in the wettest period (14.2 MJ d^{-1}) was smaller than that in the driest period (19.1 MJ d^{-1}). The diurnal amplitudes of air temperature and water vapour pressure deficit in the wettest period (5.6 °C and 7.3 hPa, respectively) were smaller than those in the driest period (7.3 °C and 8.9 hPa, respectively). The difference of air temperature and vapour pressure deficit

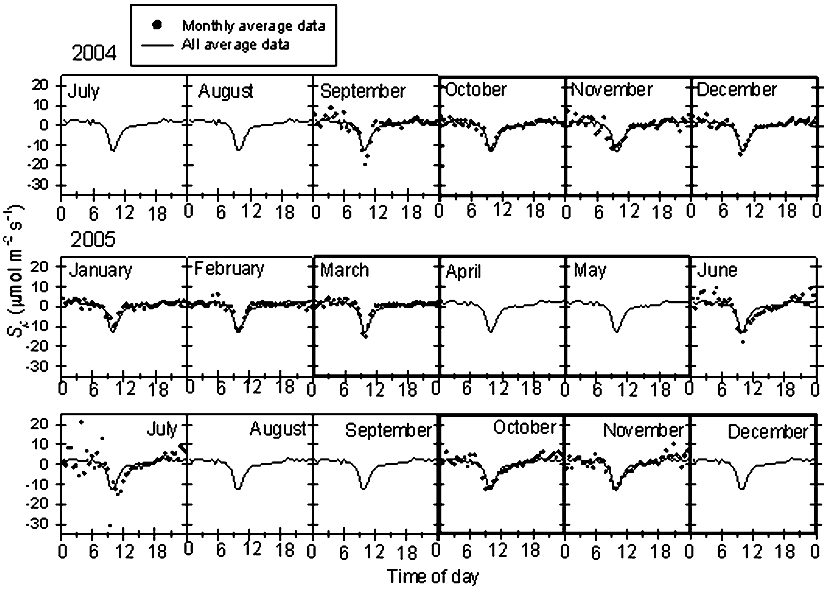

Fig. 2. Monthly ensemble averages of half-hourly values of S_c. Solid circles show the averaged value for each month, and the solid line indicates the averaged value for all available data. The rainy seasons (March to May and October to December) are enclosed by a thick line.

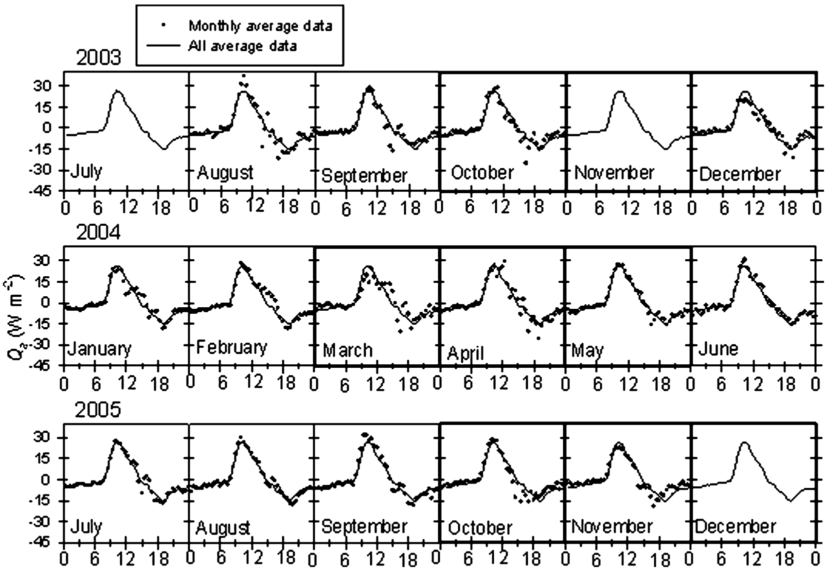

Fig. 3. Monthly ensemble averages of half-hourly values of Q_a. Solid circles show the averaged value for each month, and the solid line indicates the averaged value for all available data. The rainy seasons (March to May and October to December) are enclosed by a thick line.

between the wettest and driest periods became small in the early morning (0.7 °C and 1.3 hPa, respectively) and large in the afternoon (3.5 °C and 4.5 hPa, respectively).

Figure 5e shows that the negative peak of S_c in the wettest period was somewhat closer to zero than that in the driest period; this result may reflect the influence of a slightly smaller photosynthesis rate as a CO_2 sink due to the slightly smaller solar radiation in the wettest period (Fig. 5b). From sunset to midnight (19:00–24:00), the average S_c in the driest period (0.70 μmol m^{-2} s^{-1}) was smaller than that in the wettest period (2.92 μmol m^{-2} s^{-1}). This result corresponds to the nighttime F_c being slightly smaller under the driest condition (Kosugi et al.,

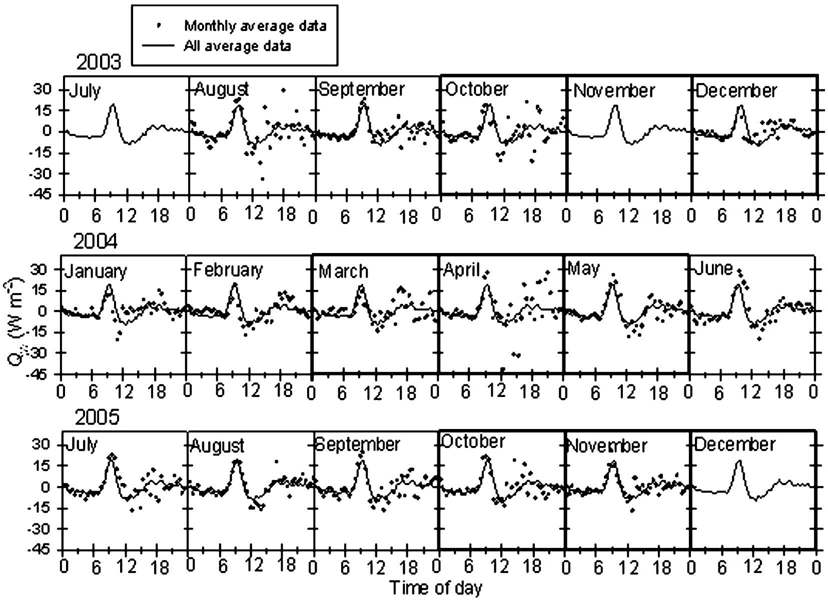

Fig. 4. Monthly ensemble averages of half-hourly values of Q_w. Solid circles show the averaged value for each month, and the solid line indicates the averaged value for all available data. The rainy seasons (March to May and October to December) are enclosed by a thick line.

2008). Kosugi et al. (2008) also reported that the soil respiration rate was low temporally, when the soil was dry. We can assume that the small nighttime S_c was due to the low soil respiration rate in the driest period, which contributed to nighttime ecosystem respiration as a CO_2 source.

In the case of Q_a, the positive peak in the morning, negative peak in the afternoon, and nighttime values in the wettest period were closer to zero than those in the driest period. The diurnal amplitude of Q_a in the wettest period (41.0 W m^{-2}) was smaller than that in the driest period (54.7 W m^{-2}; Fig. 5f), due to the lower solar radiation in the wettest period than in the driest period. On the other hand, no clear difference in the mean diurnal variation in Q_w was observed between the driest and wettest periods, although the plots scattered in the afternoon (Fig. 5g). These results correspond to the finding of no clear seasonal changes in $\lambda \boldsymbol{E}$, although $\boldsymbol{H}$ sometimes fluctuated between the dry and wet periods (Takanashi et al., unpublished).

3.2. Diurnal changes in vertical profiles and storage fluxes

3.2.1. Vertical CO_2 profiles and CO_2 storage fluxes (S_c). Figure 6 shows the mean diurnal variations in S_c, F_c and u_* (a) and the isoline of [CO_2] (b). The arrows indicate the average times of sunrise and sunset; solar noon was around 13:00 at this site. The diurnal variations shown in Fig. 6 were obtained by averaging all available data collected at 30-min intervals. From midnight to sunrise, [CO_2] increased at all heights with low u_* and was highest during the day at sunrise. After sunrise, [CO_2] rapidly decreased with increasing u_*, especially in the lower canopy, thereby reducing the vertical gradient. After 10:00, there was no clear vertical difference in [CO_2], and the concentrations throughout the forest were similar to those in the well-mixed atmosphere above the canopy space, except near the ground. From 13:00 to 18:00, [CO_2] throughout the canopy remained stable. In the afternoon, [CO_2] reached its minimum. Around 20:00, the vertical CO_2 gradient began to build again from the ground, and [CO_2] increased and became vertically stratified within the canopy. At the soil surface, [CO_2] was consistently higher than at any other level within the canopy. The S_c was greater than zero (2.2 μmol m^{-2} s^{-1} on average) at night (20:00–06:00) and dropped below zero after sunrise, whereas F_c remained positive. At 10:00, S_c reached its negative peak (-12.7 μmol m^{-2} s^{-1}), and F_c switched from positive to negative. At sunset, S_c and F_c both became positive. The average S_c over the daily cycle was 0.017 μmol m^{-2} s^{-1}, a value that was not significantly different from zero.

The diurnal vertical profiles of [CO_2] and S_c should be influenced by both air mixing and ecosystem processes. Two mechanisms can explain the rapid transition in [CO_2] after sunrise. First, much of the nocturnally stored CO_2 released during nighttime respiration may be rapidly reabsorbed by photosynthesis after sunrise, since the leaves are dispersed vertically below the canopy in this forest (i.e. there is no trunk space). This study site is located near the equator; so, solar altitude increases drastically and light can penetrate deeply into the canopy as time

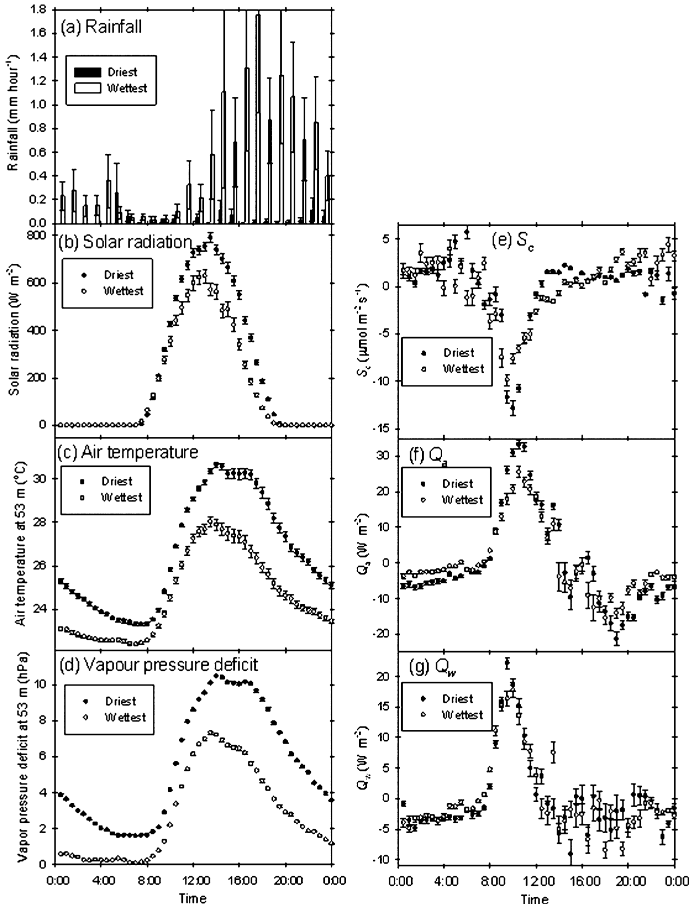

Fig. 5. Mean diurnal variations in rainfall (a), solar radiation (b), air temperature at 53 m (c), vapour pressure deficit at 53 m (d), S_c (e), Q_a (f) and Q_w (g) in the driest and wettest periods during the observation. The driest period data (black bars and solid circles) were selected from days with small volumetric soil water content (<0.22 m^3 m^{-3}, average value from nine total sensors at 0.1, 0.2 and 0.3 m depths) during the dry season, and the wettest period data (white bars and open circles) were selected from days with large volumetric soil water content (≥ 0.33 m^3 m^{-3}) during the rainy season. The error bars represent the standard errors of the means. The number of S_c values for the driest period and wettest period were 13 d (11% of available S_c data) and 23 d (20% of available S_c data), respectively. The numbers of Q_a and Q_w values in the driest period and wettest period were 36 d (11% of available Q_a and Q_w data) and 21 d (6% of available Q_a and Q_w data), respectively.

passes after sunrise. Because there is sufficient light soon after sunrise for photosynthesis to start, [CO$_2$] decreases rapidly. Second, the forest air is mixed and emitted upward from the canopy due to turbulence caused by heating of the air. Thus, u_* rapidly increased after sunrise (Fig. 6). At night, the elevated [CO$_2$] within the canopy was caused by the calm conditions, which trapped respired CO$_2$. After sunrise (around 7:00), [CO$_2$] at 10–30 m began to decrease due to photosynthetic activity. Thirty minutes later, [CO$_2$] at 0.2–5 m began to decrease. This time lag might have been due to tall trees and dense vegetation blocking light from reaching lower heights just after sunrise; thus, CO$_2$ emission from the soil may have strongly affected [CO$_2$] at lower heights. Then, [CO$_2$] at 45–53 m began to decrease. Two reasons might explain such a late decrease in [CO$_2$]. One is that there was no photosynthesis uptake above the canopy. The other is that [CO$_2$] below the canopy was still higher than [CO$_2$] above the canopy and increasing air mixing still increased [CO$_2$] above the canopy. For that reason, at 09:00, F_c was still positive whereas S_c was negative. This negative–positive difference implies that early-morning photosynthesis was not detected over the canopy by the eddy covariance measurement. The daytime [CO$_2$] was considerably lower than the nighttime [CO$_2$] because photosynthetic uptake of CO$_2$, which was greater than respiratory CO$_2$ emission and air mixing, occurred during the day, whereas respiratory efflux and accumulation of CO$_2$ by plants and soil occurred at night. The elevated [CO$_2$] near the forest floor suggests that gentle air mixing and soil respiration, which represent a large share of the respiration in the ecosystem, significantly influence this period. Larger amplitude has been found near the crown in tropical rainforests (e.g. Aoki et al., 1975; Kumagai et al., 2001), including at our site, than in other forest types (e.g. Brooks et al., 1997; Jarvis et al., 1997; Hollinger et al., 1998; Dolman et al., 2002; Kondo et al., 2005).

3.2.2. *Vertical air temperature profiles and sensible heat storage fluxes (Q_a).*

Figure 7 shows the mean diurnal variations in Q_a, $\boldsymbol{H}$ and u_* (a) and the air temperature isoline (b). At night, the air temperature decreased due to radiative cooling from the forest floor to the top of the canopy. At 07:30, the air temperature reached its minimum at every height; air temperature then reached its maximum at

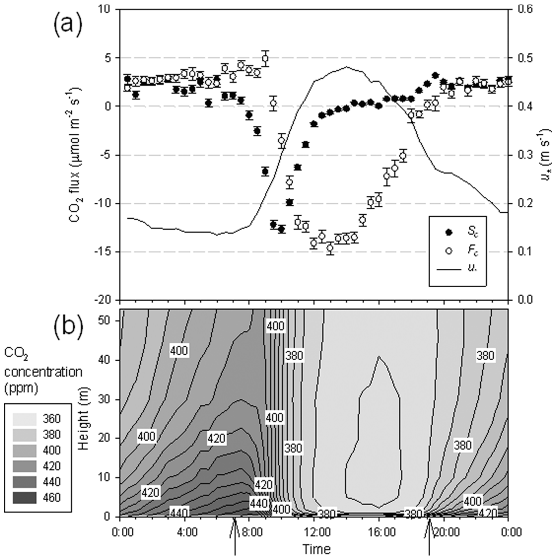

Fig. 6. (a) Mean diurnal variations in S_c (solid circles), F_c (open circles) and u_* (line), based on all available data (141 d). The error bars represent the standard errors of the means. (b) Isoline of the average CO2 concentration distributions within the canopy as a function of height and time of day ($N = 141$ d). Isolines are indicated every 5 ppm. The arrows on the x-axis represent the average times of sunrise (ranging from 06:54 to 07:25) and sunset (ranging from 18:55 to 19:26) throughout the year.

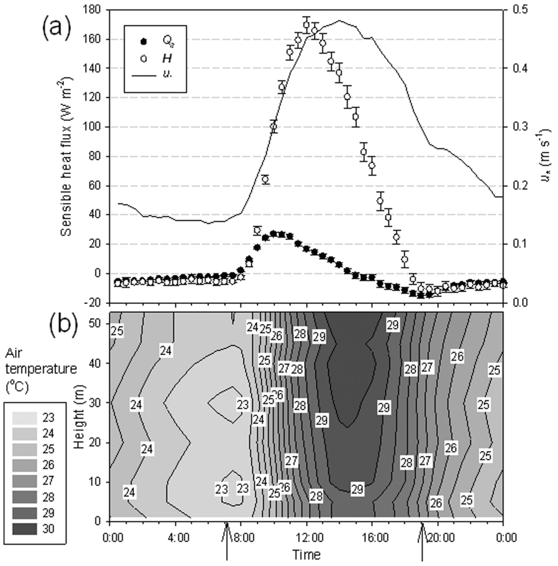

Fig. 7. (a) Mean diurnal variations in Q_a (solid circles), $\boldsymbol{H}$ (open circles) and u_* (line), based on all available data (336 d). The error bars represent the standard errors of the means. (b) Isoline of the average air temperature distributions within the canopy as a function of height and time of day ($N = 336$ d). Isolines are indicated every 0.5 °C. The arrows are as given in Fig. 6.

14:30 at all heights. The amplitude of the diurnal change in air temperature at 53 m (6.5 °C) was larger than that at 1 m (5.6 °C). The values of Q_a and $\boldsymbol{H}$ were negative at night but became positive after sunrise as the air temperature increased. This rapid increase after sunrise is due to light deeply entering the canopy, as discussed in the previous section. The positive peak of Q_a (27 W m^{-2}) occurred at 10:00, while $\boldsymbol{H}$ reached its positive peak (169 W m^{-2}) at noon. In the afternoon, Q_a dropped below zero as the air temperature decreased. Just before sunset, $\boldsymbol{H}$ also became negative, even as Q_a reached its negative peak (-15 W m^{-2}) at 19:00. The average Q_a over the daily cycle was 0.00029 W m^{-2}, a value that can be regarded as zero.

The deep penetration of light into the forest accounts for the amplitude difference in air temperature being small between the top (53 m) and bottom (1 m) of the forest. The diurnal pattern of Q_a (i.e. a positive peak for Q_a in the morning and negative peak in the afternoon) is similar to the patterns found at several other sites in various forest types (e.g. McCaughey and Saxton, 1988; Vogt et al., 1996; Silberstein et al., 2001; Turnipseed et al., 2002; Oliphant et al., 2004).

3.2.3. *Vertical water vapour pressure profiles and latent heat storage fluxes (Q_w).*

Figure 8 shows the mean diurnal variations in Q_w, $\lambda\boldsymbol{E}$ and u_* (a) and the average water vapour pressure isoline (b). The water vapour pressure decreased at all heights from midnight to sunrise, but increased rapidly after sunrise. Beginning at midday, the water vapour pressure decreased from 10:30 to 15:30, after which time it increased until midnight. This bimodal diurnal variation was observed everywhere except near the forest floor. The water vapour pressure near the forest floor was consistently higher than at any other level. Bimodal fluctuation was also found for Q_w due to the bimodal fluctuation in water vapour pressure. From 20:00 to 00:30, Q_w and $\lambda\boldsymbol{E}$ were both positive, while from 00:30 to 06:00, Q_w was negative and $\lambda\boldsymbol{E}$ was positive. After sunrise, Q_w became positive, peaking (20 W m^{-2}) at 09:30, while $\lambda\boldsymbol{E}$ reached its positive peak (250 W m^{-2}) at 13:00 and then decreased until again becoming positive in the evening. The average Q_w over the daily cycle was 0.014 W m^{-2}. Similarly to Q_a, this value can be considered zero.

Bimodal variation in Q_w depended on the $\delta e/\delta t$ at each height. Diurnal changes in the daytime water vapour pressure profile and Q_w were mainly controlled by the balance between the transpiration rate and the level of air mixing. The water vapour pressure increased from 07:30 at all levels because of the start of transpiration and low air mixing condition. It then decreased from 10:00 above the canopy (at 40–53 m), as the level of air mixing increased by the transport of water vapour upward from the canopy. Further decreases in the water vapour pressure were observed at 20–30 m from 10:30 and at 5–10 m from 11:00. The time lag reflects differences in the air mixing condition, which was weak at lower levels. In the afternoon, water vapour

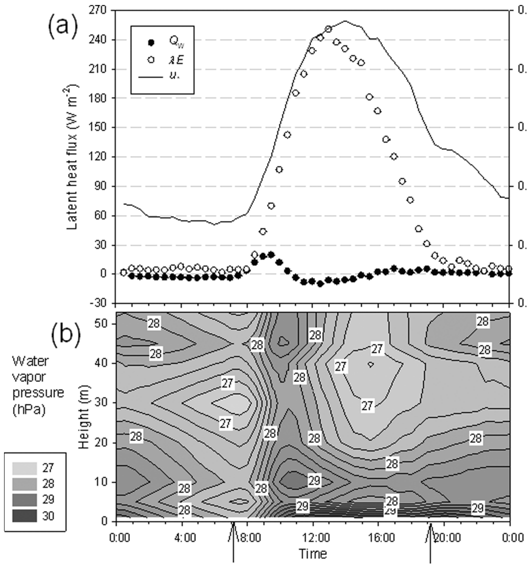

Fig. 8. (a) Mean diurnal variations in Q_w (solid circles), $\lambda \boldsymbol{E}$ (open circles) and u_* (line) based on all available data (336 d). The error bars represent the standard errors of the means. (b) Isoline of the average water vapour pressure distributions within the canopy as a function of height and time of day ($N = 336$ d). Isolines are indicated every 0.25 hPa. The arrows are as given in Fig. 6.

pressure except at 1 m started to increase due to decreasing u_*. After sunset, the evapotranspiration rate dropped, and water vapour pressure at 1 m began to decrease. At 1 m, air mixing was weak all day long, and the evapotranspiration rate mainly controlled the water vapour pressure.

Oliphant et al. (2004) also reported two positive peaks in the diurnal profile of Q_w in a temperate deciduous forest in summer. On the other hand, Q_w showed no clear bimodal diurnal variation at other sites (e.g. McCaughey and Saxton, 1988; Vogt et al., 1996; Silberstein et al., 2001; Turnipseed et al., 2002). The differences may be due to the smaller number of levels (e.g. three) and shorter observation periods used in those studies.

3.3. Differences in the storage fluxes under various meteorological conditions

Turbulent mixing and the source/sink intensity (i.e. respiration and photosynthesis, in the case of CO_2) govern the dynamics of CO_2 within a forest canopy (Brooks et al., 1997). These factors also govern the dynamics of sensible and latent heat storage fluxes. Solar radiation strongly influences photosynthesis and transpiration; therefore, solar radiation is a good index of the sources/sinks of CO_2, sensible heat and latent heat. Solar radiation also makes up a large part of the net radiation and is thus the main energy source for heat fluxes. We investigated how u_*, which is an index of turbulent mixing, and solar radiation influenced the storage fluxes S_c, Q_a and Q_w at this site.

Figure 9 shows the transition of S_c, Q_a and Q_w with u_* in panels I, II and III, respectively. Ensemble-averaged storage fluxes and eddy fluxes for each u_* range during the day and at night are shown in panels (a) and (b), respectively. The ensemble mean diurnal variations in the vertical [CO_2] profile were classified into two patterns based on the average u_* at night (Fig. 10). Similarly, the ensemble mean diurnal variations in S_c and F_c (a), Q_a and $\boldsymbol{H}$ (b) and Q_w and $\lambda \boldsymbol{E}$ (c) were classified into two patterns by the daily accumulated solar radiation patterns (Fig. 11).

Figure 9I-a, shows that the negative value of S_c approached zero as u_* increased during the day, whereas F_c decreased except when the range of u_* was very low. On the other hand, panel I-b shows that the positive value of S_c approached zero as u_* increased at night, whereas F_c increased. At night, CO_2 is emitted throughout the forest and turbulence with a high u_* value accelerates the upward emission of CO_2 from the canopy. This leads to a decrease in S_c and an increase in F_c with increasing u_* (Fig. 9I-b). As shown in Fig. 10, when the nighttime u_* was high, [CO_2] was lower than that at low u_*, especially at the lower levels. In daytime, there were no clear differences between the two accumulated daily solar radiation patterns of S_c, although the negative peak of S_c with small solar radiation was slightly closer to zero than that with large solar radiation (Fig. 11a). At this site, canopy photosynthesis and stomatal conductance did not differ between sunny and cloudy days and showed an obvious trend of decline from late morning and in the afternoon, irrespective of whether it was a sunny or cloudy day or the rainy or dry season (Takanashi et al., 2006; Kosugi et al., 2008). Thus, differences in solar radiation at this site had no obvious influence on either F_c or S_c.

Panels II-a and III-a of Fig. 9 show that Q_a and Q_w decreased with increasing u_* during the day, in contrast to the increases in $\boldsymbol{H}$ and $\lambda \boldsymbol{E}$, whereas panels II-b and III-b of Fig. 9 demonstrate that at night Q_a and Q_w were not obviously influenced by u_*. During the day, as u_* increased, Q_a and Q_w decreased while $\boldsymbol{H}$ and $\lambda \boldsymbol{E}$ increased because the turbulence above the canopy promoted the release of heat and water stored in the forest. Values of Q_a and Q_w were unaffected by increases in u_* at night, when there were no notable sinks or sources; thus vertical gradients of air temperature and water vapour pressure did not form. The diurnal amplitudes of Q_a and Q_w with larger solar radiation were larger than those with smaller solar radiation (Figs. 11b and c).

These results indicate that air mixing at night controlled the large contribution of S_c to the exchange of CO_2 between the forest and the atmosphere but did not greatly influence Q_a and Q_w. On the other hand, larger solar radiation led to larger diurnal amplitudes of Q_a and Q_w, but did not largely influence S_c. This difference in daytime coincided with that of eddy covariance fluxes measured over the canopy.

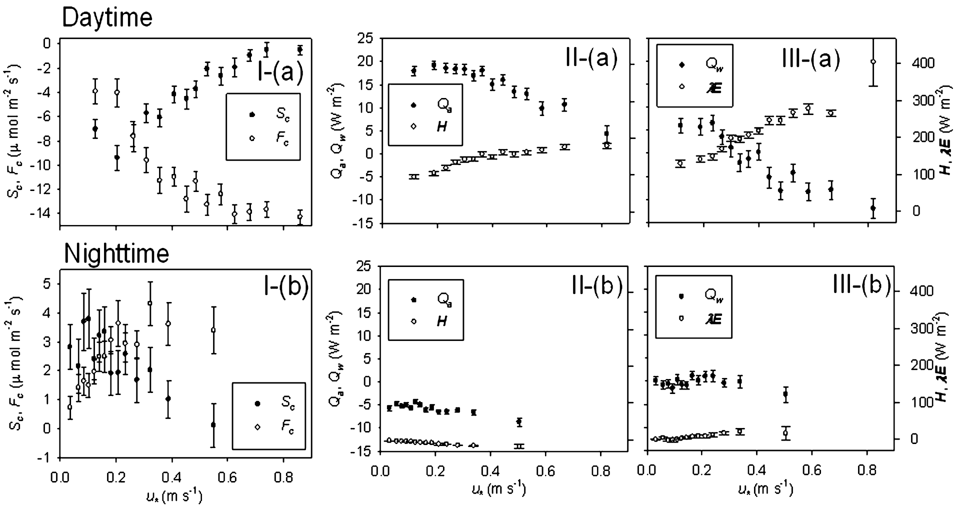

Fig. 9. Storage fluxes S_c (I), Q_a (II) and Q_w (III) (solid circles) and eddy fluxes F_c (I), $\boldsymbol{H}$ (II) and λE (III) (open circles) for each u_* range. The upper panels show daytime (09:00–15:00) data (a) and the lower panels show nighttime (21:00–03:00) data (b). The error bars represent the standard errors of the means.

(a) Low nighttime u_*

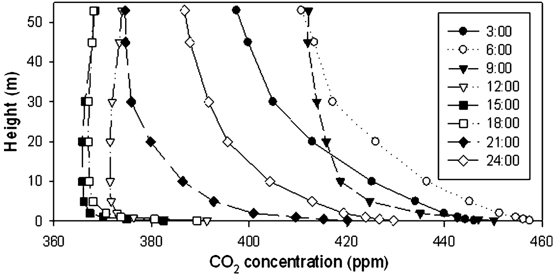

(b) High nighttime u_*

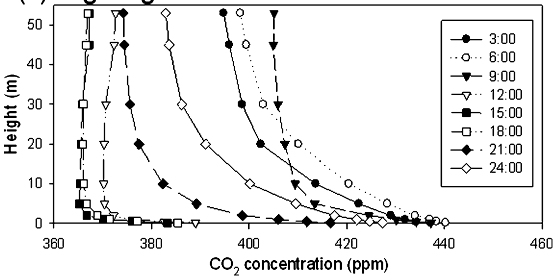

Fig. 10. Mean diurnal variations in the vertical profiles of the CO$_2$ concentration for two nighttime u_* patterns. We classified the patterns by the average u_* at night (00:00–06:00) into (a) <0.15 m s^{-1} versus (b) ≥0.15 m s^{-1}. The number of data points in (a) and (b) are 40 and 50, respectively. The [CO$_2$] profiles are based on measurements taken every 3 h.

3.4. Contribution of storage fluxes to the exchange of CO$_2$ and energy

Although storage fluxes (especially Q_a and Q_w) had a diurnal mean close to zero, they could contribute significantly to the exchange of CO$_2$ and energy on a half-hourly basis. The negative peak of the mean diurnal change in S_c (-12.7 μmol m^{-2} s^{-1}) corresponded to 86% of the negative peak of F_c (Fig. 6). Figure 6a shows that the nighttime respiratory efflux of CO$_2$ from the forest floor and the standing biomass were considerably underestimated by F_c alone. On average, the nocturnal (i.e. 20:00–06:00) value of S_c (2.2 μmol m^{-2} s^{-1}) was roughly half of the value of $F_c + S_c$ (4.7 μmol m^{-2} s^{-1}). The contribution ratio of S_c to $F_c + S_c$ ranged from -419 to 370%. The contribution became large when $F_c + S_c$ approached zero just after sunrise and before sunset. After sunrise, the contribution ratio of S_c to $F_c + S_c$ decreased with increasing $F_c + S_c$ and eventually became nearly zero.

The positive peaks of Q_a (27 W m^{-2}) and Q_w (20 W m^{-2}) were 16 and 7.8% of the positive peaks of $\boldsymbol{H}$ and λE, respectively (Figs. 7 and 8). The contribution ratios of Q_a and Q_w to $\boldsymbol{H} + \lambda E + Q_a + Q_w$ ranged from -152 to 273% and -33 to 90%, respectively, and the contribution became large when $\boldsymbol{H} + \lambda E + Q_a + Q_w$ was small during nighttime. Contributions of Q_a and Q_w were about half of $\boldsymbol{H} + \lambda E + Q_a + Q_w$ from midnight to sunrise. After sunrise, the contribution ratios of Q_a and Q_w decreased with increasing $\boldsymbol{H} + \lambda E + Q_a + Q_w$ and approached zero. Wilson et al. (2002) reported that the energy balance

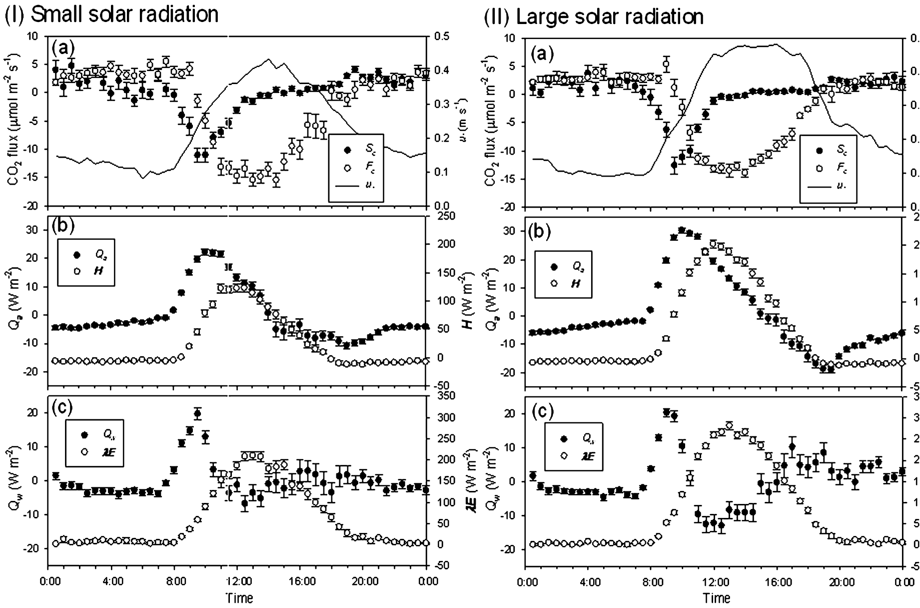

Fig. 11. Mean diurnal variations in u_* and the storage fluxes (S_c, F_c, Q_a, $\boldsymbol{H}$, Q_w and $\lambda\boldsymbol{E}$) for two daily accumulated solar radiation patterns. Using the solar radiation, we classified the values into patterns I ($<$ 17 MJ d^{-1}) and II ($\geq$ 17 MJ d^{-1}). There were 125 and 170 values in classifications I and II, respectively. (a) Mean diurnal variations in u_* (solid line), S_c (solid circles) and F_c (open circles). (b) Mean diurnal variations in Q_a (solid circles) and $\boldsymbol{H}$ (open circles). (c) Mean diurnal variations in Q_w (solid circles) and $\lambda\boldsymbol{E}$ (open circles). The error bars represent the standard errors of the means.

ratio during nighttime was smaller than that in daytime and that a weak air mixing condition decreased the energy balance ratio. Our results indicate that the contributions of Q_a and Q_w to $\boldsymbol{H} + \lambda\boldsymbol{E} + Q_a + Q_w$ were large during nighttime, and Q_a and Q_w became larger with smaller u_* (Fig. 9). We can assume that Q_a and Q_w are quite important when the energy balance ratio is small, and that other components such as advection would also largely influence the energy balance under such a condition.

To reveal which factors influence the storage fluxes and how, we compared our data from PSO in a tropical rainforest with summertime data from Kiryu Experimental Watershed (KEW) in a temperate Japanese cypress forest (Ohkubo et al., 2007; Ohkubo and Kosugi, 2008). Canopy height at PSO was about twice that at KEW. The LAI at PSO was also slightly larger than that at KEW. Leaves were distributed vertically at PSO whereas the KEW forest had a dense crown and trunk space. Further, KEW was mainly covered by *Chamaecyparis obtusa* Sieb. et Zucc. (Japanese cypress, an evergreen conifer), whereas PSO was covered by a primary forest of lowland mixed dipterocarp (tropical evergreen broadleaved forest), which included various species of *Shorea* and *Dipterocarpus*. The observation system and calculation method for storage fluxes were almost the same at both sites. Thus, we could neglect methodological differences between these two study sites.

Figure 12 presents comparisons of the diurnal variation of the air temperature and water vapour deficit (a), u_* and solar radiation (b), S_c and F_c (c), Q_a and $\boldsymbol{H}$ (d) and Q_w and $\lambda\boldsymbol{E}$ (e) at PSO to those at KEW in summer. Solar noon at PSO was about 1 h later than that at KEW. Air temperatures and water vapour deficit were almost the same at the two sites, ranging from 23.0 to 29.0 °C and 1.1 to 11.4 hPa at KEW and 23.2 to 28.7 °C and 0.7 to 9.7 hPa at PSO, respectively (Fig. 12a). At PSO, u_* was smaller especially during night and early morning and solar radiation was slightly larger than at KEW (Fig. 12b). During nighttime, average S_c from 20:00 to 06:00 at PSO (2.2 μmol m^{-2} s^{-1}) was larger than that from 20:00 to 04:00 at KEW (0.8 μmol m^{-2} s^{-1}; Fig. 12c). The diurnal amplitude of S_c at PSO (15.9 μmol m^{-2} s^{-1}) was about three times larger than that at KEW (4.8 μmol m^{-2} s^{-1}), whereas the diurnal amplitudes of Q_a and Q_w at PSO (42 W m^{-2} and 30 W m^{-2}) were also larger than those at KEW (30 W m^{-2} and 14 W m^{-2}; Figs. 12d and e). The diurnal variations of F_c, $\boldsymbol{H}$ and $\lambda\boldsymbol{E}$ at KEW were similar to those at PSO, although F_c at PSO was slightly smaller than that at KEW.

We assumed that the differences in u_* during nighttime mainly reflected differences in S_c between the two sites, because CO$_2$ emitted by ecosystem respiration would be easily stored under the condition of weak air mixing (low u_*). Negative S_c would also become larger because a large amount of stored CO$_2$ would be released upward from the canopy before sunrise. Meanwhile,

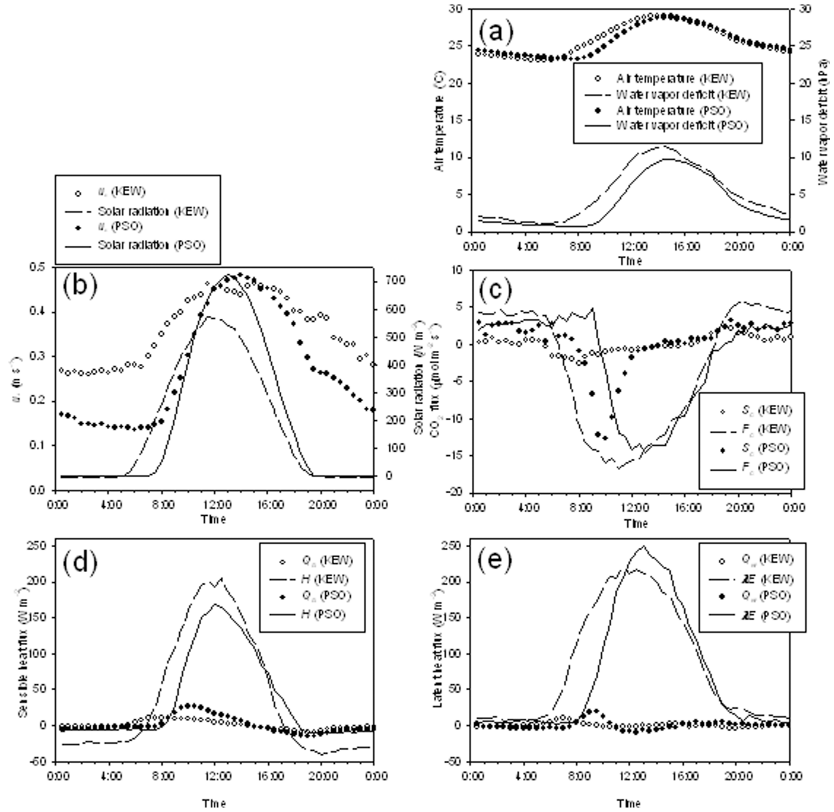

Fig. 12. (a) Diurnal variation in air temperature and water vapour pressure at Kiryu Experimental Watershed (KEW) in a temperate Japanese cypress forest (Ohkubo and Kosugi, 2008; open circles and dashed line) and at the present study site at Pasoh Forest Reserve (PSO) in a tropical rainforest (solid circles and thick line). (b) Diurnal variation in u_* and solar radiation at KEW (open circles and dashed line) and at PSO (solid circles and thick line). (c) Diurnal variation in S_c and F_c at KEW (open circles and dashed line) and at PSO (solid circles and thick line). (d) Diurnal variation in Q_a and $\boldsymbol{H}$ at KEW (open circles and dashed line) and at PSO (solid circles and thick line). (e) Diurnal variation in Q_w and $\lambda \boldsymbol{E}$ at KEW (open circles and dashed line) and at PSO (solid circles and thick line).

the strength of u_* did not seem to have much influence on Q_a and Q_w at night, because sink/source intensity was smaller in the cases of heat and water vapour compared with CO_2.

As also shown in Fig. 12, PSO and KEW had similar nighttime $F_c + S_c$ values in summer. However, we expect that nighttime ecosystem respiration at PSO was larger than that at KEW and that the larger source of CO_2 also somewhat influenced the larger S_c at PSO. Ohkubo et al. (2007) reported that nocturnal $F_c + S_c$ was nearly equal to total ecosystem respiration with high u_* at KEW, whereas Kosugi et al. (2008) reported that $F_c + S_c$ corresponded only to the component of soil respiration estimated with the chamber method, even at a moderate friction velocity ($u_* > 0.2$ m s^{-1}). We can assume that our $F_c + S_c$ data considerably underestimated nighttime ecosystem respiration at PSO even under moderate u_*, and thus, the actual mean nighttime CO_2 source, as the ecosystem respiration was likely greater than the nocturnal value of $F_c + S_c$.

Next, we compared nighttime ecosystem respiration as a CO_2 source between KEW in summer and PSO. Using the average from June to August for two summers (2003–2004), Ohkubo et al. (2007) estimated the summertime soil respiration rate at KEW to be 3.1 μmol m^{-2} s^{-1}, which represented 49.6% of the total ecosystem respiration (6.2 μmol m^{-2} s^{-1}). Kosugi et al. (2008) estimated the average soil respiration rate at PSO for 3 yr (2003–2005) to be 4.1 μmol m^{-2} s^{-1}. Total ecosystem respiration includes respiration from stem, foliage and coarse surface litter components other than soil respiration (root respiration, fine surface litter and soil organic matter decomposition) and is likely to be greater than soil respiration. The above estimates for ecosystem respiration at the two sites are consistent with the findings that $F_c + S_c$ underestimated ecosystem respiration at PSO, and that the $F_c + S_c$ values were similar at the two sites. In addition to the weak air mixing condition, a larger CO_2 source would make S_c somewhat large at PSO. The underestimation would be caused by advection over non-flat terrain with relatively small u_* compared with other forest types.

Comparison of S_c values at our study site and other forests revealed larger S_c in tropical forests than in other forest types (e.g. Jarvis et al., 1997; Hollinger et al., 1998; Dolman et al., 2002). Further, the S_c found for a central Amazonian forest (Malhi et al., 1998) was as large as that for our tropical rainforest site. We also compared Q_a and Q_w with those at other study sites (e.g. McCaughey and Saxton, 1988; Vogt et al., 1996; Silberstein et al., 2001; Turnipseed et al., 2002; Oliphant et al., 2004) but could not find clear differences between our site and other sites. This result could reflect methodological differences and the shorter observation periods in most past studies. However, we could also assume that there are no conspicuous differences in Q_a and Q_w between various forest types, unlike for S_c. The difference in S_c characteristics between two tropical rainforest sites might be caused by a combination of weaker air mixing and a larger source. On the other hand, the small differences of Q_a and Q_w would be due to the small sinks/sources of heat and water vapour among these forest sites at night.

4. Conclusions

Using 3 yr (2003–2005) of intermittent observations of $[CO_2]$, air temperature and relative humidity at several heights from the floor to the canopy top of a tropical rainforest at Pasoh, Peninsular Malaysia, we analysed the amplitude and diurnal profiles of $[CO_2]$, air temperature and water vapour pressure as well as S_c, Q_a and Q_w and their contributions to CO_2 and energy exchanges. From sunset to midnight, S_c in the driest period was slightly smaller than that in the wettest period. This result corresponds to the finding that nighttime F_c was slightly smaller under the driest condition (Kosugi et al., 2008), reflecting the low soil respiration rate in the dry period, which largely contributed to nighttime ecosystem respiration as a CO_2 source. The diurnal amplitude of Q_a in the wettest period was slightly smaller than that in the driest period. However, no clear difference was found for Q_w. These results correspond to the finding of no clear seasonal changes in $\lambda \boldsymbol{E}$, while $\boldsymbol{H}$ sometimes fluctuated between the dry and wet periods (Takanashi et al., unpublished). The small fluctuation of Q_a can be explained by the low solar radiation in the wet period.

At night, S_c contributed to the CO_2 exchange between the forest and the atmosphere, being greater under low u_* conditions than under high u_*. In contrast, the strength of air mixing (u_*) at night did not heavily influence Q_a and Q_w. In daytime, Q_a and Q_w had larger diurnal amplitudes when solar radiation was greater; in contrast, the diurnal variation of S_c did not depend greatly on solar radiation. Comparison of our data with summertime data from a temperate Japanese cypress forest suggested a much higher contribution of S_c at our tropical rainforest study site, mainly because of lower nighttime u_*. Weak air mixing would make S_c large. Further comparison with other forest sites indicated that the weak air mixing condition at our site also created a vertical gradient of CO_2, air temperature and water vapour pressure within the forest. Such a situation could induce a time lag in the diurnal variation of these meteorological factors, depending on the height from the ground. The larger source from ecosystem respiration at this site would also make S_c somewhat large. On the other hand, differences in Q_a and Q_w were smaller than the difference in S_c among sites, probably because of the lack of sizable heat and water vapour sources at nighttime. Our long-term observations revealed that the diurnal patterns of each storage flux form from a combination of the strength of air mixing (u_*) and the availability of sources and sinks.

5. Acknowledgments

We thank the Forestry Department of Negeri Sembilan and the Director General of the Forest Research Institute Malaysia (FRIM) for permitting us to work in the Pasoh Forest Reserve. We also thank the staff of the Hydrology Unit and the Pasoh Station of the FRIM for collecting data. Dr. Kaoru Niiyama provided the LAI data for the forest reserve. We also thank Dr. Toshinori Okuda, Dr. Naishen Liang and the members of a joint research project between FRIM, Universiti Putra Malaysia and the National Institute for Environmental Studies, Japan, for assisting with our fieldwork. This study was supported by the Global Environment Research Fund of the Japan Environment Agency and by scientific research grants from the Ministry of Education, Culture, Sports, Science, and Technology, Japan and also by Grants-in-Aid for Scientific Research from the Japan Society for the Promotion of Science.

References

Aoki, M., Yabuki, K. and Koyama, H. 1975. Micrometeorology and assessment of primary production of a tropical rain forest in West Malaysia. *J. Agric. Met.* **31**, 115–124.

Baldocchi, D. 2003. Assessing the eddy covariance technique for evaluating carbon dioxide exchange rates of ecosystems: past, present and future. *Global Change Biol.* **9**, 479–492.

Brooks, J. R., Flanagan, L. B., Varney, G. T. and Ehleringer, J. R. 1997. Vertical gradients in photosynthetic gas exchange characteristics and refixation of respired CO_2 within boreal forest canopies. *Tree Physiol.* **17**, 1–12.

Dolman, A. J., Moors, E. J. and Elbers, J. A. 2002. The carbon uptake of a mid-latitude pine forest growing on sandy soil. *Agric. For. Meteorol.* **111**, 157–170.

Feigenwinter, C., Bernhofer, C., Eichelmann, U., Heinesch, B., Hertel, M. and co-authors. 2008. Comparison of horizontal and vertical advective CO_2 fluxes at three forest sites. *Agric. For. Meteorol.* **148**, 12–24.

Finnigan, J. J. 2006. The storage term in eddy flux calculations. *Agric. For. Meteorol.* **136**, 108–113.

Hollinger, D. Y., Kelliher, F. M., Schulze, E.-D., Bauer, G., Arneth, A. and co-authors. 1998. Forest-atmosphere carbon dioxide exchange in eastern Siberia. *Agric. For. Meteorol.* **90**, 291–306.

Jarvis, P. G., Massheder, J. M., Hale, S. E., Moncrieff, J. B., Rayment, M. and co-authors. 1997. Seasonal variation of carbon dioxide, water vapor, and energy exchange of a boreal black spruce forest. *J. Geophys. Res.* **102**, 28 953–28 966.

Kondo, M., Muraoka, H., Uchida, M., Yazaki, Y. and Koizumi, H. 2005. Refixation of respired CO_2 by understory vegetation in a cool-temperate deciduous forest in Japan. *Agric. For. Meteorol.* **134**, 110–121.

Kosugi, Y., Takanashi, S., Ohkubo, S., Matsuo, N., Tani, M. and co-authors. 2008. CO_2 exchange of a tropical rain forest at Pasoh in Peninsular Malaysia. *Agric. For. Meteorol.* **148**, 439–452.

Kumagai, T., Kuraji, K., Noguchi, H., Tanaka, Y., Tanaka, K. and co-authors. 2001. Vertical profiles of environmental factors within tropical rainforest. *J. For. Res.* **6**, 257–264.

Lamaud, E., Ogée, J., Brunet, Y. and Berbigier, P. 2001. Validation of eddy flux measurements above the understorey of a pine forest. *Agric. For. Meteorol.* **106**, 187–203.

Law, B. E., Ryan, M. G. and Anthoni, P. M. 1999. Seasonal and annual respiration of a ponderosa pine ecosystem. *Global Change Biol.* **5**, 169–182.

Lee, X. 1998. On micrometeorological observations of surface–air exchange over tall vegetation. *Agric. For. Meteorol.* 91, 39–49.

Malhi, Y., Nobre, A. D., Grace, J., Kruijt, B., Pereira, M. G. P. and co-authors. 1998. Carbon dioxide transfer over a Central Amazonian rain forest. *J. Geophys. Res.* **103**, 31 593–31 612.

McCaughey, J. H. and Saxton, E. L. 1988. Energy balance storage terms in a mixed forest. *Agric. For. Meteorol.* **44**, 1–18.

Mölder, M., Lindroth, A. and Halldin, S. 2000. Water vapor, CO_2, and temperature profiles in and above a forest-accuracy assessment of an unattended measurement system. *J. Atmos. Ocean. Technol.* **17**, 417–425.

Noguchi, S., Nik, A. R. and Tani, M. 2003. Rainfall characteristics of tropical rainforest at Pasoh Forest Reserve, Negeri Sembilan, Peninsular Malaysia. In: *Pasoh: Ecology of a Lowland Rain Forest in Southeast Asia*, (eds T. Okuda, N. Manokaran, Y. Matsumoto, K. Niiyama, S. C. Thomas and P. S. Ashton), Springer, Tokyo, 51–58.

Ohkubo, S. and Kosugi, Y. 2008. Amplitude and seasonality of storage fluxes for CO_2, heat and water vapor in a temperate Japanese cypress forest. *Tellus* **60B**, 11–20.

Ohkubo, S., Kosugi, Y., Takanashi, S., Mitani, T. and Tani, M. 2007. Comparison of the eddy covariance and automated closed chamber methods for evaluating nocturnal CO_2 exchange in a Japanese cypress forest. *Agric. For. Meteorol.* **142**, 50–65.

Oliphant, A. J., Grimmond, C. S. B., Zutter, H. N., Schmid, H. P., Su, H.-B. and co-authors. 2004. Heat storage and energy balance fluxes for a temperate deciduous forest. *Agr. For. Meteorol.* **126**, 185–201.

Silberstein, R., Held, A., Hatton, T., Viney, N. and Sivapalan, M. 2001. Energy balance of a natural jarrah (*Eucalyptus marginata*) forest in Western Australia: measurements during the spring and summer. *Agric. For. Meteorol.* **109**, 79–104.

Sun, J., Burns, S., Delaney, A., Oncley, S., Turnipseed, A. and co-authors. 2007. CO_2 transport over complex terrain. *Agric. For. Meteorol.* **145**, 1–21.

Takanashi S., Kosugi, Y., Matsuo, N., Tani, M. and Ohte, N. 2006. Patchy stomatal behavior in broad-leaved trees grown in different habitats. *Tree Physiol.* **26**, 1565–1578.

Turnipseed, A. A., Blanken, P. D., Anderson, D. E. and Monson, R. K. 2002. Energy budget above a high-elevation subalpine forest in complex topography. *Agric. For. Meteorol.* **110**, 177–201.

Vogt, R., Bernhofer, Ch., Gay, L. W., Jaeger, L. and Parlow, E. 1996. The available energy over a Scots pine plantation: what's up for partitioning? *Theor. Appl. Climatol.* **53**, 23–31.

Webb, E. K., Pearman, G. I. and Leuning, R. 1980. Correction of flux measurements for density effects due to heat and water vapour transfer. *Quart. J. R. Met. Soc.* **106**, 85–100.

Wilson, K. B., Goldstein, A., Falge, E., Aubinet, M., Baldocchi, D. and co-authors. 2002. Energy balance closure at FLUXNET sites. *Agric. For. Meteorol.* **113**, 223–243.

Xu, L.-K., Matista, A. A. and Hsiao, T. C. 1999. A technique for measuring CO_2 and water vapor profiles within and above plant canopies over short periods. *Agric. For. Meteorol.* **94**, 1–12.

Yasuda, Y., Ohtani, Y., Watanabe, T., Okano, M., Yokota, T. and co-authors. 2003. Measurement of CO_2 flux above a tropical rain forest at Pasoh in Peninsular Malaysia. *Agric. For. Meteorol.* **114**, 235–244.

HYDROLOGICAL PROCESSES
Hydrol. Process. **24**, 472–480 (2010)

(www.interscience.wiley.com) DOI: 10.1002/hyp.7499

Water and heat fluxes above a lowland dipterocarp forest in Peninsular Malaysia

Satoru Takanashi,[1]* Yoshiko Kosugi,[2] Shinjiro Ohkubo,[3] Naoko Matsuo,[4] Makoto Tani[2] and Abdul Rahim Nik[5]

[1] *Forest Meteorology Laboratory, Department of Meteorological Environment, Forestry and Forest Products Research Institute, Ibaraki 305-0031, Japan*
[2] *Graduate School of Agriculture, Kyoto University, Kyoto 606-8502, Japan*
[3] *National Agricultural Research Center for Hokkaido Region, Sapporo 062-8555, Japan*
[4] *Faculty of Bioresources, Mie University, Tsu, Mie 514-8507, Japan*
[5] *Forest Research Institute Malaysia, Kepong, Kuala Lumpur 52109, Malaysia*

Abstract:

We measured the fluxes of sensible and latent heat between a low-land dipterocarp forest in Peninsular Malaysia and the atmosphere. No clear seasonal or interannual changes in latent heat flux were found from 2003 to 2005, while sensible heat flux sometimes fluctuated depending on the fluctuation of incoming radiation between wet and dry seasons. The evapotranspiration rates averaged for the period between 2003 and 2005 were 2·77 and 3·61 mm day^{-1} using eddy covariance data without and with an energy balance correction, respectively. Average precipitation was 4·74 mm day^{-1}. Midday surface conductance decreased with an increasing atmospheric water vapour pressure deficit and thus restricted the excess water loss on sunny days in the dry season. However, the relationship between the surface conductance and vapour pressure deficit did not significantly decline with an increase in volumetric soil water content even during a period of extremely low rainfall.

KEY WORDS tropical rainforest; eddy covariance; evapotranspiration; energy balance; Southeast Asia

Received 21 April 2009; Accepted 15 September 2009

INTRODUCTION

The exchange of heat and water vapour by terrestrial ecosystems, coupled with carbon dioxide, plays a role in the regulation of the thermal environment of the atmosphere and water cycling on the planet scale. Tropical rainforests, in particular, play an important role in climate change because of their large plant volume and complexity. It is important to understand the role played by heat and water exchanges of a tropical rain forest in global environmental changes. In recent decades, diurnal and seasonal changes in the H_2O and CO_2 exchange rates of forests have been directly detected using the eddy covariance method (Aubinet *et al*., 2000; Baldocchi, 2003). With over 140 micrometeorological flux measurement sites, FLUXNET was established to understand the mechanisms controlling the exchanges of CO_2, water vapour and energy across spectra of time and space, and to provide information for modelling carbon and water cycling across regions and across the globe (Baldocchi *et al*., 2001). A few studies have reported on long-term eddy covariance heat and H_2O flux observations in tropical rainforests, both in the Amazon (Shuttleworth, 1988; Malhi *et al*., 2002; da Rocha *et al*., 2004) and in Southeast Asia (Kumagai *et al*., 2004). There are major environmental differences between Amazonian and Southeast Asian rainforests in the patterns of rainfall. Most sites in Amazon rainforests have distinct dry and wet seasons during the year, although the magnitude of dryness depends on the location (Nepstad *et al*., 1994). In contrast, Peninsular Malaysian and Bornean rainforests do not experience distinct dry and wet seasons during the year although dry and wet periods do exist as part of the seasonal fluctuation with considerable variability between years (Tani *et al*., 2003b; Kumagai *et al*., 2005). Given that H_2O is exchanged through leaf stomata, the heat and water exchange characteristics of a forest are mainly affected by stomatal regulation. Therefore, the stomatal behaviour and surface conductance response to changing moisture availability should be investigated to clarify the effects of varying amounts and patterns of rainfall on heat and H_2O exchange in tropical rain forests. During the long dry season in the central-to-eastern Amazon, forest canopy foliage is maintained via deep roots to soil water reserves (Nepstad *et al*., 1994). Effects of drought stress on the surface conductance of Amazonian rainforest were reported for Manaus (Malhi *et al*., 2002), but were not evident at Santarém (da Rocha *et al*., 2004). Kumagai *et al*. (2004) reported that drought stress reduced surface conductance at Lambir in Borneo. It is unknown if these results are equally valid for other rain forests. Further

---

* Correspondence to: Satoru Takanashi, Forest Meteorology Laboratory, Department of Meteorological Environment, Forestry and Forest Products Research Institute, Ibaraki 305-0031, Japan.
E-mail: tnsatoru@ffpri.affrc.go.jp

study is warranted to investigate issues related to heat and H_2O exchange in tropical rain forests, especially for intercomparisons over the Amazon and Southeast Asian regions.

This paper considers 3 years of eddy covariance sensible and latent flux data for a primary tropical rain forest in the Pasoh Forest Reserve in Peninsular Malaysia, Southeast Asia. This paper assesses the footprint of flux measurement and the magnitude of the energy imbalance at this site, describes the nature and magnitude of diurnal, seasonal and interannual heat and H_2O exchanges, and analyzes whether the effects of drought stress on the surface conductance are evident at this site.

METHODS

Site description

Observations were conducted at the Pasoh Forest Reserve near Simpang Pertang in Negeri Sembilan, Peninsular Malaysia (2°58′N, 102°18′E, Figure 1). The core area (600 ha) of the reserve is a primary low-land mixed dipterocarp forest consisting of various species of *Shorea* and *Dipterocarpus*. The continuous canopy height is approximately 35 m, although some emergent trees exceed 45 m. An intensive research project by the International Biological Programme was conducted in this forest reserve from 1970 to 1974 (Soepadmo, 1978). On the basis of empirical equations obtained for the Pasoh Forest Reserve by Kato *et al.* (1978), the leaf area index estimated from tree diameter observations (Niiyama, unpublished) was 6·52. The plant area index was optically measured using a plant canopy analyzer (LAI-2000, Li-Cor Inc., Lincoln, NB, USA) on 19 September 2002, 27 November 2002, 9 March 2003, 25, 26 and 27 August 2003, 17 December 2003, 30 May 2004, and 12 September 2004. The temporally averaged plant area index was 5·76 and the standard deviation was 0·47 ($n = 15$).

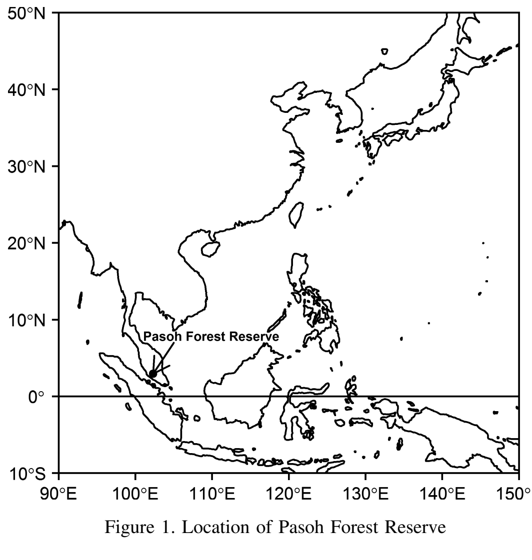

Figure 1. Location of Pasoh Forest Reserve

The core area of the forest reserve includes plot 1, a 2-ha plot used extensively to study primary productivity of the tropical rain forest by the International Biological Programme (Kato *et al.*, 1978). Biometric observations have been carried out continuously also in a 6-ha plot that extends plot 1, and a 50-ha plot (e.g. Davies *et al.*, 2003; Niiyama *et al.*, 2003; Hoshizaki *et al.*, 2004). The topography, area of the Pasoh Forest Reserve and the locations of the 6-ha plot, the 50-ha plot and the flux observation tower are shown in Figure 2. The forest reserve is widest at about 3500 m to the north and narrowest at about 800 m. The area has gently undulating topography, and the altitude of the core area ranges from 75 to 150 m a.s.l. Soil characteristics and the rainfall pattern are briefly described with citations in the paper of Kosugi *et al.* (2007a).

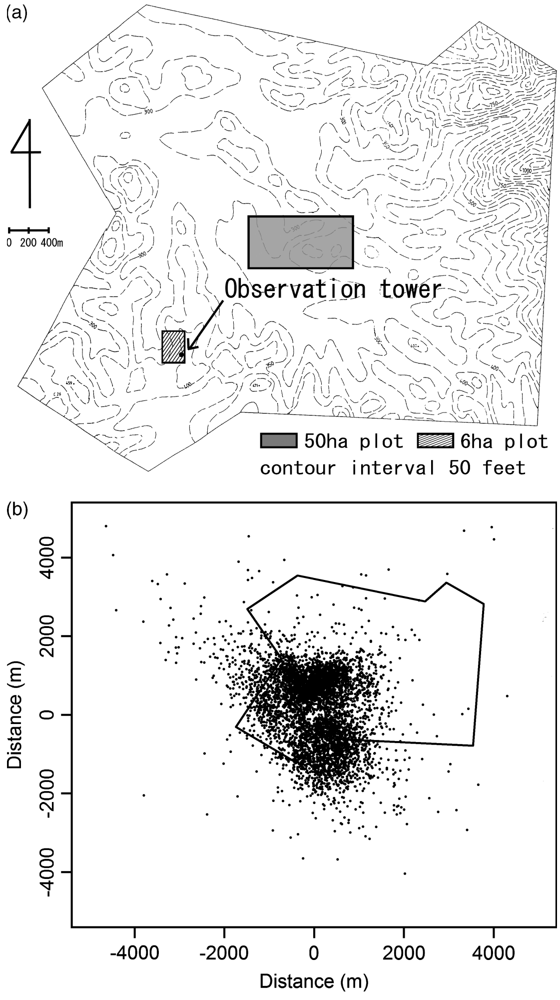

Figure 2. Location of the observation tower (a) and fetch length in the daytime and the boundary of Pasoh Forest Reserve (b). On the basis of the work of Schuepp *et al.* (1990), the fetch length for which >80% of the flux measurements are expected to come from is calculated and the points plotted

Micrometeorological measurements

Flux measurements were made at a height of 54 m from the observation tower. The wind velocity and temperature were observed with a three-axis sonic anemometer (SAT-550, Kaijo, Japan) from September 2002 (the first probe was disabled by lightning on 5 June 2004, and a new one was installed on 24 November 2004) to December 2005. Water vapour densities were monitored with an open path CO_2/H_2O analyzer (LI-7500, Li-Cor Inc., Lincoln, NB, USA) from September 2002 (the first probe was disabled by lightning on 5 June 2004, and a new one was installed on 4 September 2004) to December 2005. Analog signals from the sonic anemometer and infrared gas analyzer were sampled by a data logger (CR-5000, Campbell Scientific, Utah, USA) at 10 Hz. The averaging time for the calculation of fluxes was 30 min. The Webb, Pearman, and Leuning (WPL) correction for the effect of air density fluctuation (Webb *et al*., 1980) was made. A three-dimensional coordinate rotation for the vertical wind velocity normal to the mean wind direction (double rotation; McMillen, 1988; Kaimal and Finnigan, 1994) was applied assuming a zero mean vertical wind. This paper considers the data from 1 January 2003 to 31 December 2005. Thresholds were set for sensible heat flux ($-400 < H < 1000$, W m^{-2}) and latent heat flux ($-400 < \lambda \boldsymbol{E} < 1000$, W m^{-2}). Data were ignored from 30 min before to 1 h after rainfall (>0·5 mm) to avoid data spikes and noise caused by rainfall drops in the path of the infrared beam of the LI-7500. Valid surface fluxes were obtained during 66·2% of this period (79·1% of 2003, 46·2% of 2004 and 73·3% of 2005). The observation tower was equipped with instruments to measure downward and upward short-wave radiation (MR22, Eko, Japan), long-wave radiation (PIR, Eppley Laboratory Inc., Newport, RI, USA), air temperature, humidity (HMP45A, Visala, Helsinki, Finland), wind velocity (AC750, Makino, Japan) and rainfall (RT-5, Ikedakeiki, Japan). Soil water content at depths of 0·1, 0·2 and 0·3 m (CS615 or CS616, Campbell Scientific, Utah, USA) and soil heat flux at a depth of 0·02 m (HFP01, Hukseflux Thermal Sensors B.V., The Netherlands) were monitored at three points around the tower. Rainfall was measured by tipping bucket rain gauges (Ota Keiki 34-T, Japan) at the top of the 52-m tower and at an observatory located 430 m from the tower. The rainfall measured on the tower may be influenced by strong wind, whereas the rainfall in the observatory was sometimes different from that at the tower site owing to large spatial variability of rainfall in the region. Both types of data were carefully compared with the data for storage rain recorded at the observatory and corrected (Konishi *et al*., 2006). We used the rainfall data recorded at the observatory if that measured at the tower was not available.

Data analysis

To analyze the response of stomata to environmental factors, surface conductance was calculated using latent heat flux and the Penman–Monteith equation:

$$g_c{}^{-1} = r_c = \frac{r_a}{\gamma} \left(\frac{\Delta(R_n - G) + \rho C_P(e_s(T_a) - e_a)/r_a}{\lambda E} - (\Delta + \gamma) \right) \quad (1)$$

where R_n is the net radiation (W m^{-2}), G is the ground heat flux (W m^{-2}), λE is the latent heat flux (W m^{-2}), g_c is the surface conductance (s m^{-1}), r_c is the surface resistance (m s^{-1}), Δ is the rate of change of saturated water vapour pressure with temperature (Pa K^{-1}), ρ is the air density (mol m^{-3}), C_p is the specific heat capacity of air (J mol K^{-1}), $e_s(T_a)$ is the saturated vapour pressure at air temperature (Pa), e_a is the vapour pressure (Pa), γ is the psychrometric constant (Pa K^{-1}), and r_a is the aerodynamic resistance (s m^{-1}). Aerodynamic resistance was calculated as (Kumagai *et al*., 2004; Kosugi *et al*., 2007b):

$$r_a = \frac{u_r}{u_*{}^2} \quad (2)$$

where u_r is the wind velocity at the reference height (m s^{-1}, height of 54 m) and u_* is the friction velocity obtained from eddy covariance measurements (m s^{-1}). The decoupling factor (Ω) was calculated using the expression derived by MacNaughton and Jarvis (1983):

$$\Omega = \frac{\Delta/\gamma + 1}{\Delta/\gamma + 1 + r_c/r_a} \quad (3)$$

To avoid influences of evaporation from wet canopy, the data for which there was no rainfall in the previous 24 h were used in the analysis of the surface conductance.

RESULTS AND DISCUSSION

Footprint and energy closure analysis

Figure 2 shows the footprint of fluxes in the daytime and the boundary of Pasoh Forest Reserve. On the basis of the model developed by Schuepp *et al*. (1990), observations for which >80% of the measured flux is expected to have come from within the boundary made up 72% of the total number of measurements during the daytime. Figure 3 shows the sum of 30-min sensible heat flux (H_{eddy}, W m^{-2}) and latent heat flux (λE_{eddy}) versus the available energy that was calculated as net radiation (R_n) minus the soil heat flux (G) and canopy heat storage (S). The slope of this relationship for all data was 0·724, while for data limited to the data for which the fetch lengths were within the boundary, the slope became 0·776.

Energy balance closure provides important information on the absolute accuracy of the sensible heat flux and latent heat flux estimates derived from eddy covariance measurements. From many studies, a general concern has developed within the micrometeorological community that surface energy fluxes ($\lambda E + H$) are frequently (but not always) underestimated by about 10–30% relative to estimates of available energy ($R_n - G - S$) (Wilson

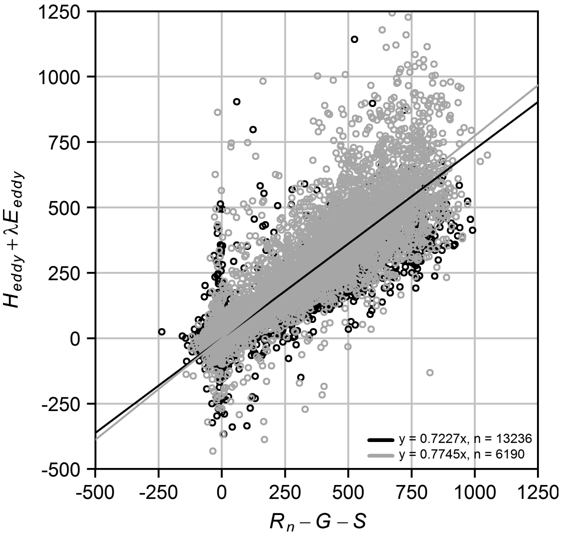

Figure 3. The sum of sensible heat flux (H_{eddy}) and latent heat flux (λE_{eddy}) vs. the available energy [net radiation (R_n) minus the sum of soil heat flux (G) and canopy heat storage (S)] for half-hourly data. Black circles represent all available data and grey circles represent the data whose fetch lengths were within the boundary of Pasoh Forest Reserve. Lines fitted by linear regression are also shown

et al., 2002). Figure 4 shows the imbalance ratios ($I_{\text{BR}} = \frac{\lambda E + H}{R_n - G - S} - 1$) and the slopes of linear regression of the sum of surface energy fluxes ($\lambda E + H$) against the available energy ($R_n - G - S$) for each of the friction velocity classes. Both the slope and the imbalance ratio increased with friction velocity up to approximately 80% of the energy balance closure. This value is within the common range of the imbalance reported for many flux observation sites covered in various types of vegetation across the world (Wilson *et al*., 2002), although it should be noted that it still indicates a considerable imbalance of energy and thus suggests the underestimation of heat and water fluxes and bulk surface conductance.

Tanaka *et al*. (2002) evaluated the total evapotranspiration from a larch forest by assuming that the energy closure deficit could be divided into sensible and latent heat advection fluxes, defined as the product of the energy difference between incoming and outgoing air and the volume of advective air. Ohta *et al*. (2001) estimated actual evapotranspiration by multiplying the ratio obtained using the energy balance closure method by the eddy latent heat flux. For a better estimation of evapotranspiration from the Pasoh forest, sensible and latent heat fluxes were corrected by assuming that the Bowen ratio deduced from the eddy covariance fluxes was conserved after correction, and closure deficits were divided into sensible and latent heat fluxes using the Bowen ratio. Available energy was divided into sensible and latent heat fluxes using the Bowen ratio as calculated from the eddy covariance fluxes; therefore, the evapotranspiration rate

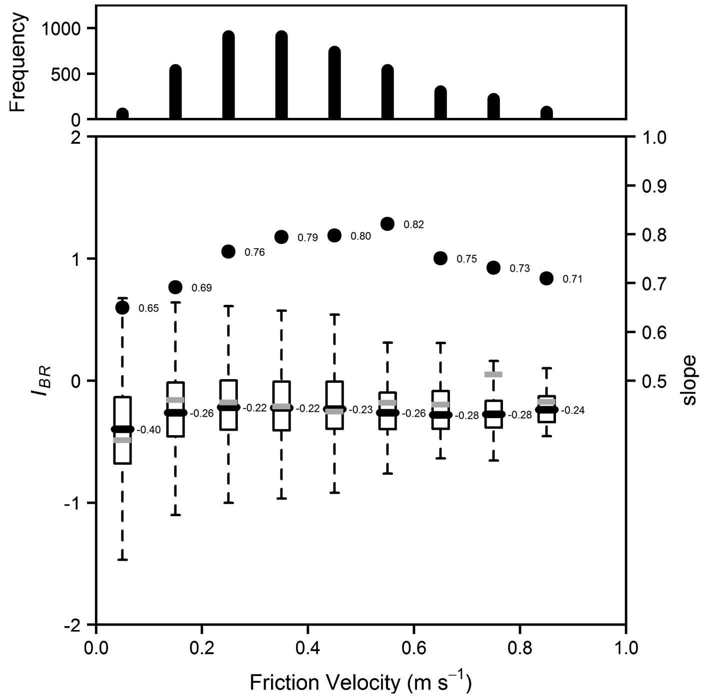

Figure 4. Effects of friction velocity (u_*) on the imbalance ratios and the linear regression slopes in the daytime. Box plots of the imbalance ratios (I_{BR}) for each different friction velocity class are shown. The medians are indicated by the black center line, and the first and third quartiles are the edges of the box. The ends of the lines extending from the boxes denote extreme values that are within 1·5 times the quartile range from the upper or lower quartile. The averages are indicated by grey lines. Black points represent the linear regression slopes between the available energy and the sum of sensible heat flux and latent heat flux

DOI: 10.1002/hyp

of a canopy was corrected as follows:

$$\lambda E = \lambda E_{\text{eddy}} \frac{R_n - G}{H_{\text{eddy}} + \lambda E_{\text{eddy}}} \quad (4)$$

where λE_{eddy} is the evapotranspiration rate measured above the forest using the eddy covariance method (W m^{-2}) and H_{eddy} is the sensible heat flux above the forest determined using the eddy covariance method (W m^{-2}).

The evapotranspiration rate averaged for the period between 2003 and 2005 was directly estimated to be 2·77 mm day^{-1} using an eddy covariance latent heat flux without correction. After the energy balance correction, it became 3·61 mm day^{-1}. As the average rainfall at this site is 4·74 mm day^{-1}, this difference is not negligible. It cannot be said that this is the best method for the energy balance correction, as there is no evidence or theory that the Bowen ratio suggested by the eddy covariance measurement is conserved after considering various factors including the mass movement other than that of the eddy. However, our results along with the results for many other flux sites reported by Wilson *et al.* (2002) strongly suggest the necessity of considering an energy imbalance correction in the estimation of evapotranspiration using the eddy covariance method.

Diurnal, seasonal and interannual fluctuation of sensible and latent heat fluxes

Annual rainfall totals in 2003, 2004 and 2005 were 1896, 1655, and 1649 mm respectively. These values were close to the mean annual rainfall from 1983 to 1997 (1804 mm) at an observation station near the site (Tani *et al.*, 2003a). The driest condition of the soil was observed in February 2005. Seasonal changes in the micrometeorological and hydrological environments at Pasoh Forest Reserve from 2003 to 2005 are shown in Figure 5. Relatively low air temperature, a low level

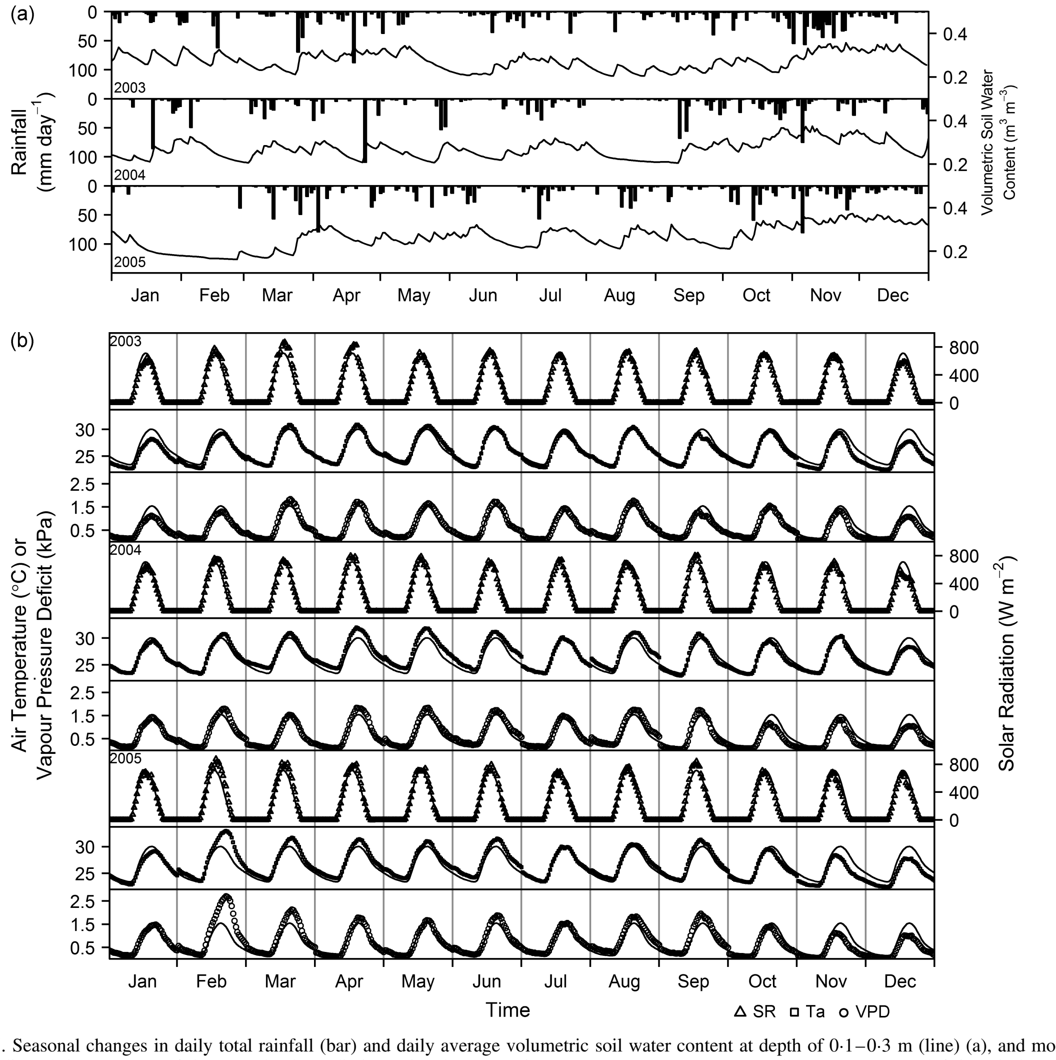

Figure 5. Seasonal changes in daily total rainfall (bar) and daily average volumetric soil water content at depth of 0·1–0·3 m (line) (a), and monthly average diurnal time courses of downward solar radiation (triangles: SR), air temperatures (squares: Ta), and vapour pressure deficits (circles: VPD) (b). Lines in (b) represent average diurnal time courses of 3 years

of solar radiation and a low vapour pressure deficit coincided with cloudy and rainy periods (January and December in 2003 and December 2004). High air temperature, a high level of solar radiation and high vapour pressure deficit coincided with sunny and dry periods (February 2005).

Figure 6 shows the monthly average diurnal changes in sensible and latent heat fluxes over the canopy after the energy balance correction from January 2003 to December 2005. The black line represents the average diurnal change for the 3 years. The grey line, which almost overlies the black line, shows the 3-year average diurnal course of the sum of sensible heat fluxes over the canopy and sensible heat storage fluxes, or latent heat fluxes over the canopy and latent heat storage fluxes. Figure 6 shows that the contributions of storage fluxes to the heat and water exchange between the forest and the atmosphere were small; Ohkubo *et al.* (2008) reported that the positive peaks of the heat and water storage fluxes were 16 and 7·8% of the positive peaks of H_{eddy} and $\lambda E_{\mathrm{eddy}}$, respectively. We see from this figure that there were no clear seasonal and interannual changes in latent heat flux from 2003 to 2005, while the sensible heat flux sometimes fluctuated depending on variations in incoming radiation between wet and dry periods. For example, the largest diurnal maximum of sensible heat flux was observed in February 2005, which was the driest and sunniest month during the 3-year observation period (Figure 5), and smaller maxima of sensible heat flux were observed in January and December 2003 and December 2004, which were cooler and cloudier months (Figure 5). We see from Figure 6 that latent heat flux and thus evapotranspiration from the forest did not increase in the driest, hottest and sunniest month (February 2005). Tanaka *et al.* (2008) reviewed evapotranspiration estimates from tropical monsoon forests of mainland Southeast Asia and reported that the dry season (from November to April) evapotranspiration rate for evergreen forests ranged from 0·6 to 5·9 mm day^{-1} and that there were relatively small differences in the wet season evapotranspiration rate (around 3 mm day^{-1}). Our results for the monthly averaged evapotranspiration rates ranging from 3·2 to 3·8 mm day^{-1} are slightly higher than those of tropical monsoon forests in the wet season and those of Bornean tropical rainforest (2·86–3·48 mm day^{-1}, Kumagai *et al.*, 2004) and similar to those of eastern Amazonian forest (wet season rate of 3·2 and dry season rate of 4·0 mm day^{-1}; da Rocha *et al.*, 2004).

Figure 7 shows the relationship between the vapour pressure deficit and surface conductance (g_c) and the decoupling coefficient calculated for the available 30-min data in the afternoon under light-saturated conditions. This relationship is shown for each year and for two groups of average volumetric soil water content at 0·1, 0·2, and 0·3 m depth (average values for nine sensors). The Lohammar equation (Lohammar *et al.*, 1980), which has often been used to represent the relationship between the stomatal conductance and vapour pressure deficit in single-leaf-scale analysis, was used here to fit curves to the data (Figure 7) to assess whether this relationship

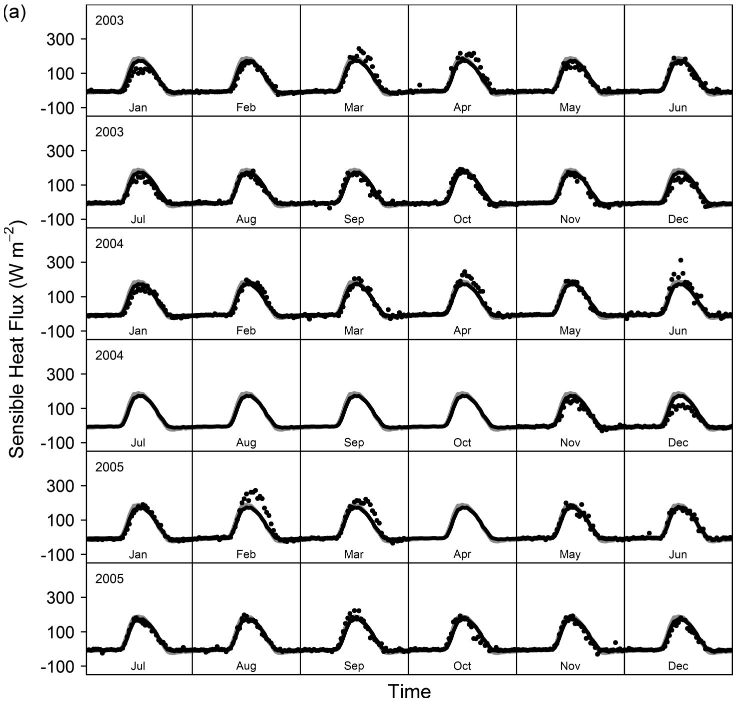

Figure 6. Diurnal changes in sensible heat flux (a) and latent heat flux (b). Monthly average time courses of each year are plotted. Black lines represent average time courses of 3 years. Grey lines represent monthly average time courses of the sum of sensible heat flux and storage or latent heat flux and storage

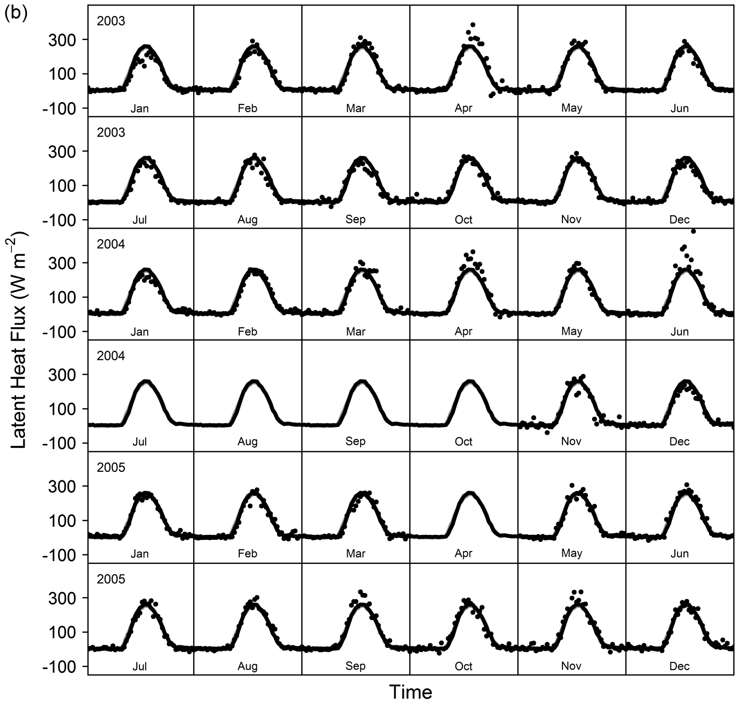

Figure 6. (*Continued*)

changed between dry and rainy seasons owing to the soil moisture condition. It is noted that surface conductance differed sharply when estimated with and without the energy balance correction. The values after correction may not be theoretically correct, but it is a better estimation than that made without the correction. One reason for this is that the value with energy balance correction is closer to the surface conductance of the same site determined using the Bowen ratio method and reported by Tani *et al.* (2003b) and Takanashi *et al.* (2003).

Figure 7 shows that the midday surface conductance decreased as the atmospheric water vapour pressure deficit increased and thus restricted the excess water loss on sunny days in the dry season, and midday stomatal control of the transpiration $(1 - \Omega)$ increased with the atmospheric water vapour pressure deficit. However, the relationship between surface conductance and vapour pressure deficit did not decline with increasing volumetric soil water content. During the extremely low rainfall period from January to February in 2005 (Figure 7h), the relationship slightly declined. Tani *et al.* (2003b) and Takanashi *et al.* (2003) estimated the surface conductance using both the Bowen ratio method and the Penman–Monteith equation at this site and showed that the conductance was consistently controlled by the same function of solar radiation and vapour pressure deficit and that evaporation did not suffer from severe stress of soil water even in the driest condition in early 1998. Our results along with those of previous studies suggest that there is no clear restriction of surface conductance by the soil moisture condition at this site, which is similar to that observed for other tropical rainforests (da Rocha *et al.*, 2004).

CONCLUSIONS

We analysed sensible and latent heat fluxes above a tropical rainforest in Peninsular Malaysia for 3 years from 2003 to 2005. The Pasoh forest did not have distinct wet and dry seasonal changes in weather conditions, such as those seen in some parts of the Amazonian forests. After considering the heat storage terms and fetch length, the energy balance closure was estimated to be approximately 78%, which improved to around 80% for periods with higher friction velocity. An energy balance correction was made for the latent heat flux measured using the eddy covariance method. With the correction, the evapotranspiration from the lowland dipterocarp forest in the Pasoh Forest Reserve was estimated to be 3·61 mm day^{-1}, which was less than the rainfall of 4·71 mm day^{-1}. There was no evidence of water stress from the diurnal changes in the latent heat flux, and the surface conductance was limited by the vapour pressure deficit but not by the volumetric soil water content.

ACKNOWLEDGEMENTS

We thank the Forestry Department of Negeri Sembilan and the Director General of Forest Research Institute Malaysia (FRIM) for granting us permission to work in the Pasoh Forest Reserve. We gratefully acknowledge the staffs of the Hydrology Unit and the Pasoh Station of

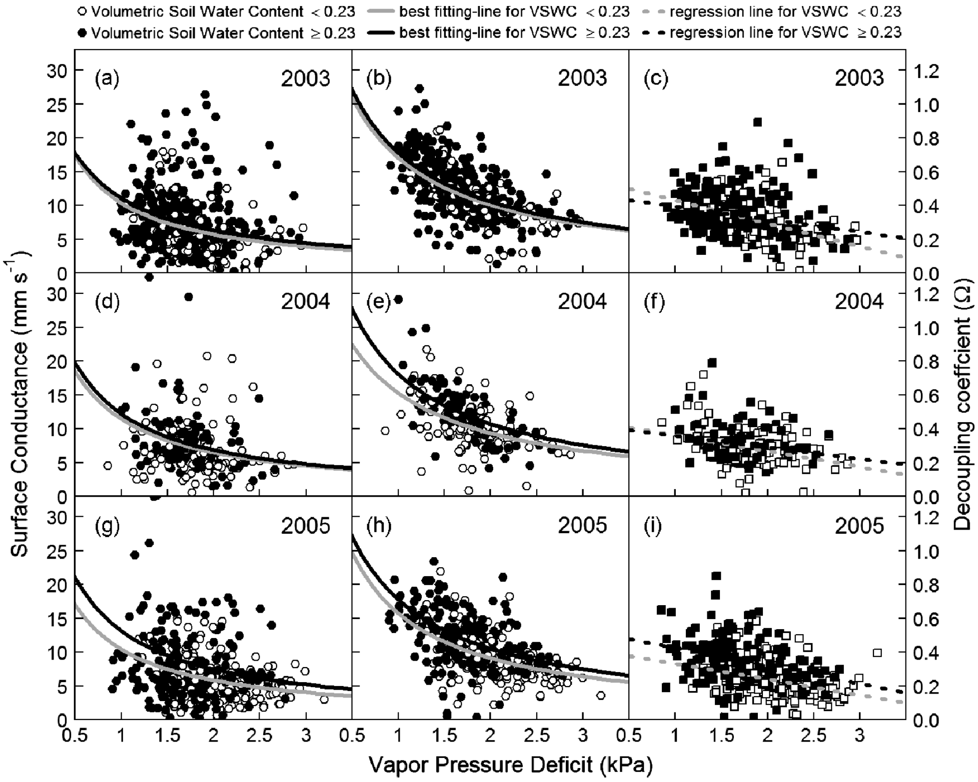

Figure 7. Relationships between the vapour pressure deficit and surface conductance in the afternoon under light-saturated conditions (with solar radiation of >800 W m^{-2}) for two average volumetric soil water content classes (white circles represent the data under low soil water content conditions and black circles represent the data for high soil water content). Lines represent best-fitting curves based on the Lohammar equation (Lohammar *et al.*, 1980): $f_d(\delta e) = \frac{f_{d\ max}}{1+\delta e/\delta e_0}$ where δe is the atmospheric vapour pressure deficit (Pa) and $f_{d\ max}$ and δe_0 are the maximum conductance of the function (mm s^{-1}) and the curvature of the function (Pa) respectively. Surface conductances calculated using λE_{eddy} and λE are shown in left panels (a, d, and g) and middle panels (b, e, and h), respectively. The decoupling coefficient (Jarvis and McNaughton, 1986), Ω, calculated using λE is plotted in right panels (c, f, and i). Dotted lines in the right panels represent the regression lines for the decoupling coefficient

FRIM for collecting field data. Dr Shoji Noguchi and Dr Jyunjiro Negishi helped install the soil moisture sensors, Dr Kaoru Niiyama provided biometric observations and leaf area index data obtained in this forest reserve, and Mr Tomonori Mitani, Dr Daizo Tsutsumi, Mr Tatsuya Katayama, Mr Takumi Wada, Mr Shinji Konishi, Mr Yusuke Fukui, Ms Rie Nakanishi, Mr Masayuki Ito and Mr Naoto Yokoyama assisted with the fieldwork. We also thank Dr Toshinori Okuda, Dr Naishen Liang and a joint research project between FRIM, University Putra Malaysia and National Institute for Environmental Studies. This work was supported by the Global Environment Research Fund of the Japan Environment Agency, and by grants for scientific research from the Ministry of Education, Culture, Sports, Science and Technology, Japan.

REFERENCES

Aubinet M, Grelle A, Ibrom A, Rannik Ü, Moncrieff J, Foken T, Kowalski AS, Martin P, Berbigier P, Bernhofer C, Clement R, Elbers J, Granier AGT, Morgenstern K, Pilegaard K, Rebmann C, Snijders W, Valentini R, Vesala T. 2000. Estimates of the annual net carbon and water exchange of European forests: the EUROFLUX methodology. *Advances in Ecological Research* **30**: 113–175.

Baldocchi DD. 2003. Assessing the eddy covariance technique for evaluating carbon dioxide exchange rates of ecosystems: past, present and future. *Global Change Biology* **9**: 479–492. DOI: 10.1046/j. 1365-2486.2003.00629.x.

Baldocchi D, Falge E, Gu L, Olson R, Hollinger D, Running S, Anthoni P, Bernhofer C, Davis K, Evans R, Fuentes J, Goldstein A, Katul G, Law B, Lee X, Malhi Y, Meyers T, Munger W, Oechel W, Paw UKT, Pilegaard K, Schmid HP, Valentini R, Verma S, Vesala T, Wilson K, Wofsy S. 2001. FLUXNET: A new tool to study the temporal and spatial variability of ecosystem-scale carbon dioxide, water vapor, and energy flux densities. *Bulletin of the American Meteorological Society* **82**: 2415–2434.

Davies SJ, Nur Supardi MN. LaFrankie JV, Ashton PS. 2003. The trees of Pasoh forest: Stand structure and floristic composition of the 50-ha forest research plot. In *Pasoh: Ecology of a Lowland Rain Forest in Southeast Asia*, Okuda T, Niiyama K, Thomas SC (eds). Springer: Tokyo, Japan; 35–50.

Hoshizaki K, Niiyama K, Kimura K, Yamashita T, Bekku Y, Okuda T, Quah ES, Noor NSM. 2004. Temporal and spatial variation of forest biomass in relation to stand dynamics in a mature, lowland tropical rainforest, Malaysia. *Ecological Research* **19**: 357–363. DOI: 10.1111/j. 1440-1703.2004.00645.x.

Jarvis PG, McNaughton KG. 1986. Stomatal control of transpiration: scaling up from leaf to region. *Advances in Ecological Research* **15**: 1–49.

Kaimal JC, Finnigan JJ. 1994. Spectra and cospectra over flat uniform terrain. In *Atmospheric Boundary Layer Flows: Their Structure and Measurement*. Oxford University Press: New York; 32–65.

Kato R, Tadaki Y, Ogawa H. 1978. Plant biomass and growth increment studies in Pasoh Forest. *The Malayan Nature Journal* **30**: 211–245.

Konishi S, Tani M, Kosugi Y, Takanashi S, Sahat MM, Abdul Rahim N, Niiyama K, Okuda T. 2006. Characteristics of spatial distribution of throughfall in a lowland tropical rainforest, Peninsular

Malaysia. *Forest Ecology and Management* **224**: 19–25. DOI: 10.1016/j.foreco.2005.12.005.

Kosugi Y, Mitani T, Itoh M, Noguchi S, Tani M, Matsuo N, Takanashi S, Ohkubo S. 2007a. Spatial and temporal variation in soil respiration in a Southeast Asian tropical rainforest. *Agricultural and Forest Meteorology* **147**: 35–47. DOI: 10.1016/j.agrformet.2007.06.005.

Kosugi Y, Takanashi S, Tanaka H, Ohkubo S, Tani M, Yano M, Katayama T. 2007b. Evapotranspiration over a Japanese cypress forest. I. Eddy covariance fluxes and surface conductance characteristics for 3 years. *Journal of Hydrology* **337**: 269–283. DOI: 10.1016/j.jhydrol.2007.01.039.

Kumagai T, Saitoh TM, Sato Y, Morooka T, Manfroi OJ, Kuraji K, Suzuki M. 2004. Transpiration, canopy conductance and the decoupling coefficient of a lowland mixed dipterocarp forest in Sarawak, Borneo: dry spell effects. *Journal of Hydrology* **287**: 237–251. DOI: 10.1016/j.jhydrol.2003.10.002.

Kumagai T, Saitoh TM, Sato Y, Takahashi H, Manfroi OJ, Morooka T, Kuraji K, Suzuki M, Yasunari T, Komatsu H. 2005. Annual water balance and seasonality of evapotranspiration in a Bornean tropical rainforest. *Agricultural and Forest Meteorology* **128**: 81–92. DOI: 10.1016/j.agrformet.2004.08.006.

Lohammar T, Larsson S, Linder S, Falk SO. 1980. FAST—Simulation models of gaseous exchange in Scots pine. *Structure and Function of Northern Coniferous Forests—An Ecosystem Study*, *Ecological Bulletin 32*, Persson T (ed): Swedish Natural Science Research Council (NFR): Stockholm; 505–523.

MacNaughton KG, Janvis PG. 1983. Predicting effects of vegetation changes on transpiration and evaporation. *In Water deficits and plant growth. Vol. VIII*, Kozlowski TT (eds). Academic Press: London; 1–47.

Malhi Y, Pegoraro E, Nobre AD, Pereira MGP, Grace J, Culf AD, Clement R. 2002. Energy and water dynamics of a central Amazonian rain forest. *Journal of Geophysical Research* **107**: 8061. DOI: 10.1029/2001JD000623.

McMillen RT. 1988. An eddy correlation technique with extended applicability to non-simple terrain. *Boundary-Layer Meteorology* **43**: 231–245.

Nepstad DC, de Carvalho CR, Davidson EA, Jipp PH, Lefebvre PA, Negreiros GH, da Silva ED, Stone TA, Trumbore SE, Vieira S. 1994. The role of deep roots in the hydrological and carbon cycles of Amazonian forests and pastures. *Nature* **372**: 666–669. DOI: 10.1038/372666a0.

Niiyama N, Abdul Rahman Kssim , Iida S, Kimura K, Ripin A, Appanah S. 2003. Regeneration of a clear-cut plot in a lowland dipterocarp forest in Pasoh Forest Reserve, Peninsular Malaysia. In *Pasoh: Ecology of a Lowland Rain Forest in Southeast Asia*, Okuda T, Niiyama K, Thomas SC (eds). Springer: Tokyo; 559–568.

Ohkubo S, Kosugi Y, Takanashi S, Matsuo N, Tani M. 2008. Vertical profiles and storage fluxes of CO_2, heat and water in a tropical rain forest at Pasoh in Peninsular Malaysia. *Tellus B* **60**: 569–582. DOI: 10.1111/j. 1600-0889.2008.00367.x.

Ohta T, Hiyama T, Tanaka H, Kuwada T, Maximov TC, Ohata T, Fukushima Y. 2001. Seasonal variation in the energy and water exchanges above and below a larch forest in eastern Siberia. *Hydrological Processes* **15**: 1459–1476. DOI: 10.1002/hyp.219.

da Rocha HR, Goulden ML, Miller SD, Menton MC, Pinto LDVO, de Freitas HC, e Silva Figueira AM. 2004. Seasonality of water and heat fluxes over a tropical forest in eastern Amazonia. *Ecological Applications* **14**: S22–S32.

Schuepp PH, Leclerc MY, MacPherson JI, Desjardins RL. 1990. Footprint prediction of scalar fluxes from analytical solutions of the diffusion equation. *Boundary-Layer Meteorology* **50**: 355–373. DOI: 10.1007/BF00120530.

Shuttleworth WJ. 1988. Evaporation from Amazonian rainforest. *Proceedings of the Royal Society of London. series B* **233**: 321–346.

Soepadmo E. 1978. Introduction to the Malaysian I. B. P. Synthesis Meetings. *The Malayan Nature Journal* **30**: 119–124.

Takanashi S, Tani M, Abdul Rahim N. 2003. Characteristics of transpiration over a tropical rainforest in Peninsular Malaysia. *Journal of the Japanese Society of Revegetation Technology* **29**: 51–55 (in Japanese with English abstract).

Tanaka N, Kume T, Yoshifuji N, Tanaka K, Takizawa H, Shiraki K, Tantasirin C, Tangtham N, Suzuki M. 2008. A review of evapotranspiration estimates from tropical forests in Thailand and adjacent regions. *Agricultural and Forest Meteorology* **148**: 807–819. DOI: 10.1016/j.agrformet.2008.01.011.

Tanaka H, Ohta T, Maximov TC, Hiyama T. 2002. Re-evaluation of the energy exchange rate including the advection in a larch forest in eastern Siberia. *Journal of Japan Society of Hydrology and Water Resources* **15**: 615–624 (in Japanese with English abstract).

Tani M, Abdul Rahim N, Ohtani Y, Yasuda Y, Sahat MM, Baharuddin K, Takanashi S, Noguchi S, Zulkifli Y, Watanabe T. 2003b. Characteristics of energy exchange and surface conductance of a tropical rain forest in Peninsular Malaysia. In *Pasoh: Ecology of a Lowland Rain Forest in Southeast Asia*, Okuda T, Niiyama K, Thomas SC (eds). Springer: Tokyo; 73–88.

Tani M, Abdul Rahim N, Sahat MM, Noguchi S, Ohtani Y. 2003a. Five-year meteorological observation at Pasoh Forest Reserve, Negeri Sembilan, Peninsular Malaysia. *Forest Research Institute Malaysia Reports* **78**: 1–27.

Webb EK, Pearman GI, Leuning R. 1980. Correction of flux measurements for density effects due to heat and water vapour transfer. *Quarterly Journal of the Royal Meteorological Society* **106**: 85–100.

Wilson K, Goldstein A, Falge E, Aubinet M, Baldocchi D, Berbigier P, Bernhofer C, Ceulemans R, Dolman H, Field C, Grelle A, Ibrom A, Law BE, Kowalski A, Meyers T, Moncrieff J, Monson R, Oechel W, Tenhunen J, Valentini R, Verma S. 2002. Energy balance closure at FLUXNET sites. *Agricultural and Forest Meteorology* **113**: 223–243. DOI: 10.1016/S0168-1923 (02) 00109-0.

J For Res
DOI 10.1007/s10310-010-0235-4

SPECIAL FEATURE: ORIGINAL ARTICLE

CO_2 flux observation in various forests of Monsoon-Asia

Effect of inter-annual climate variability on evapotranspiration and canopy CO_2 exchange of a tropical rainforest in Peninsular Malaysia

**Yoshiko Kosugi · Satoru Takanashi ·
Makoto Tani · Shinjiro Ohkubo · Naoko Matsuo ·
Masayuki Itoh · Shoji Noguchi · Abdul Rahim Nik**

Received: 27 April 2010 / Accepted: 14 October 2010

Abstract We investigated inter-annual variation of canopy CO_2 exchange (NEE) and evapotranspiration during a 7-year period over a lowland Dipterocarp forest in Pasoh, Peninsular Malaysia, using the eddy covariance method. Annual rainfall fluctuated between 1,451 and 2,235 mm during this period. Annual evapotranspiration estimated by energy budget correction and gap filling using the relationship between latent heat and available energy was 1,287 ± 52 mm. Despite inter-annual variation in rainfall, annual evapotranspiration was stable, except for a slight decrease in the driest year (2009). Evapotranspiration was roughly related to the amount of available energy, but was regulated by stomatal closure to prevent excessive water loss at high vapour pressure deficit. Even during dry periods, no significant decrease in evapotranspiration occurred, as water was supplied from soil layers deeper than 0.5 m. Ecosystem respiration (RE) increased with soil water content. Daytime NEE was also stable during the 7 years, despite climate variability. Afternoon inhibition of canopy photosynthesis was seen every month. Daytime NEE did not become more negative with increasing solar radiation, or with increasing soil water content. During dry periods, gross primary production (GPP) and thus canopy gross photosynthesis decreased slightly, coupled with decreased daytime RE. In this forest, variability in rainfall pattern resulted in seasonal and inter-annual variability in micrometeorology; evapotranspiration, photosynthesis, and RE responded to these changes, and compensated for each other and/or other components of micrometeorology, resulting in rather stable annual evapotranspiration and NEE, even during a very dry year associated with an El Nino Southern Oscillation (ENSO) event.

Keywords Dipterocarp · Ecosystem respiration · Eddy covariance method · Flux · NEE · Southeast Asia

Introduction

Clarification of the nature and magnitude of diurnal, seasonal, and annual evapotranspiration and canopy CO_2 exchange in tropical rainforests, and identification of the factors affecting these exchanges on different timescales are of primary importance to understanding the role of gas exchange in the global climate. Although relatively few

---

Y. Kosugi (✉) · M. Tani
Laboratory of Forest Hydrology, Division of Environmental Science and Technology, Graduate School of Agriculture, Kyoto University, Kyoto 606-8502, Japan
e-mail: ykosugi@kais.kyoto-u.ac.jp

S. Takanashi
Forestry and Forest Products Research Institute,
Tsukuba, Ibaraki 305-8687, Japan

S. Ohkubo
National Agricultural Research Center for Hokkaido Region,
Sapporo 062-8555, Japan

N. Matsuo
Faculty of Bioresources, Mie University,
Tsu, Mie 514-8507, Japan

M. Itoh
Center for Ecological Research,
Kyoto University, Shiga 520-2113, Japan

S. Noguchi
Forestry and Forest Products Research Institute Tohoku
Research Center, Morioka, Iwate 020-0123, Japan

A. R. Nik
Forest Research Institute Malaysia,
Kepong, Kuala Lumpur 52109, Malaysia

studies have applied eddy covariance (EC) flux measurement in tropical rainforests compared with other vegetation types (Valentini et al. 2000; Baldocchi et al. 2001; Yasuda et al. 2003), recent studies have observed 1–3 years of flux of either evapotranspiration or CO_2 exchange at several sites in Amazonian (Malhi et al. 1998, 2002; Araújo et al. 2002; Saleska et al. 2003; da Rocha et al. 2004; Goulden et al. 2004; Kruijt et al. 2004; Miller et al. 2004) and Southeast Asian (Kumagai et al. 2005, 2006; Takanashi et al. 2005; Hirano et al. 2007; Kosugi et al. 2008; Takanashi et al. 2010) tropical rainforests.

The most important environmental difference between Amazonian and Southeast Asian tropical forests with regard to factors determining the nature and magnitude of diurnal, seasonal, and annual evapotranspiration and canopy CO_2 exchanges, is rainfall pattern. For example, most Amazon rainforest sites have distinct dry and wet seasons during the year and the effect of drought stress on gas exchange is an important issue in this region (Asner et al. 2004). In contrast, Southeast Asian rainforests do not experience distinct dry and wet seasons during the year although dry and wet periods do occur with considerable variability between years (Tani et al. 2003; Kumagai et al. 2005). After examination of a year's worth of EC data for the Tapajós site of Brazil, Goulden et al. (2004) showed that canopy CO_2 exchange (NEE) became more negative during the dry season as soil respiration decreased. They also found no obvious effect of drought stress on daytime net canopy photosynthesis, probably because of deep root systems. Recently we studied 3 years of EC CO_2 flux (Kosugi et al. 2008) and latent and sensible heat fluxes (Takanashi et al. 2010) in a primary tropical rainforest in the Pasoh Forest Reserve, Peninsular Malaysia. We found a very stable monthly diurnal course of evapotranspiration and NEE during this period. Although we observed an increase in CO_2 uptake caused by a decrease in soil respiration during dry periods in this Southeast Asian rainforest similar to that reported by Goulden et al. (2004), the increase of CO_2 uptake did not have the clear seasonality it exhibited in Amazonian forests. From these results, rainfall pattern, and the closely related soil moisture, can be assumed to be among the most important environmental factors determining gas exchange in tropical forests. Other environmental factors, for example radiation, air temperature, and vapour pressure deficit, which are also related to rainfall pattern, and typically regarded as key factors in various types of global-scale carbon and water movement models used to evaluate ecosystem function, should also be considered. To clarify the effect of these environmental factors and their future changes on gas exchange processes of tropical forests, we should first evaluate the actual range of their fluctuations as affected by inter-annual climate variability.

Long-term heat, H_2O, and CO_2 flux monitoring based on EC measurements enables evaluation of the inter-annual range of fluctuation in gas exchange and detailed analysis of the factors affecting gas exchange. In this study, we examined 7 years of fluctuations in microclimate, sensible and latent heat flux, and CO_2 flux to determine the effect of daily, seasonal, and inter-annual climate variability on evapotranspiration and canopy CO_2 exchange of a tropical rainforest in Pasoh, Peninsular Malaysia.

Materials and methods

Site

The study was conducted on an observation tower in the Pasoh Forest Reserve (PSO) of the Forest Research Institute Malaysia (FRIM), located near Simpang Pertang in Negeri Sembilan, Peninsular Malaysia (2°58′N, 102°18′E, 75–150 m a.s.l.). The core area (600 ha) of the reserve (2,450 ha) is covered with primary lowland mixed dipterocarp forest and includes various species of *Shorea* and *Dipterocarpus*. The continuous canopy height is approximately 35 m, but some emergent trees exceed 45 m. The soil type around the tower is Haplic Acrisol according to FAO classifications. The A horizon is thin (0–0.05 m; Yamashita et al. 2003), and lateritic gravels are abundant below 0.3 m (Soepadmo 1978; Yamashita et al. 2003). The area has a gently undulating topography. Topographic details and a fetch analysis are reported in Takanashi et al. (2010). Additional site details are described in Kosugi et al. (2008).

Mean annual rainfall at the study site totals 1,804 mm (1983–1997; Tani et al. 2003), less than in other regions of Peninsular Malaysia (Noguchi et al. 2003). Rainfall peaks from March to May and from October to December, and mostly occurs from late afternoon to night (Kosugi et al. 2008).

Observations

Meteorological variables were monitored at a height of 52–54 m on the observation tower; these variables included downward (S_d, W m^{-2}) and upward shortwave radiation (measured using an MR22; Eko Instruments, Tokyo, Japan), downward and upward longwave radiation (model PIR; Eppley, Newport, RI, USA), net radiation as the balance of the four previous components (R_n, W m^{-2}), air temperature and humidity (models HMP45A, HMP45C; Vaisala, Helsinki, Finland), and rainfall (Fig. 1). Soil water content at depths of 0.1, 0.2, and 0.3 m (volumetric soil water content (VSWC), m^3 m^{-3}; average of the values from nine sensors; CS615 or CS616; Campbell Scientific, Logan, UT, USA), soil heat flux (G, W m^{-2}; model HFP01; Hukseflux Thermal Sensors, Delft, The Netherlands), and soil temperature

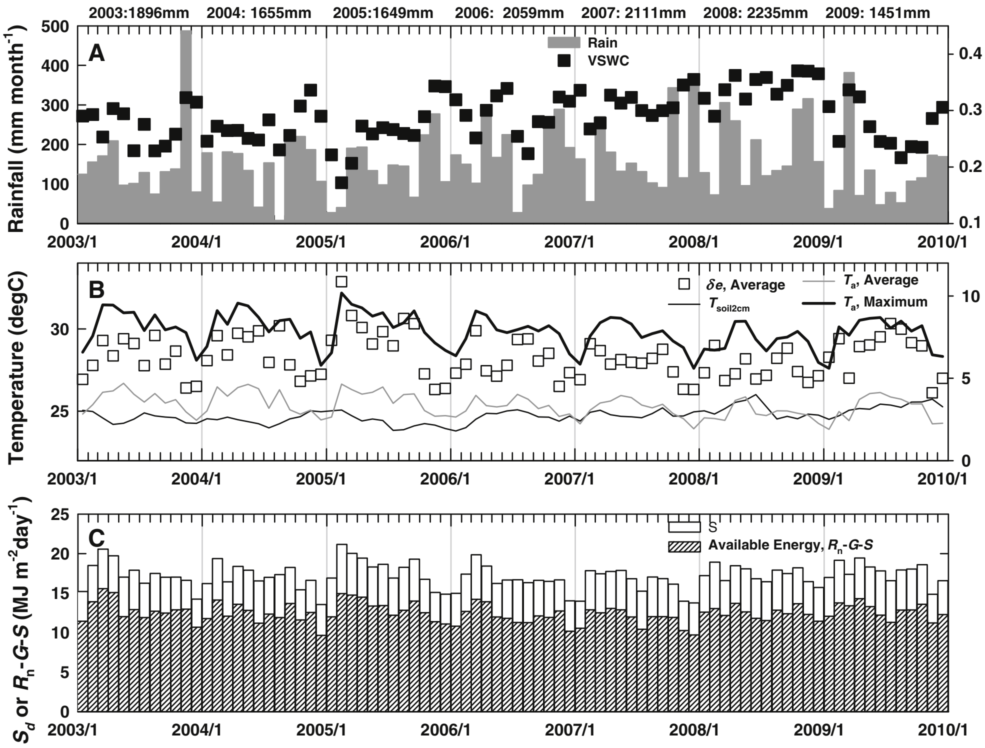

Fig. 1 **a** Monthly amount of rainfall (*grey bars*), and monthly average volumetric soil water content at 0.1, 0.2, and 0.3 m taken with nine sensors (*black squares* VSWC); **b** monthly average air temperature (*grey line*), monthly maximum air temperature (*bold black line*), monthly average vapour pressure deficit (δe, *white squares*), and monthly average soil temperature at 0.02 m depth (*black line*); **c** monthly average daily amount of solar radiation (*shadow bars*, S_d) and available energy (*white bars*, $R_n - G - S$), at the Pasoh tower site from January 2003 to December 2009

($T_{soil2cm}$, °C; thermocouple model 107; Campbell Scientific) at a depth of 0.02 m were monitored at three points around the tower. Rainfall was measured by use of tipping-bucket rain gauges (model 34-T; Ota Keiki Seisakusho, Tokyo, Japan) at the top of the tower (52 m) and at an observatory located 430 m from the tower.

Fluxes of sensible heat, water vapour, and carbon dioxide were measured at a height of 54 m on the observation tower. Wind velocity and temperature were measured with a three-axis sonic anemometer (SAT-550; Kaijo, Tokyo, Japan). CO_2 and H_2O concentrations were monitored with an open path CO_2/H_2O analyser (LI-7500; Li-Cor, Lincoln, NE, USA). Data were sampled at 10 Hz and sent to a data logger (CR-5000; Campbell Scientific). Fluxes of momentum, sensible heat (H, W m^{-2}), latent heat (λE, W m^{-2}) and CO_2 (F_c, μmol m^{-2} s^{-1}) were calculated as 30-min averages. Double rotation (McMillen 1988) was applied, assuming a zero mean vertical wind. The Webb–Pearman–Leuning (WPL) correction for the effect of air density fluctuations (Webb et al. 1980) was applied. Linear trends in temperature, water vapour, and CO_2 concentration were not removed. The eddy flux observations were described in more detail in Kosugi et al. (2008). We added two criteria after the flux data used in Kosugi et al. (2008) and Takanashi et al. (2010). Data that did not meet the stationarity criteria (Foken and Wichura 1996; Aubinet et al. 2000) were rejected. λE and F_c data obtained during periods of rainfall (from 30 min before to 60 min after a rainfall event) were rejected. Eddy flux observations have been collected since September 2002, and this study considered the 7 years of data from January 2003 to December 2009.

Vertical profiles of CO_2 concentration, air temperature and humidity were also observed to assess fluxes of sensible and latent heat and CO_2 storage (S_c, μmol m^{-2} s^{-1}). More details of the profile measurements and calculation of the storage terms are described in Ohkubo et al. (2008). The profile data available for calculating the storage terms were limited. To compensate for the lack of profile observation data, we used the differentials at one reference height for canopy heat storage fluxes and CO_2 storage flux for preparing the long-term database. Each component of biomass, sensible heat, and latent heat storage flux (S, W m^{-2}) was estimated using the relationship with the temperature or vapour pressure differential at 52-m height based on Ohtani et al. (1997). We estimated S_c using the CO_2 concentration at 54-m height, based on the relationship between $\Delta c/\Delta t$ (ppm h^{-1}) at the top of tower measured with the LI-7500 open-path sensor and S_c calculated from the profile measurement (Fig. 2). In this study, instantaneous NEE was estimated as $F_c + S_c$.

Evapotranspiration data correction and gap-filling policy

As reported by Takanashi et al. (2010), energy imbalance is a severe problem and should be considered when estimating evapotranspiration at this site, as pointed out for other tower sites (Wilson et al. 2002; Kumagai et al. 2005; Kosugi and Katsuyama 2007; Kosugi et al. 2007a). We tried several methods of data correction and gap filling to assess the effect of the imbalance correction and the gap-filling method. Because we used an open-path infrared gas analyzer (IRGA), latent heat flux data were rejected and replaced with $(R_n - G - S) - H$ during periods of rainfall and for the first hour after rainfall.

Method 1

Energy budget corrections were made for both sensible and latent heat fluxes using a Bowen ratio to produce an energy imbalance of zero. Gaps were filled using the second-order polynomial relationship between 30-min λE after the energy budget correction with Method 1 and available energy $(R_n - G - S)$ determined using all available data for each year.

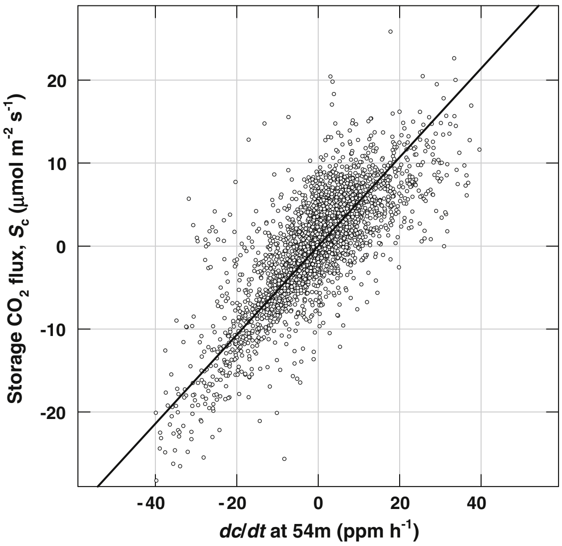

Fig. 2 The relationship between the difference in ambient CO_2 concentration at the top of the observation tower (54 m) measured using a LI7500 open-path gas analyser ($\Delta c/\Delta t$, ppm h^{-1}) and storage CO_2 flux (S_c, μmol m^{-2} s^{-1}) estimated using CO_2 concentrations from 10 different heights. All available data for 2008 were used in this analysis (n = 3,879). The median value of the relationship was used for estimation of storage CO_2 flux

Method 1′

This is the same as Method 1 for energy budget corrections, but with a different gap-filling method. The daily amount of evapotranspiration was calculated for the days the gap percentage was within 15%, and the daily base gap was filled using the second-order polynomial relationship between daily amounts of evapotranspiration (E, mm) after the energy budget correction with Method 1 and $R_n - G - S$ determined using all available data for the 7 years.

Method 2

No energy budget corrections were made. Gaps were filled using the second-order polynomial relationship between raw 30-min λE and $R_n - G - S$ determined using all available data for each year.

Method 3

Energy budget corrections were made for latent heat flux only to produce energy imbalances of zero. Gaps were filled using the second-order polynomial relationship between 30-min λE after energy budget correction with Method 3 and $R_n - G - S$ determined using all available data for each year.

Note that gap filling was only applied for the analysis with Figs. 5 and 6, and not that with Figs. 3 and 4, to prevent possible artificial bias. In Figs. 3 and 4, energy budget corrections were based on Method 1. In Fig. 4, monthly averaged daily amounts of sensible and latent heat flux were calculated for days with gap percentage values within 15%.

Data correction and gap-filling policy of NEE

Nighttime and daytime NEE gaps were filled separately. As pointed out by Kosugi et al. (2008), raw nighttime NEE data might severely underestimate nighttime ecosystem respiration (RE) at this site, even with turbulent intensity (u^*) correction. All nighttime NEE data were rejected and replaced with estimated RE. RE was estimated in two different ways. Daytime gaps were normally filled with the 7-year-average diurnal course of observed daytime NEE. Because we used open-path IRGA, F_c and S_c were rejected during periods of rainfall and for the first

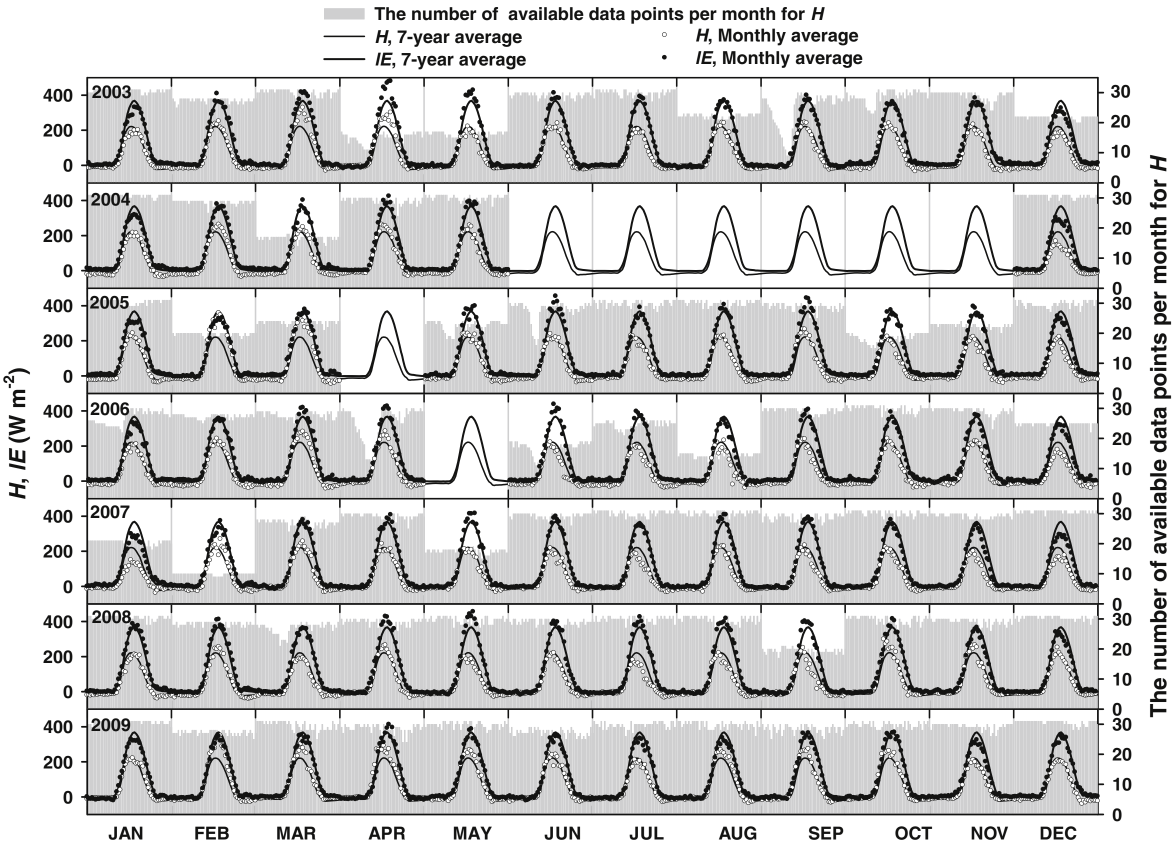

Fig. 3 Monthly averaged diurnal courses of sensible (*H*) and latent heat (λE) flux at the Pasoh tower site from January 2003 to December 2009. *Black line*, 7-year average diurnal course of sensible heat flux; *bold black line*, 7-year average diurnal course of latent heat flux; *white circles*, monthly averaged diurnal course of sensible heat flux; *black circles*, monthly averaged diurnal course of latent heat flux; *grey bars*, number of days per month with available data points for *H*

hour after rainfall. In Methods 1 and 3, described below, daytime NEE during periods of rainfall was replaced with estimated RE. We have no evidence that NEE during rainfall events equals RE, although we expect it to fall within a range between RE and the average diurnal course of daytime NEE. We examined both extremes as described in Methods 1 and 2. The effect of the different models of filling rainfall gaps was also assessed in this study.

Method 1

Nighttime NEE was replaced with estimated RE based on the relationship between "optimum" nighttime NEE with EC measurement and VSWC (bold black line in Fig. 7b). Daytime NEE during periods of rain was replaced with estimated RE. Other daytime gaps were filled with the 7-year-average diurnal course of observed daytime NEE.

Method 2

Nighttime NEE was replaced with estimated RE based on the relationship between "optimum" nighttime NEE with EC measurement and VSWC (bold black line in Fig. 7b). Daytime gaps were filled with the 7-year-average diurnal course of observed daytime NEE.

Method 3

Nighttime NEE was replaced with another estimate of RE based on the chamber method (grey line in Fig. 7b). We occasionally observed the soil respiration rate at the site, from 2002 using a 50 m × 50 m plot (Kosugi et al. 2007b) and from 2006 at a 2-ha plot matching the main fetch of the EC flux (Takanashi et al. 2010), including a wide range of VSWC. The spatially averaged soil respiration in the larger (2 ha) plot roughly showed a linear increase with increasing VSWC, as in the 50 m × 50 m plot, although the slope

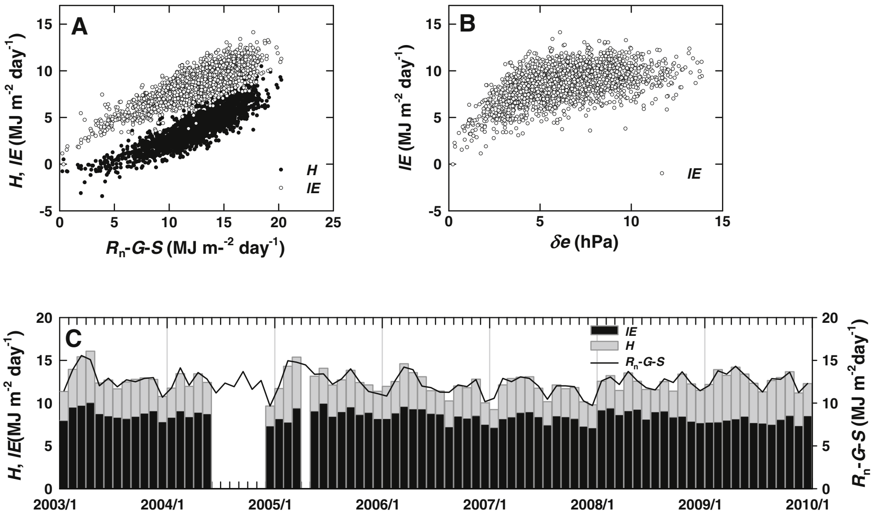

Fig. 4 **a** Relationship between daily amount of latent (*white circles*, λE) or sensible (*black circles*, H) heat flux and daily amount of available energy ($R_n - G - S$); **b** relationship between daily amount of latent heat flux (*white circles*, λE) and daily average air vapour pressure deficit (δe), and **c** monthly average daily amount of sensible (*grey bars*) and latent (*black bars*) heat flux, and available energy (*black line*) at the Pasoh tower site from January 2003 to December 2009. Energy budget correction was made for both sensible and latent heat flux to result in energy imbalances of zero. All latent heat flux data during rainfall events and for the first hour after the events were rejected and replaced with $(R_n - G - S) - H$. Daily amounts of sensible and latent heat flux were calculated for the days when gap percentage was within 15%

became milder, and the deviation became wider than in the smaller plot. We made a trial estimate of total RE, using this estimate of soil respiration in relation to VSWC from the 2-ha plot (Kosugi et al., unpublished data) and other components (leaf, trunk, forest floor trees, and coarse woody debris (CWD)) of RE reported by Chambers et al. (2004). Daytime NEE during periods of rain was replaced with estimated RE. Other daytime gaps were filled with the 7-year-average diurnal course of observed daytime NEE.

Note that gap filling was only applied for the analysis in Figs. 10, 11 and 12, and not for those in Figs. 8 and 9, to prevent possible artificial bias. In Figs. 8 and 9a, the monthly averaged diurnal course of daytime NEE was purely calculated using all available 30-min data. In Figs. 9b, c, daytime mean NEE was purely calculated using all available 30-min data for the days that the gap percentage of daytime NEE data was within 15%.

Results

Micrometeorology

Annual rainfall fluctuated between 1,451 and 2,235 mm (1,865 ± 288 mm) during the 7 study years. The study site had a constant rainy period in November and December, and mild dry periods between January and March and from July to October, although the intensity of these dry periods varied annually. The years 2003, 2004, and 2005 were rather dry, and 2006, 2007, and 2008 were wet years. Also, 2009 was a dry year, affected by an ENSO event, with only 1,451 mm rain. Figure 1 shows that variation in rainfall pattern resulted in seasonal and inter-annual variability in other components of micrometeorology. VSWC was higher during 2006, 2007, and 2008, and in November and December of every year. Air temperature, vapour pressure deficit, and radiation decreased in wet periods in November and December of every year. Because most rainfall occurred in the evening and at night, reductions in radiation during wet periods were not apparent. The driest month during the 7-year period was February 2005, the wettest and sunniest month was November 2008, and several unusual daytime storms and cloudy days occurred in December 2007.

Evapotranspiration

Approximately 70% of available energy in this forest was partitioned to the latent heat flux (Figs. 3, 4c). Latent heat flux peaked around solar noon (1300 h local time), and no obvious decline occurred in the afternoon compared with morning values (Fig. 3). The diurnal course of latent heat flux was rather stable over the 7-year period, with little fluctuation from the 7-year-average line (Fig. 3). Both daily latent and sensible heat flux were roughly related to the amount of available energy (Fig. 4a), although Figs. 3, 4a, c indicate that excess energy was disproportionately partitioned to sensible heat flux. The relationship between the daily latent heat flux and vapour pressure deficit (δe) shows the upper limit of latent heat flux at high vapour pressure deficit (Fig. 4b).

Daily and annual evapotranspiration were calculated using several data correction and gap-filling methods. Although considerable differences existed among the estimates, we are able to obtain stable annual evapotranspiration (1,287 ± 52 mm with Method 1) despite rainfall fluctuation and irrespective of correction or gap-filling method (Figs. 5, 6). At the same time, we detected a slight decrease of annual evapotranspiration in the driest year (2009). Figure 6 shows that, except in the driest year (2009), annual evapotranspiration increased with increasing annual amount of available energy ($R_n - G - S$).

We did not detect any obvious decline in monthly evapotranspiration, even in February 2005, the driest month of the study, although during the driest period of the study from January to March 2005, the amount of rainfall was much lower than the amount of evapotranspiration (Fig. 5a). Figure 5b shows the soil water budget, comparing cumulative residual evapotranspiration from rainfall and soil water storage differential between 0 and 0.5 m depth; this was calculated using the average VSWC at the depth between 0.1 and 0.3 m from nine sensors, assuming uniform soil water content between 0 and 0.5 m depth. In most periods, a decline in soil water storage between 0 and 0.5 m depth coincided well with evaporative demand (slope of decline shown by the bold black line in Fig. 5b). However, in the driest periods, for example August 2004, February 2005, July and August 2006, February 2009, and July to October 2009, the slope of evaporative demand was greater than the slope of decline for soil water storage between 0 and 0.5 m depth, indicating that water was supplied from deeper soil layers.

Nighttime NEE

Kosugi et al. (2008) compared nighttime NEE and soil respiration, but did not have enough NEE data, because S_c data were limited at that time. In this study, we were able to examine the relationship in more detail using all available NEE data for the 7-year study period after calculating S_c using the differential of CO_2 concentration at the reference height.

First, pure processing of all raw nighttime NEE data showed that it increased with increasing VSWC, although the values were lower than expected total RE (grey line in Fig. 7b), as pointed out by Kosugi et al. (2008). We have no solution for the severe imbalance problem at this site, because it was strongly suggested advection flux was involved in most nighttime gas exchange. However, we can still extract the trend of nighttime NEE (=RE) from

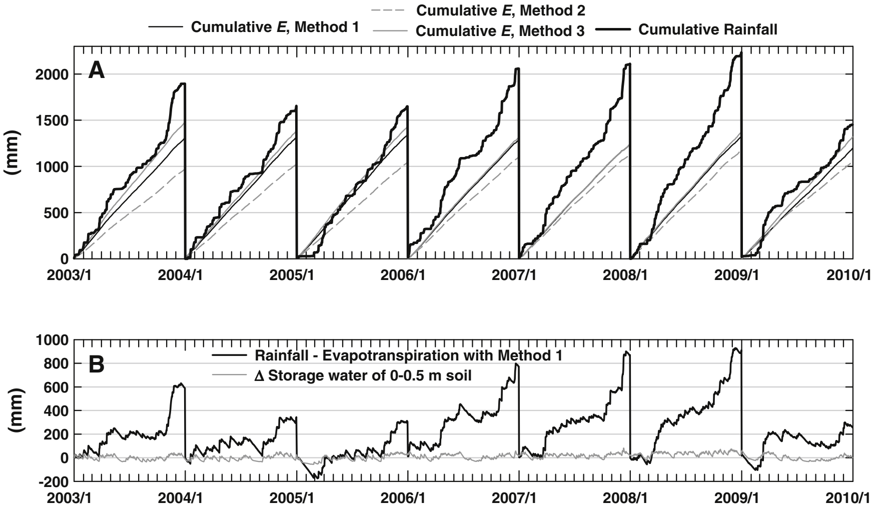

Fig. 5 **a** Annual cumulative values of rainfall and evapotranspiration (*E*, mm), and **b** the soil water budget, comparing cumulative residual evapotranspiration from rainfall and the soil water storage differential in the 0–0.5-m-deep soils at the Pasoh tower site from January 2003 to December 2009. In Method 1, energy budget corrections were made for both sensible and latent heat fluxes using the Bowen ratio, to result in energy imbalances of zero; these corrections were not made in Method 2, and in Method 3 were only made for latent heat flux, to result in energy imbalances of zero. All latent heat flux data during rainfall events and for the first hour after the events were rejected and replaced with ($R_n - G - S$) − H. Gaps were filled using the second-order polynomial relationship between 30-min λE and available energy ($R_n - G - S$) determined using all available data for each year. Evapotranspiration calculated using Method 1 was used in **b**. The soil water storage differential in 0–0.5-m-deep soil was calculated using the average volumetric soil water content at depths from 0.1 to 0.3 m from nine sensors, assuming uniform soil water content between 0 and 0.5 m depth

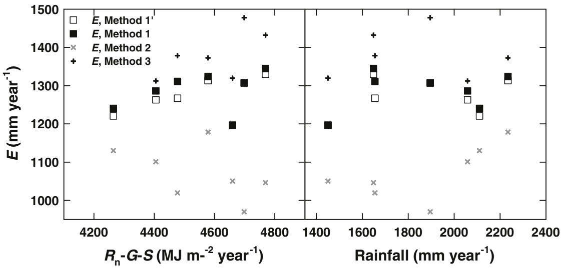

Fig. 6 Annual evapotranspiration versus available energy ($R_n - G - S$) or rainfall. Energy budget corrections were made for both sensible and latent heat flux using the Bowen ratio, to result in energy imbalances of zero in Methods 1 and 1′; these corrections were not made in Method 2, and in Method 3 were only made for latent heat flux, to result in energy imbalances of zero. During rainfall events and for the first hour after the events, all latent heat flux data were rejected and replaced with $(R_n - G - S) - H$. In Methods 1, 2, and 3, gaps were filled using the second-order polynomial relationship between 30-min λE and available energy ($R_n - G - S$) determined using all available data for each year. In Method 1′, daily amounts of evapotranspiration were calculated for the days when gap percentage was within 15%, and daily base gap was filled using the second-order polynomial relationship between the daily amount of evapotranspiration and available energy ($R_n - G - S$) determined using all available data for all 7 years

the EC data. The "optimum" sets of nighttime NEE, F_c, and S_c data matching the criteria ($F_c > 0$, $S_c > 0$, $5 < \mathrm{NEE} < 15$ μmol m^{-2} s^{-1}) were chosen for further analysis ($n = 6{,}033$, Fig. 7a, b). The NEE criteria were set to be within the range of expected RE, on the basis of information from the chamber studies. We detected an increase in F_c and a decrease in S_c with increasing u^* (Fig. 7a), and also noticed a clear dependency of VSWC on u^*, which resulted in decreasing NEE at higher u^*. As the decline of NEE at low u^* disappeared during the rise of lower criteria of NEE (Fig. 7a), we did not discard the NEE at low u^* to make the relationship between NEE and VSWC (Fig. 7b). A mild increase in NEE with increasing VSWC was detected (bold black line in Fig. 7b), and the line defined by this relationship corresponded well with the trial estimate of RE based on the chamber observations, although the range of values was lower than the estimated values of RE.

Daytime NEE

The monthly averaged diurnal course of daytime NEE (Fig. 8) was quite stable and showed no obvious variation

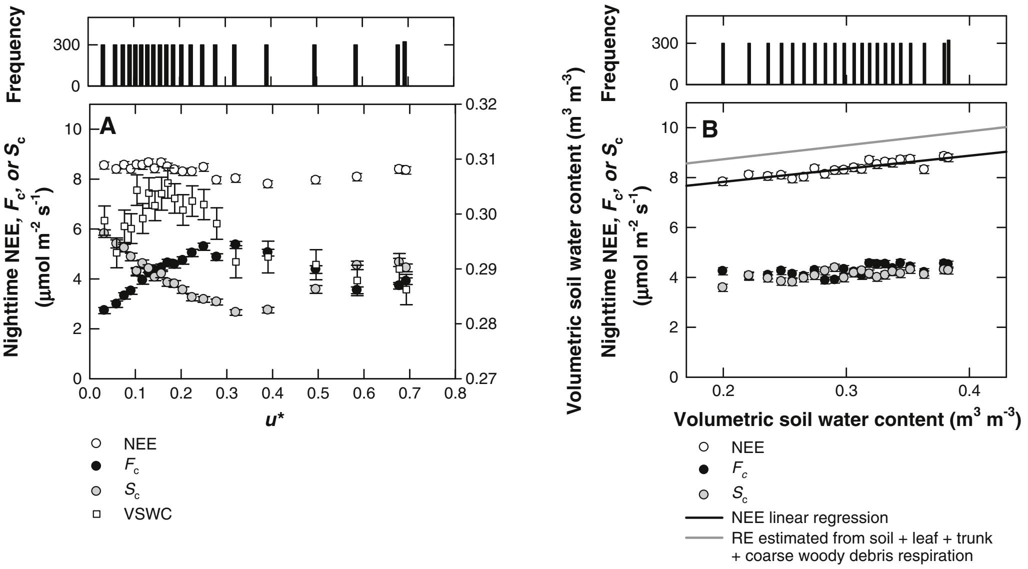

Fig. 7 **a** Relationship between turbulence intensity (u^*, m s^{-1}) and NEE (*white circles*), F_c (*black circles*), S_c (*grey circles*), and volumetric soil water content (*VSWC*) at depths between 0.1 and 0.3 m (*white square*). **b** Relationship between VSWC and NEE (*white circles*), F_c (*black circles*), and S_c (*grey circles*). "Optimum" sets of nighttime NEE, F_c, and S_c data matching the criteria ($F_c > 0$, $S_c > 0$, $5 < \mathrm{NEE} < 15$ μmol m^{-2} s^{-1}) were chosen for this analysis ($n = 6{,}033$). The data were grouped in clusters of 300 points into each class of u^* or VSWC. Average values with a standard error for each class are shown as *dots* and *error bars* in the figure. Frequencies are shown as *bar graphs* at the *top* of the diagram. The *bold black line* denotes the linear regression for NEE. The *bold grey line* indicates a trial estimate of total ecosystem respiration based on the chamber method, adding soil respiration in relation to VSWC (Kosugi et al., unpublished data), and other components (leaf, trunk, forest floor trees, and coarse woody debris) of ecosystem respiration from Chambers et al. (2004)

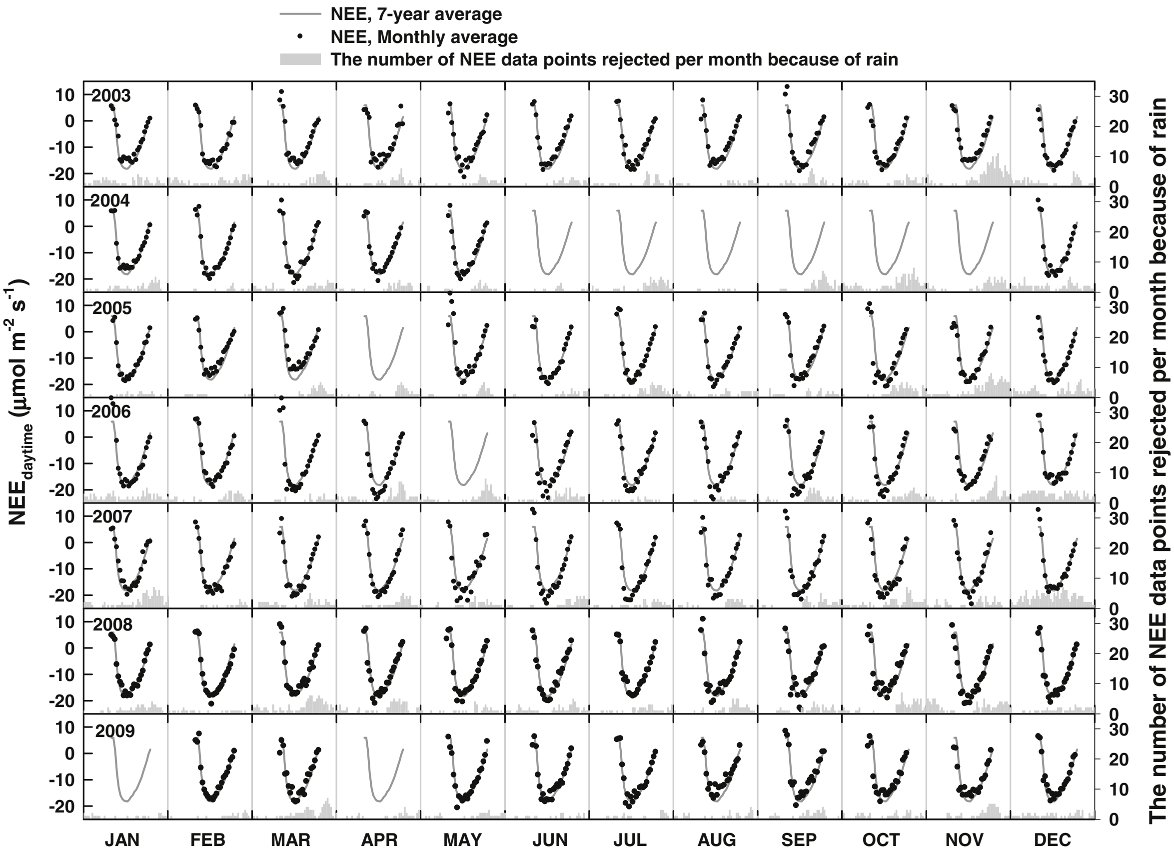

Fig. 8 Monthly averaged diurnal course of daytime NEE at the Pasoh tower site from January 2003 to December 2009. *grey line*, 7-year average diurnal course of daytime NEE; *black circles*, monthly averaged diurnal course of daytime NEE; *grey bars*, the number of NEE data points rejected per month because of rain

during the 7 years. These results agree with those of a previous study using data from 2003 and 2005 (Kosugi et al. 2008), even though the more recent years included in our study had both wetter (2006–2008) and drier conditions (2009, related to the ENSO event). Less negative values of NEE (decreased CO_2 uptake) were seen in the afternoon every month. The numbers of NEE observations omitted because of rain are shown in Fig. 8 (grey bars), and we should carefully consider the effect of these periods, even though most rainfall occurred in the evening and at night, and the numbers of daytime rain event observations were often similar between dry and wet periods, except for a few months. If we assume less negative NEE values (smaller CO_2 uptake) during rain periods, then afternoon NEE values would be even less negative.

The effect of solar radiation on NEE is shown in Fig. 9. Monthly averaged diurnal course of daytime NEE plotted against that of photosynthetic photon flux density (PPFD) (Fig. 9a) showed no obvious differences in the lower reaching point and diurnal pattern of NEE between the driest sunny period (February 2005), the wettest sunny period (November 2008), and a wet and cloudy period (December 2007), regardless of the differences in PPFD, although the afternoon decline in NEE was more severe in the driest month (February 2005). Daytime mean NEE neither became less negative with decreased daily sum of solar radiation at this site (Fig. 9b), nor became significantly less negative with the decrease in daily mean VSWC (Fig. 9c).

Carbon budget

Gap filling was performed to assess the daily, monthly, and annual sums of NEE, gross primary production (GPP), and RE and their variations in relation to variation in microclimate. Daily sum of GPP plotted against that of solar radiation (Fig. 10a; gap-filling Method 1; the daily sum of GPP is shown for the days when the percentage daytime

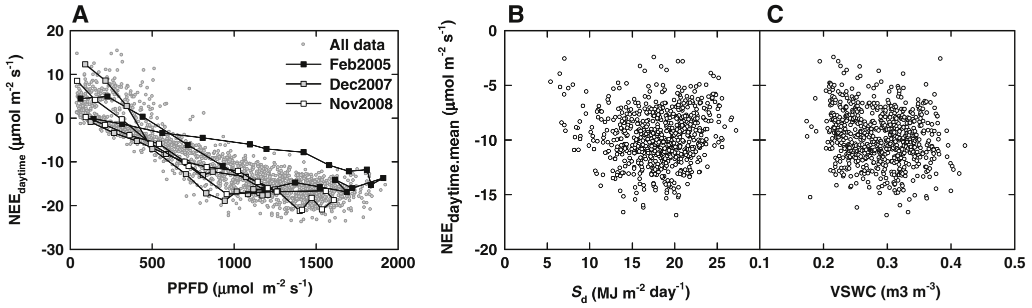

Fig. 9 **a** Monthly averaged diurnal course of daytime NEE in relation to PPFD at the Pasoh tower site from January 2003 to December 2009. The same daytime NEE data shown in Fig. 8 were used in this analysis. *Black circles*, February 2005 (dry and sunny); *grey circles*, December 2007 (wet and cloudy); *white circles*, November 2008 (wet and sunny). Daytime mean NEE per day versus **b** daily sum of solar radiation (S_d), and **c** daily average volumetric soil water content (*VSWC*) at depths between 0.1 and 0.3 m. In **b** and **c**, daytime mean NEE was calculated for the days when the daytime gap percentage was within 15%

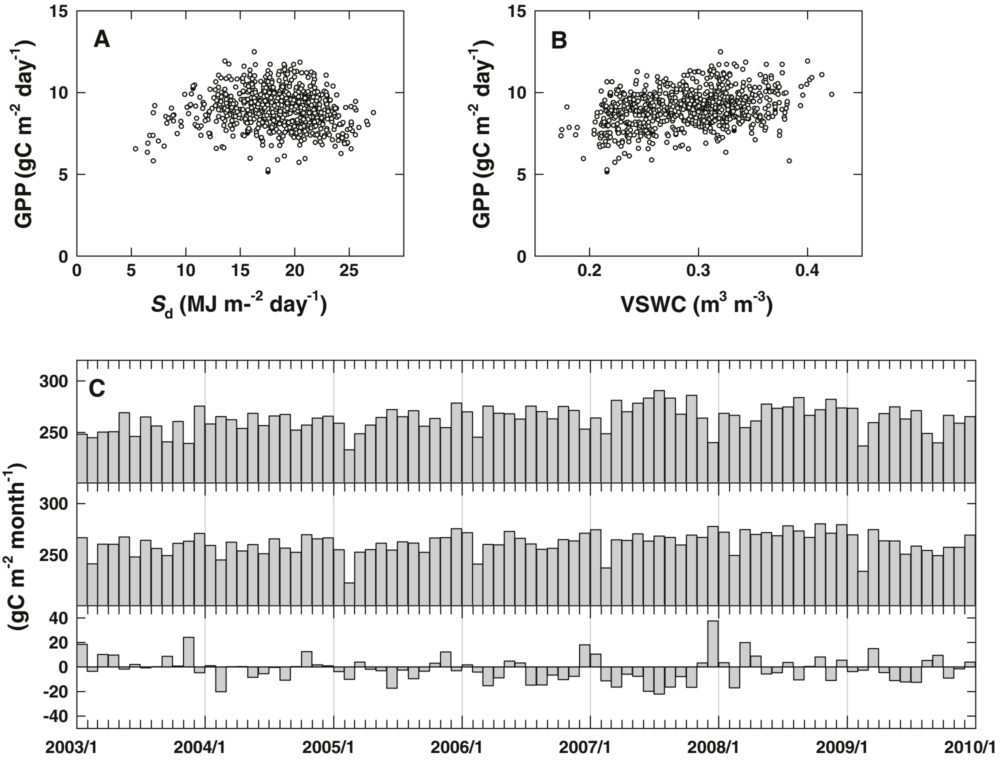

Fig. 10 Daily sum of GPP versus **a** daily sum of solar radiation (S_d), and **b** daily average volumetric soil water content (*VSWC*) at the depth between 0.1 and 0.3 m. **c** Monthly sum of GPP, RE, and NEE at the Pasoh tower site from January 2003 to December 2009. The data shown in this figure were estimated using Method 1. All nighttime NEE data were rejected and replaced with estimated RE based on the relationship with "optimum" nighttime NEE and VSWC shown in Fig. 7. Daytime NEE during rain events was replaced with estimated RE. Daytime gaps were filled with the 7-year average diurnal course of observed daytime NEE. In **a** and **b**, the daily sum of GPP is shown for the days when the daytime gap percentage of NEE was within 15%

gap of NEE was within 15%) showed no dependency of GPP on solar radiation, but showed a mild decrease with decreasing VSWC (Fig. 10b). This indicates that GPP decreased in the dry period along with the daytime decline in RE; thus, daytime NEE remained stable and showed no clear dependence on VSWC. The estimated monthly sum of GPP and RE consequently exhibited dependency on VSWC (Fig. 10c). The decline in RE during dry periods was greater than that in GPP, and thus NEE resulted in more CO_2 uptake by the whole canopy in dry periods than in wet periods.

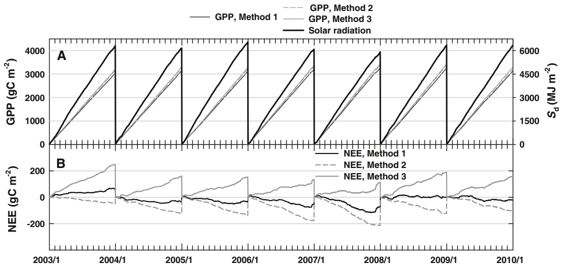

Fig. 11 Annual cumulative **a** solar radiation (S_d), GPP, and **b** NEE at the Pasoh tower site from January 2003 to December 2009. All nighttime NEE data were rejected and replaced with estimated RE based on the relationship with "optimum" nighttime NEE and VSWC (Methods 1 and 2), or replaced with another estimate of RE based on the chamber method (Method 3). Daytime gaps were filled with the 7-year average diurnal course of observed daytime NEE irrespective of method, although daytime NEE during rain events was replaced with estimated RE in Methods 1 and 3

Cumulative GPP and NEE exhibited no dependence on solar radiation, irrespective of gap-filling method (Fig. 11). In wet periods, especially in November and December of every year, cumulative NEE tended to increase (Fig. 11b), indicating net CO_2 release by the whole ecosystem. The average and standard deviation of annual GPP, RE, and NEE over the 7 years were 3,164 ± 77, 3,143 ± 59, and −21 ± 44 g C m^{-2}, respectively, with Method 1, 3,275 ± 91, 3,143 ± 60, and −132 ± 52 g C m^{-2}, respectively, with Method 2, and 3,332 ± 79, 3,498 ± 64, and 166 ± 43 g C m^{-2}, respectively, with Method 3 (Fig. 12). However, depending on the gap-filling method, interannual fluctuation in GPP, RE, and NEE was up to ± 100 g C m^{-2} (Figs. 11, 12). Neither gross nor net CO_2 uptake (GPP and negative value of NEE, respectively) exhibited any increase with increasing solar radiation on an annual basis (Fig. 12), and the annual values of GPP and RE roughly increased with increasing rainfall, and thus VSWC (Fig. 12).

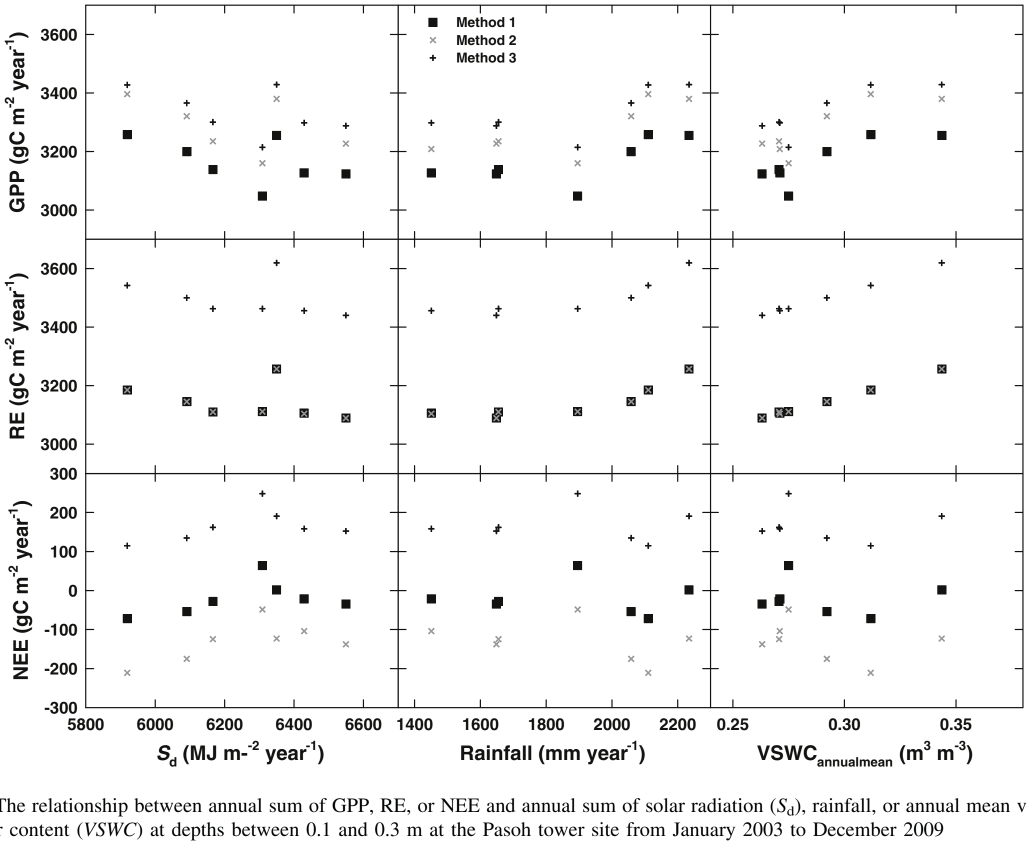

Fig. 12 The relationship between annual sum of GPP, RE, or NEE and annual sum of solar radiation (S_d), rainfall, or annual mean volumetric soil water content (*VSWC*) at depths between 0.1 and 0.3 m at the Pasoh tower site from January 2003 to December 2009

Discussion

Evapotranspiration

Annual evapotranspiration estimated with energy budget correction and gap filling using the relationship between latent heat and available energy was approximately 1,300 mm and quite stable despite inter-annual variation in rainfall (Figs. 3, 5, 6). It was roughly related to the amount of available energy. At the same time, a limitation on evapotranspiration at high vapour pressure was clearly observed (Fig. 4). This plateau in the relationship between evapotranspiration and vapour pressure deficit was evidence that stomatal closure occurred to prevent excessive water loss at high vapour pressure deficit. A decline in canopy conductance with vapour pressure deficit, irrespective of VSWC, was also reported by Takanashi et al. (2010). No increase in annual evapotranspiration with available energy occurred in the case of Method 2 (Fig. 6), probably because the periods of rainfall (including the first hour following the rain event), when raw λE was rejected and replaced with $(R_n - G - S) - H$, were fewer in sunny years. Thus the trend seen with Method 2 is considered to be artificial. The amount of annual evapotranspiration with Method 2 is also suspected to be an underestimate, based on comparisons with values of annual evapotranspiration in the tropics derived from the water budget (Oki et al. 1995).

No severe decline of evapotranspiration occurred during dry periods, because water was supplied from soil layers deeper than 0–0.5 m (Fig. 5). This phenomenon coincided well with the observed root distribution at this site. While observations of root distribution carried out in February 2009 and 2010 found most fine roots between 0 and 0.5 m, we also found fine roots as deep as 4.0 m (Yamashita et al., unpublished data).

Canopy CO_2 exchange

Nighttime NEE increased with soil water content (Fig. 7). Kosugi et al. (2007b) showed that soil respiration was lower in wetter places, but increased in wetter periods. The increase in nighttime NEE during wet periods corresponds well with the increase in spatially averaged soil respiration rate with increasing soil water content, which was detected by long-term chamber observations of soil respiration at the study site (Kosugi et al. 2007b; Fig. 7). Daytime NEE was stable during the 7 years despite climate variability (Fig. 8). In particular, we did not detect any evidence of the increasing or decreasing daytime NEE during wetter years, for example 2006 and 2008, or drier years, for example 2005 and 2009. This result indicates that no clear increase or decrease of daytime net canopy CO_2 uptake occurred within the range of observed seasonal and inter-annual differences in solar radiation and air temperature. Afternoon inhibition of canopy photosynthesis was seen every month (Fig. 8), although the magnitude of inhibition might have depended on soil moisture in the driest month (Fig. 9a). Daytime NEE neither became more negative with increasing solar radiation at this site (Fig. 9b), nor increased with increasing soil water content (Fig. 9c). This result indicates that GPP and thus canopy gross photosynthesis decreased a little during dry periods, coupling with decreased daytime RE (Fig. 10b).

The inhibition of canopy photosynthesis in the afternoon, and the slight decline in daily GPP in dry periods, corresponded well with results of single-leaf gas exchange analysis of the canopy leaves at this site (Takanashi et al. 2006; Kosugi et al. 2009). Therefore, we suggest that patchy stomatal closure induced the decline in canopy photosynthesis. The decline in RE coupled with the decline in GPP mitigated the influence of soil drought to net canopy CO_2 exchange, resulting in rather stable monthly and annual NEE. Our studies on single-leaf gas exchange also revealed that increased PPFD does not cause increased net assimilation by canopy leaves at this site in dry or wet periods (Kosugi et al. 2009). This result differed from that of Graham et al. (2003), who found that illumination resulted in increased net assimilation by a canopy leaves in an Amazonian rainforest. However, the difference might have been the result of the ambient PPFD conditions of the leaves, which were much lower in those sampled by Graham et al. (Fig. 2 in Graham et al. 2003) than in those at our site (Fig. 9a in this study, and Kosugi et al. 2009). Our data (Fig. 9a) also indicate a decline in net CO_2 uptake at lower PPFD ($<1{,}000$ µmol m^{-2} s^{-1}). Our results strongly suggest that more consideration should be given to the actual results of tower flux observations when discussing the effect of radiation on canopy CO_2 uptake; most numerical models expected to predict the effect of future climate change are apt to use simple and perhaps misleading assumptions that CO_2 uptake increases with increasing radiation, and vice versa.

More precise analysis of annual budgets requires much more information about every component of RE. Our results strongly suggest values of GPP and RE of approximately 3,000–3,400 g C m^{-2} $year^{-1}$, and NEE of around 0 ± 200 g C m^{-2} $year^{-1}$, with no clear dependence on annual differences in solar radiation or air temperature, and some dependence on rainfall pattern and soil water content.

Conclusions

Variation in rainfall pattern resulted in seasonal and inter-annual variability in micrometeorology at our Southeast

Asian primary tropical rainforest study site, in the Pasoh Forest Reserve, Peninsular Malaysia. Evapotranspiration, canopy photosynthesis, and RE responded to this variation of rainfall pattern compensating for each other and/or other components of micrometeorology to result in stable values of annual evapotranspiration and NEE. We detected a dependence of evapotranspiration on available energy, regulation of evapotranspiration at high vapour pressure deficit, and no dependence of evapotranspiration on the amount of rainfall or soil water content. Stomatal regulation occurred at high vapour pressure deficit to mitigate excessive evapotranspiration under conditions of higher available energy, irrespective of soil water content, and water supply from deeper layers supported this stable evapotranspiration even during the driest periods. However, neither net nor gross canopy CO_2 uptake showed dependence on radiation, and canopy gross photosynthesis and RE showed dependence on soil water content. These results strongly suggest that the reduction in radiation caused by factors such as haze events is not likely to cause a significant change in canopy CO_2 exchange, and that a decrease in rainfall and thus soil drought would cause decreases in both GPP and RE, and vice versa, resulting in no significant change in NEE, or a slight shift in the direction of CO_2 uptake.

Our results for 2009, an ENSO year, suggest that if more severely dry and hot years occur, the decline in evapotranspiration and GPP caused by the stomatal closure under conditions of higher vapour pressure deficit would increase substantially. Future comparison with results from other tower sites, coupled with a larger data set with wider variation in micrometeorological conditions, will be valuable for evaluating the response of tropical rainforests to possible climate change.

Acknowledgments We thank the Forestry Department of Negeri Sembilan and the director general of FRIM for granting us permission to work in the Pasoh Forest Reserve. We gratefully acknowledge the staff of the Hydrology Unit and the Pasoh Station of FRIM for collecting field data. We also thank Dr Toshinori Okuda and a joint research project between FRIM, Putra University, Malaysia, and the National Institute for Environmental Studies, Japan. This work was supported by the Global Environment Research Fund of the Japan Environment Agency, and by grants for scientific research from the Ministry of Education, Culture, Sports, Science and Technology, Japan.

References

Araújo AC, Nobre AD, Kruijt B, Dallarosa R, Stefani P, von Randow C, Manzi AO, Culf AD, Gash JHC, Valentini R, Kabat P (2002) Comparative measurements of carbon dioxide fluxes from two nearby towers in a central Amazonian rainforest: the Manaus LBA site. J Geophys Res 107:8090–8109

Asner GP, Nepstad D, Cardinot G, David R (2004) Drought stress and carbon uptake in an Amazon forest measured with spaceborne imaging spectroscopy. Proc Natl Acad Sci USA 101:6039–6044

Aubinet M, Grelle A, Ibrom A, Rannik U, Moncrieff J, Foken T, Kowalski AS, Martin PH, Berbigier P, Bernhofer Ch, Clement R, Elbers J, Granier A, Grunwald T, Morgenstern K, Pilegaard K, Rebmann C, Snijders W, Valentini R, Vesala T (2000) Estimates of the annual net carbon and water exchange of forests: the EUROFLUX methodology. Adv Ecol Res 30:113–175

Baldocchi D, Falge E, Wilson K (2001) A spectral analysis of biosphere–atmosphere trace gas flux densities and meteorological variables across hour to multi-year time scales. Agric Forest Meteorol 107:1–27

Chambers JQ, Tribuzy ES, Toledo LC, Crispim BF, Higuchi N, Santos JD, Araújo AC, Kruijt B, Nobre AD, Trumbore SE (2004) Respiration from a tropical forest ecosystem: partitioning of sources and low carbon use efficiency. Ecol Appl 14:S72–S88

da Rocha HR, Goulden ML, Miller SD, Menton MC, Pinto LDVO, de Freitas HC, e Silva Figueira AM (2004) Seasonality of water and heat fluxes over a tropical forest in eastern Amazonia. Ecol Appl 14:S22–S32

Foken T, Wichura B (1996) Tools for quality assessment of surface-based flux measurements. Agric For Meteorol 78:83–105

Goulden ML, Miller SD, da Rocha HR, Menton MC, de Freitas HC, e Silva Figueira AM, de Sousa CAD (2004) Diel and seasonal patterns of tropical forest CO_2 exchange. Ecol Appl 14:S42–S54

Graham EA, Mulkey SS, Kitajima K, Phillips NG, Wright SJ (2003) Cloud cover limits net CO_2 uptake and growth of a rainforest tree during tropical rainy seasons. PNAS 100:572–576

Hirano T, Segah H, Harada T, Limin S, June T, Hirata R, Osaki M (2007) Carbon dioxide balance of a tropical peat swamp forest in Kalimantan, Indonesia. Glob Change Biol 13:412–425

Kosugi Y, Katsuyama M (2007) Evapotranspiration over a Japanese cypress forest. II. Comparison of the eddy covariance and water budget methods. J Hydrol 334:305–311

Kosugi Y, Takanashi S, Tanaka H, Ohkubo S, Tani M, Yano M, Katayama T (2007a) Evapotranspiration over a Japanese cypress forest. I. Eddy covariance fluxes and surface conductance characteristics for three years. J Hydrol 337:269–283

Kosugi Y, Mitani T, Itoh M, Noguchi S, Tani M, Matsuo N, Takanashi S, Ohkubo S, Nik AR (2007b) Spatial and temporal variation in soil respiration in a Southeast Asian tropical rainforest. Agric For Meteorol 147:35–47

Kosugi Y, Takanashi S, Ohkubo S, Matsuo N, Tani M, Mitani T, Tsutsumi D, Nik AR (2008) CO_2 exchange of a tropical rainforest at Pasoh in Peninsular Malaysia. Agric For Meteorol 148:439–452

Kosugi Y, Takanashi S, Matsuo N, Nik AR (2009) Midday depression of leaf CO_2 exchange within the crown of Dipterocarpus sublamellatus in a lowland dipterocarp forest in Peninsular Malaysia. Tree Physiol 29:505–515

Kruijt B, Elbers JA, von Randow C, Araújo AC, Oliveira PJ, Culf A, Manzi AO, Nobre AD, Kabat P, Moors EJ (2004) The robustness of eddy correlation fluxes for Amazon rain forest conditions. Ecol Appl 14:S101–S113

Kumagai T, Saitoh TM, Sato Y, Takahashi H, Manfroi OJ, Morooka T, Kuraji K, Suzuki M, Yasunari T, Komatsu H (2005) Annual water balance and seasonality of evapotranspiration in a Bornean tropical rainforest. Agric For Meteorol 128:81–92

Kumagai T, Ichie T, Yoshimura M, Yamashita M, Kenzo T, Saitoh TM, Ohashi M, Suzuki M, Koike T, Komatsu H (2006) Modeling CO_2 exchange over a Bornean tropical rain forest using measured vertical and horizontal variations in leaf-level physiological parameters and leaf area densities. J Geophys Res 111:D10107

Malhi Y, Nobre AD, Grace J, Kruijt B, Pereira MGP, Culf A, Scott S (1998) Carbon dioxide transfer over a Central Amazonian rain forest. J Geophys Res 103:31593–31612

Malhi Y, Pegoraro E, Nobre AD, Pereira MGP, Grace J, Culf AD, Clement R (2002) Energy and water dynamics of a central Amazonian rain forest. J Geophys Res 107:8061

McMillen RT (1988) An eddy correlation technique with extended applicability to non-simple terrain. Bound Lay Meteorol 43:231–245

Miller SD, Goulden ML, Menton MC, da Rocha HR, de Freitas HC, e Silva Figueira AM, Dias de Sousa CA (2004) Biometric and micrometeorological measurements of tropical forest carbon balance. Ecol Appl 14:S114–S126

Noguchi S, Nik AR, Tani M (2003) Rainfall characteristics of tropical rainforest at Pasoh Forest Reserve, Negeri Sembilan, Peninsular Malaysia. In: Okuda T, Manokaran N, Matsumoto Y, Niiyama K, Thomas SC, Ashton PS (eds) Pasoh: ecology of a lowland rain forest in southeast Asia. Springer, Tokyo, pp 51–58

Ohkubo S, Kosugi Y, Takanashi S, Matsuo N, Tani M, Nik AR (2008) Vertical profiles and storage fluxes of CO_2, heat and water in a tropical rainforest at Pasoh, Peninsular Malaysia. Tellus B 60:569–582

Ohtani Y, Okano M, Tani M, Yamanoi T, Watanabe T, Yasuda Y, Nik AR (1997) Energy and CO_2 fluxes above a tropical rain forest in Peninsular Malaysia. J Agric Meteorol 52:453–456

Oki T, Musiake K, Matsuyama H, Masuda K (1995) Global atmospheric water balance and runoff from large river basins. Hydrol Process 9:655–678

Saleska SR, Miller SD, Matross DM, Goulden ML, Wofsy SC, da Rocha HR, de Camargo PB, Crill P, Daube BC, de Freitas HC, Hutyra L, Keller M, Kirchhoff V, Menton M, Munger JW, Pyle EH, Rice AH, Silva H (2003) Carbon in Amazonian forests: unexpected seasonal fluxes and disturbance-induced losses. Science 302:1554–1557

Soepadmo E (1978) Introduction to the Malaysian I.B.P. synthesis meetings. Malays Nat J 30:119–124

Takanashi S, Kosugi Y, Tani M, Matsuo N, Mitani T, Nik AR (2005) Characteristics of the gas exchange of a tropical rain forest in Peninsular Malaysia. Phyton 45:61–66

Takanashi S, Kosugi Y, Matsuo N, Tani M, Ohte N (2006) Patchy stomatal behavior in broad-leaved trees grown in different habitats. Tree Physiol 26:1565–1578

Takanashi S, Kosugi Y, Ohkubo S, Matsuo N, Tani M, Nik AR (2010) Water and heat fluxes above a lowland dipterocarp forest in Peninsular Malaysia. Hydrol Process 24:472–480

Tani M, Nik AR, Ohtani Y, Yasuda Y, Sahat MM, Baharuddin K, Takanashi S, Noguchi S, Zulkifli Y, Watanabe T (2003) Characteristics of energy exchange and surface conductance of a tropical rain forest in Peninsular Malaysia. In: Okuda T, Manokaran N, Matsumoto Y, Niiyama K, Thomas SC, Ashton PS (eds) Pasoh: ecology of a lowland rain forest in southeast Asia. Springer, Tokyo, pp 73–88

Valentini R, Matteucci G, Dolman AJ, Schulze E-D, Rebmann C, Moors EJ, Granier A, Gross P, Jensen NO, Pilegaard K, Lindroth A, Grelle A, Bernhofer C, Grünwald T, Aubinet M, Ceulemans R, Kowalski AS, Vesala T, Rannik Ü, Berbigier P, Loustau D, Guðmundsson J, Thorgeirsson H, Ibrom A, Morgenstern K, Clement R, Moncrieff J, Montagnani L, Minerbi S, Jarvis PG (2000) Respiration as the main determinant of carbon balance in European forests. Nature 404:861–865

Webb EK, Pearman GI, Leuning R (1980) Correction of flux measurements for density effects due to heat and water vapour transfer. Q J R Meteor Soc 106:85–100

Wilson K, Goldstein A, Falge E, Aubinet M, Baldocchi D, Berbigier P, Bernhofer C, Ceulemans R, Dolman H, Field C, Grelle A, Ibrom A, Law BE, Kowalski A, Meyers T, Moncrieff J, Monson R, Oechel W, Tenhunen J, Valentini R, Verma S (2002) Energy balance closure at FLUXNET sites. Agric For Meteorol 113:223–243

Yamashita T, Kasuya N, Kadir WR, Chik SW, Seng QE, Okuda T (2003) Soil and belowground characteristics of Pasoh Forest Reserve. In: Okuda T, Manokaran N, Matsumoto Y, Niiyama K, Thomas SC, Ashton PS (eds) Pasoh: ecology of a lowland rain forest in southeast Asia. Springer, Tokyo, pp 89–109

Yasuda Y, Ohtani Y, Watanabe T, Okano M, Yokota T, Liang N, Tang Y, Nik AR, Tani M, Okuda T (2003) Measurement of CO_2 flux above a tropical rain forest at Pasoh in Peninsular Malaysia. Agric For Meteorol 114:235–244

GEOPHYSICAL RESEARCH LETTERS, VOL. 35, L19812, doi:10.1029/2008GL035241, 2008

Methyl chloride and isoprene emissions from tropical rain forest in Southeast Asia

Takuya Saito,[1] Yoko Yokouchi,[1] Yoshiko Kosugi,[2] Makoto Tani,[2]
Elizabeth Philip,[3] and Toshinori Okuda[4]

Received 4 July 2008; revised 25 August 2008; accepted 28 August 2008; published 7 October 2008.

[1] Methyl chloride (CH_3Cl) fluxes were investigated at leaf and forest-canopy scales in tropical forests in Malaysia. Screening of CH_3Cl-emitting species showed that 21% of 117 tree species were CH_3Cl emitters; the percentage was markedly higher for dipterocarps (66%) than non-dipterocarps (6%). The dipterocarp-derived CH_3Cl was characterized by high emissions (median: 0.03 $\mu g\ g^{-1}\ h^{-1}$) and low stable carbon isotope ratios (mean: $-88.9 \pm 11.0‰$). Measurements of CH_3Cl above the canopy showed a slight decrease in the mixing ratios with increasing height. These values were used to estimate the canopy-scale flux of about 14 $\mu g\ m^{-2}\ h^{-1}$, comparable to that extrapolated from the leaf-scale emissions. Using the canopy-scale flux, global CH_3Cl emission by tropical forests was estimated to be 1.3 Tg yr^{-1}, representing approximately 30% of the global emissions. Above-canopy measurements were also made for isoprene, with a mean flux of 1.2 mg $m^{-2}\ h^{-1}$.
Citation: Saito, T., Y. Yokouchi, Y. Kosugi, M. Tani, E. Philip, and T. Okuda (2008), Methyl chloride and isoprene emissions from tropical rain forest in Southeast Asia, *Geophys. Res. Lett.*, *35*, L19812, doi:10.1029/2008GL035241.

1. Introduction

[2] Emission of methyl chloride (CH_3Cl), predominantly from natural sources, provides the dominant input of halocarbons to the atmosphere and influences stratospheric chemistry through the chlorine-catalyzed destruction of stratospheric ozone [*World Meteorological Organization* (*WMO*), 2007]. Among a variety of natural sources, tropical forest ecosystems, including living tropical plants [*Yokouchi et al.*, 2002], senescent or dead leaves [*Hamilton et al.*, 2003], and wood-rotting fungi [*Harper*, 1985], are considered a major source of CH_3Cl, whereas tropical soil may act as a net sink of CH_3Cl. In recent years, there has been growing evidence of the strong emission of CH_3Cl from tropical and subtropical terrestrial sources [*Gebhardt et al.*, 2008; *Keppler et al.*, 2005; *Moore et al.*, 2005; *Saito and Yokouchi*, 2006, 2008; *Yokouchi et al.*, 2006, 2007]. However, the actual source strength of tropical forests is still uncertain because of the lack of field observations and the extremely high species diversity of tropical plants, with variable fluxes of CH_3Cl between and within species [*Yokouchi et al.*, 2007]. Micrometeorological flux measurements, such as the gradient method [e.g., *Schween et al.*, 1997], have been applied to estimate the averaged gas flux from a whole forest ecosystem at the canopy scale, although the method has not been applied to the measurement of CH_3Cl flux.

[3] Tropical forests also play an important role in the photochemistry of the lower troposphere by emitting a variety of reactive volatile organic compounds (VOCs) such as isoprene, the most important VOC in the rural atmosphere [e.g., *Guenther et al.*, 1995]. Isoprene emission fluxes have been studied in the tropical forests of South America [e.g., *Geron et al.*, 2002; *Greenberg et al.*, 2004; *Karl et al.*, 2004; *Rasmussen and Khalil*, 1988] and Africa [e.g., *Greenberg et al.*, 1999; *Klinger et al.*, 1998], although few such studies have been conducted in Southeast Asia.

[4] To estimate whole-ecosystem CH_3Cl emissions, we conducted the first canopy-scale flux measurements of CH_3Cl above a lowland tropical rain forest in Malaysia by the micrometeorological gradient method. We also screened more than 100 tropical tree species for CH_3Cl emissions and made stable carbon isotope measurements of CH_3Cl emitted from tropical plants. In addition, we made the first canopy-scale flux measurements of isoprene in Southeast Asian tropical forests.

2. Experiments

2.1. Site Description

[5] Leaves and air were sampled at the Pasoh Forest Reserve (2°58′N, 102°18′E; elevation, 75–150 m a.s.l.), located in Negri Sembilan, about 70 km southeast of Kuala Lumpur in Peninsular Malaysia. The core area (about 600 ha) of the site is characterized by a primary lowland mixed forest dominated by Dipterocarpaceae (such as *Shorea* and *Dipterocarpus*). Mean canopy height of the primary forest is 27.4 m, with some emergent trees exceeding 45 m [*Okuda et al.*, 2003]. A 52-m tower used for the observations is located in the southwestern part of the primary forest. Continuous canopy-scale CO_2 and H_2O flux measurements with eddy covariance method have been conducted at the top of the tower since 2002 [*Takanashi et al.*, 2005; *Kosugi et al.*, 2008; *Ohkubo et al.*, 2008]. The mean annual temperature is 25.6°C and the mean annual rainfall is 1571 mm [*Tani et al.*, 2003]. Additional leaf sampling was conducted at the Dipterocarp Arboretum and along a nature trail (Engkabang Trail) at the Forest Research Institute Malaysia (FRIM), Kuala Lumpur.

---

[1] National Institute for Environmental Studies, Tsukuba, Japan.

[2] Division of Environmental Science and Technology, Graduate School of Agriculture, Kyoto University, Kyoto, Japan.

[3] Forest Research Institute Malaysia, Kepong, Malaysia.

[4] Department of Environmental Sciences, Graduate School of Integrated Arts and Sciences, Hiroshima University, Higashihiroshima, Japan.

0094-8276/08/2008GL035241$05.00

2.2. Screening of CH_3Cl-Emitting Species

[6] Leaves were collected from 117 species at Pasoh in December 2006, August 2007, and December 2007 and at FRIM in December 2006 and August 2007. During the experiments at Pasoh in 2006 and December 2007, leaves in the canopy were taken using the tower or a canopy walkway (30 m high). Sampling at Pasoh in August 2007 was conducted for infant plants at the forest floor. At FRIM, leaves of dipterocarp trees were taken at the Dipterocarp Arboretum and those of non-dipterocarp trees were gathered along the nature trail. Leaves of tall trees (>3 m height) were obtained using a sling.

[7] Foliar emission gas was collected using the vial method. Details of the sampling and analytical methods have been published elsewhere [*Yokouchi et al.*, 2007]. Whole leaves were detached from the plants and placed in a 40-ml screw-cap vial. The samples were analyzed at the National Institute for Environmental Studies (NIES; samples in 2006 and December 2007) or FRIM (August 2007). Headspace gas in the vials was analyzed by preconcentration/gas chromatography/mass spectrometry (GC/MS, HP 6890/5973) at NIES within a week after sampling or by a GC equipped with a flame ionization detector (HP 5890 Series II) and an HP-PLOT Q capillary column (30 m long) at FRIM within a few days after sampling. Quantification of CH_3Cl was made with 5 ppmv standard gas (Taiyo Toyo Sanso), which was prepared gravimetrically. The leaves of dipterocarps (obtained in December 2007) with significant CH_3Cl emissions were analyzed for stable carbon isotope ratios using preconcentration/gas chromatography/combustion/isotope ratio mass spectrometry (GC/C/IRMS, HP 6890/Finnigan MAT 252). Details for the isotope measurements were described by *Saito and Yokouchi* [2008]. After analyses, leaves were dried for 24 h at 80°C and weighed, and CH_3Cl emission rates were expressed as ng (g dry leaf weight)$^{-1}$ h^{-1}. Some preliminary tests for the reliability of the vial method had shown no significant change of the emission rates and the stable carbon isotope ratios at least for a few days after sampling [*Yokouchi et al.*, 2007; *Saito and Yokouchi*, 2008].

2.3. Micrometeorological Gradient Measurements

[8] Ambient air above the forest canopy was sampled at Pasoh in December 2007 from the tower. The tower height was temporarily extended to 60 m with a telescopic measuring pole. Air was drawn from three heights (45, 52, and 60 m) through separate ¼-inch (OD) Teflon® tubes to three sampling units at 35-m height on the tower. The air samples were pressurized into evacuated stainless steel canisters to 100 kPa above atmospheric pressure for 30 min at a constant flow rate using the sampling units, which consisted of metal bellows pumps (MB-41, Metal Bellows Inc.), mass flow controllers (Model 2203, Kofloc), back pressure regulators (Model 6800, Kofloc), and ozone scrubbers (multiple layer of MnO_2-coated copper mesh, Shimazu). Two types of canister were used: 6-L fused-silica-lined stainless steel canisters (SilicoCan, Restek Co., Ltd.) and 3-L electrochemical buffing canisters (Ultra Finish Technology). The air samples were analyzed by the preconcentration/GC/MS as described in detail by *Enomoto et al.* [2005]. Quantification was made with a gravimetrically prepared standard gas containing CH_3Cl (500 pptv) and isoprene (100 pptv). Based on replicate analyses of the standard gas, the analytical precision of CH_3Cl and isoprene was estimated to be about 0.5%.

[9] Canopy-scale flux of VOCs was estimated by the micrometeorological gradient method. The flux, F (μg m^{-2} s^{-1}), is given by:

$$F = \frac{\Delta C}{\Delta z}, \tag{1}$$

where K is the eddy diffusion coefficient (m^2 s^{-1}) and $\Delta C/\Delta z$ is the vertical concentration gradient (μg m^{-3} m^{-1}) above the forest canopy. The eddy diffusion coefficient was calculated using the modified Bowen ratio technique [*Meyers et al.*, 1996], which is based on the assumption that the eddy diffusion coefficient for VOCs is equal to that for heat. Accordingly, the flux can be calculated with the following equation:

$$F = \frac{H}{\rho C_p} \cdot \frac{\Delta C/\Delta z}{\Delta T/\Delta z}, \tag{2}$$

where H is the sensible heat flux (W m^{-2}), ρ is the density of air (kg m^{-3}), C_p is the specific heat of air (J kg^{-1} K^{-1}), and $\Delta T/\Delta z$ is the temperature gradient (K m^{-1}). The sensible heat flux was measured at 54 m from the tower by eddy correlation with a three-dimensional sonic anemometer thermometer (SAT-550, Kaijo [*Takanashi et al.*, 2005]). The temperature difference between 45 and 52 m was directly measured with an aspirated psychrometer (Meteo Electronics) composed of 10 pairs of copper-constantan thermocouples. Vertical gradients of VOC mixing ratios were estimated by a least squares fitting to the measured profile data. The uncertainty of the calculated flux was estimated by the propagation-of-error technique using the uncertainties of heat (10%), temperature (0.01 K), and the least square fitting to the concentration data.

3. Results and Discussion

3.1. CH_3Cl-Emitting Tropical Tree Species

[10] Of the 117 species screened, 24 were identified as emitters of CH_3Cl, those species that emitted CH_3Cl at rates greater than 0.01 μg g^{-1} h^{-1} (Table 1). Fluxes varied widely between and within the species, with the emission rates ranging from <0.01 to 0.23 μg g^{-1} h^{-1} (by *Shorea ochrophloria*). These values were low compared with those reported from dipterocarps growing in a tropical greenhouse (0.02 to 0.6 μg g^{-1} h^{-1}) [*Yokouchi et al.*, 2002]. As for dipterocarp trees, of the 29 species examined, 19 emitted CH_3Cl (non- CH_3Cl emitters were *Anisoptera megistocarpa, Dipterocarpus cornutus, D. costulatus, D. grandiflorus, D. kerrii, D. malaccencis, Dryobalanop aromatica, Hopea subulata, Shorea accuminata,* and *S. ovalis*). Thus, 66% of the dipterocarp species examined were CH_3Cl-emitting (with a median emission rate of 0.03 μg g^{-1} h^{-1}), which is one order of magnitude greater than the percentage for non-dipterocarp trees (6%, median: 0.01 μg g^{-1} h^{-1}). Among the dipterocarp species studied, six had been examined previously at Pasoh in June 2002 using the branch enclosure method and five were identified as emitters [*Yokouchi et al.*, 2006]. Most of these previously

Table 1. Methyl Chloride-Emitting Species and Their Emission Rates at Field Sites in Malaysia

		CH_3Cl (μg g^{-1} h^{-1})			
Family	Species	Jun 2002[a]	Dec 2006	Aug 2007	Dec 2007
Dipterocarpaceae	*Anisoptera magistocarpa*	0.01	-[b]	-	-
Dipterocarpaceae	*Dipterocarpus crinitus*	-	-	0.03	<0.01
Dipterocarpaceae	*D. rutundipolius*	-	0.01	-	-
Dipterocarpaceae	*D. sublamelatus*	0.03	<0.01	-	<0.01
Dipterocarpaceae	*D. sublamelatus*	0.04	<0.01	-	<0.01
Dipterocarpaceae	*Hopea dryobalanoides*	-	-	-	0.01
Dipterocarpaceae	*H. helferi*	-	0.09	-	-
Dipterocarpaceae	*H. odorata*	-	-	0.07	-
Dipterocarpaceae	*Neobalanocarpus hemii*	0.20	-	0.10	0.01
Dipterocarpaceae	*Neobalanocarpus hemii*	0.03	-	0.10	0.01
Dipterocarpaceae	*Shorea bracteolata*	-	-	0.04	-
Dipterocarpaceae	*S. leprosula*	<0.01	-	0.03	<0.01
Dipterocarpaceae	*S. macroptera*	-	-	<0.01	0.02
Dipterocarpaceae	*S. macroptera*	-	-	0.01	0.02
Dipterocarpaceae	*S. multiflora*	0.04	-	0.02	0.02
Dipterocarpaceae	*S. maxima*	-	0.03	-	0.01
Dipterocarpaceae	*S. maxima*	-	0.06	-	0.01
Dipterocarpaceae	*S. maxwelliana*	0.04	-	0.10	0.04
Dipterocarpaceae	*S. ochrophloria*	-	0.20	-	-
Dipterocarpaceae	*S. platyclados*	-	0.01	-	-
Dipterocarpaceae	*S. platyclados*	-	0.02	-	-
Dipterocarpaceae	*S. paruifolia*	-	-	0.01	0.07
Dipterocarpaceae	*S. pauciflora*	0.03	0.02	0.01	0.04
Dipterocarpaceae	*S. pauciflora*	0.03	0.02	0.03	0.04
Dipterocarpaceae	*Vatica bella*	-	-	-	0.01
Euphorbiaceae	*Aporusa microstachya*	-	-	0.02	<0.01
Rhizophoraceae	*Carallia brachiata*	-	-	0.02	-
Myrthaceae	*Eugenia polyantha*	-	-	0.01	-
Sumaroubaceae	*Eurycoma longifolia*	-	-	0.01	<0.01
Tiliaceae	*Pentace triptera*	-	-	0.01	-

[a] *Yokouchi et al.* [2006].

[b] Here - indicates not measured.

identified emitters (*Neobalanocarpus hemii, Shorea multiflora, S. ochrophloria*, and *S. pauciflora*) were found to emit CH_3Cl significantly in this study, with the exception of *Dipterocarpus sublamelatus*.

[11] The observed leaf-scale emission rate can be extrapolated to the flux at the canopy scale, based on the following assumptions: the coverage by dipterocarp trees is 27% of the total forest basal area [*Davies et al.*, 2003] and the remaining portion (63%) is covered by non-dipterocarps; the percentages of the CH_3Cl emitters are 66% for dipterocarps and 6% for non-dipterocarps; the leaf biomass per unit area is 900 g m^{-2} [*Kato et al.*, 1978]; and our observations are representative of tropical plants at the site. As a result, the canopy-scale median and maximum fluxes were estimated to be 5 and 39 μg m^{-2} h^{-1} (0.1 and 0.8 μmol m^{-2} h^{-1}), respectively. For both calculations, the relative contribution of dipterocarp tree species to the canopy-scale fluxes was more than 90%.

[12] Table 2 shows the stable carbon isotope measurements made for 11 dipterocarp species obtained at Pasoh in December 2007. The stable carbon isotope ratios of CH_3Cl vary widely, ranging from −65‰ for *D. sublamelatus* to −111‰ for *Neobalanocarpus hemii*. Although the measured isotope ratios for *Shorea multiflora* (−88.8‰ and −85.5‰), which is the only species that was previously studied using glasshouse-grown tropical plants [*Saito and Yokouchi*, 2008], were lower than the previous measurements for *S. multiflora* (−72.1 ± 3.9‰), the measured isotope ratio of the 11 dipterocarp species (−88.9 ± 11.0‰) was on average very similar to that of the previous study (−87.4 ± 12.3‰). Our present findings appear to support the conclusion of the previous study: global CH_3Cl emission by tropical plants accounts for 30–50% of the

Table 2. Measured Stable Carbon Isotope Ratios of Methyl Chloride Emitted From Dipterocarp Tree Species

Species	CH_3Cl (‰)
Dipterocarpus crinitus	−96.4
D. sublamelatus	−65.2
D. sublamelatus	−76.0
Hopea dryobalanoides	−78.7
Hopea dryobalanoides	−81.2
Neobalanocarpus hemii	−108.8
Neobalanocarpus hemii	−111.0
Shorea macroptera	−79.0
S. maxima	−87.4
S. maxima	−81.0
S. maxwelliana	−83.4
S. maxwelliana	−99.3
S. multiflora	−88.8
S. multiflora	−85.5
S. paruiflora	−96.2
S. paruiflora	−93.4
S. pauciflora	−94.6
S. pauciflora	−97.7
Vatica bella	−88.9
Vatica bella	−85.2
mean	−88.9 ± 11

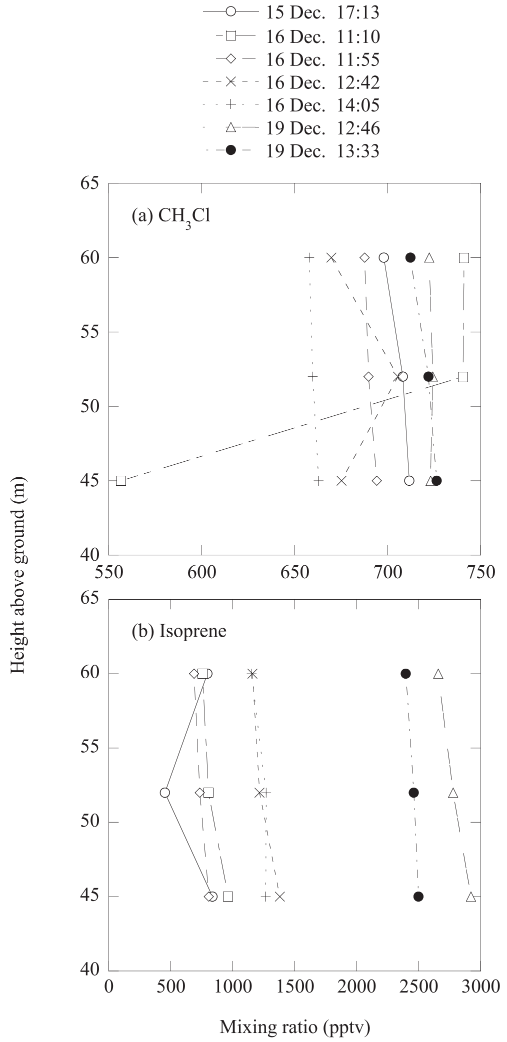

Figure 1. Measured vertical profiles of (a) methyl chloride and (b) isoprene above the forest canopy at the Pasoh Forest Reserve in Peninsular Malaysia in December 2007.

global emission, as deduced from the isotopic mass balance calculation.

3.2. Vertical Profiles of CH_3Cl and Isoprene Above the Forest Canopy

3.2.1. CH_3Cl

[13] Between 15 and 19 December 2007, CH_3Cl and isoprene concentrations were measured for eight vertical profiles above the forest canopy at Pasoh. Figure 1a shows seven profiles; one profile was excluded (taken around 12:03 on 19 December) because of the substantial influence of polluted air, as indicated by high mixing ratios of anthropogenic VOCs, such as benzene (data not shown). The measured CH_3Cl mixing ratios were mostly above 650 pptv, which exceeds the background mixing ratio in the tropics (about 550 pptv; [*Yokouchi et al.*, 2000]), and showed slightly decreasing trends with increasing measurement heights, except for the first profile on 16 December. In this profile, a background mixing ratio of 560 pptv for CH_3Cl was observed just above the canopy. This unexpectedly irregular profile was eliminated from the flux calculations, although its cause is unknown.

[14] The emission fluxes of CH_3Cl estimated by the gradient method are shown in Table 3. The estimated fluxes (5–66 μg m^{-2} h^{-1} or 0.1–1.3 μmol m^{-2} h^{-1}) were positive, indicating upward flux from the tropical forest to the atmosphere. However, it should be noted that the values were associated with large uncertainties. In particular, two estimated fluxes (66 ± 190 μg m^{-2} h^{-1} at 12:42 on 16 December and 5 ± 11 μg m^{-2} h^{-1} at 12:46 on 19 December) were associated with a relative standard error exceeding 100%. Those uncertainties were mostly attributed to the poor least-squares fit of the irregular gradient data, partly caused by low analytical precision compared to the small gradients. Thus, we considered that median flux (14 μg m^{-2} h^{-1}) is more reliable than the mean (28 μg m^{-2} h^{-1}). The median flux reasonably agrees with the estimates (median: 5 μg m^{-2} h^{-1}, maximum: 39 μg m^{-2} h^{-1}) extrapolated from the leaf-scale measurements in section 3.1. This may suggest that living tropical plants make a major contribution to the emission of CH_3Cl for the whole forest ecosystem at Pasoh; however, the large uncertainties, particularly with regard to the leaf-scale measurements by the vial method and their extrapolation to the canopy-scale flux, make it difficult to estimate the relative contribution of each terrestrial tropical source (i.e., living tropical plants, senescent or dead leaves, and fungi).

[15] We extrapolated the measured local emission of CH_3Cl at Pasoh to the global scale by simply multiplying the area-based fluxes (median: 14 μg m^{-2} h^{-1}) by the global tropical forest area (10.39 × 10^6 km^2 [*Guenther et al.*, 1995]). The resulting annual global emission of 1.3 Tg corresponds to approximately 30% of the total (about 4.4 Tg; [*WMO*, 2007]), suggesting that tropical forest is the single largest source of atmospheric CH_3Cl. This estimated flux is consistent with the recent estimate of 1.5 ± 0.6 Tg yr^{-1} by *Gebhardt et al.* [2008], which was based on the landscape-scale flux estimated by the airborne measurement of CH_3Cl over the tropical forests in South America, suggesting homogeneous emission of CH_3Cl from the global tropical forests. This may imply that CH_3Cl emission by the global tropical forests is somewhat lower than model predictions (2.4 Tg yr^{-1}, [*Lee-Taylor et al.*,

Table 3. Canopy Scale Fluxes of Methyl Chloride and Isoprene Estimated by Vertical Gradient Measurements

Date	Time	Temperature (°C)	CH_3Cl (μg m^{-2} h^{-1})	C_5H_8 (mg m^{-2} h^{-1})
15 Dec	17:13	26.0	8 ± 1	−0.03 ± 0.3
16 Dec	11:10	25.1	-[a]	0.1 ± 0.1
16 Dec	11:55	26.8	13 ± 6	0.3 ± 0.1
16 Dec	12:42	28.0	66 ± 190	1.5 ± 0.8
16 Dec	14:05	29.5	59 ± 23	2.1 ± 0.8
19 Dec	12:46	27.8	5 ± 11	2.3 ± 0.7
19 Dec	13:33	28.0	14 ± 5	1.2 ± 0.4
Median		27.8	14	1.2

[a] Here - means not calculated (see text).

2001]; 2.9 Tg yr^{-1}, [*Yoshida et al.*, 2004]). However, our estimate is based on a limited data set at a local site and its extrapolation to the global scale involves many assumptions and simplifications. Thus, more extensive field measurements in the broad range of tropical forest ecosystems are clearly required for more reliable flux estimates of CH_3Cl.

3.2.2. Isoprene

[16] Measured daytime mixing ratios of isoprene above the canopy are shown in Figure 1b. The mixing ratios (range: 700–3000 pptv) decreased with increasing height; the vertical trends were similar to the vertical gradients of CH_3Cl, but more pronounced for isoprene. The fluxes determined by the gradient method were in the range of −0.03 to 2.3 mg m^{-2} h^{-1} (Table 3). Although the flux data were very limited, a pattern of high emissions around midday (0.3 to 2.3 mg m^{-2} h^{-1}) and low emissions during the morning (0.1 mg m^{-2} h^{-1}) and the late afternoon (−0.03 mg m^{-2} h^{-1}) was observed, probably reflecting temperature and light dependency of isoprene emission [e.g., *Guenther et al.*, 1993; *Tingey et al.*, 1979]. The observed flux of isoprene (median: 1.2 mg m^{-2} h^{-1}) is consistent with previous studies conducted in tropical forests in South America (e.g., 3.09 mg m^{-2} h^{-1}, [*Zimmerman et al.*, 1988]; 1.35 mg m^{-2} h^{-1}, [*Karl et al.*, 2004]; 2.4 mg m^{-2} h^{-1}, [*Kuhn et al.*, 2007]).

[17] **Acknowledgments.** We thank En Seng Quah for his help in collecting leaf and air samples and in plant identification, and Naishen Liang for his support on air sampling. This study was supported in part by the Japanese Ministry of Education, Science, Sport and Culture through a Grant-in-Aid (18340179).

References

Davies, S. J., N. S. M. Noor, J. V. LaFrankie, and P. S. Ashton (2003), The trees of Pasoh Forest: Stand structure and floristic composition of the 50-ha forest research plot, in *Pasoh: Ecology of a Lowland Rain Forest in Southeast Asia,* edited by T. Okuda et al., pp. 35–50, Springer, Tokyo.

Enomoto, T., Y. Yokouchi, K. Izumi, and T. Inagaki (2005), Development of an analytical method for atmospheric halocarbons and its application to airborne observation, *J. Jpn. Soc. Atmos. Environ.*, *40*, 1–8.

Gebhardt, S., A. Colomb, R. Hofmann, J. Williams, and J. Lelieveld (2008), Halogenated organic species over the tropical South American rainforest, *Atmos. Chem. Phys.*, *8*(12), 3185–3197.

Geron, C., A. Guenther, J. Greenberg, H. W. Loescher, D. Clark, and B. Baker (2002), Biogenic volatile organic compound emissions from a lowland tropical wet forest in Costa Rica, *Atmos. Environ.*, *36*, 3793–3802.

Greenberg, J. P., A. B. Guenther, S. Madronich, W. Baugh, P. Ginoux, A. Druilhet, R. Delmas, and C. Delon (1999), Biogenic volatile organic compound emissions in central Africa during the Experiment for the Regional Sources and Sinks of Oxidants (EXPRESSO) biomass burning season, *J. Geophys. Res.*, *104*(D23), 30,659–30,671.

Greenberg, J. P., A. B. Guenther, G. Petron, C. Wiedinmyer, O. Vega, L. V. Gatti, J. Tota, and G. Fisch (2004), Biogenic VOC emissions from forested Amazonian landscapes, *Global Change Biol.*, *10*(5), 651–662.

Guenther, A. B., P. R. Zimmerman, P. C. Harley, R. K. Monson, and R. Fall (1993), Isoprene and monoterpene emission rate variability: Model evaluations and sensitivity analyses, *J. Geophys. Res.*, *98*(D7), 12,609–12,617.

Guenther, A., et al. (1995), A global-model of natural volatile organic compound emissions, *J. Geophys. Res.*, *100*(D5), 8873–8892.

Hamilton, J. T. G., W. C. McRoberts, F. Keppler, R. M. Kalin, and D. B. Harper (2003), Chloride methylation by plant pectin: An efficient environmentally significant process, *Science*, *301*(5630), 206–209.

Harper, D. B. (1985), Halomethane from halide ion: A highly efficient fungal conversion of environmental significance, *Nature*, *315*(6014), 55–57.

Karl, T., M. Potosnak, A. Guenther, D. Clark, J. Walker, J. D. Herrick, and C. Geron (2004), Exchange processes of volatile organic compounds above a tropical rain forest: Implications for modeling tropospheric chemistry above dense vegetation, *J. Geophys. Res.*, *109*, D18306, doi:10.1029/2004JD004738.

Kato, R., Y. Tadaki, and H. Ogawa (1978), Plant biomass and growth increment studies in Pasoh Forest Reserve, *Malayan Nature J.*, *30*, 211–224.

Keppler, F., D. B. Harper, T. Rockmann, R. M. Moore, and J. T. G. Hamilton (2005), New insight into the atmospheric chloromethane budget gained using stable carbon isotope ratios, *Atmos. Chem. Phys.*, *5*, 2403–2411.

Klinger, L. F., J. Greenberg, A. Guenther, G. Tyndall, P. Zimmerman, M. M'Bangui, and J. M. Moutsambote (1998), Patterns in volatile organic compound emissions along a savanna-rainforest gradient in central Africa, *J. Geophys. Res.*, *103*(D1), 1443–1454.

Kosugi, Y., S. Takanashi, S. Ohkubo, N. Matsuo, M. Tani, T. Mitani, D. Tsutsumi, and A. R. Nik (2008), CO_2 exchange of a tropical rainforest at Pasoh in Peninsular Malaysia, *Agric. For. Meteorol.*, *148*, 439–452.

Kuhn, U., et al. (2007), Isoprene and monoterpene fluxes from Central Amazonian rainforest inferred from tower-based and airborne measurements, and implications on the atmospheric chemistry and the local carbon budget, *Atmos. Chem. Phys.*, *7*(11), 2855–2879.

Lee-Taylor, J. M., G. P. Brasseur, and Y. Yokouchi (2001), A preliminary three-dimensional global model study of atmospheric methyl chloride distributions, *J. Geophys. Res.*, *106*(D24), 34,221–34,233.

Meyers, T. P., M. E. Hall, S. E. Lindberg, and K. Kim (1996), Use of the modified Bowen-ratio technique to measure fluxes of trace gases, *Atmos. Environ.*, *30*, 3321–3329.

Moore, R. M., A. Gut, and M. O. Andreae (2005), A pilot study of methyl chloride emissions from tropical woodrot fungi, *Chemosphere*, *58*(2), 221–225.

Ohkubo, S., Y. Kosugi, S. Takanashi, N. Matsuo, M. Tani, and A. R. Nik (2008), Vertical profiles and storage fluxes of CO_2, heat, and water in a tropical rainforest at Pasoh, Peninsular Malaysia, *Tellus, Ser. B*, *60*, 569–582.

Okuda, T., M. Suzuki, N. Adachi, K. Yoshida, K. Niiyama, N. S. M. Noor, N. A. Hussein, N. Manokaran, and M. Hashim (2003), Logging history and its impact on forest structure and species compositions in the Pasoh Forest Reserve: Implications for the sustainable management of natural resources and landscapes, in *Pasoh: Ecology of a Lowland Rain Forest in Southeast Asia*, edited by T. Okuda et al., pp. 15–34, Springer, Tokyo.

Rasmussen, R. A., and M. A. K. Khalil (1988), Isoprene over the Amazon Basin, *J. Geophys. Res.*, *93*(D2), 1417–1421.

Saito, T., and Y. Yokouchi (2006), Diurnal variation in methyl halide emission rates from tropical ferns, *Atmos. Environ.*, *40*(16), 2806–2811.

Saito, T., and Y. Yokouchi (2008), Stable carbon isotope ratio of methyl chloride emitted from glasshouse-grown tropical plants and its implication for the global methyl chloride budget, *Geophys. Res. Lett.*, *35*, L08807, doi:10.1029/2007GL032736.

Schween, J. H., R. Dlugi, C. N. Hewitt, and P. Foster (1997), Determination and accuracy of VOC-fluxes above the pine/oak forest at Castelporziano, *Atmos. Environ.*, *31*, 199–215.

Takanashi, S., Y. Kosugi, M. Tani, N. Matsuo, T. Mitani, and A. R. Nik (2005), Characteristics of the gas exchange of a tropical rain forest in peninsular Malaysia, *Phyton Ann. Rei Bot.*, *45*(4), 61–66.

Tani, M., N. A. Rahim, Y. Ohtani, Y. Yasuda, S. Mohd, K. Baharuddin, S. Takanashi, S. Noguchi, Y. Zulkifli, and T. Watanabe (2003), Characteristics of energy exchange and surface conductance of a tropical rain forest in Peninsular Malaysia, in *Pasoh: Ecology of a Lowland Rain Forest in Southeast Asia*, edited by T. Okuda et al., pp. 73–88, Springer, Tokyo.

Tingey, D. T., M. Manning, L. C. Grothaus, and W. F. Burns (1979), The influence of light and temperature on isoprene emission rates from live oak, *Physiol. Plant.*, *47*(2), 112–118.

World Meteorological Organization (WMO) (2007), Scientific assessment of ozone depletion: 2006, *Global Ozone Res. Monit. Proj. Rep. 50*, Geneva, Switzerland.

Yokouchi, Y., Y. Noijiri, L. A. Barrie, D. Toom-Sauntry, T. Machida, Y. Inuzuka, H. Akimoto, H. J. Li, Y. Fujinuma, and S. Aoki (2000), A strong source of methyl chloride to the atmosphere from tropical coastal land, *Nature*, *403*(6767), 295–298.

Yokouchi, Y., M. Ikeda, Y. Inuzuka, and T. Yukawa (2002), Strong emission of methyl chloride from tropical plants, *Nature*, *416*(6877), 163–165.

Yokouchi, Y., T. Saito, T. Okuda, and E. Phillip (2006), A preliminary study of volatile organic compounds emitted from tropical plants, in *Annual Report of the NIES/FRIM/UPM Joint Research Project on Tropical Ecology and Biodiversity 2005*, edited by T. Okuda and T. Kondo, pp. 37–43, Natl. Inst. Environ. Stud., Tsukuba, Japan.

Yokouchi, Y., T. Saito, C. Ishigaki, and M. Aramoto (2007), Identification of methyl chloride-emitting plants and atmospheric measurements on a subtropical island, *Chemosphere*, *69*(4), 549–553.

Yoshida, Y., Y. Wang, T. Zeng, and R. Yantosca (2004), A three-dimensional global model study of atmospheric methyl chloride budget and distributions, *J. Geophys. Res.*, *109*, D24309, doi:10.1029/2004JD004951.

Zimmerman, P. R., J. P. Greenberg, and C. E. Westberg (1988), Measurements of atmospheric hydrocarbons and biogenic emission fluxes in the Amazon boundary-layer, *J. Geophys. Res.*, *93*(D2), 1407–1416.

Y. Kosugi and M. Tani, Division of Environmental Science and Technology, Graduate School of Agriculture, Kyoto University, Kyoto 606-8502, Japan.

T. Okuda, Department of Environmental Sciences, Graduate School of Integrated Arts and Sciences, Hiroshima University, Higashihiroshima, Hiroshima 739-8521, Japan.

E. Philip, Forest Research Institute Malaysia, Kepong, Kuala Lumpur 52109, Malaysia.

T. Saito and Y. Yokouchi, Environmental Chemistry Division, National Institute for Environmental Studies, 16-2 Onogawa, Tsukuba, Ibaraki 305-8506, Japan. (saito.takuya@nies.go.jp)

AGRICULTURAL AND FOREST METEOROLOGY 148 (2008) 700–713

available at www.sciencedirect.com

ScienceDirect

journal homepage: www.elsevier.com/locate/agrformet

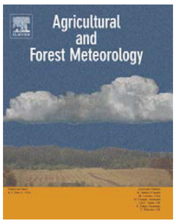

Temporal and spatial variations in the seasonal patterns of CO_2 flux in boreal, temperate, and tropical forests in East Asia

Nobuko Saigusa[a,*], *Susumu Yamamoto*[b], *Ryuichi Hirata*[c], *Yoshikazu Ohtani*[d], *Reiko Ide*[c], *Jun Asanuma*[e], *Minoru Gamo*[a], *Takashi Hirano*[f], *Hiroaki Kondo*[a], *Yoshiko Kosugi*[g], *Sheng-Gong Li*[e,h,j], *Yuichiro Nakai*[d], *Kentaro Takagi*[i], *Makoto Tani*[g], *Huimin Wang*[a,h]

[a] *National Institute of Advanced Industrial Science and Technology (AIST), 16-1 Onogawa, Tsukuba 305-8569, Japan*
[b] *Graduate School of Environmental Science, Okayama University, 3-1-1 Tsushimanaka, Okayama 700-8530, Japan*
[c] *National Institute for Environmental Studies, 16-2 Onogawa, Tsukuba 305-8506, Japan*
[d] *Forestry and Forest Products Research Institute, 1 Matsunosato, Tsukuba 305-8687, Japan*
[e] *Terrestrial Environment Research Center, University of Tsukuba, Tsukuba 305-8572, Japan*
[f] *Graduate School of Agriculture, Hokkaido University, Sapporo 060-8589, Japan*
[g] *Graduate School of Agriculture, Kyoto University, Kyoto 606-8502, Japan*
[h] *Institute of Geographic Sciences and Natural Resources Research, Chinese Academy of Sciences, 11A Datun Road, Anwai Street, Beijing 100101, China*
[i] *Teshio Experimental Forest, Field Science Center for Northern Biosphere, Hokkaido University, Toikanbetsu 098-2943, Japan*
[j] *Japan Science and Technology Agency, Kawaguchi, Saitama 332-0012, Japan*

ARTICLE INFO

Article history:
Received 2 May 2007
Received in revised form
6 December 2007
Accepted 8 December 2007

Keywords:
Asiaflux
CO_2 flux
Forest ecosystem in East Asia
Inter-annual variation
Net ecosystem production
Spatial variation

ABSTRACT

Measurements of net ecosystem production (NEP) over forest stands were conducted from 11 flux towers in sub-arctic, temperate, and tropical regions in East Asia between 2000 and 2005. The sites extend over a wide latitude, ranging from 3 to 64°N, and include sub-arctic and temperate needle-leaf deciduous forests (larch) (central Siberia, Mongolia, China, and northern Japan), temperate mixed, broadleaf deciduous, needle-leaf evergreen forests (northern and central Japan), and seasonal and tropical rain forests (Thailand and Malaysia).

The sub-arctic larch forests had short growing periods of 3–4 months. The temperate deciduous forests showed the greatest positive NEP after leaf expansion in early summer. Among the 11 sites, the maximum gross primary production (GPP) was observed in a temperate larch forest during the early stages of the growing period due to the high productivity of the larch species. The temperate evergreen sites displayed positive NEP earlier in the spring than the deciduous sites and had long growing periods (>10 months). The tropical seasonal forests showed negative NEP during the dry period from February to April, and turned positive after the rainy season started. The tropical rain forest showed a small flux ($<30\ \mathrm{g\,C\,m^{-2}\,month^{-1}}$) throughout the year without a clear seasonal change.

In 2002 and 2003, several significant weather anomalies were observed, such as increased temperature in the temperate sites and less precipitation than average in the tropical sites in the beginning of 2002, and decreased solar radiation in the temperate sites in the 2003 summer. The seasonal patterns of NEP were sensitive to the anomalies, and the variations were caused by: (1) high spring air temperature, which induced an early start of the growing period in the temperate forests, (2) summer solar radiation, which controlled the summer GPP in the temperate forests with a slight variation among sites due to different responses of

---

[*] *Corresponding author*: Tel.: +81 29 861 8347; fax: +81 29 861 8358.
E-mail address: n.saigusa@aist.go.jp (N. Saigusa).

doi:10.1016/j.agrformet.2007.12.006

GPP to the temperature and water vapor pressure deficit (VPD) conditions, and (3) a long dry season, which significantly reduced GPP in a tropical seasonal forest.

The dataset, which was obtained from a wide variety of forest ecosystems in East Asia over several years, is essential to validate ecosystem models and to generate technological developments of satellite remote sensing in the distribution of the terrestrial carbon budget in Asia.

1. Introduction

Forest ecosystems located in East Asia have several different characteristics when compared with their counterparts in the European, North, and South American continents. For example, forested areas in the East Eurasian continent exist in a wide latitude range, spreading continually from the sub-arctic, through the temperate, to the tropics (Yu et al., 2006). In addition, heat, water, and CO_2 exchanges are under the strong influence of atmospheric and water vapor circulations induced by the Asian monsoon (Kim et al., 2006). A temperature contrast between the Eurasian continent and the oceans is considered as a key factor for characterizing monsoon intensity. In addition, the influence of the Asian monsoon, which is related to El Niño Southern Oscillation (ENSO) events, has been observed in the inter-annual climatic variations of Asia, particularly land surface temperature, summer rainfall, and snow depth (Yasunari and Seki, 1992; Kitoh et al., 1999). A distinct influence of ENSO events is also observed in tropical Asian ecosystems, especially in the year-to-year change in temperature and precipitation (Malhi and Wright, 2004). After ENSO events, tropical Asian forests often experience a longer dry season. This change significantly affects the carbon and water cycles in the ecosystem and triggers the flowering of dominant species in tropical forests (Sakai et al., 2006), which are typically observed once every several years. Thus, the data gathered from the monitoring of long-term fluxes at multiple sites in addition to phenological and eco-physiological activities is indispensable for interpreting the mechanism of seasonal and year-to-year variability in heat, water, and CO_2 exchanges. This information can be applied to a wide variety of terrestrial ecosystems in Asia and used to predict long-term biological responses to climatic systems which change dynamically in the multi-year time-scale.

Recent studies using a tower flux measurement network have shown that the seasonal changes in NEP and its year-to-year variations are affected by various meteorological and biological factors, which are stated in the following. In several broadleaf deciduous forests in the boreal and temperate zones, the annual NEP is primarily controlled by the length of the growing period (Black et al., 2000; Carrara et al., 2003; Saigusa et al., 2005). Summer drought stresses greatly influence temperate ecosystems in North America and the Mediterranean region (Law et al., 2001; Irvine et al., 2002; Reichstein et al., 2002; Powell et al., 2006) while temperate forests in East Asia are relatively free from severe drought stress in summer. This difference is due to the influence of the Asian summer monsoon in the rainy season of the East Asian temperate forests during the early stages of their growing period. In addition, these forests are often exposed to natural disasters, such as destructive typhoon storms and landslides. Unexpected defoliation caused by heavy rainstorms occasionally impacts the annual carbon budget of the forests (Ito et al., 2005). The body of knowledge on the seasonal and inter-annual variations of the carbon cycle in tropical Asian forest ecosystems based on long-term flux measurements has been increasing (Yasuda et al., 2003; Saitoh et al., 2005; Kosugi et al., 2008). However, our data and understanding of these variations in a larger spatial scale are still quite limited.

Until recently, most integrated studies based on the flux tower network were developed mainly in Europe and North America. This work revealed the seasonal patterns and annual values of the net ecosystem CO_2 exchange (NEE), GPP, and ecosystem respiration (RE) in different ecosystems (Falge et al., 2002; Reichstein et al., 2005; Amiro et al., 2006; Coursolle et al., 2006; Owen et al., 2007). In Asia, studies have been started to clarify the control factors of the seasonal change and annual values of NEE based on the data obtained at several flux sites (Yamamoto et al., 2005; Yu et al., 2006). Few studies, however, have been reported using Asian ecosystems to generalize our understanding of the temporal and spatial variability of NEE, GPP, and RE from a dataset consisting of multiple sites over several years.

Thus, the objectives of the present study are: (1) to describe important characteristics of seasonal and inter-annual changes in NEP, GPP, and RE during the 2000–2005 employing more than 10 flux observation sites in sub-arctic, temperate, and tropical forests in Asia, and (2) to demonstrate how ecosystems respond to meteorological anomalies widely observed in East Asia during this same period. The results of three case studies will be presented. The first case exhibited less solar radiation in the mid-latitude temperate zone in the summer of 2003. Next, the warm winter of 2002 with unusually high air temperature in northeastern Asia and, lastly, the long dry period in tropical southeastern Asia at the beginning of 2002.

2. Methods

2.1. Study sites

The present comparative study consists of 11 forest sites in East Asia. Four deciduous coniferous forests (larch) in the high- and mid-latitudes are in the study, i.e., a sub-arctic larch forest in a continuous permafrost region of central Siberia, Russia (the site name is Tura; the abbreviated site code is TUR), a sub-arctic larch forest in a mountainous region in Mongolia (Southern Khentei Taiga; SKT), a planted temperate larch forest in northeastern China (Laoshan; LSH), and a planted temperate larch forest in Hokkaido, Japan (Tomakomai Flux

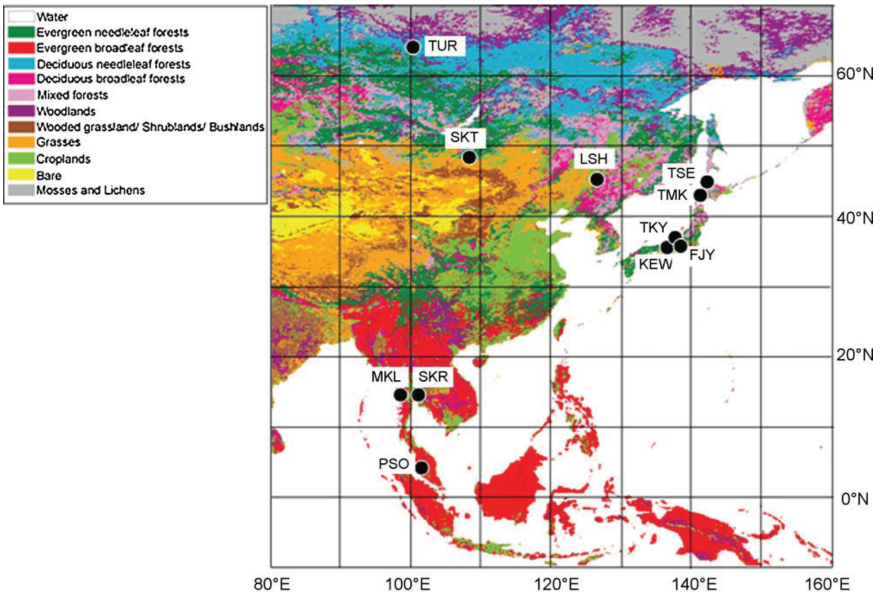

Fig. 1 – Location of study sites in East Asia plotted on a land classification map illustrated according to De Fries et al. (1998).

Research Site, TMK). Four temperate mid-latitude forests are also in the study, i.e., an old conifer-hardwood mixed forest in Hokkaido, Japan (CC-LaG Experiment Site, Teshio; TSE); a birch-oak secondary forest in central Japan (Takayama; TKY); a red pine forest in central Japan (Fujiyoshida Forest Meteorology Research Site; FJY) and a planted Japanese cypress forest (Kiryu Experiment Watershed; KEW) in central Japan. In the low-latitude, three tropical dipterocarp forests were selected, a tropical mixed deciduous forest (Mak Klong; MKL) and a tropical dry evergreen forest (Sakaerat; SKR) in Thailand, and a tropical rain forest (Pasoh Forest Reserve; PSO) in Malaysia. MKL and SKR are two seasonal forests. The locations of the study sites are shown in Fig. 1. The ecosystem type, dominant species, and approximate age are described in Table 1 and the climatic conditions are presented in Table 2.

2.2. *Measurement system*

Continuous long-term flux observations were performed at each site with the exception of TUR and maintained by different research organizations. The observation at TUR (central Siberia) was only conducted during the summer from June to September. All sites had an eddy covariance measurement system installed on a tower, which consisted of a three-dimensional sonic anemometer–thermometer, an infrared gas analyzer (IRGA) for CO_2 and water vapor, and a data acquisition system. Open and closed-path IRGAs were utilized depending on the site. Continuous high frequency (mostly from 5 to 10 Hz) data were recorded and the covariance was calculated at 30 min intervals. To test the energy balance closure and to monitor basic environmental variables, net radiation (or downward and upward short- and long-wave radiation), photosynthetically photon flux density (PPFD), ground heat flux, vertical profiles of air temperature, humidity, CO_2 concentration, and vertical profiles of soil temperature, and volumetric soil water content were measured at most sites. The measurement systems for each site as used in the study period are listed in Table 3.

2.3. *Data processing and gap filling*

The net ecosystem CO_2 exchange was estimated from the CO_2 flux over the canopy, taking into account the temporal change in CO_2 storage below the height of the flux measurement system. The total RE was estimated by the nighttime NEE with data filtering by the friction velocity (u_*). The threshold values of u_*-filtering were determined by Hirata et al. (2008) and varied slightly among sites as listed in Table 3. Site-specific differences to mitigate the effects of nighttime NEE in the estimation of RE are described in Appendix A.

For the present study, the observed nighttime NEE were fitted to the equation of Lloyd and Taylor (1994):

$$F_{RE} = F_{RE,T_{ref}} \exp\left\{\frac{E_0}{R}\left(\frac{1}{T_K + T_{ref} - T_0} - \frac{1}{T_K + T_a - T_0}\right)\right\}, \qquad (1)$$

where $F_{RE,T_{ref}}$ is the ecosystem respiration rate (F_{RE}) at the reference temperature T_{ref} (10 °C), E_0 is the activation energy (J mol^{-1}), R is the ideal gas constant (8.314 J mol^{-1} K^{-1}), T_K and T_0 are constants (273.15 K and 227.13 K), and T_a is the air temperature (°C). The two regression coefficients, E_0 and $F_{RE,T_{ref}}$, were estimated for every site and each day with a 29-day moving window using the least-squares method. Gaps in the nighttime NEE were filled by Eq. (1) as a function of the nighttime air temperature.

Table 1 – Description of the study sites

Code	Site name	Country	Location (°N, °E)	Elevation (m)	Ecosystem type	Dominant species	Age (year)	Canopy height (m)	References
TUR	Tura	Russia	64° 12′, 100° 27′	250	DC	Larch (*Larix gmelinii*)	105	3	Kajimoto et al. (2006); Nakai et al. (in press)
SKT	Southern Khentei Taiga	Mongolia	48° 21′, 108° 39′	1630	DC	Larch (*Larix sibirica*)	70–300	20	Li et al. (2005)
LSH	Laoshan	China	45° 20′, 127° 34′	370	DC	Larch (*Larix gmelinii*)	35	18	Wang et al. (2005a)
TSE	CC-LaG Experiment Site (Teshio)	Japan	45 ° 03′, 142 ° 06′	70	MX	Oak (*Quercus crispula*), Birch (*Betula ermanii*), Fir (*Abies sachalinensis*)	–	18–25	Koike et al. (2001); Takagi et al. (2005)
TMK	Tomakomai Flux Research Site	Japan	42 ° 44′, 141 ° 31′	140	DC	Larch (*Larix kaempferi*)	45	16	Hirano et al. (2003); Wang et al. (2004)
TKY	Takayama	Japan	36° 08′, 137° 25′	1420	DB	Birch (*Betula ermanii*), Oak (*Quercus crispula*)	50	15–20	Saigusa et al. (2002)
FJY	Fujiyoshida Forest Meteorology Research Site	Japan	35° 27′, 138° 46′	1030	EC	Red pine (*Pinus densiflora*)	90	20	Ohtani et al. (2005)
KEW	Kiryu Experiment Watershed	Japan	34° 58′, 135° 59′	250	EC	Japanese cypress (*Chamaecyparis obtusa*)	45	18	Takanashi et al. (2005a); Ohkubo et al. (2007)
MKL	Mae Klong	Thailand	14° 35′, 98° 51′	160	TR	Dipterocarp (*Shorea siamensis*)	–	30	Gamo et al. (2005)
SKR	Sakaerat	Thailand	14° 29′, 101° 55′	535	TR	Dipterocarp (*Hopea ferrea*)	–	35	Kondo et al. (submitted)
PSO	Pasoh Forest Reserve	Malaysia	2° 58′, 102° 18′	75-150	TR	Dipterocarp (*Hopea ferrea*)	–	35–45	Kosugi et al. (2008); Takanashi et al. (2005b)

Description of ecosystem type: DC, deciduous coniferous forest; MX, mixed forest; DB, deciduous broadleaf forest; EC, evergreen coniferous forest; TR, tropical forest.

The observed daytime NEE ($F_{\mathrm{NEE,day}}$) were fitted to the following equation based on the non-rectangular hyperbola relationship (Thornley, 1976) as a function of PPFD (Q):

$$F_{\mathrm{NEE,day}} = -\frac{\phi Q + P_{\max} - \sqrt{(\phi Q + P_{\max})^2 - 4\phi Q\theta P_{\max}}}{2\theta} + R_{\mathrm{d}} \qquad (2)$$

Here, ϕ is the initial slope, $P_{\max}$ is the maximum level of GPP at light saturation, θ (=0.9) is a parameter of convexity, and R_{d} is the intercept. The regression coefficients ϕ, $P_{\max}$, and R_{d} were determined for every site and each day with a 15-day moving window by the least-squares method. Gaps in the daytime NEE were filled by Eq. (2) as a function of PPFD.

The gross primary production (GPP; F_{GPP}) was calculated as the sum of NEP ($-F_{\mathrm{NEE}}$) and RE:

$$F_{\mathrm{GPP}} = -F_{\mathrm{NEE}} + F_{\mathrm{RE}} \qquad (3)$$

The temperature dependence of RE in the daytime was assumed to be equal to the nighttime estimation, and the daytime RE was calculated by Eq. (1) using the daytime air temperature. The procedure of gap filling and flux partitioning for the present analyses were described in detail by Hirata et al. (2008).

3. Results and discussion

3.1. *Monthly values of GPP, RE, and NEP (2000–2005)*

Fig. 2a–k represents the monthly values of GPP estimated at each site. Sites represented in Fig. 2a–d are larch forests (DC) in central Siberia (the annual air temperature is −9 °C), Mongolia (−1 °C), northeastern China (5 °C), and northern Japan (6 °C), respectively. The maximum values of GPP in the larch forests were observed during the early stages of their growing period, such as, July (Fig. 2a–c) and June (Fig. 2d). As clearly shown in Fig. 2a–d, the maximum values of GPP and the length of the growing period increased with the annual air temperature. In contrast, the seasonal variations of GPP are shown to display similar behavior (the rapid increase after leaf expansion, the peak in early growing period, and the slow decrease from mid-summer to fall). Among the eleven sites shown in Fig. 2a–k, the maximum value of GPP was the highest in the temperate larch forest TMK (~420 g C m^{-2} $month^{-1}$; Fig. 2d). This result is supported by previous eco-physiological studies, such as those by Koike et al. (2000) and Wang et al. (2005b). Both indicate that the larch species in northeastern Asia have a high photosynthetic capacity and may act as an important CO_2 sink.

Fig. 2e and h represents the monthly values of GPP estimated in a temperate mixed forest (MX), a birch-oak forest (DB), a red pine forest (EC), and a Japanese cypress forest (EC), respectively. The EC forests (Fig. 2g and h) had a longer growing season (>10 months) compared with mixed or deciduous forests (Fig. 2e–f). Even during the mid-winter (December–February), EC forests showed weak but detectable positive GPP, which is similar to the results of Ohtani et al. (2005). These results indicate a temperate red pine forest in central Japan has enough potential to assimilate CO_2 even in

Table 2 – Climatic conditions of the study sites

Code	Air temperature			Precipitation annual (mm)	Climatic zone	Observation period
	Annual mean (°C)	Monthly minimum (°C)	Monthly maximum (°C)			
TUR	−9[a]	–	–	360[a]	Sub-arctic	2004
SKT	−1	−21	16	250	Sub-arctic	2004–2005
LSH	5	−16	21	640	Temperate	2004
TSE	5	−8	16	970	Temperate	2002
TMK	6	−7	18	1040	Temperate	2001–2003
TKY	7	−8	19	2030	Temperate	2000–2004
FJY	10	−3	22	2060	Temperate	2000–2004
KEW	15	2	29	1600	Temperate	2001–2004
MKL	25	22	29	1200	Tropical	2003–2004
SKR	24	22	27	1500	Tropical	2002–2003
PSO	26	25	28	1700	Tropical	2003–2005

[a] Climatic data from TUR was obtained from a meteorological station near the site (Nakai et al., in press).

Table 3 – Measurement systems

Code	Measurement height (m)	Sonic anemometer	IRGA	u_* threshold (m s^{-1})
TUR	20	R-3, Gill[a]	LI-7500, LI-COR[b]	0.1
SKT	30	SAT-550, Kaijo[c]	LI-7500, LI-COR[b]	0.3
LSH	29	SAT-550, Kaijo[c]	LI-7000, LI-COR[b]	0.2
TSE	32	DA600-3TV, Kaijo[c]	LI-7000, LI-COR[b]	0.0
TMK	27	DA600-3TV, Kaijo[c]	LI-6262, LI-COR[b]	0.3
TKY	25	DA600-3T, Kaijo[c]	LI-6262, LI-COR[b]	0.5
FJY	26	DA600-3T, Kaijo[c]	LI-6262, LI-COR[b]	0.2
KEW	29	DA600-T, Kaijo[c]	LI-7500, LI-COR[b]	0.4
MKL	42	SAT-540, Kaijo[c]	LI-6262, LI-COR[b]	0.2
SKR	45	Wind Master, Gill[a]	LI-6262, LI-COR[b]	–[d]
PSO	54	SAT-550, Kaijo[c]	LI-7500, LI-COR[b]	–[d]

[a] Gill Instruments Ltd., Lymington, UK.
[b] LI-COR, Inc., Lincoln, NE, USA.
[c] KAIJOSONIC Corporation, Tokyo, Japan.
[d] See Appendix A for detail.

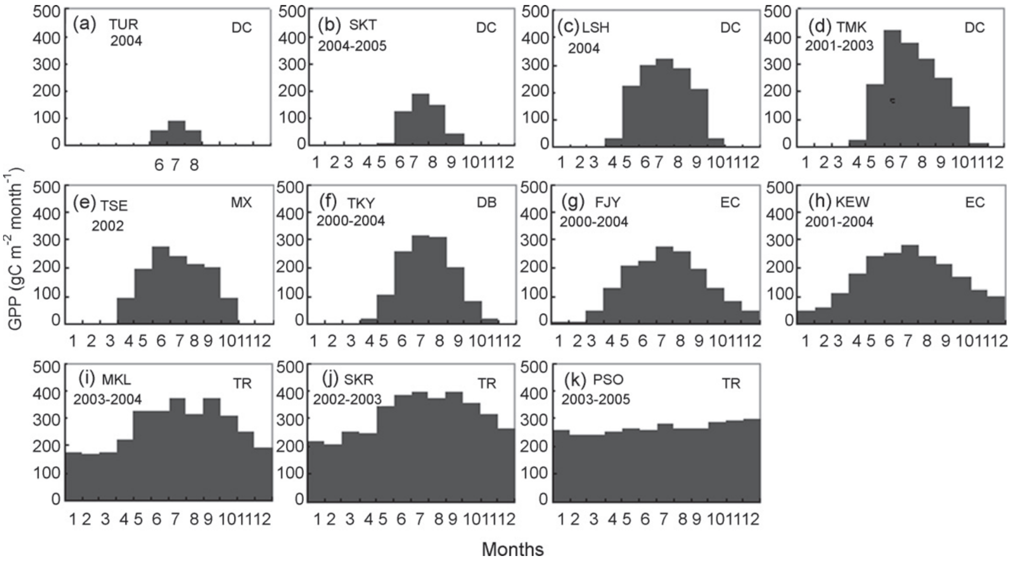

Fig. 2 – Monthly GPP observed at the 11 sites listed in Table 1. The site code, year(s) of GPP evaluation, and ecosystem type are indicated in each figure.

mid-winter when the climatic conditions are favorable. It should be also mentioned that the GPP in the temperate DC and DB forests started to increase before the leaf foliation period of canopy trees, which was typically from May to June (Fig. 2c, d, and f). This early increase in GPP was primarily caused by the photosynthetic activity of understorey plants, particularly ferns (*Dryopteris crassirhizoma*) at TMK and dwarf bamboo (*Sasa senanensis*) at TKY.

The seasonal variations of GPP estimated in tropical forests (Fig. 2i–k) had completely different aspects from sub-arctic and temperate forests. GPP values for the tropical rain forest in Malaysia (PSO; Fig. 2k) were high throughout the year with little seasonality. GPP values measured in PSO were similar to the maximum level of those observed in the temperate MX and EC forests. The GPP of tropical seasonal forests in Thailand (Fig. 2i and j) decreased from December to April, due to the dry season. Drought stress is likely the main cause for the photosynthetic rate reduction.

Fig. 3a–k displays the monthly values of the total RE. From sub-arctic to temperate (Fig. 3a–h), the maximum values of RE were observed in mid-summer (July and/or August) and the seasonal variations were quite similar. This observation is likely due to the fact that the most important controlling factor of RE in sub-arctic and temperate forests was the temperature, and other factors, such as drought stress, were not dominant. The maximum monthly value of RE was highest in the temperate larch forest in mid-summer (Fig. 3d). This high RE might be related to the high photosynthetic activity of needles during the growing period of the temperate larch forest. The RE of tropical seasonal forests (Fig. 3i and j) decreased from December to April, due to the dry season. In the tropical rain forest (Fig. 3k), the seasonality of RE was less clear.

Fig. 4a–k represents the monthly values of NEP at each site. The NEP at the sub-arctic and temperate deciduous forests (Fig. 4a–f) indicates clear seasonal change, and the maximum value of NEP tended to increase with the annual air temperature. In the TMK and TSE sites (Fig. 4d and e), the values of mid-summer NEP reduced to almost zero or negative. One reason for this reduction was the high respiratory activity in both sites during mid-summer as indicated in Fig. 3d and e. The NEP at temperate EC forests and a tropical rain forest (Fig. 4g, h, and k) had less clear seasonal changes compared with sub-arctic and temperate deciduous forests. Slight decrease in NEP was observed in winter at temperate EC forests (Fig. 4g and h) caused by low temperature conditions. In tropical seasonal forests (Fig. 4i and j), zero or negative NEP was observed from February to April due to the dry season.

Seasonal patterns for GPP, RE, and NEP estimated from the various ecosystems in East Asia are a valuable dataset, which can be used for validation and sensitivity tests of various terrestrial ecosystem models. In addition, this data can be applicable for advanced technological development of satellite remote sensing; however, the patterns still include considerable uncertainty depending on the observational conditions and the data processing, such as topography and fetch around the towers, different data correction and quality control, and so on. A critical source of uncertainty, and also the most difficult problem to be solved, lies is the nighttime underestimation of NEE and data corrections. As indicated in Appendix A, this study used the usual u_*-filtering for most sites, while site-specific data filtering was applied at two tropical sites. Currently, comparative studies are being performed for the better estimation of nighttime RE and the annual NEP by multiple methods at the sites, such as the Eddy covariance method, chamber method, and other biometric methods (Kosugi et al., 2008; Kondo et al., submitted; Hirata et al., 2008). However, the uncertainty in the nighttime flux might still be great especially for tropical forests with large year-round CO_2 emissions and frequent calm atmospheric conditions (Kosugi et al., 2008), and absolute values of GPP and RE in Figs. 2 and 3 might include some bias. Further studies are

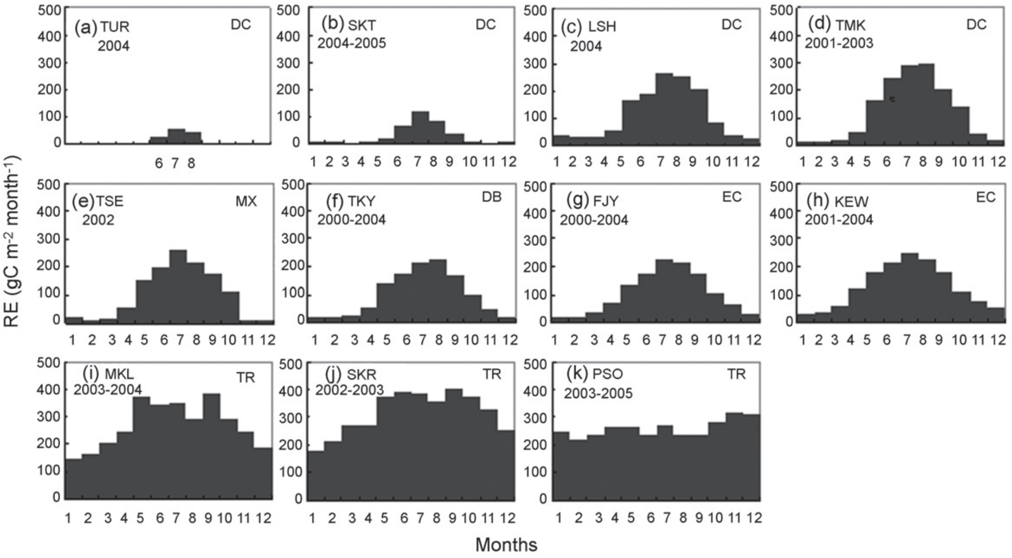

Fig. 3 – Monthly RE observed at the 11 sites listed in Table 1. The site code, year(s) of RE evaluation, and ecosystem type are indicated in each figure.

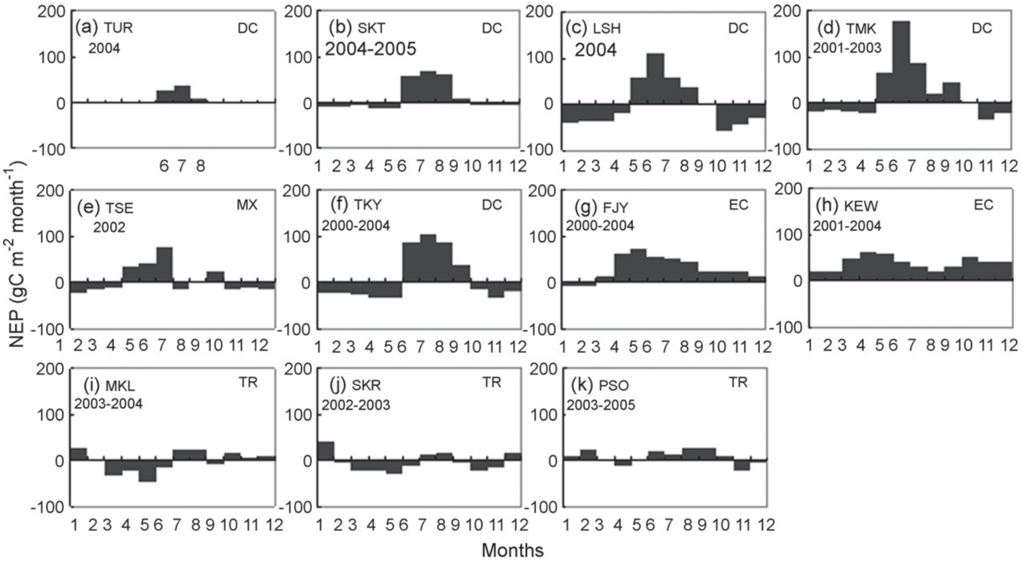

Fig. 4 – **Monthly NEP observed at the eleven sites listed in Table 1. The site code, year(s) of NEP evaluation, and ecosystem type are indicated in each figure.**

clearly necessary to establish an effective and practical way to avoid nighttime data problems.

3.2. *Meteorological anomalies and ecosystem responses*

During our study period from 2000 to 2005, several significant anomalies in the meteorological conditions were observed, such as solar radiation, air temperature, and precipitation. In the following analyses, results of three case studies are presented showing how each forest ecosystem responded to the meteorological anomalies. The first case is the negative anomaly of solar radiation observed in the mid-latitude zonal area during the 2003 summer. The second case occurred in the beginning of 2002 when unusually high surface air temperature widely appeared in northeastern Asia. The third case happened during the same period as the second case and presented as a negative precipitation anomaly in tropical Asia. The data were obtained from NCEP/NCAR reanalysis data (Kistler et al., 2001), and the anomalies in the meteorological variable refer to the 1971–2000 base period.

3.2.1. *Case 1: effect of negative anomaly of solar radiation in the 2003 summer*

To demonstrate the meteorological conditions of the first case, the spatial distribution of the anomaly within the summer solar radiation (3-month average of July–September) in 2003 is displayed in Fig. 5. In a zonal area at mid-latitude around 35–40°N from China to the main island of Japan through South Korea, a clear negative anomaly of solar radiation was observed. The anomaly was stationary during the 2003 summer with a wide longitude range from 80° to 150°E, under the influence of an active rain front which remained for an unusually long period. In the 2003 summer, several meteorological stations on the main island of Japan broke records for the minimum daylight hours, especially in July 2003 (Japan Meteorological Agency, 2005).

We examined PPFD at each site and found that a significant negative anomaly was observed in the 2003 summer at three temperate forests in the central part of the main island of Japan. Fig. 6a–c shows monthly values of GPP from 2001 to 2003 at the three sites: TKY, FJY and KEW, respectively. At two of the three sites (TKY and FJY), a significant decrease was observed in GPP especially in July 2003 compared with previous years. The mean GPP of July was 19% (TKY) and 32% (FJY) lower in 2003 than in other years. The significant

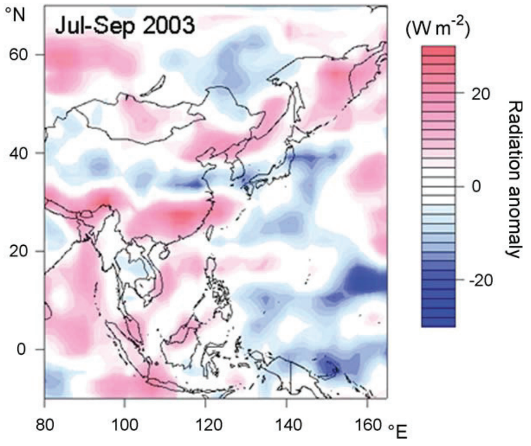

Fig. 5 – **The spatial distribution of the anomaly in summer solar radiation (3-month average of July–September) in 2003 obtained from NCEP/NCAR reanalysis data (base period 1971–2000).**

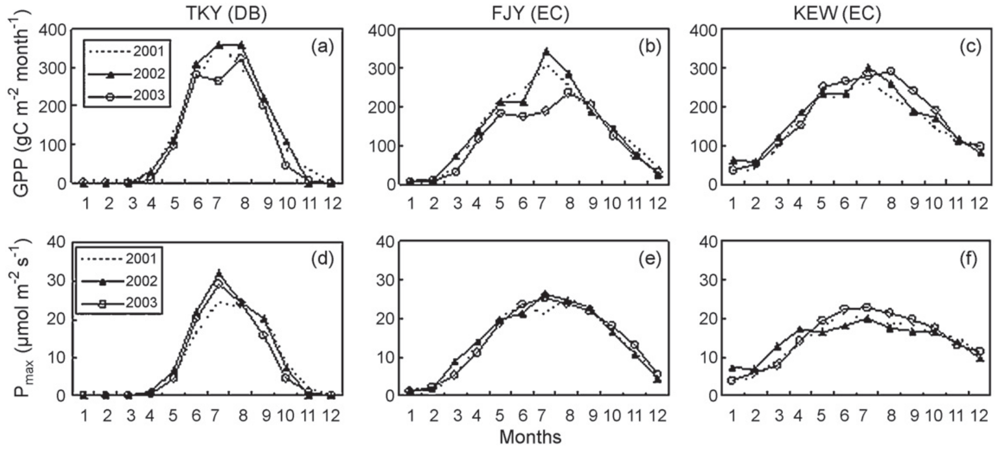

Fig. 6 – Monthly GPP at (a) TKY, (b) FJY, and (c) KEW, and monthly mean P_{max} at (d) TKY, (e) FJY, and (f) KEW from 2001 to 2003.

decrease in GPP was mainly due to an unusually low PPFD in July, which was 32% (TKY) and 44% (FJY) lower in 2003 than in previous years. Monthly values of GPP in the KEW site, however, did not show a clear decrease in the 2003 summer, even though the monthly PPFD in July was 35% lower in 2003 than in other years.

To investigate the cause for the different responses to summer GPP, we compared monthly mean P_{max} (the maximum level of GPP at light saturation condition) among the three sites. Fig. 6d–f indicates the monthly P_{max} at the first two sites (TKY and FJY) did not show systematic year-to-year difference from 2001 to 2003. In contrast, the values of P_{max} at the KEW site were obviously higher in the 2003 summer than in other years from June to September. To discuss the cause for different year-to-year changes in P_{max}, the monthly mean daytime air temperature and daytime water vapor pressure deficit (VPD) were shown in Fig. 7a–f for the three sites. A clear decrease was observed in daytime temperature in the 2003 summer especially in July for each site. Here, it should be noted that the monthly mean daytime VPD was relatively lower at the TKY and FJY sites (<0.9 kPa) even during mid-summer due to cool climatic conditions in high altitude (>1000 m a.s.l.), while those at KEW site had higher VPD (>1.2 kPa) in July and August except for 2003. The decreased daytime VPD and decreased water stress in the 2003 summer are possible causes for the increased P_{max} at the KEW site.

These results suggest the following interpretations of the different response seen among the three forests to the negative anomaly of solar radiation during the 2003 summer: (1) at the TKY and FJY sites, the decrease in the monthly GPP in 2003 summer was caused mainly by a significant reduction (from 32 to 44%) in monthly PPFD, which was lower than observed in previous years; (2) at the KEW site, a similar level of decrease (35%) in the monthly PPFD was also observed, however, a decrease in the monthly GPP was not obvious. The effect of low PPFD may have been compensated by the increase in P_{max} in this forest.

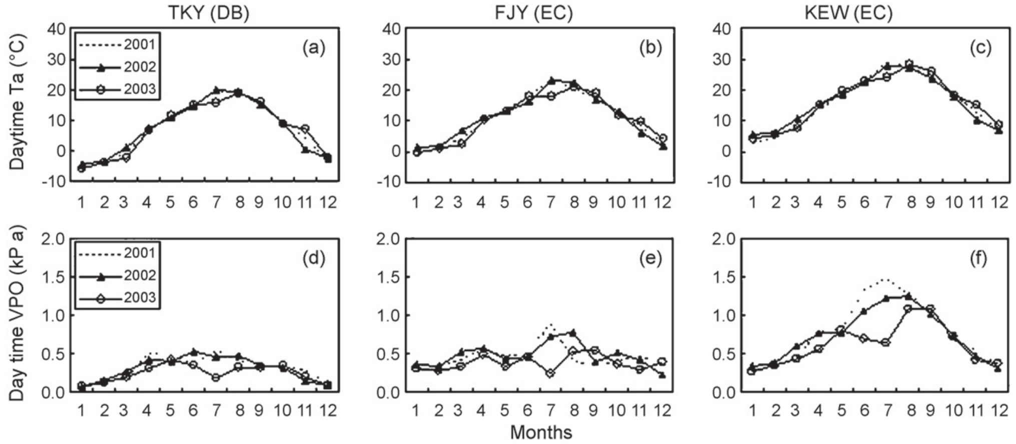

Fig. 7 – Monthly averaged daytime (PPFD > 0) air temperature at (a) TKY, (b) FJY, and (c) KEW, and monthly averaged daytime VPD at (d) TKY, (e) FJY, and (f) KEW from 2001 to 2003.

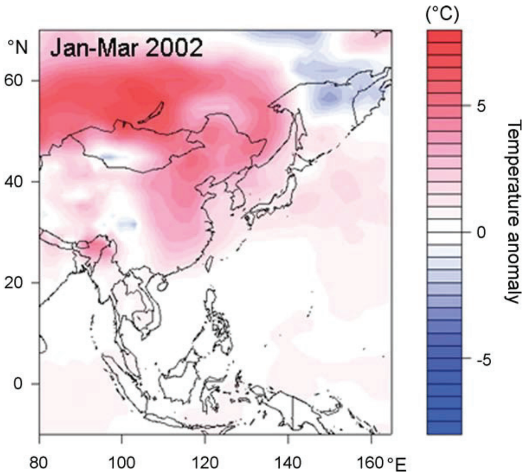

Fig. 8 – The spatial distribution of the anomaly in a 3-month mean surface air temperature (January–March) in 2002 obtained by NCEP/NCAR Reanalysis data (base period 1971–2000).

3.2.2. *Case 2: effects of the positive anomaly of surface air temperature in the beginning of 2002*

The second case is the effect of a positive anomaly of surface air temperature. Fig. 8 shows a spatial distribution of the anomaly in the surface air temperature from the winter to spring 2002 (3-month average of January–March). A significant anomaly of positive surface air temperature was observed over a large area which encompasses the eastern part of China, North- and South-Korea, Japan, Mongolia, and the southern part of Russia. A significant high spring air temperature anomaly was observed in northeastern Asia during the El Niño year of 1998. The high temperature anomaly observed in the beginning of 2002 was, however, slightly before the onset of the 2002/2003 El Niño. The winter air temperature in North Eurasia is highly influenced not only by ENSO events but also by the arctic atmospheric pressure pattern and polar atmospheric circulation, which varies with a period of several years or longer (Yamazaki, 2004). Currently, the mechanism of unusually high (or low) temperature anomalies in northeastern Asia has not been clarified.

Responding to the positive temperature anomaly at the beginning of 2002, NEP in several forests increased during the early stage of the growing period. Fig. 9a–d shows the monthly values of NEP at four temperate forests in central Japan from 2001 to 2003. The deviation of monthly mean air temperature in 2002 from the 3-year average (2001–2003) is shown in Fig. 9e–h. At two EC forests (Fig. 9c and d), a higher NEP was observed from March to April, probably due to the enhancement of needle photosynthetic activity under the warm weather condition. On the other hand, at two deciduous forests (Fig. 9a and b), no obvious year-to-year difference was observed from January to April, since the forests were leafless. The monthly NEP was higher in 2002 than observed in 2001 and 2003 at the beginning of the growing season (May in TMK, and June in TKY) for the deciduous forests. At the TKY site, the NEP in the beginning of the growing season (June) was highest in 2002 compared to 2001 and 2003 though the high temperature deviation was finished by May.

The main cause for this result was due to the earlier timing of leaf expansion during 2002 than had occurred in 2001 and 2003. At the TKY site, the leaf expansion had a year-to-year variation for about 2–3 weeks, and the timing of the expansion in 2002 was earlier than normal years (Saigusa et al., 2005). At the TMK site, Hirata et al. (2007) reported that the larch needles foliated 2-weeks earlier in 2002 than in 2001 and 2003.

As a result, the unusually warm winter in 2002 affected temperate forests as follows: (1) the warm weather condition enhanced photosynthesis rates of temperate evergreen coniferous forests and increased NEP, (2) in the temperate deciduous forests, the high air temperature caused early leaf expansion, which enhanced NEP at the beginning of the growing period even after the high temperature deviation was over.

3.2.3. *Case 3: effects of negative precipitation anomaly at the early stage of 2002*

The third case is the effects of less precipitation in tropical Asia during the same period that unusually high temperature was observed in northeastern Asia (from January to March 2002). Fig. 10 indicates the spatial distribution of the anomaly of 3-month averaged precipitation in January–March in 2002. There was a significant negative precipitation anomaly in Southeast Asia, ranging from around 0° to 20°N and from 90° to 150°E. The area of the negative precipitation anomaly covered

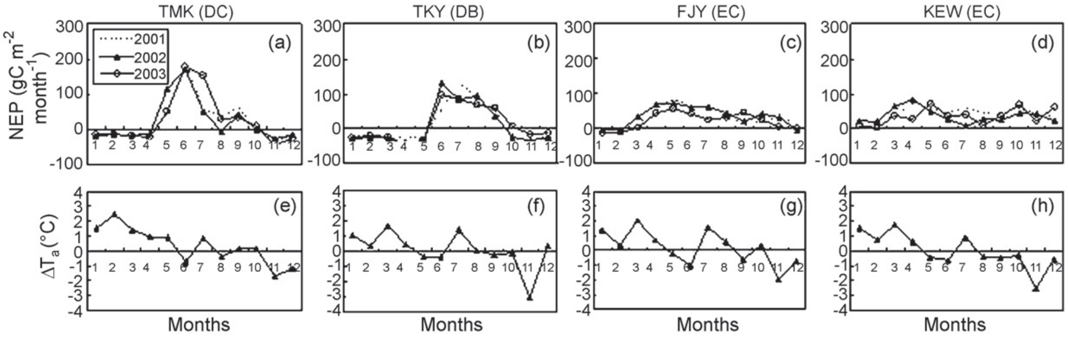

Fig. 9 – Monthly NEP from 2001 to 2003 at four temperate forests (a) TMK, (b) TKY, (c) FJY, and (d) KEW. The deviation of monthly mean air temperature of 2002 (ΔT_a) from the 3-year average (2001–2003) was also shown at each forest.

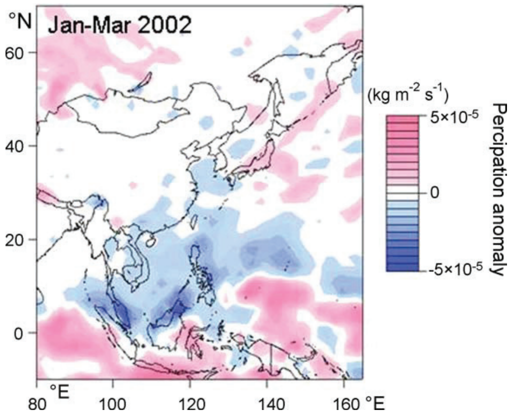

Fig. 10 – The spatial distribution of the anomaly in 3-month mean precipitation (January–March) in 2002 obtained by NCEP/NCAR reanalysis data (base period 1971–2000) (5×10^{-5} kg m^{-2} s^{-1} is equivalent to 4.3 mm day^{-1}).

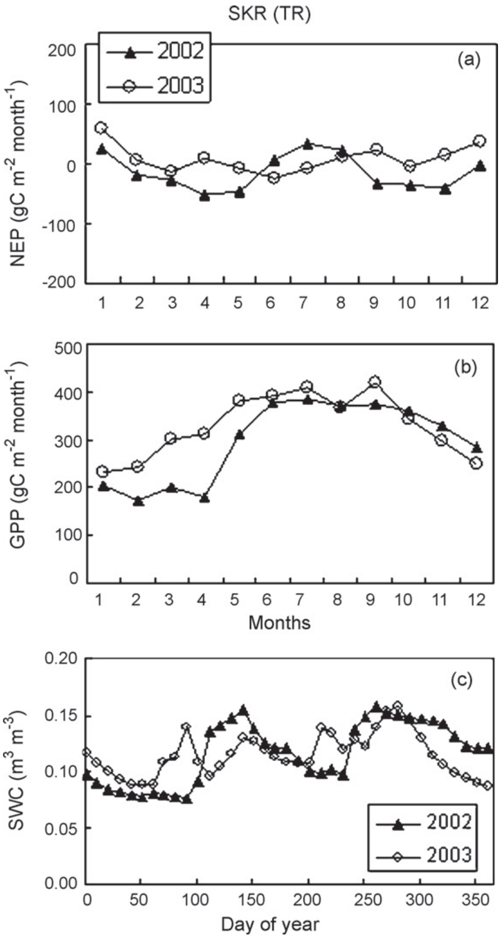

Fig. 11 – Seasonal changes in the monthly values of (a) NEP and (b) GPP, and (c) 10-day mean values of volumetric soil water content at 10 cm deep in tropical seasonal forest site (SKR).

the northern part of Kalimantan, Philippine Islands, the northern part of Sumatra, the Malay Peninsula, and Indochinese Peninsula.

As a response to decreased precipitation, Fig. 11a and b showes that the monthly values of GPP at the tropical seasonal forest in Thailand (SKR) were reduced from January to April 2002 compared with 2003, and the monthly NEP was negative (carbon release) from February to May. This forest has a dry season in winter (December–February) in a normal year; however, there was an unusually longer dry season at the beginning of 2002, which continued until the end of April. Fig. 11c shows the 10-day mean volumetric soil water content (SWC) measured at 10 cm depth. Values of SWC was quite low (<0.1) from January to April (day of year (DOY) <110) in 2002. The long dry period with low SWC at the early stage of 2002 was probably a main cause for the reduction in GPP.As observed in the tropical seasonal forests in Thailand, recent studies have reported that significant reductions in the CO_2 uptake of tropical forests have been widely observed in Southeast Asia caused by severe droughts and wild fires every several years. Hirano et al. (2007) reported that the highest CO_2 release was observed in 2002 at a tropical peat swamp forest in Indonesia during their study period from 2002 to 2004, due to dry condition and a dense smoke emitted from large forest fires associated with severe droughts. Kobayashi et al. (2005) estimated the net primary production (NPP) by satellite images, and suggested that the year-to-year variations of NPP in Southeast Asia were affected by El Niño drought years. Patra et al. (2005) mentioned that changes in meteorology (i.e., rainfall and air temperature) associated with ENSO events were the most dominant controlling factors of CO_2 flux in tropical Asia, based on the estimation of global distribution of source/sink of CO_2 using atmospheric transport models.

Inter-annual variation of CO_2 uptake in tropical Asia is, as discussed above, closely related to the large scale climatic variations, and further studies are necessary to generalize our understandings of a variety of interactions between terrestrial ecosystems and the atmosphere in tropical Asia. The focus of the analysis in this section was on the seasonal and year-to-year changes in the CO_2 flux observed from 2002 to 2003 at a tropical seasonal forest, and more thorough analyses are clearly necessary using multiple years and sites to investigate spatial variations in the seasonal patterns of CO_2 flux in tropical Asia. In addition to the strong negative anomaly for precipitation discussed in this section, some positive anomalies appeared simultaneously to the south of the equator and in the mid- and high-latitudes, as shown in Fig. 10. Further studies should focus more on the spatial distributions of CO_2 flux and such effects as phenological changes in severe droughts, reduction in photosynthesis, and respiration by water limitations, forest fire, and the recovery process from such disturbances. Studies should be based not only on the ground observation network, but also on satellite remote sensing and modeling analyses. Clarifying the variety of ecosystem responses to climatic variations in tropical Asia is indispensable for a better prediction of future changes in the terrestrial carbon cycle processes and also in the growth rate of atmospheric CO_2 concentration.

4. Conclusion

In East Asia, where few long-term and multi-site datasets have been available, continuous flux observations were made for 1–5 years during the study period from 2000 to 2005 at 11 forest sites distributed in the sub-arctic, temperate, and tropical zone. In addition, the seasonal patterns and amplitudes of GPP, RE, and NEP were discussed.

Larch forests, distributed over a vast area in northeastern Asia, have a characteristic that the maximum values of GPP and the length of the growing period clearly increased with the annual air temperature. Among the 11 study sites, the maximum values of the monthly GPP were the highest in the temperate larch forest (TMK) ($\sim$420 g C m^{-2} $month^{-1}$). The high maximum GPP was probably caused by the high photosynthetic capacity of the larch species achieved during their short growing period. This result reveals the important role of larch species, which produce seasonal and year-to-year variations of carbon uptake by the boreal ecosystems.

The seasonal patterns of RE were compared among 11 sites and found to be similar at eight sites from the sub-arctic to temperate zone and in different ecosystems (DC, MX, DB, and EC). This result was interpreted to indicate that the temperature was the most important factor controlling RE and that other factors, such as drought stress, were not dominant in the sub-arctic to temperate forests. These ecosystems are relatively free from severe drought stress in summer, due to the influence of the Asian summer monsoon in the rainy season of the East Asian temperate forests during the early stages of their growing period.

Three case studies were presented to illustrate how GPP and NEP for several ecosystems responded to significant meteorological anomalies observed in East Asia from 2002 to 2003. The productivity in the temperate forests (TMK, TKY) typically decreased when summer solar radiation was unusually less than normal years, due to an active rain front stationary during the 2003 summer. However, the effect of a decrease in PPFD could be compensated for by the increased maximum level of photosynthetic activity due to less VPD and less water stress depending on the site.

The effects of unusually high air temperatures at the beginning of 2002 differed between evergreen and deciduous forests in the temperate zone. For evergreen forests, photosynthesis was directly enhanced in March and April under warm weather conditions. On the other hand, unusually early leaf expansion was observed in deciduous forests, which increased NEP at the beginning of the growing season. The earlier timing of leaf expansion during 2002 enhanced NEP in deciduous forests from May to June even after the high temperature deviation was over.

Finally, decreased precipitation at the early stage of 2002, which happened during the same period as the unusually high air temperature in the temperate zone, significantly decreased GPP in a tropical seasonal forest due to a long dry period and severe drought stress. Year-to-year change in CO_2 uptake in tropical forests in Southeast Asia is closely related to the large scale climatic variation such as El Niño events and also large forest fires associated with severe droughts.

Although this study is still preliminary as an integrated study of Asian scale, the results showed some important aspects, i.e., that forest ecosystems in Asia responded dynamically to meteorological anomalies depending on the climatic zone and forest type, particularly, summer solar radiation in temperate forests, air temperature at the early stage of year in temperate and sub-arctic forests, and severe drought that is typically observed once every several years in tropical forests.

Acknowledgements

This study was financially supported by the Global Environment Research Fund from the Japanese Ministry of the Environment (Integrated study for the terrestrial carbon management of Asia in the 21st century on the basis of scientific advancements: Project leader, Prof. Takehisa Oikawa (University of Tsukuba, Japan)). The authors would like to thank the project investigators, their co-workers, and students for providing data and valuable comments. Especially, Drs. Y. Matsuura, Y. Mizoguchi, S. Takanashi and Y. Yasuda (Forestry and Forest Products Research Institute, Japan), Y. Fujinuma, A. Ito, E. Kato, and Y. Yamagata (National Institute for Environmental Studies, Japan), Y. Kobayashi (National Institute for Agro-Environmental Sciences, Japan), S. Murayama, T. Maeda, and T. Sasai (National Institute of Advanced Industrial Science and Technology, Japan), T. Nakano (Yamanashi Institute of Environmental Sciences, Japan), K. Nishida and M. Sugita (University of Tsukuba, Japan), T. Akiyama, H. Koizumi and H. Muraoka (Gifu University, Japan), A. Kotani (Nagoya University, Japan), S. Ohkubo (Kyoto University, Japan), N. Matsuo (Mie University, Japan), and N. Monji (Osaka Prefecture University, Japan). The authors also wish to thank their co-workers in overseas observational sites for their support and for providing data. Especially, Drs. O.A. Zyryanova (V.N. Sukachev Institute of Forest, Russia), Y. Zu and W. Wang (Northeast Forestry University, China), S. Panuthai (National Park, Wildlife and Plant Conservation Department, Thailand), G. Davaa and D. Oyunbaatar (Institute of Meteorology and Hydrology, Mongolia), and A.R. Nik (FRIM, Malaysia).

Appendix A

nighttime data correction is one of the most critical sources of uncertainty at many sites. Several effects such as complex topography in mountainous regions and horizontal advection in tall canopies are expected to be important sources of error; however, effective protocols for data correction have not been established. We applied u_*-filtering method for most sites in the present study. Practical validations of the method have been conducted in some sites, for example, u_*-filtering worked well so that the values of nocturnal NEE in high u_* conditions were almost equivalent to those estimated by the integration of chamber measurements for soil, trunk, and foliar respiration at a temperate site (KEW) (Ohkubo et al., 2007). However, the nocturnal NEE estimated by the eddy covariance method showed a serious underestimation even in high u_* conditions in the following two tropical forests.

At a tropical seasonal forest (SKR) where the mean tree height was approximately 35 m, the value of u_*-threshold was not determined successfully because the relationship between the nighttime NEE and u_* under the same temperature conditions were unclear. The values of nighttime NEE were not ‘‘saturated’’ even in turbulent (high u_*) conditions (Gamo et al., 2005).

Kondo et al. (submitted) tested three methods of data filtering to estimate RE. One technique was originally proposed by van Gorsel et al. (2007). This method used the maximum value of the nighttime NEE each night to construct a temperature response function (such as Eq. (1)) instead of using all the nighttime NEE data of windy (high u_*) conditions. Using biometric estimations (Kondo et al., submitted) as the standard, the annual RE estimation based on van Gorsel's filtering was more realistic than u_*-filtering. Therefore, the present study used regression parameters of Eq. (1), which are estimated based on the van Gorsel's filtering, for the SKR site.

At tropical forest PSO, where mean canopy height was higher than 35 m, RE by the eddy covariance measurement was difficult to estimate (Kosugi et al., 2008). Estimation of total RE based on detailed chamber measurements was first attempted. The results suggested a serious underestimation of RE when calculated using the eddy covariance with u_*-filtering. In addition, an original method of data filtering was used in which all nighttime NEE data were replaced with the values estimated based on the chamber measurements. They concluded that the values of annual NEP estimated by their method were more reliable compared to the estimations based on biometric studies in their forest. Therefore, the present study used nighttime NEE data which were estimated with differing techniques depending on the site.

REFERENCES

Amiro, B.D., Barr, A.G., Black, T.A., Iwashita, H., Kljun, N., McCaughey, J.H., Morgenstern, K., Murayama, S., Nesic, Z., Orchansky, A.L., Saigusa, N., 2006. Carbon, energy and water fluxes at mature and disturbed forest sites, Saskatchewan, Canada. Agric. Forest Meteorol. 136, 237–251.

Black, T.A., Chen, W.J., Barr, A.G., 2000. Increased carbon sequestration by a boreal deciduous forest in years with a warm spring. Geophys. Res. Lett. 27, 1271–1274.

Carrara, A., Kowalski, A.S., Neirynck, J., Janssens, I.A., Yuste, J.C., Ceulemans, R., 2003. Net ecosystem CO_2 exchange of mixed forest in Belgium over 5 years. Agric. Forest. Meteorol. 119, 209–227.

Coursolle, C., Margolis, H.A., Barr, A.G., Black, T.A., Amiro, B.D., McCaughey, J.H., Flanagan, L.B., Lafleur, P.M., Roulet, N.T., Bourque, C.P.-A., Arain, M.A., Wofsy, S.C., Dunn, A., Morgenstern, K., Orchansky, A.L., Bernier, P.Y., Chen, J.M., Kidston, J., Saigusa, N., Hedstrom, N., 2006. Late-summer carbon fluxes from Canadian forests and peatlands along an east–west continental transect. Can. J. Forest Res. 36, 783–800.

De Fries, R.S., Hansen, M., Townshend, J.R.G., Sohlberg, R., 1998. Global land cover classifications at 8 km spatial resolution: the use of training data derived from Landsat imagery in decision tree classifiers. Int. J. Remote Sens. 19, 3141–3168.

Falge, E., Baldocchi, D., Tenhunen, J., Aubinet, M., Bakwin, P., Berbigier, P., Bernhofer, C., Burba, G., Clement, R., Davis, K.J., Elbers, J.A., Goldstein, A.H., Grelle, A., Granier, A., Guðmundsson, J., Hollinger, D., Kowalski, A.S., Katul, G., Law, B.E., Malhi, Y., Meyers, T., Monson, R.K., Munger, J.W., Oechel, W., Paw, U.K.T., Pilegaard, K., Rannik, Ü., Rebmann, C., Suyker, A., Valentini, R., Wilson, K., Wofsy, S., 2002. Seasonality of ecosystem respiration and gross primary production as derived from FLUXNET measurements. Agric. Forest Meteorol. 113, 53–74.

Gamo, M., Panuthai, S., Maeda, T., Toma, T., Ishida, A., Hayashi, M., Warsudi, Dianna, R., Diloksumpun, S., Phanumard, L., Staporn, D., Ishizuka, M., Saigusa, N., Kondo, H., 2005. Carbon flux observation in the tropical seasonal forests and tropical rain forest. In: Proceedings of the International Workshop on Advanced Flux Network and Flux Evaluation (AsiaFlux Workshop 2005), Fujiyoshida, Japan, p. 86.

Hirano, T., Hirata, R., Fujinuma, Y., Saigusa, N., Yamamoto, S., Harazono, Y., Takada, M., Inukai, K., Inoue, G., 2003. CO_2 and water vapor exchange of a larch forest in northern Japan. Tellus 55B, 244–257.

Hirano, T., Segah, H., Harada, T., Limin, S., June, T., Hirata, R., Osaki, M., 2007. Carbon dioxide balance of a tropical peat swamp forest in Kalimantan, Indonesia. Global Change Biol. 13, 412–425.

Hirata, R., Hirano, T., Saigusa, N., Fujinuma, Y., Inukai, K., Kitamori, Y., Yamamoto, S., 2007. Seasonal and inter-annual variations in carbon dioxide exchange of a temperate larch forest. Agric. Forest Meteorol. 147, 110–124.

Hirata, R., Saigusa, N., Yamamoto, S., Ohtani, Y., Ide, R., Asanuma, J., Gamo, M., Hirano, T., Kondo, H., Kosugi, Y., Li, S.-G., Nakai, Y., Takagi, K., Tani, M., Wang, H., 2008. Spatial distribution of carbon balance in forest ecosystems across East Asia. Agric. For. Meteorol. 148, 761–775.

Irvine, J., Law, B.E., Anthoni, P.M., Meinzer, F.C., 2002. Water limitations to carbon exchange in old-growth and young ponderosa pine stands. Tree Physiol. 22, 189–196.

Ito, A., Saigusa, N., Murayama, S., Yamamoto, S., 2005. Modeling of gross and net carbon dioxide exchange over a cool-temperate deciduous broad-leaved forest in Japan: Analysis of seasonal and inter-annual change. Agric. Forest Meteorol. 134, 122–134.

Japan Meteorological Agency, 2005. Report on Abnormal Weather 2005, 383 pp. (in Japanese). http://www.data.kishou.go.jp/climate/cpdinfo/climate_change/2005/pdf/2005_all.pdf.

Kajimoto, T., Matsuura, Y., Osawa, A., Abaimov, A.P., Zyryanova, O.A., Isaev, A.P., Yefremov, D.P., Mori, S., Koike, T., 2006. Size–mass allometry and biomass allocation of two larch species growing on the continuous permafrost region in Siberia. Forest Ecol. Manage. 222, 314–325.

Kim, J., Lee, D., Hong, J.Y., Kang, S.Y., Kim, S.J., Moon, S.K., Lim, J.H., Son, Y., Lee, J., Kim, S., Woo, N., Kim, K., Lee, B., Lee, B.L., Kim, S., 2006. HydroKorea and CarboKorea: cross-scale studies of ecohydrology and biogeochemistry in a heterogeneous and complex forest catchment of Korea. Ecol. Res. 21, 881–889.

Kistler, R., Kalnay, E., Collins, W., Saha, S., White, G., Woollen, J., Chelliah, M., Ebisuzaki, W., Kanamitsu, M., Kousky, V., Van Den Dool, H., Jenne, R., Fiorino, M., 2001. The NCEP-NCAR 50-year reanalysis: monthly means CD-ROM and documentation. Bull. Am. Meteorol. Soc. 82, 247–267.

Kitoh, A., Yukimoto, S., Noda, A., 1999. ENSO-monsoon relationship in the MRI coupled GCM. J. Meteorol. Soc. Jpn. 77, 1221–1245.

Kobayashi, H., Matsunaga, T., Hoyano, A., 2005. Net primary production in Southeast Asia following a large reduction in photosynthetically active radiation owing to smoke. Geophys. Res. Lett. 32, L02403, doi:10.1029/2004GL021704.

Koike, T., Yazaki, K., Funada, R., Maruyama, Y., Mori, S., Sasa, K., 2000. Forest health and vitality in northern Japan: A history of larch plantation. Res. Notes, Fac. Forest., Univ. Joensuu 92, 49–60.

Koike, T., Hojyo, H., Naniwa, A., Ashiya, D., Sugata, S., Sugishita, Y., Kobayashi, M., Nomura, M., Akibayashi, Y., Nakajima, J., Takagi, K., Shibata, H., Satoh, F., Wang, W., Takada, M., Fujinuma, Y., Shi, F., Matsuura, Y., Sasa, K., 2001. Basic data of the study site for CO_2 flux monitoring of a young larch plantation located in the border between northern Japan and far east Russia—Current status of a mature mixed conifer-hardwood forest stand. Eurasian J. Forest Res. 2, 65–79.

Kondo, H., Gamo, M., Hirata, R., Maeda, T., Panuthai, S., Saigusa, N., submitted. CO_2 flux observation in a dry evergreen forest in Thaiiland.

Kosugi, Y., Takanashi, S., Ohkubo, S., Matsuo, N., Tani, M., Mitani, T., Tsutsumi, D., Nik, A.R., 2008. CO_2 exchange of a tropical rainforest at Pasoh in Peninsular Malaysia. Agric. For. Meteorol. 148, 439–452.

Law, B.E., Kelliher, F.M., Baldocchi, D.D., Anthoni, P.M., Irvine, J., Moore, D., Van Tuyl, S., 2001. Spatial and temporal variation in respiration in a young ponderosa pine forests during a summer drought. Agric. Forest Meteorol. 110, 27–43.

Li, S.-G., Asanuma, J., Kotani, A., Eugster, W., Davaa, G., Oyunbaatar, D., Sugita, M., 2005. Year-round measurements of net ecosystem CO_2 flux over a montane larch forest in Mongolia. J. Geophys. Res. 110, D09303, doi:10.1029/2004JD005453.

Lloyd, J., Taylor, J.A., 1994. On the temperature dependence of soil respiration. Funct. Ecol. 8, 315–323.

Malhi, Y., Wright, J., 2004. Spatial patterns and recent trends in the climate of tropical rainforest regions. Phil. Trans. Roy. Soc. Lond. B Biol. Sci. 359, 311–329.

Nakai, Y., Matsuura, Y., Kajimoto, T., Abaimov, A.P., Yamamoto, S., and Zyryanova, O.A., in press. Eddy covariance CO_2 flux above a Gmelin larch forest on continuous permafrost of central Siberia during a growing season. Theor. Appl. Climatol.

Ohkubo, S., Kosugi, Y., Takanashi, S., Mitani, T., Tani, M., 2007. Comparison of the eddy covariance and automated closed chamber methods for evaluating nocturnal CO_2 exchange in a Japanese cypress forest. Agric. Forest Meteorol. 142, 50–65.

Ohtani, Y., Saigusa, N., Yamamoto, S., Mizoguchi, Y., Watanabe, T., Yasuda, Y., Murayama, S., 2005. Characterictics of CO_2 fluxes in cool-temperate coniferous and deciduous broadleaf forests in Japan. Phyton 45, 73–80.

Owen, K.E., Tenhunen, J., Reichstein, M., Wang, Q., Falge, E., Geyer, R., Xiao, X., Stoy, P., Ammann, C., Arain, A., Aubinet, M., Aurela, M., Bernhofer, C., Chojnicki, B.H., Granier, A., Gruenwald, T., Hadley, J., Heinesch, B., Hollinger, D., Knohl, A., Kutsch, W., Lohila, A., Meyers, T., Moors, E., Moureaux, C., Pilegaard, K., Saigusa, N., Verma, S., Vesala, T., Vogel, C., 2007. Linking flux network measurements to continental scale simulations: ecosystem CO_2 exchange capacity under non-water-stressed conditions. Global Change Biol. 13, 734–760.

Patra, P.K., Ishizawa, M., Maksyutov, S., Nakazawa, T., Inoue, G., 2005. Role of biomass burning and climate anomalies for land-atmosphere carbon fluxes based on inverse modeling of atmospheric CO_2. Global Biogeochem. Cycles 19, GB3005, doi:10.1029/2004GB002258.

Powell, T.L., Bracho, R., Li, J., Dore, S., Hinkle, C.R., Drake, B.G., 2006. Environmental controls over net ecosystem carbon exchange of scrub oak in central Florida. Agric. Forest Meteorol. 141, 19–34.

Reichstein, M., Tenhunen, J.D., Roupsard, O., Ourcival, J.M., Rambal, S., Dore, S., Valentini, R., 2002. Ecosystem respiration in two Mediterranean evergreen Holm Oak forests: drought effects and decomposition dynamics. Funct. Ecol. 16, 27–39.

Reichstein, M., Falge, E., Baldocchi, D., Papale, D., Aubinet, M., Berbigier, P., Bernhofer, C., Buchmann, N., Gilmanov, T., Granier, A., Grunwald, T., Havrankova, K., Ilvesniemi, H., Janous, D., Knohl, A., Laurila, T., Lohila, A., Loustau, D., Matteucci, G., Meyers, T., Miglietta, F., Ourcival, J.M., Pumpanen, J., Rambal, S., Rotenberg, E., Sanz, M., Tenhunen, J., Seufert, G., Vaccari, F., Vesala, T., Yakir, D., Valentini, R., 2005. On the separation of net ecosystem exchange into assimilation and ecosystem respiration: review and improved algorithm. Global Change Biol. 11, 1424–1439.

Saigusa, N., Yamamoto, S., Murayama, S., Kondo, H., Nishimura, N., 2002. Gross primary production and net ecosystem production of a cool-temperate deciduous forest estimated by the eddy covariance method. Agric. Forest Meteorol. 112, 203–215.

Saigusa, N., Yamamoto, S., Murayama, S., Kondo, H., 2005. Inter-annual variability of carbon budget components in an AsiaFlux forest site estimated by long-term flux measurements. Agric. Forest Meteorol. 134, 4–16.

Saitoh, T.M., Kumagai, T., Sato, Y., Suzuki, M., 2005. Carbon dioxide exchange over a Bornean tropical rainforest. J. Agric. Meteorol. 60, 553–556.

Sakai, S., Harrison, R.D., Momose, K., Kuraji, K., Nagamasu, H., Yasunari, T., Chong, L., Nakashizuka, T., 2006. Irregular droughts trigger mass flowering in a seasonal tropical forests in Asia. Am. J. Bot. 93, 1134–1139.

Takagi, K., Nomura, M., Ashiya, D., Takahashi, H., Sasa, K., Fujinuma, Y., Shibata, H., Akibayashi, Y., Koike, T., 2005. Dynamic carbon dioxide exchange through snowpack by wind-driven mass transfer in a conifer-broadleaf mixed forest in northernmost Japan. Global Biogeochem. Cycles 19, GB2012, doi:10.1029/2004GB002272.

Takanashi, S., Kosugi, Y., Tanaka, Y., Yano, M., Katayama, T., Tanaka, H., Tani, M., 2005a. CO_2 exchange in a temperate Japanese cypress forest compared with that in a cool-temperate deciduous broad-leaved forest. Ecol. Res. 20, 313–324.

Takanashi, S., Kosugi, Y., Tani, M., Matsuo, N., Mitani, T., Nik, A.R., 2005b. Characteristics of the gas exchange of a tropical rain forest in peninsular Malaysia. Phyton 45, 61–66.

Thornley, J.H.M., 1976. Mathematical Models in Plant Physiology. Academic Press, London, 318.

van Gorsel, E., Leuning, R., Cleugh, H.A., Keith, H., Suni, T., 2007. Nocturnal carbon efflux: reconciliation of eddy covariance and chamber measurements using an alternative to the u_*-threshold filtering technique. Tellus 59B, 397–403.

Wang, H., Saigusa, N., Yamamoto, S., Kondo, H., Hirano, T., Toriyama, A., Fujinuma, Y., 2004. Net ecosystem CO_2 exchange over a larch forest in Hokkaido, Japan. Atmos. Environ. 38, 7021–7032.

Wang, H., Saigusa, N., Zu, Y., Yamamoto, S., Kondo, H., Yang, F., Wang, W., Hirano, T., Fujinuma, Y., 2005a. Response of CO_2 flux to environmental variables in two larch forest ecosystems in East Asia. Phyton 45, 339–346.

Wang, W., Zu, Y., Wang, H., Matsuura, Y., Sasa, K., Koike, T., 2005b. Plant biomass and productivity of *Larix gmelinii* forest ecosystems in northeast China: Intra- and inter-species comparison. Eurasian J. Forest Res. 8, 21–41.

Yamamoto, S., Saigusa, N., Murayama, S., Gamo, M., Ohtani, Y., Kosugi, Y., Tani, M., 2005. Synthetic analysis of the CO_2 fluxes at various forests in East Asia. In: Omasa, K., Nouchi, I., DeKok, L.J. (Eds.), Plant Responses to Air Pollution and Global Change. Springer–Verlag, Tokyo, pp. 215–225.

Yamazaki, K. (Ed.), 2004. *Arctic oscillation*. Meteorological Research Note 206, Meteorological Society of Japan, 181 pp. (in Japanese).

Yasuda, Y., Ohtani, Y., Watanabe, T., Okano, M., Yokota, T., Liang, N., Tang, Y., Nik, A.R., Tani, M., Okuda, T., 2003. Measurement of CO_2 flux above a tropical rain forest at Pasoh in Peninsular Malaysia. Agric. Forest Meteorol. 114, 235–244.

Yasunari, T., Seki, Y., 1992. Role of the Asian Monsoon on the inter-annual variability of the global climate system. J. Meteorol. Soc. Jpn. 70, 177–189.

Yu, G.-R., Wen, X.-F., Sun, X.-M., Tanner, B.D., Lee, X.H., Chen, J.-Y., 2006. Overview of ChinaFLUX and evaluation of its eddy covariance measurement. Agric. Forest Meteorol. 137, 125–137.

AGRICULTURAL AND FOREST METEOROLOGY 148 (2008) 761–775

available at www.sciencedirect.com

journal homepage: www.elsevier.com/locate/agrformet

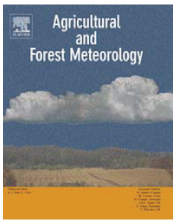

Spatial distribution of carbon balance in forest ecosystems across East Asia

Ryuichi Hirata [a,*], *Nobuko Saigusa* [b], *Susumu Yamamoto* [c], *Yoshikazu Ohtani* [d], *Reiko Ide* [a], *Jun Asanuma* [e], *Minoru Gamo* [b], *Takashi Hirano* [f], *Hiroaki Kondo* [b], *Yoshiko Kosugi* [g], *Sheng-Gong Li* [e,h,j], *Yuichiro Nakai* [d], *Kentaro Takagi* [i], *Makoto Tani* [g], *Huimin Wang* [b,j]

[a] *National Institute for Environmental Studies, Tsukuba, Japan*
[b] *National Institute of Advanced Industrial Science and Technology, Tsukuba, Japan*
[c] *Graduate School of Environmental Science, Okayama University, Okayama, Japan*
[d] *Forestry and Forest Products Research Institute, Tsukuba, Japan*
[e] *Terrestrial Environment Research Center, University of Tsukuba, Tsukuba, Japan*
[f] *Graduate School of Agriculture, Hokkaido University, Sapporo, Japan*
[g] *Graduate School of Agriculture, Kyoto University, Kyoto, Japan*
[h] *Japan Science and Technology Agency, Kawaguchi, Japan*
[i] *Field Science Center for Northern Biosphere, Hokkaido University, Sapporo, Japan*
[j] *Institute of Geographic Sciences and Natural Resources Research, Chinese Academy of Sciences, Beijing, China*

ARTICLE INFO

Article history:
Received 16 May 2007
Received in revised form
21 November 2007
Accepted 30 November 2007

Keywords:
AsiaFlux
Inter-site comparison
Eddy covariance
Net ecosystem production (NEP)
Gross primary production (GPP)
Ecosystem respiration (RE)

ABSTRACT

The objective of this paper is to clarify what kind of environmental factors that regulate net ecosystem production (NEP), gross primary production (GPP), and ecosystem respiration (RE) in forest ecosystems across East Asia. Study sites were widely distributed and included diverse ecosystems, such as evergreen and deciduous, coniferous and broadleaf, planted and natural forests, from subarctic to tropical zones. We measured NEP using the eddy covariance technique at 13 forest sites in East Asia.

Annual values of GPP and RE are simply regulated by annual mean air temperature across East Asia. There is a clear linear relationship between annual GPP and annual mean air temperature because the air temperature influences both growing period length and the seasonal variation of the maximum photosynthetic capacity, which, together, regulate the annual GPP. On the other hand, there is a strong exponential relationship between annual RE and annual mean air temperature on an East Asia scale, which is quite similar to the relation obtained on a canopy scale. The dependency of annual RE on air temperature on the East Asia scale was similar to that of monthly RE on air temperature on an individual site scale excepting for temperate larch and mixed forests in northern Japan.

The reason why the relation is simple is that severe stress, which affects GPP or RE, is small in East Asia. The present study suggests that RE is sensitive to non-climate environmental factors when compared to GPP, thus the annual RE–air temperature relationship is more scattered than the annual GPP–air temperature relationship. The NEP is small at high latitude, relatively large at mid-latitude, and scattered at low latitude. As a whole, the NEP is more influenced by RE than GPP in East Asia. Compared to North America and Europe, the

---

* *Corresponding author at*: Agro-Meteorology Division, National Institute for Agro-Environmental Sciences, 3-1-3 Kannondai, Tsukuba, Ibaraki 305-8604, Japan. Tel.: +81 29 838 8239; fax: +81 29 838 8211.
E-mail address: hiraryu@affrc.go.jp (R. Hirata).

doi:10.1016/j.agrformet.2007.11.016

increase in the ratio of GPP to air temperature is slightly higher in East Asia. One of the possible reasons for this is that GPP in East Asia is not exposed to severe environmental stresses, such as summer drought.

1. Introduction

The Kyoto protocol, which accounts for offsetting reduced targets of CO_2 emission by carbon sequestration in forests through forest management, became effective in February 2005. The rules, which were determined at COP6 and COP7 (Schulze et al., 2002), have focused attention on the role of the terrestrial biosphere in global scale carbon cycles. Therefore, accurate data are required for net ecosystem production (NEP) over various terrestrial ecosystems. However, uncertainty remains about the change in carbon stock from forest management and the response of the ecosystem CO_2 exchange to climate change.

Recently, several studies have been made of the inter-comparison of CO_2 fluxes on regional and global scales as continuous data for CO_2 fluxes from the eddy covariance technique have been accumulated. Valentini et al. (2000) showed the relationship between carbon accumulation and geography in Europe. Law et al. (2002) investigated the response of vegetation to environmental variables using the North American and European flux data collected by FLUXNET. Falge et al. (2002) compared seasonal variations in net ecosystem exchange (NEE) for various vegetations. Amiro et al. (2006) studied the affect of disturbance on carbon balance in boreal forests by the comparing flux data for several sites in Canada. However, systematic inter-comparative studies of CO_2 fluxes in Asia have been limited.

In East Asia, which is the East Eurasian continent in the Northern Hemisphere, a humid region spreads continuously from the arctic to the tropics because of the East Asian monsoon and rain front (Kohyama, 2006). Seasonal variation in temperature is clear in the subarctic and temperate zones while it is small in the tropical zone. Snow covers the land for 1–7 months in the subarctic and cool-temperate zones. There is also a permafrost period in the subarctic and cool-temperate zones. The temperate zone has four seasons and a rainy period for about 1 month before the summer dry season. Typhoons hit marine countries at mid-latitude. In the tropical zone; the year is divided into rainy and dry seasons. Drought occurs every few years in an El Niño event in the tropical zone (Hirano et al., 2007).

In East Asia, forest ecosystems, which adjust for humid regions, are continuously distributed from subarctic, through temperate, to tropical climate zones from north to south (Ohta et al., 1993; Kohyama, 2006). In the present study, sites are distributed widely from the subarctic to tropical zones in East

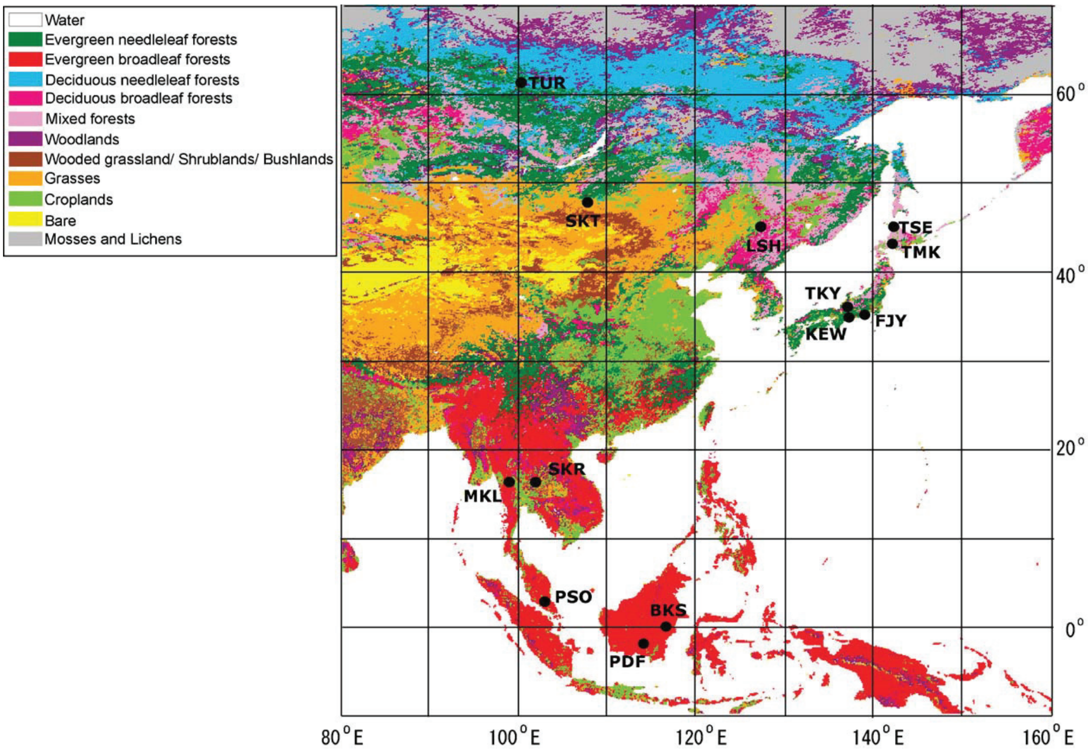

Fig. 1 – Location of study sites in East Asia in a land classification map (De Fries et al., 1998).

Asia, and cover typical vegetation types found in East Asia. Boreal forests are considered to play an important role in global climate and the global scale carbon cycle, as they are large carbon stocks (e.g. Bonan et al., 1992; Otto-Bliesner and Upchurch, 1997). The eastern Siberian boreal forest is dominated by deciduous conifer forest (larch: *Larix*) over permafrost (Gower and Richards, 1990; Matsuura et al., 2005). However, there are few studies for CO_2 exchange between forest ecosystems and the atmosphere over larch forest (Hollinger et al., 1998). Therefore, we have collected data at four larch forest sites. There are many forest types in the temperate zone. Deciduous broadleaf, larch, mixed, and evergreen forest were examined in this report. The tropical zone is mainly dominated by evergreen broadleaf forest. However, reports on NEE are still limited from Asian tropical ecosystems (Yasuda et al., 2003; Saitoh et al., 2005). Therefore, we collected data for five different types of tropical forest.

The objectives of this paper are to clarify environmental control factors that regulate NEP, gross primary production (GPP), and ecosystem respiration (RE) in various forest ecosystems across East Asia and to compare these with those in the North America and Europe.

2. Materials and methods

2.1. Sites description

We analyzed CO_2 flux data from 13 flux tower sites, which are distributed geographically from 2°S to 64°N in latitude and from 98°E to 141°E in longitude. Fig. 1 shows the site location, and Table 1 shows the details of the site characteristics. The climatic zones include subarctic (2 sites), temperate (6 sites) and tropical (5 sites) zones. The forest biomes are constituted of deciduous coniferous (4 sites), deciduous broadleaf (1 site), mixed evergreen and deciduous (1 site), evergreen coniferous (2 sites), and tropical forests (5 sites). Eleven sites in the present study are relatively close to the ocean, and two sites are located deeper within the continent.

Most sites are natural forests, secondary forests, or planted forests with a tree age more than approximately 45 years. This study also includes two naturally or artificially disturbed sites in the tropics; one is a young forest regenerating after a severe wild fire (BKS), and the other is a peat swamp forest where the ground water level is artificially controlled (PDF). At the BKS site, forest burned severely in 1998 and most of the trees were killed. During our study period, a shrub species *Macaranga gigantea* was re-growing with a tree age of 4 years or less. At the PDF site, a drainage canal was built near the study site in the late 1990s. The ground water level slowly reduced and the soil surface layer became dry (Hirano et al., 2007).

2.2. Measurements

Net ecosystem CO_2 exchange (NEE = −NEP) was calculated as the sum of the eddy CO_2 flux (F_C) and the rate of change in CO_2 storage below the flux measurement height (F_S). F_C was measured using the eddy covariance technique with three-dimensional sonic anemometer–thermometers and open- or closed-path CO_2/H_2O analyzers. Measurement systems and calculation protocols were mostly based on EUROFLUX methodology (Aubinet et al., 2000). The CO_2 storage change was calculated by the vertical profile of the atmospheric CO_2 concentration or a single height measurement of CO_2 concentration at the flux measurement height. At KEW and PSO sites, F_S was neglected since the measurement of CO_2 concentration was not conducted at the site. The measurement instruments used at each site are shown in Table 2.

2.3. Estimation of GPP and RE, gap filling, and data procedure

At each site, principal investigators performed quality control for high frequency data (4–10 Hz) including the removal of spikes, raw data tests (Vickers and Mahrt, 1997), a non-stationary test and an integral turbulence test (Foken and Wichura, 1996) and calculated 30-min or 60-min fluxes. The detailed protocols used at each site are described in the references listed in Table 1. This study collected 30-min- or 60-min-average meteorological observations and CO_2 fluxes with data gaps, and applies nighttime correction and gap-filling. Positive or negative NEP represents the forest ecosystem absorbing or releasing CO_2, respectively. NEP data with low turbulence were excluded using the threshold of friction velocity (u_*) (Massman and Lee, 2002). We examined whether temperature-normalized nighttime NEE responds to turbulent intensity from all nighttime data categorized into u_* classes of 0.1 m s^{-1}. We statistically distinguish the u_* classes for dropping RE from each other (Tukey's HSD, $p < 0.05$) (Hirata et al., 2007), and obtained the threshold of u_*, which varied among the sites (Table 2).

At the TUR site (a larch forest in central Siberia), measurement periods were limited to the growing season. Therefore, we used long-term (1968–1992) meteorological data from a meteorological station near the site for annual mean air temperature and annual precipitation data. An eddy covariance measurement was performed from June to the first half of September 2005 (Nakai et al., in press). NEP estimated by the eddy covariance technique at TUR is not based on year-round data but on the measurement in the growing season from June to early September. At the site, GPP during the dormant season can be ignored because the larch trees were leafless, and winter CO_2 efflux from the snow surface estimated by chamber measurement was negligibly small for a whole-year estimation (Matsuura et al., 2007). Therefore, we considered the NEP and RE in the growing season at TUR to be almost equivalent to the annual NEP and RE, however, the annual values might have some overestimation (NEP) and underestimation (RE) due to disregarding RE in the dormant season.

We used the following equation of Lloyd and Taylor (1994) to fill gaps in nighttime NEE ($F_{\mathrm{NEE,\,night}}$):

$$F_{\mathrm{NEE,night}} = F_{\mathrm{RE},T_{\mathrm{ref}}} \exp\left\{\frac{E_0}{R}\left(\frac{1}{T_K + T_{\mathrm{ref}} - T_0} - \frac{1}{T_K + T_a - T_0}\right)\right\} \quad (1)$$

Here T_a is the air temperature (°C), E_0 is activation energy (J mol^{-1}), R is ideal gas constant (J mol^{-1} K^{-1}). $F_{\mathrm{RE,\,Tref}}$ is $F_{\mathrm{NEE,\,night}}$ at the reference temperature (T_{ref}), which was 10 °C. T_K and T_0 are 273.15 and 227.13 K, respectively. F_{RE}; T_{ref} and E_0

Table 1 – Site characteristics

Site name (Site code), Country	Location	Elevation (m)	Forest type	Soil type	Maximum LAI ($m^2\ m^{-2}$)	Tree height (m)	Tree age (years)	Dominant species	Reference
Tura (TUR), Russia	64°12′N, 100° 27′E	250	Subarctic larch forest (DC)	Gelisol	<0.3	3	105	Gmelin larch (*Larix gmelinii*), lichen and moss (*Cladina stellaris*, *Pleurozi schreberi*)	Kajimoto et al. (2006) Nakai et al. (in press)
Southern Khentei Taiga (SKT), Mongolia	48°21′N, 10S°39′E	1630	Subarctic larchforest (DC)	Alfisol (Soil Survey Staff (1999))	2.7	20	70–300	Siberian larch (*Larix sibirica*), White birch (*Betula platyphylla*)	Li et al. (2005)
Laoshan (LSH), China	45°20′N, 127°34′E	370	Temperate planted larch forest (DC)	Alfisol	2.5	IS	35	Gmelin larch (*Larix gmelinii*)	Wang et al. (2005)
CC-LaG experiment site (TSE), Teshio, Japan	45°03′N, 142°06′E	70	Conifer-Hardwood mixed forest (MX)	Inceptisol	7.5 (PAI) (Canopy3, Forest floor 4.5)	25	–	Oak (*Quercus crispula*), Birch (*Betula ermanii*), Sakhalin fir (*Abies sachalinensis*), Bamboo grass (*Sasa senanensis*)	Koike et al. (2001) Takagi et al. (2005)
Tomakomai Flux Research Site (TMK), Japan	42°44′N,141°31′E	140	Temperate planted larch forest (DC)	Entisol	9.2 (Canopy 5.6, Forest floor 3.6)	16	45	Japanese larch (*Larix Kaempferi*), Birch (*Betula ermanii*, *Betula platyphylla*), fern (*Dryopteris crassirhizoma*)	Hirano et al. (2003) Wang et al. (2004) Hirata et al. (2007)
Takayama (TKY), Japan	36°0S′N, 137°25′E	1420	Temperate deciduous forest (DB)	Inceptisol	3.5 (PAI)	15-20	50	Deciduous oak (*Quercus crispula*), Bamboo grass (*Sasa veitchii*)	Saigusa et al. (2002) Saigusa et al. (2005)
Fujiyoshida forest meteorology research site (FJY), Japan	35°27′N, 138°46′E	1030	Naturally regenerated red pine forest (EC)	Entisol	5.5	20	90	Japanese redpine (*Pinus densiflora*), Japanese holly (*Ilex pedunculosa*)	Ohtani et al. (2005)
Kiryu Experiment Watershed (KEW), Japan	34°58′N 135°59′E	250	Temperate planted Japanese cypress forest (EC)	Entisol	5.5 (PAI)	IS	45	Japanese cypress (*Chamaecyparis obtusa*)	Takanashi et al. (2005a) Ohkubo et al. (2007)
Mae Klong (MKL), Thailand	14°35′N, 98°51′E	160	Tropical seasonal deciduous forest (TR)	Ultisol	4.0 (PAI)	30	–	*Dipterocarp* (*Shorea siamensis*, *Vitex peduncularis*, *Xylia xylocarpa*)	Kondo et al. (submitted for publication)
Sakaerat (SKR), Thailand	14°29′N, 101°55′E	535	Tropical dry evergreen forest (TR)	Ultisol	4.0 (PAI)	35	–	Dipterocarp (*Hopea ferrea*)	Gamo et al. (2005)
Pasoh Forest Reserve (PSO), Malaysia	2°58′N, 102°18′E	75–150	Tropical rain forest (TR)	Ultisol	6.5 (PAI)	35–45	–	Dipterocarp (*Hopea ferrea*)	Takanashi et al. (2005b) Kosugi et al. (2008)
Bukit Soeharto (BKS), Indonesia	0°52′S, 117°03′E	20	Tropical secondary forest (TRF)	Ultisol	3.0 (PAI)	11	4	Dipterocarp (*Macaranga gigantea*)	Gamo et al. (2005)
Palangkaraya drained forest (PDF), Indonesia	2°21′S, 114°02′E	30	Tropical peat swamp forest (TRD)	Histosol	5.6 (PAI)	26	–	Tumih (*Combretocarpus rotundatus*), Clusiaceae (*Cratoxylum arborescens*), Buchanania (*Buchanania sessifolia*) Entuyut (*Tetramerista glabra*)	Hirano et al. (2007)

Description of ecosystem type—DC: deciduous coniferous forest; MX: mixed forest; DB: deciduous broadleaf forest; EC: evergreen coniferous forest; TR: tropical forest; TRF: tropical forest disturbed by forest fire; TRD: tropical forest influenced by drainage changes from a constructed canal. Soils were classified into soil orders of the USDA Taxomony (Soil Survey Staff, 1999). For soils that lacked information in the articles, we determined soil orders by soil map.

Table 2 – Measurement systems

Site code	Sonic anemometer model	IRGA model	Flux measurement height (m)	Sampling frequency (Hz)	Average period for flux calculation (min)	u_* threshould ($m\ s^{-1}$)
TUR	R-3, Gill[a]	LI-7500, Licor[d]	20	10	30	0.1
SKT	SAT-550, Kaijo[b]	LI-7500, Licor[d]	30	10	30	0.3
LSH	SAT-550, Kaijo[b]	LI-7000, Licor[d]	29	10	30	0.2
TSE	DA600-3TV, Kaijo[b]	LI-7000, Licor[d]	32	10	30	0.0
TMK	DA600-3TV, Kaijo[b]	LI-6262, Licor[d]	27	10	30	0.3
TKY	DA600-3TV, Kaijo[b]	LI-6262, Licor[d]	25	5	30	0.5
FJY	DA600-3TV, Kaijo[b]	LI-6262, Licor[d]	26	5	30	0.2
KEW	DA-600T, Kaijo[b]	LI-7500, Licor[d]	29	10	30	0.4
MKL	SAT540, Kaijo[b]	LI-6262, Licor[d]	42	4	30	0.2
SKR	Wind Master, Gill[a]	LI-6262, Licor[d]	45	4	30	–
PSO	SAT-550, Kaijo[b]	LI-7500, Licor[d]	54	10	30	–
BKS	Wind Master, Gill[a]	LI-6262, Licor[d]	14	10	30	0.2
PDF	CSAT3, Campbell[c]	LI-7500, Licor[d]	41	10	60	0.1

[a] Gill Instruments Ltd., Lymington, UK.
[b] KAIJOSONIC Corporation, Tokyo, Japan.
[c] Campbell Scientific, Inc., Logan, USA.
[d] LI-COR Inc., Lincoln, USA.

were determined each day for a 29-day moving window by the least-squares method.

Data gaps in daytime NEE ($F_{NEE,\ day}$) were filled by the following non-rectangular hyperbola equation as a function of photosynthetic photon flux density (PPFD; Q) (Prioul and Chartier, 1977).

$$F_{NEE,day} = \frac{-\phi Q - P_{max} + \sqrt{(\phi Q + P_{max})^2 - 4\phi Q \theta P_{max}}}{2\theta} + R_d \qquad (2)$$

In the equation, P_{max}, ϕ, θ(=0.9) and R_d are the maximum GPP at light saturation ($\mu mol\ m^{-2}\ s^{-1}$), the initial slope ($mol\ mol^{-1}$), the convexity of the light-response curve and daytime respiration ($\mu mol\ m^{-2}\ s^{-1}$), respectively. The parameters for Eq. (2) were determined each day for a 15-day moving window by the least-squares method. Gaps of observed NEP were filled by estimated NEP using non-linear empirical models (Eqs. (1) and (2)).

The relationship between the net ecosystem exchange, NEE (F_{NEE}), the net ecosystem production, NEP (F_{NEP}), the gross primary production, GPP (F_{GPP}), and the total ecosystem respiration, RE (F_{RE}), is expressed:

$$F_{NEP} = -F_{NEE} = F_{GPP} - F_{RE} \qquad (3)$$

In this equation, where GPP represents CO_2 assimilation by photosynthesis in vegetation. RE represents CO_2 release by soil, stem, branch, and foliage respiration. The values of NEE in nighttime and winter season are identical to RE because GPP equals zero. Daytime RE was estimated by extrapolation using Eq. (1). GPP was calculated by the subtraction of daytime NEE from daytime RE.

Here we explain some site specific procedures for flux calculation (Saigusa et al., 2008). Flux measurement involves particular problems caused by advection and low turbulence at night (Massman and Lee, 2002). The effects of these factors are different at each site, because they relate to site specific conditions such as complex topography, canopy structure and frequency of calm nights. We applied u_* correction to nighttime NEE for most sites. However, at two tropical forest sites (SKR and PSO), there was a significant underestimation of nighttime NEE even if u_* filtering was applied. At both sites, the annual NEP was estimated by biometric methods, and the underestimation in the total ecosystem respiration estimated by the eddy covariance method was obvious from the comparison with these other methods (Saigusa et al., 2008). At the PSO site, we replaced all the nighttime NEE values by values of ecosystem respiration that was calculated by an empirical equation based on the chamber method (Kosugi et al., 2008). van Gorsel et al. (2007) proposed a method for correction of nighttime NEE, which uses the maximum value of nighttime NEE of each night to construct a temperature response function (such as Eq. (1)). At the SKR site, in addition of this method, we used nighttime data only during turbulent night (high u_*) in order to exclude low turbulent data continuing whole night (Saigusa et al., 2008).

3. Results

3.1. Annual values of GPP, RE and NEP

Annual values of carbon budget components and meteorological variables are listed in Table 3 for each site and year. GPP ranged from 40 to 2 tC ha^{-1} $year^{-1}$ and RE from 40 to 1 tC ha^{-1} $year^{-1}$. In the tropical forest (< 20°N), values of GPP reached 33.3 ± 3.3 tC ha^{-1} $year^{-1}$, while RE varied from 23 tC ha^{-1} $year^{-1}$ at BKS (TRF; 1°S) to 40 tC ha^{-1} $year^{-1}$ at PDF (TRD; 2°S) (Table 3).

The annual values of NEP ranged widely from −7 to 5 tC ha^{-1} $year^{-1}$ from 2°S to 64°N in latitude. NEP was small at high latitude, relatively large at mid-latitude, and there was large scattering at low latitude. Above 40°N, CO_2 exchange was almost balanced or absorbed slightly with small scatter. The NEP of evergreen forests (FJY, KEW) was larger than that of

Table 3 – Climatic conditions of the study sites including annual sum of NEP, GPP, RE, photosynthetic photon flux density (PPFD) and precipitation (P), annual mean air temperature, soil water content (SWC), daytime vapor pressure deficit (VPD), P_{max}, and maximum P_{max}, and growing season length for NEP and GPP

Site	Year	NEP (tC ha^{-1})	GPP (tC ha^{-1})	RE (tC ha^{-1})	PPFD (mol m^{-2})	P (mm)	T_a (°C)	SWC (m^3 m^{-3})	Daytime VPD (kPa)	Annual mean P_{max} (μmol m^{-2} s^{-1})	Maximum P_{max} (μmol m^{-2} s^{-1})	Growing season length (days)
TUR	2004	0.7[a]	2.1[a]	1.5[a]	1918[b]	360[b]	−9.0[b]	0.48[b]	1.6[b]	4.0[a]	5.8	102[b]
SKT	2003[c]	1.2	4.5	3.4	11582	276	−2.0	0.07	0.5	2.8	12.0	115
	2004	1.5	6.0	4.5	11582	267	−1.2	0.07	0.7	4.0	14.1	187
	2005	1.5	5.2	3.7	11929	230	−1.7	0.05	0.6	3.9	13.2	168
LSH	2004	0.1	14.3	14.2	9295	639	4.8	0.28	1.1	9.2	27.0	198
TSE	2002	0.7	13.3	12.6	7546	973	5.4	0.39	0.7	9.9	25.4	223
TMK	2001	2.4	17.1	14.7	8125	1208	5.9	0.33	0.6	14.0	42.6	202
	2002	2.7	17.6	14.9	8433	885	6.7	0.35	0.6	13.5	41.8	224
	2003	3.2	18.8	15.6	9028	1034	6.4	0.29	0.6	14.8	47.6	199
TKY	2000	0.6	15.8	15.1	10012	1912	6.4	0.39	0.5	9.0	28.1	227
	2001	1.1	14.1	13.0	10003	1655	6.3	0.39	0.5	8.4	25.7	202
	2002	1.0	15.0	14.0	9840	1912	6.5	0.40	0.5	9.5	35.9	195
	2003	1.4	12.2	10.8	9307	2294	6.3	0.40	0.4	8.3	31.9	215
	2004	1.5	9.3	7.8	10337	2392	7.3	0.39	0.5	5.9	20.5	238
FJY	2000	3.0	16.8	13.8	10464	1599	9.6	–	0.8	14.8	28.2	365
	2001	3.7	16.8	13.1	10344	2414	9.1	–	0.7	14.0	29.3	361
	2002	4.2	17.1	12.9	10576	1858	9.5	–	0.8	14.4	28.5	364
	2003	2.5	13.7	11.2	9777	2201	9.2	–	0.6	14.2	26.8	363
	2004	4.6	17.3	12.7	10883	2201	10.4	–	0.8	15.6	30.3	366
KEW	2001	4.9	18.2	13.2	9493	1437	14.0	–	1.2	13.9	22.9	365
	2002	4.4	20.1	15.8	9424	1179	14.4	–	1.2	14.4	21.5	364
	2003	4.3	20.7	16.4	8430	1971	14.8	–	1.1	15.0	26.3	362
	2004	5.4	22.3	16.8	9239	1797	17.4	–	1.5	15.4	23.5	365
MKL	2003	0.6	33.8	33.1	11941	1708	25.3	0.32	1.8	33.3	55.4	365
	2004	−0.8	30.7	31.5	11449	–	25.5	0.26	2.0	30.9	49.1	365
SKR	2002	−1.8	35.6	37.4	13660	1813	24.5	1.42	1.4	22.0	32.8	365
	2003	0.9	39.6	38.7	14570	1152	24.3	0.12	1.4	25.0	39.2	365
PSO	2003	−0.4	31.4	31.8	12603	1896	25.9	0.25	1.3	21.6	25.9	365
	2004	2.4	33.7	31.3	12335	1655	26.6	0.26	1.3	24.4	29.2	366
	2005	0.8	31.4	30.5	13100	1649	26.5	0.25	1.4	23.1	27.4	365
BKS	2002	4.4	27.1	22.7	11853	2015	25.3	0.27	1.3	22.4	37.0	365
PDF	2002	−7.2	32.9	40.1	6425	1853	26.7	0.30	1.5	23.7	31.8	365
	2003	−5.8	33.1	38.8	7197	2291	26.4	0.28	1.5	25.5	34.1	365

Daytime VPD is the annual mean VPD for PPFD above 1000 μmol m^{-2} s^{-1}. Growing season length is the number of days of positive GPP.

[a] Data are from June to early September 2005.

[b] Data are from long-term (1968–1992) meteorological data at a meteorological station near the site.

[c] Data are from April 2003 to March 2004.

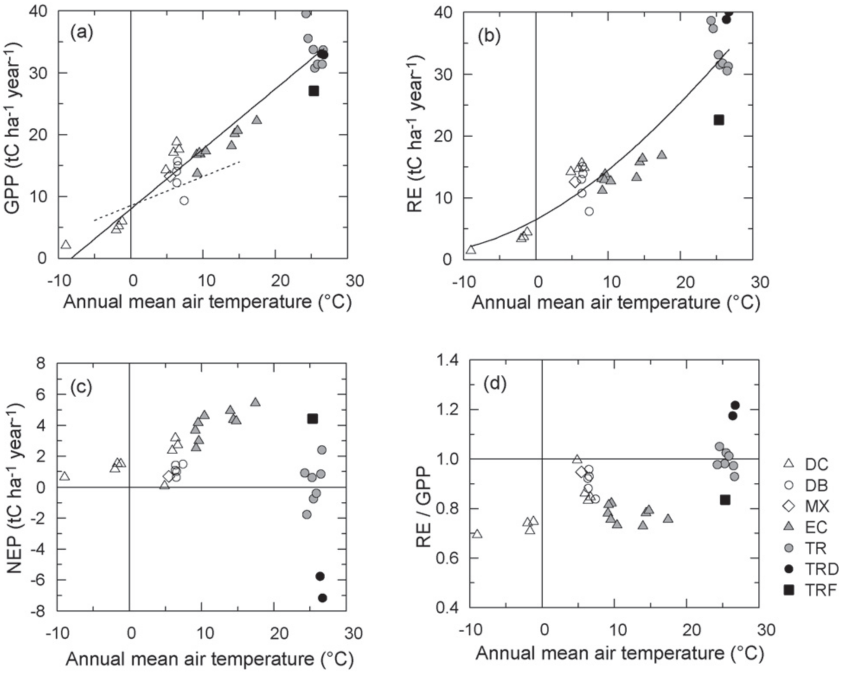

Fig. 2 – Relationships between annual mean air temperature (T_a) and (a) GPP, (b) RE, (c) NEP and (d) ratio of RE to GPP (RE/GPP). Data is categorized by forest type (Table 2) using symbols. A solid line in (a) is the regression line, which is calculated from non-disturbed forests (that is, except for disturbed sites (TRF, TRD)); GPP = 0.97T_a + 7.99, r^2 = 0.92, RMS = 2.84 tC ha^{-1} year^{-1}. The dashed line in (a) is the regression between annual GPP and annual mean air temperature in North America and Europe (Law et al., 2002); GPP = 0.42T_a + 8.53, r^2 = 0.50. The solid line in (b) is the regression curve, which is calculated from non-disturbed forests excluding disturbed sites (TRF, TRD); $F_{\mathrm{night,Tref}} = F_{\mathrm{RE,Tref}}\, e^{E_0/R[(1/(T_K+T_{ref}-T_0))-(1/(T_K+T_0-T_a))]}$, $F_{\mathrm{RE,Tref}}$ = 14.47 tC ha^{-1} year^{-1}, E_0 = 24.99 J mol^{-1} K^{-1}, r^2 = 0.89, RMS = 3.45 tC ha^{-1} year^{-1}.

deciduous forests (LSH, TMK, TKY) at mid-latitude. At low latitude, NEP varied from being a large CO_2 sink in tropical secondary forest BKS (TRF; 1°S), almost at equilibrium in tropical rain forest PSO (TR; 3°N) and a large CO_2 source (−5.8–−7.2 tC ha^{-1} year^{-1}) in tropical peat swamp forest PDF (TRD; 2°S). This large negative NEP was mainly caused by enhanced ecosystem respiration due to the affect of the artificial disturbance, in which the ground water level decreased due to excavated drains, and the decomposition of soil organic matter significantly accelerated as the surface soil dried (Hirano et al., 2007). This resulted in the highest RE/GPP value of 1.2 of all sites. The values of RE/GPP ranged from 0.8 to 1.0 in other tropical forests (<20°N), from 0.7 to 1.0 in temperate forests (30–45°N), and were about 0.7 for subarctic forests (>48°N). In the young tropical secondary forest BKS (TRF; 1°S), RE/GPP was about 0.8, which was smaller than other tropical forests due to low RE.

3.2. *Relationships between air temperature and GPP, RE and NEP*

The responses of annual values of NEP, GPP, RE, and RE/GPP to environmental factors are examined in the following sections. Fig. 2 shows the relationships between annual carbon fluxes and annual mean air temperature. Data was categorized by forest types, which were deciduous coniferous (DC; TUR, SKT, LSH, TMK), deciduous broadleaf (DB; TKY), mixed (MX; TSE), evergreen coniferous (EC; FJY, KEW), tropical (TR; MKL, SKR, PSO), tropical swamp (TRD; PDF), and tropical secondary (TRF; BKS) (Table 2). As is clearly shown in Fig. 2(a), the annual values of GPP linearly increased with the air temperature, which varied between −10 and 27 °C from the subarctic zone to the tropical zone. The solid line in Fig. 2(a) shows the result of linear regression between GPP and the annual temperature obtained in the present study (GPP = 0.97 × T_a + 8.4, r^2 = 0.92, RMS = 2.84 tC ha^{-1} year^{-1}), except for the two disturbed sites: BKS (TRF) and PDF (TRD) (Table 4). The dashed line shows the result based on forests in North America and Europe from Law et al. (2002) (GPP = 0.47 × T_a + 8.52, r^2 = 0.50).

The annual values of RE also had a significant positive correlation with the annual air temperature (Fig. 2(b)), however, the relation was rather more exponential than linear. The solid curve in Fig. 2(b) was the result of regression with the Lloyd and Taylor equation. The determination coefficient of the regression curve was 0.89 and RMS was 3.45 tC ha^{-1} year^{-1}, which indicates the RE–temperature relationship was relatively more scattered than the GPP–temperature relationship.

It should be noted that the regression lines shown in Fig. 2(a) and (b) were calculated only from the data of mature forests, not using data from the two disturbed forests; BKS (TRD) and PDF

Table 4 – Regression results where the equation is $y = aX + b$

Y variable	X variable	Slope, a	Intercept, b	r^2	RMS
Annual GPP (tC ha year^{-1})	Annual mean air temperature (°C)	0.97	7.99	0.92	2.84
Annual GPP (tC ha year^{-1})	Annual cumulative PPFD (mol m^{-2} year^{-1})	0.00	−7.64	0.37	7.83
Annual GPP (tC ha year^{-1})	Annual mean P_{max} (μmol m^{-2} s^{-1})	1.17	2.09	0.87	3.63
Annual GPP (tC ha year^{-1})	Maximum P_{max} (μmol m^{-2} s^{-1})	0.54	3.07	0.38	7.78
Annual GPP (tC ha year^{-1})	Maximum LAI (PAI) (m^2 m^{-2})	3.09	7.42	0.23	10.23
Annual GPP (tC ha year^{-1})	Annual mean SWC (m^3 m^{-3})	−16.15	23.61	0.03	11.68
Annual RE (tC ha year^{-1})	Annual mean SWC (m^3 m^{-3})	−17.40	22.94	0.03	12.11

The data includes non-disturbed sites (DC, DB, MX, EC and TR) and excludes disturbed sites (TRF and TRD).

(TRF). The data from the disturbed sites was also plotted in Fig. 2(a) and (b), and the relations between GPP and the annual temperature at the disturbed forests were quite similar to those for the mature forests (Fig. 2(a)), however, the relations between RE and the annual temperature at the disturbed forests were much more scattered (Fig. 2(b)).

Fig. 2(c) shows the relationship between annual NEP and annual mean air temperature. Observed annual NEP rapidly increased with air temperature, when the temperature was lower than about 10 °C, from 1 to 5 tC ha^{-1} year^{-1}, and stayed at 4–5 tC ha^{-1} year^{-1} in the temperature range between 10 and 20 °C. In the tropical zone with a temperature from 24 to 27 °C, the annual NEP showed a large scatter from −7 to 4 tC ha^{-1} year^{-1}.

The ratio of RE to GPP increased with temperature (Fig. 2(d)). RE/GPP was almost 0.7 when the annual mean temperature was below 0 °C. In the temperate zone with a temperature range between 5 and 20 °C, values of RE/GPP ranged from 0.7 to 1.0, where the values of RE/GPP for temperate deciduous coniferous (temperate larch) (DC) and temperate mixed (MX) forests (~1.0) were higher than that for temperate deciduous (DB) and temperate evergreen coniferous (EC) forests (0.7–0.8). In the tropical zone, the RE/GPP of mature forests ranged between 0.8 and 1.0; 0.8 for young secondary forest (TRF, BKS sites), was the smallest and 1.2 for drainage forest (TRD, PDF sites) was the largest.

3.3. Maximum GPP at light saturation (P_{max})

The forest sites included in the present study have different dominant species, different light-photosynthesis responses for individual leaves, and different growing periods. In order to make clear the controlling factors for the annual GPP, we examined the significance of the parameters for the maximum and the mean levels of photosynthetic ability. Table 4 shows the regression results for the relationship between the annual GPP and the maximum P_{max} and the annual mean P_{max}, respectively. Annual mean P_{max} clearly increased with annual GPP (Fig. 3, Table 4), although maximum P_{max} had a poor relationship with annual GPP (Table 4). In Section 4.1, we discuss the reason that the annual mean P_{max} correlates strongly with annual GPP.

3.4. Other climatic factors

Table 4 shows linear regression results for the annual values of several variables with GPP and RE. Annual PPFD did not influence annual GPP, although PPFD influenced seasonal or interannual variations of GPP at a specific site (e.g. Li et al., 2005; Hirano et al., 2007; Hirata et al., 2007). These results were because GPP saturated at high PPFD and PPFD had no affect during the defoliated season.

The annual GPP had a positive correlation with the maximum leaf area index (LAI), although the correlation coefficient was poor ($r^2 = 0.23$). A caution should be given that the LAI data at several sites included not only leaf area but also plant area such as stems and branches. Moreover, the evaluation method for LAI was different among the sites.

The correlation was also relatively low between the annual values of soil water content (SWC) and both GPP and RE across East Asia, although SWC influenced the RE of tropical forests at a site scale (Gamo et al., 2005; Hirano et al., 2007; Kosugi et al., 2008). In contrast, it did not influence the RE of a subarctic forest (SKT) (Li et al., 2005) or a temperate larch forest (TMK) (Liang et al., 2004) at a site scale.

Both GPP and RE decreased with annual precipitation when precipitation was below 1000 mm year^{-1}. However, there was no significant relationship between NEP and precipitation (Table 3).

4. Discussion

4.1. GPP

This study clearly shows that annual GPP has a significant positive correlation with the annual air temperature across East Asia, and the relationship is quite linear even though the study sites covered diverse forest ecosystems with a wide climatic range from subarctic to tropical zones and different

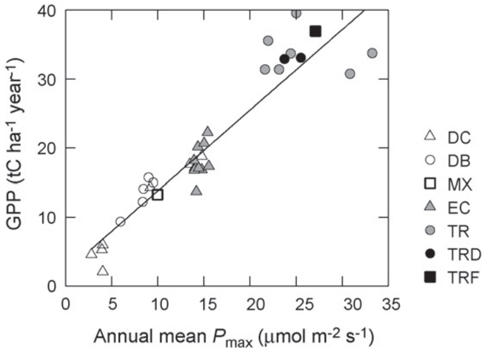

Fig. 3 – Relationship between annual GPP and annual mean P_{max}; Y = 1.17X + 2.09, r^2 = 0.87, RMS = 3.63 tC ha^{-1} year^{-1}.

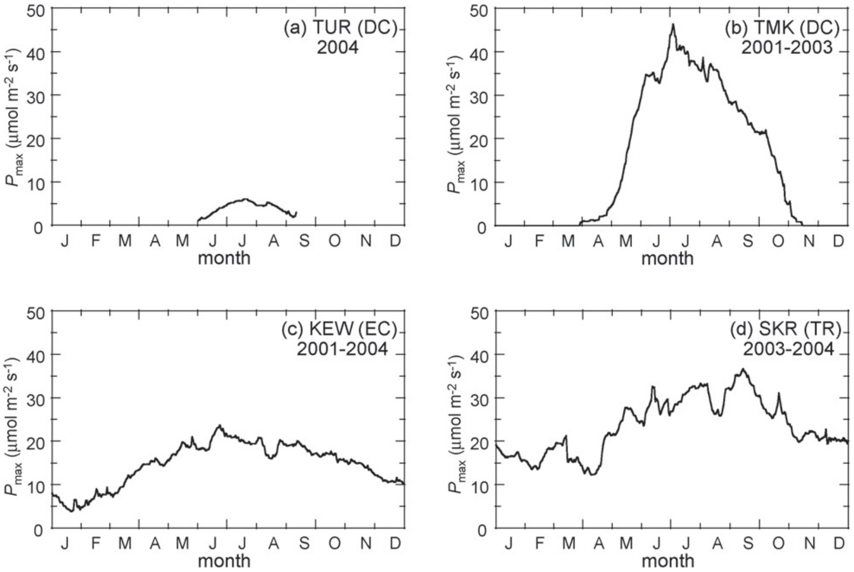

Fig. 4 – Seasonal variation in P_{max} at the (a) TUR, (b) TMK, (c) KEW and (d) SKR sites.

ecosystem types such as deciduous, evergreen, broadleaved, and coniferous (Fig. 2(a)). At the same time, the annual GPP shows a strong linear relationship with the annual mean P_{max} (Fig. 3). We are, therefore, able to hypothesize that there is a significant interdependence among the annual air temperature, the annual mean P_{max}, and the annual GPP in the forest ecosystems across East Asia. In the following sections, we discuss how meteorological elements and biological characteristics regulate annual GPP.

It is generally said that GPP is determined by growing season length, photosynthetic capacity, and LAI (Chapin et al., 2002). The annual air temperature can influence all three of the above conditions, and in particular, the temperature is the most important factor in regulating the growth period length (Saigusa et al., 2008). As listed in Table 3, the growing season length for GPP, which means the number of days when GPP was positive, could be longer than 360 days when the annual air temperature was above 9 °C for evergreen forests in temperate and tropical zones, and decreased to only about 100 days with the decrease in annual temperature in temperate and subarctic zones.

The seasonal change of the photosynthetic capacity was an important factor in regulating the annual GPP. Seasonal changes in P_{max}, which represents the highest level of photosynthetic capacity, are plotted in Fig. 4 for a subarctic larch forest in central Siberia (TUR), a temperate larch forest in northern Japan (TMK), a temperate evergreen coniferous forest in central Japan (KEW), and a tropical evergreen forest in Thailand (SKR). In the larch forest in central Siberia (TUR), the growing season was quite short (from June to August), and the maximum value of P_{max}, which appeared in the early stage of the growing period (July), was the lowest of all sites. At the temperate larch forest (TMK), the growing season was longer than TUR (from May to October), with the highest P_{max} observed in June. At the evergreen site (KEW), the growing season was the longest (the whole year), however, the maximum value of P_{max} was less than the temperate deciduous forest. P_{max} of the tropical dry evergreen forest (SKR) peaked at the end of the rainy season or the beginning of the dry season (September to October), but kept relatively high throughout the year.

According to Table 3, P_{max} values observed in the temperate larch forest (44.0 μmol m^{-2} s^{-1} at TMK) was higher than those in the two tropical forests (SKR, PSO) where the annual values of GPP were extreme (>30 tC ha^{-1} year^{-1}). This result was interpreted to mean that higher annual GPP in the tropical forests was mainly attributable to relatively high P_{max} maintained throughout the year. The strong positive correlation between the annual mean P_{max} and the annual GPP supports this. The reason the annual mean P_{max} showed higher correlation with the annual GPP compared to the maximum P_{max} was that the annual mean P_{max} takes into account the affect of growing period length.

In previous studies, Law et al. (2002) found that there is a significant positive correlation between the annual air temperature and the annual GPP estimated at various flux sites in North America and Europe. The regression lines of both studies are plotted in Fig. 2(a), with a dashed line for Law's result and a solid line for the present study. The present study covers a wide temperature range from −9 to 27 °C, and the determination coefficient of the regression line was much higher (0.92) than that in Law's study (0.57). This result suggests that the annual GPP in East Asian forests is primarily related to annual temperature.

One of the reasons the annual GPP so strongly correlates with temperature was possibly that forests in East Asia are not exposed to severe stresses other than temperature. For example, photosynthetic capacity of forests in North America and Europe is influenced by the limitation of soil water content and high vapor pressure deficit (VPD) caused by summer

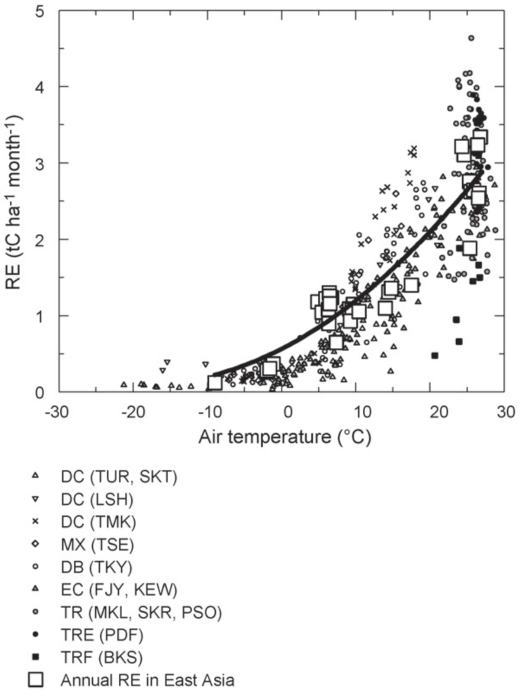

Fig. 5 – Relationship between monthly RE and air temperature. Relationship between annual RE and annual mean air temperature represented by white square symbols, and its regression curve ($F_{\mathrm{night,Tref}} = F_{\mathrm{RE,Tref}}\mathrm{e}^{E_0/R[(1/(T_K+T_{\mathrm{ref}}-T_0))-(1/(T_K+T_0-T_a))]}$, $F_{\mathrm{RE,\ Tref}}$ = 1.20 tC ha^{-1} month^{-1}, E_0 = 25.73 J mol^{-1} K^{-1}), represented by a solid line, are the same as those in Fig. 2(b) except that the annual RE has been converted from annual to monthly.

drought (e.g., Anthoni et al., 1999; Scott et al., 2004). In comparison, the annual precipitation at the present study sites in East Asia was mostly higher than 600 mm, up to 2400 mm, except for the two subarctic sites (230–270 mm at SKT; 360 mm at TUR). This is fairly high compared to North America and Europe (198–1700 mm). Furthermore, there is a rainy season at mid-latitudes in East Asia in the early stage of the growing season typically from June to July, which provides sufficient water to ecosystems every year. As a result, less summer drought stress is a strong candidate for the main cause of the simple relationship between the annual GPP and the annual air temperature in East Asia. On a site scale, the diurnal, seasonal or interannual variation of GPP is affected by VPD conditions (Gamo et al., 2005; Li et al., 2005; Wang et al., 2004; Hirano et al., 2007).

4.2. *RE*

A strong exponential relationship between the annual RE and the annual mean air temperature was observed throughout East Asia (Fig. 2(b)). Similar results were observed at a site scale. In Fig. 5, we superimpose the monthly RE–air temperature relationship on the annual relationship (Fig. 2(b)) (the unit of RE has been converted from annual to monthly) in order to compare the dependency of RE on air temperature between an East Asia scale and an individual site scale. The white squares and solid curve represent the relationship between annual RE and air temperature. Most monthly RE–air temperature relationships almost overlap annual RE–air temperature relationships, except for temperate larch and mixed forests in northern Japan (TMK; DC, TSE; MX), which have ratios of GPP to air temperature that increase at a quicker rate than those of other forests. At TMK site, RE values should be enhanced by the high photosynthetic activity of larch forest during the growing season (Hirata et al., 2007).

In contrast, previous studies such as Law et al. (2002) reported a less clear relationship between annual RE and annual mean temperature in North America and Europe. One of the advantages of this study was that the sites were distributed over a wide latitude range from 2°S to 64°N with an annual temperature from −9 to 27 °C, while the previous study sites in North America and Europe typically covered from 30 to 70°N. The wide latitude range of the present study enabled us to detect a clear temperature dependence of the annual RE in East Asia in a wide temperature band.

The annual RE is regulated by numerous components, such as respiration in the stem (Liang et al., 2005; Miyama et al., 2006), branch (Miyama et al., 2003), root (Lee et al., 2003; Dannoura et al., 2006), foliage (Miyama et al., 2003), microorganisms (Uchida et al., 2005), and decomposition of litter (Kim et al., 2005a, Kim et al., 2005b), soil organic carbon (Lee et al., 2003; Dannoura et al., 2006) and coarse wood debris (Jomura et al., 2007). The total annual ecosystem respiration is affected by various processes, not only by meteorological factors such as temperature and soil water content, but also by biological and biochemical factors such as plant biomass, soil organic matter content, nutrient resources, chemical substances and physical characteristics of the soil, type of disturbance, tree age, seasonal changes in photosynthesis, leaf area, and other phenological events. Responses of the ecosystem respiration to the environment are different depending on the ecosystem (Bond-Lamberty et al., 2004; Subke et al., 2006; Trumbore, 2006). Thus, the respiratory processes could be far more influenced by any number of factors other than the photosynthetic processes. This interpretation is supported by the fact that the RE–temperature relationship was more scattered than the GPP–temperature relationship.

Although the respiration processes includes complicated mechanisms, the annual total ecosystem respiration from diverse ecosystems across East Asia was expressed by one simple curve as a function of the annual mean air temperature. On the other hand, the seasonal or interannual variation of RE was affected by seasonal changes in water resources in some tropical forests such as MKL, SKR (Gamo et al., 2005), PSO (Kosugi et al., 2008) and PDF (Hirano et al., 2007).

4.3. *NEP*

In the present study, the NEP–temperature relationship in Fig. 2(c) shows that NEP is close to zero in subarctic larch forests (DC) with low annual temperatures (<0 °C). In the mid-temperature zone (5–20 °C), the annual NEP tends to increase with temperature, and the CO_2 uptake rate is highest in the temperature range around 10–20 °C. For high temperatures (>20 °C) the values of annual NEP show a significant scatter from a large CO_2 source (-8 tC ha^{-1} year^{-1} at TRD) to a large sink (4 tC ha^{-1} year^{-1} at TRF). The large scatter in the annual NEP in the high temperature zone was due to the large scatter in the annual RE, not in GPP.

The influence of disturbance was more significant on RE than on GPP. A large CO_2 release was observed at the PDF site (TRD) affected by the artificial drainage and acceleration of peat decomposition by drying soil, although the annual GPP of the PDF site was relatively close to those of non-disturbed natural forests (TR). The annual GPP of BKS (TRF) is also close to that of other natural tropical forests; however, the annual RE of the BKS site was smaller than that of non-disturbed natural tropical forest, probably because the trees were quite young (<4 years old) and the above-ground and below-ground plant biomass was less than those at the mature forests. Except for the two disturbed sites, the annual NEP in tropical mature sites was mostly less than that in the mid-temperature zone, due to the increased rate of annual RE with temperature being much higher than that of GPP in higher temperature conditions. In the Amazon region, Saleska et al. (2003) also reported that recent disturbance influences RE rather than GPP; old-growth forests lost CO_2, which was mainly released from large coarse wood debris (CWD) pools despite high growth rates (Rice et al., 2004) because of the recent disturbance such as drought associated with a strong El Niño event.

While annual GPP is simply regulated by annual mean air temperature (Section 4.1), annual RE is much more sensitive to factors other than air temperature when compared to GPP (Section 4.2). The annual NEP was not simply determined by annual mean air temperature only. Caution should be exercised as NEP is small in comparison to large gross fluxes such as GPP and RE. Therefore, factors other than annual mean air temperature (e.g. site history, disturbance, and soil characteristic) are responsible for the scatter in the RE–temperature relationship (Figs. 2(b) and 5), and that they have a great impact on the resultant NEP. Consequently, annual NEP should be understood in terms of a wide variety factors via RE. In temperate and boreal European forests, which are N-limited, Magnani et al. (2007) reported that NEP was strongly driven by nitrogen deposition resulting from anthropogenic activities while GPP and RE were regulated by air temperature.

4.4. *Validity of NEP*

It is important to evaluate the uncertainty of the annual NEP by crosschecking with different methods. In this section, we compare the annual NEP estimated by the eddy covariance technique with that obtained by the biometric and chamber methods in order to evaluate the uncertainty.

There are many sources of uncertainty in the eddy covariance technique: horizontal advection and nighttime data correction, topography, surface roughness, and night-time atmospheric stability (e.g. Massman and Lee, 2002). Moreover, the different instrumentation and installation of the measurement system among sites may cause systematic errors when we use the data for the purpose of inter-site comparisons (Loescher et al., 2005). In addition, even though the flux measurement was ideally conducted on flat and horizontal-homogeneous surfaces, the temporal average of fluxes observed at a single point may have an inherent distortion compared with the spatial average (Kanda et al., 2004).

Here we use data from the biometric and chamber methods to evaluate uncertainty in the annual NEP, since both methods have advantages and disadvantages. The advantage of the biometric method for NEP evaluation is that long-term changes in plant biomass and carbon stock in the soil are detectable and is, hence, suitable for verification of long-term integration of NEP (Jia and Akiyama, 2005; Ohtsuka et al., 2005). The disadvantage is that the method still has a large uncertainty in estimating carbon stock in the soil, such as soil organic matter and fine root production (Satomura et al., 2006; Fukuzawa et al., 2007). The advantage of the chamber method is that we can use the data for validation of specific processes on a short time scale such as nighttime ecosystem respiration and daytime canopy photosynthesis, while the disadvantage is that it requires an enormous number of measurements to establish spatial heterogeneity and there are large uncertainties in the process of scaling up space and time because many assumptions need to be made (Malhi et al., 1999).

Other sources of uncertainty may be in the carbon loss from the foliage as volatile organic compounds (Tani et al., 2002; Ieda et al., 2006), and from the soil through leaching by herbivores (Chapin et al., 2002). We neglected these affects in the present study.

It is important to point out that the spatial and temporal results of ground research such as micrometeorological, biometric, and chamber method base analysis are limited. For instance, our eddy flux data was obtained within about 1 km. Therefore, our observation data cannot completely cover the long-term and wide areas including whole forests, tree age, and disturbance in East Asia. Our results are, however, informative and useful to validate terrestrial ecosystem models to investigate the response of forest to climate and disturbance (Sasai et al., 2005; Friend et al., 2007; Ito et al., 2007).

Since the early 2000s, many studies have been conducted in various terrestrial ecosystems in Asia to estimate the annual values of carbon budget components using biometric measurements and the chamber method. The annual NEP had been estimated by the biometric method at the TUR (Matsuura et al., 2007), TMK (Yone et al., 2005; Yone et al., 2006; Hirata et al., 2007), TKY (Ohtsuka et al., 2007), FJY (Sugita, 2005), SKR (Yamamoto et al., 2005), and PSO sites (Yamamoto et al., 2005). Fig. 6 shows the annual NEP from micrometeorological and biometric methods and the difference between the two. Both methods resulted in similar variation of NEP between sites. The differences of NEP between the two methods were 0.4 ± 1.0 tC ha^{-1} year^{-1}. Attention should be paid to uncertainty arising from the difference of measuring period for the eddy covariance technique and the biometric method at each site. If we simply scaled the difference (0.4 ± 1.0 tC ha^{-1} year^{-1}) over the present study area (2.1 Gha; East and Southeast Asia and Russia (FAO, 2006)), the uncertainty in the different methods

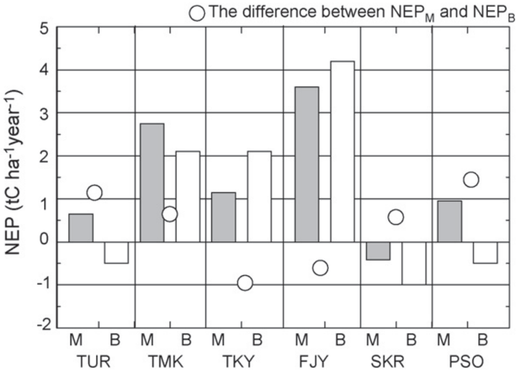

Fig. 6 – Comparison of NEP between the meteorological (M) and the biometric method (B). Circles show the subtraction of NEP obtained by the biometric method from that calculated by the meteorological method.

reached 0.86 ± 2.05 PgC year^{-1}. Ground measurement of NEP still contains uncertainties in the present study; these should be minimized by improving long-term measurements for both methods in future study.

The chamber method for soil, trunk and foliar respiration was applied to the KEW and TMK sites. Ohkubo et al. (2007) validated that nighttime NEP of the KEW site by chamber method with identical results to that by eddy covariance technique with a u_* threshold. At the TMK site, Liang et al. (2006) also verified that total NEP of the eddy covariance technique was close to that of the chamber method (Hirata et al., 2007).

In the temperate zone, some sites, such as TKY and KEW, were located in mountainous regions and the topography around the tower was quite complex. The uncertainty caused by the horizontal advection and nighttime data correction is large, however, the annual NEP estimated by the two methods were relatively close at both sites (Ohtsuka et al., 2007; Ohkubo et al., 2007). This result suggests that the eddy covariance data can be used for estimating ecosystem carbon cycle components even in complex topography if the data is well validated by other methods (Hammerle et al., 2006).

Kosugi et al. (2008) reported that many calm nights caused continuous underestimation of nighttime NEP by the eddy covariance technique at the PSO site. In contrast, at the PDF site, Hirano et al. (2007) observed large nighttime NEE by eddy covariance technique with small u_* similar to that at the PSO site. Nighttime NEE estimation remained difficult and the uncertainty was significantly higher in tropical forests for reasons such as a large amount of respiration under high temperature conditions throughout the year, many calm nights (Kosugi et al., 2008), and tall canopy with a wide variety of tree height (Finnigan, 2004).

5. Conclusions

This paper compares annual values of NEP, GPP, and RE among 11 mature forests and 2 disturbed forests across East Asia including different ecosystem types such as evergreen and deciduous, coniferous and broadleaf, planted and natural forests, with a wide climatic range from subarctic, through temperate, to tropical zones.

In East Asia, where sufficient precipitation is supplied to most ecosystems in every growing season, summer drought stress is less severe than in North America and Europe. Thus the environmental influence on forest NEP, GPP, and RE differs in several aspects between these areas.

The findings we obtained from the present inter-site comparison are summarized as follows:

(1) The annual GPP and RE are simply regulated by annual mean air temperature across East Asia. The annual GPP has a very strong linear relationship with the annual air temperature, and the annual RE also has a clear exponential relationship with temperature.
(2) There is a clear inter-dependency among the annual GPP, annual mean P_{max}, and the annual temperature; which means that the annual GPP is regulated by both growing period length and the seasonal variation in maximum photosynthetic ability. Air temperature is the most important influence on these values.
(3) The RE–temperature relationship is more complicated than the GPP–temperature relationship. This is because annual RE is much more sensitive to factors other than the annual temperature compared to GPP. Some factors other than annual mean air temperature (e.g. site history, disturbance, and soil characteristic) are responsible for the scatter in the RE–temperature relationship (Figs. 2(b) and 5), and that they have a great impact on the resultant NEP. This indicates that annual NEP should be understood in terms of a wide variety factors via RE.
(4) Annual NEP is small at high latitude, relatively large at mid-latitude, and is widely scattered at low latitude. The site-specific characteristics of NEE are influenced more by RE than GPP.
(5) Compared with North America and Europe, the regression coefficients of the GPP–temperature and RE–temperature relationships are high. Moreover, the slope of the GPP–temperature relationship in East Asia is greater than that of North America and Europe. One of the reasons for this relates to less restriction of GPP and RE by severe environmental stresses such as summer drought. As a result, the temperature dependence of the annual values of GPP and RE can be expressed in a relatively simple form in East Asia.

Acknowledgements

This study was supported by funding from:

- The Japan Ministry of the Environment (Integrated study for the terrestrial carbon management of Asia in the 21st Century on the basis of scientific advancements: Project leader, Takehisa Oikawa (University of Tsukuba)) for TUR, LSH, TKY, FJY, KEW, MKL, SKR, PSO, and BKS sites.
- The rangelands atmosphere–hydrosphere–biosphere interaction study experiment in north-eastern Asia (RAISE)

project through financial support from Japan Science and Technology Agency (2003–2006) for the SKT site.

- JSPS Core University Program and a Grant-in-Aid for Scientific Research (Nos. 13375011 and 15255001) from the Japanese Ministry of Education, Culture, Sports, Science and Technology for the PDF site.
- Hokkaido Electric Power Co., Inc., JP for the TSE site.

We acknowledge Drs. Y. Matsuura, Y. Mizoguchi, S. Takanashi and Y. Yasuda (Forestry and Forest Products Research Institute, Japan), Y. Fujinuma (National Institute for Environmental Studies), Y. Kobayashi (National Institute for Agro-Environmental Sciences), T. Maeda and S. Murayama (National Institute of Advanced Industrial Science and Technology), T. Nakano (Yamanashi Institute of Environmental Sciences), K. Sasa (Hokkaido University), M. Sugita (University of Tsukuba, Japan), T. Akiyama, H. Koizumi, and H. Muraoka (Gifu University, Japan), A. Kotani (Nagoya University, Japan), N. Matsuo (Mie University, Japan), S. Ohkubo (Kyoto University, Japan), Y. Zu and W. Wang (Northeast Forestry University, China), Samreong Panuthai (National Park, Wildlife and Plant Conservation Department, Thailand), G. Davaa and D. Oyunbaatar (Institute of Meteorology and Hydrology, Mongolia), O.A. Zyryanova (V.N. Sukachev Institute of Forest, Russian Academy of Science), A.R. Nik (FRIM, Malaysia), and the staff of each institute for data provided.

REFERENCES

Amiro, B.D., Barr, A.G., Black, T.A., Iwashita, H., Kljun, N., McCaughey, J.H., Morgenstern, K., Murayama, S., Nesic, Z., Orchansky, A.L., Saigusa, N., 2006. Carbon, energy and water fluxes at mature and disturbed forest sites, Sskatchewan, Canada. Agric. Forest Meteorol. 136, 237–251.

Anthoni, P.M., Law, B.E., Unsworth, M.H., Huxman, M.H., 1999. Carbon and water vapor exchange of an open-canopied ponderosa pine ecosystem. Agric. Forest Meteorol. 95, 151–168.

Aubinet, M., Grelle, A., Ibrom, A., Rannik, Ü., Moncrieff, J., Foken, T., Kowalski, A.S., Martin, P.H., Berbigier, P., Bernhofer, Ch., Clement, R., Elbers, J., Granier, A., Grunwald, T., Morgenstern, K., Pielegaard, K., Rebmann, C., Snijders, W., Valentini, R., Vesala, T., 2000. Estimates of the annual net carbon and water vapor exchange of forests: the EUROFLUX methodology. Adv. Ecol. Res. 30, 113–175.

Bonan, G.B., Pollard, D., Thompson, S.L., 1992. Effects of boreal forest vegetation on global climate. Nature 359, 716–718.

Bond-Lamberty, B., Wang, C., Gower, S., 2004. A global relationship between the heterotrophic and autotrophic components of soil respiration? Global Change Biol. 10, 1756–1766.

Chapin III, F.S., Matson, P.A., Mooney, H.A., 2002. Principles of Terrestrial Ecosystem Ecology. Springer Science and Business Media, Inc., 436 p.

Dannoura, M., Kominami, Y., Tamai, K., Jomura, M., Miyama, T., Goto, Y., Kanazawa, Y., 2006. Development of an automatic chamber system for long-term measurements of CO_2 flux from roots. Tellus 50B, 502–512.

De Fries, R.S., Hansen, M., Townshend, J.R.G., Sohlberg, R., 1998. Global land cover classifications at 8 km spatial resolution: the use of training data derived from Landsat imagery in decision tree classifiers. Int. J. Remote Sens. 19, 3141–3168.

Falge, E., Baldocchi, D.D., Tenhunen, J., Aubinet, M., Bakwin, P., Berbigier, P., Bernhofer, C., Burba, G., Ceulemans, R., Davis, K.J., Elbers, J.A., Goldstein, A.H., Grelle, A., Granier, A., Guðmundsson, J., Hollinger, D., Kowalski, A.S., Katul, G., Law, B.E., Malhi, Y., Meyers, T., Monson, R., Munger, J.W., Oechel, W., Paw, U.K.T., Pielegaard, K., Rannik, Ü., Rebmann, C., Suyker, A., Valentini, R., Wilson, K., Wofsy, S., 2002. Seasonality of ecosystem respiration and gross primary production as derived from FLUXNET measurements. Agric. Forest Meteorol. 113, 53–74.

FAO, 2006. Global forest resources assessment 2005. Progress towards sustainable forest management, p. 320.

Finnigan, J.J., 2004. Advection and modeling. In: Handbook of Micrometeorology, Kluwer Academic Publishers, Dordrecht, pp. 209–244.

Foken, T., Wichura, B., 1996. Tools for quality assessment of surface-based flux measurements. Agric. Forest Meteorol. 78, 83–105.

Friend, A., Arneth, A., Kiang, N., Lomas, M., Ogee, J., Rodenbeck, C., Running, S.W., Santaren, J.D., Sitch, S., Viovy, N., Woodward, F.I., Zaehle, S., 2007. FLUXNET and modelling the global carbon cycle. Global Change Biol. 13, 610–633.

Fukuzawa, K., Shibata, H., Takagi, K., Satoh, F., Koike, T., Sasa, K., 2007. Vertical distribution and seasonal pattern of fine-root dynamics in a cool-temperate forest in northern Japan: implication of the understory vegetation, *Sasa* dwarf bamboo. Ecol. Res. 22, 435–495.

Gamo, M., Panuthai, S., Maeda, T., Toma, T., Ishida, A., Hayashi, M., Warsudi, Dianna, R., Diloksumpun, S., Phanumard, L., Staporn, D., Ishizuka, M., Saigusa, N., Kondo, H., 2005. Carbon flux observation in the tropical seasonal forests and tropical rain forest. In: Proceedings of the International Workshop on Advanced Flux Network and Flux Evaluation (AsiaFlux Workshop 2005), Fujiyoshida, Japan, p. 86.

Gower, S.T., Richards, J.H., 1990. Larches: deciduous conifers in an evergreen world. Bioscience 40, 818–826.

Hammerle, A., Haslwanter, A., Schmitt, M., Bahn, M., Tappeiner, U., Cernusca, A., Wohlfahrt, G., 2006. Eddy covariance measurements of carbon dioxide, latent and sensible energy fluxes above a meadow on a mountain slope. Bound-Layer Meteorol. 122, 397–416.

Hirano, T., Hirata, R., Fujinuma, Y., Saigusa, N., Yamamoto, S., Harazono, Y., Takada, M., Inukai, K., Inoue, G., 2003. CO_2 and water vapor exchange of a larch forest in northern Japan. Tellus 55B, 244–257.

Hirano, T., Hendrik, S., Harada, T., Limin, S., June, T., Hirata, R., Osaki, M., 2007. Carbon dioxide balance of a tropical peat swamp forest in Kalimantan, Indonesia. Global Change Biol. 13, 412–425.

Hirata, R., Hirano, T., Saigusa, N., Fujinuma, Y., Inukai, K., Kitamori, Y., Yamamoto, S., 2007. Seasonal and interannual variations in carbon dioxide exchange of a temperate larch forest. Agric. Forest Meteorol. 147, 110–124.

Hollinger, D.Y., Kelliher, F.M., Schulze, E.-D., Bauer, G., Arneth, A., Byers, J.N., Hunt, J.E., McSeveny, T.M., Kobak, K.I., Milukova, I., Sogatchev, A., Tatarinov, F., Varlargin, A., Ziegler, W., Vygodskaya, N., 1998. Forest-atmosphere carbon dioxide exchange in eastern Siberia. Agric. Forest Meteorol. 90, 291–306.

Ieda, T., Kitamori, Y., Mochida, M., Hirata, R., Hirano, T., Inukai, K., Fujinuma, Y., Kawamura, K., 2006. Diurnal variations and vertical gradients of biogenic volatile and semi-volatile organic compounds at the Tomakomai larch forest station in Japan. Tellus 59B, 177–186.

Ito, A., Inatomi, M., Mo, W., Lee, M., Koizumi, H., Saigusa, N., Murayama, S., Yamamoto, S., 2007. Examination of model-estimated ecosystem respiration by use of flux measurement data from a cool-temperate deciduous broad-leaved forest in central Japan. Tellus 59B, 616–624.

Jia, S., Akiyama, T., 2005. A precise, unified method for estimating carbon storage in cool-temperate deciduous forest ecosystems. Agric. Forest Meteorol. 134, 70–80.

Jomura, M., Kominami, Y., Tamai, K., Miyama, T., Goto, Y., Dannoura, M., Kanazawa, Y., 2007. The carbon budget of coarse woody debris in a temperate broad-leaved secondary forest in Japan. Tellus 59B, 211–222.

Kajimoto, T., Matsuura, Y., Osawa, A., Abaimov, A.P., Zyryanova, O.A., Isaev, A.P., Yefremovf, D.P., Mori, S., Koike, T., 2006. Size-mass allometry and biomass allocation of two larch species growing on the continuous permafrost region in Siberia. Forest Ecol. Manage. 222, 314–325.

Kanda, M., Inagaki, A., Letzel, M.O., Raasch, S., Watanabe, T., 2004. LES study of the energy imbalance problem with eddy covariance fluxes. Bound-Layer Meteorol. 110, 381–404.

Kim, H., Hirano, T., Koike, T., Urano, S., 2005a. Contribution of litter CO_2 production to total soil respiration in two different deciduous forests. Phyton-Ann. REI Bot. 45, 385–388.

Kim, H., Hirano, T., Urano, S., 2005b. Seasonal variation in CO_2 production of leaf liter from different deciduous forests at the early decomposition stage. J. Agric. Meteorol. 61, 95–104.

Kohyama, T., 2006. The characteristic of terrestrial ecosystems in East Asia and environmental response. (Kyoritsu Shuppan), Global environment and trestrial ecosystems, Tokyo 243–253 (in Japanese).

Koike, T., Hojyo, H., Naniwa, A., Ashiya, D., Sugata, S., Sugishita, Y., Kobayashi, M., Nomura, M., Akibayashi, Y., Nakajima, J., Takagi, K., Shibata, H., Satoh, F., Wang, W., Takada, M., Fujinuma, Y., Shi, F., Matsuura, Y., Sasa, K., 2001. Basic data of the study site for CO_2 flux monitoring of a young larch plantation located in the border between northern Japan and far east Russia-Current status of a mature mixed conifer-hardwood forest stand. Eurasian J. Forest Res. 2, 65–79.

Kondo, H., Gamo, M., Hirata, R., Maeda, T., Panuthai, S., Saigusa, N., submitted for publication. Carbon flux observation in the tropical forests in South East Asia.

Kosugi, Y., Takanashi, S., Ohkubo, S., Matsuo, N., Tani, M., Mitani, T., Tsutsumi, D., Nik, A.R., 2008. CO_2 exchange of a tropical rain forest at Pasoh in Peninsular Malaysia. Agric. Forest Meteorol. 148, 439–452.

Law, B.E., Falge, E., Gu, L., Baldocchi, D.D., Bakwin, P., Berbigier, P., Davis, K., Dolman, A.J., Falk, M., Fuentes, J.D., Goldstein, A., Granier, A., Grelle, A., Hollinger, D., Janssens, I.A., Jarvis, P., Jensen, N.O., Katul, G., Mahli, Y., Matteucci, G., Meyers, T., Monson, R., Munger, W., Oechel, W., Olson, R., Pielegaard, K., Paw, U.K.T., Thorgeirsson, H., Valentini, R., Verma, S., Vesala, T., Wilson, K., Wofsy, S., 2002. Environmental controls over carbon dioxide and water vapor exchange of terrestrial vegetation. Agric. Forest Meteorol. 113, 97–120.

Lee, M.-S., Nakane, K., Nakatsubo, T., Koizumi, H., 2003. Seasonal changes in the contribution of root respiration in a cool-temperate deciduous forest. Plant Soil 255, 311–318.

Li, S.-G., Asanuma, J., Kotani, A., Eugster, W., Davaa, G., Oyunbaatar, D., Sugita, M., 2005. Year-round measurements of net ecosystem CO_2 flux over a montane larch forest in Mongolia. J. Geophys. Res. 110, D09303, doi:10.1029/2004JD005453.

Liang, N., Nakadai, T., Hirano, T., Qu, L., Koike, T., Fujinuma, Y., Inoue, G., 2004. In situ comparison of four approaches to estimating soil CO_2 efflux in a northern larch (*Larix kaempferi* Sarg). Agric. Forest Meteorol. 123, 97–117.

Liang, N., Fujinuma, Y., Inoue, G., 2005. Measurement of wood CO_2 efflux using a multichannel automated chamber system. Phyton-Ann. REI Bot. 45, 109–115.

Liang, N., Takagi, K., Kosugi, Y., Tani, M., Okuda, T., Fujinuma, Y., 2006. Comparison of ecophysiological technique with eddy covariance method and biometric approach for estimating carbon balance of forest ecosystems. In: Proceedings of the AsiaFlux Workshop 2006, Chiang Mai, Thailand, p. 23.

Lloyd, J., Taylor, J.A., 1994. On the temperature dependence of soil respiration. Funct. Ecol. 8, 315–323.

Loescher, H.W., Ocheltree, T., Tanner, B., Swiatek, E., Dano, B., Wong, J., Zimmerman, G., Campbell, J., Stock, C., Jacobsen, L., Shiga, Y., Kollas, J., Liburdy, J., Law, B.E., 2005. Comparison of temperature and wind statistics in contrasting environments among different sonic anemometer–thermometers. Agric. Forest Meteorol. 133, 119–139.

Magnani, F., Mencuccini, M., Borghetti, M., Berbigier, P., Berninger, F., Delzon, S., Grelle, A., Hari, P., Jarvis, P.G., Kolari, P., Kowalski, A.S., Lankreijer, H., Law, B.E., Lindroth, A., Loustau, D., Manca, G., Moncrieff, J.B., Rayment, M., Tedeschi, V., Valentini, R., Grace, J., 2007. The human footprint in the carbon cycle of temperate and boreal forests. Nature 447, 848–850.

Malhi, Y., Baldocchi, D.D., Jarvis, G., 1999. The carbon balance of tropical, temperate and boreal forests. Plant Cell Environ. 22, 715–740.

Massman, W.J., Lee, X., 2002. Eddy covariance flux corrections and uncertainties in long-term studies of carbon and energy exchanges. Agric. Forest Meteorol. 113, 121–144.

Matsuura, Y., Kajimoto, T., Osawa, A., Abaimov, A.P., 2005. Carbon storage in larch ecosystems in continuous permafrost region of Siberia. Phyton-Ann. REI Bot. 45, 51–54.

Matsuura, Y., Kajimoto, T., Nakai, Y., Osawa, A., Morishita, T., Zyryanova, O.A., Abaimov, A.P., 2007. In: Proceedings of the Seventh International Conference on Global Change: Connection to the Arctic (GCCA-7) International Arctic Research Center. University of Alaska Fairbanks 312 p., 258–261.

Miyama, T., Kominami, Y., Tamai, K., Tamai, K., Tatsuhko, N., Goto, Y., 2003. Automated foliage chamber method for long-term measurement of CO_2 flux in the uppermost canopy. Tellus 55B, 322–330.

Miyama, T., Kominami, Y., Tamai, K., Goto, Y., Kawahara, T., Jomura, M., Dannoura, M., 2006. Components and seasonal variation of night-time total ecosystem respiration in a Japanese broad-leaved secondary forest. Tellus B 58B, 550–559.

Nakai, Y., Matsuura, Y., Kajimoto, T., Abaimov, A.P., Yamamoto, S., Zyryanova, O.A., in press. Eddy covariance CO_2 flux above a Gmelin larch forest in continuous permafrost of central Siberia during a growing season. Theor. Appl. Climatol.

Ohkubo, N., Kosugi, Y., Takanashi, S., Mitani, T., Tani, M., 2007. Comparison of the eddy covariance and automated chamber method for evaluating nocturnal CO_2 exchange in Japanese cypress forest. Agric. Forest Meteorol. 142, 50–65.

Ohta, S., Uchijima, Z., Oshima, Y., 1993. Probale effects of CO_2-induced climate changes on net primary productivity of terrestrial vegetation in East Asia. Ecol. Res. 8, 199–213.

Ohtani, Y., Saigusa, N., Yamamoto, S., Mizoguchi, Y., Watanabe, T., Yasuda, Y., Murayama, S., 2005. Characterictics of CO_2 fluxes in cool-temperate coniferous and deciduous broadleaf forests in Japan. Phyton-Ann. REI Bot. 45, 73–80.

Ohtsuka, T., Akiyama, T., Hashimoto, Y., Inatomi, M., Sakai, T., Jia, S., Mo, W., Tsuda, S., Koizumi, H., 2005. Biometric based estimates of net primary production (NPP) in a cool-temperate deciduous forest stand beneath a flux tower. Agric. Forest Meteorol. 134, 27–38.

Ohtsuka, T., Mo, W., Satomura, T., Inatomi, M., Koizumi, H., 2007. Biometric-based carbon flux measurements and net ecosystem production (NEP) in a temperate deciduous broad-leaved forest beneath a flux tower. Ecosystems 10, 324–334.

Otto-Bliesner, B.L., Upchurch Jr., G.R., 1997. Vegetation-induced warming of high latitude regions during the late cretaceous period. Nature 385, 804–807.

Prioul, J.L., Chartier, P., 1977. Partitioning of transfer and carboxylation components of intracellular resistance to photosynthetic CO_2 fixation. Ann. Bot. 41, 789–800.

Rice, A.H., Pyle, E.H., Saleska, S.R., Hutyra, L., Palace, M., Keller, M., De Camargo, P.B., Portilho, K., Marques, D.F., Wofsy, S.C., 2004. Carbon balance and vegetation dynamics in an old-growth Amazonian forest. Ecol. Appl. 14, S55–S71.

Saigusa, N., Yamamoto, S., Murayama, S., Kondo, H., Nishimura, N., 2002. Gross primary production and net ecosystem production of a cool-temperate deciduous forest estimated by the eddy covariance method. Agric. Forest Meteorol. 112, 203–215.

Saigusa, N., Yamamoto, S., Murayama, S., Kondo, H., 2005. Inter-annual variability of carbon budget components in an AsiaFlux forest site estimated by long-term flux measurements. Agric. Forest Meteorol. 134, 4–16.

Saigusa, N., Yamamoto, S., Hirata, R., Ohtani, Y., Ide, R., Asanuma, J., Gamo, M., Hirano, T., Kondo, H., Kosugi, Y., Li, S.-G., Nakai, Y., Tani, M., Wang, H., 2008. Temporal and spatial variations in the seasonal patterns of CO2 flux in boreal, temperate, and tropical forests in East Asia. Agric. Forest Meteorol. 148, 700–713.

Saitoh, T.M., Kumagai, T., Sato, Y., Suzuki, M., 2005. Carbon dioxide exchange over a Bornean tropical rainforest. J. Agric. Meteorol. 60, 553–556.

Saleska, S.R., Miller, S.D., Matross, D.M., Goulden, M.L., Wofsy, S.C., Da Rocha, H.R., De Camargo, P.B., Crill, P., Daube, B.C., De Freitas, H.C., Hutyra, L., Keller, M., Kirchhoff, V., Menton, M., Munger, J.W., Pyle, E.H., Rice, A.H., Silva, H., 2003. Carbon in Amazon forests: unexpected seasonal fluxes and disturbance-induced losses. Science 302, 1554–1557.

Sasai, T., Ichii, K., Nemani, R.R., Yamaguchi, Y., 2005. Simulating terrestrial carbon fluxes using the new biosphere model "biosphere model integrating eco-physiological and mechanistic approaches using satellite data" (BEAMS). J. Geophys. Res. 110, G02014, doi:10.1019/2005JG000045.

Satomura, T., Hashimoto, Y., Koizumi, H., Nakane, K., Horikoshi, T., 2006. Seasonal patterns of fine root demography in a cool-temperate deciduous forest in central Japan. Ecol. Res. 21, 741–753.

Schulze, E.-D., Valentini, R., Sanz, M.-J., 2002. The long way from Kyoto to Marrakesh: implications of the Kyoto protocol negotiations for global ecology. Global Change Biol. 8, 505–518.

Scott, R.L., Edwards, E.A., Shuttleworth, W.J., Huxman, M.H., Watts, T.E., Goodrich, D.C., 2004. Interannual and seasonal variation in fluxes of water and carbon dioxide from a riparian woodland ecosystem. Agric. Forest Meteorol. 122, 65–84.

Soil Survey Staff, 1999. Soil Taxonomy. In: A Basic System of Soil Classification for Making and Interpreting Soil Survey, 2nd ed. U.S. Government Printing Office, Washington, DC 20402, 869 p.

Subke, J.-A., Inglima, I., Cotrufo, M.F., 2006. Trends and methodological impacts in soil CO_2 efflux partitioning: a metaanalytical review. Global Change Biol. 12, 921–943.

Sugita, K., 2005. Inter-annual variability of net ecosystem production in a temperate pine forest on the north slopes of Mt.Fuji. Master Thesis, Ibaraki University, 78 p.

Takagi, K., Nomura, M., Ashiya, D., Takahashi, H., Sasa, K., Fujinuma, Y., Shibata, H., Akibayashi, Y., Koike, T., 2005. Dynamic carbon dioxide exchange through snowpack by wind-driven mass transfer in a conifer-broadleaf mixed forest in northernmost Japan. Global Biogeochem. Cycles 19, GB2012, doi:10.1029/2004GB002272.

Takanashi, S., Kosugi, Y., Tanaka, Y., Yano, M., Katayama, T., Tanaka, H., Tani, M., 2005a. CO_2 exchange in a temperate Japanese cypress forest compared with that in a cool-temperate deciduous broad-leaved forest. Ecol. Res. 20, 313–324.

Takanashi, S., Kosugi, Y., Tani, M., Matsuo, N., Mitani, T., Nik, A.R., 2005b. Characteristics of the gas exchange of a tropical rain forest in peninsular Malaysia. Phyton-Ann. REI Bot. 45, 61–66.

Tani, A., Nozoe, S., Aoki, M., Hewitt, C.N., 2002. Monoterpene fluxes measured above a Japanese red pine forest at Oshiba plateau, Japan. Atmos. Environ. 36, 3391–3402.

Trumbore, S., 2006. Carbon respired by terrestrial ecosystems–recent progress and challenges. Global Change Biol. 12, 141–153.

Uchida, M., Mo, W., Nakatsubo, T., Tsuchiya, Y., Horikoshi, T., Koizumi, H., 2005. Microbial activity and litter decomposition under snow cover in a cool-temperate broad-leaved deciduous forest. Agric. Forest Meteorol. 134, 102–109.

Valentini, R., Matteucci, G., Dolman, A.J., Schulze, E.-D., Rebmann, C., Moors, E.J., Granier, A., Gross, P., Jensen, N.O., Pielegaard, K., Lindroth, A., Grelle, A., Bernhofer, C., Grünwald, T., Aubinet, M., Ceulemans, R., Kowalski, A.S., Vesala, T., Rannik, Ü., Berbigier, P., Loustau, D., Guomundsson, J., Thorgirsson, H., Ibrom, A., Morgenstern, K., Clement, R., Moncrieff, J., Montagnani, L., Minebi, S., Jarvis, O.G., 2000. Respiration as the main determinant of carbon balance in Europe forests. Nature 404, 861–865.

van Gorsel, E., Leuning, R., Cleugh, H.A., Keith, H., Suni, T., 2007. Nocturnal carbon efflux: reconciliation of eddy covariance and chamber measurements using an alternative to the u_*-threshold filtering technique. Tellus 59B, 397–403.

Vickers, D., Mahrt, L., 1997. Quality control and flux sampling problems for tower and aircraft data. J. Atmos. Ocean. Technol. 14, 512–526.

Wang, H., Saigusa, N., Yamamoto, S., Kondo, H., Hirano, T., Toriyama, A., Fujinuma, F., 2004. Seasonal variation of net ecosystem CO_2 exchange over a larch forest in Hokkaido, Japan. Atmos. Environ. 38, 7021–7032.

Wang, H., Saigusa, N., Zu, Y., Yamamoto, S., Kondo, H., Yang, F., Wang, W., Hirano, T., Fujinuma, Y., 2005. Response of CO_2 flux to environmental variables in two larch forest ecosystems in East Asia. Phyton-Ann. REI Bot. 45, 339–346.

Yamamoto, S., Saigusa, N., Murayama, S., Gamo, M., Ohtani, Y., Kosugi, Y., Tani, M., 2005. Synthetic analysis of the CO_2 fluxes at various forest in East Asia. In: Plant Responses to Air Pollution and Global Change, Springer-Verlag, Tokyo, pp. 215–225.

Yasuda, Y., Ohtani, Y., Watanabe, T., Okano, M., Yokota, T., Liang, N., Tang, Y., Nik, A.R., Tani, M., Okuda, T., 2003. Measurement of CO_2 flux above a tropical rain forest at Pasoh in Peninsular. Malaysia. Agric. Forest Meteorol. 114, 235–244.

Yone, Y., Oguma, H., Yamagata, Y., Fujinuma, Y., 2005. Development of measurement system for evaluating forest ecosystems: measurement method of aboveground biomass growth by using airborne laser survery. Phyton-Ann. REI Bot. 45, 517–524.

Yone, Y., Fukushi, R., Hirata, R., Oguma, H., Fujinuma, Y., 2006. Estimation of NPP in a Larix kaempfer stand—comparison of field surveying, airborne laser surveying and Eddy fluxes. J. Jpn. Forest. Soc. Hokkaido 54, 82–84 in Japanese.

Tree Physiology 26, 1565–1578

Patchy stomatal behavior in broad-leaved trees grown in different habitats

SATORU TAKANASHI,[1,2] YOSHIKO KOSUGI,[1] NAOKO MATSUO,[1] MAKOTO TANI[1] and NOBUHITO OHTE[1]

[1] *Laboratory of Forest Hydrology, Division of Environmental Science and Technology, Graduate School of Agriculture, Kyoto University, Kyoto 606–8502, Japan*

[2] *Corresponding author (takanash@kais.kyoto-u.ac.jp)*

Received April 18, 2005; accepted January 17, 2006; published online September 1, 2006

Summary Effects of heterogeneity in stomatal behavior on gas-exchange characteristics of leaves from four tree species growing in different climates, including temperate, tropical monsoon and tropical rain forest, were investigated by combining gas-exchange measurements and the pressure-infiltration method. Field observations indicated linear relationships between whole-leaf conductance and the ratio of infiltrated to non-infiltrated leaf area (open stomata area) in *Dipterocarpus sublamellatus* Foxw. and *Neobalanocarpus heimii* (King) Ashton in a tropical rain forest in Peninsular Malaysia, whereas the ratio of infiltrated to non-infiltrated area rapidly increased up to the whole-leaf conductance at which the entire leaf was infiltrated in *Cinnamomum camphora* Sieb. in a temperate evergreen forest in Japan and in *Azadirachta indica* Juss. in a tropical monsoon area in Thailand. These results strongly suggest small ranges in bell-shaped stomatal conductance distributions in *C. camphora* and *A. indica* and bimodal stomatal conductance distributions in *D. sublamellatus* and *N. heimii.* The values of normalized maximum carboxylation rate at 25 °C (V_{cmax25}) derived from gas-exchange measurements were not constant, but decreased with decreasing whole-leaf conductance in *D. sublamellatus* and *N. heimii.* A gas-exchange model analysis revealed a linear relationship between whole-leaf conductance and the ratio of infiltrated to non-infiltrated leaf area for bimodal stomatal conductance distributions, whereas for bell-shaped distributions, the relationships were nonlinear. Midday depression of apparent V_{cmax25} in these species was mainly caused by bimodal stomatal closure. The bimodal stomatal distribution model could also explain diurnal changes in photosynthetic assimilation and transpiration rates in these species.

Keywords: Azadirachta indica, Cinnamomum camphora, Dipterocarpus sublamellatus, heterobaric leaf, Neobalanocarpus heimii, pressure infiltration methods, stomatal patchiness, V_{cmax}.

Introduction

The rate of gas exchange between plants and the atmosphere is determined mainly by the rates of photosynthesis and transpiration in individual leaves, both of which vary in response to environmental factors such as water and nutrient supplies, temperature and light. In most plants, diurnal changes in photosynthetic rate within a horizontal leaf can be described by a time-course with a single peak that is determined by the light environment. However, in some plants in arid environments or in habitats where transpirational demand is high, diurnal changes in photosynthetic rates follow a bimodal time course. Based on a cost (transpiration) versus benefit (assimilation) analysis, Cowan (1977) showed that the assumption of optimized regulation of stomatal opening results in a midday depression of transpiration and photosynthesis when the ratio of the change in transpiration to the change in assimilation is small. The midday depression is the result of stomatal closure during the period of the day when evaporative demand is highest owing to a large difference in water vapor pressure between the leaf and the air. The theoretical time courses calculated by Cowan (1977) agree with changes in the metabolism of C_3 and C_4 plants in dry environments, where midday depressions of transpiration and photosynthesis are common (Lambers et al. 1998). However, although the optimization approach provides a reasonably good explanation of stomatal behavior, it does not provide an explicit solution for optimal water use by a whole plant and does not take into account the effects of water deficits on physiological processes such as growth or water transport (Jones 1998).

Declines in photosynthesis during the afternoon have been reported for plants in many ecosystems. These declines have been attributed to a variety of causes, including (but not limited to) stomatal regulation in response to low humidity or low leaf-water potential, the effects of elevated temperature on photosynthesis, the accumulation of starch and metabolites, intrinsic circadian rhythms and increased leaf respiration in response to elevated temperature (Jones 1992, Larcher 2003). A midday depression in gas exchange was observed in the tropical rain forest trees *Dipterocarpus sublamellatus* Foxw. and *Neobalanocarpus heimii* (King) Ashton in Pasoh on the Malaysian peninsula (Toma et al. 1995) and in *Macaranga conifera* (Zoll.) Muell. Arg. in East Kalimantan on the island of Borneo in Indonesia (Ishida et al. 1999*a*, Ishida et al. 1999*b*).

Ishida et al. (1999*b*) analyzed changes in net assimilation rate for a given electron transport rate at different temperatures throughout the day (including early morning and afternoon) and reported that internal CO_2 concentrations (C_i) estimated by whole-leaf gas exchange probably increase at midday. As this finding is consistent with the heterogeneous closure of stomata, a low net assimilation rate at midday would appear to be the result of increases in both metabolic and stomatal limitations to photosynthesis.

To understand the link between plant responses and environmental factors, the measurement of CO_2 and H_2O gas exchange has been carried out for many plant species. Parameterization of the Farquhar-von Caemmerer-Berry model (Farquhar et al. 1980) of biochemical photosynthesis with empirical data obtained by the gas-exchange method has revealed insights into the gas exchange process in leaves (e.g., Wullschleger 1993, Wohlfahrt et al. 1999). Within the context of the Farquhar-von Caemmerer-Berry model, characteristics such as the activity of ribulose-1,5-bisphosphate carboxylase/oxygenase, the rate of ribulose-1,5-bisphosphate regeneration by electron transport and the rate of triose phosphate utilization are taken into account. The normalized maximum rate of carboxylation at 25 °C (V_{cmax25}) reflects photosynthetic capacity independent of stomatal conductance. A positive correlation between V_{cmax25} and the normalized maximum potential rate of electron transport has been used to model leaf and canopy photosynthesis (Wullschleger 1993, Harley and Baldocchi 1995, Leuning et al. 1995, Leuning 1997, Baldocchi and Meyers 1998, Baldocchi et al. 2002, Tanaka et al. 2002).

Measurement of gas exchange allows estimation of V_{cmax25}. Because the midday depression in photosynthesis is normally analyzed under conditions of either stomatal or nonstomatal limitations, V_{cmax25} is often used instead of net assimilation rate to estimate photosynthetic capacity because it avoids the effects of stomatal regulation. The value of V_{cmax25} is derived from the relationship between photosynthesis and C_i (the $A-C_i$ curve) under the assumption that gas exchange within the leaf is homogeneous. However, Laisk (1983) showed that failure to consider the statistical distribution of stomatal apertures may cause significant error in the calculated photosynthetic parameters of leaves when the diffusion resistance between neighboring substomatal cavities is large and when stomatal apertures vary over a wide range. In the conventional calculation of the intercellular partial pressure of CO_2, it is assumed that photosynthesis and transpiration are uniform over the leaf area under consideration (Terashima et al. 1988). This results in an overestimation of the intercellular partial pressure of CO_2 and, consequently, an underestimation of V_{cmax25}. Wide variation has been reported in stomatal apertures, even for leaves with small surface areas (Laisk et al. 1980, van Gardingen et al. 1989, Smith et al. 1989, Weyers and Lawson 1997). The heterogeneity in stomatal apertures is attributed to "patchy" stomatal behavior and has been reviewed in several articles (Terashima 1992, Weyers and Lawson 1997, Beyschlag and Eckstein 1998, Mott and Buckley 1998).

There are several methods to evaluate the heterogeneity of stomatal apertures (see Terashima 1992, Weyers and Lawson 1997), including starch–iodine staining (Terashima et al. 1988), infiltration (Beyschlag and Pfanz 1990), measurements from silicon rubber impressions (Smith et al. 1989), ^{14}C autoradiography (Wise et al. 1992), fluorescence imaging (Daley et al. 1989, Mott et al. 1993, Cardon et al. 1994, Meyer and Genty 1998), thermography (Jones 1999) and direct microscopic observation (van Gardingen et al. 1989). Patchy stomatal behavior has been documented under conditions of water stress (Sharkey and Seeman 1989, Gunasekera and Berkowitz 1992), low humidity (Loreto and Sharkey 1990, Beyschlag et al. 1992, Mott et al. 1993), sudden changes from high to low irradiance (Cardon et al. 1994, Eckstein et al. 1996), sudden transition from darkness to bright light (Bro et al. 1996) and in response to exogenous abscisic acid (ABA) application (Downton et al. 1988, Terashima et al. 1988, Daley et al. 1989). The hydraulic interactions among stomata have been proposed as one mechanism to explain many aspects of patchy stomatal behavior (Haefner et al. 1997, Mott et al. 1997, Mott and Buckley 1998, Buckley and Mott 2000), and the effects of several different distributions of stomatal apertures on gas exchange have been modeled (Cheeseman 1991, Buckley et al. 1997). However, under the same climatic conditions, there are species that show patchy stomatal aperture and species that do not (e.g., Beyschlag et al. 1992, Wise et al. 1992).

Although several studies have revealed that plants in natural environments repeatedly undergo heterogeneous stomatal closure during specific periods of the day (Beyschlag and Pfanz 1990, Beyschlag et al. 1992, Düring and Loveys 1996), relatively few studies have examined the effects of patchy stomatal behavior on gas-exchange characteristics in the field. One reason for the paucity of field observations is that direct observation of individual stomatal pores is technically difficult and laborious. The infiltration method is especially suitable for gross surveys of patchy closure of stomata in the field (Weyers and Lawson 1997). However, infiltration is an all-or-nothing event, which means that this technique essentially results in the classification of groups of stomata as either open or closed according to whether some or all of the stomata are above or below a particular threshold for liquid conductance. To estimate the distribution of stomatal apertures in our study, we combined gas-exchange measurements with the infiltration method. The relationship between whole-leaf conductance and the infiltration ratio was also simulated by computer modeling. We used our empirical data and our model to investigate the effect of heterogeneity in stomatal opening on the apparent photosynthetic capacity of leaves and, thus, were able to evaluate the main factor that causes midday depression of photosynthesis.

Materials and methods

Field observations

To investigate the effects of patchy stomatal behavior on gas exchange in trees from different habitats, we studied the leaves of four species: *Cinnamomum camphora* Sieb. in a temperate evergreen forest in Japan; *Azadirachta indica* Juss. in a tropical monsoon area in Thailand; and *Dipterocarpus sublamellatus* and *Neobalanocarpus heimii* in a tropical rain forest on the Malaysian peninsula (Table 1). Whole-leaf conductance and pressure infiltration were measured for *C. camphora* on September 26, 2000, for *A. indica* on November 16 2000, for *N. heimii* on September 19 and 20, 2002 and for *D. sublamellatus* on September 20, 2002 and March 8, 2003. Gas-exchange measurements were made on leaves of the two tropical trees (*D. sublamellatus* and *N. heimii*) on September 18–20, 2002 and March 9, 2003, and the electron transport rates in these species were measured on March 8 and 9, 2003.

For *C. camphora* and *A. indica*, whole-leaf conductance was measured in situ with an LI-1600 steady-state porometer (Li-Cor, Lincoln, NE). For *N. heimii* and *D. sublamellatus*, whole-leaf conductance and net assimilation rates were measured in situ with a Li-Cor LI-6400 gas-exchange measurement system equipped with a 2 × 3 cm clear-top chamber.

We calculated V_{cmax25} to evaluate the effect of heterogeneous stomatal behavior on gas exchange and to determine directly the apparent depression in photosynthetic capacity in the field. Maximum carboxylation rate (V_{cmax}) was calculated by a "one-point method" (Wilson et al. 2000, Kosugi et al. 2003, Grassi et al. 2005), which can be used to determine the actual responses of leaves in the field. By contrast, determining the $A{-}C_{\mathrm{i}}$ curve with a controlled environment chamber is time-consuming and involves a number of technical difficulties (Kosugi et al. 2003). To measure V_{cmax25} for *N. heimii* and *D. sublamellatus*, we used a 2 × 3 cm light-emitting diode (LED) chamber and a Li-Cor LI-6400-40 leaf chamber fluorometer. The measurements were conducted under ambient conditions except for light, which was controlled at a photosynthetically active radiation (PAR) of 1000 μmol m^{-2} s^{-1}. To estimate V_{cmax25}, we used data, including measurements made with the clear-top chamber, obtained at a PAR of > 500 μmol m^{-2} s^{-1} and $C_{\mathrm{i}} < 320$ ppm. The intercellular CO_2 concentration was estimated with Equation 4 and the whole-leaf assimilation and conductance values. The electron transport rates for *N. heimii* and *D. sublamellatus* were measured with a Li-Cor LI-6400-40 leaf chamber fluorometer. The periods during which gas-exchange and pressure infiltration measurements were conducted for *N. heimii* and *D. sublamellatus* are presented in Figure 1. Figure 1 also shows the micrometeorological environments, including solar radiation, air temperature and relative humidity, above a canopy of *N. heimii* and *D. sublamellatus*.

A pressure infiltration technique similar to that of Beyschlag and Pfanz (1990) was used to evaluate patchy stomatal behavior. Immediately after the measurement of leaf conductance, the leaf was detached from the tree and placed in a 50-ml plastic syringe that was filled with a 1% acid fuchsin solution. Air within the syringe was expelled through the syringe outlet. The outlet was then closed and the plunger was forcefully pulled outward to evacuate the internal air spaces of the leaf. The syringe was simultaneously shaken to remove gas bubbles that emerged from the leaf surface. The water column in the syringe was then set under pressure by carefully pushing the plunger back into the syringe, with the outlet closed. After careful extraction from the syringe, the leaf was washed with water and blotted dry between two pieces of absorbent paper. The degree of acid fuchsin infiltration was recorded by digital photography. The digital photographs of acid fuchsin-infiltrated leaves were analyzed with Adobe Photoshop (Adobe Systems, San Jose, CA) to measure the ratio of acid fuchsin-infiltrated area to uninfiltrated area.

Model description

We used a stomatal conductance distribution model to evaluate the effect of the distribution of stomatal apertures on gas exchange. In this model, the leaf is subdivided into many isolated patches. A stomatal conductance is allocated to each patch according to the distributions described below. The C_{i} and the net assimilation rate in each patch were estimated using this stomatal conductance model and the Farquhar-von Caemmerer-Berry model of biochemical photosynthesis, in which we assumed that the photosynthetic parameters were uniform throughout the whole leaf. Mean stomatal conductance (g_{sleaf}) and mean net assimilation rate (A_{leaf}) for the whole leaf were calculated by integrating the stomatal conductance and net assimilation rate of each patch; thereafter, the "apparent" V_{cmax25} to be measured by the chamber method (V_{cmax25}*) was calculated. We estimated the infiltrated leaf area that would result for each modeled distribution of stomatal conductance by assuming that a patch would infiltrate if its stomatal conductance were above some threshold value, corresponding to the liquid-phase conductance allowing infiltration.

Buckley et al. (1997) showed that, for most conductance distributions, there are fairly small differences between homogeneous and patchy assimilation rates at a given C_{i}. However, differences between homogeneous and patchy assimilation rates are greater for conductance distributions that (a) span re-

Table 1: Summary information about the trees used for gas-exchange and pressure infiltration measurements.

Climate, vegetation type	Location	Mean annual air temperature (°C), precipitation (mm), years (range)	Species	Tree height (m)	Observation height (m)
Temperate, evergreen broad-leaved tree	34.73° N, 134.36° E	15.2, 1159, 1995–1999	*Cinnamomum camphora*	9	8
Tropical monsoon, deciduous broad-leaved tree	16.94° N, 99.43° E	26.9, 822, 1998–1999	*Azadirachta indica*	10	3.5
Tropical, evergreen broad-leaved tree	2.96° N, 102.3° E	25.6, 1571, 1996–1999	*Neobalanocarpus heimii* *Dipterocarpus sublamellatus*	46 43	32 32

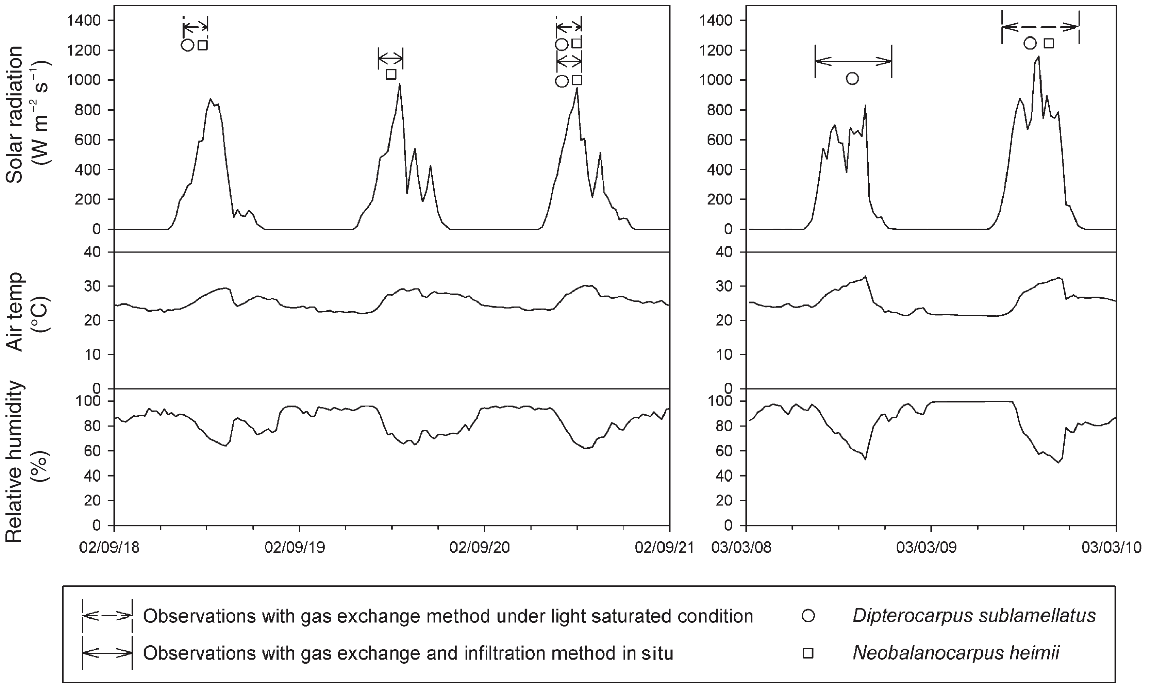

Figure 1. Diurnal variations in solar radiation, air temperature and relative humidity. Arrows indicate periods when the experiments were carried out with *Dipterocarpus sublamellatus* and *Neobalanocarpus heimii.*

gions of lower conductance; (b) extend over a larger range of conductances; (c) are more nearly bimodal; and (d) are right-skewed. In this study, we simulated stomatal conductance using two distributions of stomatal apertures, namely a bimodal distribution (which indicates that whole-leaf conductance reflects either open or closed stomatal conductance) and a normal (bell-shaped) distribution. For both types of distributions, we analyzed the relationships between g_{sleaf}, the infiltration ratio and V_{cmax25}*. A leaf was subdivided into 10,000 patches of equal area and equivalent photosynthetic characteristics. For the bimodal distribution, the stomatal conductance for an open or a closed patch was g_{smax} or g_{smin}, respectively. For the normal distribution, mean whole-leaf stomatal conductance (g_{sleaf}) was equal to a given conductance (stomatal conductance values that were smaller than g_{smin} were made equal to g_{smin}). The normal distribution that we used was truncated at a value of g_{smin}. We adjusted the peak of the distribution to make the g_{sleaf} equal to the given conductance. The modeled leaf was perfectly heterobaric, i.e., no lateral flow of CO_2 between patches was allowed. Leaf temperature was assumed to be homogeneous.

In this model, the assimilation rate for each patch was determined with a Farquhar-von Caemmerer-Berry model in which stomatal conductance values for each patch were given by the two types of distributions. This model was also used to calculate the value of V_{cmax25} by the one-point method.

The partial pressure of CO_2 at the sites of carboxylation ($p(C_{\mathrm{c}})$) was calculated assuming that this parameter was related to C_{i} as:

$$C_{\mathrm{i}} = \frac{\left(g_{\mathrm{t}}^{\mathrm{CO_2}} - \frac{E}{2}\right)C_{\mathrm{a}} - A}{g_{\mathrm{t}}^{\mathrm{CO_2}} + \frac{E}{2}} \tag{1}$$

$$\frac{1}{g_{\mathrm{t}}^{\mathrm{CO_2}}} = \frac{1}{g_{\mathrm{b}}^{\mathrm{CO_2}}} + \frac{1}{g_{\mathrm{s}}^{\mathrm{CO_2}}} \tag{2}$$

$$p(C_{\mathrm{c}}) = P_{\mathrm{atm}}\left(C_{\mathrm{i}} - \frac{A}{g_{\mathrm{i}}}\right) \tag{3}$$

where C_{i} is intercellular CO_2 concentration (μmol CO_2 mol^{-1} air); C_{a} is ambient CO_2 concentration (μmol CO_2 mol^{-1} air); A is assimilation rate (μmol m^{-2} s^{-1}); $g_{\mathrm{t}}^{\mathrm{CO_2}}$ is total conductance of CO_2 (mol CO_2 m^{-2} s^{-1}); E is transpiration rate (mol H_2O m^{-2} s^{-1}); P_{atm} is atmospheric pressure (MPa); and g_{i} is internal conductance of CO_2 (mol CO_2 m^{-2} s^{-1}). The variable $g_{\mathrm{b}}^{\mathrm{CO_2}}$ is boundary layer conductance of CO_2 (mol CO_2 m^{-2} s^{-1}) such that $g_{\mathrm{b}}^{\mathrm{CO_2}} = g_{\mathrm{b}}^{\mathrm{H_2O}}/1.6^{2/3}$, and $g_{\mathrm{s}}^{\mathrm{CO_2}}$ is stomatal conductance of CO_2 (mol CO_2 m^{-2} s^{-1}) such that $g_{\mathrm{s}}^{\mathrm{CO_2}} = g_{\mathrm{s}}^{\mathrm{H_2O}}/1.6$, where $g_{\mathrm{b}}^{\mathrm{H_2O}}$ is the boundary layer conductance of H_2O (mol H_2O m^{-2} s^{-1}) and $g_{\mathrm{s}}^{\mathrm{H_2O}}$ is stomatal conductance of H_2O (mol H_2O m^{-2} s^{-1}). Equation 1 uses the correction described by Jarman (1974) and von Caemmerer and Farquhar (1981) to account for the convective effects of transpiration at stomatal pores.

In the one-point method, the apparent partial pressure of CO_2 at the sites of intercellular space ($p(C_i)^*$) was estimated from variables measured by the gas-exchange method, including the mean total conductance of CO_2 for the whole leaf (g_{tleaf}), C_a, A_{leaf}, P_{atm} and E. Assuming that $p(C_i)^*$ could substitute for $p(C_c)$ (the infinite g_i), the value of V_{cmax25}^* was calculated from the values of A_{leaf}, $p(C_i)^*$ and the leaf temperature (T_l) as:

$$p(C_i)^* = P_{\mathrm{atm}} \frac{\left(g_{\mathrm{tleaf}}^{\mathrm{CO_2}} - \frac{E}{2}\right) C_a - A_{\mathrm{leaf}}}{g_{\mathrm{tleaf}}^{\mathrm{CO_2}} + \frac{E}{2}} \tag{4}$$

$$V_{\mathrm{cmax25}}^* = (A_{\mathrm{leaf}} + R_d) \frac{p(C_i)^* + K_c\left(1 + \dfrac{p(O)}{K_o}\right)}{p(C_i)^* - \dfrac{p(O)}{2\tau}} \times \frac{1 + \exp\left[\dfrac{\Delta S(V_{\mathrm{cmax}})(T_l + 273) - \Delta H_d(V_{\mathrm{cmax}})}{R(T_l + 273)}\right]}{\exp\left[\dfrac{\Delta H_a(V_{\mathrm{cmax}})(T_l - 25)}{298R(T_l + 273)}\right]} \tag{5}$$

where R_d is non-photorespiratory respiration rate (μmol m^{-2} s^{-1}); τ is the specificity factor of Rubisco; $p(O)$ (21,000 Pa) is the partial pressure of O_2 at the sites of oxygenation; K_c and K_o are the Michaelis-Menten constants of Rubisco for CO_2 and O_2, respectively; T_l is leaf temperature (°C); R is the gas constant (8.31 J K^{-1} mol^{-1}); $\Delta H_a(V_{\mathrm{cmax}})$ is the activation energy for V_{cmax}; $\Delta H_d(V_{\mathrm{cmax}})$ is the deactivation energy for V_{cmax}; and $\Delta S(V_{\mathrm{cmax}})$ is an entropy term.

The Arrhenius function was used for the temperature dependences of parameters K_c, K_o, τ, V_{cmax} and R_d as:

$$K_c = K_{c25} \exp\left[\frac{\Delta H_a(K_c)}{298R}\left(1 - \frac{298}{T_l + 273}\right)\right] \tag{6}$$

$$K_o = K_{o25} \exp\left[\frac{\Delta H_a(K_o)}{298R}\left(1 - \frac{298}{T_l + 273}\right)\right] \tag{7}$$

$$\tau = \tau_{25} \exp\left[\frac{\Delta H_a(\tau)}{298R}\left(1 - \frac{298}{T_l + 273}\right)\right] \tag{8}$$

$$R_d = R_{d25} \exp\left[\frac{\Delta H_a(R_d)}{298R}\left(1 - \frac{298}{T_l + 273}\right)\right] \tag{9}$$

where τ_{25}, K_{c25}, K_{o25}, V_{cmax25} and R_{d25} are τ, K_c, K_o and R_d at 25 °C, respectively. Terms $\Delta H_a(\tau)$, $\Delta H_a(K_c)$, $\Delta H_a(K_o)$ and $\Delta H_a(R_d)$ are the activation energies for τ, K_c, K_o and R_d, respectively.

In the model simulation, the net assimilation rate of each patch was calculated as:

$$A_c = V_{\mathrm{cmax25}} \frac{\exp\left[\dfrac{\Delta H_a(V_{\mathrm{cmax}})(T_l - 25)}{298R(T_l + 273)}\right]}{1 + \exp\left[\dfrac{\Delta S(V_{\mathrm{cmax}})(T_l + 273) - \Delta H_d(V_{\mathrm{cmax}})}{R(T_l + 273)}\right]} \times \frac{p(C_c) - \dfrac{p(O)}{2\tau}}{p(C_c) + K_c\left(1 + \dfrac{p(O)}{K_o}\right)} - R_d \tag{10}$$

where A_c is net assimilation rate limited by the RuBP saturated rate of carboxylation (μmol m^{-2} s^{-1}).

The net RuBP-limited CO_2 assimilation rate (A_j) was expressed as:

$$A_j = \frac{J}{4} \times \frac{p(C_c) - \dfrac{p(O)}{2\tau}}{p(C_c) + \dfrac{p(O)}{\tau}} - R_d \tag{11}$$

where J is potential electron transport rate. We expressed J as the smaller root of the following nonrectangular hyperbola representing the relationship to absorbed PAR (Farquhar and Wong 1984).

$$\theta J^2 - \left[J_{\max} + \frac{\varepsilon(1-f)}{2}Q\right]J + J_{\max}\frac{\varepsilon(1-f)}{2}Q = 0 \tag{12}$$

where θ is a convexity factor; $J_{\max}$ is maximum potential rate of electron transport; Q is incident PAR (μmol m^{-2} s^{-1}); ε is leaf absorbance of Q; and f is the fraction of light loss not used photosynthetically at chloroplast lamellae. The values of θ (0.9) and $1 - f$ (0.593) were approximated from the results of light curve measurements of electron transport rate. The value of ε (0.842) was approximated from measurements of the light penetration of the canopy leaves. Based on Wullschleger (1993), $J_{\max}$ is related to V_{cmax} as:

$$J_{\max} = k_j V_{\mathrm{cmax}} \tag{13}$$

Disregarding the possible limitation imposed on photosynthesis at high CO_2 concentrations by the rate of triose phosphates utilization, the net assimilation rate is:

$$A = \min\{A_c, A_j\} \tag{14}$$

The corresponding values of A and $p(C_c)$ are determined as the point of intersection of the "demand function" described by Equation 14 and the "supply function" described by Equation 3 following the Newton-Raphson method.

To estimate the value of V_{cmax25}*, we have to know the value of R_d. Accordingly, the temperature dependency of the respiration rate in darkness was determined from the net assimilation data obtained in September 2002 with a covered chamber and the parameter $\Delta H_a(R_d)$ (= 66,405 J mol^{-1}), and we then scaled R_d using the relationship with the dark respiration rate based on the results of Brooks and Farquhar (1985). The value of V_{cmax25} (25 μmol CO_2 mol^{-1}) was tentatively used considering the patchy effects. We used the parameters V_{cmax25} and R_{d25} obtained from the observed data for *D. sublamellatus* and *N. heimii* in September 2002 and other parameters that were reported in the literature listed in Table 2.

Figure 2 shows the response of net CO_2 assimilation to apparent internal CO_2 concentration for *D. sublamellatus* and V_{cmax25}* calculated with Equation 5. Observations were conducted on February 14, 2005. The value of V_{cmax25}* was also determined by nonlinear regression based on the biochemical photosynthesis model and parameters described in this section (not using Equation 5). The value of 14.9 μmol m^{-2} s^{-1} is slightly smaller than values calculated with Equation 5. At a range of apparent C_i (C_i*) from 100 to 320 ppm, the mean and the standard deviations of V_{cmax25}* were 15.5 and 0.6 μmol m^{-2} s^{-1}, respectively. Figure 2 also shows that the model simulated acceptable values of R_d.

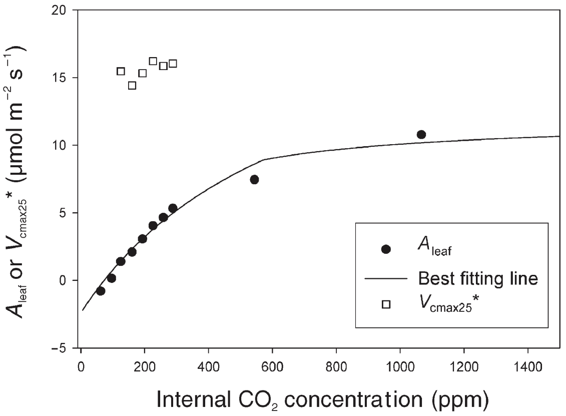

Figure 2. Responses of net CO_2 assimilation (A_{leaf}) to apparent internal CO_2 concentration and apparent photosynthetic capacity (V_{cmax25}*) for *D. sublamellatus*. Mean whole-leaf stomatal conductance was 0.09 mol m^{-2} s^{-1} during the observation. The solid line is a model fit to measured data of A_{leaf}. Symbols: ● = measured values of A_{leaf}; and □ = measured values of V_{cmax25}*.

Results

By microscopic observation, we confirmed that all leaves studied were heterobaric. The acid fuchsin-infiltrated areas of the leaves always corresponded to intercostal areas. This was expected because, in the leaves we studied, leaf veins subdivided the intercellular space into many isolated units (Figure 3). Infiltrated areas were spatially randomly distributed for all leaves. Therefore, we assumed that the conductance measured by the chamber method was approximately equal to true whole-leaf conductance.

Figures 4 and 5 show the relationship between observed g_{leaf} and the infiltration ratio as well as diurnal changes in this rela-

Table 2. List of parameters used in the biochemical photosynthesis model.

Parameter	Units	Value	Reference
K_c			
K_{c25}	Pa CO_2	27.5	Harley and Baldocchi (1995)
$\Delta H_a(K_c)$	J mol^{-1}	80470	Harley et al. (1992)
K_o			
K_{o25}	Pa O_2	42000	Harley and Baldocchi (1995)
$\Delta H_a(K_o)$	J mol^{-1}	14510	Harley et al. (1992)
τ			
τ_{25}		2321	Harley and Baldocchi (1995)
$\Delta H_a(\tau)$	J mol^{-1}	–29000	Harley and Baldocchi (1995)
R_d			
R_{d25}	μmol m^{-2} s^{-1}	1.00*{0.50–0.05*ln(Q)}	This study
$\Delta H_a(R_d)$	J mol^{-1}	66405	Farquhar et al. (1980)
V_{cmax}			
V_{cmax25}	μmol m^{-2} s^{-1}	25	This study
$\Delta H_a(V_{cmax})$	J mol^{-1}	65000	Tenhunen et al. (1990)
$\Delta H_d(V_{cmax})$	J mol^{-1}	250000	Tenhunen et al. (1990)
$\Delta S(V_{cmax})$	J mol^{-1}	600	Tenhunen et al. (1990)
J_{max}			
k_j		2.2	This study
g_i	mol^{-1} CO_2 m^{-2} s^{-1}	0.05, 0.2, 0.5, ∞	This study

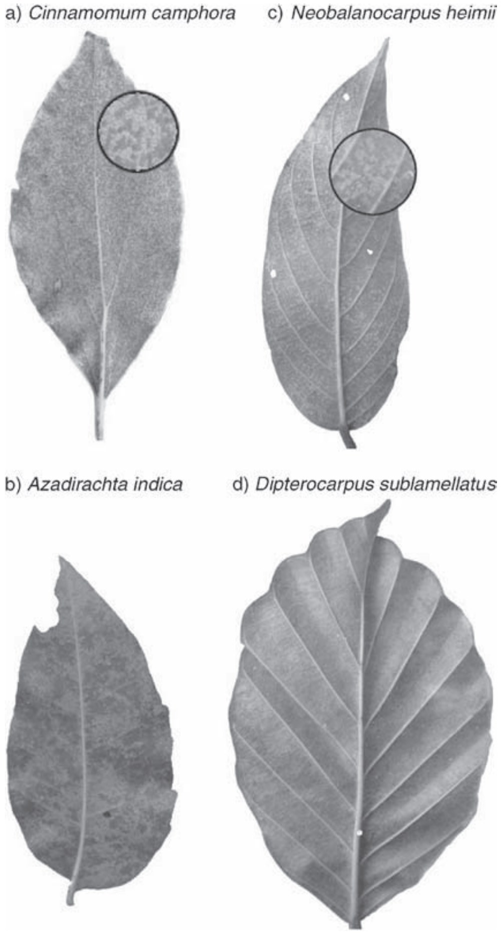

Figure 3. Photographs of leaves from (a) *Cinnamomum camphora*; (b) *Azadirachta indica*; (c) *Neobalanocarpus heimii*; and (d) *Dipterocarpus sublamellatus* immediately after the infiltration of a 1% acid fuchsin solution.

tionship. Whole-leaf conductance and the infiltration ratio of the temperate evergreen leaves of *C. camphora* and the tropical deciduous leaves of *A. indica* gradually decreased from about 1000 h; the leaves of the tropical rain forest trees *N. heimii* and *D. sublamellatus* also exhibited depression of whole leaf conductance and the infiltration ratio before noon.

Figure 6 shows diurnal changes in A_{leaf}, g_{leaf}, electron transport rate, $C_{\mathrm{i}}*$ and $V_{\mathrm{cmax25}}*$ under saturated light conditions (PAR = 1000 μmol $\mathrm{m^{-2}\ s^{-1}}$) for *N. heimii* and *D. sublamellatus*. The diurnal changes in g_{sleaf} and A_{leaf} were similar in both species, and the changes in g_{sleaf} resembled the changes in A_{leaf}. Parameter A_{leaf} peaked at 0800 h with values of ~8 and 6 μmol $\mathrm{m^{-2}\ s^{-1}}$ for *D. sublamellatus* and *N. heimii*, respectively, and decreased gradually thereafter, reaching a minimum at 1400 h (~0 and 1 μmol $\mathrm{m^{-2}\ s^{-1}}$ for *D. sublamellatus* and *N. heimii*, respectively). A small recovery in net photosynthesis occurred in the late afternoon. Values of $C_{\mathrm{i}}*$ (calculated by Equation 4) were relatively constant throughout the day, but tended to be higher in the afternoon. For *N. heimii*, the mean values of $C_{\mathrm{i}}*$ before and after noon were 291.6 ppm (± 7.43 standard deviation, $n = 27$) and 293.8 ppm (± 7.11, $n = 14$); the corresponding values for *D. sublamellatus* were 316.1 ppm (± 5.02, $n = 25$) and 342.0 ppm (± 13.4, $n = 15$). There were no significant diferences between the before and the after noon data for each species at $P = 0.05$ (Student's *t* test). There was no clear diurnal change in electron transport rate, but there were marked diurnal changes in $\mathrm{V_{cmax25}}*$ that resembled the changes in g_{sleaf}.

Discussion

The heterogeneity of stomatal behavior in the leaves of trees from different climates is discussed by considering the relationship between g_{sleaf} and the infiltration ratio. In addition, the effects of these parameters on gas exchange in a model of stomatal conductance are described.

Heterogeneity of stomatal apertures

To examine the distribution of stomata in leaves from each of the four tree species we studied, we compared the actual relationship between g_{sleaf} and the infiltration ratio as determined from data measured in the field with the simulated relationship obtained with a computer model. Pressure infiltration of acid fuchsin revealed a patchy distribution of stomatal openings. However, this did not necessarily reflect a bimodal distribution of stomatal apertures, because such a patchy distribution of infiltrated areas can be observed for normally distributed stomatal apertures near the threshold of infiltratable conductance (Figure 7). The results of a simulation of stomatal apertures based on a stomatal conductance distribution model revealed that, if the stomatal apertures are distributed bimodally, the relationship between g_{sleaf} and the infiltration ratio would be linear (i.e., the infiltration ratio is 100% when $g_{\mathrm{sleaf}} = g_{\mathrm{smax}}$ and 0% when $g_{\mathrm{sleaf}} = g_{\mathrm{smin}}$; Figure 7a). By contrast, for normally distributed stomatal apertures, the smaller the deviation of the distribution from normality, the greater the increase in the infiltration ratio near the threshold for conductance (Figure 7b). Figure 8 shows a comparison between the observed and simulated relationships of g_{sleaf} and the infiltration ratio for each of the species examined. The observed relationship between these two parameters suggests that stomatal apertures follow a normal distribution in *C. camphora* and *A. indica*; a difference in thresholds might account for the apparent discrepancy between the observed and simulated relationship. The threshold values, corresponding to the liquid-phase conductance allowing infiltration, were not clarified because of insufficient measurements, although these values may range around the values of single stomata for several reasons, including plant species, type of liquid and surface tension (e.g., 0.065–0.069 mol $\mathrm{m^{-2}\ s^{-1}}$; leaves of Mediterranean evergreen sclerophylls infiltrated by double-distilled water at an infiltration pressure of 300 kPa; Beyschlag et al. 1992). By contrast, the relationship between g_{sleaf} and the infiltration ratio is linear for *N. heimii* and *D. sublamellatus*, indicating that stomatal apertures are bimodally

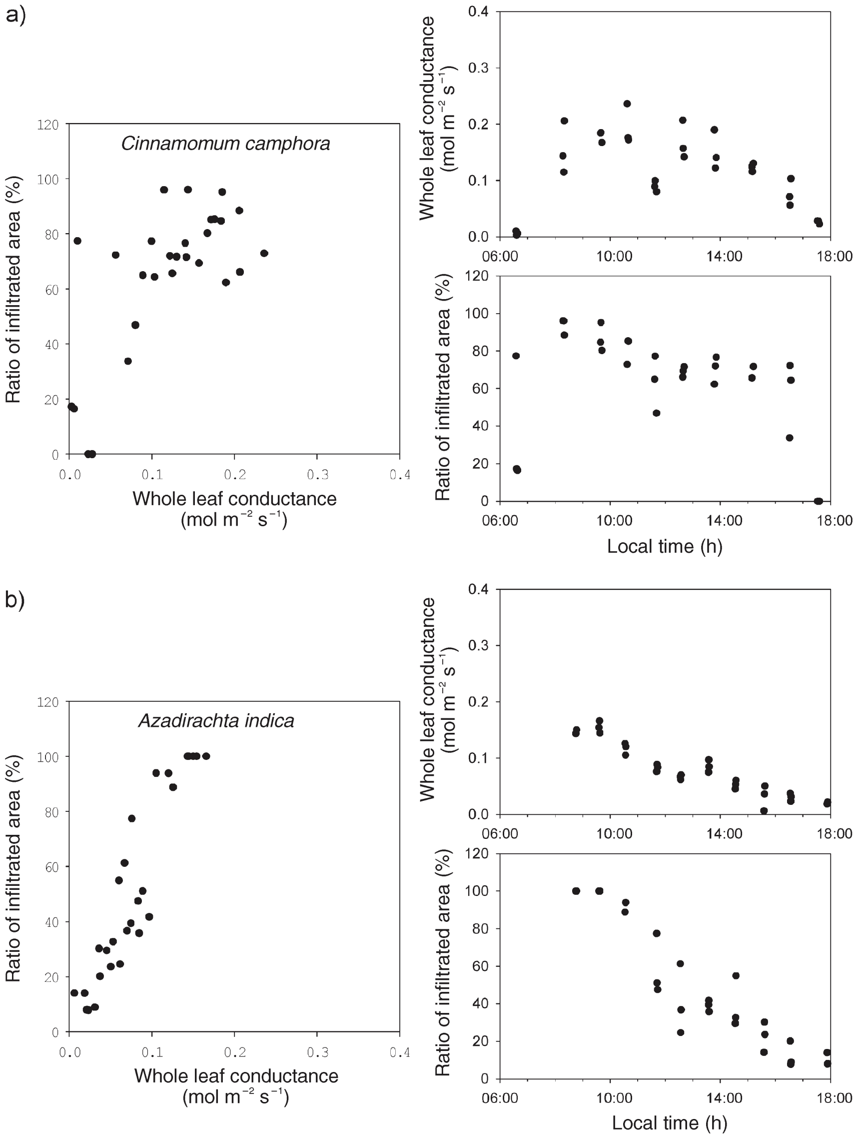

Figure 4. Diurnal relationships between mean whole-leaf stomatal conductance and the infiltration ratio for (a) *Cinnamomum camphora* and (b) *Azadirachta indica*.

distributed in these species. We estimated g_{smax} for *N. heimii* and *D. sublamellatus*—as the value of whole-leaf conductance for a leaf entirely infiltrated—from the relationships between whole-leaf conductance and the ratio of infiltrated to non-infiltrated area by linear-regression. The values of g_{smax} for *N. heimii* and *D. sublamellatus* were 0.34 and 0.25 mol m^{-2} s^{-1}, respectively. These results are similar to those reported by Beyschlag et al. (1992), who described a linear relationship between whole-leaf conductance and the amount of liquid per unit area that infiltrated potted plants of the Mediterranean sclerophylls, *Arbutus unedo* L. and *Quercus suber* L. (leaf thickness was similar among the leaves of the species). A bimodal distribution of stomatal apertures probably causes a depression in the efficiency of carboxylation at midday. Our data on the distribution of stomatal apertures in *N. heimii* and *D. sublamellatus* are consistent with the relationship between transpiration rate and the infiltration ratio in canopy tree species (Dipterocarpaceae) in the lowland rain forests of Malaysia (Lambir, Sarawak; Hiromi et al. 1999).

Effects of patchy stomatal behavior on gas exchange

To analyze the effects of patchy stomatal behavior on the characteristics of leaf gas exchange, we compared the observed and simulated values of the maximum carboxylation rate, V_{cmax25}*. We integrated stomatal conductance and assimilation rate over patches using both the patchy stomatal distribution model and a model of biochemical photosynthesis, and then calculate C_i* and V_{cmax25}*. Figure 9 shows the relationship between g_{sleaf} and V_{cmax25}* for *D. sublamellatus* and *N. heimii*. Both a bimodal distribution and a normal distribution (with

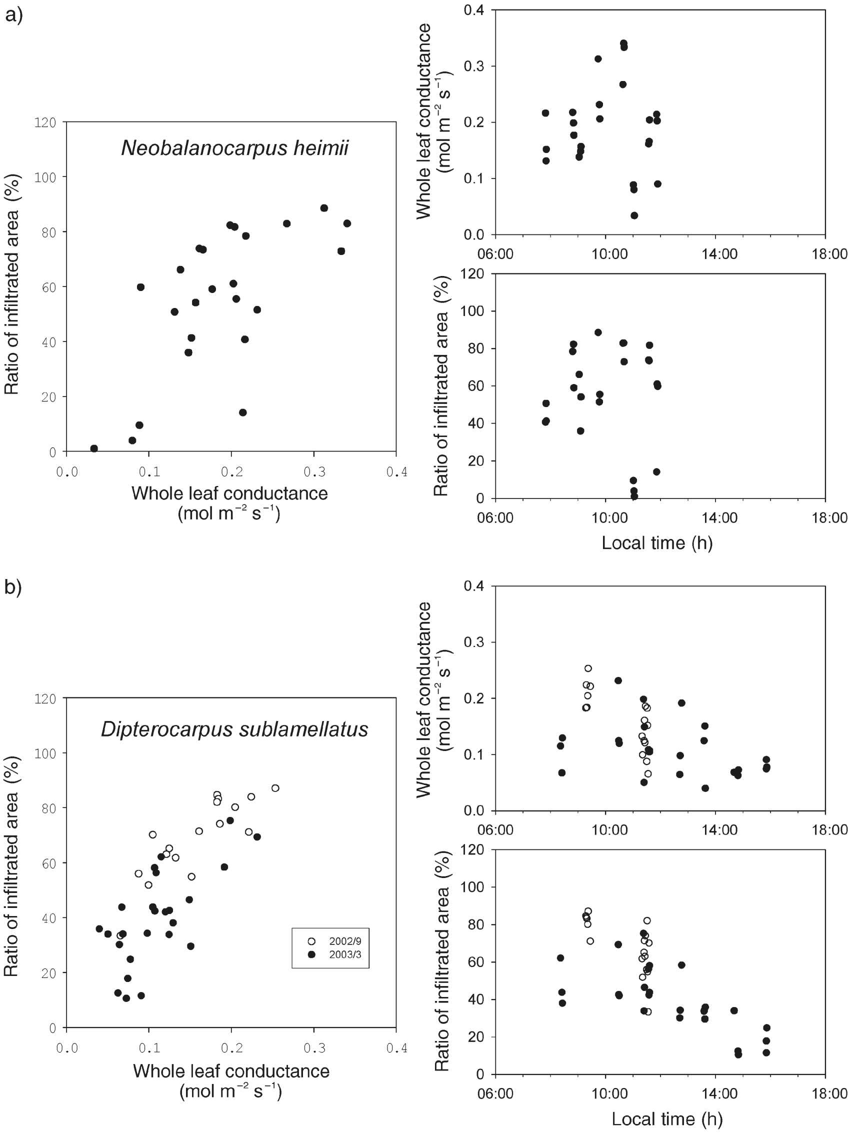

Figure 5. Diurnal relationships between mean whole-leaf stomatal conductance and the infiltration ratio for (a) *Neobalanocarpus heimii* and (b) *Dipterocarpus sublamellatus*.

two different standard deviations) of stomatal apertures were simulated with $V_{\mathrm{cmax25}}^* = 25$ μmol m^{-2} s^{-1}, $g_{\mathrm{smin}} = 0.016$ mol m^{-2} s^{-1} and $g_{\mathrm{smax}} = 0.25$ mol m^{-2} s^{-1}. The values of V_{cmax25}^* were calculated under constant conditions of leaf temperature (30 °C), ambient CO_2 concentration (380 ppm), boundary layer conductance (4.64 mol m^{-2} s^{-1}), ambient vapor pressure (20 hPa), and PAR (1000 μmol m^{-2} s^{-1}). For the bimodal distribution of stomatal apertures, V_{cmax25}^* decreased from 25 μmol m^{-2} s^{-1} to about 10 μmol m^{-2} s^{-1} as g_{sleaf} decreased, although the actual value of V_{cmax25}^* in this model was constant (25 μmol m^{-2} s^{-1}). The relationship between g_{sleaf} and V_{cmax25}^* was linear for the bimodal distribution; the value of V_{cmax25}^* decreased as g_{sleaf} decreased. The reduction in V_{cmax25}^* was greater at greater deviations for the normal distribution, but the reduction was smaller than that shown for the bimodal distribution. The minimum values of V_{cmax25}^* were ~16 μmol m^{-2} s^{-1} for a standard deviation of 0.09 and ~23 μmol m^{-2} s^{-1} for a standard deviation of 0.01. The observed and simulated values of V_{cmax25}^* were similar for the bimodal distribution, except at low values of V_{cmax25}^* (Figure 10). This does not imply that all changes in V_{cmax25}^* are the result of patchy stomatal behavior, especially at low V_{cmax25}^* values (low g_{sleaf}). The changes may also result from changes in mesophyll functioning such as: (a) a decline in the rate of electron transport caused by photoinhibition; (b) a reduction in transfer conductance from the intercellular space to the site of carboxylation; or (c) an increase in photorespiration. However, the observed electron transport rates were not sufficiently low to explain the reduction in V_{cmax25}^* (Figure 6c), and the model simulation revealed that the larger the range of stomatal conductance, the more lin-

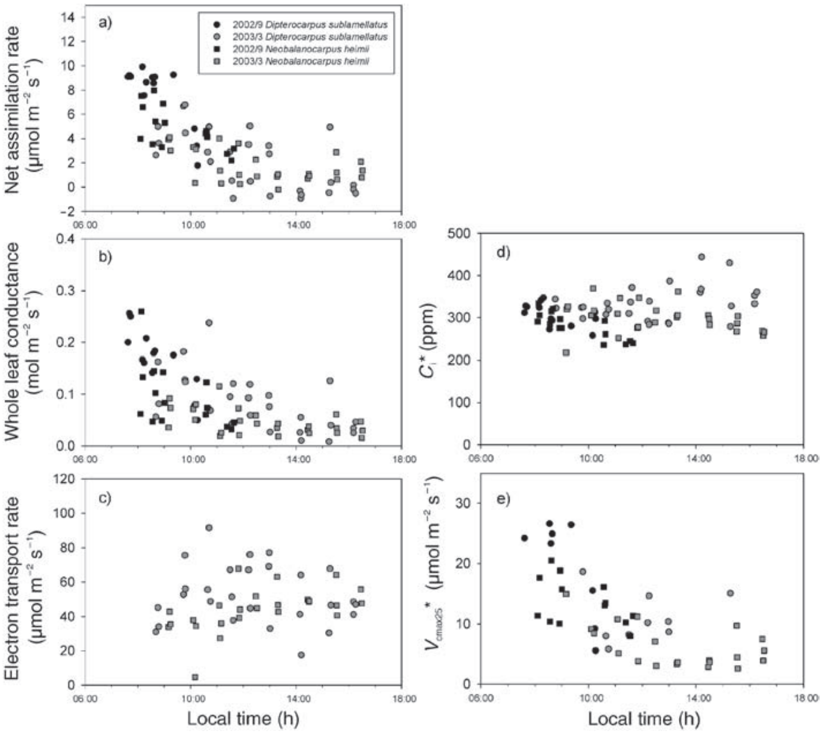

Figure 6. Diurnal changes in (a) net assimilation rate; (b) mean whole-leaf stomatal conductance; (c) electron transport rate; (d) apparent intercellular CO$_2$ concentration (C_i*); and (e) apparent normalized maximum carboxylation rate at 25 °C (V_{cmax25}*) under light-saturated conditions for *Neobalanocarpus heimii* and *Dipterocarpus sublamellatus*.

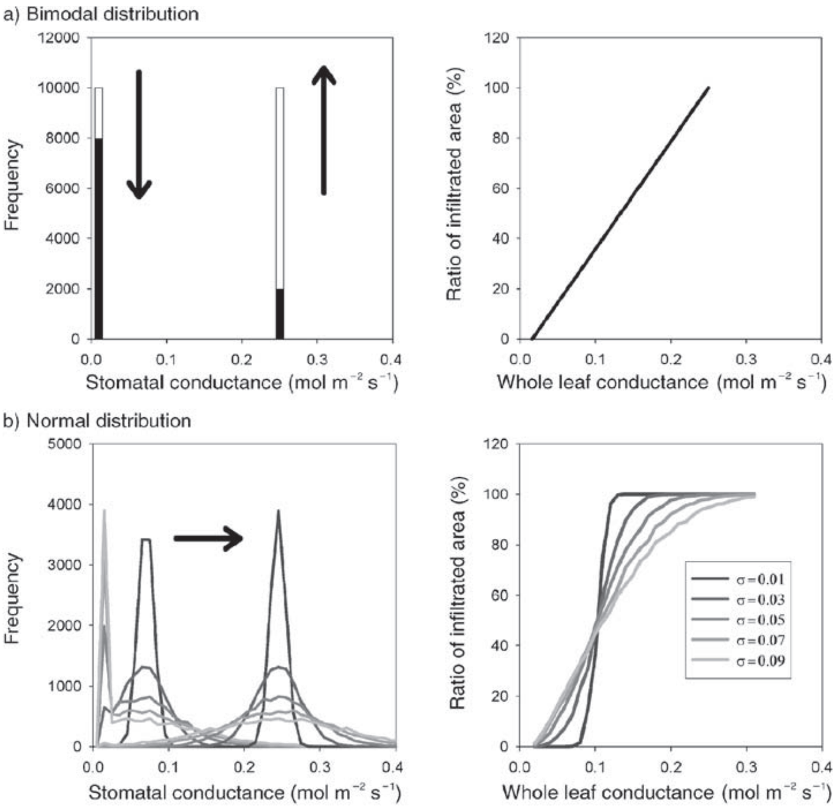

Figure 7. Relationships between simulated mean whole-leaf stomatal conductance and the simulated ratio of infiltrated area for (a) bimodal and (b) normal distributions of stomatal apertures. The values of stomatal conductance for a closed patch (g_{smin}) and for an open patch (g_{smax}) were 0.016 and 0.25 mol m^{-2} s^{-1}, respectively. The threshold value of mean whole-leaf stomatal conductance (g_{sleaf}) was 0.1 mol m^{-2} s^{-1}. Arrows represent the direction of changes in the distribution when the value of g_{sleaf} increased. There are peaks around g_{smin} for the normal distribution because stomatal conductance values that were smaller than g_{smin} were made equal to g_{smin}.

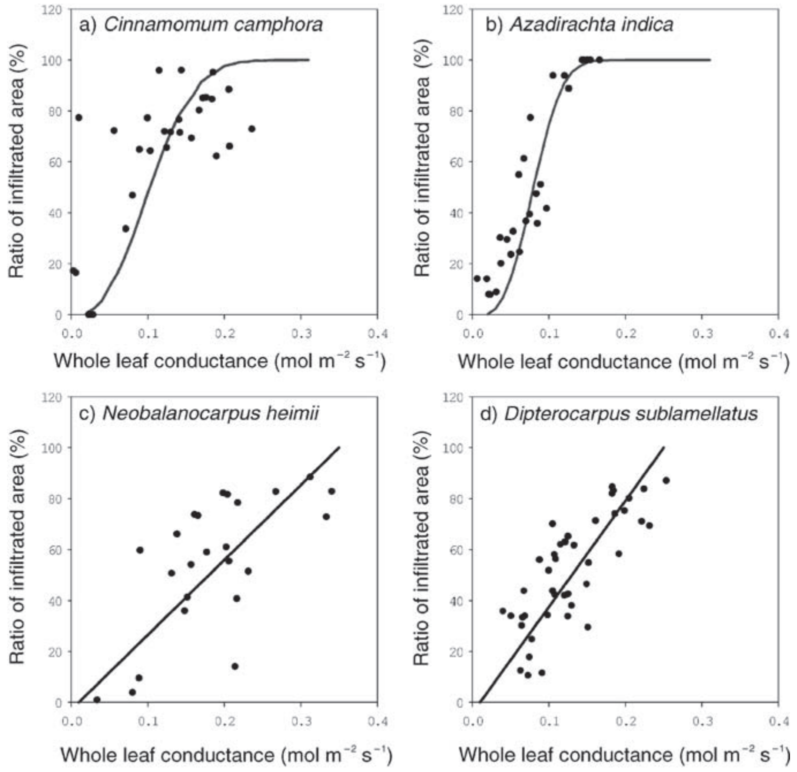

Figure 8. Comparison of the simulated (lines) and observed (●) relationship between mean whole-leaf stomatal conductance and the infiltration ratio in: (a) *Cinnamomum camphora*; (b) *Azadirachta indica*; (c) *Dipterocarpus sublamellatus*; and (d) *Neobalanocarpus heimii*. The lines in (a) and (b) represent the simulated relationship under a normal distribution of stomatal conductance with standard deviations of 0.05 and 0.03, respectively, and threshold value of 0.1 mol m^{-2} s^{-1}, whereas those in (c) and (d) represent the relationship under a bimodal distribution. The solid lines in (c) and (d) were fitted from linear regressions, and the values of stomatal conductance for an open patch (g_{smax}) for *N. heimii* and *D. sublamellatus* were 0.34 and 0.25 mol m^{-2} s^{-1}, respectively.

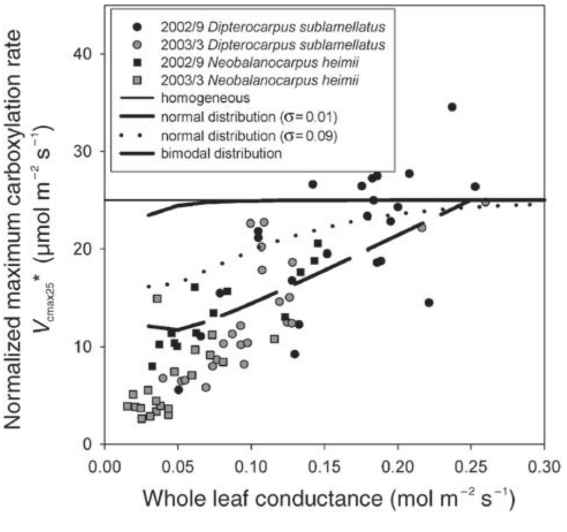

Figure 9. Relationships between mean whole-leaf stomatal conductance and normalized maximum carboxylation rate (V_{cmax25}*) for *Dipterocarpus sublamellatus* and *Neobalacarpus heimii*. A bimodal and a normal distribution (with two different standard deviations) of stomatal apertures were simulated. For the simulations, V_{cmax25} = 25 μmol m^{-2} s^{-1}; stomatal conductance for a closed patch (g_{smin}) = 0.016 mol m^{-2} s^{-1}; and stomatal conductance for an open patch (g_{smax}) = 0.25 mol m^{-2} s^{-1}. The simulated values of V_{cmax25}* were calculated for different values of mean whole-leaf stomatal conductance (g_{sleaf}) under constant conditions.

ear the relationship between g_{sleaf} and the infiltration ratio. Figure 11 shows the sensitivity of V_{cmax25}* to changes in internal conductance (g_i) and g_{sleaf}. Internal conductance has no important influence on the relationships between g_{sleaf} and V_{cmax25}*, although it affects the absolute value of V_{cmax25}*. The relationships between g_{sleaf} and V_{cmax25}* could be explained if g_i dynamically decreases with decreasing g_{sleaf}. Many articles report that g_i is affected by leaf anatomy, including the chloroplast surface area facing the intercellular airspaces and the thickness of mesophyll cell walls (e.g., Terashima et al. 2001, Evans et al. 1994, Kogami et al. 2001), although few articles report that g_i could change as rapidly as g_{sleaf} in response to a protein-mediated process; possibly involving a carbonic anhydrase or aquaporins (Bernacchi et al. 2002, Centritto et al. 2003). The absolute values of V_{cmax25} and g_i can be determined by the isotopic method or by chlorophyll fluorescence analysis combined with gas-exchange measurements.

The observed relationships strongly suggest that stomatal conductance in *D. sublamellatus* and *N. heimii* follows a bimodal distribution. Ishida et al. (1999*b*) reported that the depression of net photosynthesis at a given electron transport rate in tropical trees was caused by photorespiration or patchy stomatal behavior, or both, when the influences of nitrogen assimilation and photoinhibition were small. The strong correlation between g_{sleaf} and V_{cmax25}* in our study suggests that the afternoon depression of V_{cmax25}* in *D. sublamellatus* and *N. heimii* is caused mainly by bimodal closure of stomata.

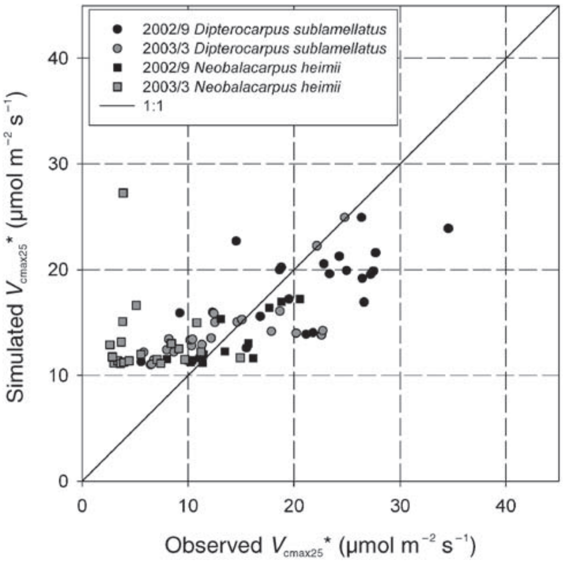

Figure 10. Comparison of simulated normalized apparent maximum carboxylation rate at 25 °C (V_{cmax25}*) under a bimodal distribution of stomatal apertures and the observed values for *Dipterocarpus sublamellatus* and *Neobalacarpus heimii*.

In conclusion, to investigate the effect of a heterogeneous distribution of stomatal apertures on the characteristics of gas exchange in the leaves of trees from different climates (temperate, tropical monsoon and tropical rain forest habitats), we combined the measurement of gas exchange with the pressure infiltration method in the field and also carried out computer model-based simulations. The field observations revealed that the relationship between g_{sleaf} and the infiltration ratio is linear in leaves from *D. sublamellatus* and *N. heimii*, which grow in the tropical rain forests of the Malaysian peninsula. By contrast, in leaves from *C. camphora* (which grows in temperate evergreen forests in Japan) and *A. indica* (from the tropical monsoon area of Thailand), the infiltration ratio increased rapidly beyond a point that corresponded to the whole-leaf stomatal conductance threshold. In *D. sublamellatus* and *N. heimii*, the value of V_{cmax25}* (derived from field observations by the one-point method) was not constant but rather decreased as g_{sleaf} decreased. The patchy stomatal conductance distribution model revealed that, when the stomatal conductance followed a bimodal distribution, there was a linear relationship between g_{sleaf} and the infiltration ratio; when the stomatal conductance followed a normal distribution, increasingly smaller deviations from normal distribution were associated with increasingly greater increases in the infiltration ratio near the threshold conductance. Simulated V_{cmax25}* decreased as g_{sleaf} decreased, and this decline was greater for a bimodal distribution of stomatal apertures than for a normal distribution. These results suggest that the stomatal conductance distribution has a relatively narrow range in *C. camphora* and *A. indica*, whereas stomatal conductance is distributed bimodally in *D. sublamellatus* and *N. heimii*. The midday depression of V_{cmax25}* in *D. sublamellatus* and *N. heimii* would result mainly from the bimodal closure of stomata. The bimodal stomatal distribution model could also explain the rates of photosynthetic assimilation and transpiration in these species.

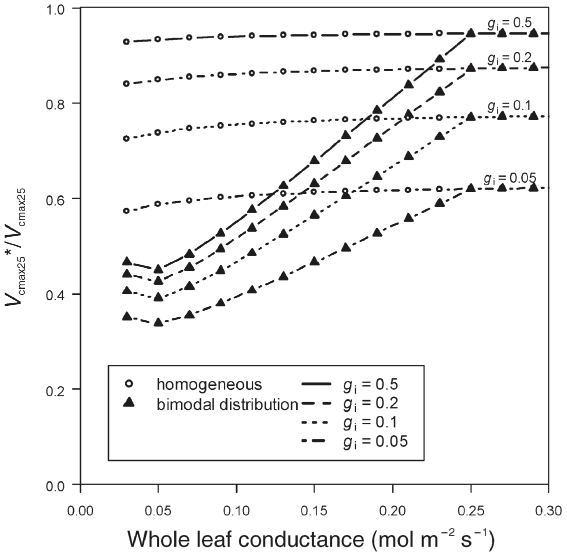

Figure 11. Sensitivity of normalized apparent maximum carboxylation rate at 25 °C (V_{cmax25}*) to changes in internal conductance (g_i) and whole-leaf conductance (g_{sleaf}) expressed as the ratio of V_{cmax25}* to V_{cmax25}. Symbols represent different stomatal conductance distributions and line-types represents different values.

Acknowledgments

This work was partially supported by the Global Environmental Research Fund. We thank the Forestry Department of Negeri Sembilan and the Director General of the Forest Research Institute of Malaysia for permission to work at the Pasoh Forest Reserve in Malaysia. We thank the Kansai Electric Power Co., Inc. and Kansai Environmental Engineering Center Co., Ltd. (KANSO), especially Mr. Masayuki Yamauchi, for assistance with the field observations at the Akou Power Station in Japan. We also thank Dr. Motomu Toda for assistance with the field observations in Thailand.

References

Baldocchi, D. and T. Meyers. 1998. On using ecophysiological, micrometeorological and biogeochemical theory to evaluate carbon dioxide, water vapor and trace gas fluxes over vegetation: a perspective. Agric. For. Meteorol. 90:1–25.

Baldocchi, D.D., K.B. Wilson and L. Gu. 2002. How the environment, canopy structure and canopy physiological functioning influence carbon, water and energy fluxes of a temperate broadleaved deciduous forest—an assessment with the biophysical model CANOAK. Tree Physiol. 22:1065–1077.

Bernacchi, C.J., A.R. Portis, H. Nakano, S. von Caemmerer and S.P. Long. 2002. Temperature response of mesophyll conductance. Implications for the determination of Rubisco enzyme kinetics and for limitations to photosynthesis in vivo. Plant Physiol. 130: 1992–1998.

Beyschlag, W. and H. Pfanz. 1990. A fast method to detect the occurrence of nonhomogeneous distribution of stomatal aperture in heterobaric plant leaves. Oecologia 82:52–55.

Beyschlag, W. and J. Eckstein. 1998. Stomatal patchiness. *In* Progress in Botany. Eds. H.-D. Behnke, K. Esser, J.W. Kadereit, U. Lüttge and M. Runge. Springer-Verlag, Berlin, pp 283–298.

Beyschlag, W., H. Pfanz and R.J. Ryel. 1992. Stomatal patchiness in Mediterranean evergreen sclerophylls: phenomenology and consequences for the interpretation of the midday depression in photosynthesis and transpiration. Planta 187:546–553.

Bro, E., S. Meyer and B. Genty. 1996. Heterogeneity of leaf CO_2 assimilation during photosynthetic induction. Plant Cell Environ. 19:1349–1358.

Brooks, A. and G. Farquhar. 1985. Effect of temperature on the CO_2/O_2 specificity of ribulose-1,5-bisphosphate carboxylase/oxygenase and the rate of respiration in the light. Planta 165: 397–406.

Buckley, T.N. and K.A. Mott. 2000. Stomatal responses to non-local changes in PFD: evidence for long-distance hydraulic interactions. Plant Cell Environ. 23:301–309.

Buckley, T.N., G.D. Farquhar and K.A. Mott. 1997. Qualitative effects of patchy stomatal conductance distribution features on gas-exchange calculations. Plant Cell Environ. 20:867–880.

Cardon, Z.G., K.A. Mott and J.A. Berry. 1994. Dynamics of patchy stomatal movements, and their contribution to steady-state and oscillating stomatal conductance calculated using gas-exchange techniques. Plant Cell Environ. 17:995–1007.

Centritto, M., F. Loreto and K. Chartzoulakis. 2003. The use of low [CO_2] to estimate diffusional and non-diffusional limitations of photosynthetic capacity of salt-stressed olive saplings. Plant Cell Environ. 26:585–594.

Cheeseman, J.M. 1991. PATCHY: simulating and visualizing the effects of stomatal patchiness on photosynthetic CO_2 exchange studies. Plant Cell Environ. 14:593–599.

Cowan, I.R. 1977. Stomatal behavior and environment. Adv. Bot. Res. 4:117–228.

Daley, P.F., K. Raschke, J.T. Ball and J.A. Berry. 1989. Topography of photosynthetic activity of leaves obtained from video images of chlorophyll fluorescence. Plant Physiol. 90:1233–1238.

Downton, W.J.S., B.R. Loveys and W.J.R. Grant. 1988. Stomatal closure fully accounts for the inhibition of photosynthesis by abscisic acid. New Phytol. 108:263–266.

Düring, H. and B.R. Loveys. 1996. Stomatal patchiness of field-grown Sultana leaves: diurnal changes and light effects. Vitis 35: 7–10.

Eckstein, J., W. Beyschlag, K.A. Mott and R. Ryel. 1996. Changes in photon flux induce stomatal patchiness. Plant Cell Environ. 19: 1066–1074.

Evans, J.R., S. von Caemmerer, B.A. Setchell and G.S. Hudson. 1994. The relationship between CO_2 transfer conductance and leaf anatomy in transgenic tobacco with a reduced content of Rubisco. Aust. J. Plant Physiol. 21:475–495.

Farquhar, G.D. and S.C. Wong. 1984. An empirical model of stomatal conductance. Aust. J. Plant Physiol. 11:191–210.

Farquhar, G.D., S. von Caemmerer and J.A. Berry. 1980. A biochemical model of photosynthetic CO_2 assimilation in leaves of C_3 species. Planta 149:78–90.

Grassi, G., E. Vicinelli, F. Ponti, L. Cantoni and F. Magnani. 2005. Seasonal and interannual variability of photosynthetic capacity in relation to leaf nitrogen in a deciduous forest plantation in northern Italy. Tree Physiol. 25:349–360.

Gunasekera, D. and G.A. Berkowitz. 1992. Heterogenous stomatal closure in response to leaf water deficits is not a universal phenomenon. Plant Physiol. 98:660–665.

Haefner, J.W., T.N. Buckley and K.A. Mott. 1997. A spatially explicit model of patchy stomatal responses to humidity. Plant Cell Environ. 20:1087–1097.

Harley, P.C. and D.D. Baldocchi. 1995. Scaling carbon dioxide and water vapor exchange from leaf to canopy in a deciduos forest. I. Leaf model parameterization. Plant Cell Environ. 18:1146–1156.

Hiromi, T., I. Ninomiya, T. Koike and K. Ogino. 1999. Regulation of transpiration by patchy stomatal opening in canopy tree species of dipterocarpaceae in tropical rain forest, Sarawak, Malaysia. Jpn. J. Ecol. 49:83–90. In Japanese with English abstract.

Ishida, A., T. Toma and Marjenah. 1999*a*. Leaf gas exchange and cholorphyll fluorescence in relation to leaf angle, azimuth, and canopy position in the tropical pioneer tree, *Macaranga conifera*. Tree Physiol. 19:117–124.

Ishida, A., T. Toma and Marjenah. 1999*b*. Limitation of leaf carbon gain by stomatal and photochemical processes in the top canopy of *Macaranga conifera*, a tropical pioneer tree. Tree Physiol. 19: 467–473.

Jarman, P.D. 1974. The diffusion of carbon dioxide and water vapour through stomata. J. Exp. Bot. 25:927–936.

Jones, H.G. 1992. Plants and microclimate: a quantitative approach to environmental plant physiology. 2nd Edn. Cambridge Univ. Press, Cambridge, 428 p.

Jones, H.G. 1998. Stomatal control of photosynthesis and transpiration. J. Exp. Bot. 49:387–398.

Jones, H.G. 1999. Use of thermography for quantitative studies of spatial and temporal variation of stomatal conductance over leaf surface. Plant Cell Environ. 22:1043–1055.

Kogami, H., Y.T. Hanba, T. Kibe, I. Terashima and T. Masuzawa. 2001. CO_2 transfer conductance, leaf structure and carbon isotope composition of *Polygonum cuspidatum* leaves from low and high altitudes. Plant Cell Environ. 24:529–538.

Kosugi, Y., S. Shibata and S. Kobashi. 2003. Parameterization of the CO_2 and H_2O gas exchange of several temperate deciduous broad-leaved trees at the leaf scale considering seasonal changes. Plant Cell Environ. 26:285–301.

Laisk, A. 1983. Calculation of leaf photosynthetic parameters considering the statistical distribution of stomatal apertures. J. Exp. Bot. 34:1627–1635.

Laisk, A., V. Oja and K. Kull. 1980. Statistical distribution of stomatal apertures of *Vicia faba* and *Hordeum vulgare* and the *Spannungsphase* of stomatal opening. J. Exp. Bot. 31:49–58.

Lambers, H., F.S. Chapin, III and T.L. Pons. 1998. Plant water relations. *In* Plant Physiological Ecology. Eds. H. Lambers, F.S. Chapin, III and T.L. Pons. Springer-Verlag, New York, pp 154–209.

Larcher, W. 2003. Physiological plant ecology: ecophysiology and stress physiology of functional groups. 4th Edn. Springer-Verlag, Berlin, 513 p.

Leuning, R. 1997. Scaling to a common temperature improves the correlation between the photosynthesis parameters J_{max} and V_{cmax}. J. Exp. Bot. 48:345–347.

Leuning, R., F.M. Kelliher, D.G.G. De Pury and E.-D. Schulze. 1995. Leaf nitrogen, photosynthesis, conductance and transpiration: scaling from leaves to canopies. Plant Cell Environ. 18:1183–1200.

Loreto, F. and T.D. Sharkey. 1990. Low humidity can cause uneven photosynthesis in olive (*Olea europea* L.) leaves. Tree Physiol. 6: 409–415.

Meyer, S. and B. Genty. 1998. Mapping intercellular CO_2 mole fraction (C_i) in *Rosa rubiginosa* leaves fed with abscisic acid by using chlorophyll fluorescence imaging. Plant Physiol. 116:947–957.

Mott, K. and T. Buckley. 1998. Stomatal heterogeneity. J. Exp. Bot. 49:407–417.

Mott, K.A., Z.G. Cardon and J.A. Berry. 1993. Asymmetric patchy stomatal closure for the two surfaces of *Xanthium strumarium* L. leaves at low humidity. Plant Cell Environ. 16:25–34.

Mott, K.A., F. Denne and J. Powell. 1997. Interactions among stomata in response to perturbations in humidity. Plant Cell Environ. 20: 1098–1107.

Sharkey, T.D. and J.R. Seemann. 1989. Mild water stress effects on carbon-reduction-cycle intermediates, ribulose bisphosphate carboxylase activity, and spatial homogeneity of photosynthesis in intact leaves. Plant Physiol. 89:1060–1065.

Smith, S., J.D.B. Weyers and W.G. Berry. 1989. Variation in stomatal characteristics over the lower surface of *Commelina communis* leaves. Plant Cell Environ. 12:653–659.

Tanaka, K., Y. Kosugi and A. Nakamura. 2002. Impact of leaf physiological characteristics on seasonal variation in CO_2, latent and sensible heat exchanges over a tree plantation. Agric. For. Meteorol. 114:103–122.

Terashima, I. 1992. Anatomy of non-uniform leaf photosynthesis. Photosynth. Res. 31:195–212.

Terashima, I., S.C. Wong, C.B. Osmond and G.D. Farquhar. 1988. Characterization of non-uniform photosynthesis induced by abscisic acid in leaves having different mesophyll anatomies. Plant Cell Physiol. 29:385–394.

Terashima, I., S. Miyazawa and Y.T. Hanba. 2001. Why are sun leaves thicker than shade leaves? Consideration based on analyses of CO_2 diffusion in the leaf. J. Plant Res. 114:93–105.

Toma, T. and A. Furukawa. 1995. CO_2 assimilation rate of canopy leaves in rain forest trees: high or low? Tropics 4:287–296. In Japanese with English abstract.

van Gardingen, P.R., C.E. Jeffree and J. Grace. 1989. Variation in stomatal aperture in leaves of *Avena fatua* L. observed by low-temperature scanning electron microscopy. Plant Cell Environ. 12: 887–898.

von Caemmerer, S. and G.D. Farquhar. 1981. Some relationships between the biochemistry of photosynthesis and the gas exchange of leaves. Planta 153:376–387.

Weyers, J.D.B. and T. Lawson. 1997. Heterogeneity in stomatal characteristics. Adv. Bot. Res. 26:317–352.

Wilson, K.B., D.D. Baldocchi and P.J. Hanson. 2000. Spatial and seasonal variability of photosynthetic parameters and their relationship to leaf nitrogen in a deciduous forest. Tree Physiol. 20: 565–578.

Wise, R.R., S. Oritiz-Lopez and D.R. Ort. 1992. Spatial distribution of photosynthesis during drought in field-grown and acclimated and nonacclimated growth chamber-grown cotton. Plant Physiol. 100:26–32.

Wohlfahrt, G., M. Bahn, E. Haubner, I. Horak, W. Michaeler, K. Rottmar, U. Tappeiner and A. Cernusca. 1999. Inter-specific variation of the biochemical limitation to photosynthesis and related leaf traits of 30 species from mountain grassland ecosystems under different land use. Plant Cell Environ. 22:1281–1296.

Wullschleger, S.D. 1993. Biochemical limitations to carbon assimilation in C_3 plants—a retrospective analysis of the A/C_i curves from 109 species. J. Exp. Bot. 44:907–920.

Tree Physiology 29, 505–515
doi:10.1093/treephys/tpn041

Midday depression of leaf CO_2 exchange within the crown of *Dipterocarpus sublamellatus* in a lowland dipterocarp forest in Peninsular Malaysia

YOSHIKO KOSUGI,[1,2] SATORU TAKANASHI,[3] NAOKO MATSUO[4] and ABDUL RAHIM NIK[5]

[1] *Graduate School of Agriculture, Kyoto University, Kyoto 606-8502, Japan*

[2] *Corresponding author (ykosugi@kais.kyoto-u.ac.jp)*

[3] *Forestry and Forest Products Research Institute, Tsukuba, Ibaraki 305-8687, Japan*

[4] *Graduate School of Bioresources, Mie University, Tsu, Mie 514-8507, Japan*

[5] *Forest Research Institute Malaysia, Kepong, Kuala Lumpur 52109, Malaysia*

Received October 6, 2008; accepted November 23, 2008; published online January 30, 2009

Summary We observed diurnal and seasonal patterns of leaf-scale gas exchange within the crown of a *Dipterocarpus sublamellatus* Foxw. tree growing in a lowland dipterocarp forest at Pasoh, Peninsular Malaysia. Observations were carried out nine times over 6 years, from September 2002 to December 2007. Observation periods included both wet and mild-dry periods, and natural and saturated photosynthetic photon flux density (PPFD) light conditions. In situ measurements of the diurnal change in net photosynthetic rate and in stomatal conductance were carried out on canopy leaves of a 40-m-tall *D. sublamellatus* tree, which was accessed from a canopy corridor. A diurnal change in electron transport rate was observed under saturated PPFD conditions. The maximum net assimilation rate was $\sim 10\ \mu\text{mol m}^{-2}\ \text{s}^{-1}$. There was a clear inhibition of the net assimilation rate coupled with stomatal closure after late morning and this inhibition occurred year-round. Although the electron transport rate decreased alongside this inhibition, it sometimes followed on. Numerical analysis showed that the main factor in the inhibition of the net assimilation rate was patchy bimodal stomatal closure, which occurred in both mild-dry and wet periods. The midday depression occurred year-round, though there are fluctuations in soil moisture during the mild-dry and wet periods. The magnitude of the inhibition was not related to soil water content but was related to vapor pressure deficit (VPD): that is, whether the days were sunny and hot or cloudy and cool. On cloudy, cool days in the wet period, the net photosynthesis was only moderately inhibited, but it still decreased in the afternoon and was coupled with patchy stomatal closure, even in quite moderate VPD, leaf temperature and PPFD conditions. Our results suggest that patchy stomatal closure signaled by the increase in VPD, in transpiration and by circadian rhythms, was the key factor in constraining midday leaf gas exchange of the *D. sublamellatus* canopy leaves.

Keywords: electron transport rate, net assimilation rate, patchy stomatal closure, stomatal conductance, tropical rainforest.

Introduction

Tropical rainforests play a major role in the global carbon budget because they are the greatest global source of net primary production from photosynthesis of canopy tree leaves. To better understand the roles of tropical rainforests in the global carbon budget, we need to clarify the nature and the magnitude of diurnal, seasonal and annual CO_2 exchanges in tropical rainforests and to determine the factors that control the CO_2 exchanges at different timescales.

In many tropical forests, the diurnal pattern of CO_2 exchange at the canopy-scale shows a clear restriction of canopy photosynthesis in the afternoon (Malhi et al. 1998, 1999, Araujo et al. 2002, Saleska et al. 2003, Goulden et al. 2004, Vourlitis et al. 2004, Kumagai et al. 2006, Kosugi et al. 2008). Vourlitis et al. (2004) conducted their study in a Brazilian transitional tropical forest with clear dry and rainy seasons, and reported differences in net ecosystem exchange (NEE) and the magnitude of midday depression among trees during wet, wet–dry transition, dry and dry–wet transition periods. Kosugi et al. (2008) carried out their study in a primary tropical rainforest at Pasoh (Peninsular Malaysia) that receives relatively less rainfall (1804 mm) during two moderate-wet and mild-dry periods. They found that the diurnal pattern of NEE and the magnitude of midday depression were similar every month for 3 years, and there were no differences related to soil moisture or wet and mild-dry periods. These two studies provide some data, but the seasonal and the inter-annual trends coupled with various rainfall patterns in the tropical forest ecosystems remain unclear because of the lack of a long-term dataset.

Canopy-scale photosynthesis is mainly determined by gas exchange of leaves at the top of the canopy. Therefore, we should investigate the gas exchange characteristics of the canopy leaves to identify the factors affecting midday depression and its seasonal, inter-annual and regional variations and the effects of rainfall patterns. Some aspects of the leaf gas exchange are well understood, such as the relationship between leaf nitrogen content/nitrogen allocation and gas exchange (e.g., Field 1983, Evans 1987, Evans 1993, Hikosaka and Terashima 1995, Niinemets and Tenhunen 1997, Takashima et al. 2004). However, instantaneous leaf gas exchange in natural conditions is a dynamic process that is affected by many micrometeorological and physiological factors. Ishida et al. (1999) reported severe midday depression of photosynthesis coupled with stomatal closure in the upper canopy leaves of a tropical pioneer tree during a severe ENSO-related drought. As summarized by Ishida et al. (1996, 1999), midday depression may be caused by both stomatal and non-stomatal factors, although stomatal limitations can be obscured because of the patchy stomatal behavior (Terashima et al. 1988). When the pattern of stomatal closure is patchy, the stomatal effects on midday depression of photosynthesis can be underestimated in analyses that rely on uniform leaf intercellular CO_2 concentrations. Using a pressure-infiltration method and a numerical analysis, Takanashi et al. (2006) showed that patchy stomatal closure with a bimodal closure pattern explained the midday depression in top canopy leaves of a tropical rainforest at Pasoh, Peninsular Malaysia. It is still unclear whether midday depression occurs year-round, whether patchy stomatal closure is always the main limiting factor and which environmental or physiological factors induce patchy stomatal closure.

To better understand gas exchange of canopy leaves in tropical rainforests, we carried out long-term observations of diurnal changes in CO_2 exchange in crown leaves of *Dipterocarpus sublamellatus* Foxw., which is one of the dominant species in the Southeast Asian lowland dipterocarp forest at Pasoh, Peninsular Malaysia. The focus of this paper is (1) to describe the magnitude and the fluctuations of CO_2 exchange among crown leaves of *D. sublamellatus*, (2) to describe the midday depression of photosynthesis and its variations during mild-dry and wet periods and (3) to determine which factors limit the net assimilation rate of canopy leaves during mild-dry and wet periods, using a numerical analysis based on the Farquhar–von Caemmerer–Berry model (Farquhar et al. 1980) and taking into account the patchy stomatal behavior (Takanashi et al. 2006).

Materials and methods

Site and materials

The study site was located in the Pasoh Forest Reserve of the Forest Research Institute Malaysia (FRIM), near Simpang Pertang in Negeri Sembilan, in Peninsular Malaysia (2°58′N and 102°18′E, 75–150 m asl). The core area (600 ha) of the reserve (2450 ha) is covered with a primary lowland mixed dipterocarp forest (tropical evergreen broad-leaved forest), which consists of various species of *Shorea* and *Dipterocarpus*. The continuous canopy height is $\sim$ 35 m, although some emergent trees exceed 45 m. Soil type around the tower is Haplic Acrisol (FAO classification). The A horizon is thin (0–5 cm). Lateritic gravels are abundant below a depth of 30 cm (Yamashita et al. 2003). The mean annual rainfall is 1804 mm (1983–1997; Tani et al. 2003).

In situ leaf gas exchange and chlorophyll fluorescence measurements were conducted on intact leaves within the canopy of a 40-m-tall *D. sublamellatus*. This tree is one of the dominant species in this forest and was accessible from a triangle canopy corridor at 31 m height (Figure 1). This forest has two rainy periods that occur from March to May and from October to December, although there are considerable inter-annual fluctuations (Kosugi et al. 2008). We carried out observations nine times during the period from September 2002 to December 2007 to obtain data under a range of environmental and physiological conditions related to mild-dry and wet periods.

Measurements of leaf gas exchange, chlorophyll fluorescence and microclimate

We measured the diurnal change of net photosynthetic rate (A, μmol m^{-2} s^{-1}) and the stomatal conductance for water vapor (g_s, mol m^{-2} s^{-1}) of canopy leaves at the canopy corridor. Photosynthetic photon flux density (PPFD, μmol m^{-2} s^{-1}) conditions were considered to be ‘natural’ on nine measurement days using a clear top chamber: September 19, 2002; March 8, 2003; August 23, 2003; September 10, 2004; November 24, 2004; February 11, 2005; July 3, 2005; October 19, 2005 and December 8, 2007. Saturated PPFD conditions occurred on the other seven measurement days using light-emitting diode chambers: September 20, 2002; March 9, 2003; August 23, 2003; November 23, 2004; July 5, 2005; October 17, 2005 and December 14, 2007. A diurnal change in the maximum electron transport rate (J, μmol m^{-2} s^{-1}) was also observed in saturated PPFD conditions. There is only one individual with sunlit branches that can be accessed from the canopy corridor, so sampling leaves were selected from the sunlit leaves of these branches. Sunlit mature leaves from the upper canopy were chosen. In rainy periods (November 2004 and December 2007), both newly expanded young leaves and older leaves coexisted at the

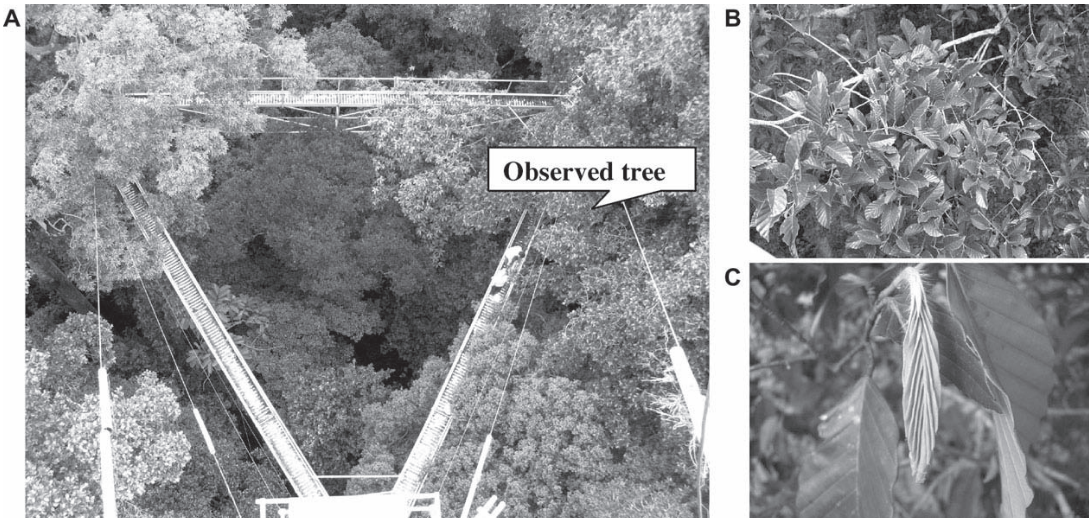

Figure 1. Canopy corridor and tree (*D. sublamellatus*). (A) Canopy corridor and sampled tree. (B) Sunlit foliage of sampled tree. (C) Newly expanding leaves and mature leaves in wet period. A color version of this figure is available as Supplementary Data at *Tree Physiology* Online.

top part of the sunlit branch, so we sampled both leaf types. On each observation day, we sampled 3–5 leaves in saturated PPFD conditions and 3–10 leaves in natural PPFD conditions. Gas exchange of these leaves was measured several times during the daytime. In the natural PPFD conditions, we sometimes included additional leaf samples (1–5 leaves each measurement) which were cut after each observation to measure infiltration ratio or leaf water potential. In that case, we chose new samples from the immediate vicinity at each observation. Each observation was carried out for several minutes under saturated PPFD conditions and immediately under natural PPFD conditions. Observations were conducted every 30–60 min during daytime. The instrument must be set up after dawn (around 7:00 am), so data from the early morning is not included in the dataset. Data from after 5:00 pm is also not included in the dataset, because we left the forest before sunset for safety reasons. In September 2002, it rained in the afternoon, so diurnal observations were discontinued.

An LI-6400 gas-exchange measurement system (Li-Cor Inc., Lincoln, NE) with a 2 × 3 cm clear-top chamber was used to measure the diurnal change of A and g_s under natural PPFD conditions. In saturated PPFD conditions, we used a 2 × 3 cm light-emitting diode chamber or a 6400-40 leaf chamber fluorometer (Li-Cor Inc., Lincoln, NE) to measure the diurnal changes in A, g_s and J. The measurements were conducted under ambient conditions except for light, which was controlled at a PPFD value of 1000 $\mu mol\ m^{-2}\ s^{-1}$. Based on the preliminary test, this PPFD level was usually sufficient to obtain maximum values of A, although some leaves showed depression of A under 1500 or 2000 $\mu mol\ m^{-2}\ s^{-1}$ PPFD. The intercellular CO_2 concentration (C_i, $\mu mol\ mol^{-1}$) was estimated assuming that whole-leaf A and g_s values were uniform.

Meteorological variables monitored at a height of 52 m on the tower included downward short-wave radiation (MR22, Eko, Japan) and rainfall. Soil water content (SWC) at depths of 0.1, 0.2 and 0.3 m were monitored at three points around the tower (CS615 or CS616, Campbell Scientific, Logan, UT). The accumulated precipitation index for 60 days (API_{60}) was defined as $\sum_{i=1}^{60} P_i/i$, where P_i is daily precipitation (mm) and i is the number of preceding days (Kosugi et al. 2007). The API_{60} is used in this study to show the rainfall pattern at the site, and this corresponded well with the average SWC at depths of 0.1, 0.2 and 0.3 m (Figure 2). Canopy-scale gas exchange observed at the top of the flux tower was reported by Takanashi et al. (2005), Kosugi et al. (2008) and Ohkubo et al. (2008).

Numerical analysis

We calculated the ‘apparent’ normalized maximum carboxylation rate (V_{cmax25}*, $\mu mol\ m^{-2}\ s^{-1}$) to evaluate the effect of heterogeneous stomatal behavior on gas exchange, and to directly determine the apparent depression in photosynthetic capacity in the field (Takanashi et al. 2006). The ‘apparent’ maximum carboxylation rate (V_{cmax}*) was calculated using a one-point method (Wilson et al. 2000, Kosugi et al. 2003, Grassi et al. 2005, Kosugi and Matsuo 2006, Takanashi et al. 2006), an inverse method based on the Farquhar–von Caemmerer–Berry model (Farquhar et al. 1980) that can be used to determine the actual responses of leaves in the field. In the one-point method, the apparent partial pressure of CO_2 within the intercellular space ($p(C_i)$*) was estimated from variables measured by the

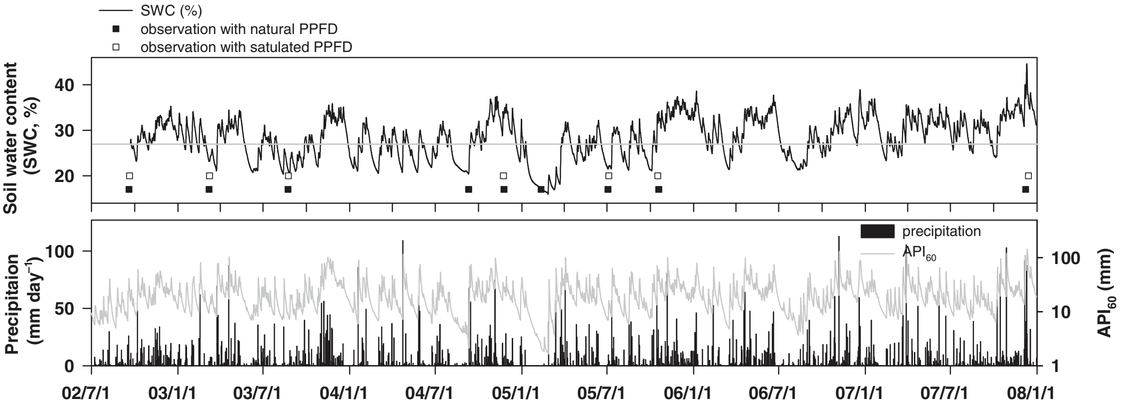

Figure 2. Fluctuation of daily rainfall, % SWC (average value from nine sensors at 0.1-, 0.2- and 0.3-m depth), API_{60} for 6 years from 2002 to 2007, and dates of leaf gas exchange observations under natural PPFD conditions (nine times) and saturated PPFD (seven times). The API_{60} was defined as $\sum_{i=1}^{60} P_i/i$, where P_i is daily precipitation (mm) and i is the number of preceding days. Gray line shows SWC = 27%, which was designated as the cut-off point between wet and mild-dry periods in this study.

gas-exchange method, and the value of V_{cmax25}* was calculated from the values of A, $p(C_i)$* and leaf temperature (T_l) as follows:

$$V_{\mathrm{cmax25}}* = (A+R_{\mathrm{d}})\frac{p(C_i)^* + K_{\mathrm{c}}\left(1+\frac{p(\mathrm{O})}{K_{\mathrm{o}}}\right)}{p(C_i)^* - \frac{p(\mathrm{O})}{2\tau}} \times \frac{1+\exp\left[\frac{\Delta S(V_{\mathrm{cmax}})(T_l+273)-\Delta H_{\mathrm{d}}(V_{\mathrm{cmax}})}{R(T_l+273)}\right]}{\exp\left[\frac{\Delta H_{\mathrm{a}}(V_{\mathrm{cmax}})(T_l-25)}{298R(T_l+273)}\right]}, \tag{1}$$

where R_{d} is the non-photorespiratory respiration rate (μmol $\mathrm{m}^{-2}\ \mathrm{s}^{-1}$), τ is the specificity factor of Rubisco, $p(\mathrm{O})$ (21,000 Pa) is the partial pressure of O_2 at the sites of oxygenation, K_{c} and K_{o} are the Michaelis–Menten constants of Rubisco for CO_2 and O_2, T_l is the leaf temperature (°C), R is the gas constant (8.31 J $\mathrm{K}^{-1}\ \mathrm{mol}^{-1}$), $\Delta H_{\mathrm{a}}(V_{\mathrm{cmax}})$ is the activation energy for V_{cmax}, $\Delta H_{\mathrm{d}}(V_{\mathrm{cmax}})$ is the deactivation energy for V_{cmax} and $\Delta S(V_{\mathrm{cmax}})$ is an entropy term. The Arrhenius function was used to estimate temperature dependence of parameters K_{c}, K_{o}, τ, V_{cmax} and R_{d} (detailed in Kosugi et al. 2003, Kosugi and Matsuo 2006, Takanashi et al. 2006). Here, we calculated V_{cmax25}* assuming that the infinite internal conductance ($g_{\mathrm{i}} = \infty$) and thus the CO_2 concentration in the chloroplast ($p(C_{\mathrm{c}})$) was the same as $p(C_i)$*. A possible error in V_{cmax25} resulting from this assumption has been discussed by Takanashi et al. (2006) and Kosugi and Matsuo (2006).

We simulated the predicted values of the net assimilation rate at a given stomatal conductance, under both uniform stomatal behavior and bimodal patchy stomatal behavior (Takanashi et al. 2006). A bimodal distribution means that the whole-leaf conductance reflects either open or closed stomatal conductance. For the bimodal distribution, the stomatal conductance for an open or a closed patch was g_{smax} or g_{smin}, respectively, and the open/closed patch ratio was determined from the observed g_{s} for a whole leaf. The net assimilation rate and the intercellular CO_2 concentration for each patch were determined using the same Farquhar–von Caemmerer–Berry model that was used to determine the stomatal conductance values for each patch. We assumed that the photosynthetic parameters were uniform throughout the whole leaf. The average net assimilation rate for the whole leaf was calculated by integrating the net assimilation rate of each patch.

In the model simulation, the net assimilation rate of each patch or the whole leaf was calculated as described by Kosugi et al. (2003), Kosugi and Matsuo (2006) and Takanashi et al. (2006). Briefly, A was determined from the minimum value between the (ribulose 1,5-bisphosphate) RuBP-saturated rate or carboxylation-limited net assimilation rate (A_{c}) and electron transport- or RuBP regeneration-limited net assimilation rate (A_j) as follows:

$$A_{\mathrm{c}} = V_{\mathrm{cmax25}}\frac{\exp\left[\frac{\Delta H_{\mathrm{a}}(V_{\mathrm{cmax}})(T_l-25)}{298R(T_l+273)}\right]}{1+\exp\left[\frac{\Delta S(V_{\mathrm{cmax}})(T_l+273)-\Delta H_{\mathrm{d}}(V_{\mathrm{cmax}})}{R(T_l+273)}\right]} \times \frac{p(C_{\mathrm{c}})-\frac{p(\mathrm{O})}{2\tau}}{p(C_{\mathrm{c}})+K_{\mathrm{c}}\left(1+\frac{p(\mathrm{O})}{K_{\mathrm{o}}}\right)} - R_{\mathrm{d}}, \tag{2}$$

$$A_j = \frac{J}{4}\frac{p(C_{\mathrm{c}})-\frac{p(\mathrm{O})}{2\tau}}{p(C_{\mathrm{c}})+\frac{p(\mathrm{O})}{\tau}} - R_{\mathrm{d}}. \tag{3}$$

Here V_{cmax25} is the intrinsic value that represents the carboxylation ability of the leaves and is not always the same as the apparent value (V_{cmax25}*), which shows significant diurnal fluctuations coupled with patchy stomatal closure (Takanashi et al. 2006). A J value was required to evaluate the influence of depression in electron transport rate on the net assimilation rate. To estimate J, we used both observed J values measured with the chlorophyll fluorescence method and the optimal J_{max} values estimated from the relationship between V_{cmax} and J_{max} as follows:

$$J_{max} = k_j V_{cmax}. \quad (4)$$

Observed values of V_{cmax25} (25.0 μmol m^{-2} s^{-1}), R_{d25} (1.0 μmol m^{-2} s^{-1}) k_j (2.4), g_{smax} (0.2 mol m^{-2} s^{-1}) and g_{smin} (0.0005 mol m^{-2} s^{-1}) were used to calculate uniform photosynthetic parameters. We also used 55,200 J mol^{-1} for $\Delta H_a(V_{cmax})$, 220,000 J mol^{-1} for $\Delta H_d(V_{cmax})$, 650 J mol^{-1} for $\Delta S(V_{cmax})$ and 41,500 μmol m^{-2} s^{-1} for $\Delta H_a(R_d)$ based on the average line or the median value for evergreen broadleaved trees listed by Kosugi and Matsuo (2006). Other parameters were as listed in Takanashi et al. (2006).

Results

Microclimate

Figure 2 shows the fluctuation of daily rainfall, % SWC (average value from nine sensors at 0.1-, 0.2- and 0.3-m depth) and API_{60} for 6 years from 2002 to 2007, and dates on which leaf gas exchange observations were carried out under natural PPFD conditions (nine times) and saturated PPFD conditions (seven times). During the 6 years from 2002 to 2007, the average and the standard deviation of annual rainfall were 1755 ± 183 mm. This exceeded the 4-year average (1571 mm) from 1996 to 1999, which included an El Niño event from 1997 to early 1998 (Tani et al. 2003), but was close to the normal average (1804 mm, 1983–1997; Tani et al. 2003). The SWC and the API_{60} showed rather complex seasonal fluctuations, corresponding with mild-dry and wet periods twice each year. Average SWC at each gas exchange observation day ranged from 18% to 37%. This range included the lowest 5% (SWC $<$ 21%) and the highest 5% (SWC $>$ 35%) of recorded values during the 6 years. The driest period in the 6 years occurred in February 2005. We defined 'mild-dry period' as a period with SWC $<$ 27%, and 'wet period' as one with SWC $\geq$ 27%. Five gas exchange observations were carried out during mild-dry periods (March 2003, August 2003, September 2004, February 2005 and July 2005) and four during wet periods (September 2002, November 2004, October 2005 and December 2007). The September 2002 measurement day fell immediately after the first rainfall at the end of the mild-dry period, so it was very difficult to assign this measurement to either a rainy or a dry period.

At the site, the median daily average of SWC over the 6 years was 28.5%. On 30% of measurement days SWC exceeded 31.1%, and on 30% of days it was $<$ 25.8%. Therefore, the observation days were grouped according to their SWC as follows: November 2004, October 2005 and December 2007 had SWC values within the highest 24% of all the measured SWC values. These were designated as 'wet' periods. The other periods except September 2002 were designated as 'mild-dry' periods (SWC on these measurement days were among the lowest 14% of measured values). It was very difficult to designate days with SWC between 25.8% and 31.1% as 'wet' or 'mild-dry' using only the SWC value. We designated 27% SWC as the cut-off value between 'wet' and 'mild-dry', which means that the September 2002 observation day was considered to be a 'wet period'. However, it is more accurate to consider it as a dry–wet transition period.

Diurnal pattern of leaf CO_2 exchange with saturated PPFD

Figure 3 shows the diurnal change of A, g_s, J, V_{cmax25}*, T_l and vapor pressure deficit (VPD, hPa) measured on the 7 days with saturated PPFD conditions (1000 μmol m^{-2} s^{-1}). The averaged diurnal change from several leaves (n = 3–5) is shown in this figure. Daily diurnal change of solar radiation measured at the top of the tower is also shown. Note that solar noon is around 13:00 pm local time at this site. Figure 4 shows the relation between (A) g_s and A, (B) J and A and (C) g_s and V_{cmax25}* during mild-dry (closed squares) and wet periods (open squares).

Maximum A and g_s under saturated PPFD conditions were ~ 10 μmol m^{-2} s^{-1} and 0.2 mol m^{-2} s^{-1}, respectively. The corresponding V_{cmax25}* at that time was ~ 20–30 μmol m^{-2} s^{-1}. These values were recorded in the early morning of three of the four observations that were conducted during wet periods (September 2002, October 2005 and December 2007). In the wet period in November 2004, and also in the mild-dry period (March 2003, August 2003 and July 2005), both A and g_s were slightly lower than their maximum values recorded in the morning (Figure 3). The J ranged between ~ 50 and 100 μmol m^{-2} s^{-1} in mature leaves (Figure 4). In the middle of wet periods (November 2004 and December 2007), the newly expanding leaves had lower A, J and V_{cmax25}* values than the older mature leaves. Maximum g_s values of these young leaves within a day were greater than or the same as those of the older leaves, while the minimum g_s in a day was lower than that of older leaves (Figure 3).

The diurnal change of A showed a clear depression after late morning, coupled with depression of g_s, J and V_{cmax25}*. This midday depression occurred on every observation day, irrespective of mild-dry or wet conditions. On cloudy cool days in wet periods (October 2005 and December 2007), depression was moderate and occurred more slowly than in other periods. On sunny hot days, even in wet periods (September 2002 and November 2004), depression was immediate and severe (Figure 3). Both g_s and J were significantly correlated with A (P $<$ 0.0001), and had similar correlation coefficients (R = 0.69 for g_s, R = 0.61 for J). In mild-dry periods, A, g_s and J tended to be lower than in wet periods. The J did not markedly decrease alongside

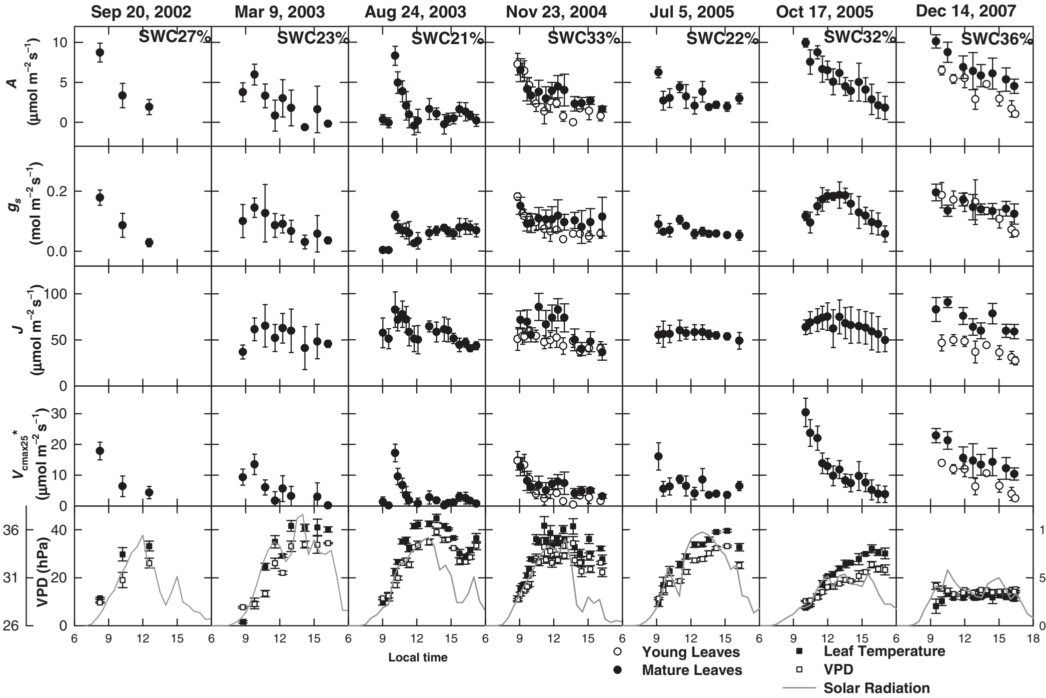

Figure 3. Diurnal change of net assimilation rate (A), stomatal conductance (g_s), electron transport rate (J), V_{cmax25}*, leaf temperature (T_l) and VPD measured under saturated PPFD conditions (1000 μmol m^{-2} s^{-1}) on seven observation days during mild-dry and wet periods from 2002 to 2007. Averaged diurnal change from several leaves (n = 3–5) sampled from sunlit branches of an individual *D. sublamellatus* tree is shown. Error bars represent standard deviation. Daily diurnal change of solar radiation measured at the top of the tower is shown (gray line). Top panel shows SWC on each observation day.

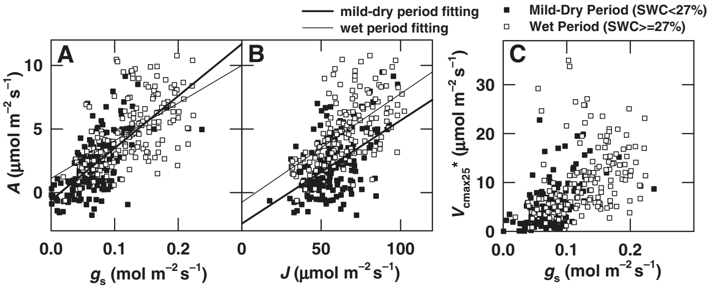

Figure 4. Relation between (A) stomatal conductance (g_s) and net assimilation rate (A), (B) electron transport rate (J) and net assimilation rate (A) and (C) stomatal conductance (g_s) and V_{cmax25}* during mild-dry (closed squares) and wet periods (open squares). All data were collected from mature leaves under saturated PPFD conditions (1000 μmol m^{-2} s^{-1}).

the severe depression of A and g_s that occurred in mild-dry periods. This suggests that the relation between J and A differed between mild-dry and wet periods (Figure 4). There was a clear midday depression in V_{cmax25}* that corresponded with g_s both in mild-dry and wet periods. This phenomenon was also reported by Takanashi et al. (2006), whose simulations showed that depression of V_{cmax25}* was associated with depression of g_s during the patchy stomatal closure.

Figure 5 shows the numerical analysis based on the Farquhar–von Caemmerer–Berry model. In this model, it is assumed that assimilation rate is affected by (A) the decrease of observed electron transport rate while stomata remain open ($g_s = 0.2$ mol m^{-2} s^{-1}), (B) uniform stomatal closure while the electron transport rate remains at its optimal value, (C) the patchy bimodal stomatal closure while electron transport rate remains at its optimal value and (D) the patchy bimodal stomatal closure coupled with a decrease in observed electron transport rate. The results show that neither the decrease in J nor the uniform stomatal closure can explain the magnitude of the depression of A. On the other hand, the patchy bimodal stomatal closure largely explained the observed depression in both mild-dry and wet periods. A slightly better estimation could be obtained by including the decrease of electron transport rate as well as the patchy bimodal stomatal closure. During

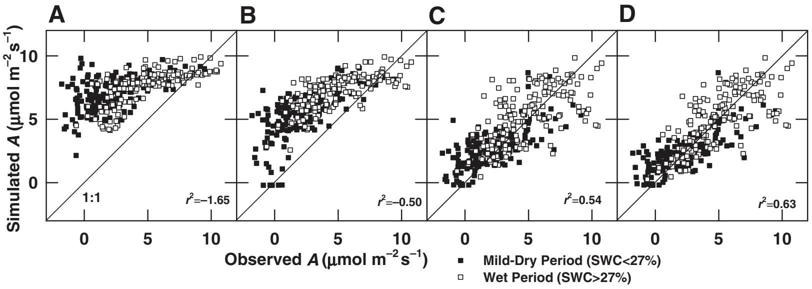

Figure 5. Comparison between observed and simulated net assimilation rate (A) by numerical analysis based on Farquhar–von Caemmerer–Berry model. In this model, it is assumed that the A is restricted by (A) decrease in the observed electron transport rate while stomata remain open ($g_s = 0.2$ mol m^{-2} s^{-1}), (B) uniform stomatal closure while electron transport rate remains at optimal value, (C) patchy bimodal stomatal closure while electron transport rate remains at optimal value and (D) patchy bimodal stomatal closure coupled with a decrease in the observed electron transport rate; r^2 is defined here as follows: $1-\Sigma(A_{obs}-A_{sim})^2/\Sigma(A_{obs}-A_{avg})^2$, where A_{obs} is the observed A, A_{sim} is the simulated A, and A_{avg} is the average value of the observed A.

the most severe depression of A, the A values obtained using these assumptions were slightly larger than observed A values.

Diurnal pattern of leaf CO_2 exchange under natural PPFD conditions

Figure 6 shows the diurnal changes of A, g_s and C_i/C_a (the ratio of C_i to the ambient CO_2 concentration, C_a), measured under natural PPFD conditions in (A) mild-dry and (B) wet periods. Figure 7 shows the relation between A or g_s and PPFD or VPD, using the same mature-leaf dataset, and the simulation results assuming uniform stomatal closure and patchy bimodal stomatal closure.

Maximum values of A and g_s were in the same range as those measured under saturated PPFD conditions (i.e., ~ 10 µmol m^{-2} s^{-1} and 0.2 mol m^{-2} s^{-1}, respectively). However, the maximum value of stomatal conductance sometimes exceeded 0.2 mol m^{-2} s^{-1}. These maximum values were observed under natural PPFD conditions in mild-dry periods, and slightly lower maximum values were observed under saturated PPFD conditions (March 2003, August 2003 and July 2003). Compared with saturated PPFD conditions, maximum values occurred later in the day under natural PPFD conditions, but varied depending on environmental conditions such as instantaneous PPFD at each measured leaf. On cloudy days in wet periods (October 2005 and December 2007), the maximum A was sometimes lower than that observed under saturated PPFD conditions. Moreover, in December 2007, maximum A occurred in the afternoon, during periods of sunshine. In November 2004, we observed significantly lower A, g_s and larger C_i/C_a values in newly expanding leaves than that in older mature leaves ($P < 0.001$). In December 2007, young leaves had larger A and g_s values on cloudy mornings, while the maximum A values in the afternoon were smaller than those of mature leaves (Figure 6). Among all observations, the minimum value of C_i/C_a, which represents the intrinsic water use efficiency of leaves, ranged between ~ 0.6 and 0.7. We did not observe a decrease in C_i/C_a coupled with midday depression of A.

Midday depression of A occurred on observation days in both mild-dry and wet periods, except in December 2007 (Figure 6). The relation between A or g_s and PPFD or VPD (Figure 7) showed a clear decline of A in the afternoon compared with the pattern observed in the morning. The hyperbolic curves of both A and g_s in the relation with PPFD showed considerable scattering, and a decline in maximum values in the afternoon. The relation between A or g_s and VPD showed declining curves, similar to those observed in Lohammer's equation (Lohammer et al. 1980), which is often used to describe the relation between g_s and VPD. There were no significant differences in these relations between mild-dry and wet periods. Even in wet periods, A and g_s became lower in high VPD conditions. Furthermore, in wet periods A and g_s were lower in the afternoon than in the morning, even in cloudy conditions with only moderate VPD (Figure 7).

The numerical analysis (Figure 7) showed that patchy bimodal stomatal closure could explain the depression in A, whereas uniform stomatal closure could not. Uniform stomatal closure only explained the depression in A in the mornings of mild-dry periods, and simulation with patchy stomatal closure overestimated the depression in A compared with that of the observed values.

Discussion

Photosynthetic ability and its temporal variations

Maximum A values of ~ 10 µmol m^{-2} s^{-1} were frequently observed under both saturated and natural PPFD conditions, thus we can assume that this value represents the maximum photosynthetic ability of mature canopy leaves of *D. sublamellatus*. In the wet period, this maximum value was observed only under saturated PPFD conditions,

A Mild-Dry Period (SWC<27%)

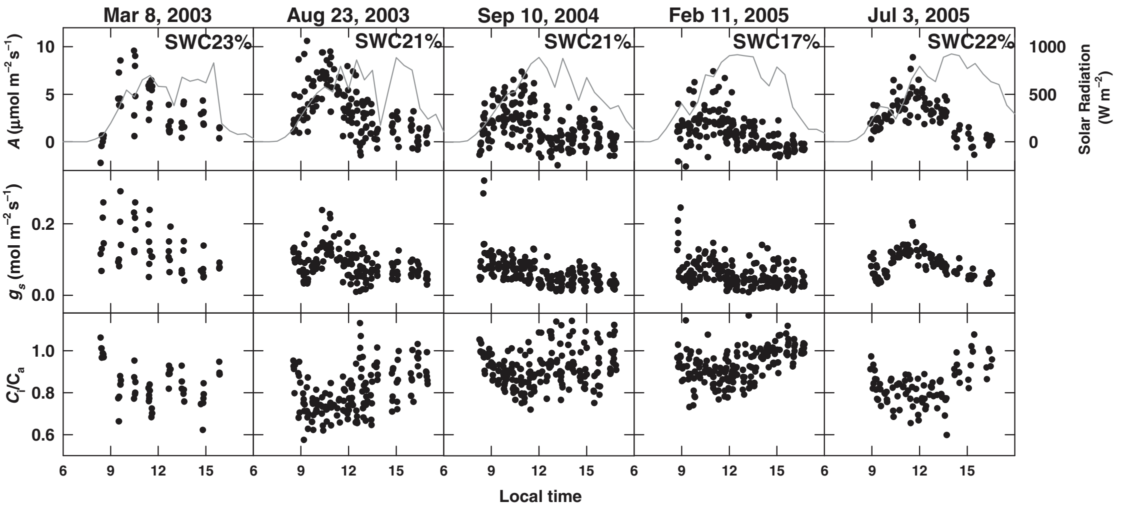

B Wet Period (SWC>=27%)

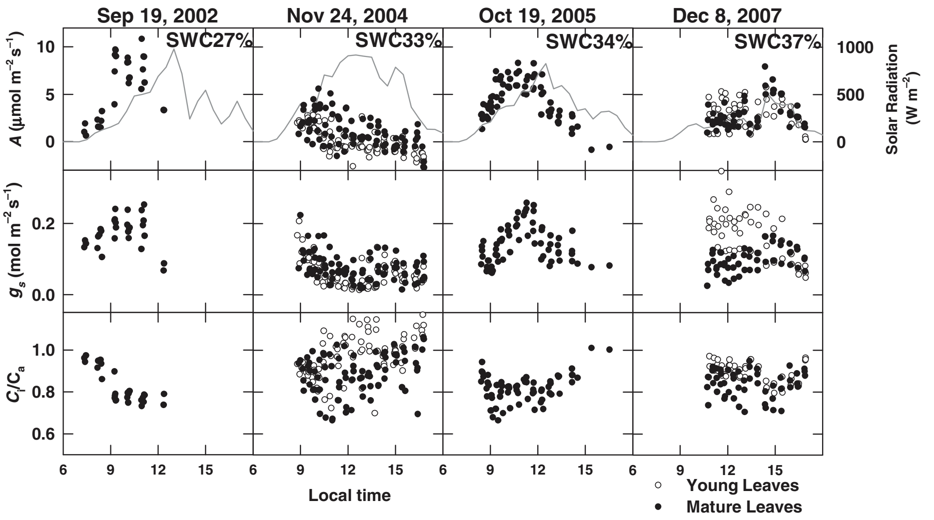

Figure 6. Diurnal changes in net assimilation rate (*A*), stomatal conductance (g_s) and ratio of intercellular CO_2 concentration (C_i) to ambient CO_2 concentration (C_a) measured under natural PPFD conditions on nine observation days during (A) mild-dry and (B) wet periods from 2002 to 2007. All instantaneous gas exchange data from several leaves (n = 3–10) sampled from sunlit branches of an individual *D. sublamellatus* tree are shown. Measurements were taken immediately every 30–60 min during daytime in leaves under natural PPFD conditions. Additional leaf samples (1–5 leaves each observation) were sometimes included. These additional sampling leaves were cut immediately after each observation and the next leaf was sampled at the following measurement time. Daily diurnal change of solar radiation measured at the top of the tower is shown (gray line). The SWC at each observation day is shown in the top panel.

whereas in the dry period it was sometimes observed under natural PPFD conditions (Figures 3 and 6). This finding suggests that we may have missed any higher *A* values that occurred under saturated PPFD conditions in the mild-dry period, because the depression occurred immediately after sunshine and was coupled with increases in leaf temperature, VPD, PPFD and water loss through transpiration. In September 2004 and February 2005 in the mild-dry period, and in November 2004 in the wet period, the maximum *A* was lower than that observed in other periods. The data alone do not provide sufficient evidence to determine whether the photosynthetic ability was lower during these periods than during other periods. However, the numerical analysis showed that the patchy stomatal closure largely explained the lower than expected net assimilation rate. This resulted from the constant photosynthetic ability of

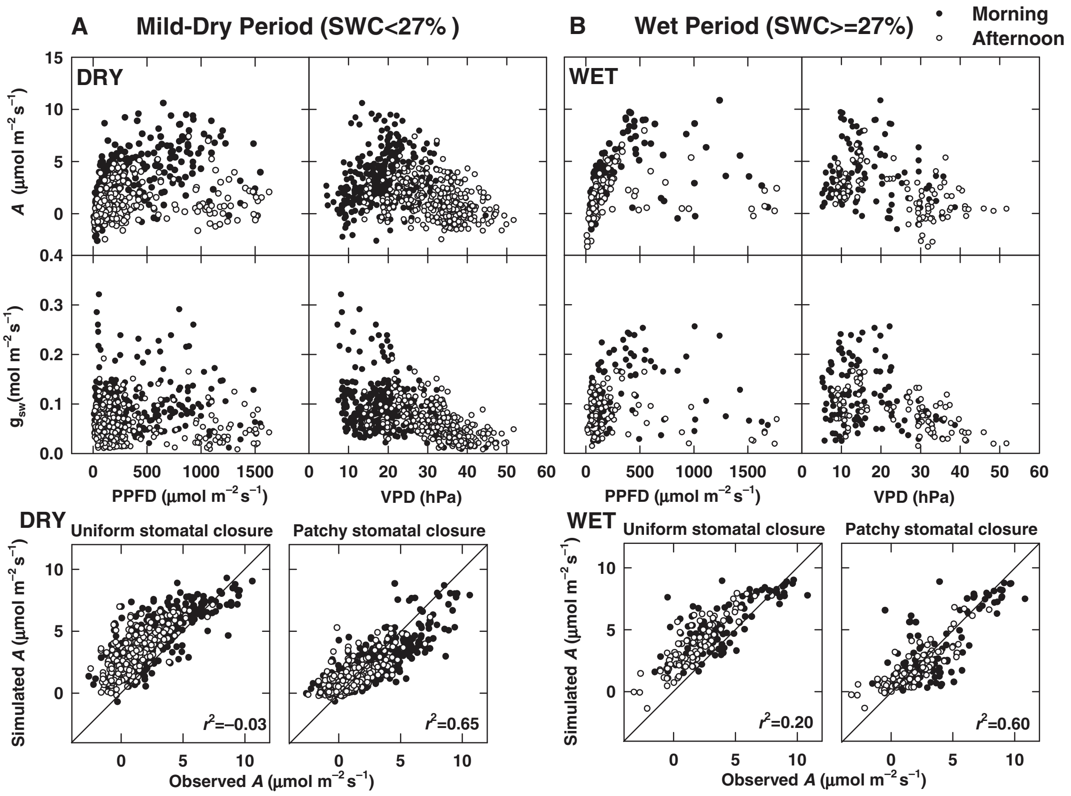

Figure 7. Relation between net assimilation rate (A) or stomatal conductance (g_s) and PPFD or VPD, and simulation results assuming uniform stomatal closure and patchy bimodal stomatal closure during (A) mild-dry and (B) wet periods. Closed circles show morning data and open circles show afternoon data. All data were collected from mature leaves under natural PPFD conditions; r^2 is defined here as $1-\Sigma(A_{obs}-A_{sim})^2/\Sigma(A_{obs}-A_{avg})^2$, where A_{obs} is the observed A, A_{sim} is the simulated A, and A_{avg} is the average value of the observed A.

the canopy leaves, which is represented with constant V_{cmax25} value (25 μmol m^{-2} s^{-1}) in the simulations (Figures 5 and 7). From this result we can assume that photosynthetic ability of canopy leaves showed no significant temporal variations during the observation periods over various seasons at this site. Photosynthetic ability differed only in the newly expanding young leaves in wet periods. Compared with those in the mature leaves, the values of A, J and V_{cmax25}* were lower, the maximum g_s was the same or larger, and the response of g_s to VPD was more rapid in young leaves (Figures 3 and 6). Occasional leaf flashes were observed in *D. sublamellatus* corresponding with the rainfall pattern. Although the data were limited, they suggested that in the wet period there are some newly expanding leaves that have lower photosynthetic ability than mature leaves. Further research is required to clarify the seasonal variations in photosynthetic capacity.

Does midday depression occur year-round?

Midday depression of A was observed on almost every observation day, whether light conditions were saturated or natural PPFD. The only exception was on a cloudy day during the wet period (December 2007) under natural PPFD conditions (Figures 3 and 6). In the diurnal change of A under both saturated and natural PPFD conditions in December 2007, A gradually decreased after late morning under natural PPFD conditions. Under natural PPFD conditions, A reached its maximum daily value during the sunshine hours in the afternoon, but this value was lower than that observed in the early morning under saturated PPFD conditions (Figures 3 and 6). This result strongly suggests that midday depression also occurred in this period. From these data, we can conclude that midday depression of photosynthesis of canopy leaves occurred year-round, even on cloudy days in the wettest period.

Was patchy stomatal closure always the main factor limiting midday net assimilation?

We investigated the influence of stomatal and non-stomatal factors on midday depression of A. Similar correlation coefficients were observed when comparing both g_s and A, and J and A, although J sometimes decreased more slowly than

g_s and A (Figure 3). These relations alone cannot determine whether stomatal or non-stomatal factors induce midday depression of A. However, the numerical analysis using the saturated PPFD data (Figure 5) showed that neither the decrease in J nor the uniform stomatal closure could explain the depression of A. Instead, the patchy bimodal stomatal closure largely explained midday depression of A, both in dry and in wet periods. This finding strongly suggests that patchy stomatal closure was always the main factor limiting midday net assimilation in canopy leaves of *D. sublamellatus*. Patchy stomatal closure with a bimodal pattern was also observed in another emergent tree in this forest, *Neobalanocarpus heimii* (King) Ashton (Takanashi et al. 2006). We observed similar depression of A and g_s in all five trees that are accessible from the corridor (unpublished data). Diurnal CO_2 exchange at the canopy scale also showed midday depression every month, irrespective of mild-dry and wet periods (Kosugi et al. 2008).

The numerical analysis also showed that when low values of A were observed during the mild-dry period, patchy bimodal stomatal closure could not explain the more severe depression in A, which sometimes reached negative values (Figure 5). At that time, A at a given J became lower than that in the wetter period (Figure 4). Ishida et al. (1999) reported similar differences in the relation of J and A between dry and wet seasons, and they suggested that the photorespiration rate might increase during the dryer and the hotter periods. During the mild-dry period, estimating depression using the patchy bimodal pattern of stomatal closure sometimes overestimated the depression of A, compared with the value measured under natural PPFD conditions (Figure 7). This corresponded to the period during the early morning when stomata opened, and sunshine first fell on leaves. In this case, uniform g_s and C_i explained A, suggesting that the pattern of stomatal closure was not patchy at that time.

Which environmental or physiological factors induced patchy stomatal closure?

The data showed that there were some differences in diurnal patterns of A and g_s among the observation periods. Although numerical analyses showed that there were no significant fluctuations in photosynthetic ability of canopy mature leaves among the different observation periods and that patchy stomatal closure occurring irrespective of mild-dry and wet periods was always the main factor causing midday depression of net assimilation.

We attempted to determine which environmental or physiological factors induced the patchy stomatal closure and resulted in the different diurnal patterns of A and g_s among the observation periods. On sunny, hot days, leaf temperature, VPD and thus transpiration rate increased rapidly when direct radiation reached the canopy leaves in the morning. On those days, we observed a rapid and severe decrease or a low value of g_s from the beginning of the day (Figures 3 and 6). This occurred during both mild-dry and wet periods, irrespective of SWC. On the other hand, slower and moderate depression of A and g_s were observed on cloudy and cool days. We observed a strong dependence of g_s on VPD (Figure 7). Our results indicate that the magnitude of midday depression among observation periods was not related to SWC, but rather to atmospheric conditions such as whether the day was sunny and hot or cloudy and cool. Thus midday depression was related to VPD. However, moderate depression of A occurred even on cloudy cool days in wet periods, coupled with patchy stomatal closure in quite moderate VPD, leaf temperature and PPFD conditions. These results suggest that patchy stomatal closure was also signaled by circadian rhythms (Doughty et al. 2006). We have collected some data on leaf water potential, determined with a pressure chamber (unpublished) and a hygrometer (Fukui et al. 2007). The pressure chamber method did not accurately measure the leaf water potential because water was already moving when we cut the *D. sublamellatus* leaves, indicating that the leaf water potential was quite high. Using the hygrometer, we observed that leaf water potential at midday decreased to –1.1 MPa, a value that is not particularly low. Our results strongly suggest that low leaf water potential did not trigger midday depression. Further research is required to determine which ‘circadian rhythms’ induced the patchy stomatal closure.

Midday depression coupled with patchy stomatal closure was more moderate on cloudy and cool days in the wet period than on sunny and hot days in the mild-dry period. However, the lower A values observed in newly expanding leaves with lower photosynthetic ability might mitigate this difference, and result in similar diurnal CO_2 exchange at the canopy scale year-round, as reported by Kosugi et al. (2008).

Supplementary Data

Supplementary data for this article are available at *Tree Physiology* Online.

Acknowledgments

We thank the Forestry Department of Negeri Sembilan and the Director General of FRIM for permission to work in the Pasoh Forest Reserve. We thank Mr. Quah Eng Seng for assistance with species identification, Dr. Shoji Noguchi and Dr. Jyunjiro Negishi for their assistance in installing soil moisture sensors, and Miss Rie Nakanishi, Mr. Yusuke Fukui and Mr. Kenta Nakagawa for their help with field work. We also thank Dr. Makoto Tani, Dr. Toshinori Okuda and a joint research project between FRIM, UPM and NIES. This work was supported by the Global Environment Research Fund of the Japan Environment Agency, and by grants for scientific research from the Ministry of Education, Culture, Sports, Science and Technology, Japan.

References

Araujo, A.C., A.D. Nobre, B. Kruijt et al. 2002. Comparative measurements of carbon dioxide fluxes from two nearby towers in a central Amazonian rainforest: the Manaus LBA site. J. Geophys. Res. 107:8090.

Doughty, C.E., M.L. Goulden, S.D. Miller and H.R. da Rocha. 2006. Circadian rhythms constrain leaf and canopy gas exchange in an Amazonian forest. Geophys. Res. Lett. 33:L15404.

Evans, J.R. 1987. The dependence of quantum yield on wavelength and growth irradiance. Aust. J. Plant Physiol. 14: 69–79.

Evans, J.R. 1993. Photosynthetic acclimation and nitrogen partitioning within a lucerne canopy. I. Canopy characteristics. Aust. J. Plant Physiol. 20:55–67.

Farquhar, G.D., S. von Caemmerer and J.A. Berry. 1980. A biochemical model of photosynthetic CO_2 assimilation in leaves of C_3 species. Planta 149:78–90.

Field, C. 1983. Allocating leaf nitrogen for the maximization of carbon gain: lead age as a control on the allocation program. Oecologia 56:341–347.

Fukui, Y., Y. Kosugi, N. Matsuo, S. Takanashi and M. Tani. 2007. Comparison of water use of various trees grown in several different habitats. J. Jpn. Soc. Hydrol. Water Resour. 20:265–277 (in Japanese).

Goulden, M.L., S.D. Miller, H.R. da Rocha, M.C. Menton, H.C. de Freitas, A.M. e Silva Figueira and C.A. Dias de Sousa. 2004. Diel and seasonal patterns of tropical forest CO_2 exchange. Ecol. Appl. 14:S42–S54.

Grassi, G., E. Vicinelli, F. Ponti, L. Cantoni and F. Magnani. 2005. Seasonal and interannual variability of photosynthetic capacity in relation to leaf nitrogen in a deciduous forest plantation in northern Italy. Tree Physiol. 25:349–360.

Hikosaka, K. and I. Terashima. 1995. A model of the acclimation of photosynthesis in the leaves of C3 plants to sun and shade with respect to nitrogen use. Plant Cell Environ. 18:605–618.

Ishida, A., T. Toma, Y. Matsumoto, S.K. Yap and Y. Maruyama. 1996. Diurnal changes in leaf gas exchange characteristics in the uppermost canopy of a rain forest tree, *Dryobalanops aromatica* Gaertn. F. Tree Physiol. 16:779–785.

Ishida, A., T. Toma and Marjenah. 1999. Limitation of leaf carbon gain by stomatal and photochemical processes in the top canopy of *Macaranga conifera*, a tropical pioneer tree. Tree Physiol. 19:467–473.

Kosugi, Y. and N. Matsuo. 2006. Seasonal fluctuations and temperature dependence of leaf gas exchange parameters of co-occurring evergreen and deciduous trees in a temperate broad-leaved forest. Tree Physiol. 26:1173–1184.

Kosugi, Y., S. Shibata and S. Kobashi. 2003. Parameterization of the CO_2 and H_2O gas exchange of several temperate deciduous broad-leaved trees at the leaf scale considering seasonal changes. Plant Cell Environ. 26:285–301.

Kosugi, Y., T. Mitani, M. Itoh, S. Noguchi, M. Tani, N. Matsuo, S. Takanashi, S. Ohkubo and N. Abdul Rahim. 2007. Spatial and temporal variation in soil respiration in a Southeast Asian tropical rainforest. Agric. For. Meteorol. 147:35–47.

Kosugi, Y., S. Takanashi, S. Ohkubo, N. Matsuo, M. Tani, T. Mitani, D. Tsutsumi and N. Abdul Rahim. 2008. CO_2 exchange of a tropical rainforest at Pasoh in Peninsular Malaysia. Agric. For. Meteorol. 148:439–452.

Kumagai, T., T. Ichie, M. Yoshimura, M. Yamashita, T. Kenzo, T.M. Saitoh, M. Ohashi, M. Suzuki, T. Koike and H. Komatsu. 2006. Modeling CO_2 exchange over a Bornean tropical rain forest using measured vertical and horizontal variations in leaf-level physiological parameters and leaf area densities. J. Geophys. Res. 111:D10107.

Lohammer, T., S. Larsson, S. Linder and S.O. Falk. 1980. FAST-simulation models of gaseous exchange in Scots Pine. Ecol. Bull. 32:505–523.

Malhi, Y., A.D. Nobre, J. Grace, B. Kruijt, M.G.P. Pereira, A. Culf and S. Scott. 1998. Carbon dioxide transfer over a Central Amazonian rain forest. J. Geophys. Res. 103: 31593–31612.

Malhi, Y., D.D. Baldocchi and P.G. Jarvis. 1999. The carbon balance of tropical, temperate and boreal forests. Plant Cell Environ. 22:715–740.

Niinemets, U. and J.D. Tenhunen. 1997. A model separating leaf structural and physiological effects on carbon gain along light gradients for the shade-tolerant species *Acer saccharum*. Plant Cell Environ. 20:845–866.

Ohkubo, S., Y. Kosugi, S. Takanashi, M. Tani, N. Matsuo and N. Abdul Rahim. 2008. Vertical profiles and storage fluxes of CO_2, heat, and water in a tropical rainforest at Pasoh, Peninsular Malaysia. Tellus 60B:569–582.

Saleska, S.R., S.D. Miller, D. M. Matross et al. 2003. Carbon in Amazonian forests: unexpected seasonal fluxes and disturbance-induced losses. Science 302:1554–1557.

Takanashi, S., Y. Kosugi, M. Tani, N. Matsuo, T. Mitani and N. Abdul Rahim. 2005. Characteristics of the gas exchange of a tropical rain forest in Peninsular Malaysia. Phyton 45: 61–66.

Takanashi, S., Y. Kosugi, N. Matsuo, M. Tani and N. Ohte. 2006. Patchy stomatal behavior in broad-leaved trees grown in different habitats. Tree Physiol. 26:1565–1578.

Takashima, T., K. Hikosaka and T. Hirose. 2004. Photosynthesis or persistence: nitrogen allocation in leaves of evergreen and deciduous *Quercus* species. Plant Cell Environ. 27: 1047–1054.

Tani, M., N. Abdul Rahim, Y. Ohtani, Y. Yasuda, S. Mohd Md, K. Baharuddin, S. Takanashi, S. Noguchi, Y. Zulkifli and T. Watanabe. 2003. Characteristics of energy exchange and surface conductance of a tropical rain forest in Peninsular Malaysia. *In* Pasoh: Ecology of a Lowland Rain Forest in Southeast Asia. Eds. T. Okuda, N. Manokaran, Y. Matsumoto, K. Niiyama, S.C. Thomas and P.S. Ashton. Springer, Tokyo, pp. 73–88.

Terashima, I., S.C. Wong, C.B. Osmond and G.D. Farquhar. 1988. Characterization of non-uniform photosynthesis induced by abscisic acid in leaves having different mesophyll anatomies. Plant Cell Physiol. 29:385–394.

Vourlitis, G.L., N.P. Filho, M.M.S. Hayashi, J.S. Nogueira, F. Raiter, W. Hoegel and J.H. Campelo Jr. 2004. Effects of meteorological variations on the CO_2 exchange of a Brazilian transitional tropical forest. Ecol. Appl. 14:S89–S100.

Wilson, K.B., D.D. Baldocchi and P.J. Hanson. 2000. Spatial and seasonal variability of photosynthetic parameters and their relationship to leaf nitrogen in a deciduous forest. Tree Physiol. 20:565–578.

Yamashita, T., N. Kasuya, K. Wan Rasidah, C. Suhaimi Wan, S. Quah Eng and T. Okuda. 2003. Soil and belowground characteristics of Pasoh forest reserve. *In* Pasoh: Ecology of a Lowland Rain Forest in Southeast Asia. Eds. T. Okuda, N. Manokaran, Y. Matsumoto, K. Niiyama, S.C. Thomas and P.S. Ashton. Springer, Tokyo, pp. 89–109.

Tree Physiology 31, 160–168
doi:10.1093/treephys/tpq102

Research paper

Patchy stomatal behavior during midday depression of leaf CO_2 exchange in tropical trees

Mai Kamakura[1,7], Yoshiko Kosugi[2], Satoru Takanashi[3], Kazuho Matsumoto[4], Motonori Okumura[5], and Elizabeth Philip[6]

[1]*KYOUSEI* Science Center for Life and Nature, Nara Women's University, Kita-uoya Higashimachi, Nara 630-8506, Japan; [2]Laboratory of Forest Hydrology, Division of Environmental Science and Technology, Graduate School of Agriculture, Kyoto University, Kyoto 606-8502, Japan; [3]Forestry and Forest Products Research Institute, Tsukuba, Ibaraki 305-8687, Japan; [4]Laboratory of Ecohydrology, Kasuya Research Forest, Kyushu University, Sasaguri, Fukuoka 811-2415, Japan; [5]Department of Socio-Environmental Energy Science, Graduate School of Energy Science, Kyoto University, Kyoto 606-8501, Japan and [6]Forest Research Institute Malaysia, Kepong, Kuala Lumpur 52109, Malaysia; [7]Corresponding author (mkamakura@cc.nara-wu.ac.jp)

Received July 14, 2010; accepted October 8, 2010; published online March 7, 2011; handling Editor Guillermo Goldstein

We investigated effects of heterogeneous stomatal behavior on diurnal patterns of leaf gas exchange in 10 tree species. Observations were made in middle and upper canopy layers of potted tropical rainforest trees in a nursery at the Forest Research Institute Malaysia. Measurements were taken from 29 January to 3 February 2010. We measured in situ diurnal changes in net photosynthetic rate and stomatal conductance in three leaves of each species under natural light. In both top-canopy and sub-canopy species, midday depression of net assimilation rate occurred in late morning. Numerical analysis showed that patchy bimodal stomatal behavior occurred only during midday depression, suggesting that the distribution pattern of stomatal apertures (either uniform or non-uniform stomatal behavior) varies flexibly within single days. Direct observation of stomatal aperture using Suzuki's Universal Micro-Printing (SUMP) method demonstrated midday patchy stomatal closure that fits a bimodal pattern in *Shorea leprosula* Miq., *Shorea macrantha* Brandis. and *Dipterocarpus tempehes* V.Sl. Inhibition of net assimilation rate and stomatal conductance appears to be a response to changes in vapor pressure deficit (VPD). Variable stomatal closure with increasing VPD is a mechanism used by a range of species to prevent excess water loss from leaves through evapotranspiration (viz., inhibition of midday leaf gas exchange). Bimodal stomatal closure may occur among adjacent stomata within a single patch, rather than among patches on a single leaf. Our results suggest the occurrence of patches at several scales within single leaves. Further analysis should consider variable spatial scales in heterogeneous stomatal behavior between and within patches and within single leaves.

Keywords: heterobaric leaf, net assimilation rate, stomatal aperture distribution, stomatal conductance, vapor pressure deficit

Introduction

Plants regulate the exchange of CO_2 and water vapor with the atmosphere by adjusting their photosynthetic capacity and changing the apertures of stomata on the epidermis of their leaves. To prevent water loss and facilitate CO_2 diffusion to mesophyll cells, the stomatal aperture mechanism responds variably to environmental factors including light intensity, water status, temperature and nutrient supply.

Responses to environmental stimuli usually differ between adaxial and abaxial stomata on amphistomatous leaves (e.g., Travis and Mansfield 1981, Wang et al. 1998). Moreover, heterogeneous or 'patchy' stomatal behavior occurs on the surface of single leaves in response to water stress (Sharkey and Seemann 1989, Gunasekera and Berkowitz 1992), low humidity (Loreto and Sharkey 1990, Beyschlag et al. 1992, Mott et al. 1993) and exogenous abscisic acid (ABA) application (Downton et al. 1988, Terashima et al. 1988). This phenomenon, as well as non-uniform photosynthesis in response to environmental stimuli, has been observed in plants with heterobaric leaves, in which vertical extensions of bundle sheath cells delimit the mesophyll and restrict the diffusion of CO_2 (Mott and Buckley 1998, 2000, West et al. 2005), whereas uniform stomatal behavior occurs in homobaric leaves that lack these vertical extensions (Terashima 1992). Concerning the differences in growth environment between the two leaf types, Wylie (1952) reported that plants with heterobaric leaves were found in temperate and dry areas, whereas those with homobaric leaves were found in warmer and wet regions. Kenzo et al. (2007) postulated that bundle sheath extensions might give heterobaric leaves an advantage over homobaric leaves in the severe stress canopy environment; this argument is based on the occurrence of different leaf types across the steep vertical microenvironmental gradient from forest floor to tree top. The bundle sheath extensions in heterobaric leaves may respond quickly to drought signals by, for example, reducing mesophyll water potential or increasing concentrations of ABA transported via the transpiration stream in bundle sheath extensions (Terashima 1992).

Heterogeneous stomatal behavior can be seen in plants under natural ecosystems during midday depression of photosynthesis (Beyschlag and Pfanz 1990, Beyschlag et al. 1992, Takanashi et al. 2006). The existence of this phenomenon under natural conditions is important because algorithms commonly used to calculate leaf conductance from water vapor exchange measurements assume homogeneously open stomata (see von Caemmerer and Farquhar 1981). If there is stomatal patchiness, then it results in error in the calculations, and the effects of stomatal behavior on midday depression of photosynthesis are underestimated. A few studies determined the effects of patchy stomatal behavior on gas exchange in the field. Using a pressure-infiltration method and numerical analysis, Takanashi et al. (2006) demonstrated that patchy stomatal closure with a bimodal closure pattern may explain midday depression in top canopy leaves of a tropical rainforest (at Pasoh, Peninsular Malaysia). Moreover, application of numerical analyses to these canopy leaves shows that patchy bimodal stomatal closure is the main determinant of photosynthetic rate inhibition year round (Kosugi et al. 2009). Brodribb and Holbrook (2004) argued that hydraulic dysfunction at midday is linked to gas exchange depression, which may explain some of the spatial variation in stomatal aperture. However, it is still unclear whether patchy bimodal stomatal behavior actually occurs under field conditions (because the infiltration method is an all-or-nothing procedure that classifies groups of stomata as either open or closed depending on whether some or all of the stomata are above or below a particular threshold for liquid conductance), and whether the distribution of stomatal aperture on a single leaf (either uniform or non-uniform stomatal behavior) varies flexibly in response to stress factors within a single day.

To better understand the effects of stomatal dynamics on the midday depression of photosynthesis, we measured diurnal changes in leaf CO_2 exchange in 10 tree species; measurements were taken from middle to upper canopy layers in a tropical rainforest, and observations were made on individual stomatal apertures. We analyzed the relationships between diurnal changes in photosynthetic rate and patterns of stomatal aperture distribution on single leaves. We used a numerical procedure based on the Farquhar–von Caemmerer–Berry model (Farquhar et al. 1980) and Suzuki's Universal Micro-Printing (SUMP) method for stomatal observation.

Materials and methods

Site and materials

The study was conducted in a nursery at the Forest Research Institute Malaysia (FRIM), in Kepong, Peninsular Malaysia (3°23′N, 101°63′E). We measured in situ leaf gas exchange and observed the stomatal aperture distribution of leaves of potted trees (pot size: 18 cm diameter, 20 cm deep) of 10 species. The species selected were located at the middle and upper canopy levels (see Table 1). All species had heterobaric leaves. Data were collected from 29 January to 3 February 2010. Plants were watered several times during observations to prevent the soil from drying.

Measurement of leaf gas exchange

Diurnal changes in net assimilation rate (A, μmol m^{-2} s^{-1}) and stomatal conductance of water vapor (g_s, mol m^{-2} s^{-1}) of intact

Table 1. List of tree species of a Malaysian lowland tropical rainforest measured in this study. Height and ground diameter of each plant are shown.

Forest stratification	Family	Species	Height, cm	Ground diameter, cm	Measurement date
Upper layer	Dipterocarpaceae	*Shorea leprosula*	200	3.30	1 Feb. 2010
		S. macrantha	90	1.30	1 Feb. 2010
		S. hemsleyana	85	1.70	2 Feb. 2010
		S. sumatrana	180	2.90	1 Feb. 2010
		Dipterocarpus tempehes	175	2.00	2 Feb. 2010
		D. grandiflorous	200	2.70	2 Feb. 2010
Middle layer	Dipterocarpaceae	*Hopea glaucescens*	180	1.80	3 Feb. 2010
		H. subalata	185	1.30	3 Feb. 2010
		Vatica nitens	265	2.70	29 Jan. 2010
	Clusiaceae	*Mesua ferrea*	120	1.80	30 Jan. 2010

leaves were measured under natural photosynthetic photon flux density (PPFD, µmol m^{-2} s^{-1}), using an LI-6400 gas exchange measurement system (Li-Cor, Inc., Lincoln, NE, USA) with a 2 × 3 cm clear-top chamber. Gas exchange measurements were made on three leaves per plant. Photosynthetic photon flux density and leaf-to-air vapor pressure deficit (VPD, kPa) conditions on five measurement days are presented in Figure 1. Leaf temperature was 37.3 ± 4.1 °C (mean ± SD). The ambient CO_2 concentration was 397 ± 20 µmol mol^{-1} (mean ± SD).

Model description

We calculated normalized maximum rates of carboxylation at 25 °C (V_{cmax25}, µmol m^{-2} s^{-1}) to evaluate the effects of heterogeneous stomatal behavior on gas exchange, and to determine directly the apparent depression of photosynthetic capacity in the field (Takanashi et al. 2006). Maximum carboxylation rate (V_{cmax}) was calculated with a one-point method (Wilson et al. 2000, Kosugi et al. 2003, 2009, Grassi et al. 2005, Kosugi and Matsuo 2006, Takanashi et al. 2006), which is an inverse method based on the Farquhar–von Caemmerer–Berry model (Farquhar et al. 1980) that can be used to determine the actual responses of leaves in the field. In the one-point method, the apparent partial pressure of CO_2 within the intercellular space ($p(C_i)^*$) is estimated from variables measured using a gas exchange methodology, and the 'apparent' normalized maximum carboxylation rate ($V_{cmax25}{}^*$) is calculated from the values of A, $p(C_i)^*$ and leaf temperature (T_1). Here, we calculated $V_{cmax25}{}^*$, assuming that the infinite internal conductance ($g_i = \infty$), and thus the CO_2 concentration in the chloroplast ($p(C_c)$) was the same as $p(C_i)^*$. A possible influence of error in V_{cmax25} resulting from the estimation of g_i has been discussed by Takanashi et al. (2006) and Kosugi and Matsuo (2006). Although V_{cmax} is generally calculated assuming that $g_i = \infty$, lower values of g_i (<0.1 CO_2 mol m^{-2} s^{-1}) affect the absolute value of V_{cmax25}. Thus, $V_{cmax25}{}^*$ was calculated as follows:

$$V_{cmax25}{}^* = (A + R_d)\frac{p(C_c) + K_c(1 + (p(O) / K_o))}{p(C_c) - (p(O) / 2\tau)} \times \frac{1 + \exp[(\Delta S(V_{cmax})(T_1 + 273) - \Delta H_d(V_{cmax})) / (R(T_1 + 273))]}{\exp[\Delta H_a(V_{cmax})(T_1 - 25) / (298R(T_1 + 273))]} \quad (1)$$

where R_d is the non-photorespiratory respiration rate (µmol m^{-2} s^{-1}), τ is the specificity factor of RuBisCo, $p(O)$ (21,000 Pa) is the partial pressure of O_2 at the sites of oxygenation, K_c and K_o are the Michaelis–Menten constants of RuBisCo for CO_2 and O_2, respectively, T_1 is leaf temperature (°C), R is the gas constant (8.31 J K^{-1} mol^{-1}), $\Delta H_a(V_{cmax})$ is the activation energy for V_{cmax}, $\Delta H_d(V_{cmax})$ is the deactivation energy for V_{cmax} and $\Delta S(V_{cmax})$ is an entropy term. The Arrhenius function was used to estimate the temperature dependence of parameters K_c, K_o, τ, V_{cmax} and R_d (detailed in Kosugi et al. 2003, Kosugi and Matsuo 2006, Takanashi et al. 2006).

To determine the effects of stomatal aperture distribution on gas exchange, we performed simulations to predict net assimilation rates at a given stomatal conductance for both uniform and patchy bimodal stomatal distributions (Takanashi et al. 2006). A patchy bimodal distribution indicates that whole-leaf conductance reflects either open or closed stomatal conductance. For patchy bimodal distribution, stomatal conductance for open and closed patches was g_{smax} and g_{smin}, respectively, and the open/closed patch ratio (r_{oc}) was determined from the observed g_s for a whole leaf. Net assimilation rate and intercellular CO_2 concentration for each patch were estimated with the Farquhar–von Caemmerer–Berry model used for determining patch stomatal conductance values. We assumed uniform photosynthetic parameters through the

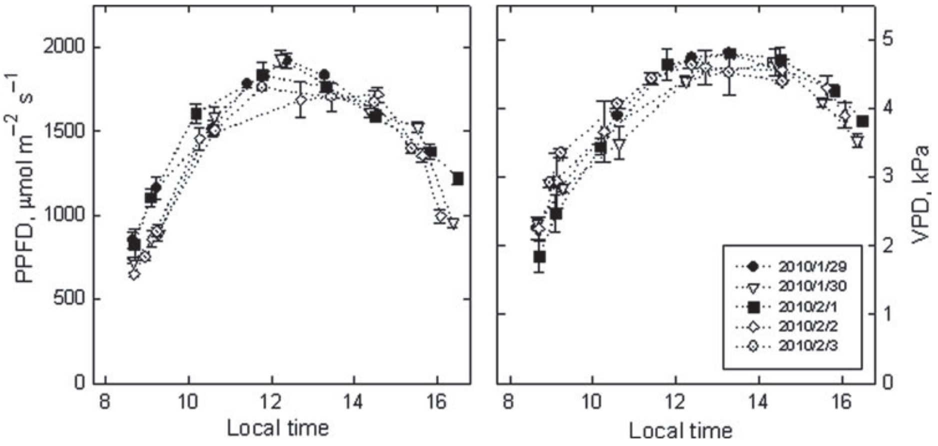

Figure 1. Averaged diurnal change in PPFD (µmol m^{-2} s^{-1}) and VPD (kPa) on each measurement day. Values are means ± SD.

whole leaf. The average net assimilation rate for the whole leaf was calculated by integrating net assimilation rates of individual patches.

In the model simulations, the net assimilation rate of each patch was calculated following Kosugi et al. (2003), Kosugi and Matsuo (2006) and Takanashi et al. (2006). Briefly, A of open (A_{op}) and closed (A_{cl}) patches were determined from the minimum value between the RuBP-saturated rate or carboxylation-limited net assimilation rate (A_c) and the electron transport- or RuBP regeneration-limited net assimilation rate (A_j), respectively, as follows:

$$A_c = V_{cmax25} \times \frac{\exp[\Delta H_a(V_{cmax})(T_1 - 25)/(298R(T_1+273))]}{1+\exp[(\Delta S(V_{cmax})(T_1+273) - \Delta H_d(V_{cmax}))/(R(T_1+273))]} \times \frac{p(C_c) - p(O)/2\tau}{p(C_c)+K_c(1+p(O)/K_o)} - R_d. \quad (2)$$

$$A_j = \frac{J}{4} \times \frac{p(C_c) - (p(O)/2\tau)}{p(C_c)+(p(O)/\tau)} - R_d. \quad (3)$$

Here V_{cmax25} is the intrinsic value that represents the carboxylation ability of leaves and is not always identical to the apparent value (V_{cmax25^*}), which exhibits significant diurnal fluctuations coupled with patchy stomatal closure (Takanashi et al. 2006). CO_2 concentration in the chloroplast of open patches ($p(C_c)_{op}$) was determined from A_{op} and g_{smax}, and that for closed patches ($p(C_c)_{cl}$) was determined from A_{cl} and g_{smin}. A J value was required to estimate the influence of depression in the electron transport rate on the net assimilation rate. To estimate J, we used optimal J_{max} values estimated from the relationship between V_{cmax} and J_{max} as follows:

$$J_{max} = k_j V_{cmax}. \quad (4)$$

The net assimilation rate (A_{leaf}) and CO_2 concentration in the chloroplasts ($p(C_c)_{leaf}$) of the whole leaf were calculated as follows:

$$A_{leaf} = r_{oc}A_{op} + (1 - r_{oc})A_{cl} \quad (5)$$

$$p(C_c)_{leaf} = r_{oc}p(C_c)_{op} + (1 - r_{oc})p(C_c)_{cl}. \quad (6)$$

The estimated maximum rate of carboxylation at 25 °C (V_{cmax25}^*) was determined by substituting values of A_{leaf} and $p(C_c)_{leaf}$ into equation (1).

For photosynthetic parameters, we used the observed optimal values of V_{cmax25} and g_{smax} of each species (listed in Table 2), and also used 0.0005 mol m^{-2} s^{-1} for g_{smin} and 2.2 for k_j. Based on the average line or the median value for evergreen broadleaved trees listed by Kosugi and Matsuo (2006), we used the following parameterizations: 55,200 J mol^{-1} for ΔH_a (V_{cmax}), 220,000 J mol^{-1} for ΔH_d (V_{cmax}), 650 J mol^{-1} for ΔS (V_{cmax}) and 41,500 µmol m^{-2} s^{-1} for ΔH_a (R_d). Other parameters were as listed in Takanashi et al. (2006).

Table 2. List of parameters used in the biochemical photosynthetic model.

Species	V_{cmax25}, µmol m^{-2} s^{-1}	g_{smax}, mol m^{-2} s^{-1}
S. leprosula	48.9	0.28
S. macrantha	17.4	0.16
S. hemsleyana	26.7	0.08
S. sumatrana	16.1	0.09
D. tempehes	14.6	0.12
D. grandiflorous	20.3	0.10
H. glaucescens	17.3	0.05
H. subalata	21.0	0.06
V. nitens	10.9	0.09
M. ferrea	18.4	0.09

Observation of stomatal aperture distribution

To evaluate patchy stomatal behavior, we obtained the frequency distributions of stomatal aperture for single leaves of three top-canopy tree species (*Shorea leprosula* Miq., *Shorea macrantha* Brandis. and *Dipterocarpus tempehes* V.Sl.) from observations made using the SUMP method, which uses amyl acetate and thin celluloid plates (2 cm in diameter; SUMP Laboratory, Tokyo). Observations were made twice a day, once immediately following the onset of midday depression of A, and then halfway through the midday depression. Immediately after measuring leaf gas exchange, we made impressions of the surface of one of the three experimental leaves by fastening the celluloid plate dissolved by amyl acetate to the abaxial leaf surface (the site at which the gas exchange rate was measured). Then stomatal behavior was observed under a digital microscope (Model VH-Z450; Keyence, Osaka). A total of 35–40 microscopic fields per leaf (10–17 stomata in each field of vision) were observed. The widths of individual stomatal pores were determined from static images using NIH image software (National Institutes of Health, Bethesda, MD, USA). Because the leaves used for making impressions were destroyed, we used adjacent leaves with similar photosynthetic rates for leaf gas exchange measurements after treatment.

Results

Diurnal pattern of leaf CO_2 exchange

The averaged diurnal changes in PPFD (µmol m^{-2} s^{-1}) and VPD (kPa) on each measurement day are presented in Figure 1 (n = 3–9). The measurements were made on clear days.

Stomatal conductance (g_s) and A for all plant species varied within single days (Figure 2), and every leaf showed midday depressions of both parameters. Figure 3 compares the observed and simulated plots (simulated by numerical analysis based on the Farquhar–von Caemmerer–Berry model) of diurnal changes in A for three leaves of each plant species. The model assumes that the assimilation rate is affected by uniform or patchy bimodal distribution of stomatal aperture. In top-canopy species, the observed diurnal change in A was clearly depressed in late morning (Figure 3a). With the exception of *S. leprosula* and *S. hemsleyana*, observed A values recovered in the afternoons, but the rates were lower than morning rates. Midday depression of observed A also occurred in all sub-canopy species (Figure 3b). Observed A usually recovered in the afternoon, and for some species, increased to the morning level. Comparisons of observed and simulated A values clearly show that patchy bimodal distribution of stomatal aperture explains the severe depression of A, regardless of species, whereas uniform distribution of stomatal aperture explains optimum A in the early morning and recovery in the afternoon.

Distribution of stomatal aperture

Figures 4–6 present images (captured by the SUMP method) of individual stomatal apertures immediately following the onset of midday depression and during the midday depression; frequency distributions of stomatal aperture are also presented. In *S. leprosula* and *S. macrantha*, two peaks in the frequency distributions of stomatal aperture indicate that a patchy bimodal distribution of stomatal aperture (observed stomata were either widely open or almost closed) occurred immediately following the onset of midday depression (Figures 4a and 5a). These bimodal distributions occurred within single isolated leaf patches, rather than between patches. In these two species, most stomata closed during midday depression (Figures 4b and 5b). A few stomata in each patch still remained open during the midday depression; however, between-patch differences were not apparent. In *D. tempehes*, the frequency distribution of stomatal aperture was bimodal during the midday depression (Figure 6b), but the frequency distribution immediately following the onset of midday depression was normal (Figure 6a). Between-patch differences were not observed.

Discussion

Midday depression in A clearly occurred in leaves of all observed plant species distributed in the upper and middle canopy layers. Numerical analysis showed that patchy bimodal stomatal closure largely explained this depression (Figure 3). Kosugi et al. (2009) also argued that patchy stomatal closure was the main factor limiting midday net assimilation in another top-canopy species (*Dipterocarpus sublamellatus* Foxw.) in a lowland dipterocarp forest in Peninsular Malaysia. The diurnal pattern in A differed slightly between plant species, but was similar among the three leaves of each species. Depressed values of A recovered to morning levels in sub-canopy tree species, but not in top-canopy tree species. In top-canopy

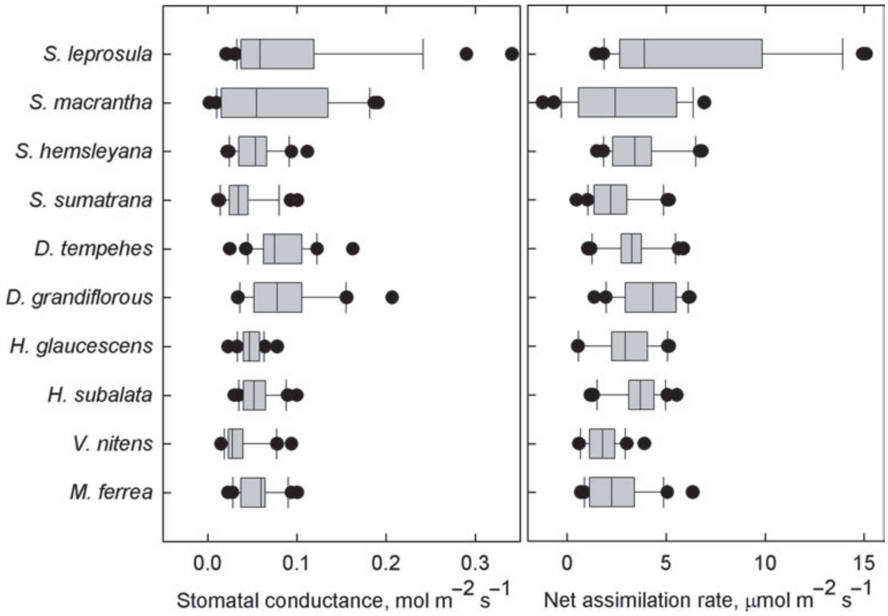

Figure 2. Variation in stomatal conductance (g_s) and net assimilation rate (A) for each plant species within single days (medians, 10th, 25th, 75th and 90th percentiles with error bars in box and whisker plots).

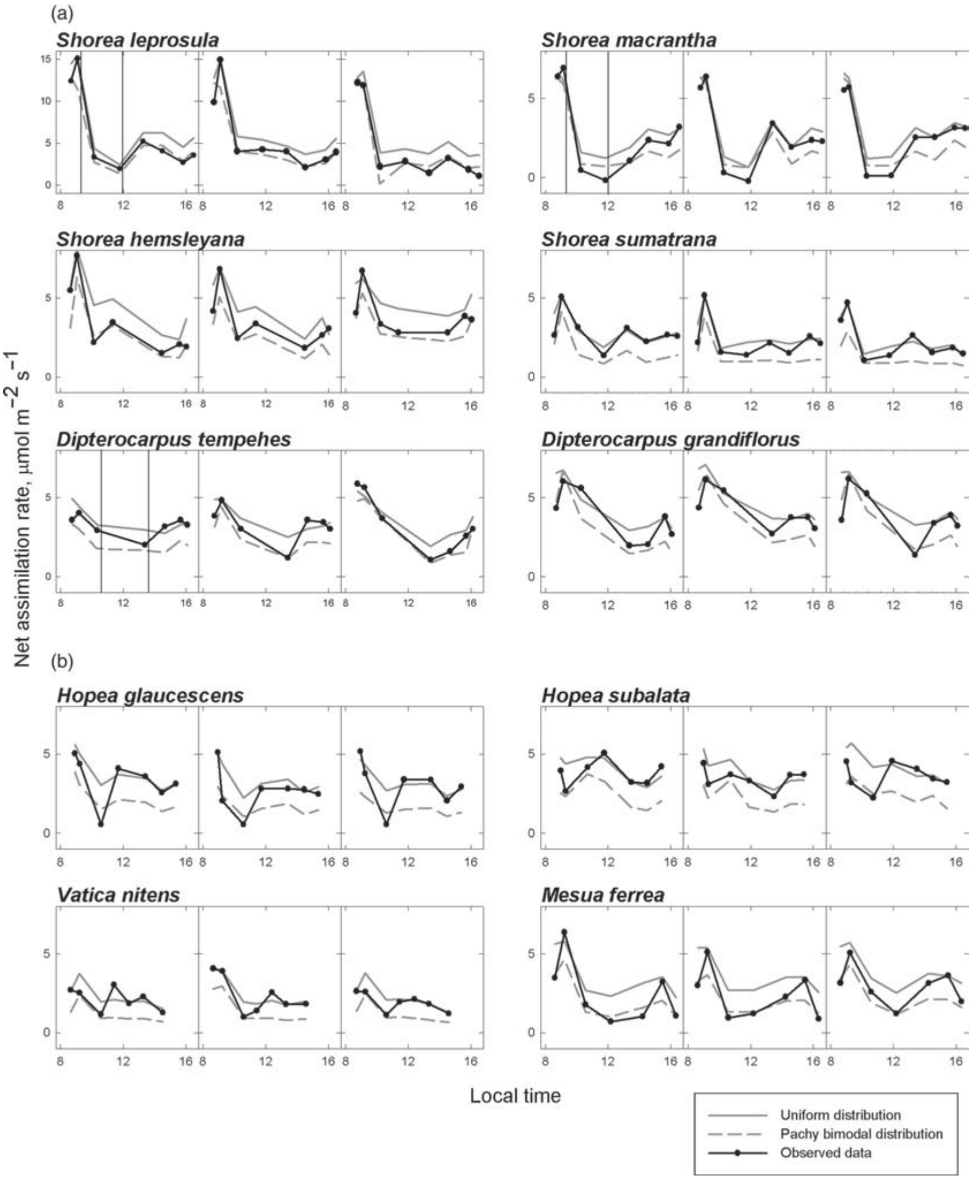

Figure 3. Diurnal changes in observed net assimilation rate (*A*), and simulation results assuming uniform stomatal closure and patchy bimodal stomatal closure [$n = 3$ leaves each of top-canopy species (a) and sub-canopy species (b)]. Solid vertical lines for *S. leprosula*, *S. macrantha* and *D. tempehes* indicate times when impressions were made of the abaxial leaf surfaces using the SUMP method.

conditions of tropical rainforests, tree leaves suffer severe environmental conditions through higher radiation, VPD and temperature than leaves in the lower forest layers (Chazdon et al. 1996, Kenzo et al. 2007). Thus, values of *A* in leaves of top-canopy tree species may be depressed more strongly than those of sub-canopy tree species.

Our numerical analysis demonstrated that patchy bimodal stomatal behavior occurred only during the midday depression, which strongly suggests that distribution patterns of stomatal aperture (uniform vs. non-uniform stomatal behavior) vary flexibly within single days. Patchy stomatal closure might be induced by environmental factors (Kosugi et al. 2009) and/or circadian rhythms (Doughty et al. 2006). Kosugi et al. (2009) showed that severe midday depression of *A* and g_s on hot, sunny days is related to VPD, whereas moderate depression on cloudy and cool days is induced by circadian rhythms. In our study, all measurements were made on sunny, hot days. On those days, leaf temperature, VPD and thus transpiration rate increased quickly with radiation in the morning (Figure 1), followed by rapid and severe depression of *A* and g_s over the

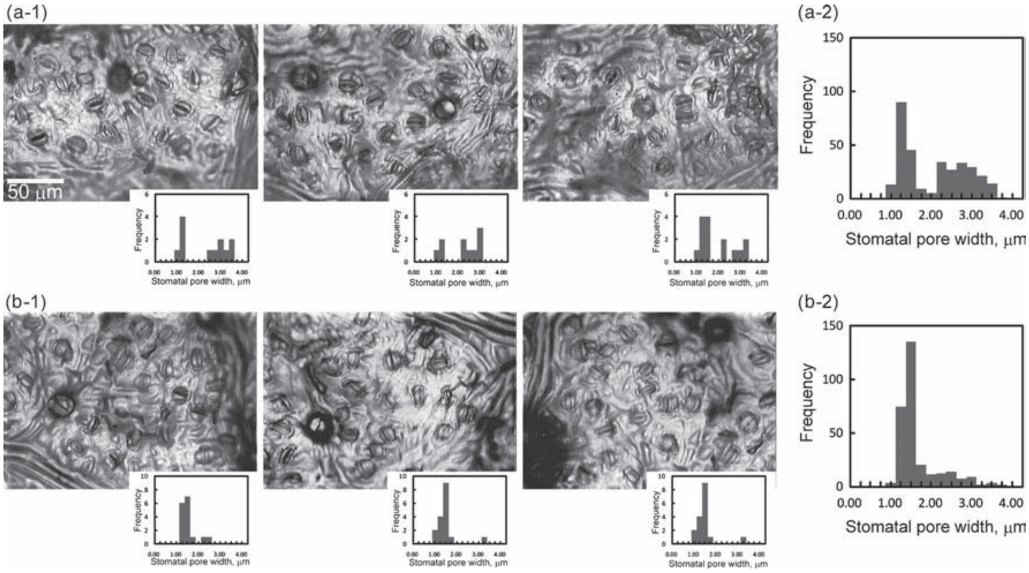

Figure 4. Images of individual stomatal behavior and frequency distribution of stomatal pore width (a-1) in leaves of *S. leprosula* immediately following the onset of midday depression (09:15) and (b-1) in the middle of the midday depression (12:00). Pooled frequency distribution data for stomatal pore width across times are shown to the right (a-2 and b-2).

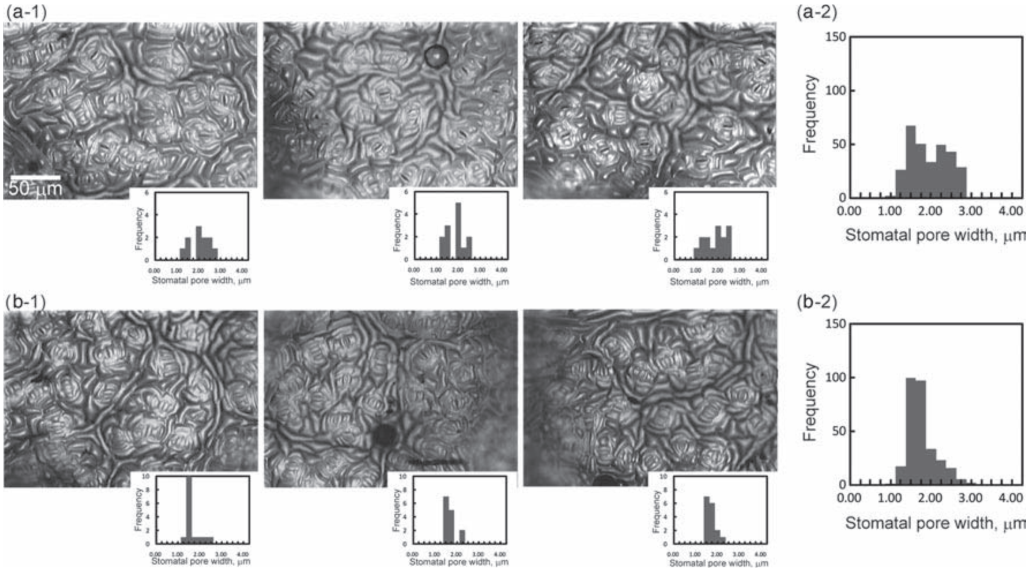

Figure 5. Images of individual stomatal behavior and frequency distribution of stomatal pore width (a-1) in leaves of *S. macrantha* immediately following the onset of midday depression (09:15) and (b-1) in the middle of the midday depression (12:00). Pooled frequency distribution data for stomatal pore width across times are shown to the right (a-2 and b-2).

midday period (Figure 3). Previous studies have reported strong correlations between midday depression of photosynthesis and VPD (e.g., Brodribb and Holbrook 2004, Tay et al. 2007). In most plant species observed, both A and g_s recovered in the afternoon (Figure 3), coupled with the depression of radiation and VPD (Figure 1). Our data suggest that patchy bimodal stomatal closure occurs with increased VPD to prevent excess water loss from leaves through evapotranspiration, with concomitant severe depression of photosynthesis.

Patchy stomatal closure has been detected in some species with heterobaric leaves using the infiltration method (e.g., Beyschlang and Pfanz 1990, Küppers et al. 1999). However,

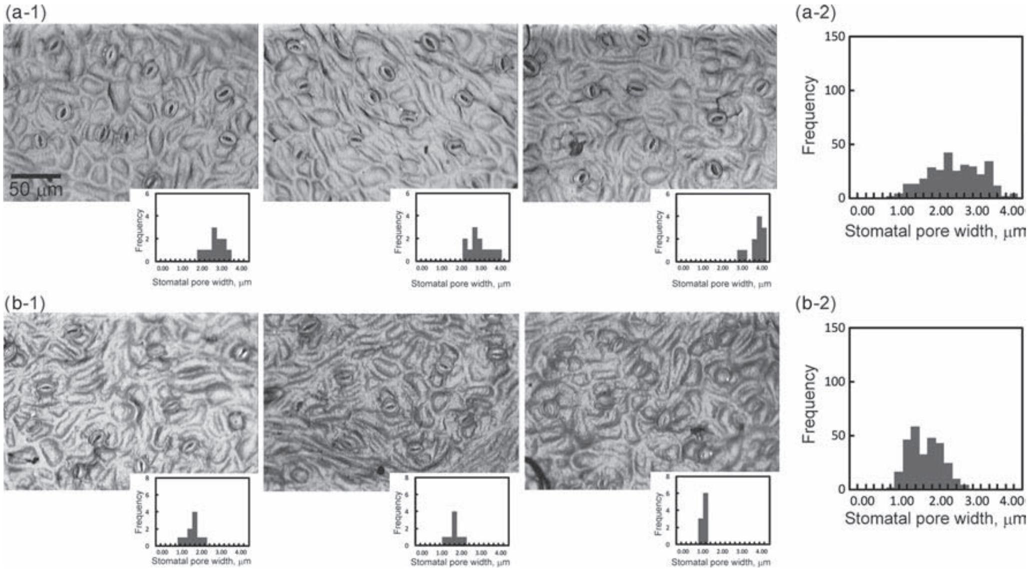

Figure 6. Images of individual stomatal behavior and frequency distribution of stomatal pore width (a-1) in leaves of *D. tempehes* immediately following the onset of midday depression (10:30) and (b-1) in the middle of midday depression (13:30). Pooled frequency distribution data for stomatal pore width across times are shown to the right (a-2 and b-2).

correlations between distribution of stomatal aperture and gas exchange characteristics remained unclear, because direct observation of individual stomatal movements under field conditions was technically difficult. Kaiser and Kappen (2000) observed in situ stomatal movements by video microscopy while simultaneously measuring leaf gas exchange in the field. They observed between 5 and 40 stomata in each experiment, but this methodology did not permit comparisons of stomatal aperture distribution on a single leaf. Our observation of patchy bimodal stomatal closure using the SUMP method allowed us to discern patterns of patchiness. We observed a bimodal stomatal closure pattern during midday depression of *A* in top-canopy leaves of the tropical rainforest species, *S. leprosula*, *S. macrantha* and *D. tempehes* (Figures 4–6). Although, bimodal distribution of stomatal aperture occurred within patches, rather than between patches. Within a bundle sheath extension (at least a small one having a few dozen stomata), lateral diffusion of CO_2 would be sufficiently rapid. Assuming uniform C_i within a patch, a bimodal distribution of stomatal aperture between patches is required to explain the midday depression of *A* induced by 'bimodal stomatal closure'. A bimodal frequency distribution of stomatal aperture in a small area within a patch would not cause serious overestimation of C_i (Cheeseman 1991). However, our data suggest that bimodal stomatal closure occurred among adjacent stomata within patches, rather than among patches within a single leaf, and still coupling with the depression of *A* induced by patchy stomatal closure that fits a bimodal frequency pattern. When the pattern of stomatal closure is patchy bimodal, homogeneous behavior between adjacent stomata within a patch is predicted. A possible explanation for this is that the heterogeneity of C_i might occur within a patch, although the details remain unclear. Kamakura and Furukawa (2008) reported from direct observations that, in some cases, heterogeneous responses to CO_2 occur between adjacent stomata in leaves of homobaric species that lack bundle sheath extensions. Further analyses should take into account scale differences in the heterogeneity of stomatal behavior between and within patches and within single leaves.

We used saplings in this study, and it is possible that the behavior of these small trees differs from that of mature trees. Further studies of midday depression should be extended to mature trees.

Acknowledgments

We thank Ms Lillian Chua and Mr Qua Eng Seng for organizing our research in a nursery at FRIM. We also thank Dr Makoto Tani, Dr Abdul Rahim Nik and Dr Toshinori Okuda and a joint research project between FRIM, UPM and NIES.

Funding

This research was partially supported by the Japan Society for the Promotion Science (JSPS), Grant-in-Aim for Scientific Research.

References

Beyschlag, W. and H. Pfanz. 1990. A fast method to detect the occurrence of nonhomogeneous distribution of stomatal aperture in heterobaric plant leaves. Oecologia 82:52–55.

Beyschlag, W., H. Pfanz and R.J. Ryel. 1992. Stomatal patchiness in Mediterranean evergreen sclerophylls: phenomenology and consequences for the interpretation of the midday depression in photosynthesis and transpiration. Planta 187:546–553.

Brodribb, T.J. and N.M. Holbrook. 2004. Diurnal depression of leaf hydraulic conductance in a tropical tree species. Plant Cell Environ. 27:820–827.

Chazdon, R.L., R.W. Pearcy, D.W. Lee and N. Fetcher. 1996. Photosynthetic responses of tropical forest plants to contrasting light environments. In Tropical Forest Plant Ecophysiology. Eds. S.S. Mulkey, R.L. Chazdon and A.P. Smith. Chapman and Hall, New York, USA, pp 5–55.

Cheeseman, J.M. 1991. PATCHY: simulating and visualizing the effects of stomatal patchiness on photosynthetic CO_2 exchange studies. Plant Cell Environ. 14:593–599.

Doughty, C.E., M.L. Goulden, S.D. Miller and H.R. da Rocha. 2006. Circadian rhythms constrain leaf and canopy gas exchange in an Amazonian forest. Geophys. Res. Lett. 33:L15404.

Downton, W.J.S., B.R. Loveys and W.J.R. Grant. 1988. Stomatal closure fully accounts for the inhibition of photosynthesis by abscisic acid. New Phytol. 198:263–266.

Farquhar, G.D., S. von Caemmerer and J.A. Berry. 1980. A biochemical model of photosynthetic CO_2 assimilation in leaves of C_3 species. Planta 149:79–90.

Grassi, G., E. Vicinelli, F. Ponti, L. Cantoni and F. Magnani. 2005. Seasonal and interannual variability of photosynthetic capacity in relation to leaf nitrogen in a deciduous forest plantation in northern Italy. Tree Physiol. 25:349–360.

Gunasekera, D. and G.A. Berkowitz. 1992. Heterogeneous stomatal closure in response to leaf water deficits is not a universal phenomenon. Plant Physiol. 98:660–665.

Kaiser, H. and L. Kappen. 2000. In situ observation of stomatal movements and gas exchange of *Aegopodium podagraria* L. in the understory. J. Exp. Bot. 51:1741–1749.

Kamakura, M. and Furukawa, A. 2008. Responses of individual stomata in *Ipomoea pes-caprae* to various CO_2 concentrations. Physiol. Plant. 132:255–261.

Kenzo, T., T. Ichie, Y. Watanabe and T. Hiromi. 2007. Ecological distribution of homobaric and heterobaric leaves in tree species of Malaysian lowland tropical rainforest. Am. J. Bot. 94:764–775.

Kosugi, Y. and N. Matsuo. 2006. Seasonal fluctuations and temperature dependence of leaf gas exchange parameters of co-occurring evergreen and deciduous trees in a temperate broad-leaved forest. Tree Physiol. 26:1173–1184.

Kosugi, Y., S. Shibata and S. Kobashi. 2003. Parameterization of the CO_2 and H_2O gas exchange of several temperate deciduous broad-leaved trees at the leaf scale considering seasonal changes. Plant Cell Environ. 26:285–301.

Kosugi, Y., S. Takanashi, N. Matsuo and N. Abdul Rahim. 2009. Midday depression of leaf CO_2 exchange within the crown of *Dipterocarpus sublamellatus* in a lowland dipterocarp forest in Peninsular Malaysia. Tree Physiol. 29:505–515.

Küppers, M., I. Heiland, H. Schneider and P.J. Neugebauer. 1999. Light-flecks cause non-uniform stomatal opening-studies with special emphasis on *Fagus sylvatica* L. Trees 14:130–144.

Loreto, F. and T.D. Sharkey. 1990. Low humidity can cause uneven photosynthesis in olive (*Olea europea* L.) leaves. Tree Physiol. 6:409–415.

Mott, K.A. and T. Buckley. 1998. Stomatal heterogeneity. J. Exp. Bot. 49:407–417.

Mott, K.A. and T. Buckley. 2000. Patchy stomatal conductance: emergent collective behavior of stomata. Trends Plant Sci. 5:258–262.

Mott, K.A., Z.G. Cardon and J.A. Berry. 1993. Asymmetric patchy stomatal closure for the two surfaces of *Xanthium strumarium* L. leaves at low humidity. Plant Cell Environ. 20:1098–1107.

Sharkey, T.D. and J.R. Seemann. 1989. Mild water stress effects on carbon-reduction-cycle intermediates, ribulose bisphosphate carboxylase activity, and spatial homogeneity of photosynthesis in intact leaves. Plant Physiol. 89:1060–1065.

Takanashi, S., Y. Kosugi, N. Matsuo, M. Tani and N. Ohte. 2006. Patchy stomatal behavior in broad-leaved trees grown in different habitats. Tree Physiol. 26:1565–1578.

Tay, A.C., A.M. Abdullah, M. Awang and A. Furukawa. 2007. Midday depression of photosynthesis in *Enkleia malaccensis*, a woody climber in a tropical rainforest. Photosynthetica 45:189–193.

Terashima, I. 1992. Anatomy of non-uniform leaf photosynthesis. Photosynth. Res. 31:195–212.

Terashima, I., S.C. Wong, C.B. Osmond and G.D. Farquhar. 1988. Characterization of non-uniform photosynthesis induced by abscisic acid in leaves having different mesophyll anatomies. Plant Cell Physiol. 29:385–394.

Travis, A.J. and T.A. Mansfield. 1981. Light saturation of stomatal opening on the adaxial and abaxial epidermis of *Commelina communis*. J. Exp. Bot. 32:1169–1179.

von Caemmerer, S. and G.D. Farquhar. 1981. Some relationships between biochemistry of photosynthesis and the gas exchange of leaves. Planta 153:376–387.

Wang, X.Q., W.H. Wu and S.M. Assmann. 1998. Differential responses of abaxial and adaxial guard cells of broad bean to abscisic acid and calcium. Plant Physiol. 118:1421–1429.

West, J.D., D. Peak, J.Q. Peterson and K.A. Mott. 2005. Dynamics of stomatal patches for a single surface of *Xanthium strumarium* L. leaves observed with fluorescence and thermal images. Plant Cell Environ. 28:633–641.

Wilson, K.B., D.D. Baldocchi and P.J. Hanson. 2000. Spatial and seasonal variability of photosynthetic parameters and their relationship to leaf nitrogen in a deciduous forest. Tree Physiol. 20:565–578.

Wylie, R.B. 1952. The bundle sheath extension in leaves of dicotyledons. Am. J. Bot. 39:645–651.

水文・水資源学会誌
J. Japan Soc. Hydrol. & Water Resour.
Vol. 20, No.4, Jul. 2007　pp. 265 - 277

原著論文

生育地，生活形態の多様な樹種における水利用様式の比較

福井 佑介[1)]　小杉 緑子[1)]　松尾 奈緒子[1)]
高梨　聡[1)]　谷　誠[1)]

[1)]京都大学大学院農学研究科地域環境科学専攻森林水文学分野
（〒606-8502　京都市左京区北白川追分町）

生育地，生活形態の多様な樹種の樹冠葉における蒸散速度，気孔コンダクタンス，葉・土壌の水ポテンシャル等を測定した．また，*P*−*V*曲線法を用いて葉の水分特性を評価した．そして，得られた通水コンダクタンス，葉の水分特性および蒸散速度を関連づけて解析することにより，多様な樹種の高木個体における水利用様式を明らかにした．冷温帯落葉広葉樹種のブナは通水コンダクタンスが高い反面，葉の初発原形質分離点の水ポテンシャルは高く，脱水を避ける水利用様式を採っていた．温帯常緑針葉樹種のヒノキでは，乾燥期に通水コンダクタンスおよび蒸散速度の低下が見られ，通水障害に対して気孔閉鎖を起こしていたと思われる．暖温帯常緑広葉樹種4種では常に気孔コンダクタンスを低く抑制していた．また，乾燥期には浸透調節を行って葉の耐乾性を高めるなど，乾燥条件下での生存に有利な水利用様式を採っていた．熱帯常緑広葉樹種2種は通水コンダクタンスが低かったが，*Dipterocarpus sublamellatus* Foxw.は他の2種と比較して通水コンダクタンスが高く，通水距離の増大を克服する給水システムを有している可能性が示唆された．

キーワード：水利用様式，蒸散，通水コンダクタンス，水ポテンシャル，*P*−*V*曲線法

I．はじめに

植物がどのように蒸散と給水を行うか，すなわち植物の水利用様式を知ることは，水環境がどのように植生に制約を与えているのか，また植生がどのように水循環過程に影響を与えているのかといった，水環境と植生との相互作用を明らかにする上で非常に重要である．

植物の蒸散を介した土壌から大気中への一連の水輸送系（Soil-Plant-Atmosphere Continuum；SPAC）にオームの法則を適用すると，蒸散速度は下記の(1)，(2)式で表すことができる．

$$E = K_{s-l} \times \Delta\psi \tag{1}$$

$$\Delta\psi = (\psi_s - \psi_l) \tag{2}$$

E：蒸散速度（mmol m^{-2} s^{-1}），$K_{s\text{-}l}$：土壌−葉間の通水コンダクタンス（mmol m^{-2} s^{-1} MPa^{-1}），ψ_s，ψ_l：土壌および葉の水ポテンシャル（MPa），$\Delta\psi$：土壌−葉間の水ポテンシャル差（MPa）である．

(1) 式中の$K_{s\text{-}l}$は植物の耐乾強度を決定する大きな要因の1つである．なぜなら，それが蒸散による水分損失を補填し，葉が過剰な脱水状態に陥るのを回避する能力だからである．水ストレスが進行するにつれ，植物と土壌に生じる障害によって土壌−葉間の通水パイプラインを無傷に保っておくことが困難になる．このパイプラインすなわち道管組織の水輸送特性が，葉への水供給速度，また気孔の蒸散速度を物理的に制限する（Tyree and Sperry 1989）．さらに，このことは気孔制御を通して植物の光合成速度を制限することにつながる（Ryan *et al.*, 2000）．Hubbard *et al.*（2001）は$K_{s\text{-}l}$の低下に伴って，気孔コンダクタンス，光合成速度，Eが低下することを幼樹における実験によって示した．また，Hubbard *et al.*（1999）は自然条件下に生育する樹木についても，$K_{s\text{-}l}$の一時的な向上が気孔コンダクタンスの向上をもたらすことを実証している．いっぽう，樹木はマスバランスの変化や道管自体の透水性の向上（Phillips *et al.*, 2002）や辺材貯留水の利用（Goldstein *et al.*, 1998）

によって樹高生長による通水性の低下を軽減させることも分かっている．Ryan and Yoder（1997）は樹木の生長速度が樹齢とともに低下するのは樹高の伸長に伴うK_{s-l}の低下が原因であるとする説（Hydraulic Limitation Hypothesis）を提唱した．このように，葉への水供給を司るK_{s-l}は植物の生育に重大な影響を及ぼす．

また一方で，（1）式において$\Delta\psi$を大きくすれば，Eも大きくなる．ψ_sとψ_lでは後者のほうが2オーダー大きく，また前者が環境要因によるものであるため，$\Delta\psi$の種間差あるいは個体差は事実上，ψ_lとそれをもたらす葉の水分特性によって決定される．したがって，葉の水分特性および耐乾性も乾燥条件下での生育の可否を決定する要因である．脱水に耐えて膨圧を維持する能力の高い葉を有すれば，乾燥条件下においても安定したEおよび光合成速度維持することができるからである．葉の水分特性において，ψ_lの低下がおこった時に原形質分離を防ぎ膨圧を維持するためのメカニズムとして，主に細胞壁の弾性特性や浸透調節が挙げられる（Tyree and Jarvis, 1982）．乾燥に対する細胞壁の弾性特性の適応には2パターンーすなわち，①弾性特性を低く，つまり柔軟な細胞壁にして，水分を失っても膨圧を維持させる方法（Kikuta and Richter, 1986）と，②弾性特性を高く，つまり硬い細胞壁にして，わずかな脱水で膨圧を大きく下げ，吸水力を向上させる方法（Cheung *et al*., 1975）ーがあると考えられている．前者は乾燥に長期間耐えうる点で，後者は短期的な乾燥に対して敏感であるという点で有利である（吉川，2004）．なお，生育段階によってもどちらの方法が有利になるかは異なる（Saito and Terashima, 2004）．また，浸透調節とは液胞中に糖類あるいはK^+やCl^-などのイオンを蓄積させて細胞にはたらく浸透圧（ポテンシャル）を低くすることにより，膨圧維持能力を高めることである（吉川，2004）．このことにより，脱水で細胞代謝が不安定になるのが抑制され，水ストレスからの回復も助長される（Morgan, 1984）．

以上に述べてきたように，（1）式はψ_lおよびK_{s-l}の両方が気孔制御を通じてEを制御していることを示唆する．したがって，植物の水利用様式を理解し記述する方法として，$\Delta\psi$，K_{s-l}そしてEの相互関係を総合的に解析する手法が非常に有効である（石田・谷，2003）．

Ishida *et al*.（1992）は落葉広葉樹林の林床に生育する低木10種と樹冠構成樹種2種について研究し，自然条件に生育する低木がいくつかの水利用様式をもつことを明らかにした．さらに，それらの$\Delta\psi$あるいはK_{s-l}の変化に基づいたEの順応について解析している．また，Saito *et al*.（2003）は日本の冷温帯林に生育する8種の主要な落葉広葉樹種について研究を行っている．この研究では，観測地に建設されたタワーを用いて地上約4 mの高さで観測が行われた．彼らは供試木を同齢・同生育条件に管理して各樹種の最大蒸散速度の違いについて解析し，それらの樹種間ではK_{s-l}よりも葉の耐乾性により最大蒸散速度の多様性が説明できたと報告している．

これらの研究は同生育地の樹木（おもに中低木）について水利用様式を調べた研究であり，生育地，生活形態の異なるいくつかの植物種を対象に比較を行った例は，わずかに石田・谷（2003）があるのみである．異なる生育地，生活形態の下において，樹木の水利用様式がどの程度の幅を持つのかを調べることは，それぞれの生育地の水環境に樹木がどの程度まで適応できるのかを知るために重要である．また，樹冠を構成する高木類は低木や草本，作物など他の植生に比べて水輸送の面で様々な制約を受けるため，これら樹冠構成木における水利用様式が，樹高や生活形態，さらには様々な環境下における植生タイプの決定や陸域の水循環過程にも大きな影響を与えていると予想される．そこで，本研究では生育地，生活形態の異なる，樹冠構成個体の水利用様式を比較するため，冷温帯落葉広葉樹種1種，温帯常緑針葉樹種1種，暖温帯常緑広葉樹種4種そして熱帯常緑広葉樹種3種（いずれも樹冠構成個体）を対象に，E，ψ_s，ψ_lおよびK_{s-l}を測定・算出した．また同時に葉の水分特性について測定を行い，それらの相互関係を解析することで，生育地，生活形態の多様な樹木が有する水利用様式の一端を明らかにすることを目的とした．

Ⅱ．材料と方法

1．調査地と供試木の概要

生育地・生活形態の多様な樹種を対象とするため，特徴的な森林タイプを有する4調査地を設定した．各調査地で観測対象とした樹木個体，調査日および各調査日におけるAPI（先行降雨指数）を**表ー1**に示す．

1）冷温帯落葉広葉樹林（金糞岳ブナ林）

本調査地は滋賀県東浅井郡浅井町の金糞岳に位置

表－1　各調査地で観測対象とした樹種，樹高，観測日および各観測日におけるAPI，正午頃の平均E, g_s, ψ_l, およびP-V曲線の$\psi_{w\text{-}tlp}$, $\psi_{s\text{-}sat}$

Table 1　List of examined tree species in each habitat, tree height, date, API, E, g_s, ψ_l, around noon of each observation day, and $\psi_{w\text{-}tlp}$, and $\psi_{s\text{-}sat}$ of P-V curve of each species.

Site	Tree	Height (m)	E, g_s, ψ_l, $K_{s\text{-}1}$						P-V curve			
			Date of observation (API)	n	E	g_s	ψ_l	$K_{s\text{-}l}$	Date of sampling	n	$\psi_{w\text{-}tlp}$	$\psi_{s\text{-}sat}$
Cool-temperate deciduous broad-leaved forest (Kanakuso-dake N35° 32′ E136° 20′ a.s.l. 1050 m)	*Fagus crenata*	16	16 May, 2005	3	2.57	0.16	-1.07	2.59	16 May, 2005	3	-1.07	-0.83
Temperate evergreen coniferous forest (Kiryu N34° 58′ E136° 00′ a.s.l. 190-255 m)	*Chamaecyparis obtusa*	19	6 Jul, 2004* (12.7)	6	2.52	0.08	-1.51	1.67	13 Sep, 2005	3	-2.11	-1.48
			22 Jul, 2004* (8.5)	6	2.65	0.09	-1.59	1.70				
			28 Jul, 2004* (5.2)	6	2.35	0.08	-1.39	1.69				
			24 Aug, 2004* (51.5)	6	1.73	0.16	-1.10	1.57				
			2 Nov, 2004** (37.0)	6	0.93	0.11	-1.21	0.76				
			16 Jul, 2005* (38.6)	6	1.67	0.05	-1.52	1.10				
			9 Aug, 2005* (8.4)	6	1.12	0.05	-1.43	0.80				
			10 Aug, 2005* (6.3)	6	0.76	0.03	-1.35	0.57				
			13 Sep, 2005** (17.6)	6	0.37	0.02	-1.31	0.28				
Warm-temperate evergreen broad-leaved forest (Akou N34° 44′ E134° 22′ a.s.l. 0-20 m)	*Castanopsis cuspidata*	8-9	23 Aug, 2000** (0.8)	3	0.40	0.08	-2.47	0.17	25 Jan, 2005	2	-1.80	-1.05
			11 Jul, 2001** (9.6)		1.57	0.19	-1.15	4.17				
	Quercus glauca	8-9	23 Aug, 2000** (0.8)	3	0.81	0.02	-2.08	0.40		1	-2.62	-1.81
			11 Jul, 2001** (9.6)		2.21	0.09	-0.82	2.89				
	Quercus Phillyraeoides	8-9	23 Aug, 2000** (0.8)	3	2.97	0.06	-2.31	1.32		2	-2.39	-1.14
			11 Jul, 2001** (9.6)		2.52	0.13	-0.87	3.08				
	Cinnamomun camphora	8-9	23 Aug, 2000** (0.8)	3	1.07	0.02	-1.65	0.67		2	-2.40	-1.72
			11 Jul, 2001** (9.6)		2.90	0.14	-1.24	2.46				
Tropical evergreen broad-leaved forest (Pasoh N2° 58′, E102° 18′ a.s.l. 75-150 m)	*Xanthophyllum stipitatum*	32	12 Feb, 2005** (0.1)	3	1.20	0.03	-1.21	1.04	6-13 Feb, 2005	3	-2.10	-1.56
	Dipterocarpus sublamellatus	40	10 Sep, 2004** (1.5)	5	2.49	0.07	-	-	6-13 Feb, 2005	2	-1.88	-1.41
			13 Feb, 2005** (0.1)	3	4.30	0.17	-	-	8 May, 2005	2		
			25 Oct, 2005** (18.5)	8	3.66	0.11	-1.07	3.56				
	Ptychopyxis caput-medusae	32	11 Sep, 2004** (1.3)	3	2.14	0.05	-1.50	1.46	6-13 Feb, 2005	2	-1.92	-1.49

* the day that E, g_s and Ψ_1 were observed one time around noon　** the day that diurnal change of E, g_s and Ψ_1 were observed　n : sampling number

Fagus crenata：ブナ、*Chamaecyparis obtuse*：ヒノキ、*Castanopsis cuspidata*：シイノキ、*Quercus glauca*：アラカシ、*Quercus. Phillyraeoides*：ウバメガシ、*Cinnamomun camphora*：クスノキ、*Xanthophyllum stipitatum*：ヒメハギ科、*Dipterocarpus sublamellatus*：フタバガキ科、*Ptychopyxis caput-medusae*：トウダイグサ科

する落葉広葉樹二次林（北緯35° 32′，東経136° 20′，標高約1,050 m）である．周辺の年平均気温は12-13 ℃，年降水量は2,500-3,000 mm（武田，1991）である．年最大積雪深は平均で80-100 cm，多い年には4 m以上にもなる多雪地域である．そのため，年降水量の約30 %が冬季の降水で占められる（武田，1991）．植生区分は，滋賀県植物地理区の中で湖北植物区に分類され（村瀬，1979），北方系要素の植物や日本海要素の植物が多いことが特徴である．優占する高木はブナ・ミズナラであり，中下層にはヤマボウシやマルバマンサク，カエデ類などが見られる．

本観測地では，樹高約16 mの*Fagus crenata* Blume（ブナ）1個体を対象とした．

2）温帯ヒノキ林（桐生水文試験地）

本調査地は滋賀県南部（北緯34° 58′，東経136° 00′ 標高190-255 m）に位置し，田上山系に属する．本研究は，試験地源頭部の小流域であるマツ沢流域にて行った．この流域の流域面積は0.68 ha，植生は主に1959年に植栽されたヒノキである．観測を行った2004年，2005年の年平均気温および年降水量は，そ

れぞれ13.9 ℃, 1,797 mmと13.0 ℃, 1,151 mmであった．本調査地では①乱流変動法を用いた樹冠上のフラックス測定（Takanashi *et al.*, 2005a），②土壌呼吸量の時空間変動（三谷ら，2003），③樹体貯熱量の推定（和田ら，2002），④降雨中および降雨後の森林における蒸発散過程（高梨ら，2003）など，森林生態系によるガス交換の総合的な研究が行われている．

ここでは，マツ沢流域に生育する約30年生の *Chamaecyparis obtusa* Sieb. et Zucc.（ヒノキ）1個体を対象とした．樹高は約19 mである．

3）暖温帯常緑広葉樹林（赤穂緩衝緑地）

本調査地は，兵庫県赤穂市（北緯34° 44′，東経134° 22′，標高0-20 m）に位置する人工照葉樹林である．赤穂市の年平均気温および年平均降水量（1995-1999）は15.2 ℃および1,159 mmである（松尾・小杉，2002）．また，夏季に高温少雨となるのが特徴である．本観測地では，1987年に温帯常緑広葉樹種12種と温帯落葉広葉樹種4種の3年生の苗木が，1-2本 m^{-2} 程度の密度で植栽された．2002年1月現在では，全個体（劣勢木を含む）の平均樹高は5.3 mである（松尾・小杉，2002）．本研究では2000年および2001年の観測データを用いる．この間の年平均気温および年降水量は，それぞれ16.0 ℃，788 mm（2000）および，15.3 ℃，1,078 mm（2001）であった（松尾・小杉，2002）．本調査地では① 樹冠における炭素・熱フラックスの季節あるいは年変動（Tanaka *et al.*, 2002; Kosugi *et al.*, 2005），② 個葉レベルのガス交換特性や炭素安定同位体を用いた水利用効率に関する研究（松尾・小杉，2002；松尾ら，2002；Kosugi and Matsuo,2006）などが行われている．

ここでは，*Castanopsis cuspidata* Shottky（シイノキ），*Quercus glauca* Thunb.（アラカシ），*Quercus. phillyraeoides A.* Gray（ウバメガシ），*Cinnamomun camphora* Sieb.（クスノキ）を対象とした．樹高は約8-9 mである．

4）熱帯常緑広葉樹林（Pasoh森林保護区）

本調査地は半島マレーシア，首都クアラ・ルンプールの南東約70 km（北緯2° 58′，東経102° 18′，標高75-150 m）に位置する（Soepadmo 1978）．気温の変化は年間を通じてほとんど見られず，1970年から1974年における年平均気温は24.8 ℃，年平均降水量は2,054 mmであった（Soepadmo 1978）．また，2003年の年平均気温および年降水量は，それぞれ25.9 ℃および1,896 mmであった．半島マレーシアでは，南西モンスーンの影響を受ける4-5月と，北東モンスーンの影響を受ける10-11月が雨季にあたり，降水量が多い．しかし，本保護区は半島内陸部に位置するため半島マレーシアの中では比較的少雨の地域となっている．保護区内の中心部約650 haは，*Shorea*属や*Dipterocarpus*属を中心とした多くのフタバガキ科樹種により構成される低地性林である．連続した樹冠の高さは約35 mであるが，エマージェントと呼ばれ，樹冠から突出する高木は樹高45 mに達する．本調査地では乱流変動法を用いた熱帯林のガス交換特性（Takanashi *et al.*, 2005b），加圧浸潤法による熱帯樹種の個葉気孔動態（Takanashi *et al.*, 2006），遮断降雨量の空間分布（Konishi *et al.*, 2006）等の研究が行われている．

ここでは，*Xanthophyllum stipitatum* Benn.（ヒメハギ科），*Dipterocarpus sublamellatus* Foxw.（フタバガキ科），*Ptychopyxis caput-medusae*（Hk.f.）Ridl.（トウダイグサ科）の各1個体を対象とした．各樹木の樹高は，*X. stipitatum* と*P. caput-medusae*がそれぞれ約32 m，*D. sublamellatus*が約40 mである．

2. 観測方法

1）蒸散速度および気孔コンダクタンス

各調査地に建設されている観測タワーから供試木の樹冠にアクセスした．そして，上層の日当たりの良い当年葉で携帯型の光合成蒸散測定装置（Li-1600あるいはLi-6400, Li-Cor）を用いて，蒸散速度（E_{inner}，mmol m^{-2} s^{-1}）および気孔コンダクタンス（g_s，mol m^{-2} s^{-1}）等を測定した．ブナおよびヒノキの観測にはLi-1600，暖温帯常緑広葉樹種4種と熱帯常緑広葉樹種3種の測定にはLi-6400を用いた．また，同時にこれらの光合成蒸散測定装置で気温，相対湿度および葉温（T_{leaf}，℃）などの条件も測定し，g_sおよびEについて再計算を行った（本章3節－2項で詳述）．

2）葉の水ポテンシャル（ψ_l）

光合成蒸散測定装置による測定の後，サンプル葉あるいはその近傍の葉を切り取り，プレッシャーチャンバー（Model 3005, Soilmoistureあるいは Model 600, PMS Instrument）を用いて速やかにψ_lを測定した．ただし2005年10月25日の*D. Sablamellatus*における測定では，ハイグロメーター（HR-33T, Wescor）を用いた．

3）土壌の水ポテンシャル（ψ_s）

供試木周辺の林床土壌において，土壌深30 cm（赤穂では40 cm）にテンシオメーター（DIK 3150-12，大起理化工業）を埋設してψ_sを連続測定した

（冷温帯落葉広葉樹林を除く）．冷温帯落葉広葉樹林では，滋賀県立大学陸圏生態系研究室によって2003年からADRプロファイルプローブ（PR1/4，池田計器製作所）が設置され，林床土壌の体積含水率（$m^3\,m^{-3}$）が測定されている．本研究ではこのデータの土壌深30 cmにおける値と兵庫県六甲山におけるブナ林土壌の水分特性曲線（林祐妃，私信）からψ_sを推定し，解析に供した．はじめにで述べた理由から，ψ_sの推定誤差による$\Delta\psi$への影響はほとんど無い．

4）葉の水分特性（*P-V*曲線）

樹冠において日当たりの良い場所の葉が数枚程度ついた枝をサンプリングして直後に水切りを行い，黒いビニール袋をかけてガス交換を抑制したまま一晩以上吸水させた．そして，プレッシャーチャンバー（Model 3005, Soilmoisture）あるいはハイグロメーター（HR-33T, Wescor）を用いて樹種ごとにそれぞれ1-6サンプルの*P-V*曲線を作成（Scholander *et al.*, 1965; 丸山・森川，1983）した．なお，実験中の蒸散を防ぐため，葉身はアルミホイルで覆った．そして，徐々に失水させたときに最初に細胞が膨圧を失って原形質分離を起こす時点（初発原形質分離点）の水ポテンシャル（$\psi_{w\text{-}tlp}$），充分吸水した時の浸透ポテンシャル（$\psi_{s\text{-}sat}$）などを求めた．

5）観測日およびサンプリング方法

観測日およびサンプリング方法の概要を**表一1**にしめす．

冷温帯落葉広葉樹林のブナでは，2005年5月16日に地上高約15 mの3枚の個葉で1）と2）の日変化観測を行った．また同日に樹冠葉3サンプルを採取して4）の実験を行った．温帯常緑針葉樹林のヒノキでは，2004年7月6日，7月22日，7月28日，8月24日および2005年7月16日，8月9日，8月10日，9月13日に地上高約16 mの当年葉（2004年7月時点）6枚で1）と2）の観測（正午一回のみ）を行った．2004年11月2日および2005年9月13日には6枚の個葉で1）と2）の日変化観測を行った．また，2005年9月13日に採取したヒノキの樹冠葉（枝部を含む）3サンプルで4）の実験を行った．暖温帯常緑広葉樹林の4樹種では，2000年8月23日および2001年7月11日に，地上高約9 mの葉各3枚で1）と2）の日変化観測を行った．また，2005年1月25日に採取した4樹種の樹冠葉1-2サンプルで4）の実験を行った．熱帯常緑広葉樹林では，2004年9月10日（*D. sablamellatus*），2004年9月11日（*P. caput-medusae*），2005年2月12日（*X. stipitatum*），2005年2月13日および2005年10月25日（両日とも*D. sablamellatus*）に，いずれも地上高約31 mの葉3-8枚で1）と2）の日変化観測を行った．また，2005年2月6, 10, 13日に採取した*X. Stipitatum*，*D. sablamellatus*，*P. caput-medusae*の樹冠葉各2-3サンプル，さらに2005年5月8日に採取したD. sablamellatusの樹冠葉2サンプルで4）の実験を行った．

3. 計算方法

1）API

個葉観測当日の林床土壌の乾燥を表す指標として，下記の（3）式で定義されるAPI（Antecedent Precipitation Index；先行降雨指数）を算出した．

$$\mathrm{API}=\sum_{k=1}^{n}(P_k/k) \tag{3}$$

k：個葉観測日のk日前，P_k：その日の日降水量（mm）を表す．本研究では，個葉観測日の30日前までの降水を対象（n=30）にAPIを算定した（**表一1**）

2）気孔コンダクタンスおよび蒸散速度

光合成と蒸散が同時に起こる点を考慮するため，光合成蒸散測定装置による蒸散速度（E_{inner}, $\mathrm{mmol\,m^{-2}\,s^{-1}}$）と下記の（4）式（von Caemmerer and Farquhar, 1981）を用いてg_s（$\mathrm{mol\,m^{-2}\,s^{-1}}$）を再計算した．

$$\frac{E_{inner}}{1000}\left(1-\frac{W_i+W_a}{2}\right)=\frac{g_s g_{b-inner}}{g_s+g_{b-inner}}\left(W_i-W_a\right) \tag{4}$$

ここで，W_i：葉面上での飽和水蒸気モル分圧，W_a：大気の水蒸気モル分圧，$g_{b\text{-}inner}$：チャンバー内の葉面境界層コンダクタンス（$\mathrm{mol\,m^{-2}\,s^{-1}}$）である．$W_i$および$W_a$については，光合成蒸散測定装置によって同時測定された気温，葉温，大気の相対湿度から算出した．また，$g_{b\text{-}inner}$は，チャンバー内の風速が一定であることから1.5 $\mathrm{mol\,m^{-2}\,s^{-1}}$とした（高梨ら，2001）．しかし，チャンバー外の風速は刻々と変化する．そのため，E_{inner}は実際のEよりも過大評価されがちである（谷・石田，2003）．そこで，Eを下記の（5）式および（6）式（Pearcy *et al.*, 1989）によって算出した．

$$\frac{E}{1000}=\Delta W\left(\frac{g_s g_b}{g_s+g_b}\right) \tag{5}$$

$$g_b=0.446\left[0.715\left(\frac{u}{d}\right)^{0.5}\right]\left(\frac{273}{T_{leaf}+273}\right)\left(\frac{P}{101.3}\right)\times 10^3 \tag{6}$$

ΔW：T_{leaf}における飽和水蒸気濃度と周辺大気の水蒸

気濃度の差（mol mol^{-1}），g_b：葉面境界層コンダクタンス（mol m^{-2} s^{-1}），u :風速（m s^{-1}），d：葉長（m），P：大気圧（kPa）である．以下，本研究で扱う樹木葉の平均的な葉長を想定してd =0.1 mと仮定し，またP =101.3 kPaとして解析を行った．また，uは風速計（AC750, 牧野応用測器研究所あるいはModel 6071, KANOMAX）を用いて測定した．uが得られなかった場合はその値を1 m s^{-1}と仮定して計算した．

3）通水コンダクタンスの算出

単位葉面積あたりのK_{s-l}は，（1）式をK_{s-l}について解いた下記の（7）式から算出した．

$$K_{s-l}=\frac{E}{\Delta\psi} \qquad (7)$$

Ⅲ．結果

1．各樹種の個葉蒸散日変化

図ー1に，4つの生育地における9樹種（（a）冷温帯落葉広葉樹種1種，（b）温帯常緑針葉樹種（ヒノキ），（c）暖温帯常緑広葉樹種4種，（d）熱帯常緑広葉樹種3種）で行ったE，g_s，ψ_l，K_{s-l}の日変化測定・算出結果を示す．また**表ー1**に，各樹種の各測定日正午頃におけるE，g_s，ψ_l，K_{s-l}の測定・算出結果を示す．

1）冷温帯落葉広葉樹種（ブナ）

冷温帯落葉広葉樹種（ブナ）では，Eは13時頃が日最大値となる山型の変化を示した（**図ー1（a1）**）．g_sは11時頃から0.16 mol m^{-2} s^{-1}程度でほぼ頭打ちとなり，15時以降緩やかに低下した（**図ー1（a2）**）．ψ_lは12時頃に日最低値の約－1.1 MPaとなった（**図ー1（a3）**）．また，K_{s-l}は日中2-3 mmol m^{-2} s^{-1} MPa^{-1}前後の値をとった（**図ー1（a4）**）．

2）温帯常緑針葉樹種（ヒノキ）

温帯常緑針葉樹種（ヒノキ）では，2004年11月2日においては朝方のψ_lが－0.1 MPa以上と高かった（**図ー1（b3）**）．この日を湿潤日と位置づける．Eは

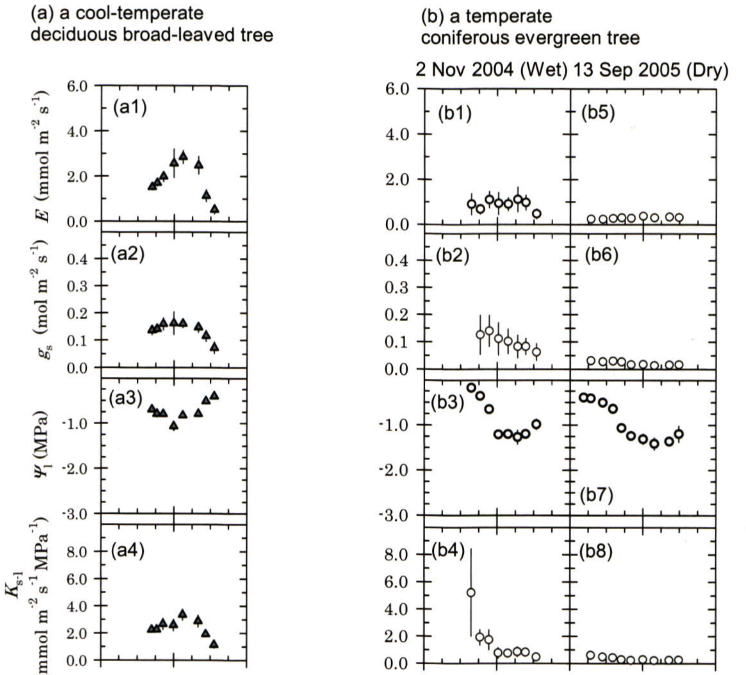

図ー1　各調査地に生育する樹木（a：冷温帯落葉広葉樹種1種，b：温帯常緑針葉樹種1種）の蒸散速度（E），気孔コンダクタンス（g_s），葉の水ポテンシャル（ψ_l），土壌-葉間の通水コンダクタンス（K_{s-l}）の日変化（図中のエラーバーは標準偏差を表す）．

Fig.1 Diurnal change of transpiration rate (E), leaf water potential (ψ_l), stomatal conductance (g_s), soil-leaf hydraulic conductance (K_{s-l}) in various trees grown in several different habitats (a : a cool-temperate deciduous broad-leaved tree, b : a temperate coniferous evergreen tree). Bars within the graph represent standard deviation.

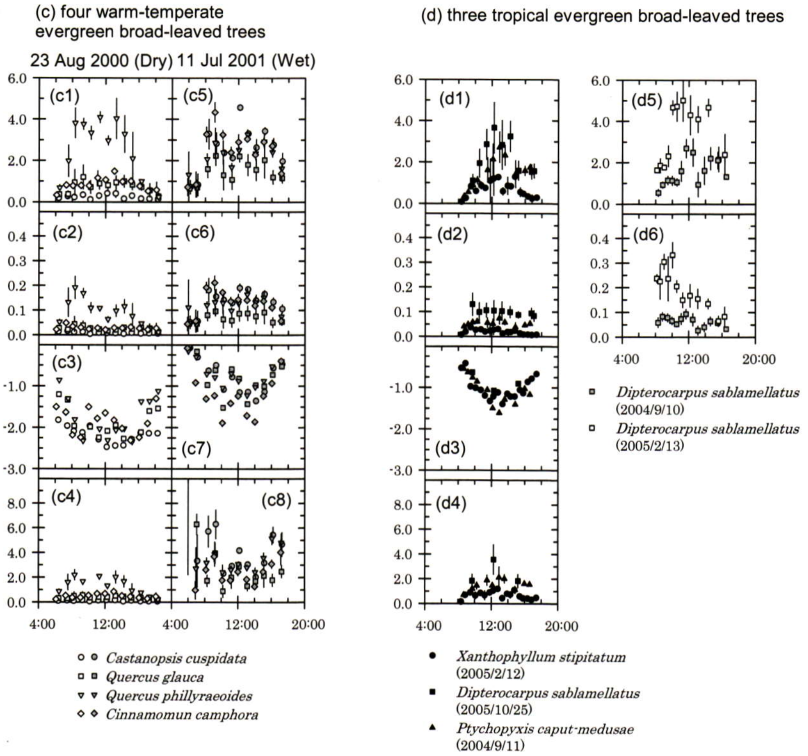

図－1　各調査地に生育する樹木（c：暖温帯常緑広葉樹種4種，d：熱帯常緑広葉樹種3種）の蒸散速度（E），気孔コンダクタンス（g_s），葉の水ポテンシャル（ψ_l），土壌-葉間の通水コンダクタンス（$K_{s\text{-}l}$）の日変化（図中のエラーバーは標準偏差を表す）．

Fig.1 Diurnal change of transpiration rate (E), leaf water potential (ψ_l), stomatal conductance (g_s), soil-leaf hydraulic conductance ($K_{s\text{-}l}$) in various trees grown in several different habitats (c : four warm-temperate evergreen broad-leaved trees, d : tropical evergreen broad-leaved trees). Bars within the graph represent standard deviation.

日最大値が1 mmol m^{-2} s^{-1}程度であった（図－1（b1））．g_sは正午前に日最大値0.11 mol m^{-2} s^{-1}を取り，午後になると徐々に低下した図－1（b2））．ψ_lは日中に約-1.3 MPaまで低下した（図－1（b3））．$K_{s\text{-}l}$は午前中高かったが，徐々に低下して正午頃以降には約0.8 mmol m^{-2} s^{-1} MPa^{-1}でほぼ一定になった（図－1（b4））．一方，2005年9月13日においては土壌の乾燥をうけて給水が阻害され夜明け前のψ_lが－0.4 MPa程度までしか回復していなかった（図－1（b7））．この日を乾燥日と位置づける．Eおよびg_sは湿潤日（2004年11月2日）に比べて低かった（図－1（b5, b6））．しかしψ_lの日中の最低値は約－1.4 MPaで湿潤日（2004年11月2日）と同程度であった（図－1（b7））．日中の$K_{s\text{-}l}$は0.3 mmol m^{-2} s^{-1} MPa^{-1}以下であった（図－1（b8））．

3）暖温帯常緑広葉樹種4種

暖温帯常緑広葉樹種4種では，2001年7月11日においてはAPIは9.6でψ_lが全樹種において朝方までに充分高くなっていた（図－1（c7））．この日を湿潤日と位置づける．Eは日中に約2.5-4 mmol m^{-2} s^{-1}まで上昇した（図－1（c5））．また，g_sは0.1-0.2 mol m^{-2} s^{-1}であった（図－1（c6））．日最低ψ_lは樹種によって差が大きく，最高値がウバメガシの－1.2 MPa，最低値がクスノキの－1.9 MPaであった（図－1（c37））．$K_{s\text{-}l}$は日中までに2-3 mmol m^{-2} s^{-1} MPa^{-1}まで低下したが，夕方には上昇に転じた（図－1（c8））．一方，2000年8月23日においてはAPIが0.8で強度の土壌乾燥が見られ，夜明け直後のψ_lが十分回復していなかった（図－1（c3））．この日を乾燥日と位置づける．Eはウバメガシを除く3樹種で概ね1 mmol m^{-2} s^{-1}以下であったが，ウバメガシは湿潤日（2001年7月11日）と同程度のEを維持していた（図－1（c1））．g_sはウバメガシを除いた3種で一日を通してほぼ0.03 mol m^{-2} s^{-1}未満であった（図－1（c2））．夜明け直後のψ_lは，高くてもウバメガシの－0.9 MPaまでしか回復していなかった．またψ_lの日最低値はシイノ

キの−2.5 MPaを最低値として4樹種とも−2.2 MPaを下回り，湿潤日（2001年7月11日）に較べて大きく低下していた（図−1(c3)）．$K_{s\text{-}l}$はウバメガシを除く3樹種で湿潤日（2001年7月11日）に較べて極めて小さかった（図−1(c4)）．

4）熱帯常緑広葉樹種3種

熱帯常緑広葉樹種3種では，観測日のAPIはそれぞれ，1.5（2004年9月10日），1.3（2004年9月11日），0.1（2005年2月12日），0.1（2005年2月13日）および18.5（2005年10月25日）であった．2005年10月25日は雨季であったので，APIは他の観測日よりもかなり高かった． *X. stipitatum*と*P. caput-medusae*におけるEの日最大値は，それぞれ1.3 mmol m^{-2} s^{-1}，2.7 mmol m^{-2} s^{-1}であった（図−1(d4)）．また，*D. sablamellatus*におけるEの日最大値は2.7 mmol m^{-2} s^{-1}（2004年9月10日），5.0 mmol m^{-2} s^{-1}（2005年2月13日），3.7 mmol m^{-2} s^{-1}（2005年10月25日）であった（図−1(d1)，(d5)）．g_sは*X. stipitatum*と*P. caput-medusae*で一日中概ね0.05 mol m^{-2} s^{-1}程度であったが，*D. sablamellatus*ではやや高く（0.1 mol m^{-2} s^{-1}），2005年2月13日には最大で0.33 mol m^{-2} s^{-1}になった（図−1(d2)，(d6)）．ψ_lは3樹種とも午前から日中にかけて徐々に低下し，その後回復する日変化を示した（図−1(d3)）．日最低ψ_lは*X. stipitatum*と*P. caput-medusae*で約−1.5 MPaであったが，*D. sablamellatus*では−1.1 MPaであった．また，APIの大小に関らず*D. sablamellatus*の葉サンプルの切り口から水が滲み出てくるため，プレッシャーチャンバーでのψ_l測定は困難であった．$K_{s\text{-}l}$の日最大値は*X. stipitatum*で 1.2， *P. caput-medusae*で 2.1， *D. sablamellatus*で は 3.6 mmol m^{-2} s^{-1} MPa^{-1}と，*D. sablamellatus*が他の2樹種に比べて高い値をとった（図−1(d4)）．

2. 多様な樹種の葉の水分特性

P-V曲線法から得られた各樹種の樹冠葉の$\psi_{w\text{-}tlp}$と$\psi_{s\text{-}sat}$を図−2に示す．暖温帯常緑広葉樹種4種の$\psi_{w\text{-}tlp}$は，アラカシ，ウバメガシ，クスノキで−2.5 MPa程度であり，シイノキでも−1.80 MPaであった．またヒノキや熱帯常緑広葉樹種3種の$\psi_{w\text{-}tlp}$は−2.0 MPa前後の値を示した．いっぽう，冷温帯落葉広葉樹種であるブナの$\psi_{w\text{-}tlp}$は−1.1 MPaであり，他生育地の樹種に較べてかなり高かった．$\psi_{s\text{-}sat}$は最低値であるアラカシの−1.8 MPaから，最高値であるブナの−0.8 MPaに亘った．全体として，$\psi_{s\text{-}sat}$が低いほど$\psi_{w\text{-}tlp}$も低下していた．これらの点から，暖温帯林常緑広葉樹林の各樹種が初発原形質分離点の葉水ポテンシャル$\psi_{w\text{-}tlp}$が低く，低い葉水ポテンシャルまで膨圧を維持できること，またこのことは浸透調整（$\psi_{s\text{-}sat}$を低めること）によって達成されていることがわかる．

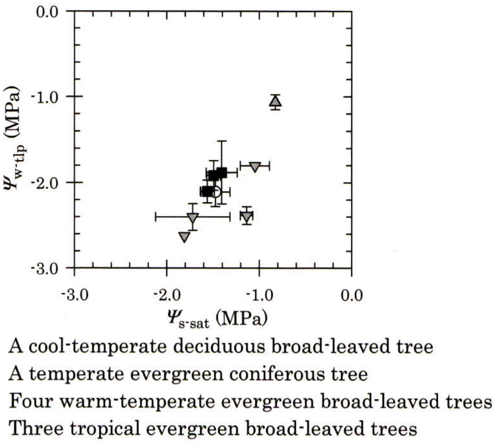

図−2　多様な樹種における，葉の飽和浸透ポテンシャル（$\psi_{s\text{-}tlp}$）と初発原形質分離水ポテンシャル（$\psi_{w\text{-}tlp}$）の関係（エラーバーは標準偏差を表す）．

Fig.2 The relationship between osmotic potential when leaves were fully saturated with water ($\psi_{s\text{-}tlp}$) and water potential at turgor loss point ($\psi_{w\text{-}tlp}$) in various trees. Bars within the graph represent standard deviation.

3. 多様な樹種の水利用様式

観測によって得られた正午頃のEと$\Delta\psi$および(3)式によって算出された$K_{s\text{-}l}$を**表−1**に，これらの相互関係（＝水利用様式）を図−3に示す．また，Saito *et al.*（2003）による冷温帯落葉広葉樹種8種のデータ（Eは最大蒸散速度，ψ_lは日最低値，また$K_{s\text{-}l}$は10点以上の$\Delta\psi$とEデータセットの回帰より算出された）も図−3に参照する．ψ_lは着葉位置によって重力により0.01 MPa m^{-1}程度低下するが，本研究では樹高の違いも含めた水利用様式を考慮するため，この影響を含めている．

$K_{s\text{-}l}$は全体的に冷温帯落葉広葉樹種9種で高い（3-8 mmol m^{-2} s^{-1} MPa^{-1}）傾向にあった．暖温帯常緑広葉樹種がそれに次いで高かったが，乾燥期にはそれらの値は著しく低下した．ヒノキおよび熱帯常緑広葉樹種3種のうち*X. stipitatum*と*P. caput-medusae*では1~2 mmol m^{-2} s^{-1} MPa^{-1}程度の$K_{s\text{-}l}$を有していたが，*D. sablamellatus*の$K_{s\text{-}l}$は3 mmol m^{-2} s^{-1} MPa^{-1}前後と同生育地の他の2種と比べて高い値であった．

$\Delta\psi$は乾燥期の暖温帯常緑広葉樹種4種で大きく，

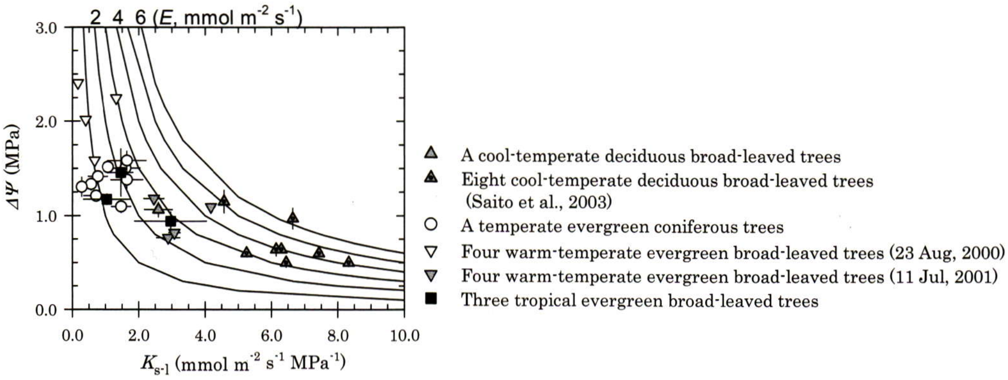

図－3　多様な樹種における通水コンダクタンス($K_{s\text{-}l}$)，土壌－葉間の水ポテンシャル差($\Delta\psi$)および蒸散速度(E)の関係（正午の観測で得られた成熟葉のデータ）と，Saito *et al.*（2003）の結果（ただし，Eは日最大値，$K_{s\text{-}l}$は日平均値）．また，エラーバーは標準偏差を表す．

Fig.3 The relationship among hydraulic conductance ($K_{s\text{-}l}$), soil to leaf water potential difference ($\Delta\psi$) and transpiration rate (E) in various trees (data in this study were obtained from measurements with mature leaves at noon). With the data in the reference paper (Saito *et al.* 2003), E was daily maximum value and $K_{s\text{-}l}$ was daily average value. Bars within the graph represent standard deviation.

冷温帯落葉広葉樹種9種で小さかった．また，ヒノキにおける$\Delta\psi$は，Eおよび$K_{s\text{-}l}$の多寡に関らずほとんど変化が無かった．いっぽう暖温帯常緑広葉樹種4種では，$K_{s\text{-}l}$の低下に伴い$\Delta\psi$が大幅に増大した．

Eは冷温帯落葉広葉樹種の数種においてやや大きく，4-6 mmol m^{-2} s^{-1}まで上昇した．その他の樹種では概ね1-3 mmol m^{-2} s^{-1}であった．

Ⅳ．考察

1．冷温帯落葉広葉樹種（ブナ）

本研究のブナおよびSaito *et al.*（2003）の冷温帯落葉広葉樹種8種は**図－3**において，他の生育地の樹種に比べて$K_{s\text{-}l}$が高く，$\Delta\psi$が低い領域に位置した．しかしながらその中では，本研究で観測を行ったブナにおける$K_{s\text{-}l}$がSaito *et al.*（2003）の冷温帯樹種8種のそれらに較べて低かった．このことには，幾つかの原因が考えられる．まず1つ目に，前者は後者に較べて樹高が10 m以上高く，通水距離の増大による$K_{s\text{-}l}$の低下が生じているかもしれない．また，後者の供試木では相互被陰を避ける目的で樹冠を剪定されているため，水消費器官の相対的な減少によって一時的に$K_{s\text{-}l}$が向上している可能性がある（Hubbard *et al.* 1999）．

ブナにおける2005年5月16日の樹冠葉の$\psi_{w\text{-}tlp}$は他の樹種に比べて高かったので，比較的早い脱水段階で膨圧を失うと考えられる（**表－1**，**図－2**）．*P-V*曲線法を用いて冷温帯落葉広葉樹種の葉の水分特性を評価した先行研究は幾つか見られる（Saito and Terashima 2004; 渥美ら，2000; 多賀ら，1993; 丸山・森川，1984）．これらの先行研究によると冷温帯落葉広葉樹種の$\psi_{w\text{-}tlp}$は－1.5MPa程度であるが，浸透調節によって変動する．以上のことから，冷温帯落葉広葉樹種は脱水によって原形質分離を起こしやすいため，高い$K_{s\text{-}l}$を有して葉の脱水を回避する水利用様式を採っていることが示唆される．

2．温帯常緑針葉樹種（ヒノキ）

本研究の結果から，測定日の条件に関らずψ_lの日最低値の変動幅が非常に小さいことが，ヒノキの大きな特徴として挙げられる．このことは，給水の不足による葉の脱水に対して有効な順応である浸透調節が行われていないことを示唆する．このため，ヒノキは過剰な脱水状態になるのを回避するために，気孔を閉鎖（**図－1(b7)**）して失水を最小限に抑制することで環境変化に対応するという水利用様式をとっていると考えられる．

土壌水分が湿潤な条件下においては，ψ_lは夜明け前までに根表面のψ_sとほぼ平衡すると言われてきた．実際には平衡に達していないとする報告もあるが，それには葉細胞の基質濃度による浸透ポテンシャルあるいは吸水に必要な$\Delta\psi$の閾値の存在など（Donovan *et al.*, 2001; Sellin, 1999）が関与しているとされる．本研究の結果では，2005年9月13日にはψ_lの回復が－0.4 MPaまでであった（**図－1(b6)**）．サンプル葉の着生位置による重力ψ（－0.16 MPa）で

説明しきれない水ポテンシャルの低下があり，2004年11月2日と比較してもψ_lの回復が充分でないことから，前日までの脱水状態が解消されていないと考えられる．先行研究では，土壌の乾燥によって最も通水性が低下するのは土壌−根系間であるとされている（小林ら，1993）．また，樹体内における通水性の低下は道管内での気泡（キャビテーション）の発生（Zimmermann, 1983）に起因する．キャビテーションは葉に水ストレスを起こすため，これまで植物にとって不利益だと考えられてきたが，近年の研究で気孔の調節による蒸散抑制に寄与することが分かってきた（Sperry, 2000）．Sperry（2000）はキャビテーションの発生によって$K_{s\text{-}l}$が低下することで，乾燥に対する気孔反応がより敏感になり，乾燥条件下で生存できる期間を延ばすことにつながると結論付けている．

3. 暖温帯常緑広葉樹種4種

暖温帯常緑広葉樹種でも，乾燥期には湿潤期と較べて$K_{s\text{-}l}$が低下した（図－1（c4），（c8），図－3）．また，夜明け直後のψ_lは4樹種全てで低下しており（図－1（c3），（c7）），同日のg_sもウバメガシを除いた3樹種では非常に低い（図－1（c2），（c6））．このことからヒノキと同様に，ウバメガシを除く暖温帯常緑広葉樹種3種でも乾燥期には脱水状態が解消されず，失水を抑制するために気孔閉鎖が生じていたと考えられる．しかし，乾燥期の日最低ψ_lは湿潤期のそれよりも大幅に低下させることができた（図－1（c3），（c7））．このことより，これらの樹種では給水の不足に対して浸透調節を行うことで，葉の耐乾性を強化していたと考えられる．なお，これらの樹種は湿潤期においてもg_sが比較的小さく（図－1（c7）），常に失水を制御していることが示唆される．これらの水利用様式の特徴は，恒常的に水ストレスに曝されるような地域で生存していく上で有効であると考えられる．

4. 熱帯常緑広葉樹種3種

観測を行った熱帯常緑広葉樹種3種はいずれも樹高が30 m以上の高木であったが，これらのうち2樹種のEは低く，$K_{s\text{-}l}$も小さかった（図－1（d1），（d4））．このことには樹高伸長に伴う通水距離の増大が関与していると思われる（Ryan and Yoder 1997）．一方で，エマージェント（突出木）となる優占樹種の*D. Sablamellatus*は同サイトの他の2種と比較して高い$K_{s\text{-}l}$を有していた．*D. Sablamellatus*における$K_{s\text{-}l}$の測定日が他の2樹種に比較してAPIの高い湿潤日であったのでその影響である可能性も考えられる．しかしながら，測定日の条件に関らずサンプリングの際に常に切り口から水が滲み出てくること，APIのより低い測定日においても，Eおよびg_sが他樹種に比較して高かった（図－1（d1），（d2），（d5），（d6））こと，また*D. Sablamellatus*についてAPIの違う3回の測定日の結果を比較した場合にEおよびg_sが最も大きい日が必ずしもAPIの一番大きな湿潤日ではなかった（図－1（d1），（d2），（d5），（d6））ことなどから，*D. Sablamellatus*はAPIによらず他の2種と比較して高い$K_{s\text{-}l}$を有していることが強く示唆される．このような樹種は通水距離の問題を克服するため，他樹種と異なる給水システムを有している可能性がある．Goldstein *et al.*（1998）は樹液流観測によって熱帯高木の水利用を調査し，幹貯留水が通水抵抗の増大を緩和して，樹冠部の葉への給水に重要な役割を果たしていることを明らかにした．また，Stratton *et al.*（2000）は幹貯水能力の指標として辺材の飽和含水比を調査し，高飽和含水比の辺材を有する熱帯乾燥林樹種ではψ_lの日変化が小さく，最大光合成速度は大きかったことを報告している．本研究の*D.Sablamellatus*でも，樹幹などの樹冠に近い場所に水を蓄えておき迅速に給水を行うことで水収支の一時的なインバランスを緩和している可能性が示唆される．

Ⅴ．結論

多様な水環境条件下に生育し，樹冠を構成している4サイト9樹種の高木個体について，樹冠葉における蒸散速度等および水ポテンシャルを測定し，通水コンダクタンスを算出した．また，*P-V*曲線法を用いて葉の水分特性を評価した．

冷温帯落葉広葉樹種は$K_{s\text{-}l}$が大きく一方で$\psi_{w\text{-}tlp}$や実際の野外でのψ_lが高いことから，水供給能力に優れ，かつ葉の脱水を回避する水利用様式を採っていると考えられた．温帯のヒノキは，ψが一定値以下にならないよう気孔を閉じてg_sやEを調整し失水を最小限に抑制することで環境変化に対応するという水利用様式をとっていると考えられる．暖温帯常緑広葉樹種は，乾燥条件から湿潤条件まで水ポテンシャル差を幅広く調整していたことから，夏季の強い乾燥ストレスに対して脱水に耐えながら，葉の水ポテンシャルを下げて吸水を促進すると考えられ

た．また，湿潤条件下においても，気孔を閉じ気味にして失水を抑制していた．熱帯常緑広葉樹種のうち*X. stipitatum*と*P. caput-medusae*では，一日を通してEが低く抑制されていた．これらの2樹種のK_{s-l}が小さいのは，通水距離の長さが影響しているのではないかと考えられる．いっぽう，*D. sablamellatus*は他の2樹種と比較してK_{s-l}が大きく，独特な水供給システムを有している可能性が示唆された．

本研究の結果から，樹冠への水供給能力を表す通水コンダクタンスと個葉の耐乾性に基づく土壌－葉間の水ポテンシャル差のバランスにより，対象樹木の個体としての水利用様式が特徴付けられた．今後，季節やフェノロジーの変化によって，どのようにどの程度各樹木の水利用様式が変動するのかを調査すれば，各生育地の樹木の水環境への適応様式がさらに詳細に明らかになるものと期待される．

謝辞

本研究の一部は環境省地球環境研究総合推進費（GERF）により行われているNIES-FRIM-UPM熱帯林多様性プロジェクトの成果によるものである．Pasoh森林保護区の調査に際しては，Dr. Abdul Rahim Nikや奥田敏統氏をはじめとする多くのプロジェクト関係者の方々に多大なご助力をいただいた．赤穂緩衝緑地での観測の際には，㈱関西電力赤穂発電所ならびに㈱環境総合テクノスにご協力いただいた．岡山大学農学部の吉川賢教授と三木直子助手には，ハイグロメーターを長期に亘って使用させていただいた．滋賀県立大学環境科学部の籠谷泰行助手には，金糞岳ブナ林における土壌水分データを提供していただいた．京都大学大学院農学研究科の林祐妃氏には，ブナ林土壌の水分特性に関するデータを提供していただいた．ここに記して，謝意を表する．

参考文献

渥美裕子・玉井重信・山本福壽・山中典和（2002）：冷温帯林構成樹種20種の葉の水分特性，日林誌，84，pp.271-275.

Cheung YNS, Tyree MT, Dainty J. 1975. Water relations parameters on single leaves obtained in a pressure bomb and some ecological interpretations. *Can. J. Bot.* 53: 1342-1346.

Donovan LA, Linton MJ, Richards JH. 2001. Predawn plant water potential does not necessarily equilibrate with soil water potential under well-watered conditions. *Oecologia* 129: 328-335.

Goldstein G, Andrade JL, Meinzer FC, Holbrook NM, Cavelier J, Jackson P, Celis A. 1998. Stem water storage and diurnal patterns of water use in tropical forest canopy trees. *Plant, Cell Environ.* 21: 397-406.

Hubbard RM, Bond BJ, Ryan MG. 1999. Evidence that hydraulic conductance limits photosynthesis in old *Pinus ponderosa trees. Tree Physiol.* 19: 165-172.

Hubbard RM, Ryan MG, Stiller V, Sperry JS. 2001. Stomatal conductance and photosynthesis vary linearly with plant hydraulic conductance in ponderosa pine. *Plant, Cell Environ.* 24: 113-121.

石田　厚・谷　享（2003）：植物の水利用の評価1　陸上植物と水，光と水と植物のかたち（種生物学会　編）III-5，文一総合出版，pp.271-291.

Ishida A, Yamamura Y, Hori Y. 1992. Roles of leaf water potential and soil-to-leaf hydraulic conductance in water use by understory woody plants. *Ecol. Res.* 7: 213-223.

Kikuta SB, Richter H. 1986. Graphical evaluation and partitioning of turgor responses to drought in leaves of durum wheat. *Planta* 168: 36-42.

小林達明・吉川　賢・小橋澄治・増田拓朗（1993）：土壌水分条件の異なる立地に生育するハンリュウ（Salix matsudana）の水分動態の比較解析，日林誌，75（3），pp.165-175.

Konishi S, Tani M, Kosugi Y, Takanashi S, Sahat MM, Nik AR, Niiyama K, Okuda T. 2006. Characteristics of spatial distribution of throughfall in a lowland tropical rainforest, Peninsular Malaysia. *Forest Ecology and Management224*: 19-25.

Kosugi Y, Matsuo N. 2006. Seasonal fluctuations and temperature dependence of leaf gas exchange parameters of co-occurring evergreen and deciduous trees in a temperate broad-leaved forest. *Tree Physiol.*26: 1173-1184.

Kosugi Y, Tanaka H, Takanashi S, Matsuo N, Ohte N, Shibata N, Tani M. 2005. Three years of carbon and energy fluxes from Japanese evergreen broad-leaved forest. *Agric. For. Meteorol.* 132: 329-343.

松尾奈緒子・小杉緑子（2002）：暖温帯性広葉樹における個葉のガス交換制御の季節変化について，日本緑化工学会誌，28（1），pp.14-19.

松尾奈緒子・小杉緑子・大手信人・木庭啓介（2002）：炭素安定同位対比を用いた暖温帯性常緑広葉樹の水利用効率に関する解析，水文・水資源学会誌，15（3），pp.229-242.

丸山　温・森川　靖（1983）：葉の水分特性の測定　－P-V曲線法－，日林誌，65，pp.23-28.

丸山　温・森川　靖（1984）：ミズナラ，ダケカンバ，ウラジロモミの葉の水分特性の季節変化，日林誌，66（2），pp.499-505.

三谷智典・小杉緑子・谷　誠・高梨　聡・片山辰弥・和田卓巳（2003）：ヒノキ（Chamaecyparis obtusa）人工林における土壌呼吸量の時間的・空間的変動，日本緑化工学会誌，29（1），pp.153-158.

Morgan JM. 1984. Osmoregulation and water stress in higher plants. *Annu. Rev. Plant Physiol.* 35: 299-319.

村瀬忠義（1979）：滋賀県の植物地理概説，滋賀県の自然（滋賀自然環境研究会　編），滋賀県自然保護財団，pp. 899-929

Pearcy RW, Schulze ED, Zimmermann R. 1989. Measurement of transpiration and leaf conductance. In Plant Physiological Ecology: Field Methods and Instrumentation（Eds. Pearcy RW, Ehleringer J, Mooney HA and Rundel PW.）. Chapman and Hall: pp. 137-160.

Phillips N, Bond BJ, Mcdowell NG, Ryan MG. 2002. Canopy and hydraulic conductance in young, mature and old Douglas-fir trees. *Tree Physiol.* 22: 205-211.

Ryan MG, Yoder BJ. 1997. Hydraulic limits to tree height and tree growth. *Bioscience* 47: 235-242.

Ryan MG, Bond BJ, Law BE, Hubbard RM, Woodruff D, Cienciala E, Kucera J. 2000. Transpiration and whole-tree conductance in ponderosa pine trees of different heights. *Oecologia* 124: 553-560.

Saito T, Terashima I. 2004. Reversible decreases in the bulk elastic modulus of mature leaves of deciduous Quercus species subjected to two drought treatments. *Plant, Cell Environ.* 27: 863-875.

Saito T, Tanaka T, Tanabe H, Matsumoto Y, Morikawa Y. 2003. Variations in transpiration rate and leaf cell turgor maintenance in saplings of deciduous broad-leaved tree species common in cool temperate forests in Japan. Tree *Physiol.* 23: 59-66.

Scholander PF, Hammel HT, Bradstreet ED, Hemmingsen EA. 1965. Sap pressure in vascular plants. Science 148: 339-346.

Sellin A. 1999. Does pre-dawn water potential reflect conditions of equilibrium in plant and soil water status? *Acta Oecologia* 20: 51-59.

Soepadmo E. 1978. Introduction to the Malaysian I.B.P. Synthesis Meetings. *The Malayan Nature Journal* 30: 119-124.

Sperry JS. 2000. Hydraulic constraints on plant gas exchange. *Agric. For. Meteorol.* 104: 13-23.

Stratton L, Goldstein G, Meinzer FC. 2000. Stem water storage capacity and efficiency of water transport their functional significance in a Hawaiian dry forest. *Plant, Cell Environ.* 23: 99-106.

多賀敦司・小林達明・沖中建（1993）：水分条件適正の異なる樹木4種の湛水ストレスに対する生理的反応、第24回日本緑化工学会研究発表会要旨集, pp.22-25.

Takanashi S, Kosugi Y, Matsuo N, Tani M, Ohte N. 2006. Patchy stomatal behavior in broad-leaved trees grown in different habitats. *Tree Physiol* 26 : 1565-1578.

Takanashi S, Kosugi Y, Tanaka Y, Yano M, Katayama T, Tanaka H, Tani M. 2005a. CO_2 exchange in a temperate Japanese cypress forest compared with that in a cool-temperate deciduous broad-leaved forest. *Ecol. Res.* 20: 313-324.

高梨　聡・小杉緑子・谷　誠・大手信人・矢野雅人・田中広樹・田中克典（2003）：ヒノキ林における降雨中および降雨後の蒸発散過程, 水文・水資源学会誌, 16（3）, pp.268-283.

Takanashi S, Kosugi Y, Tani M, Matsuo N, Mitani T, Nik AR. 2005b. Characteristics of the gas exchange of a tropical rain forest in Peninsular Malaysia. *Phyton* 45: 61-66.

高梨　聡・大手信人・小杉緑子・松尾奈緒子（2001）：加圧浸潤法を用いた気孔コンダクタンスの推定手法に関する考察, 日本緑化工学会誌, 27（1）, pp.324-326.

武田栄夫（1991）：滋賀県の気候, 滋賀県自然誌（滋賀県自然誌編集委員会　編）, 滋賀県自然保護財団, pp.1-104

Tanaka K, Kosugi Y, Nakamura A. 2002. Impact of leaf physiological characteristics on seasonal variation in CO_2, latent and sensible heat exchanges over a tree plantation. *Agric. For. Meteorol.* 114: 103-122.

谷　享・石田　厚（2003）：植物の水利用の評価2　水ポテンシャルと通導性の測定, 光と水と植物のかたち（種生物学会　編）III-6, 文一総合出版, pp.293-308.

Tyree MT, Jarvis PG. 1982. Water in tissues and cells. In *Encyclopedia of Plant Physiology, New Series, Vol. 12B. Physiological Plant Ecology II* (eds Lange, Nobel, Osmond, Ziegler), Springer, pp. 35-77.

Tyree MT, Sperry JS. 1989. Vulnerability of xylem to cavitation and embolism. *Annu. Rev. Plant Physiol.* 40: 19-38

von Caemmerer S, Farquhar GD. 1981. Some relationships between the biochemistry of photosynthesis and the gas exchange of leaves. *Planta* 153: 376-387.

和田卓巳・谷　誠・小杉緑子・高梨　聡（2002）：ヒノキ林における樹体貯熱量の推定, 森林研究, 74, pp.69-76.

吉川　賢（2004）：乾燥地の植物, 乾燥地の自然と緑化（吉川賢・山中典和・大手信人　編著）2.3, 共立出版, pp.56-89.

Zimmermann MH. 1983. Xylem structure and the Ascent of Sap. Springer, pp.143

（受付：2006年3月22日，受理：2006年12月4日）

Comparison of Water Use of Various Trees Grown in Several Different Habitats

Yusuke FUKUI [1] Yoshiko KOSUGI [1] Naoko MATSUO [1]
Satoru TAKANASHI [1] Makoto TANI [1]

[1] Graduate School of Agriculture, Kyoto University
(Kitashirakawa Oiwake-cho, Sakyo-ku, Kyoto 606-8502, Japan)

To evaluate the water use of various trees in several different habitats, we measured leaf transpiration rate, stomatal conductance, and leaf and soil water potential to calculate leaf-specific hydraulic conductance and difference between soil and leaf water potentials. We also made *P-V* curve measurement to evaluate leaf water relations of these trees. Explicating leaf-specific hydraulic conductance, leaf water characteristics and transpiration rate together, we illustrated the manner of water use in several tall trees that compose their forest canopy. Although *Fagus crenata* Blume, a cool-temperate deciduous broad-leaved species, had higher leaf-specific hydraulic conductance, its leaf water potential at turgor loss point is higher indicating dehydration-postpone strategy. In *Chamaecyparis obtusa* Sieb. et Zucc., a temperate conifer, declines of leaf-specific hydraulic conductance and transpiration in dry period suggest occurrence of hydraulic disorder and stomatal regulation. Four warm-temperate evergreen species maintained low stomatal conductance even in wet period, and improved leaf dehydrate-tolerance by Osmo-regulation in dry period. Two tropical evergreen broad-leaved species have low leaf-specific hydraulic conductance, whereas *Dipterocarpus sublamellatus* Foxw., one emergent species, have higher leaf-specific hydraulic conductance compared to other two species, suggesting that it have a feed-water system overcome distant water transport.

Key words : Tree water use, Transpiration, Leaf-specific hydraulic conductance, Water potential, *P-V* curve

ELSEVIER

Available online at www.sciencedirect.com
SCIENCE DIRECT®

Forest Ecology and Management 210 (2005) 455–459

Forest Ecology and Management

www.elsevier.com/locate/foreco

Short communication

Required sample size for estimating soil respiration rates in large areas of two tropical forests and of two types of plantation in Malaysia

Minako Adachi[a,*], Yukiko Sakata Bekku[b], Akihiro Konuma[c], Wan Rasidah Kadir[d], Toshinori Okuda[e], Hiroshi Koizumi[a]

[a] *River Basin Research Center, Gifu University, Yanagido 1-1, Gifu 501-1193, Japan*
[b] *Department of Primary Education, Tsuru University, Tahara 3-8-1, Tsuru 402-8555, Japan*
[c] *National Institute for Agro-Environmental Sciences, Kannondai 3-1-3, Tsukuba 305-8604, Japan*
[d] *Forest Research Institute Malaysia, Kepong 51209, Malaysia*
[e] *National Institute for Environmental Studies, Onogawa 16-2, Tsukuba 305-8506, Japan*

Received 26 May 2004; received in revised form 26 November 2004; accepted 7 February 2005

Abstract

We estimated the required sample sizes for estimating large-scale soil respiration (for areas from 1 to 2 ha) in four ecosystems (primary and secondary forests, and oil palm and rubber plantations) in Malaysia. The soil respiration rates were 769 ± 329 mg CO_2 m^{-2} h^{-1} in the primary forest (2 ha, 50 sample points), 708 ± 300 mg CO_2 m^{-2} h^{-1} in the secondary forest (2 ha, 50 points), 815 ± 363 mg CO_2 m^{-2} h^{-1} in the oil palm plantation (1 ha, 25 points), and 450 ± 178 mg CO_2 m^{-2} h^{-1} in the rubber plantation (1 ha, 25 points). According to our sample size analysis, the number of measurement points required to determine the mean soil respiration rate at each site with an error in the mean of no more than 10% ranged from 67 to 85 at the 95% probability level. These results suggest that evaluating the spatial heterogeneity of soil respiration rates in the tropics may require more measurement points than in temperate forests.

Keywords: Tropical forest; Oil palm plantation; Rubber plantation; Spatial variability

1. Introduction

Soil respiration, which represents the CO_2 efflux from the soil surface, is one of the most important processes in the carbon cycle of terrestrial ecosystems. Soil respiration rate varies spatially and temporally because the environmental factors that affect this rate can vary dramatically over large areas. Tropical forests in Southeast Asia are rapidly being changed into secondary forests or plantations, and despite the large number of studies on soil respiration rates, few studies have compared soil respiration rates in forest and

---

* Corresponding author. Tel.: +81 58 293 2077; fax: +81 58 293 2062.
E-mail address: minako@green.gifu-u.ac.jp (M. Adachi).

0378-1127/$ – see front matter
doi:10.1016/j.foreco.2005.02.011

plantation ecosystems using a consistent methodology. In addition, we must be able to account for spatial heterogeneity before we can reliably estimate the mean value of soil respiration in target ecosystems. Larger sample sizes generally permit more accurate estimation, but the number of measurement points in studies of soil respiration rate is often limited by labor or time constraints. For these reasons, we must be able to estimate the sample size required to adequately estimate soil respiration over large areas, but few studies have provided sufficient data to estimate the required sample size (Yim et al., 2003; Davidson et al., 2002).

The objective of the present study was to estimate the number of measurement points required to adequately describe mean soil respiration rates in four different ecosystems.

2. Methods

We selected the four major types of ecosystem in the Pasoh area of Negeri Sembilan, Malaysia, as our study sites: primary and secondary forests in the Pasoh Forest Reserve (2°5′N, 102°18′W), and oil palm and rubber plantations adjacent to the Reserve. In 1996, these ecosystems respectively occupied 27.6, 1.8, 20.6, and 33.7%, of the 3600 km^2 Pasoh area (Okuda et al., 2003a). The monthly mean air temperature remained nearly constant between 1991 and 1997, ranging from 26 to 28 °C, and annual precipitation averaged 1788 mm at our study sites from 1975 to 1998 (Fig. 1; data provided by the Malaysian Meteorological Services for the 1977–2000 period, as cited in Manokaran et al., 2004). Members of the Dipterocarpaceae dominate the forests of the Pasoh Forest Reserve (Tang et al., 1996; Okuda et al., 2003b). In the oil palm plantation, *Elaeis guineensis* were planted around 1975. In the rubber plantation, *Hevea brasiliensis* were planted around 1989. The soil taxonomy is a Typic Paleudult in the Pasoh Forest Reserve (Yamashita et al., 2003), and the soil texture at a depth of 5 cm based on the Malaysian and FAO classification systems is a heavy clay at the forest sites and a sandy clay loam at the plantation sites (Adachi, unpublished data).

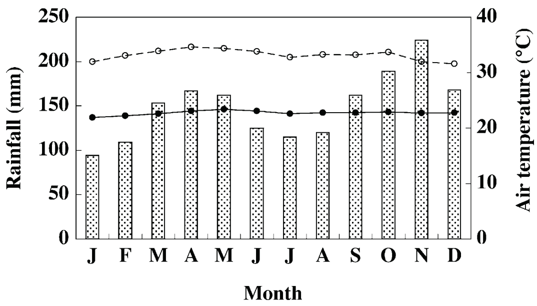

Fig. 1. Climatic data for the Pasoh Forest Reserve (from Manokaran et al., 2004). Bars indicate total monthly rainfall (1975–1998); (○) and (●) represent the maximum and minimum daily air temperatures (1991–1997).

The soil respiration rate was measured at 50 lattice positions within a 100 m × 200 m plot at 20 m intervals in the primary and secondary forests, and at 25 lattice positions within a 100 m × 100 m plot at 20 m intervals in the oil palm and rubber plantations. The research areas in the oil palm and rubber plantations were half the size of those in the primary and secondary forests because topography and vegetation conditions in the monoculture plantations were relatively homogeneous compared with those in the natural forests.

Soil respiration rate was measured using a portable soil respiration system (LI-6400, LI-COR, Lincoln, NE, USA). We measured soil respiration rates on 6 and 7 March 2000 in the primary forest, on 8 and 9 March 2000 in the secondary forest, on 14 February 2001 in the oil palm plantation, and on 28 February 2003 in the rubber plantation. The measurement duration was 6 h (from 11:00 to 17:00) on each day at the forest study sites and 4 h (from 9:00 to 13:00) at the plantation study sites. Diurnal variation in soil respiration was not detected at the four study sites in preliminary observations (Adachi, unpublished data). Soil temperatures at depths of 1 and 5 cm were measured using a thermometer (TM-150, Custom, Tokyo, Japan) and average soil water content at a depth of 5 cm was measured simultaneously using a time-domain-reflectometry sensor (TDR; TRIME-FM, IMKO, Ettlingen, Germany).

We conducted all statistical analyses using the Stat View 5.0 software package (SAS Institute, Cary, NC, USA). The distributions of soil respiration values were tested for normality using the Kolmogorov–Smirnov test, and we found that the data for each study site followed a normal distribution. We used an equation described in Petersen and Calvin (1986) to estimate the number of measurement points required to estimate soil respiration rate within a specified confidence interval:

$$n = t_\alpha^2 s^2 / D^2 \quad (1)$$

where n is the required sample size, t_α is the Student's t statistic with degrees of freedom at the α confidence level, s is the standard deviation of soil respiration, and D is the specified error limit. The specified error limit denotes the allowable margin of error in the sample mean. In the present study, we estimated the required number of measurement points at the 95% confidence level (α) and with specified error limits equal to 10 and 20% of the sample mean.

3. Results and discussion

Soil respiration rates in the primary and secondary forests and in the oil palm and rubber plantations averaged 769 ± 329, 708 ± 300, 815 ± 363, and 450 ± 178 (mean ± S.D.) mg CO_2 m^{-2} h^{-1}, respectively (Table 1). The soil respiration rate in the rubber plantation was significantly lower than at the other three study sites (Scheffe's test, $P < 0.05$). The coefficient of variation (CV) for the soil respiration rate ranged from 40 to 45% across the four study sites, and was not significantly different between the monoculture plantations and the two forests (Table 1). Soil water content was significantly lower in the rubber plantation than at the other three sites. Soil temperature did not have spatial variation over at each site, because the CV values at depth of 1 cm ranged between 3 and 5% (Table 1). The CV values for soil water content ranged between 18 and 23% in this study; these values were higher than the level of 5.4% reported for a bare tropical soil (La Scala et al., 2000).

Table 2 shows the correlations between soil respiration and the three environmental factors that we measured at each site. Soil temperature (at depths of 1 and 5 cm) was not correlated with soil respiration rate at any site. However, we detected a significant negative correlation between soil respiration rate and soil water content in the primary and secondary forests and in the rubber plantation, though not in the oil palm plantation.

The results in Table 3 show the required number of measurement points in each of the four ecosystems. The required number of measurement points was more than 50 for an allowable margin of error of 10% in the sample mean at the 95% probability level. Yim et al. (2003) estimated that the required number of measurement points for estimating soil respiration rates ranged from 27 to 33 with the same margin of error and probability level for a larch (*Larix kaempferi*) plantation in Japan. Davidson et al. (2002) reported that the required number of measurement points was 41 for the same error and probability level in a temperate mixed hardwood forest in central Massachusetts, USA. These results suggest that more measurement points are required to evaluate the spatial heterogeneity of soil respiration rates in Asian tropical forests than are required in temperate forests (Yim et al., 2003; Davidson et al., 2002). Certainly, it is clear that the number of measurement points required for reliable estimation of CO_2 emissions from a target ecosystem depends on the degree of spatial heterogeneity in soil respiration rates. Further investigations are needed for us to describe the annual and seasonal fluctuations and spatial variations in soil respiration rates; this information is essential if we are to reliably estimate annual carbon efflux from a soil.

Table 1
Descriptive statistics for soil respiration rates and three environmental factors in the four ecosystems in the study

	Primary forest (March 2000)		Secondary forest (March 2000)		Oil palm plantation (February 2001)		Rubber plantation (February 2003)	
	Mean	CV (%)	Mean	CV (%)	Mean	CV (%)	Mean	CV (%)
Soil respiration (mg CO_2 m^{-2} h^{-1})	769.2 a	42.7	707.9 a	42.3	815.3 a	44.5	449.8 b	39.6
Soil temperature (1 cm) (°C)	26.3 a	2.5	25.3 b	3.5	26.0 a	4.5	27.1 c	3.5
Soil temperature (5 cm) (°C)	25.9 ab	2.0	25.1 c	2.9	25.6 a	2.7	26.1 b	2.0
Soil water content (%)	27.3 ab	17.5	26.7 a	19.1	30.6 b	19.2	23.0 c	22.8

Means within a row followed by the same letters are not significantly different (Scheffe's test, $P < 0.05$).

Table 2
Correlations between soil respiration rate and three environmental factors in the four ecosystem in the study

	Soil respiration rate	Soil water content	Soil temperature (depth 1 cm)	Soil temperature (depth 5 cm)
Primary forest				
Soil respiration rate	1.00			
Soil water content	−0.41**	1.00		
Soil temperature (depth 1 cm)	0.23	−0.24	1.00	
Soil temperature (depth 5 cm)	0.17	−0.24	0.93***	1.00
Secondary forest				
Soil respiration rate	1.00			
Soil water content	−0.55***	1.00		
Soil temperature (depth 1 cm)	0.09	0.03	1.00	
Soil temperature (depth 5 cm)	0.09	0.03	0.97***	1.00
Oil palm plantation				
Soil respiration rate	1.00			
Soil water content	0.10	1.00		
Soil temperature (depth 1 cm)	0.15	−0.15	1.00	
Soil temperature (depth 5 cm)	0.19	−0.13	0.99***	1.00
Rubber plantation				
Soil respiration rate	1.00			
Soil water content	−0.62**	1.00		
Soil temperature (depth 1 cm)	−0.14	0.04	1.00	
Soil temperature (depth 5 cm)	−0.05	−0.04	0.849***	1.00

** $P < 0.01$.
*** $P < 0.001$.

Table 3
Required sample size for estimating soil respiration rates within ±10 and ±20% of the sample mean at the 95% probability level

	Primary forest	Secondary forest	Oil palm plantation	Rubber plantation
Sample number	50	50	25	25
S.D.	328.6	299.7	363.2	178.1
Required sample size (±10%)	75	72	85	67
Required sample size (±20%)	19	18	21	17

The present study did not provide sufficient data for this purpose because our research was conducted only once in each ecosystem type.

Acknowledgments

This work is a part of a joint research project of the Forest Research Institute Malaysia (FRIM), University Putera Malaysia, and National Institute for Environmental Studies of Japan (funded by the Global Environment Research Program, supported by the Ministry of the Environment, Japan). We thank Dr. H. Muraoka for his helpful suggestions. We also thank E. S. Quah, S.M. Wang, and other staff members of FRIM for their assistance during the field investigations at the Pasoh Forest Reserve.

References

Davidson, E.A., Savage, K., Verchot, L.V., Navarro, R., 2002. Minimizing artifacts and biases in chamber-based measurements of soil respiration. Agric. For. Meteorol. 113, 21–37.

La Scala Jr., N., Marques Jr., J., Pereira, G.T., Cora, J.E., 2000. Carbon dioxide emission related to chemical properties of a tropical bare soil. Soil Biol. Biochem. 32, 1469–1473.

Manokaran, N., Quah, E.S., Ashton, P.S., LaFrankie, J.V., Nur Supardi, M.N., Ahmad, W.M.S.W., Okuda, T., 2004. Pasoh forest dynamics plot, Peninsular Malaysia. In: Losos, E.C, Leigh, J.E.G. (Eds.), Tropical Forest Diversity and Dynamism. The University of Chicago Press, Chicago, pp. 585–598.

Okuda, T., Suzuki, M., Adachi, N., Yoshida, K., Niiyama, K., Nur Supardi, M.N., Manokaran, N., Mazlan, H., 2003a. Logging history and its impact on forest structure and species composition in the Pasoh Forest Reserve—Implications for the sustainable management of natural resources and landscapes. In: Okuda, T., Niiyama, K., Thomas, S.C., Ashton, P.S. (Eds.), Pasoh: Ecology of a Rainforest in South East Asia. Springer, Tokyo, pp. 15–34.

Okuda, T., Suzuki, M., Adachi, N., Quah, E.S., Hussein, N.A., Manokaran, N., 2003b. Effect of selective logging on canopy and stand structure and tree species composition in a lowland dipterocarp forest in peninsular Malaysia. For. Ecol. Manage. 175, 297–320.

Petersen, R.G., Calvin, L.D., 1986. Sampling. In: Campbell, G.S., Nielsen, D.R., Jackson, R.D., Klute, C.A., Mortland, M.M. (Eds.), Methods of Soil Analysis. Part 1. Physical and Mineralogical Methods. Agronomy Monograph No. 9. 2nd ed. American Society of Agronomy Inc. and Soil Science Society of America, Inc., Madison, WI, USA, pp. 33–51.

Tang, Y., Kachi, N., Furukawa, A., Muhamad, A., 1996. Light reduction by regional haze and its effect on simulated leaf photosynthesis in a tropical forest of Malaysia. For. Ecol. Manage. 89, 205–211.

Yamashita, T., Kasuya, N., Rasidah, W., Wan, C.S., Quah, E.S., Okuda, T., 2003. Soil and belowground characteristics of Pasoh Forest Reserve. In: Okuda, T., Niiyama, K., Thomas, S.C., Ashton, P.S. (Eds.), Pasoh: Ecology of a Lowland Rainforest in South East Asia. Springer, Tokyo, pp. 89–109.

Yim, M.H., Joo, S.J., Shutou, K., Nakane, K., 2003. Spatial variability of soil respiration in a larch plantation: estimation of the number of measurement points required. For. Ecol. Manage. 175, 585–588.

Available online at www.sciencedirect.com

ScienceDirect

Applied Soil Ecology 34 (2006) 258–265

Applied Soil Ecology

www.elsevier.com/locate/apsoil

Differences in soil respiration between different tropical ecosystems

Minako Adachi [a,*], Yukiko Sakata Bekku [b], Wan Rashidah [c], Toshinori Okuda [d], Hiroshi Koizumi [e]

[a] *National Institute for Agro-Environmental Science, Department of Global Resources, 3-1-3 Kannondai, Tsukuba 305-8604, Japan*
[b] *Department of Primary Education, Tsuru University, Tahara 3-8-1, Tsuru, Yamanashi 402-8555, Japan*
[c] *Forest Research Institute Malaysia, Kepong, 51209 Kuala Lumpur, Malaysia*
[d] *National Institute for Environmental Studies, Onogawa 16-2, Tsukuba, Ibaraki 305-0053, Japan*
[e] *Institute for Basin Ecosystem Studies, Gifu University, Yanagido 1-1, Gifu, Gifu 501-1193, Japan*

Received 4 April 2004; accepted 3 January 2006

Abstract

We examined the relationship between soil respiration rate and environmental determinants in three types of tropical forest ecosystem—primary forest, secondary forest, and an oil palm plantation in the Pasoh Forest Reserve on the Malaysian Peninsula. In August 2000, the soil respiration rate and environmental factors (soil temperature, soil water content, soil C and N contents, biomass of fine roots, and microbes) were measured at 12–16 points in research quadrats. Soil respiration rates were 831 ± 480, 1104 ± 995, 838 ± 143, 576 ± 374, and 966 ± 578 (mean ± S.D.) mg CO_2 m^{-2} h^{-1} in the primary forest canopy and gap site, secondary forest canopy and gap site, and oil palm plantation, respectively. Although the mean soil respiration rates in the three forest ecosystems did not differ significantly, differences were evident in the environmental factors affecting the soil respiration. The major causes of spatial variation in soil respiration were fine root biomass, soil water content, and soil C content in the primary and secondary forests and oil palm plantation, respectively.

Keywords: Land-use change; Secondary forest; Oil palm plantation; Soil C content; Root biomass; Microbial biomass

1. Introduction

The capacity of forests to absorb atmospheric CO_2 has been debated in previous studies (e.g., Dixon et al., 1994; Bousquet et al., 1999). A recent study has estimated that the annual net primary production of tropical regions is 32% of global terrestrial photosynthesis (Field et al., 1998). Tropical forests contain large amounts of C in the vegetation and soil, equivalent to 37% of global terrestrial C pools (Dixon et al., 1994). Tropical forests are estimated to represent a C sink of 1–3 Pg C y^{-1} (1 Pg = 10^{15} g) (Malhi and Grace, 2000). However, these studies were based on the micrometeorological method, which does not yield much insight into the contribution of each component to the C cycle. Malhi and Grace (2000) pointed out that net biotic C sinks can be over- or underestimated, because of insufficient sample areas for statistical analysis, especially in Asia and Africa. Tropical forests in Asia are rapidly being changed into secondary forests or plantations, and deforestation to create permanent croplands has accounted for approximately 75% of the total CO_2 emission from tropical Asia in the 1980s (Houghton and Hackler, 1999). Annual C flux to the atmosphere from changes in land use in tropical Asia

---

* Corresponding author. Tel.: +81 29 838 8202; fax: +81 29 838 8202.
E-mail address: minacoa@niaes.affrc.go.jp (M. Adachi).

0929-1393/$ – see front matter © 2006 Elsevier B.V. All rights reserved.
doi:10.1016/j.apsoil.2006.01.006

was 0.88 Pg C y^{-1} in the 1980s and 1.09 Pg C y^{-1} in the 1990s (Houghton, 2003). Schimel et al. (2001) calculated net carbon flux using an atmospheric inverse model, and indicated that tropical areas offset emissions due to tropical deforestation.

Soil respiration, or CO_2 efflux from the soil surface, is one of the most important components of the C cycle in forest ecosystems. Many studies of soil respiration have been reported in many ecosystems; temperate forest (Xu and Qi, 2001), boreal forest (Rayment and Jarvis, 2000; Søe and Buchmann, 2005), neotropical rain forest (Schwendenmann et al., 2003), semi-arid steppe (Maestre and Cortina, 2003), subalpine forest (Scott-Denton et al., 2003), tropical bare soil (La Scala et al., 2000), cropland (Rochette et al., 1991; Stoyan et al., 2000), and plantation (Epron et al., 2004; Fang et al., 1998). Generally, soil respiration varies with time and space, and soil temperature and water content are key factors responsible for the variation in soil respiration. In tropical forests, the most influential factor affecting temporal variation of the soil respiration rate is not so much the soil temperature as the soil water content or rainfall, because the soil temperature is relatively constant (Kursar, 1989; Davidson et al., 2000). On the other hand, soil respiration is composed of respiration from both roots and microbes, and some studies have reported the relationship between soil respiration and the underground environment (e.g., root biomass (Søe and Buchmann, 2005; Fang et al., 1998) and soil microbial biomass (Neergaard et al., 2002)). However, there are few data on soil respiration and the environment for forests and plantations in Southeast Asia.

Understanding the factors responsible for soil respiration is essential for predicting changes in this variable caused by changes in land use. Although there have been many studies on soil respiration rates, few have compared soil respiration in forest and plantation ecosystems using the same method. The objectives of the present study were to (1) identify small-scale spatial variations in soil respiration, and (2) examine the factors affecting the variation in soil respiration rates in primary and secondary forests and in an oil palm plantation in tropical Southeast Asia.

2. Materials and methods

2.1. Site description

Our study was conducted in primary and secondary forests in the Pasoh Forest Reserve in the state of Negeri Sembilan, Malaysian Peninsula (2°5′N, 102°18′W), and in an oil palm plantation adjacent to the Reserve. Here, the primary and secondary forests are dominated by Dipterocarpaceae (Tang et al., 1996). The total above-ground biomass was 403 Mg ha^{-1} (1 Mg = 10^3 kg) in the primary forest (Hoshizaki et al., 2004). The secondary forest site is located in an area where all trees with a DBH (diameter of trunk at breast height) of $\geq$45 cm were selectively logged in 1958, and then left to regenerate naturally (Okuda et al., 2003). In the oil palm plantation, *Elaeis guineensis* (African oil-palm) seedlings were planted in 1976, and since then the site has been fertilized and weeded every year. Mean monthly maximum air temperature is 32.5 ± 1.1 °C and minimum air temperature is 22.5 ± 0.5 °C (Manokaran et al., 2004). Mean annual precipitation is 1450–2341 mm y^{-1} in the Pasoh Forest Reserve (Malaysian Meteorological Services, 1995–2000). The pH of the topsoil (0–5 cm) was 3.8 ± 0.2 (mean ± S.D., $n = 28$) in the primary forest, 4.2 ± 0.2 ($n = 32$) in the secondary forest, and 4.7 ± 0.4 ($n = 16$) in the oil palm plantation.

2.2. Measurement of soil respiration

We selected the three different ecosystems (primary and secondary forests, and oil palm plantation) and established two quadrats (under the canopy and gap) in the primary and secondary forests to consider the spatial variability of the forest ecosystems. Canopy and gap sites in the primary and secondary forests were established to compare the soil respiration and environmental factors between the two sites. Soil respiration rate was measured in a grid pattern at 16 points in a 64-m^2 quadrat (under the canopy) and at 12 points in a 48-m^2 quadrat (under the gap) in the primary forest ($n = 28$), at 16 points in two 64-m^2 quadrats (under the canopy and gap) in the secondary forest ($n = 32$), and at 16 points in a 64-m^2 quadrat in the oil palm plantation ($n = 16$); all points were at least 2 m apart. The required sample size for estimating large-scale soil respiration rates within ±20% at the 95% probability level were 19, 18, and 21 in the primary and secondary forests, and oil palm plantation, respectively (Adachi et al., 2005). The required sample size in the oil palm plantation was thus greater than in the forest sites. However, we selected the canopy and gap sites in the primary and secondary forests to consider the difference in the soil environment between the canopy and gap.

Soil respiration was measured between 09:00 and 14:00 on 26 August 2000 in the primary forest, 28 August in the secondary forest, and 30 August in the oil palm plantation. To minimize the effects of chamber installation, 24 h before the soil respiration measurements were made a soil collar (5 cm high and 13 cm in diameter) was set into the soil to a depth of about 1 cm at each sampling point, taking care not to disturb the soil structure. The soil respiration rate was measured with a portable soil respiration rate measuring system (LI-6400, LI-COR, Lincoln, NB, USA) fitted with a soil respiration chamber (6400-09, LI-COR, NB, USA).

2.3. Measurement of environmental factors

Simultaneously with the soil respiration measurements, soil temperatures at depths of 1 and 5 cm and soil water content at 5 cm depth were measured at each point. Soil temperatures were measured using a thermometer (TM-150, Custom, Tokyo, Japan), and the soil water content was measured with a time domain reflectometry sensor (TDR; TRIME-FM, IMKO, Ettlingen, Germany). At the same sites where soil respiration had been measured in the three ecosystems, soil, and plant roots were sampled to a depth of 10 cm in a circular area 13 cm in diameter during 4–7 September 2000. Fine roots (diameter <1 mm) were collected by handpicking, rinsed with water, dried at 85 °C for 24 h, and weighed. The soil samples were sieved with a 2-mm mesh and mixed well, then part of each soil sample was stored at $-20\,^{\circ}\mathrm{C}$ for later measurement of soil microbial biomass by an adenosine triphosphate (ATP) method (Jenkinson and Oades, 1979). The ATP concentrations in the soil (nmol g^{-1} soil dry weight) were measured by an ATP taster (AF-70, TOA DKK, Tokyo, Japan). The rest of the soil sample was dried at room temperature (about 25 °C) for a week, and then soil C and N contents were measured with a N/C analyzer (C-R6A, Shimadzu, Kyoto, Japan).

2.4. Statistical analyses

All statistical analyses were conducted using the StatView 5.0 software package (SAS Institute, NC, USA). The distributions of soil respiration values were tested for normality using the Kolmogorov–Smirnov test, and we found that the data for each study site showed a normal distribution. ANOVA (Scheffé's test) was used to determine the differences in average soil respiration and environmental factors between the primary and secondary forests, and the oil palm plantation, respectively (Table 1). Pearson Product–Moment correlations were used to clarify the relationship between soil respiration and environmental factors (Figs. 1 and 2). However, this analysis was done using the data for canopy and gap sites together in the primary and secondary forests, since these were treated as a single ecosystem. Step-wise selection analyses were used to examine the relationships between soil respiration rates and environmental factors. The soil N content was not included in this analysis, because the results of multiple regression analysis were strongly biased due to the strong correlation between the soil N and C contents at all sites.

3. Results

Soil respiration rates were 831 ± 480, 1104 ± 995, 838 ± 143, 576 ± 374, and 966 ± 578 (mean ± S.D.) mg CO_2 m^{-2} h^{-1} in the primary forest canopy and gap sites, secondary forest canopy and gap sites and oil palm plantation, respectively (Table 1). There was no significant difference in soil respiration among the sites (Scheffé's test, $p < 0.05$). Soil water content at the secondary forest gap site was significantly lower than at the other sites. Soil C and N contents at the primary forest canopy site were significantly greater than at the other sites.

Table 1
Descriptive statistics (mean ± standard deviation) for soil respiration rate and environmental factors in the three ecosystems in this study

	Primary forest		Secondary forest		Oil palm plantation
	Canopy ($n = 16$)	Gap ($n = 12$)	Canopy ($n = 16$)	Gap ($n = 16$)	($n = 16$)
Soil respiration (mg CO_2 m^{-2} h^{-1})	830.6 ± 480.0a	1103.7 ± 995.4a	837.8 ± 142.8a	575.6 ± 373.7a	965.7 ± 577.7a
Soil temperature (1 cm) (°C)	24.3 ± 0.3a	26.7 ± 0.6c	25.5 ± 0.5b	24.5 ± 0.5a	25.4 ± 0.5b
Soil water content (%)	17.5 ± 7.6a	20.0 ± 5.7a	15.2 ± 2.7a	29.5 ± 5.2b	15.6 ± 4.5a
Soil C content (%)	2.92 ± 0.9a	2.10 ± 0.8b	1.70 ± 0.3b	1.36 ± 0.4b	1.55 ± 0.8b
Soil N content (%)	0.2 ± 0.05a	0.15 ± 0.04bc	0.11 ± 0.02bcd	0.09 ± 0.02bd	0.12 ± 0.05bcd
Fine root biomass (g)	1.78 ± 0.8a	1.60 ± 1.0a	2.05 ± 0.5a	0.97 ± 0.6ab	2.60 ± 2.3ac
Microbial biomass (nmol ATP/g d.w. soil)	0.79 ± 0.2a	0.45 ± 0.07b	0.58 ± 0.15ab	0.65 ± 0.13abc	0.8 ± 0.3ac

Means followed by the different letters (a–d) within a factor are significantly different (Scheffé's test, $p < 0.05$).

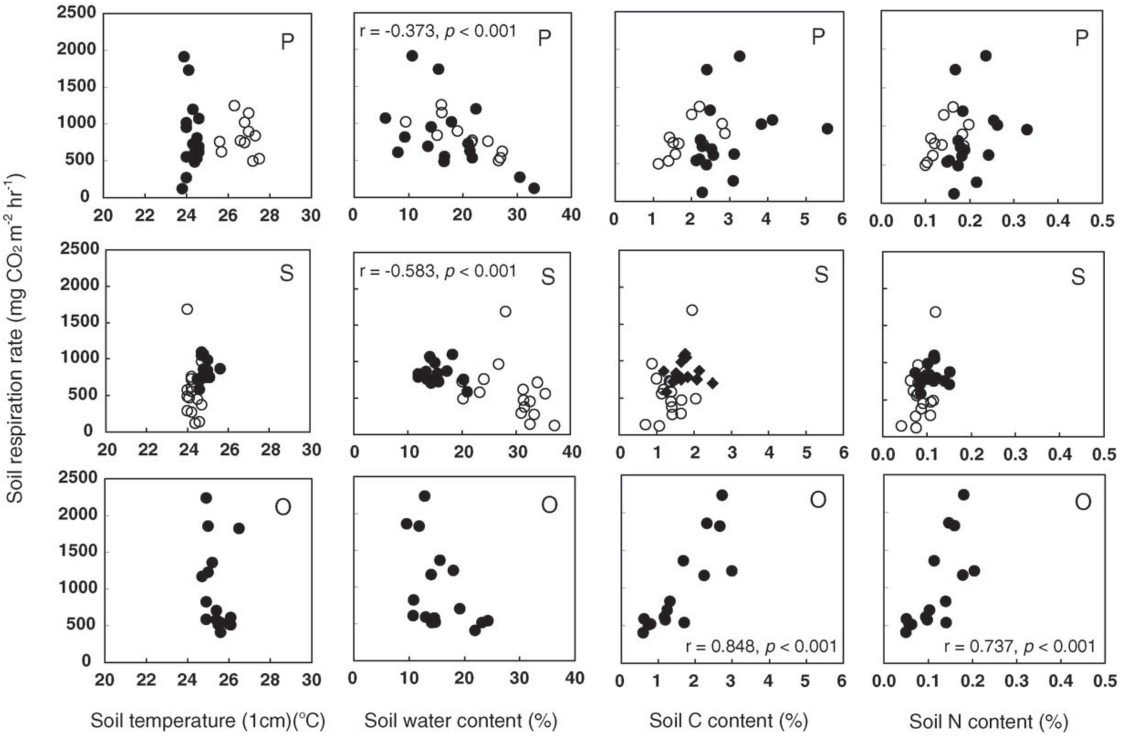

Fig. 1. The relationships between soil respiration and environmental factors (soil temperature, soil water content, soil C content and soil N content) in the three different ecosystems. P, S, and O indicate primary forest, secondary forest, and oil palm plantation, respectively. In the primary and secondary forests, canopy and gap sites are indicated by solid and clear circles, respectively. The correlation coefficient and p-value indicate significant relationships in the figure. In the primary and secondary forests, the correlation coefficient and p-value were evaluated using data for canopy and gap sites together.

Soil temperature did not correlate with the spatial variation in soil respiration rate, because soil temperatures (1 and 5 cm depths) were nearly the same in all the ecosystems (Fig. 1). In the primary forest, soil respiration had a significantly negative correlation with soil water content and a positive correlation with fine root biomass (Fig. 2). In the secondary forest, soil respiration had a negative correlation with soil water content and a positive correlation with soil C and N contents. In the oil palm plantation, soil respiration had a strong positive correlation with soil C and N contents, and a weaker positive correlation with biomass of fine roots and microbes. In the primary and secondary forests, soil water content had a strong negative correlation with fine root biomass (Fig. 3). Table 2 shows the best single- and multiple-factor models using stepwise independent variable selection in the three different ecosystems. The major causes of soil respiration were fine root biomass, soil water content, and soil C content in the primary and secondary forests and oil palm plantation, respectively.

4. Discussion

Table 3 shows a comparison of soil respiration among tropical regions. Soil respiration rates observed in the present study were greater than in the previous studies. Although we did not obtain any data that might explain the higher rates observed in our study, Yamashita and Takeda (1998) reported that the litter decomposition rate ($k = 2.15$) in the primary forest study site we investigated was greater than those reported for other tropical forest ecosystems. Therefore, the high soil respiration observed in the present study may have been due to high microbial activity.

Soil respiration rates were negatively correlated with soil water content in the primary and secondary forests. The point to be considered is the influence of soil water content on soil gas diffusiveness and underground biotic activity. A higher soil water content decreases soil gas diffusiveness. Linn and Doran (1984) have suggested that aerobic microbial activity may be inhibited by low O_2 concentration when the soil water

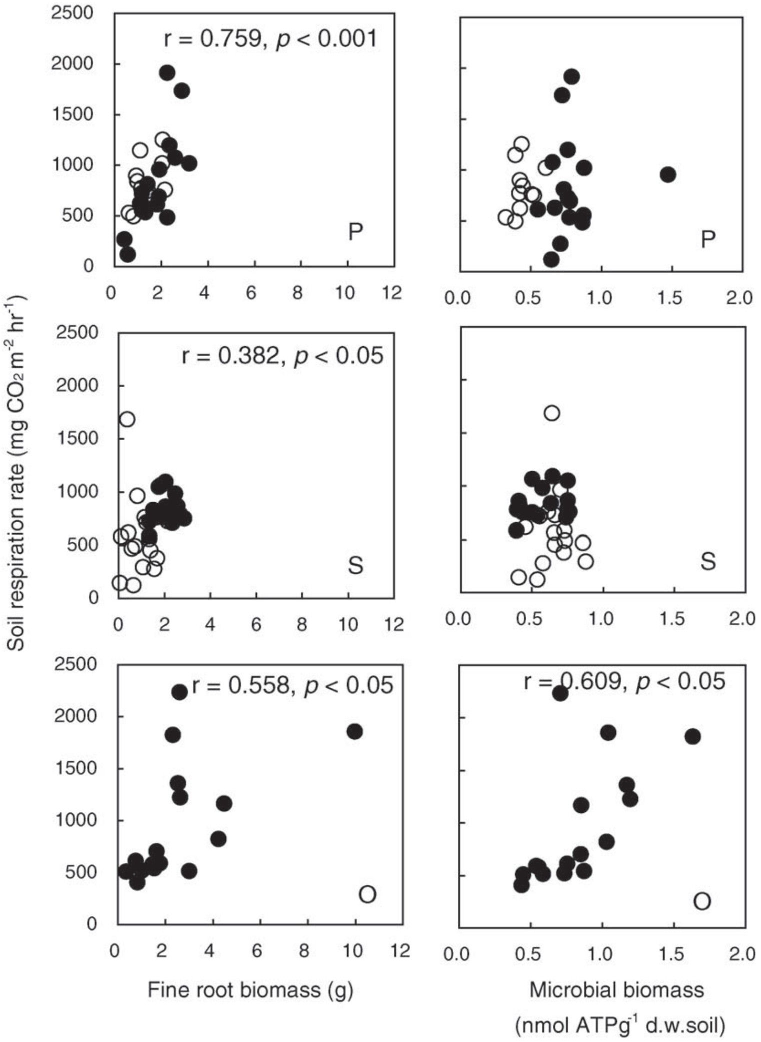

Fig. 2. The relationships between soil respiration and root biomass and microbial biomass in the three different ecosystems. P, S, and O indicate primary forest, secondary forest, and oil palm plantation, respectively. In the primary and secondary forests, canopy and gap sites are indicated by solid and clear circles, respectively. The correlation coefficient and p-value indicate significant relationships in the figure.

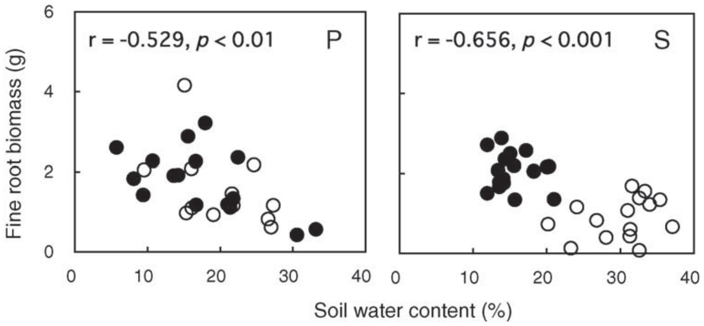

Fig. 3. The relationships between soil water content and fine root biomass in primary forest (P) and secondary forest (S). Canopy and gap sites are indicated by solid and clear circles, respectively.

Table 2
Best single and multiple-factors models were generated using stepwise independent variable selection

Site	Independent variables	Regression coefficient	Standardized partial regression coefficient	R^2	Adj-R^2	Regression ANOVA	
						F	p
Primary forest ($n = 28$)	Intercepts	282.74	282.738	0.638	0.609	22.070	<0.001
	Fine root biomass	706.02	0.824				
	Microbial biomass	−818.36	−0.258				
Secondary forest ($n = 32$)	Intercepts	1189.82	1189.818	0.340	0.318	15.481	<0.001
	Soil water content	−21.58	−0.583				
Oil palm plantation ($n = 16$)	Intercepts	650.02	650.021	0.788	0.755	24.156	<0.001
	Soil water content	−34.60	−0.272				
	Soil C content	551.97	0.778				

content is high. In the present study, soil water content was not significantly correlated with soil microbial biomass in any of the three sites, although it had a significant negative correlation with fine root biomass (diameter <1 mm) in the primary and secondary forests. Although in our study it is not clear why fine root biomass was low in soils with a higher water content, it is probable that a greater soil water content causes a lack of soil aeration, which inhibits the respiratory activity of plant roots. Gaertig et al. (2002) have reported that in German oak forests the density of fine roots showed a positive correlation with gas diffusion coefficient at the soil surface. This suggests that a high soil water content may directly or indirectly depress the soil respiration rate by affecting root biomass and soil gas diffusion.

The soil respiration rate showed a significant positive correlation with fine root biomass in the primary forest and the oil palm plantation. However, the magnitude and mode of contribution of fine root biomass to the soil respiration rate might differ between the two sites.

In the analysis of soil respiration versus fine root biomass between the natural forest (primary forest) and plantation (oil palm plantation), the regression equations for the primary forest (1), secondary forest (2), and oil palm plantation (3) were as follows:

$$y = 650.05x - 150.27 \qquad (r^2 = 0.576,\ p < 0.01) \tag{1}$$

$$y = 155.42x + 472.41 \qquad (r^2 = 0.146,\ p = 0.0309) \tag{2}$$

$$y = 140.60x + 603.29 \qquad (r^2 = 0.311,\ p = 0.0247) \tag{3}$$

As the regression equations for the primary forest and oil palm plantation were very different, we compared them. The y intercept of the regression equation for the primary forest was close to 0 mg CO_2 m^{-2} h^{-1}, indicating that the soil respiration rate falls to almost 0 when fine root biomass is removed. However, in the oil palm plantation, the y intercept was about 600 mg CO_2 m^{-2} h^{-1}, indicating that soil respiration in the absence of fine roots may be close to this value. In addition, the slopes of the regression lines show that the soil respiration rate per unit of fine root biomass was

Table 3
Soil respiration rate in different vegetation types in the tropical regions

Soil respiration rate (mg CO_2 m^{-2} h^{-1})	Vegetation/location	References
948	Tropical forest (primary forest)/Malaysia	This study
707	Tropical forest (secondary forest)/Malaysia	This study
966	Oil palm plantation/Malaysia	This study
625	Tropical semi deciduous forest/Thailand	Tulaphitak et al. (1983)
338–503	Three types tropical forest/Australia	Kiese and Butterbach-Bahl (2002)
469–914	Tropical forest/Panama	Kursar (1989)
231–444	Tropical bare soil/Brazil	La Scala et al. (2000)
216–510	Tropical forest/Brazil	Fernandes et al. (2002)
183–1162	Pasture/Brazil	Fernandes et al. (2002)
430–675	Tropical forest/Costa Rica	Schwendenmann et al. (2003)

The values of soil respiration in primary and secondary forest in this study are average of canopy and gap sites.

greater in the primary forest than in the oil palm plantation. The difference in the regression intercepts and slopes was significant ($p < 0.01$). These results suggest that the respiration rate per unit of fine root biomass and/or microbial respiration associated with roots (e.g., mycorhizae) are greater in the primary forest. In the oil palm plantation, we can consider that respiration by soil microbes that decompose soil organic matter is a more important factor affecting the soil respiration rate. This hypothesis is supported by the fact that soil respiration in the oil palm plantation was significantly correlated with soil microbial biomass and soil C content. Soil organic C is used by degradable microbes as the primary resource in litter decomposition (Singh and Gupta, 1977). Soil respiration in the oil palm plantation would be affected relatively strongly by the distribution of saprophagous microbes and soil organic matter. Therefore, even though the soil respiration rate in both the primary forest and the oil palm plantation showed a positive relationship with fine root biomass, the magnitude and mode of the contribution of fine root biomass and associated soil microbes to soil respiration might differ, reflecting the different forms of land use. This supposition is supported by the results of multiple regression analysis of the data from the two sites; in the oil palm plantation, soil C content (the major energy source for soil microbes) was the major contributor to soil respiration rate.

In the present study, the mean soil respiration rate in the three ecosystems did not differ significantly; however, the environmental factors affecting soil respiration could be different. Differences in land use almost always lead to differences in the vegetation, density of above- and below-ground biomass, the amount of resources available for soil microbes, the physical and chemical characteristics of the soil, and so on. The mean soil respiration rate in each ecosystem is therefore of primary importance when considering the C cycle. However, alterations in the relationships between soil respiration and environmental factors caused by land-use changes are important when estimating variations in the C cycle and its response to environmental change.

Acknowledgements

This paper is a part of a joint research project undertaken by the Forest Research Institute Malaysia (FRIM), Universiti Putera Malaysia, and National Institute for Environmental Studies of Japan (Global Environment Research Program supported by the Ministry of the Environment, Japan). We thank Dr. H. Muraoka of Gifu University, Dr. Konuma of National Institute for Agro-Environmental Science and Dr. Ohtsuka of Ibaraki University for their helpful suggestions. We also thank Dr. Nur Supardi M.N. and Dr. S. Numata for information of climate data in Pasoh. We thank E.S. Quah, S.M. Wang, and other staff members of FRIM in the Pasoh Forest Reserve for assistance during the field investigations.

References

Adachi, M., Bekku, Y.S., Konuma, A., Kadir, W.R., Okuda, T., Koizumi, H., 2005. Required sample size for estimating soil respiration rates in large areas of two tropical forests and of two types of plantation in Malaysia. For. Ecol. Manage. 210, 455–459.

Bousquet, P., Peylin, P., Ciais, P., Ramonet, M., Monfray, P., 1999. Inverse modeling of annual atmospheric CO_2 source and sinks. 2. Sensitivity study. J. Geophy. Res. 104, 26179–26193.

Davidson, E.A., Verchot, L.V., Cattanio, J.H., Ackerman, I.L., Carvalho, J.E.M., 2000. Effect of soil water content on soil respiration in forests and cattle pastures of eastern Amazonia. Biogeochemistry 48, 53–69.

Dixon, R.K., Brown, S., Houghton, R.A., Solomon, A.M., Trexler, M.C., Wisniewski, J., 1994. C pools and flux of global forest ecosystems. Science 263, 185–190.

Epron, D., Nouvellon, Y., Roupsard, O., Monuvondy, W., Mabiala, A., Saint-André, L., Joffre, R., Jourdan, C., Bonnefond, J.M., Berbigier, P., Hamel, O., 2004. Spatial and temporal variations of soil respiration in a Eucalyptus plantation in Congo. For. Ecol. Manage. 202, 149–160.

Fang, C., Moncrieff, J.B., Gholz, H.L., Clark, K.L., 1998. Soil CO_2 efflux and its spatial variation in a Florida slash pine plantation. Plant Soil 205, 135–146.

Fernandes, S.A.P., Bernoux, M., Cerri, C.C., Feigl, J., Piccolo, M.C., 2002. Seasonal variation of soil chemical properties and CO_2 and CH_4 fluxes in unfertilized and P-fertilized pastures in an Ultisol of the Brazilian Amazon. Geoderma 107, 227–241.

Field, C.B., Behrenfeld, M.J., Randerson, J.T., Falkowski, P., 1998. Primary production of the biosphere: integrating terrestrial and oceanic components. Science 281, 237–240.

Gaertig, T., Schack-Kirchner, H., Hildebrand, E.E., Wilpert, K.V., 2002. The impact of soil aeration on oak decline in southwestern Germany. For. Ecol. Manage. 159, 15–25.

Hoshizaki, H., Niiyama, K., Kimura, K., Yamashita, T., Bekku, Y., Okuda, T., Quah, E.S., Nur Supardi, M.N., 2004. Recent biomass change in relation to stand dynamics in a lowlamd tropical rain forest, Pasoh Forest Reserve, Malaysia. Ecol. Res. 19, 357–363.

Houghton, R.A., Hackler, J.L., 1999. Emissions of C from forestry and land-use change in tropical Asia. Global Change Biol. 5, 481–492.

Houghton, R.A., 2003. Revised estimates of the annual net flux of C to the atmosphere from changes in land use and land management 1850–2000. Tellus 55B, 378–390.

Jenkinson, D.S., Oades, J.M., 1979. A method for measuring adenosine triphosphate in soil. Soil Biol. Biochem. 11, 193–199.

Kiese, R., Butterbach-Bahl, K., 2002. N_2O and CO_2 emissions from three different tropical forest sites in the wet tropics of Queensland, Australia. Soil Biol. Biochem. 34, 975–987.

Kursar, T.A., 1989. Evaluation of soil respiration and soil CO_2 concentration in a lowland moist forest in Panama. Plant Soil 113, 21–29.

La Scala Jr., N., Marques Jr., J., Pereira, G.T., Cora, J.E., 2000. C dioxide emission related to chemical properties of a tropical bare soil. Soil Biol. Biochem. 32, 1469–1473.

Linn, D.M., Doran, J.W., 1984. Effect of water-filled pore space on C dioxide and nitrous oxide production in tilled and nontilled soils. Soil Sci. Soc. Am. J. 48, 1267–1272.

Maestre, F.T., Cortina, J., 2003. Small-scale spatial variation in soil CO_2 efflux in a Mediterranean semiarid steppe. Appl. Soil Ecol. 23, 199–209.

Malhi, Y., Grace, J., 2000. Tropical forests and atmospheric carbon dioxide. Tree 15, 332–337.

Manokaran, N., Quah, E.S., Ashton, P.S., LaFrankie, J.V., Nur Supardi, M.N., Ahmad, W.M.S.W., Okuda, T., 2004. Pasoh forest dynamics plot, Peninsular Malaysia. In: Losos, E.C., Leigh, J.E.G. (Eds.), Tropical Forest Diversity and Dynamism. pp. 585–598.

Neergaard, A., Porter, J.R., Gorissen, A., 2002. Distribution of assimilated carbon in plants and rhizosphere soil of basket willow (*Salix viminalis* L.) Plant Soil 245, 307–314.

Okuda, T., Suzuki, M., Adachi, N., Quah, E.S., Hussein, N.A., Manokaran, N., 2003. Effect of selective logging on canopy and stand structure and tree species composition in a lowland dipterocarp forest in peninsular Malaysia. For. Ecol. Manage. 175, 297–320.

Rayment, M.B., Jarvis, P.G., 2000. Temporal and spatial variation of soil CO_2 efflux in a Canadian boreal forest. Soil Biol. Biochem. 32, 35–45.

Rochette, P., Desjardins, R.L., Pattry, E., 1991. Spatial and temporal variability of soil respiration in agricultural fields. Can. J. Soil Sci. 71, 189–196.

Schimel, D.S., House, J.I., Hibbard, K.A., Bousquet, P., Ciais, P., Peylin, P., Braswell, B.H., Apps, M.J., Baker, D., Bondeau, A., Canadell, J., Churkina, G., Cramer, W., Denning, A.S., Field, C.B., Friedlimgstein, P., Goodale, C., Heimann, M., Houghton, R.A., Melillo, J.M., Moore III, B., Murdiyarso, D., Noble, I., Pacala, S.W., Prentice, I.C., Raupach, M.R., Rayner, P.J., Scholes, R.J., Steffen, W.L., Wirth, C., 2001. Recent patterns and mechanisms of carbon exchange by terrestrial ecosystems. Nature 414, 169–172.

Schwendenmann, L., Veldkamp, E., Brenes, T., O'Bien, J., Mackensen, J., 2003. Spatial and temporal variation in soil CO_2 efflux in an old-growth neotropical rain forest, La Selva, Costa Rica. Biogeochemistry 64, 111–128.

Scott-Denton, L.E., Sparks, K.L., Monson, R.K., 2003. Spatial and temporal controls of soil respiration rate in a high-elevation, subalpine forest. Soil Biol. Biochem. 35, 525–534.

Singh, J.S., Gupta, S.R., 1977. Plant decomposition and soil respiration in terrestrial ecosystems. Bot. Rev. 43, 449–528.

Søe, A.R.B., Buchmann, N., 2005. Spatial and temporal variations in soil respiration in relation to stand structure and soil parameters in an unmanaged beech forest. Tree Physiol. 25, 1427–1436.

Stoyan, H., De-Polli, H., Böhm, S., Robertson, G.P., Paul, E.A., 2000. Spatial heterogeneity of soil respiration and relates properties at the plant scale. Plant Soil 222, 203–214.

Tang, Y., Kachi, N., Furukawa, A., Muhamad, A., 1996. Light reduction by regional haze and its effect on simulated leaf photosynthesis in a tropical forest of Malaysia. For. Ecol. Manage. 89, 205–211.

Tulaphitak, T., Pairintra, C., Kyuma, K., 1983. Soil fertility and tilth. In: Kyuma, K., Pairintra, C. (Eds.), Shifting Cultivation. Faculty of Agriculture, Kyoto University, Japan, pp. 63–83.

Xu, M., Qi, Y., 2001. Soil-surface CO_2 efflux and its spatial and temporal variation in a young ponderosa pine plantation in northern California. Global Change Biol. 7, 667–677.

Yamashita, T., Takeda, H., 1998. Decomposition and nutrient dynamics of leaf litter in litter bags of two mesh size set in two dipterocarp forest sites in Peninsular Malaysia. Pedobiologia 42, 11–21.

Available online at www.sciencedirect.com
ScienceDirect
Agricultural and Forest Meteorology 147 (2007) 35–47
AGRICULTURAL AND FOREST METEOROLOGY
www.elsevier.com/locate/agrformet

Spatial and temporal variation in soil respiration in a Southeast Asian tropical rainforest

Yoshiko Kosugi [a,*], Tomonori Mitani [b], Masayuki Itoh [a], Shoji Noguchi [c], Makoto Tani [a], Naoko Matsuo [d], Satoru Takanashi [e], Shinjiro Ohkubo [a], Abdul Rahim Nik [f]

[a] Laboratory of Forest Hydrology, Division of Environmental Science and Technology, Graduate School of Agriculture, Kyoto University, Kyoto 606-8502, Japan
[b] Forestry Agency Japan, Tokyo 100-8952, Japan
[c] Forestry and Forest Products Research Institute Tohoku Research Center, Morioka, Iwate 020-0123, Japan
[d] Faculty of Bioresources, Mie University, Tsu, Mie 514-8507, Japan
[e] Forestry and Forest Products Research Institute, Tsukuba, Ibaraki 305-8687, Japan
[f] Forest Research Institute Malaysia, Kepong, Kuala Lumpur 52109, Malaysia

Received 14 February 2007; received in revised form 11 June 2007; accepted 12 June 2007

Abstract

The influence of soil temperature and water content on soil respiration rate, and its spatio-temporal variation, were evaluated for a lowland dipterocarp forest in Peninsular, Malaysia. Soil respiration rate, temperature and water content were measured in a 50-m × 50-m plot with a nested sampling design of varying grid size. The variation in soil respiration rate increased with plot size. Geostatistical analysis indicated that the range of spatial autocorrelation for soil respiration rate and water content fell between 4.4 and 24.7 m. Spatially, the soil respiration rate was low where soil water content was high. In contrast, temporally, the soil respiration rate was low when the soil was dry. During dry periods, the soil respiration rate was still lower in wetter areas. These results suggest that a physical factor such as the restriction of gas diffusivity in water-saturated soil is not the primary cause of the low soil respiration rates in wetter places, and that several physical, biological and chemical properties co-varying with soil water drive the bipolar spatial and temporal variation of soil respiration rate.

Keywords: Soil respiration rate; Spatial variation; Geostatistics; Temporal variation; Soil water content; Soil temperature; Southeast Asian tropical rainforest

1. Introduction

Global warming caused by increased concentrations of greenhouse gases (including CO_2) is currently one of the most important issues to be addressed at a global scale. Because tropical forests are the greatest global source of net primary production (NPP), they are important contributors to global carbon cycling (International Panel on Climate Change IPCC, 2001). It is important to evaluate the efficiency of forest ecosystems in tropical regions as carbon sinks to contribute to our understanding of both global carbon cycling and the prevention of deforestation in these regions. The efficacy of forest ecosystems to function as carbon sinks is evaluated as the difference between total carbon

---

* Corresponding author. Tel.: +81 75 753 6089; fax: +81 75 753 6088.
E-mail address: ykosugi@kais.kyoto-u.ac.jp (Y. Kosugi).

0168-1923/$ – see front matter © 2007 Elsevier B.V. All rights reserved.
doi:10.1016/j.agrformet.2007.06.005

assimilation from photosynthesis and carbon lost from ecosystem respiration, disturbance, and herbivory. In forest ecosystems, the largest component of the net flux of CO_2 is the efflux from the soil surface, i.e., soil respiration, followed by uptake for photosynthesis (Raich and Schlesinger, 1992). Soil respiration accounts for 40–70% of total respiration (Goulden et al., 1996; Chambers et al., 2004; Ohkubo et al., 2007); therefore, it is important to evaluate this component.

The eddy covariance method is a widely used technique for measuring the net exchange of energy and trace gases such as CO_2 between an ecosystem and the atmosphere (Kimball et al., 1997; Kramer et al., 2002; Baldocchi, 2003). This method allows for spatially integrated measurements of the total night-time respiration of the ecosystem. However, nocturnal measurements of net ecosystem CO_2 exchange are sometimes unreliable, especially when the atmosphere is stable (Goulden et al., 1996; Lavigne et al., 1997; Law et al., 1999; Baldocchi, 2003). An alternative way to measure nocturnal CO_2 flux is the chamber method, along with techniques to extrapolate these measurements to entire ecosystems (Anthoni et al., 1999). However, a sufficient number of measurements taking spatiotemporal variation into consideration is needed to permit a comparison with the spatially integrated eddy covariance technique (Drewitt et al., 2002), because soil respiration, which accounts for a high proportion of total respiration, exhibits high spatiotemporal variation (Hanson et al., 1993; Davidson et al., 1998; Buchmann, 2000; Rayment and Jarvis, 2000; Stoyan et al., 2000; Law et al., 2001; Xu and Qi, 2001). To quantify spatially averaged soil respiration, the extent of spatial variation in soil respiration should be evaluated, and this is especially important for quantifying soil respiration using the chamber method, because the area covered by one chamber is very small, whereas the spatial variation in soil respiration is quite large.

To estimate the annual amount of soil respiration and its temporal variability, it is essential to evaluate the relationship between soil respiration and environmental variables that can be continuously monitored, such as temperature and soil moisture content. Differences in soil temperature and water content may explain most of the temporal variation in soil respiration (Davidson et al., 1998; Qi and Xu, 2001; Reichstein et al., 2002; Rey et al., 2002). In tropical regions, Davidson et al. (2000) reported that soil respiration rate was high during the rainy period and low during the dry period in an Amazonian tropical rainforest. Hashimoto et al. (2004) reported that soil respiration rate increased with increasing soil moisture in a tropical monsoon forest in Thailand. In boreal regions, seasonal variation in soil respiration rate was determined to a large degree by that of soil temperature; differences in soil water content had almost no effect on variation in soil respiration rate (Goulden et al., 1998; Morén and Lindroth, 2000; Rayment and Jarvis, 2000). In temperate regions, the soil respiration rate exponentially increased with soil temperature, and soil water content suppressed soil respiration rate under dry conditions (e.g., Dong et al., 1998; Londo et al., 1999; Kosugi et al., 2005; Mitani et al., 2007), or under both dry and wet conditions (e.g., Martin and Bolstad, 2005), or did not have a significant effect on soil respiration (e.g., Fang et al., 1998; Ohashi et al., 1999). Therefore, soil temperature plays a greater role than water content in governing soil respiration rate in temperate regions where the range of temperatures is wider. However, in tropical regions where seasonal variation in soil temperature is small, soil water content should be tested as the most effective index to estimate the seasonal variation of soil respiration rate.

Although, previously reported effects of soil water content on soil respiration rate varied with site and study design. This is because both temporal and spatial variability of soil respiration is driven by many biological, chemical and physical properties that may co-vary with soil water, such as root biomass (Hanson et al., 1993; Adachi et al., 2006), microbial biomass (Scott-Denton et al., 2003), N availability (Prasolova et al., 2000), gas diffusivity of soil, and so on. For the better understanding and estimation of temporal variability in and the annual amount of soil respiration, the spatial and temporal effects of soil water content on respiration rate should be investigated separately, in comparison with previous results (e.g., Davidson et al., 1998; Schwendenmann et al., 2003; Sotta et al., 2004, 2006; Ohashi and Gyokusen, 2007).

The objectives of this study were to evaluate: (1) spatial variation in soil respiration to assess the observational design in terms of sampling size and distance between sampling points and (2) the effects of soil water content on spatial and temporal variation in soil respiration separately, in an old-growth lowland dipterocarp forest at Pasoh in Peninsula Malaysia (a Southeast Asian tropical rainforest).

2. Methods

2.1. Site

The study area was located in the Pasoh Forest Reserve (2°59′N, 102°18′E) of the Forest Research Institute Malaysia (FRIM) in Peninsula Malaysia. An intensive research project by the International Biological Programme (IBP) was conducted in this forest reserve from 1970 to 1974 (e.g., Soepadmo, 1978). The core area (600 ha) of the reserve is primary lowland mixed dipterocarp forest, consisting of various species of *Shorea* and *Dipterocarpus* (Soepadmo, 1978). Soil characteristics of the area were described in detail by Yamashita et al. (2003). The FAO soil type around a 52-m-tall tower near IBP Plot 1 is Haplic Acrisol, and the A horizon is thin (0–5 cm). Lateritic gravels are abundant below a depth of 30 cm (Soepadmo, 1978; Yamashita et al., 2003). In the core area, micrometeorological and CO_2 flux data were collected at the top of the tower near IBP Plot 1 (Tani et al., 2003; Yasuda et al., 2003). Details of the vegetation, micrometeorology, and eddy flux measurements were described by Takanashi et al. (2005).

2.2. Observations

A 50-m × 50-m plot (50-m plot) was established north of the tower within the 6-ha long-term ecological research plot established by Niiyama et al. (2003; Fig. 1a). The entire area in the 50-m plot has rather flat topography (Fig. 1a). In this plot, measurements were made at 36 points on a 10-m grid in September 2002, March 2003, August 2003, December 2003, September 2004, November 2004, February 2005, July 2005 and October 2005 (Fig. 1b). Subplots were established within the 50-m plot to investigate smaller-scale spatial variation in soil respiration rates (Fig. 1b). In September 2002, a 10-m × 10-m plot (10-m plot) with a 2-m grid and a 5-m × 5-m plot (5-m plot) with a 1-m grid were prepared; in August 2003, a 10-m plot and a 3-m × 3-m plot (3-m plot) with a 0.5-m grid were prepared; in December 2003, a 10-m plot was prepared, and in September 2004, a 10-m plot and a 5-m plot were prepared. A 10-m plot was established in the 50-m plot, a 5-m plot in the 10-m plot, and a 3-m plot in the 5-m-plot to avoid bias in the spatial autocorrelation of the limited sample.

Measurements were conducted on 16–19 September 2002, 8 March 2003, 23–25 August 2003, 15–17 December 2003, 7–11 September 2004, 22 November 2004, 12 February 2005, 3 July 2005 and 18 October 2005. With respect to antecedent precipitation index (API_n) and transience of seasons, we defined these nine measurements as measurements of the rainy, dry and transient periods. API_n was used here as a widely used index to represent both short-term and seasonal trends of rainfall pattern and also soil moisture condition. It was defined as $\sum_{i=1}^{n} P_i/i$, where P_i is daily precipitation (mm) and i is days beforehand. We tested 10, 30, 45, 60 and 75 days as the n value in the relationship with soil water content at depths of 10, 20 and 30 cm (the average of nine sensors; see below). Here, 60 days was used as the value of n, because the correlation with soil water content was highest with $n = 60$. The measurements of December 2003 ($API_{60} = 30.6$ mm), November 2004 ($API_{60} = 28.4$ mm) and October 2005

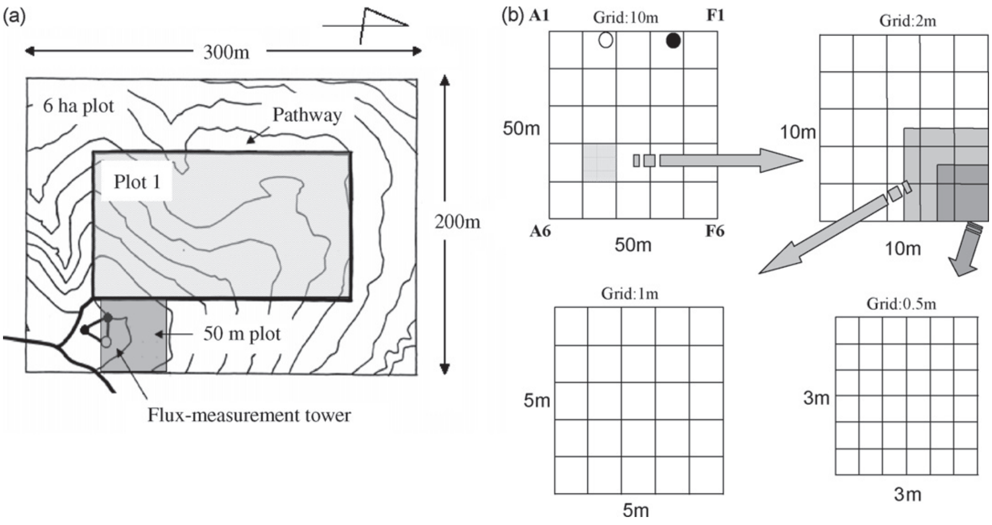

Fig. 1. (a) Locations of plots used in this study (dark-shaded). The 50-m × 50-m plot (50-m plot) was established north of the flux-measurement tower within the 6-ha plot established by Niiyama et al. (2003). The triangle is a tower-bridge system including a flux-measurement tower (○) and two other towers (●). The lightly shaded area indicates IBP Plot 1. The contour interval is 1 m. (b) Plan of the nested plot. The circles indicate two of the towers in the tower-bridge system.

($API_{60} = 37.2$ mm) were defined as those of the rainy period, the measurement of September 2002 ($API_{60} = 41.6$ mm) as that of the transient period, and the measurements of March 2003 (API = 9.3 mm), August 2003 ($API_{60} = 9.5$ mm), September 2004 ($API_{60} = 4.3$ mm), February 2005 ($API_{60} = 2.1$ mm) and July 2005 ($API_{60} = 7.8$ mm) as those of the dry period (Fig. 2d). September 2002 was defined as the transient period despite having the largest API_{60} because it was just after a sudden interruption of a dry period with heavy rains on the previous 3 days. In each plot, soil respiration rate, temperature and water content were measured at all points between about 09:00 and 16:00. No rainfall occurred during the point observations in each plot. We also avoid early morning and just after rain to prevent the influence of rapid transition of the soil respiration rate during the observation. The observation of diurnal variation of soil respiration rate at four points of the 50-m plot in August 2003 (a dry period) and September 2004 (a wet period) revealed that little diurnal variation in soil respiration rate occurred during these observations.

Soil respiration rate was measured using an infrared gas analyser (IRGA, LI-6262 or LI-820, LI-COR, Lincoln, NE, USA) equipped with a closed dynamic chamber system made of PVC. The collars of the chambers, which had an internal diameter of 13 cm and a height of 16 cm, were inserted previously 3–5 cm into the soil. Disturbance of soil when the collar was inserted was minimized. At the time of measurement, the lid of the chamber was closed and air was circulated in a loop between the chamber headspace and an IRGA. The air was circulated within the system at a flow rate of 1.0 L min^{-1} using a pump (MP-15CF, Shibata, Tokyo, Japan). After the chamber was closed and the increased CO_2 concentration in the chamber had stabilised (approximately 30 s after the chamber top had been placed on the soil collar), the concentration was recorded for about 90 s; soil respiration rate was calculated from the increase in CO_2 concentration using a linear regression of the linear section of the record. We used brief measurement periods (90 s) and linearity was checked for each measurement to avoid the noise due to pressure artifacts or disturbance of diffusion gradients (Davidson et al., 2002). The zero and span of the IRGA were calibrated in the laboratory before and after each observation campaign.

Soil temperature was measured at the same time as soil respiration rates with a thermistor (Thermo Recorder RT-10, Espec Mic Corp., Aichi, Japan) at a

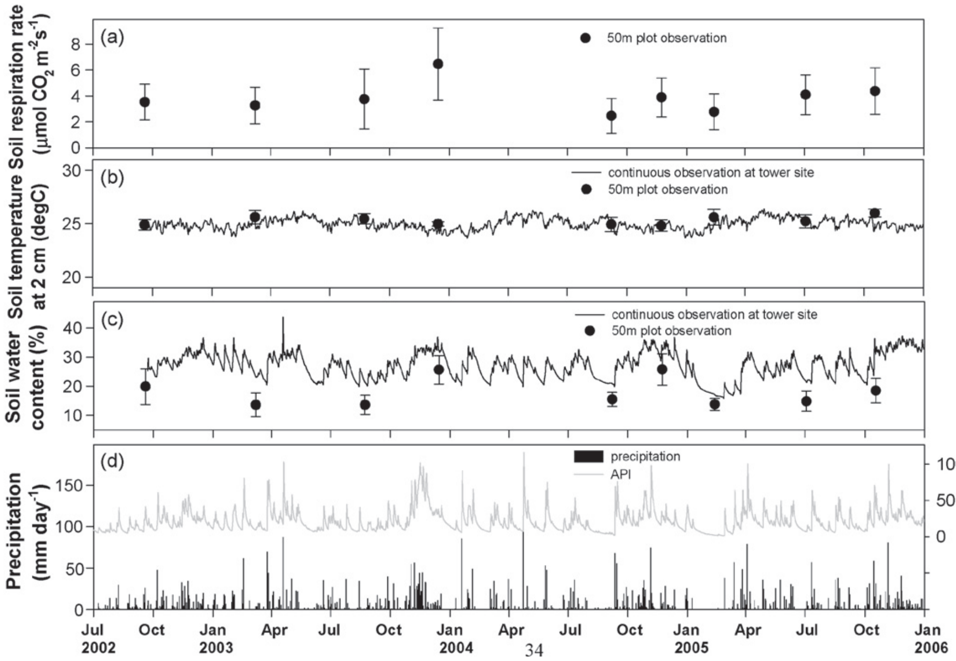

Fig. 2. Seasonal variation in soil respiration rate, temperature, water content and daily precipitation. (a) Observed (50-m plot) soil respiration rate. (b) Soil temperature at a depth of 2 cm. (c) Soil water content based on continuous observations at three points near the flux tower (average values for 10, 20 and 30 cm, $n = 9$; lines) and based on the 50-m plot manual observations at a depth of 0–12 cm (circles). (d) Daily amount of precipitation (black bars) and antecedent precipitation index (API; grey line). Bars represent standard deviations.

depth of 2 cm adjacent to each chamber. Soil water content was measured with a HydroSense Soil Water Content Measurement System (CS-620, Campbell Scientific, Inc., Logan, UT, USA) at a depth of 0–12 cm and at three points very close to each chamber, but not in the chamber, to prevent disturbance.

In addition to these manual measurements, soil temperature and water content were continuously measured at three points near the flux observation tower at 10-min intervals. Soil temperature was measured at a depth of 2 cm with three thermistors (model 107, Campbell Scientific, Inc.). Soil water content was measured at depths of 10, 20 and 30 cm with nine water content reflectometers (CS-615 or CS-616, Campbell Scientific, Inc.). These data were recorded using a data logger (CR-10X, Campbell Scientific, Inc.).

Soil mineral samples were collected at depths of 0–5 cm in each grid (36 points) of the 50-m plot in August 2006. Soils were sieved through a 2-mm mesh sieve to remove coarse fragments and then homogenised. Total N and C concentrations in the soil samples were measured using the combustion method (Bremner, 1996) in an NC-analyser (Sumigraph NC-900, Sumigraph Co. Japan).

Maps of the spatial distributions of soil respiration, soil water content, total C and N content and C/N ratio were generated with the 50-m plot data. SigmaPlot ver.9.01 software (Systet Software Inc., Richmond, USA) was used for graphical analysis of the data. The intervals of (x,y) data was 10 m. For the z-coordinate, eight major contours were used for soil respiration, six for soil water content, five for the total N and C content and C/N ratio.

2.3. Geostatistics

We used geostatistics to evaluate spatial variation, as it allows for the determination of the magnitude of spatial dependence and the scale of spatial autocorrelation among measurement points (Robertson, 1987). The measurement points estimated within this scale should be spatially dependent. Therefore, the essential spatial variation can only be efficiently detected when measurements for a given factor are made at a spatial interval beyond this scale.

The patterns of spatial variation in soil respiration rate and soil water content were analysed geostatistically (Robertson et al., 1988; Stenger et al., 2002; Franklin and Mills, 2003). The calculation of semivariances from field data and fitting the models to semivariograms was performed using the geostatistics software GS+ (Robertson, 1998). The semivariance, $\gamma(h)$, was calculated for each specific lag distance h:

$$\gamma(h) = \frac{1}{2N(h)}\sum_{i=1}^{N(h)}[z(x_i) - z(x_i + h)]^2$$

where $N(h)$ is the number of pairs of points separated by distance h, $z(x_i)$ the measured value at point x_i and $z(x_i + h)$ is the measured value at point $x_i + h$. A log-normal transformation was applied to normalise skewed frequency distributions.

Only isotropic semivariograms were considered and the semivariance data were fit to a spherical function. In this analysis, the default active lag distance was set as 80% of the maximum lag distance, and each specific lag distance was set as one-tenth of the maximum active lag distance. A typical semivariogram has a nugget variance (C_0). With increasing lag distance, the variance will increase up to the sill variance ($C_0 + C$). The nugget represents either random error or spatial dependence at scales smaller than the minimum distance examined (Robertson, 1987). The sill represents spatially independent variance. The distance at which the sill is reached is called the range. The measurement points estimated within this range are spatially autocorrelated, whereas points outside this range are considered independent (Robertson, 1998). The values of the semivariance, and thus C_0 and $C_0 + C$, were scaled to sample variance. The proportion of the structural variance (C) to sill ($C_0 + C$) is calculated to evaluate the magnitude of the spatial dependence (Robertson and Freckman, 1995; Morris, 1999; Hirobe et al., 2001; Mori and Takeda, 2003).

3. Results

3.1. Spatial distribution

The coefficient of variation (CV) for soil respiration rate was between 26 and 62%, and increased with grid size, being largest in the 50-m plot (Table 1). Spatial variation in soil temperature, with a CV of 0.8–2.7%, was much less than that of soil respiration rate, suggesting that the effect of soil temperature on spatial variation in soil respiration rate was minimal. Conversely, spatial variation in soil water content was much greater. The CV for soil water content was between 12 and 31%, and increased with plot size except in September 2004 (Table 1).

The spatial distribution maps of soil respiration rate show this variation (Fig. 3). In these maps, large-scale distribution of low and high soil respiration rate can be seen. This scale of soil respiration rate was evaluated

Table 1
Summary of mean, standard deviation (S.D.) and coefficient of variation (CV) of soil respiration, temperature and water content for four intensive observation periods

Date	Plot[a]	Soil respiration rate			Soil temperature			Soil water content		
		Mean	S.D.	CV	Mean	S.D.	CV	Mean	S.D.	CV
September 2002	5 m	3.3	1.0	30	24.9	0.54	2.2	15	2.7	18
	10 m	3.1	0.9	29	24.6	0.49	2.0	17	3.5	21
	50 m	3.5	1.4	39	24.9	0.50	2.0	20	6.2	31
August 2003	3 m	4.2	1.1	26	25.7	0.44	1.7	11	1.4	12
	10 m	3.1	1.2	38	25.6	0.35	1.4	12	2.4	21
	50 m	3.8	2.3	62	25.5	0.48	1.9	14	3.3	24
December 2003	10 m	6.8	2.3	33	24.3	0.25	1.0	27	4.8	17
	50 m	6.5	2.8	43	25.0	0.19	0.8	26	4.9	19
September 2004	5 m	3.4	1.2	35	25.2	0.49	1.9	14	2.2	16
	10 m	2.8	1.0	39	25.7	0.64	2.5	14	2.1	15
	50 m	2.5	1.4	55	24.9	0.68	2.7	15	2.4	15

The units for mean and S.D. of soil respiration rate, temperature and water content are μmol CO_2 m^{-2} s^{-1}, °C and %, respectively. The unit for CV is %.

[a] Sample sizes were 36 in the 5, 10 and 50-m plots, and 49 in the 3-m plot.

using a geostatistical analysis. A summary of the semivariogram model parameters is shown in Table 2. The spatial autocorrelation for soil respiration rate ranged between 4.4 m in the rainy period and 24.7 m in the transient periods (Table 2). The spatial distribution of soil respiration rate in the 50-m plot was significantly negatively correlated with soil water content in September 2002, August 2003, November 2004 (Fig. 4) and the average of the nine observations (Fig. 6), although this negative correlation was not significant in the other periods. Soil water content was relatively high in the centre and the lower right of the plot in all periods, and soil respiration rate was also low at this point (Fig. 3). The ranges of spatial autocorrelation for soil water content ranged between about 5.3 m in the dry period and 28.1 m in the transient period, a scale similar to that for soil respiration rate (Table 2); in the transient period when soil water content was highly correlated with soil respiration rate, the range of soil water content was in accord with that of soil respiration rate.

The C/N ratio ranged narrowly, with a mean and standard deviation of 15.5 ± 1.6. Neither of the C/N ratio nor total C content had a significant correlation with the spatial distribution of soil respiration rate of either the individual observation periods or the average of the nine observations (Fig. 5). Total N content had a weak significant correlation with soil respiration rate at September 2002 ($P < 0.05$), July 2005 ($P < 0.05$), and the average of the nine observations ($P < 0.05$. Fig. 5). With the spatial distribution of soil water content, C/N ratio had a week significant correlation only at October 2005 ($P < 0.05$), while total C content had a significant correlation at December 2003 ($P < 0.05$), November 2004 ($P < 0.05$), July 2005 ($P < 0.05$), October 2005 ($P < 0.005$), and the average of the nine observations ($P < 0.005$, Fig. 5), and total N content also had a significant correlation at November 2004 ($P < 0.005$), February 2005 ($P < 0.05$), July 2005 ($P < 0.005$), October 2005 ($P < 0.005$), and the average of the nine observations ($P < 0.001$, Fig. 5). Total N and C content were relatively high in the left part of the map. At these points, soil water content was low, and soil respiration rate was high (Fig. 3).

3.2. Seasonal variation

Seasonal variation in soil respiration rate, temperature and water content was investigated using the spatially averaged values from 36 points in the 50-m plot, because measurements in this plot were considered to capture the spatial variation in soil respiration rate most efficiently among the study plots. The spatially averaged value of soil respiration rate showed clear seasonal variation; the maximum was 6.5 μmol CO_2 m^{-2} s^{-1} in a rainy period (December 2003) and the minimum was 2.5 μmol CO_2 m^{-2} s^{-1} in a dry period (September 2004; Fig. 2a). Seasonal variation in daily average soil temperature was low, with an average and standard deviation of 24.9 ± 0.5 °C, a maximum of 26.3 °C and a minimum of 23.7 °C (Fig. 2b). In contrast, seasonal variation in spatially averaged soil water content (presented as the average value of nine sensors at 10, 20 and 30 cm at three locations) was high, with an average and standard deviation of 27.4 ± 3.9%, a maximum of 43.8% and a minimum of 20.4% (Fig. 2c). The seasonal variation in soil respiration rate spatially averaged over 36 points in

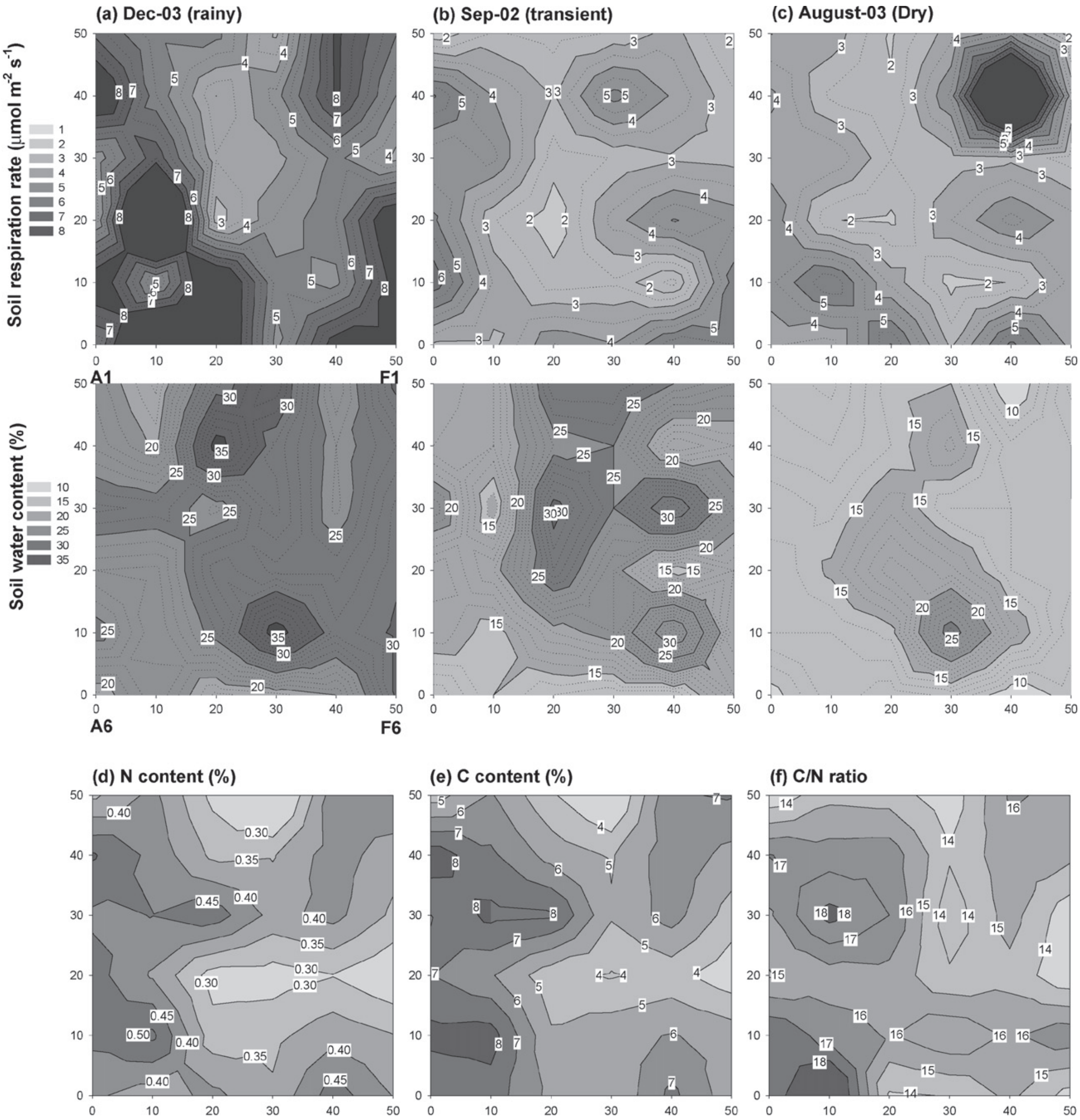

Fig. 3. Maps of the spatial distribution of soil respiration rate (upper figures, μmol CO_2 m^{-2} s^{-1}) and water content (lower figures, %) during (a) a rainy period (December 2003), (b) a transient period (September 2002) and (c) a dry period (August 2003), and spatial distribution of (d) total N content (%), (e) total C content (%), (f) C/N ratio.

the 50-m plot indicated a significant positive correlation ($r = 0.71$, $P < 0.001$) with the spatially averaged soil water content (Fig. 6b). In contrast, the spatial variation in soil respiration rate seasonally averaged across nine observations showed a significant negative correlation ($r = -0.46$, $P < 0.005$) with temporary averaged soil water content at each location (Fig. 6a).

4. Discussion

4.1. Spatial distribution of soil respiration

La Scale et al. (2000) reported that the CV for soil respiration rate was between 30 and 43% in tropical bare soil for 65 points in a 100-m × 200-m plot. At our

Table 2
Summary of semivariogram model parameters for soil respiration rate and soil water content

Date	Soil respiration rate						Soil water content					
	Model	r^2	Nugget C_0	Sill $C_0 + C$	Range (m)	Proportion $C/(C_0 + C)$	Model	r^2	Nugget C_0	Sill $C_0 + C$	Range (m)	Proportion $C/(C_0 + C)$
Rainy period												
December 2003	Spherical	0.013	0.209	0.997	4.4	0.790	Spherical	0.581	0.308	1.105	16.6	0.721
Transient period												
September 2002	Spherical	0.556	0.481	1.255	24.7	0.616	Spherical	0.832	0.119	1.489	28.1	0.920
Dry period												
August 2003	Spherical	0.293	0.073	1.058	7.9	0.931	Spherical	0.502	0.167	1.014	11.5	0.835
September 2004	Spherical	0.543	0.135	1.255	14.1	0.892	Spherical	0.090	0.069	1.055	5.3	0.935

site, Adachi et al. (2005) reported that the CV for soil respiration rate was 42.7% for 50 lattice positions within a 100-m × 200-m plot. Our study showed that the CV for soil respiration rate was between 26 and 62% (Table 1). High spatial variation in soil respiration rate has also been reported at various scales, ranging from the microscale to the catchment area or landscape level (Hanson et al., 1993; Davidson et al., 1998; Stoyan et al., 2000; Xu and Qi, 2001). Soil respiration rate may vary spatially by up to 100% at locations only 1 m apart (Nakayama, 1990). Rayment and Jarvis (2000) reported that spatial heterogeneity in soil respiration rate increased with distances greater than 1 m, but did not increase substantially with further increases in distance. In our study, soil respiration rate also varied by up to about 100% at locations 0.5 m apart in the 3-m plot.

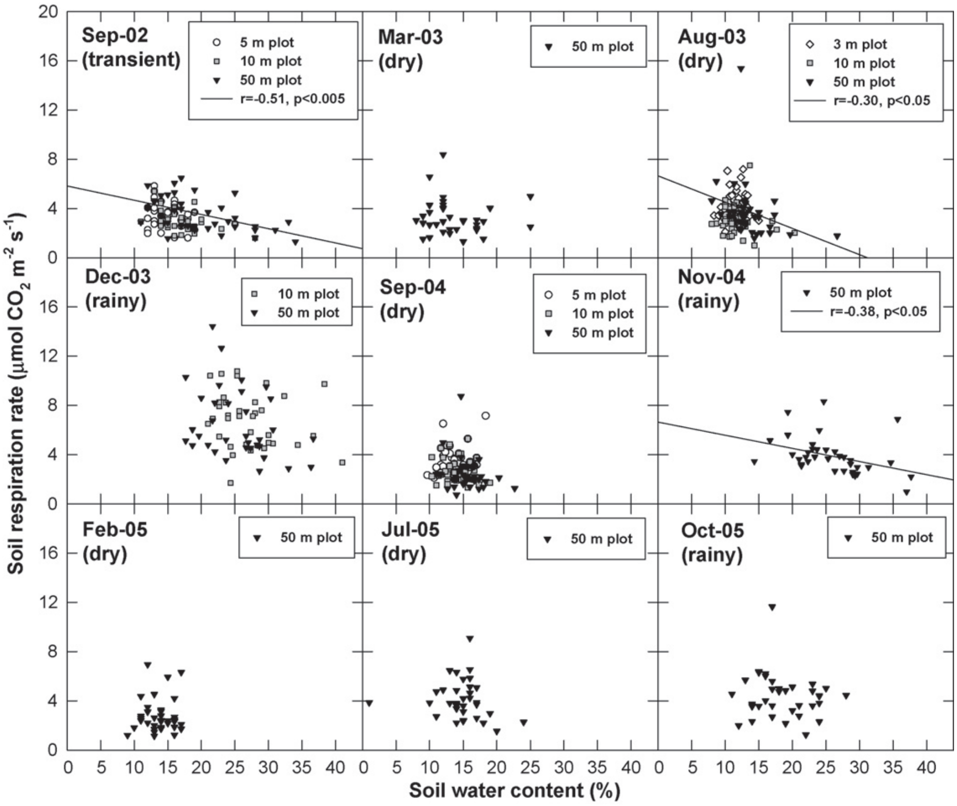

Fig. 4. Relationship between the spatial distribution of soil respiration rate and water content for nine sets of observations. Soil water content was measured manually with CS-620 at depths from 0 to 12 cm.

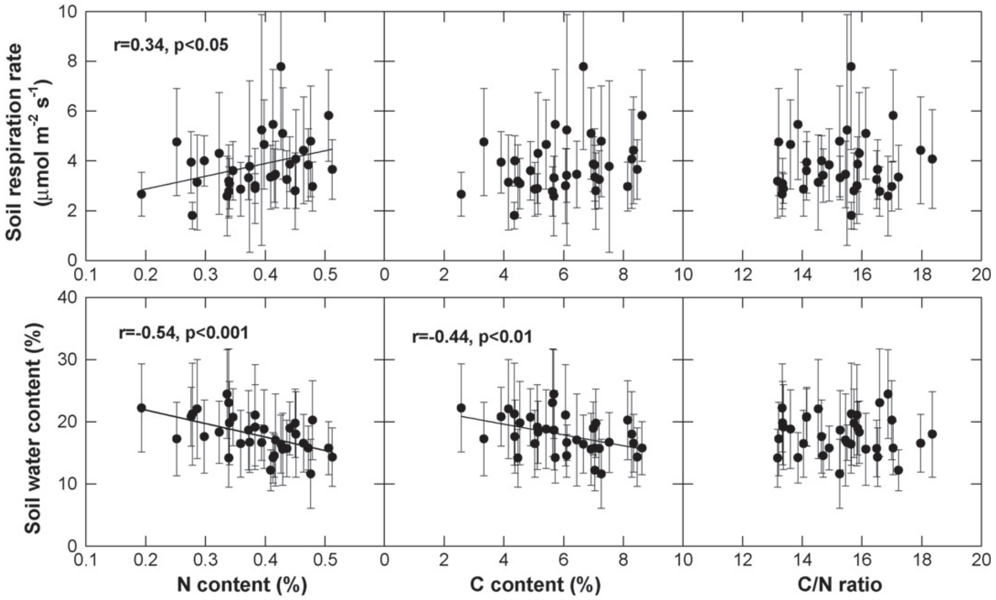

Fig. 5. Relationship between total N or C content, or C/N ratio in August 2006 and soil respiration rate or soil water content as the average of nine observations. Soil water content was measured manually with CS-620 at depths from 0 to 12 cm. Bars represent standard deviations.

However, the CVs of soil respiration rate increased with plot size, and spatial variation in soil respiration rate was considered to increase with distance (Table 1). The spatial autocorrelation for soil respiration rate ranged between 4.4 and 24.7 m, corresponded to the range reported by Savin et al. (2001), which was 18 m in a 20-m × 40-m plot subdivided into 4-m × 4-m plots in old field soil, and that by Ishizuka et al. (2005), which was 10 m in a 27-m × 21-m plot with a 3 m grid in a tropical rainforest in Indonesia. These results indicate the importance of evaluating soil respiration rate at larger scales. Soil respiration rate at this scale was also considered comparable to values determined using the eddy covariance technique, which mainly represents scales of approximately 10^1–10^3 m in the upwind direction

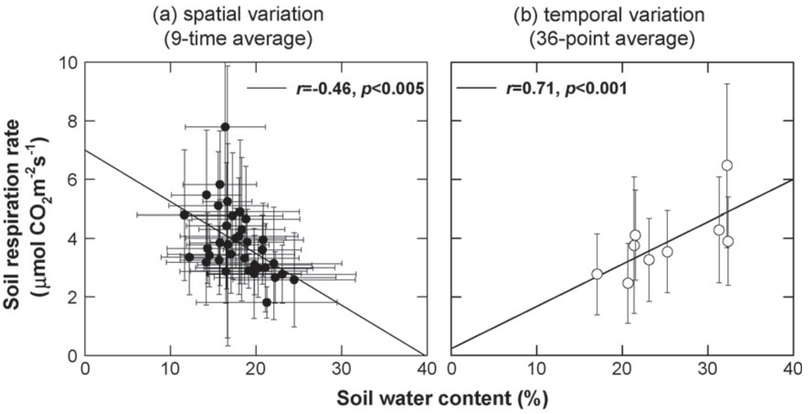

Fig. 6. (a) Relationship between spatial variation in temporally averaged soil respiration rate and water content ($r = -0.46$, $P < 0.005$). The average of nine observations was used for the values at each location. Soil water content was measured manually with CS-620 at depths from 0 to 12 cm. Bars: standard variation. (b) Relationship between temporal variation in spatially averaged soil respiration rate and water content ($r = 0.71$, $P < 0.001$). Soil respiration rate on each observation day shown in this figure was the spatially averaged value of 36 points in the 50-m plot. The average value of nine CS-615/CS-616 sensors at 10, 20 and 30 cm for soil water content at three locations continuously measured near the flux observation tower were used as the reference values indicating the temporal characteristics of each observation period. Bars: standard deviation.

and is thus considered to be on the ecosystem scale (Schmid, 1997; Schmid and Lloyd, 1999).

Our results suggest that soil water content was one of the major factors determining the spatial variation in soil respiration rate at this site. Regarding spatial variability, similar results were reported for other sites, and the restriction of gas diffusivity and few fine roots and low microbial biomass were suggested as possible causes (Hanson et al., 1993; Davidson et al., 1998). It should be noticed that at wet place such as D5, E5 and other places in the middle part of the map in Fig. 3, soil respiration rate was lower than at other places in the wet period, and it did not increase in dry periods when soil water content became low everywhere. If the decline in soil respiration in wetter places was due to the restriction of gas diffusivity in the wet period, then it should increase during the dry period. These results suggest that a physical factor such as the restriction of gas diffusivity in water-saturated soil is not the primary cause of the low soil respiration rates in wetter places.

Our results show that total N content correlates with soil water content and soil respiration rate. Because soil C and N cycling processes are closely coupled and soil C and N dynamics are tightly linked (Prasolova et al., 2000), soil N availability can influence soil respiration and C dynamics in forest ecosystems. The availability of N can also influence fine root biomass. Rasse (2002) reviewed numerous studies reporting local proliferation of fine roots when exposed to higher levels of available N, whereas increased availability of inorganic N in the soil profile can drastically reduce the root-to shoot ratio of temperate woody species. Thus, the influence of C/N ratio and total C and N contents on soil respiration is complicated and sometimes obscures a clear relationship. A previous study at this site also reported that the spatial distribution of soil respiration rate had a significant negative correlation with soil water content, a positive correlation with fine root biomass, and was not significantly correlated with soil temperature, soil C content or microbial biomass (Adachi et al., 2006). These results suggest that several chemical and biological factors such as fine root biomass, N and C dynamics co-varying with soil water content control the spatial distribution of soil respiration rate in this site, though we need more data to confirm this.

4.2. Seasonal variation in soil respiration and the effect of soil water content

Soil respiration rate was positively related to soil water content when considering the seasonal variation in spatially averaged data of soil respiration rate and water content (Fig. 6b). Regarding spatial distribution, soil respiration rate was negatively correlated with soil water content (Fig. 6a). Moreover, in the dry period when soil water content was low across all plots, soil respiration rate was still lower in the wet areas than elsewhere (Fig. 3). If the spatial and temporal relationship between soil water content and soil respiration rate can be explained with one parabolic function, the soil respiration rate at a wet place should become higher than in other places in dry periods, because soil water content becomes optimal at these places in dry periods. So these results alert us that we should not mix up the influences of soil water content on seasonal and spatial variation of soil respiration rate.

In tropical regions, Schwendenmann et al. (2003) reported the parabolic relationship between soil water content and seasonal variation of soil respiration rate. Sotta et al. (2004, 2006) also reported the parabolic relationship, although they combined the seasonal and spatial variation of soil respiration rate in one dataset. On the other hand, Davidson et al. (2000) reported the temporal positive relationship between soil water content and respiration rate at a primary forest in eastern Amazonia. Our result in a Southeast Asian primary rainforest also showed a positive linear relationship. This disaccord might be because of the limited range of soil moisture in our measurement. Although, soil water content of 33% as the average value of nine sensors at 10, 20 and 30 cm at three locations, which was observed in December 2003 and November 2004, was in the range of upper 10% of every 30-min interval data at our site, for 3 years during 2003–2005 (Fig. 2c). From this, it can at least be said that the seasonal trend of soil respiration at our site related positively with soil water content is similar to the result by Davidson et al. (2000), and different from the results for an old-growth eastern Amazonian rainforest (Sotta et al., 2006) and in an old-growth neotropical rainforest in Costa Rica (Schwendenmann et al., 2003) which showed obvious decline of soil respiration rate at the time of high soil water content. Several factors such as rainfall pattern, annual amount of rainfall, and soil texture should be considered to be possible causes of this difference. Our site has relatively smaller annual rainfall (1733 mm, 2003–2005) among tropical rainforests. It was suggested that the restriction of gas diffusivity in water-saturated soil did not occur at this site in the wet period, at least within the 50-m plot and at the time of nine observations, and that the other factors such as the decline in fine root and microbe activity under dry conditions might determine the low soil respiration rate in the dry period.

5. Conclusions

The CV of soil respiration rate increased with plot size, and geostatistical analysis indicated that soil respiration rate at this site had a strong spatial dependence. The range of spatial autocorrelation for soil respiration rates was between 4.4 and 24.7 m. These results indicate the importance of evaluating soil respiration rate at a large scale, especially when the soil respiration rate is being compared to that determined using the eddy covariance technique, which represents the ecosystem scale.

Soil respiration rate was high in the rainy period and low in the dry period. The rainy and dry period cycle is considered to determine seasonal variation in soil respiration rates in tropical regions where seasonal variation in soil temperature is low. On the other hand, spatially, soil respiration rate was low where soil water content was high. In the dry period when soil water content was low in all plots, soil respiration rate was still lower in wetter areas than elsewhere, suggesting that the restriction of gas diffusivity in water-saturated soil is not the primary cause of the low soil respiration rates in wetter places, and that continuous wetness co-varied with several physical, biological and chemical properties and thus reduced soil respiration rate. This paradox of soil respiration rate in relation to soil water content should be considered when assessing the spatio-temporal variability of soil respiration rate to estimate the seasonal variation and annual amount of ecosystem-scale soil respiration.

Acknowledgements

We thank the Forestry Department of Negri Sembilan and the Director General of the Forest Research Institute Malaysia (FRIM) for giving us permission to work in the Pasoh Forest Reserve. We gratefully acknowledge the staffs of the Hydrology Unit and the Pasoh Station of FRIM for helping field observations. Dr. Jyunjiro Negishi helped install the soil moisture sensors, Drs. Minako Adachi and Hiroshi Koizumi provided the information on their results of soil respiration observation, and Dr. Tamon Yamashita provided the information on soil properties. We also thank Drs. Toshinori Okuda, and Naishen Liang and a joint research project between FRIM, University Pertanian Malaysia (UPM) and the National Institute for Environmental Studies (NIES). This study was supported by the Global Environment Research Program granted by the Ministry of the Environment, Japan.

References

Adachi, M., Bekku, Y.S., Konuma, A., Kadir, W.R., Okuda, T., Koizumi, H., 2005. Required sample size for estimating soil respiration rates in large areas of two tropical forests and of two types of plantation in Malaysia. Forest Ecol. Manage. 210, 455–459.

Adachi, M., Bekku, Y.S., Rashidah, W., Okuda, T., Koizumi, H., 2006. Differences in soil respiration between different tropical ecosystems. Appl. Soil Ecol. 34, 258–265.

Anthoni, P.M., Law, B.E., Unsworth, M.H., 1999. Carbon and water vapor exchange of an open-canopied ponderosa pine ecosystem. Agric. For. Meteorol. 95, 151–168.

Baldocchi, D.D., 2003. Assessing the eddy covariance technique for evaluating carbon dioxide exchange rates of ecosystems: past, present and future. Global Change Biol. 9, 479–492.

Bremner, J.M., 1996. N-total. In: Sparks, D.L. (Ed.), Methods of Soil Analysis. Part 3. Soil Sci. Soc. Am., Madison, pp. 1085–1121.

Buchmann, N., 2000. Biotic and abiotic factors controlling soil respiration rates in Picea abies stands. Soil Biol. Biochem. 32, 1625–1635.

Chambers, J.Q., Tribuzy, E.S., Toledo, L.C., Crispim, B.F., Higuchi, N., Santos, J.D., Araújo, A.C., Kruijt, B., Nobre, A.D., Trumbore, S.E., 2004. Respiration from a tropical forest ecosystem: partitioning of sources and low carbon use efficiency. Ecol. Appl. 14, S72–S88.

Davidson, E.A., Belk, E., Boone, R.D., 1998. Soil water content and temperature as independent or confounded factors controlling soil respiration in a temperate mixed hardwood forest. Global Change Biol. 4, 217–227.

Davidson, E.A., Verchot, L.V., Cattânio, J.H., Ackerman, I., Carvalho, J.E.M., 2000. Effects of soil water content on soil respiration in forests and cattle pastures of eastern Amazonia. Biogeochemistry 48, 53–69.

Davidson, E.A., Savage, K., Verchot, L.V., Navarro, R., 2002. Minimizing artifacts and biases in chamber-based measurements of soil respiration. Agric. For. Meteorol. 113, 21–37.

Dong, Y., Scharffe, D., Lobert, J.M., Crutzen, P.J., Sanhueza, E., 1998. Fluxes of CO_2 CH_4 and N_2O from a temperate forest soil: the effects of leaves and humus layers. Tellus 50B, 243–252.

Drewitt, G.B., Black, T.A., Nesic, Z., Humphreys, E.R., Jork, E.M., Swanson, R., Ethier, G.J., Griffis, T., Morgenstern, K., 2002. Measuring forest floor CO_2 fluxes in a Douglas-fir forest. Agric. For. Meteorol. 110, 299–317.

Fang, C., Moncrieff, J.B., Gholz, H.L., Clark, K.L., 1998. Soil CO_2 efflux and its spatial variation in a Florida slash pine plantation. Plant Soil 205, 135–146.

Franklin, R.B., Mills, A.L., 2003. Multi-scale variation in spatial heterogeneity for microbial community structure in an eastern Virginia agricultural field. FEMS Microbiol. Ecol. 44, 335–346.

Goulden, M.L., Munger, J.W., Fan, S.M., Daube, B.C., Wofsy, S.C., 1996. Measurements of carbon sequestration by long-term eddy covariance: methods and a critical evaluation of accuracy. Global Change Biol. 2, 169–182.

Goulden, M.L., Wofsy, S.C., Harden, J.W., Trumbore, S.E., Crill, P.M., Gower, S.T., Fries, T., Daube, B.C., Fan, S.-M., Sutton, D.J., Bazzaz, A., Munger, J.W., 1998. Sensitivity of boreal forest carbon balance to soil thaw. Science 279, 214–217.

Hanson, P.J., Wullschleger, S.D., Bohlman, S.A., Todd, D.E., 1993. Seasonal and topographic patterns of forest floor CO_2 efflux from an upland oak forest. Tree Physiol. 13, 1–15.

Hashimoto, S., Tanaka, N., Suzuki, M., Inoue, A., Takizawa, H., Kosaka, I., Tanaka, K., Tantasirin, C., Tangtham, N., 2004. Soil respiration and soil CO_2 concentration in a tropical forest, Thailand. J. Forest Res. 9, 75–79.

Hirobe, M., Ohte, N., Karasawa, N., Zhang, G.S., Wang, L.H., Yoshikawa, K., 2001. Plant species effect on the spatial patterns of soil properties in the Mu-us desert ecosystem, Inner Mongolia. Chin. Plant Soil 234, 195–205.

IPCC, 2001. Climate Change 2001: The Scientific Basis. Cambridge University Press, Cambridge. 881 pp.

Ishizuka, S., Iswandi, A., Nakajima, Y., Yonemura, S., Sudo, S., Ysuruta, H., Muriyarso, D., 2005. Spatial pattern of green house gas emission in a tropical rainforest in Indonesia. Nutr. Cycling Agroecosyst. 71, 55–62.

Kimball, J.S., Thornton, P.E., White, M.A., Running, S.W., 1997. Simulating forest productivity and surface-atmosphere carbon exchange in the BOREAS study region. Tree Physiol. 17, 589–599.

Kosugi, Y., Tanaka, H., Takanashi, S., Matsuo, N., Ohte, N., Shibata, S., Tani, M., 2005. Three years of carbon and energy fluxes from Japanese evergreen broad-leaved forest. Agric. For. Meteorol. 132, 329–343.

Kramer, K., Leinonen, I., Bartelink, H.H.K., Berbigier, P., Borghetti, M., Bernhofer, Ch., Cienciala, E., Dolman, A.J., Froer, O., Gracia, C.A., Granier, A., Grünwald, T., Hari, P., Jans, W., Kellomäki, S., Loustau, D., Magnani, F., Markkanen, T., Matteucci, G., Mohren, G.M.J., Moors, E., Nissinen, A., Peltola, H., Sabaté, S., Sanchez, A., Sontag, M., Valentini, R., Vesala, T., 2002. Evaluation of six process-based forest growth models using eddy-covariance measurements of CO_2 and H_2O fluxes at six forest sites in Europe. Global Change Biol. 8, 213–230.

La Scale Jr., N., Marques Jr., J., Pereira, G.T., Cora, J.E., 2000. Carbon dioxide emission related to chemical properties of a tropical bare soil. Soil Biol. Biochem. 32, 1469–1473.

Lavigne, M.B., Ryan, M.G., Anderson, D.E., Baldocchi, D.D., Crill, P.M., Fitzjarrald, D.R., Goulden, M.L., Gower, S.T., Massheder, J.M., McCaughey, J.H., Rayment, M., Striegl, R.G., 1997. Comparing nocturnal eddy covariance measurements to estimates of ecosystem respiration made by scaling chamber measurements at six coniferous boreal sites. J. Geophys. Res. 102, 28977–28985.

Law, B.E., Ryan, M.G., Anthoni, P.M., 1999. Seasonal and annual respiration of a ponderosa pine ecosystem. Global Change Biol. 5, 169–182.

Law, B.E., Kelliher, F.M., Baldocchi, D.D., Anthoni, P.M., Irvine, J., Moore, D., Van Tuyl, S., 2001. Spatial and temporal variation in a young ponderosa pine forest during a summer drought. Agric. For. Meteorol. 110, 27–43.

Londo, A.J., Messina, M.G., Schoenholtz, S.H., 1999. Forest harvesting effects on soil temperature, moisture and respiration in a bottomland hardwood forest. Soil Sci. Soc. Am. J. 63, 637–644.

Martin, J.G., Bolstad, P.V., 2005. Annual soil respiration in broadleaf forests of northern Wiscons influence of moisture site biological chemical physical characteristics. Biogeochemistry 73, 149–182.

Mitani, T., Kosugi, Y., Osaka, K., Ohkubo, S., Takanashi, S., Tani, M., 2007. Spatial and temporal variability of soil respiration rate at a small watershed revegetated with Japanese cypress. J. Jpn. Forest Soc. 88, 496–507 (Japanese in English abstract).

Morén, A.S., Lindroth, A., 2000. CO_2 exchange at the floor of a boreal forest. Agric. For. Meteorol. 101, 1–14.

Mori, A., Takeda, H., 2003. Light-related competitive effects of overstory trees on the understory conifer saplings in a subalpine forest. J. Forest Res. 8, 163–168.

Morris, S.J., 1999. Spatial distribution of fungal and bacterial biomass in southern Ohino hardwood forest soils: fine scale variability and microscale patterns. Soil Biol. Biochem. 31, 1375–1386.

Nakayama, F.S., 1990. Soil respiration. Remote Sens. Rev. 5, 311–321.

Niiyama, K., Kassim, A.R., Iida, S., Kimura, K., Azizi, R., Appanah, S., 2003. Regeneration of clear-cut plot in a lowland dipterocarp forest in Pasoh Forest Reserve, Peninsular Malaysia. In: Okuda, T., Manokaran, Y., Matsumoto, Y., Niiyama, K., Thomas, S.C., Ashton, P.S. (Eds.), Pasoh: Ecology of a Lowland Rain Forest in Southeast. Springer-Verlag, Tokyo, Asia, pp. 559–568.

Ohashi, M., Gyokusen, K., Saito, A., 1999. Measurement of carbon dioxide evolution from a Japanese cedar (*Cryptomeria japonica* D. Don) forest floor using an open-flow chamber method. Forest Ecol. Manage. 123, 105–114.

Ohashi, M., Gyokusen, K., 2007. Temporal change in spatial variability of soil respiration on a slope of Japanese cedar (*Cryptomeria japonica* D. Don) forest. Soil Biol. Biochem. 39, 1130–1138.

Ohkubo, S., Kosugi, Y., Takanashi, S., Mitani, T., Tani, M., 2007. Comparison of the eddy covariance and automated closed chamber methods for evaluating nocturnal CO_2 exchange in a Japanese cypress forest. Agric. For. Meteorol. 142, 50–65.

Prasolova, N., Xu, Z.H., Saffigna, P.G., Dieters, M., 2000. Spatial-temporal variability of soil moisture, nitrogen availability indices and other chemical properties in hoop pine (*Araucaria cunninghamii*) plantations of subtropical Australian forest plantations. Forest Ecol. Manage. 136, 1–10.

Qi, Y., Xu, M., 2001. Separating the effects of moisture and temperature on soil CO_2 efflux in a coniferous forest in the Sierra Nevada mountains. Plant Soil 237, 15–23.

Raich, J.W., Schlesinger, W.H., 1992. The global carbon dioxide flux in soil respiration and its relationship to vegetation and climate. Tellus 44B, 81–99.

Rasse, D.P., 2002. Nitrogen deposition and atmospheric CO_2 interactions on fine root dynamics in temperate forests: a theoretical model analysis. Global Change Biol. 8, 486–503.

Rayment, M.B., Jarvis, P.G., 2000. Temporal and spatial variation of soil CO_2 efflux in a Canadian boreal forest. Soil Biol. Biochem. 32, 35–45.

Reichstein, M., Tenhunen, J.D., Roupsard, O., Ourcival, J.M., Rambal, S., Dore, S., Valentini, R., 2002. Ecosystem respiration in two Mediterranean evergreen Holm Oak forests: drought effects and decomposition dynamics. Funct. Ecol. 16, 27–39.

Rey, A., Pegoraro, E., Tedeschi, V., De Parri, I., Jarvis, P.G., Valentini, R., 2002. Annual variation in soil respiration and its components in a coppice oak forests in Central Italy. Global Change Biol. 8, 851–866.

Robertson, G.P., 1987. Geostatistics in ecology: interpolating with known variance. Ecology 68, 744–748.

Robertson, G.P., Huston, M.A., Evans, F.C., 1988. Spatial variability in a successional plant community: patterns of nitrogen availability. Ecology 69, 1517–1524.

Robertson, G.P., Freckman, D.W., 1995. The spatial distribution of nematode trophic groups across a cultivated ecosystem. Ecology 76, 1425–1432.

Robertson, G.P., 1998. GS+: Geostatistics for the Environmental Sciences. Gamma Design Software, Plainwell, MI, USA, 152 pp.

Savin, M.C., Görres, J.H., Neher, D.A., Amador, J.A., 2001. Biogeophysical factors influencing soil respiration and mineral nitrogen content in an old field soil. Soil Biol. Biochem. 33, 429–438.

Schmid, H.P., 1997. Experimental design for flux measurements: matching scales of observations and fluxes. Agric. For. Meteorol. 87, 179–200.

Schmid, H.P., Lloyd, C.R., 1999. Location bias of flux measurements over inhomogeneous areas. Agric. For. Meteorol. 93, 195–209.

Schwendenmann, L., Veldkamp, E., Brenes, T., O'brien, J., Mackensen, J., 2003. Spatial and temporal variation in soil CO_2 efflux in an old-growth neotropical rain forest, La Salva Costa Rica. Biogeochemistry 64, 111–128.

Scott-Denton, L.E., Kimberlee, L.S., Monson, R.K., 2003. Spatial and temporal controls of soil respiration rate in a high-elevation, subalpine forest. Soil Biol. Biochem. 35, 525–534.

Soepadmo, E., 1978. Introduction to the Malaysian I. B. P. Synthesis Meetings. The Malayan Nat. J. 30, 119–124.

Sotta, E.D., Meir, P., Malhi, Y., Nobre, A.D., Hodnett, M., Grace, J., 2004. Soil CO_2 efflux in a tropical forest in the central Amazon. Global Change Biol. 10, 601–617.

Sotta, E.D., Valdkamp, E., Guimarães, B.R., Paixão, R.K., Ruivo, M.L.P., Almeida, S.S., 2006. Landscape and climatic controls on spatial and temporal variation in soil CO_2 efflux in an Eastern Amazonian Rainforest, Caxiuanã Brazil. Forest Ecol. Manage. 237, 57–64.

Stenger, R., Priesack, E., Beese, F., 2002. Spatial variation of nitrate-N and related soil properties at the plot scale. Geoderma 105, 259–275.

Stoyan, H., De-Polli, H., Böhm, S., Robertson, G.P., Paul, E.A., 2000. Spatial heterogeneity of soil respiration and related properties at the plant scale. Plant Soil 222, 203–214.

Takanashi, S., Kosugi, Y., Tani, M., Matsuo, N., Mitani, T., Rahim Nik, A., 2005. Characteristics of the gas exchange of a tropical rain forest in Peninsular Malaysia. Phyton 45, 61–66.

Tani, M., Rahim Nik, A., Ohtani, Y., Yasuda, Y., Mohd Md, S., Baharuddin, K., Takanashi, S., Noguchi, S., Zulkifli, Y., Watanabe, T., 2003. Characteristics of energy exchange and surface conductance of tropical rain forest in Peninsular Malaysia. In: Okuda, T., Manokaran, Y., Matsumoto, Y., Niiyama, K., Thomas, S.C., Ashton, P.S., Pasoh:, (Eds.), Ecology of a Lowland Rain Forest in Southeast. Springer-Verlag, Tokyo, Asia, pp. 73–88.

Xu, M., Qi, Y., 2001. Soil-surface CO_2 efflux and its spatial and temporal variations in a young ponderosa pine plantation in northern California. Global Change Biol. 7, 667–677.

Yamashita, T., Kasuya, N., Wan Rasidah, K., Suhaimi Wan, C., Quah Eng, S., Okuda, T., 2003. Soil and belowground characteristics of Pasoh Forest Reserve. In: Okuda, T., Manokaran, Y., Matsumoto, Y., Niiyama, K., Thomas, S.C., Ashton, P.S., Pasoh, (Eds.), Ecology of a Lowland Rain Forest in Southeast. Springer-Verlag, Tokyo, Asia, pp. 89–109.

Yasuda, Y., Ohtani, Y., Watanabe, T., Okano, M., Yokota, T., Liang, N., Tang, Y., Rahim Nik, A., Tani, M., Okuda, T., 2003. Measurement of CO_2 flux above a tropical rain forest at Pasoh in Peninsular Malaysia. Agric. For. Meteorol. 114, 235–244.

TROPICS Vol. 17 (1) Issued November 30, 2007

Emission of nitrous oxide from tropical forest and plantation soils in Peninsular Malaysia

Yuichiro YASHIRO[1], Wan Rashidah KADIR[2], Minako ADACHI[3], Toshinori OKUDA[4] and Hiroshi KOIZUMI[1]

[1] River Basin Research Center, Gifu University, Gifu 501–1193, Japan
[2] Forest Research Institute Malaysia, Kepong 52109, Kuala Lumpur, Malaysia
[3] National Institute for Agro-Environmental Science, Department of Global Resources, 3–1–3 Kannondai, Tsukuba 305–8604, Japan
[4] Graduate School of Integrated Arts and Sciences, Hiroshima University, 1–7–1 Higashi-Hiroshima 739–8521, Japan
* Corresponding author: Yuichiro Yashiro, River Basin Research Center, Gifu University, Yanagido 1–1, Gifu 501–1193, Japan
Tel.: +81–58–293–2077, Fax: +81–58–293–2062, E–mail: yashiro@green.gifu–u.ac.jp

ABSTRACT We measured the flux of nitrous oxide (N_2O) in three different land uses (primary forest, oil palm plantation, and rubber plantation) in Peninsular Malaysia. The N_2O emission rate in the primary forest was higher than those in the plantations throughout the experimental period. This result suggests that primary forest soil is a greater source of N_2O than that of oil palm and rubber plantations. The rate of N_2O emission in the primary forest showed a clear variation during the experimental period, with higher values from wet soils and lower values from dry soils, whereas N_2O emission rates in the plantations showed little variation. The proportions of soil surface carbon and nitrogen in primary forest were three times those in the plantations. The difference in soil carbon and nitrogen contents between the primary forest and plantations may have affected the rates of N_2O emission from the soils.

Key words: N_2O emission, primary forest, oil palm plantation, rubber plantation, Southeast Asia

INTRODUCTION

The atmospheric concentration of nitrous oxide (N_2O) has increased by about 27 ppbv (9.4%) over the last century (Khalil et al. 2002). As a greenhouse gas, atmospheric N_2O has important impacts on the global environment because the global warming potential of N_2O is 340 times that of carbon dioxide when calculated for a time horizon of 100 yr (Jain et al. 2000). Atmospheric N_2O also contributes to the depletion of stratospheric ozone (Beauchamp, 1997), which absorbs harmful UV-B radiation. Therefore, it is important to accurately estimate the global N_2O budget, about which large uncertainties still remain despite considerable research.

Soils of tropical forests contribute a significant fraction of the total atmospheric N_2O (Keller, 1986; Bouwman, 1990). The N_2O emissions from humid tropical forest soils have been reported to account for approximately 10–40% of all global sources of atmospheric N_2O (Matson & Vitousek, 1990; Davidson, 1991; Prather et al. 1995), and studies of N_2O emission have long focused on tropical areas. During the last few decades, however, large areas of tropical forest have been logged and converted into agricultural lands or plantations (Myers, 1991).

Studies of N_2O emission from soils concluded that this land-use change in the tropics has the potential to affect the global budget of N_2O. In the Atlantic lowlands of Costa Rica, Keller et al. (1993) found that N_2O emissions following the conversion of forest to pasture were elevated for approximately 10 yr and then declined. This pattern in N_2O emissions was caused by a combination of rapid decomposition of soil organic matter following deforestation (Keller et al. 1993; Veldkamp, 1994) and the high soil water content in pastures, which is related to compaction of the topsoil (Keller et al. 1993). Matson and Vitousek (1990) estimated that the conversion of tropical forest to pasture would lead to a global N_2O source of approximately 0.7 Tg N yr^{-1}. As such, land-use change may have a strong effect on the global N_2O budget.

The field sites of most previous reports on N_2O emissions were distributed in the Amazon basin and Costa Rica, and there is a lack of data for N_2O emissions in other tropical areas. In particular, little work on N_2O emission has been carried out in Southeast Asia, which is one of the largest tropical regions in the world and an area that has experienced significant conversion of forests to agricultural fields during the last three decades. For example, the area of agricultural fields in Malaysia increased from 4,808,000 ha in 1979–1981 to 7,585,000 ha in 2002 (FAO, 2005) because of the conversion of original forests to plantations. To accurately estimate the N_2O budget in tropical areas, it is important to measure and analyze N_2O fluxes in both tropical primary forests and agricultural lands that were converted from forests.

The aims of the present study were to evaluate N_2O fluxes in a primary forest, an oil palm plantation, and a rubber plantation in Peninsular Malaysia to better understand the effects of land-use change on N_2O emission in tropical Asia. This comparative study will provide insight into local and global variations in tropical N_2O fluxes.

MATERIALS AND METHODS

Site description

We performed the investigation in three different land uses: primary forest in the Pasoh Forest Reserve (2°58–59'N, 102°16–20'E), about 70 km southeast of Kuala Lumpur, Malaysia, and an oil palm plantation and a rubber plantation near the reserve. The Pasoh Forest Reserve is a 2450–ha lowland tropical rain forest. The average annual minimum and maximum temperatures are 22.7 and 33.2 °C, and the annual rainfall is about 1800 mm, with a peak in April-May and one in November-December. In 1998 the Pasoh Forest Reserve had 403.2 Mg total aboveground biomass ha^{-1} (Hoshizaki et al. 2004). The forest is dominated by *Shorea* spp. and *Dipterocarpus* spp. The study site in primary forest has an Oxisol soil, classified as a Petroplinthic Haplorthox (Yamashita et al. 2003). The oil palm plantation was converted from primary forest and planted with oil palms (*Elaeis guineensis*) in 1975; about 22–27 kg ha^{-1} of nitrogen has been supplied every year as fertilizer (10% N, 1000–1200 kg for 4.5 ha). The rubber plantation was converted from secondary forest and planted with rubber trees (*Hevea brasiliensis*) in 1994; about 9 kg ha^{-1} of nitrogen has been supplied every year as fertilizer (9 % N, 400 kg for 4 ha).

Since the 1970s, a large area of tropical rain forest around our study site, the Pasoh Forest Reserve, has been converted to agricultural uses, mainly oil palm and rubber plantations. Between 1971 and 1996, the proportion of primary forest around the reserve changed from 65.6% to 29.4%, that of oil palm plantations from 4.5% to 18.9%, and that of rubber plantations from 22.7% to 31.0% (Okuda et al. 2003). The area of primary forest continues to decrease and those of oil palm and rubber plantations to increase.

In June 2003, we established a 10–m by 10–m quadrat in the primary forest, oil palm plantation, and rubber plantation, respectively. The primary forest is 5 km from the plantations, and both plantations are located within a square of 1 km^2.

Sampling design

Nine flux chambers (described below) were placed in a grid pattern in each quadrat, and N_2O fluxes were measured twice (within 10 days) per month in June 2003, December 2003, June 2004, and November 2004. Because the variations of soil temperature and moisture conditions between the two monthly samples were much less than the seasonal variations (within 0.8 °C for mean soil temperature, within 6.6 % WFPS for mean soil moisture), we summed the data for the two monthly sampling times and present the average as the N_2O efflux in each sampling month ($N = 18$). At the same time as the flux measurement, soil temperature (5–cm depth) and soil moisture (0– to 5–cm depth) were measured near each chamber. All measurements were performed from 09:00 to 16:00 local time.

Soil moisture

Soil moisture was measured with time-domain reflectometry probes (TRIME-FM, IMKO, Ettlingen, Germany) inserted vertically into the soil surface (5–cm depth) to measure the dielectric constant of the soil. The dielectric constant was then converted to the percent water-filled pore space (%WFPS) based on the soil porosity at each chamber. The soil porosities were measured using a pycnometer (DIK–1121, Daiki, Saitama, Japan).

N_2O flux from the soil surface

The closed-chamber method (Bekku et al. 1995) was used to directly determine N_2O flux in situ. A closed chamber was placed over the soil surface and the increase in N_2O concentration within the chamber was measured as a function of time.

A PVC cylinder (15–cm height, 21–cm internal diameter) was placed upright on the soil the day before the flux measurement. On the measurement day, a PVC lid was fitted to the cylinder top. A rubber-capped needle was fitted onto an air sample port on the top of the lid. Air in the chamber was aspirated through the needle into an evacuated vial (5 ml) four times (at 0.5, 10, 20, 30 min), and vials were brought to the lab to measure N_2O concentrations.

The concentrations of N_2O in the air samples were quantified by a gas chromatograph (GC-14B, Shimadzu, Kyoto, Japan) equipped with a ^{63}Ni electron capture detector. From each vial, 2 ml of air was withdrawn into a gas-tight syringe. The withdrawn air was injected into the gas chamber and purged with pure N_2 gas at a flow rate of 40 ml min^{-1}.

The N_2O concentration in each closed chamber increased or decreased linearly with time. The N_2O flux was calculated as the rate of the linear change in N_2O concentration; data showing an unclear linear change in N_2O concentration ($R^2 < 0.7$) were excluded.

General soil properties

For determination of the general soil properties, 10 soil samples were taken in 100–ml stainless steel rings at 5–cm depth at each quadrat. The soil samples were gathered in September 2001 for primary forest and in June 2003 for oil palm and rubber plantations. The soils were sieved (2–mm mesh) for measurement of pH and total carbon and nitrogen. The pH (H_2O) of fresh soil was measured in a 1:2 (w/w) soil:water mixture using a portable pH meter (DKK HM-20P, Toa, Tokyo, Japan). Total soil carbon and nitrogen at 0– to 5–cm depths were measured in air-dried soil using an NC analyzer (C-R6A, Shimadzu, Kyoto, Japan). To measure soil bulk densities, samples were dried in an oven for more than 24 h at 105 °C and the dry weight was measured to represent soil bulk density.

Statistical analyses

All statistical analyses were performed using the StatView 5.0 software (SAS Institute, Cary, NC, USA). ANOVA (Kruskall-Wallis test) and the Games-Howell test (a *post hoc* test) were used to analyze the significance ($P < 0.05$) of differences in mean N_2O flux values and environmental factors between primary forest, oil palm plantation, and rubber plantation.

RESULTS

Table 1 lists the general soil properties in each land use. All soils were acidic, with the primary forest soil being the most acidic. The soil surface carbon and nitrogen concentrations in the primary forest were about three times those in the plantations. The soil bulk density was

Table 1. The general soil properties (0–5 cm) in each land use.

	pH (H_2O)	Total C mg C g soil^{-1}	Total N mg N g soil^{-1}	C/N	Bulk Density g cm^{-3}
Primary forest	3.8 ± 0.1	31.7 ± 10.9	2.2 ± 0.6	14.4 ± 1.2	0.74 ± 0.06
Oil Palm	5.0 ± 0.3	9.4 ± 2.2	0.7 ± 0.1	13.9 ± 0.9	1.06 ± 0.08
Rubber	5.4 ± 0.3	7.7 ± 2.2	0.7 ± 0.1	11.1 ± 0.7	1.24 ± 0.08

Values are mean ± standard deviation. $N = 10$.

Table 2. The N_2O emission rate and environmental factors in each land use

	Jun. 2003	Dec. 2003	Jun. 2004	Nov. 2004
N_2O flux (μg N m^{-2} h^{-1})				
Primary Forest	9.8 ± 9.8 (18) a	100.3 ± 55.7 (18) a	8.7 ± 8.3 (17) a	153.1 ± 86.5 (18) a
Oil Palm	–0.9 ± 5.0 (16) b	–0.9 ± 10.5 (17) b	–0.1 ± 6.5 (17) b	1.6 ± 4.0 (17) b
Rubber	5.5 ± 6.9 (16) a	6.7 ± 5.7 (17) c	7.1 ± 6.0 (17) a	12.0 ± 11.0 (16) c
Soil temperature (℃)				
Primary Forest	25.6 ± 0.3 (18) a	24.4 ± 0.2 (18) a	25.0 ± 0.2 (18) a	24.8 ± 0.2 (18) a
Oil Palm	26.7 ± 0.4 (18) b	25.7 ± 0.2 (18) b	26.0 ± 0.4 (18) b	26.1 ± 0.5 (18) ab
Rubber	25.6 ± 0.2 (18) a	24.6 ± 0.1 (18) c	26.1 ± 0.3 (18) b	27.2 ± 0.5 (18) b
Soil moisture (%WFPS)				
Primary Forest	38.7 ± 3.6 (18) a	52.7 ± 5.2 (18) a	40.3 ± 3.2 (18) a	67.0 ± 6.4 (17) a
Oil Palm	51.5 ± 2.4 (18) b	53.5 ± 1.8 (18) a	33.4 ± 2.7 (18) b	61.1 ± 5.6 (18) b
Rubber	51.6 ± 2.0 (18) b	54.0 ± 2.6 (18) a	45.0 ± 4.8 (18) c	60.5 ± 5.3 (18) b

Values are mean ± standard deviation. The numbers of observations are given in parentheses.
Different letters indicate significant differences among the land uses in the mean N_2O flux value and environmental factors according to a Games-Howell test ($P < 0.05$). The soil temperatures and moistures were measured at 5–cm depth and 0– to 5–cm depth, respectively.

lower in the primary forest than in the plantations.

The N_2O emission rates and environmental factors (soil temperature and soil moisture) in each land use over the course of the experimental period are listed in Table 2. Significant differences in the N_2O emission rates among the three land uses were noted in December 2003 and November 2004 ($P < 0.05$). The N_2O emission rate in primary forest was higher than those in the plantations throughout the experimental period, especially in December 2003 and November 2004, and the rubber plantation had the second highest efflux. The oil palm plantation had a slightly negative N_2O efflux, except in November 2004. The N_2O emission rate in primary forest showed clear variation during the experimental period, with higher values in December 2003 and November 2004 and lower values in June 2003 and June 2004. The oil palm and rubber plantations had a relatively large N_2O flux only in November 2004. The soil temperature (5–cm depth) in all land uses changed only slightly during the experimental period, whereas the %WFPS in each land use changed clearly over time (Table 2). N_2O emissions from the forest soil were correlated with %WFPS, whereas those from the plantations were not (Fig. 1).

DISCUSSION

During the experimental period, the mean N_2O flux in the primary forest ranged from 8.7 to 153.1 μg N m^{-2} h^{-1}, and wet soils in the forest emitted a larger amount of N_2O than dry soils (Table 2). The N_2O emission rate in wet forest soil is the highest among values reported for humid tropical forest soils, which range from −4.2 to 207.0 μg N m^{-2} h^{-1} (Breuer et al. 2000; Kises and Butterbach-Bahl, 2002; Ishizuka et al. 2005). Ishizuka et al. (2002, 2005) reported that the N_2O effluxes in tropical humid forests in Sumatra, Indonesia, were relatively low (range, 1.5 to 9.3 μg N m^{-2} h^{-1}). These values in Sumatra were equal to the N_2O flux from dry forest soils in the present study, but were much lower than that from wet forest soils.

The rates of N_2O emission in the primary forest were larger than those in the oil palm and rubber plantations throughout the experimental period (Table 2). The results suggest that primary forest is a greater source of N_2O than oil palm and rubber plantations. In the case of pasture converted from tropical forest in the central Amazon basin, Luizao et al. (1989) estimated that a 3-yr-old pasture emitted three times the amount of N_2O over a year compared to forest soils. Keller et al. (1993) also reported that N_2O fluxes from pasture in Costa

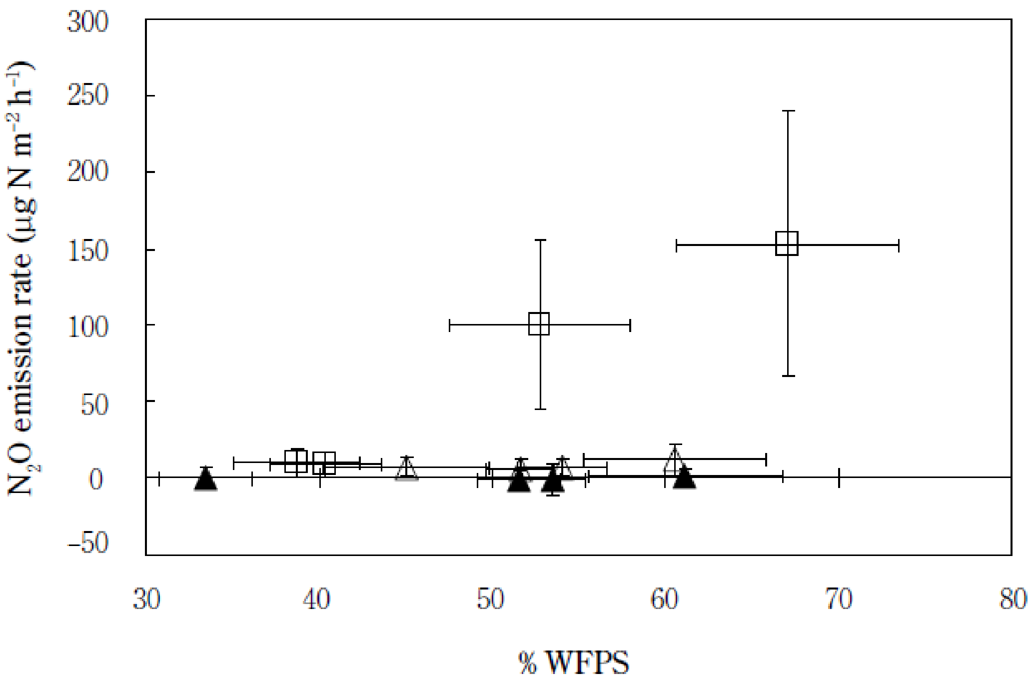

Fig. 1. The relationship between N_2O flux and percent water-filled pore space (%WFPS) in each land use. Symbols indicate the mean N_2O flux in each quadrat (open square, primary forest; closed triangle, oil palm plantation; open triangle, rubber plantation). Bars indicate standard deviation. N = 16–18.

Rica peaked during the first 10 yr after conversion, but declined thereafter to values that were lower than the original forest fluxes. These results suggest that the effect of land-use change on N_2O emission differs according to pasture age and that mature pasture emits less N_2O than forest. At the time of our study, the oil palm and rubber plantations had been in place for 28 and 9 yr, respectively. Thus, the N_2O emission rates in these plantations may have been decreasing from the peak after conversion.

Ishizuka et al. (2002) found that a primary forest emitted more N_2O than a rubber plantation in Sumatra. In another study in Indonesia, Ishizuka et al. (2005) reported that the average N_2O fluxes at a rubber plantation older than 10 yr and an oil palm plantation less than 10 yr old were 11.5 and 11.8 μg N m^{-2} h^{-1}, respectively, which were similar to the N_2O flux of a forest stand (8.6 μg N m^{-2} h^{-1}). In the present study, the N_2O emission rates in the plantations were equal to or much lower than those in the primary forest soils. Our results also suggest that primary forest soil, especially wet forest soil, has the potential to be a greater N_2O source than plantation soil after the initial 10 yr or so since plantation establishment.

N_2O emissions from the forest soil varied over time and were correlated with soil moisture (Fig. 1). The variation in N_2O emissions from the forest soil was explained by variations in %WFPS. In the forest, the soil temperature (5–cm depth) changed only slightly during the experimental period (from 24 to 26 °C) and therefore did not strongly affect N_2O emissions. Verchot et al. (1999) also found a strong log-linear relationship between N_2O and %WFPS in primary and secondary forests in eastern Amazonia, but they found a weak relationship in active pastures and none in degraded pastures. These results suggest that the importance of soil moisture to N_2O emission differs among ecosystems and that other factors limit N_2O emission rates in plantation ecosystems.

In the present study, the soil surface carbon and nitrogen concentrations in primary forest were about three times those in the plantations (Table 1), and this difference may be due to the conversion to plantation. Deforestation and conversion of forest to plantation increases soil temperature and promotes decomposition in the soil. According to Veldkamp (1994), after conversion from forest to pasture, soil organic carbon rapidly decreased and stabilized after about 5 yr in the Atlantic Zone of Costa Rica mainly because of decomposing litter and roots. Keller et al. (1993) suggested that the N_2O flux from pasture peaks during the first 10 yr after conversion but declines thereafter because forest-derived organic matter decomposes rapidly during the first decade. The oil palm and rubber plantations in the present study were 28 and 9 yr old, respectively. Therefore, the forest-derived organic matter in these plantations had already nearly disappeared, which may have resulted in the decrease of soil nutrients for N_2O production in the plantations.

Microbial nitrification and denitrification dominate N_2O production in soils (Matson and Vitousek, 1990; Bouwman et al. 1993). The low carbon and nitrogen content in the plantations suggests low organic matter content, which may have restricted nitrification and resulted in the low NO_3^- pool in the plantations. Denitification can release N_2O in low quantities with insufficient NO_3^- and metabolizable organic carbon even if low-oxygen environments, which promote denitrification. Therefore, low organic matter contents in the oil palm and rubber plantations likely restricted microbial nitrification and denitrification and contributed to the reduction of N_2O emissions.

Soil pH and compaction can affect N_2O emission because these factors also can affect nitrification and denitrification rates. Low soil pH ($pH < 4.0$) markedly inhibits nitrification and denitrification activity (Simek et al. 2002; Sierra, 2006). In the present study, the low soil pH in primary forest compared with that in the plantations would be unfavorable for N_2O production. The plantation soils emitted little N_2O, however, suggesting that soil pH does not strongly restrict N_2O emission in these ecosystems. Several studies reported that soil compaction promotes N_2O emission rates from soils (Sitaula et al. 2000; Keller et al. 2005) due to higher denitrification activity under anaerobic conditions. In the present study, however, the soil in the primary forest was in an aerated condition compared with the compacted soils of the plantations, and aeration favors nitrification rather than denitrification. Therefore, the differences in soil compaction among the land uses also did not directly affect N_2O emission.

According to Linn and Doran (1984) the optimum soil moisture content for nitrification is about 60 %WFPS, and nitrification rates are decreased as aeration is reduced above this value. In contrast, denitrification activity begins above 60 %WFPS and approaches the maximum level in saturated soil. In the primary forest of the present study, soil moisture from 52.7 to 67.0 %WFPS can favor nitrification and result in high N_2O emission rates, whereas values from 38.7 to 40.3 %WFPS can restrict nitrification and led to low N_2O emission rates. Therefore, the high %WFPS in primary forest might have promoted nitrification, which resulted in high N_2O emission in this land use. In contrast, the N_2O emissions in the plantations were consistently low even when the %WFPS values were sufficient for nitrification activity. The reason might be low nutrient content in the plantation soil.

This study had several limitations. First, our findings are based on only one example of each land use. In addition, fertilizer management varies with landowner, so our results may not be directly applicable to other plantations in the region. Because we collected our data only twice per year, we might have missed any effects of the fertilizer supply in the plantations. For example, the effect of nitrogen fertilizer on N_2O emission in the tropics was studied for only 20 days (Veldkamp et al. 1998). Based on this preliminary case study of three land uses in Peninsular Malaysia, primary tropical forest has the potential to be a greater source of N_2O than oil palm and rubber plantations in this region. More accurate and frequent N_2O flux measurements in plantations will help us to better understand the effect of land-use change on N_2O emission in tropical Southeast Asia.

ACKNOWLEDGMENTS We thank Dr. Hideshige Toda, Shinshu University, for his help and advice in this study. We also thank E.S. Quah, S.M. Wang, and other staff members of Forest Research Institute Malaysia in the Pasoh Forest Reserve for assistance during the field investigations. The present study is part of a joint research project undertaken by the Forest Research Institute Malaysia, Universiti Putra Malaysia, and the National Institute for Environmental Studies of Japan (Global Environment Research Program supported by the Ministry of the Environment, Japan).

REFERENCES

Beauchamp, E.G. 1997. Nitrous oxide emission from agricultural soils. *Canadian Journal of Soil Science*, **77:** 113–123.

Bekku, Y., Koizumi, H., Nakadai, T. & Iwaki, H. 1995. Measurement of soil respiration using closed chamber method: an IRGA technique. *Ecological Research*, **10:** 369–373.

Bouwman, A.F. ed. 1990. Exchange of greenhouse gases between terrestrial ecosystems and the atmosphere. In: *Soils and the Greenhouse Effect*, pp. 61–127. John Wiley and Sons, New York.

Bouwman, A.F., Fung, I., Matthews, E. & John, J. 1993. Global analysis of the potential for N_2O production in natural soils. *Global Biogeochemical Cycles*, **7:** 557–597.

Breuer, L., Papen, H. & Butterbach–Bahl, K. 2000. N_2O emission from tropical forest soils of Australia. *Journal of Geophysical Research*, **105:** 26353–26367.

Davidson, E.A.1991. Fluxes of nitrous oxide and nitric oxide from terrestrial ecosystems. In: *Microbial Production and Consumption of Greenhouse Gases: Methane, Nitrogen Oxide and Halomethanes* (eds. Rogers J.E. and Whitman W.B.), pp. 219–235. American Society for Microbiology, Washington DC.

FAO. 2005. Food and agriculture indicators, Country: Malaysia. http://www.fao.org/es/ess/compendium_2005/pdf/ESS_MAL.pdf

Hoshizaki, K., Niiyama, K., Kimura, K., Yamashita, T., Bekku, Y., Okuda, T., Quah, E.S. & Nur Supardi, M.N. 2004. Temporal and spatial variation of forest biomass in relation to stand dynamics in a mature, lowland tropical rainforest, Malaysia. *Ecological Research*, **19:** 357–363.

Ishizuka, S., Tsuruta, H. & Murdiyarso, D. 2002. An intensive field study on CO_2, CH_4, and N_2O emissions from soils at four land–use types in Sumatra, Indonesia. *Global Biogeochemical Cycles*, **16:** 1049; doi:10.1029/2001GB001614.

Ishizuka, S., Iswandi, A., Nakajima, Y., Yonemura, S., Sudo, S., Tsuruta, H & Murdiyarso, D. 2005. The variation of greenhouse gas emissions from soils of various land use/cover types in Jambi province, Indonesia. *Nutrient Cycling in Agroecosystems*, **71:** 17–32.

Jain, A.K., Briegleb, B.P., Minschwaner, K. & Wuebbles, D.J. 2000. Radiative forcing and global potentials of 39 greenhouse gases. *Journal of Geophysical Research D*, **16:** 20773–20790.

Keller, M. 1986. Emission of N_2O, CH_4 and CO_2 from tropical forest soils. *Journal of Geophysical Research*, **91:** 11791–11802.

Keller, M., Veldkamp, E., Weitz, A.M. & Reiners W.A. 1993. Effect of pasture age on soil trace-gas emissions from a deforested area of Costa Rica. *Nature*, **365:** 244–246.

Keller, M., Varner, R., Dias, J.D., Silva, H., Crill, P., de Oliveria Jr., R.C. & Asner, G.P. 2005. Soil-atmosphere exchange of nitrous oxide, nitric oxide, methane, and carbon dioxide in logged and undisturbed forest in the Tapajos National Forest, Brazil. *Earth Interactions*, **9:** 1–28.

Khalil, M.A.K., Rasmussen, R.A. & Shearer, M.J. 2002. Atmospheric nitrous oxide: patterns of global change during recent decades and centuries. *Chemosphere*, **47:** 807–821.

Kises, R. & Butterbach-Bahl, K. 2002. N_2O and CO_2

emissions from three different tropical forest sites in the wet tropics of Queensland, Australia. *Soil Biology and Biochemistry*, **34:** 975–987.

Linn, D.M. & Doran, J.W. 1984. Effect of water-filled pore space on carbon dioxide and nitrous oxide production in tilled and non-tilled soils. *Journal of the Soil Science Society of America*, **48:** 1267–1272.

Luizao, F., Matson, P., Livingston, G., Luizao, R. & Vitousek, P. 1989. Nitrous oxide flux following tropical land clearing. *Global Biogeochemical Cycles*, **3:** 281–285.

Matson, P.A. & Vitousek, P.M. 1990. Ecosystem approach to a global nitrous oxide budget. *Bioscience*, **40:** 672 –677.

Myers, N. 1991. Tropical forests: present status and future outlook. *Climatic Change*, **19:** 3–32.

Okuda, T., Suzuki, M., Adachi, N., Yoshida, K., Niiyama, K., Nur Supardi, M. N., Nor Azman, H., Manokaran, N. & Hashim, M., eds. 2003. Logging history and its impact on forest structure and species composition in the Pasoh Forest Reserve: implication for the sustainable management of natural resources and landscapes. In: *Pasoh: Ecology of a Lowland Rain Forest in Southeast Asia*, 15–34. Springer, Tokyo.

Prather, M., Derwent, R., Ehhalt, D., Fraser, P., Sanhuneza, E. & Zhou, X. 1995. Other trace gases and atmospheric chemistry. In: *Climate change 1994* (eds. Houghton, J.T., Meira Filho, L.G. & Callander, B.), pp. 74–126. Cambridge University Press, New York.

Sierra, J. 2006. A hot spot approach applied to nitrification in tropical acid soils. *Soil Biology & Biochemistry*, **38:** 644–652.

Simek, M., Jísová, L. & Hopkins, D.W. 2002. What is so-called optimum pH for denitrification in soil? *Soil Biology & Biochemistry*, **34:** 1227–1234.

Sitaula, B.K., Hansen, S., Sitaula, J.I.B. & Bakken, L.R. 2000. Effects of soil compaction on N_2O emission in agricultural soil. *Chemosphere: Global Change Science*, **2:** 367–371.

Veldkamp, E. 1994. Organic carbon turnover in three tropical soils under pasture after A., Harris, N., Kattenberg, A. & Maskell, K., eds. Climate Change 1994, 73–126. deforestation. *Journal of the Soil Science Society of America*, **58:** 175–180.

Veldkamp, E., Keller, M. & Nunez, M. 1998. Effects of pasture management on N_2O and NO emissions from soils in the humid tropics of Costa Rica. *Global Biogeochemical Cycles*, **12:** 71–79.

Verchot, L.V., Davidson, E.A., Cattanio, J.H., Ackerman, I.L., Erickson, H.E. & Keller, M. 1999. Land use change and biogeochemical controls of nitrogen oxide emissions from soils in eastern Amazonia. *Global Biogeochemical Cycles*, **10:** 31–46.

Yamashita, T., Kasuya, N., Wan Rasidah, K., Suhaimi, W.C., Quah, E.S. & Okuda, T., eds. 2003. Soil and belowground characteristics of Pasoh Forest Reserve. In: *Pasoh: Ecology of a Lowland Rain Forest in Southeast Asia*, pp. 89–109. Springer, Tokyo.

Received 31st Jan. 2007
Accepted 29th May 2007

AGRICULTURAL AND FOREST METEOROLOGY 148 (2008) 799–806

available at www.sciencedirect.com

journal homepage: www.elsevier.com/locate/agrformet

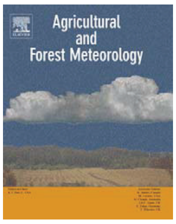

The effects of logging on soil greenhouse gas (CO_2, CH_4, N_2O) flux in a tropical rain forest, Peninsular Malaysia

Yuichiro Yashiro[a,*], *Wan Rashidah Kadir*[b], *Toshinori Okuda*[c], *Hiroshi Koizumi*[a]

[a] *River Basin Research Center, Gifu University, Yanagido 1-1, Gifu, Gifu 501-1193, Japan*
[b] *Forest Research Institute Malaysia, Kepong, 52109 Kuala Lumpur, Malaysia*
[c] *Graduate School of Integrated Arts and Sciences, Hiroshima University, 1-7-1 Higashi-Hiroshima 739-8521, Japan*

ARTICLE INFO

Article history:
Received 30 April 2007
Received in revised form
10 January 2008
Accepted 17 January 2008

Keywords:
Greenhouse gases
Carbon dioxide
Methane
Nitrous oxide
Tropical rain forest
Logging

ABSTRACT

To evaluate the effects of logging on soil greenhouse gas flux in a tropical rain forest, we measured CO_2, CH_4, and N_2O fluxes at logged and unlogged sites in Peninsular Malaysia ($N = 7–27$ at each site). Although soil temperature at the logged sites was higher than at unlogged sites, soil CO_2 flux did not differ between sites. The CH_4 consumption at the logged sites tended to be less than that at unlogged sites, and some soils at the logged sites emitted CH_4. These results suggest that logging can decrease CH_4 consumption or even convert CH_4 sinks into sources. The increase in soil bulk density after logging might lowered the effective diffusivity of CH_4 and O_2 availability in soils, which might limit the CH_4 consumption at the logged sites. N_2O fluxes were increased significantly for at least 1 year after logging because of an increase in soil nitrogen availability. Logging decreased the CH_4 absorption rate and increased the N_2O emission rate of the soil. Based on these findings, we conclude that logging in tropical rain forests increases the emission of CH_4 and N_2O for at least 1 year after logging, thus potentially contributing to global warming.

1. Introduction

Quantifying soil carbon dioxide (CO_2) flux is critical to understand the overall response of global carbon cycle to human perturbation. It is also essential to understand the effects of land-use change on the rate of increase in radiative forcing of the climate system (i.e., the greenhouse gas effect), particularly because CO_2 accounts for most of the anthropogenically driven increase in radiative forcing. Schimel et al. (1996) reported that estimated anthropogenic contributions to the global carbon cycle commonly include a major net flux to the atmosphere resulting from land-use change in the tropics (ca. 1.6 Gt C year^{-1}) as well as fossil fuel combustion and cement production (ca. 5.5 Gt C year^{-1}). Moreover, methane (CH_4) and nitrous oxide (N_2O) are also important greenhouse gases whose concentrations in the atmosphere have increased due to human activities. Although the atmospheric CH_4 concentration (1.8 ppmv) is much less than that of CO_2 (370 ppmv), CH_4 is 23 times more effective per molecule as a greenhouse gas than is CO_2 in a period of 100 years (Ramaswamy et al., 2001). The CH_4 increase accounts for 20% of the increased greenhouse warming potential of the atmosphere. Likewise, N_2O is a long half-life gas in atmosphere that is 296 times as effective as CO_2 in a period of 100 years as a greenhouse gas and accounts for about 6% of the greenhouse effect (Ramaswamy et al., 2001).

Recent studies of greenhouse gas emissions concluded that land-use changes and logging can affect the global budget of greenhouse gases. For instance, deforestation and land-use change caused by humans add large amounts of CO_2 to the

---

[*] *Corresponding author*. Tel.: +81 58 293 2077; fax: +81 58 293 2062.
E-mail address: yashiro@green.gifu-u.ac.jp (Y. Yashiro).

0168-1923/$ – see front matter © 2008 Elsevier B.V. All rights reserved.
doi:10.1016/j.agrformet.2008.01.010

atmosphere, whereas recovery of the forest following disturbance withdraws carbon from the atmosphere as the forest matures (Houghton and Hacker, 1999). Tropical forest soils can change from sinks to sources of CH_4 depending on land use (Keller and Reiners, 1994; Steudler et al., 1996). In the case of N_2O, Keller et al. (1993) reported that N_2O fluxes from pasture peak during the first 10 years after conversion from forest, but thereafter decline to values that are even lower than the original forest fluxes. In addition, Matson and Vitousek (1990) estimated that the conversion of tropical forest to pasture would lead to a global N_2O source of approximately 0.7 Tg N $year^{-1}$. Thus, land-use change and management can strongly affect the global budget of greenhouse gases.

Soils are important sources and sinks of the greenhouse gases CO_2, CH_4, and N_2O. In particular, soils of the humid tropical zone are recognized as major natural sources of carbon and nitrogen trace gas emission into the atmosphere (e.g., Keller et al., 1986). Therefore, many field studies have focused on greenhouse gas flux between soil and the atmosphere in tropical areas. During the last few decades, large areas of tropical forest have been logged (Myers, 1991). Generally, logging practices, including selective logging, affect, e.g. the forest canopy, soil physical condition, and nutrient cycling and so on (Pereira et al., 2002; Jakobsen, 1983; Wetson and Attiwill, 1996), which can have a strong impact on greenhouse gas fluxes between soil and atmosphere. It is important to evaluate the effect of logging practice on soil greenhouse gas fluxes in tropical area.

Most studies on greenhouse gas budgets in tropical zones were distributed in the Amazon Basin and Costa Rica, and there is a lack of qualitative and quantitative information on the flux of greenhouse gases in other tropical areas. In particular, little work on trace gas fluxes has been performed in Southeast Asia, which is one of the largest tropical regions in the world and an area of significant logging during the last three decades. To estimate the trace gas budget in tropical areas, it is important to measure and analyze trace gas fluxes in both logged and unlogged forests in Southeast Asia. The objective of this study was thus to quantify the effects of logging on soil greenhouse gas (CO_2, CH_4, N_2O) fluxes in tropical rain forests in Southeast Asia.

2. Materials and methods

2.1. Site description

Our study sites were located in the Pasoh forest (2°58–59′N, 102°16–20′E), about 70 km southeast of Kuala Lumpur in Peninsular Malaysia. This forest is a lowland tropical rain forest with an area of 2450 ha. The climate is characteristic of tropical rain forests, with average annual minimum and maximum temperatures of 22.7 and 33.2 °C, respectively, and annual rainfall of about 1800 mm (Manokaran et al., 2004). The forest is dominated by *Shorea* spp. and *Dipterocarpus* spp., the native vegetation of this region. The Pasoh forest had 403.2 Mg ha^{-1} aboveground biomass in 1998 (Hoshizaki et al., 2004). In mid-January 2005, the part of the Pasoh forest, which had been primary forest, was selectively logged. The logged area covers about 37 ha, and 1004 trees were collected from this area.

In February 2005, we set up one quadrat at a logged site and one at an unlogged site and conducted a preliminary study. In May 2005, we selected six study sites, consisting of three replicates of logged and unlogged sites, in the Pasoh forest. The logged sites were strongly disturbed by heavy machinery during the logging operation; the aboveground parts of trees were removed, although stumps and tree materials that could not be used for timber were left *in situ* (look like clear cutting). To avoid the confounding influences of topography, all the study sites had gentle slopes (0–3°), were at the same elevation (about 140 m a.s.l.), and were situated within 0.25 km^2. All the sites had Ultisol soils (USDA soil taxonomy). The soil pH (H_2O) at 0–5 cm depth was 4.3 ± 0.2 for logged sites and 4.1 ± 0.3 for unlogged sites (mean ± S.D., $n = 15$) in March 2006.

2.2. Field sampling of soil gas fluxes and environmental factors

The closed-chamber method (Bekku et al., 1995) was used to directly determine greenhouse gas flux *in situ*. A PVC cylinders (15-cm height, 21-cm internal diameter) was placed upright on the soil (around 5-cm depth) the day before the flux measurement. On the measurement day, a PVC lid was fitted to the cylinder top (the cylinder was insulated by the lid) and a rubber-capped needle was fitted onto an air sample port on the top of the lid. At each sampling, air in the chamber was aspirated through the needle into an evacuated 5-ml vial (at 0.5, 3, 6, 9 min for CO_2 and CH_4; 0.5, 10, 20, 30 min for N_2O). The concentrations of greenhouse gases in the air samples were quantified by gas chromatography (GC-7A, Shimadzu, Kyoto, Japan, for CO_2 and CH_4; GC-14B, Shimadzu, Kyoto, Japan, for N_2O), and the concentrations were plotted against time. Because the gas concentrations in the closed-chamber increased or decreased linearly with time. We excluded outliers from the dataset that did not fit the linear change in gas concentrations ($R^2 < 0.7$). The frequency of outliers was 1.4% for CO_2, 9.4% for CH_4 and 6.6% for N_2O, respectively. We note that currently most studies use infrared gas analyzers to measure CO_2 fluxes, which is a better one than the air sampling method associated with gas chromatography used in the present study, given the availability of the instrument. We emphasize the comparison of CO_2 flux in between the logged sites and the unlogged sites rather than that of the present study with the other studies.

Volumetric soil moisture content was measured using TDR probes and converted to water-filled pore space (WFPS, $m^3\,m^{-3}$) using soil porosity data. All soil water content data are expressed as WFPS in the present paper.

Nine chamber bases were placed in a grid pattern (about 5-m interval) at each of the six sites, and soil greenhouse gas fluxes were measured in February, May–July 2005 and March and August 2006 ($n = 9$ in February 2005 and $n = 27$ in the other months for the logged and unlogged sites). At the same time, soil temperature (1-cm depth) and water content (0–5-cm depth) were measured adjacent to each chamber. In addition, soil samples were taken inner or near the chamber after the flux measurement to assess soil physical and chemical properties (as described later). Each logged–unlogged site pair ($n = 3$) was sampled on the same day each month, and all measurements were performed from 9:00 to 15:00 h (local time).

Table 1 – The soil temperature and moisture content at the unlogged and logged sites

	February 2005	May	June	July	March 2006	August
Soil temperature (°C, 1-cm depth)						
Unlogged	24.4 ± 0.4 (7)	25.6 ± 0.3 (27)	25.1 ± 0.4 (27)	24.7 ± 0.3 (27)	24.4 ± 0.5 (27)	24.9 ± 0.3 (27)
Logged	25.0 ± 0.4 (8)	31.1 ± 1.2 (27)	30.6 ± 2.0 (27)	30.4 ± 1.5 (26)	31.0 ± 2.1 (27)	31.7 ± 2.0 (27)
WFPS ($m^3\ m^{-3}$, 0–5-cm depth)						
Unlogged	0.43 ± 0.04 (7)	0.34 ± 0.07 (27)	0.36 ± 0.07 (27)	0.32 ± 0.06 (27)	0.23 ± 0.05 (27)	0.28 ± 0.05 (18)
Logged	0.48 ± 0.09 (8)	0.42 ± 0.08 (27)	0.42 ± 0.11 (27)	0.42 ± 0.10 (25)	0.23 ± 0.04 (27)	0.28 ± 0.04 (18)

Values are mean ± standard deviation. The numbers of observations are given in parentheses.

2.3. *Soil properties*

Soil samples were taken inner or near the chambers after the gas flux measurements. Soil cores were collected at 0–5-cm depth using a 100-ml stainless steel ring at each site. One sample from each chamber (five samples at each site only in February 2005) was oven-dried at 105 °C for more than 24 h to measure the soil bulk density. The other five soil samples at each site were air-dried and sieved (2-mm mesh) to measure total carbon, total nitrogen, and mineral nitrogen (NH_4^+, NO_3^-) concentrations. Total carbon and total nitrogen in the air-dried soil samples were measured using an NC analyzer (Sumigraph NC-800, Sumika Chemical Analysis Service Ltd., Osaka, Japan). The mineral nitrogen concentrations were measured using the indophenol blue method for NH_4^+ (Hidaka, 1997) and Cataldo's method for NO_3^- (Cataldo et al., 1975).

2.4. *Statistical analysis*

All statistical analyses were performed using the StatView 5.0 software (SAS Institute, Cary, NC, USA). Mann–Whitney *U*-tests were used to analyze the significance of differences in median greenhouse gas fluxes, mineral nitrogen concentration values between unlogged and logged sites. Values of $P < 0.05$ were considered to be significant.

3. Results

3.1. *Soil conditions and general properties*

Because all measurements were made during the daytime, the soil temperature (1-cm depth) at the logged sites was always higher than at the unlogged sites (Table 1). The soil temperature measured at the logged site in February 2005 was lower than at the other dates because this site was shaded and the measurement time was relatively early in the day. Until July 2005, the WFPS values were higher at the logged sites than at the unlogged sites, although these values were nearly the same at the logged and unlogged sites in March and August 2006.

Soil bulk density at the logged sites was about 1.2 times greater than at the unlogged sites (Fig. 1A), and the high soil bulk density at the logged sites remained stable throughout the experimental period. Total carbon and nitrogen stocks in the 0–5-cm layer were consistently higher at the unlogged sites than at the logged sites except for February 2005 (Fig. 1B and C). The total carbon and nitrogen stocks at the logged sites decreased slightly with time, whereas those at the unlogged sites were stable. The mean C:N ratios of the logged and unlogged sites were similar and ranged from 13 to 17 (data not shown).

Inorganic nitrogen pools were dominated by NH_4^+ at both the logged and unlogged sites, compared with NO_3^- (Fig. 2A and B). The NH_4^+ pools varied from 16.0 to 33.9 $\mu g\,N\,g_{soil}^{-1}$ at the logged sites and 13.9 to 31.0 $\mu g\,N\,g_{soil}^{-1}$ at the unlogged sites. Until July 2005, the NH_4^+ pools at the logged sites were higher

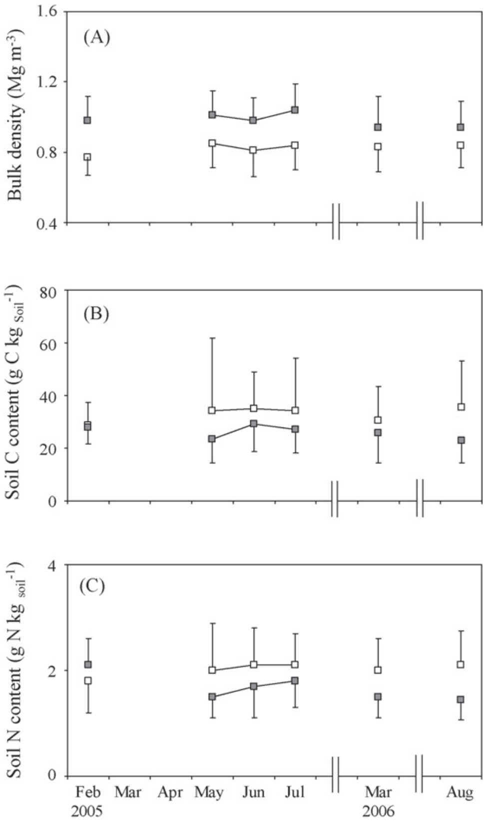

Fig. 1 – Soil bulk density (A), total carbon content (B), and total nitrogen content (C) at the logged sites (gray squares) and the unlogged sites (open squares). Error bars indicate standard deviation; *n* = 5 in February 2005 and *n* = 27 in the other months for bulk density. *n* = 5 in February 2005 and *n* = 15 in the other months for soil carbon and nitrogen content.

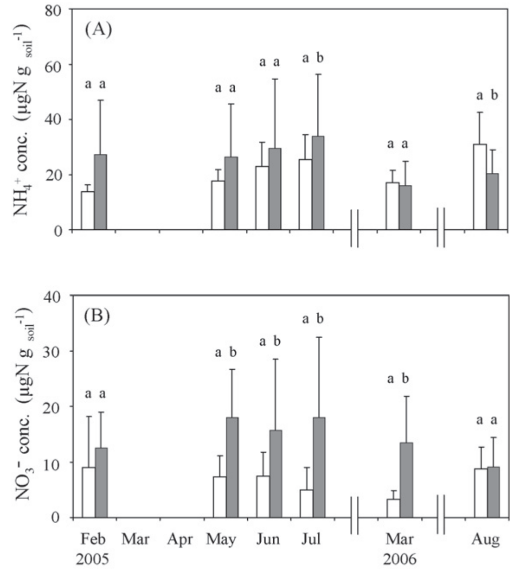

Fig. 2 – Soil NH_4^+ (A) and NO_3^- (B) concentrations at the logged sites (gray) and the unlogged sites (white). Error bars indicate standard deviation; $n = 5$ in February 2005 and $n = 15$ in the other months. Different letters indicate median values that are significantly different between the logged and unlogged sites (Mann–Whitney *U*-test, $P < 0.05$).

than those at the unlogged sites, whereas the values were equal to or lower than those at the unlogged sites in March and August 2006. The NH_4^+ pools differed unclearly between the logged sites and the unlogged sites. Soil NO_3^- content at the logged sites was highest in May 2005 ($18.1\,\mu g\,N\,g_{soil}^{-1}$) and the lowest in August 2006 ($9.2\,\mu g\,N\,g_{soil}^{-1}$). The NO_3^- pools at the unlogged sites ranged from 3.3 to $9.0\,\mu g\,N\,g_{soil}^{-1}$ and were relatively stable over time. The NO_3^- pools at the logged sites were consistently higher than those at the unlogged sites throughout the experimental period.

3.2. *Greenhouse gas fluxes*

The mean CO_2 emission rates ranged from 111.9 to $168.0\,mg\,C\,m^{-2}\,h^{-1}$ at the logged sites (Fig. 3A and Table 2). The CO_2 emission rates at the logged sites tended to be relatively low during the initial period after logging and increased gradually with time. The soil CO_2 emission rates at the unlogged sites were relatively stable throughout the experimental period. The CO_2 flux values at the logged sites were lower than those at the unlogged sites until June 2006 and were higher thereafter.

The soils at the unlogged sites absorbed CH_4 throughout the experimental period except for February 2005, whereas those at the logged sites both absorbed and emitted CH_4 (Fig. 3B and Table 2). The mean CH_4 absorption rates at the logged sites tended to be less than those at the unlogged sites, except in February 2005. At both the logged and the unlogged sites, we found CH_4 hot spots, where CH_4 emission rates were higher than other points at the site.

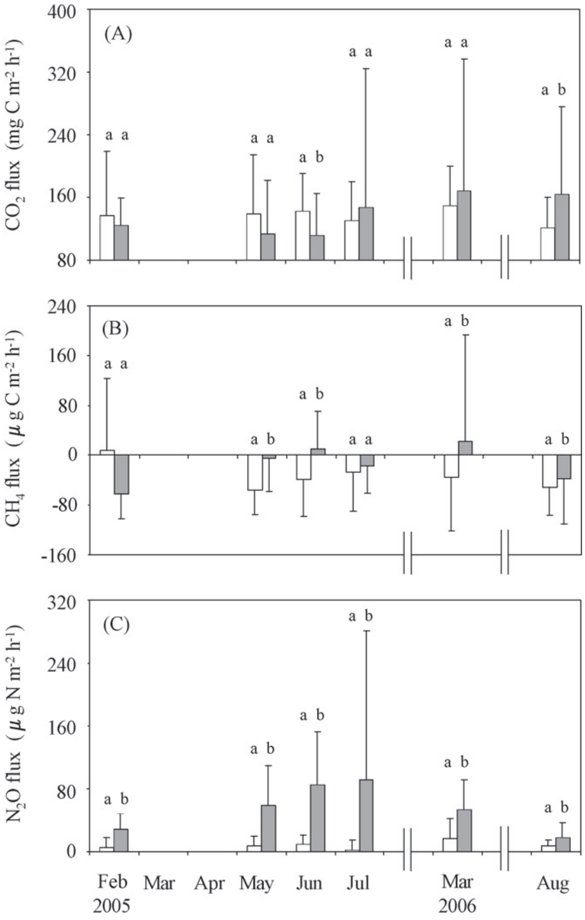

Fig. 3 – Soil CO_2 (A), CH_4 (B), and N_2O (C) flux at the logged sites (gray) and the unlogged sites (white). Error bars indicate standard deviation; $n = 9$ in February 2005 and $n = 27$ in the other months. Different letters indicate median flux values that are significantly different between the logged and unlogged sites (Mann–Whitney *U*-test, $P < 0.05$).

The mean N_2O emission rates varied temporally from 17.7 to $92.0\,\mu g\,N\,m^{-2}\,h^{-1}$ at the logged sties and from 1.6 to $17.0\,\mu g\,N\,m^{-2}\,h^{-1}$ at the unlogged sties (Fig. 3C and Table 2). The mean N_2O emission rates at the logged sites were highest in July 2005 and lowest in August 2006. The N_2O emission rate at the unlogged sites was relatively stable. The soil N_2O emission rates at the logged sites were between 3 and 100 times those at the unlogged sites throughout the experimental period ($P < 0.05$). Some negative fluxes of N_2O were observed at individual chambers in each ecosystem and during each period. Negative N_2O flux was commonly observed at the unlogged sites, and made up 3–30% of the individual chamber observations. At the logged sites, however, a negative N_2O flux was observed in only one chamber in February 2005.

Table 2 – The flux of greenhouse gases at the unlogged and logged sites

	CO_2 fluxes (mg C m^{-2} h^{-1})			CH_4 fluxes (μg C m^{-2} h^{-1})			N_2O fluxes (μg N m^{-2} h^{-1})		
	Mean (S.D.)	Median (range)	*n*	Mean (S.D.)	Median (range)	*n*	Mean (S.D.)	Median (range)	*n*
February 2005									
Unlogged	137.3 (81.7)	104.2 (61.4–333.0) a	9	7.7 (116.5)	−50.1 (−76.2–245.8) a	9	4.8 (13.6)	2.1 (−4.7–34.6) a	7
Logged	124.6 (34.3)	115.5 (85.9–186.1) a	8	−63.3 (39.8)	−47.8 (−133.2 to −26.1) a	8	28.3 (20.5)	25.0 (−5.7–53.3) b	8
May 2005									
Unlogged	138.7 (75.7)	127.1 (63.3–448.3) a	27	−55.4 (40.7)	−54.6 (−165.1–32.8) a	25	7.7 (12.2)	3.4 (−12.9–48.5) a	25
Logged	114.2 (67.5)	93.1 (44.4–325.7) a	26	−5.5 (52.5)	−11.4 (−96.6–104.3) b	22	59.0 (51.0)	47.7 (7.2–162.9) b	25
June 2005									
Unlogged	141.7(48.5)	129.2 (89.8–311.3) a	27	−39.8 (58.5)	−54.6 (−126.9–93.0) a	24	9.5 (11.6)	8.5 (−6.3–44.6) a	21
Logged	111.9 (53.0)	106.9 (32.8–252.3) b	27	9.9 (60.2)	−6.2 (−65.8–157.9) b	24	84.9(67.8)	60.9 (10.4–279.0) b	26
July 2005									
Unlogged	130.6 (49.1)	118.1 (62.3–281.9) a	26	−27.4 (63.4)	−50.6 (−109.4–122.6) a	25	1.6 (12.7)	4.5 (−36.5–21.4) a	24
Logged	147.6(176.9)	92.2 (32.7–935.1) a	27	−17.0 (44.0)	−22.6 (−91.9–73.6) a	24	92.0(189.5)	42.0 (11.1–203.8) b	26
March 2006									
Unlogged	149.7(50.8)	153.8 (84.5–321.0) a	27	−34.7 (86.9)	−55.7 (−119.7–349.4) a	25	17.0 (25.4)	9.1 (−0.1–101.9) a	27
Logged	168.0 (169.2)	120.9 (65.7–934.9) a	27	22.7 (171.3)	−19.5 (−203.7–718.3) b	22	53.2 (38.8)	41.8 (3.0–193.6) b	27
August 2006									
Unlogged	121.3 (38.5)	116.7 (64.3–208.5) a	27	−52.2 (44.7)	−55.3 (−114.1–50.5) a	26	7.8 (6.7)	5.8 (1.2–31.3) a	26
Logged	163.9(112.4)	134.2 (77.6–669.6) b	26	−38.7 (71.3)	−54.1 (−197.8–90.6) a	26	17.7 (18.8)	12.5 (1.5–96.9) b	27

Different letters indicate median values that are significantly different between the logged and unlogged sites (Mann–Whitney *U*-test, $P < 0.05$).

4. Discussion

4.1. Soil conditions and general properties

Several studies have documented significant increases in soil compaction following logging operations (e.g., Jakobsen, 1983; Jakobsen and Greacen, 1985). In the present study, the increase in the soil bulk density immediately after the logging was probably due to the compaction caused by the heavy machinery (e.g., earthmover). Soil compaction by heavy machinery decreases the air-filled space in soils, resulting in the higher WFPS of the logged sites compared to the unlogged sites.

The total soil carbon and nitrogen contents at the logged sites were lower than unlogged sites. The logging practice tilled the soil at the logged sites and decrease C and N content. The deeper soil has lower C and N content comparing with surface soils in primary forest stand (Yamashita et al., 2003). The surface soils were stirred with deeper soils by logging practice, resulting in decreasing soil C and N content at the logged sites. The total soil carbon and nitrogen contents at the logged sites decreased slightly with time after the logging operation, whereas those at the unlogged sites were stable throughout the experimental period. Due to the removal of aboveground biomass, logging restricts the continual supply of litter to soils. Nakane et al. (1986) reported that the accumulation of the A_0 layer (rich organic matter layer) decreased after felling because of the lack of litter being supplied to the stand floor. In addition, logging stimulates decomposition in soils due to the increase in soil temperature. These factors likely contributed to the slight reduction in soil carbon and nitrogen contents at the logged sites. Increased NH_4^+ and NO_3^- concentrations or production rates after logging were observed in several studies (Vitousek and Matson, 1985; Wetson and Attiwill, 1996) as well as in the present study (Fig. 2). These findings indicate that logging can increase mineral nitrogen (NH_4^+ and NO_3^-) in soil and stimulate N_2O production. Wetson and Attiwill (1996) reported that the increased total inorganic nitrogen in soil in a clearfelled, unburnt forest returned rapidly (6–9 months) to a concentration equal to that in undisturbed forest. This also suggests that logging practices increase mineral nitrogen concentration in soil for a short period of time.

4.2. CO_2 flux

Mean soil CO_2 emission rates ranged from 121.3 to 149.7 mg C m^{-2} h^{-1} at the unlogged sites. These values are in the range of those reported for tropical rain forests (58.9–184.2 mg C m^{-2} h^{-1}; Fernandes et al., 2002; Kiese and Butterbach-Bahl, 2002; Schwendenmann et al., 2003). Adachi et al. (2006) reported that the mean CO_2 fluxes from primary forest soil in Pasoh were 226.6 mg C m^{-2} h^{-1}, a value much higher than those measured in the present study. The reason for this discrepancy may be caused by the errors associated with closed-chamber methods in this study. This increase in concentration inside the chamber could decrease the concentration gradient between inside the soil and the surface, resulting in underestimation of fluxes. The errors were applicable for CH_4 and N_2O flux. However, these errors were greater with CO_2 than other gases because of the magnitude of the concentration changes.

Generally, soil respiration correlates positively with soil temperature. Although soil temperature at the logged sites was clearly higher than that at the unlogged sites, soil respiration was not significantly different between the sites, except in June 2005 and March 2006. Most root respirations may have stopped at the logged sites because tree roots were likely killed during the logging operation. Some reports suggest that soil respiration was lower in a felling forest than an intact forest due to the death of tree roots (Nakane et al., 1986; Strigel and Wickland, 1998). Bowden et al. (1993) reported the contribution of root respiration to be 33% of the total soil respiration in mixed hardwood forest soil, and Lee et al. (2005) reported a value of 45% in cool-temperate deciduous forest. According to Kuzyakov (2002), microbial decomposition of root exudates and other rhizodeposits makes a large contribution to the total root-derived CO_2 efflux from soil, indicating that roots and organisms in the rhizosphere play an important role in soil respiration. The death of tree roots during logging operations would inhibit the microbial decomposition of root exudates, which may have offset the effect of increased soil temperature on soil respiration at the logged sites. In addition, soil CO_2 emissions are promoted by well-aerated, moist conditions (Linn and Doran, 1984). In the present study, soil compaction at the logged sites limited soil aeration, which also may have offset the effect of higher soil temperature on soil respiration at the logged sites.

Soil CO_2 emission rates at the logged sites were lower than those at the unlogged sites until June 2005, when rates became higher at the logged sites, especially in March and August 2006. The soil moisture (WFPS) at the logged sites was higher prior than after July 2005. This result suggests that well-aerated soil emitted the greater amount of CO_2 at the logged sites.

4.3. CH_4 *flux*

Generally, well-drained forests, including tropical forest, act as sinks for CH_4 (Singh et al., 1997; Le Mer and Roger, 2001). In the present study, the unlogged sites were in a well-drained condition and generally consumed CH_4. The CH_4 consumption at the logged sites tended to be less than that at the unlogged sites, and some chambers at the logged sites emitted CH_4. Thus, our findings indicate that logging can decrease CH_4 consumption or convert CH_4 sinks to sources for at least 1 year afterward.

Methanotrophs are soil organisms that use CH_4 as their sole carbon and energy source (Le Mer and Roger, 2001). The rate of CH_4 consumption by methanotrophs is limited mainly by the effective diffusivity of CH_4 and O_2 availability in the soil (Dörr et al., 1993; Le Mer and Roger, 2001). In the present study, the increase of soil bulk density after the logging operation likely lowered both the effective diffusivity of CH_4 and O_2 availability in soils, which would have limited CH_4 consumption at the logged sites. According to Le Mer and Roger (2001), upland forests are usually efficient CH_4 sinks, as we found for the unlogged sites in this study. Logging practices appears to accelerate global warming because these decrease CH_4 uptake.

It is noteworthy, however, that we found often CH_4 emission hot spots at both the logged and the unlogged sites. At the logged sites, ruts produced by heavy machinery were submerged temporarily, and after these areas drained, an impermeable layer persisted under the ruts. In waterlogged upland soils, methanogenesis is initiated and methanogenic populations increase (Mayer and Conrad, 1990) because methanogenesis requires strictly anaerobic conditions (Le Mer and Roger, 2001). The ruts probably caused soil to become waterlogged (i.e., anaerobic conditions) and increased the emission of CH_4 at the logged sites. At the unlogged sites, however, we found no submerged soils. At these sites, the CH_4 hot spots may indicate the presence of termite nests in the soil, and several termite mounds were found at the unlogged sites. Tropical termites emit CH_4 and can contribute substantially to atmospheric CH_4 (Hackstein and Stumm, 1994).

Laboratory measurements and field studies have demonstrated that nitrogen fertilization reduces the ability of soil to absorb and oxidize CH_4 (e.g., Adamsen and King, 1993; Castro et al., 1994). An increase in the NH_4^+ content of soil has an inhibitory effect on CH_4 oxidation through the fertilization because this shifted the relative activities of the CH_4 oxidizing by methanotrophs to that by nitrifying bacteria (Castro et al., 1994). In the present study, the soils at the logged sites had more NH_4^+ than those at the unlogged sites at the initial period after the logging. Thus, the relatively high NH_4^+ concentration likely had an inhibitory effect on CH_4 oxidation at the logged sites.

4.4. N_2O *flux*

Our estimate of mean N_2O emission rates during the experimental period ranged from 1.6 to 17.0 $\mu g\,N\,m^{-2}\,h^{-1}$ at the unlogged sites. These values fall within the lower range of N_2O emission rates reported for humid tropical forest (−4.2 to 207.0 $\mu g\,N\,m^{-2}\,h^{-1}$; Breuer et al., 2000; Ishizuka et al., 2002, 2005; Kiese and Butterbach-Bahl, 2002). Ishizuka et al. (2002, 2005) reported that the N_2O fluxes in tropical rain forests in Sumatra, Indonesia, were relatively low, ranging from 1.5 to 9.3 $\mu g\,N\,m^{-2}\,h^{-1}$, and this range was similar to that of the unlogged sites in the present study. According to Yashiro et al. (2008), the mean N_2O flux in the Pasoh forest ranged from 8.7 to 153.1 $\mu g\,N\,m^{-2}\,h^{-1}$, and wet soils (WFPS $> 0.52\,m^3\,m^{-3}$, from 100.3 to 153.1 $\mu g\,N\,m^{-2}\,h^{-1}$) in the forest emitted a much larger amount of N_2O than dry soils (WFPS $< 0.40\,m^3\,m^{-3}$, from 8.7 to 9.8 $\mu g\,N\,m^{-2}\,h^{-1}$). The N_2O emission rates at the unlogged sites were similar to those recorded for the dry soils of the Pasoh forest, because these sites were located along a ridgeline and their soils were dry throughout the experimental period (WFPS ranged from 0.23 to 0.43 $m^3\,m^{-3}$).

Our results showed that logging increased N_2O fluxes for at least 1 year. The mean N_2O emission rates at the logged sites ranged from 17.7 to 92.0 $\mu g\,N\,m^{-2}\,h^{-1}$, and these values were significantly larger than those at the unlogged sites ($P < 0.05$) at all the sampling dates. Keller et al. (2005) reported that selective logging increased emissions of N_2O by 30–350%, depending on conditions, in the Brazilian Amazon region. Both

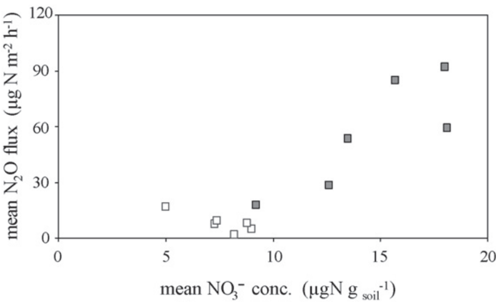

Fig. 4 – Relationship between mean N_2O flux and NO_3^- concentration at the logged (gray) and unlogged (open) sites.

these and our results suggest that logging markedly increases N_2O emission in tropical forest, at least for a short period.

N_2O production in soils is mainly dominated by microbial nitrification and denitrification. N_2O production correlates with nitrogen availability in soil, because nitrification and denitrification rely on NH_4^+ and NO_3^-, respectively (Bouwman, 1990). We found a positive correlation between the N_2O emission rate and NO_3^- pools at the logged sites (Fig. 4, $R^2 = 0.71$). Soil NO_3^- concentration represents an index of nitrogen availability because nitrification supplies and denitrification uses NO_3^- in the soil. Thus, our results suggest that logging increases soil nitrogen availability and favors N_2O production, at least for a short time.

Keller et al. (2005) noted that the areas of strong soil compaction in selectively logged forest – the skid trails and logging decks – were prone to greater emission of N_2O. Sitaula et al. (2000) also reported that N_2O emission was higher in soil compacted by tractors than in uncompacted soil in Norwegian cropland. At the logged sites, soils were compacted during the logging operation (by the heavy machinery). These studies agree with our results and suggest that the soil compaction enhanced N_2O emission.

Soil compaction decreases the air-filled space in soils, and this resulted in higher WFPS at the logged sites compared to the unlogged sites. Or, the decrease in transpiration tares due to tree removal might contribute to high WFPS at the logged sites. Many studies have reported that N_2O production and emission increase exponentially with WFPS (e.g., Keller and Reiners, 1994; Verchot et al., 1999). According to Linn and Doran (1984), the optimum WFPS for nitrification is about $0.60\ m^3\ m^{-3}$, because of water supply for microorganisms in soil. At values above $0.60\ m^3\ m^{-3}$, O_2 infiltration into the soil is reduced and denitrification activity approaches the maximum level obtained in saturated soil. In the present study, WFPS at 0–5-cm depth at the logged sites ranged from 0.23 to $0.48\ m^3\ m^{-3}$, which are relatively low values. Thus, O_2 infiltration was not limited strongly and the WFPS would favor nitrification within this soil layer. Our findings suggest that soil compaction increased WFPS and caused a shift to an environment favorable for nitrification and N_2O production.

5. Conclusions

Logging practices decreased the soil CH_4 absorption and increased the soil N_2O emission but did not strongly affect CO_2 flux. Our study also demonstrated that selectively logged forest may be converted into a weaker sink of CH_4 and greater source of N_2O than tropical rain forest, at least for a short period, because of the increased soil nitrogen availability and soil compaction due to disturbance by heavy machinery. The weaker CH_4 uptake and greater N_2O emission due to logging in tropical rain forest can accelerate global warming, for at least 1 year after the logging operation.

Acknowledgements

We thank Dr. Niiyama (FFPRI) and Dr. Yamanshita (Shimane University) for kindly advising us during this study. We also thank Dr. Toda (Shinshu University) for helping with the gas analysis. The present study was a part of a joint research project of the Forest Research Institute Malaysia, Universiti Putra Malaysia, and the National Institute for Environmental Studies (Global Environment Research Program supported by the Japan Environmental Agency, Grant No. E-4). The present study was also financially supported by a Sasakawa Scientific Research Grant from the Japan Science Society.

REFERENCES

Adachi, M., Bekku, Y.S., Kadir, W.R., Okuda, T., Koizumi, H., 2006. Differences in soil respiration between different tropical ecosystems. Appl. Soil Ecol. 34, 258–265.

Adamsen, A.P.S., King, G.M., 1993. Methane consumption in temperate and subarctic forest soils: rates, vertical zonation, and response to water and nitrogen. Appl. Environ. Microbiol. 59, 485–490.

Bekku, Y., Koizumi, H., Nakadai, T., Iwaki, H., 1995. Measurement of soil respiration using closed chamber method: an IRGA technique. Ecol. Res. 10, 369–373.

Bouwman, A.F., 1990. Exchange of greenhouse gases between terrestrial ecosystems and the atmosphere. In: Bouwman, A.F. (Ed.), Soils and the Greenhouse Effect. John Wiley and Sons, New York, pp. 61–127.

Bowden, R.D., Boone, R.D., Melillo, J.M., Garrison, J.B., 1993. Contributions of aboveground litter, belowground litter, and root respiration to total soil respiration in a mixed hardwood forest. Can. J. For. Res. 23, 1402–1407.

Breuer, L., Papen, H., Butterbach-Bahl, K., 2000. N_2O emission from tropical forest soils of Australia. J. Geophys. Res. 105, 26353–26367.

Castro, M.S., Peterjohn, W.T., Melillo, J.M., Gholz, H.L., Lewis, D., 1994. Effects of nitrogen fertilization on the fluxes of N_2O, CH_4, and CO_2 from soils in Florida slash pine plantation. Can. J. For. Res. 24, 9–13.

Cataldo, D.A., Horoon, M., Schrader, L.E., Youngs, V.L., 1975. Rapid colorimetric determination of nitrate in plant tissue by nitration of salicylic acid. Commun. Soil Sci. Plant Anal. 6, 71–86.

Dörr, H., Kartruff, L., Levin, I., 1993. Soil texture parameterization of the methane uptake in aerated soils. Chemosphere 26, 697–713.

Fernandes, S.A.P., Bernoux, M., Cerri, C.C., Feigl, J., Piccolo, M.C., 2002. Seasonal variation of soil chemical properties and CO_2 and CH_4 fluxes in unfertilized and P-fertilized pastures in Ultisol of the Brazilian Amazon. Geoderma 107, 227–241.

Hackstein, J.H., Stumm, C.K., 1994. Methane production in terrestrial arthropods. Proc. Natl. Acad. Sci. U.S.A. 91, 5441–5445.

Hidaka, 1997. Nitrogen analysis. In: Japanese Society of Soil Science and Plant Nutrition, Analysis of Soil Environment, Hakuyu Sha, Tokyo, pp. 231–254 (in Japanese).

Hoshizaki, K., Niiyama, K., Kimura, K., Yamashita, T., Bekku, Y., Okuda, T., Quah, E.S., Supardi, N.M.N., 2004. Temporal and spatial variation of forest biomass in relation to stand dynamics in a mature, lowland tropical rainforest, Malaysia. Ecol. Res. 19, 357–363.

Houghton, R.A., Hacker, J.L., 1999. Emissions of carbon from forestry and land-use change in tropical Asia. Global Change Biol. 5, 481–492.

Ishizuka, S., Tsuruta, H., Murdiyarso, D., 2002. An intensive field study on CO_2, CH_4, and N_2O emissions from soils at four land-use types in Sumatra, Indonesia. Global Biogeochem. Cycles 16 (3), 1049 doi:10.1029/2001GB001614.

Ishizuka, S., Iswandi, A., Nakajima, Y., Yonemura, S., Sudo, S., Tsuruta, H., Murdiyarso, D., 2005. The variation of greenhouse gas emissions from soils of various land use/cover types in Jambi province, Indonesia. Nutr. Cycling Agroecosyst. 71, 17–32.

Jakobsen, B.F., 1983. Persistence of compaction effects in a forest Kraznozen. Aust. For. Res. 13, 305–308.

Jakobsen, B.F., Greacen, E.L., 1985. Compaction of sandy forest soils by forwarder operation. Soil Tillage Res. 5, 55–70.

Keller, M., Reiners, W.A., 1994. Soil-atmosphere exchange of nitrous oxide, nitric oxide, and methane under secondary succession of pasture to forest in the Atlantic lowlands of Costa Rica. Global Biogeochem. Cycles 8, 399–409.

Keller, M., Kaplan, W.A., Wofsy, S.C., 1986. Emissions of N_2O, CH_4 and CO_2 from tropical forest soils. J. Geophys. Res. 91, 11791–11802.

Keller, M., Veldkamp, E., Weitz, A.M., Reiners, W.A., 1993. Effect of pasture age on soil trace-gas emissions from a deforested area of Costa Rica. Nature 365, 244–246.

Keller, M., Varner, R., Dias, J.D., Silva, H., Crill, P., de Oliveria Jr., R.C., Asner, G.P., 2005. Soil-atmosphere exchange of nitrous oxide, nitric oxide, methane, and carbon dioxide in logged and undisturbed forest in the Tapajos National Forest, Brazil. Earth Interact. 9, 1–28.

Kiese, R., Butterbach-Bahl, K., 2002. N_2O and CO_2 emissions from three different tropical forest sites in the wet tropics of Queensland, Australia. Soil Biol. Biochem. 34, 975–987.

Kuzyakov, Y., 2002. Separating microbial respiration of exudates from root respiration in non-sterile soils: a comparison of four methods. Soil Biol. Biochem. 34, 1621–1631.

Le Mer, J., Roger, P., 2001. Production, oxidation, emission and consumption of methane by soils: a review. Eur. J. Soil Biol. 37, 25–50.

Lee, M., Nakane, K., Nakatsubo, T., Koizumi, H., 2005. The importance of root respiration in annual soil carbon fluxes in a cool-temperate forest. Agric. For. Meteorol. 134, 95–101.

Linn, D.M., Doran, J.W., 1984. Effect of water filled pore space on carbon dioxide and nitrous oxide production in tilled and nontilled soils. Soil Sci. Soc. Am. J. 48, 1267–1272.

Manokaran, N., Quah, E.S., Ashton, P.S., LaFrankie, J.V., Nur Supardi, M.N., Ahmad, W.M.S.W., Okuda, T., 2004. Pasoh forest dynamics plot, peninsular Malaysia. In: Losos, E.C., Leigh, J.E.G. (Eds.), Tropical Forest Diversity and Dynamism. University of Chicago Press, Chicago, IL, USA, pp. 585–598.

Matson, P.A., Vitousek, P.M., 1990. Ecosystem approach to a global nitrous oxide budget. Bioscience 40, 672–677.

Mayer, H.P., Conrad, R., 1990. Factors influencing the population of methanogenic bacteria and the initiation of methane production upon flooding of rice paddy. FEMS Microbiol. Ecol. 73, 103–112.

Myers, N., 1991. Tropical forests: present status and future outlook. Clim. Change 19, 3–32.

Nakane, K., Tsubota, H., Ymamoto, M., 1986. Cycling of soil carbon in a Japanese red pine forest. II. Change occurring in the first year after a clear-felling. Ecol. Res. 1, 47–58.

Pereira, R., Zweede, J.C., Asner, G.P., Keller, M.M., 2002. Forest canopy damage and recovery in reduced impact and conventional logging in eastern Para, Brazil. For. Ecol. Manage. 168, 77–89.

Ramaswamy, V., Boucher, O., Haigh, J., Hauglustaine, J., Haywood, G., Mythe, T., Nakajima, T., Shi, G.Y., Solomon, S., 2001. Radiative forcing of climate change. In: Houghton , J.T., Ding, Y., Griggs, D.J., Noguer, M., van der Linden, X., Dai, K., Maskell, K., Johnson, C.A. (Eds.), Climate Change 2001: The Scientific Basis. Cambridge University Press, Cambridge, UK, pp. 349–416.

Schimel, D., Alves, D., Enting, I., Heimann, M., Joos, F., Raynaud, D., Wigley, T., 1996. Radiative forcing of climate change. In: Houghton, J.T., Meira Filho, L.G., Callander, B.A., Harris, N., Kattenberg, A., Maskell, K. (Eds.), Climate Change 1995: The Science of Climate Change. Cambridge University Press, Cambridge, UK, pp. 65–86.

Schwendenmann, L., Veldkamp, E., Brenes, T., O'Brien, J.J., Mackensen, J., 2003. Spatial and temporal variation in soil CO_2 efflux in an old-growth neotropical rain forest, La Selva, Costa Rica. Biogeochemistry 64, 111–128.

Singh, J.S., Singh, S., Raghubanshi, A.S., Singh, S., Kashyyap, A.K., Reddy, V.S., 1997. Effect of soil nitrogen, carbon and moisture on methane uptake by dry tropical forest soils. Plant Soil 196, 115–121.

Sitaula, B.K., Hansen, S., Sitaula, J.I.B., Bakken, L.R., 2000. Effects of soil compaction on N_2O emission in agricultural soil. Chemosphere-Global Change Sci. 2, 367–371.

Steudler, P.A., Melillo, J.M., Feigl, B.J., Neill, C., Piccolo, M.C., Cerri, C.C., 1996. Consequence of forest-to-pasture conversion on CH_4 fluxes in the Brazilian Amazon Basin. J. Geophys. Res. 101, 18547–18554.

Strigel, R.G., Wickland, K.P., 1998. Effect of a clear-cut harvest on soil respiration in a jack pine-lichen woodland. Can. J. For. Res. 28, 534–539.

Verchot, L.V., Davidson, E.A., Cattânio, J.H., Ackerman, I.L., Erickson, H.E., Keller, M., 1999. Land use change and biogeochemical controls of nitrogen oxide emissions from soils in eastern Amazonia. Global Biogeochem. Cycles 10, 31–46.

Vitousek, P.M., Matson, P.A., 1985. Disturbance, nitrogen availability, and nitrogen losses in an intensively managed loblolly pine plantation. Ecology 66, 1360–1376.

Wetson, C., Attiwill, P.M., 1996. Clearfelling and burning effects on nitrogen mineralization and leaching in soils of old age *Eucalyptus regnans* forests. For. Ecol. Manage. 89, 13–24.

Yamashita, T., Kasuya, N., Wan Rashidah, K., Suhaimi, W.C., Quah, E.S., Okuda, T., 2003. Soil and belowground characteristics of Pasoh forest reserve. In: Okuda, T., Manokaran, N., Matsumoto, Y., Niiyama, K., Thomas, S.C., Ashton, P.S. (Eds.), Pasoh: Ecology of a Lowland Rain Forest in Southeast Asia. Springer, Tokyo, pp. 89–109.

Yashiro, Y., Wan Rashidah, K., Adachi, M., Okuda, T., Koizumi, H., 2008. Emission of nitrous oxide from tropical forest and plantation soils in Peninsular Malaysia. Tropics 17, 17–23.

4 Rainfall Characteristics of Tropical Rainforest at Pasoh Forest Reserve, Negeri Sembilan, Peninsular Malaysia

Shoji Noguchi[1], Abdul Rahim Nik[2] & Makoto Tani[3]

Abstract: We investigated the rainfall at the Pasoh Forest Reserve (Pasoh FR), Peninsular Malaysia. Pasoh FR is located in the Southwest rainfall regime, in which the average annual rainfall (1,500–2,000 mm) is less than that in other regions of Peninsular Malaysia. Monthly rainfall in 1996 and 1997 ranged from 2.2 to 206.7 mm with a mean of 115.6 mm. The rainfall in 1997 was much smaller due to the El Niño Southern-Oscillation (ENSO) event. The longest period of dry days was 49 days. Dry periods as well as fluctuation in rainfall are major factors affecting the growth of vegetation. A distinct diurnal cycle in rainfall, in which 52% of the rainfall occurred between 13:00 and 19:00 h, was apparent. The frequency of the amount of rainfall in each event was an inverse J-shaped type distribution. The amount of rainfall in one event ranged from 1.2 and 93.1 mm with a mean of 11.4 mm and a median of 5.6 mm. The rainfall was characterized by a short duration (range:1.0–22.0 h, mean: 3.8 h) and high intensity. The maximum hourly rainfall intensity during a rain event ranged from 0.6 to 63.8 mm h^{-1} with a mean of 7.8 mm h^{-1} and a median of 3.8 mm h^{-1}.

Key words: amount, diurnal cycle, duration, rainfall intensity, seasonal variation, tropical rain forest.

1. INTRODUCTION

Rainfall data can be applied immediately to water resource planning and consumption. The Drainage and Irrigation Department and Malaysian Meteorological Service collect rainfall at more than 650 stations, which cover most of Peninsular Malaysia. However, there are a few stations in the hilly forested regions (Abdul Rahim 1983).

A tropical rain forest contributes to the prevention of sediment disaster as well as to the conservation of water resources. Understanding hydrological characteristics in a tropical rain forest is very important from a scientific point of view. Hydrological characteristics such as streamflow, soil moisture, suspended sediment yield, and nutrient cycling depend on the rainfall characteristics in tropical rain forests (Baharuddin & Abdul Rahim 1994; Noguchi et al. 1997; Zulkifli 1996). Therefore, it is important to understand the rainfall characteristics in order to elucidate the hydrological processes in a tropical rain forest.

The Pasoh Forest Reserve (Pasoh FR) has been a site of ongoing research on lowland rain forest ecology since the early 1970s. Rainfall data obtained from this site provides important information on ecology as well as hydrology. Hydrological observations for elucidation of rainfall-runoff responses, soil water

---

[1] Forestry and Forest Products Research Institute (FFPRI), Ibaraki 305-8687, Japan. E-mail: noguchi@affrc.go.jp

[2] Forest Research Institute Malaysia (FRIM), Malaysia.

[3] Kyoto University, Japan.

Fig. 1 Locations of Pasoh FR, Bukit Tarek Experimental Watershed (BTEW), and mean annual rainfall (mm) in Peninsular Malaysia (modified from Robiah et al. 1988).

storage, and nutrient cycling have been conducted at Bukit Tarek Experimental Watershed (BTEW) in Peninsular Malaysia (Noguchi et al. 1997, 2000; Zulkifli 1996). A comparison of the rainfall characteristics at Pasoh FR and BTEW would be helpful for understanding the hydrological characteristics at Pasoh FR.

The primary objective of this study was to analyze the temporal distribution of rainfall at Pasoh FR. A comparison of rainfall characteristics (duration, amount and intensity) at Pasoh FR and BTEW based on 3-year records was also carried out.

2. METHODS AND MATERIALS

The Pasoh FR is located in Negeri Sembilan of Peninsular Malaysia (2°59' N, 102°19' E: Fig. 1). The core area (600 ha) of the reserve (2,450 ha) is covered with a primary lowland mixed dipterocarp forest, which consists of various species of *Shorea* and *Dipterocarpus* (Manokaran et al. 1992). The emergent layer averages 46 m and the main canopy is 20–30 m in height (Manokaran & Swaine 1994). A 52-m high tower was established in the core area for meteorological observation (Color plate 3). Rainfall data was collected at 30-min intervals at a height of 52.6 m using a tipping-bucket rain gauge. The amount of rainfall collected at the tower was calibrated by a tatlizing rain gauge at a climate station in Pasoh FR. Details of the locations and the tower in Pasoh FR are shown in the Color Plates and Chaps. 1 and 2.

Bukit Tarek Experimental Watershed (BTEW) is located in Selangor Darul Ehsan, Peninsular Malaysia (3°31' N, 101°35' E: Fig. 1). The forest was logged in the early 1960s by MUS (Malayan Uniform System) and has now been fully regenerated. The vegetation is dominated by *Koompassia malaccensis*, *Eugenia* spp. and *Canarium* spp. Rainfall data were obtained at 10-min intervals using a weightingtype recording rain gauge and a tipping bucket rain gauge near weir C1. Details of the locations BTEW presented by Noguchi et al. (1996).

A rain event is defined as rainfall of more than 1 mm with an interval of more than six hours from the last recorded rainfall using hourly data.

3. RESULTS AND DISCUSSION

3.1 Diurnal and seasonal variations in rainfall

Figuar 2 shows monthly rainfall based on 13-year records (1983–1995) at Federal Land Depelopment Authority (FELDA) Pasoh Dua, which is located 3 km to the south of the tower in Pasoh FR. The annual rainfall at this site ranged from 1,468.6 to 2,349.5 mm with a mean of 1,810.7 mm. The monthly rainfall ranged from 3.4 to 430 mm with a mean of 150.9 mm. The monthly rainfall had a two-peak distribution (Mar.–May and Sep.–Dec.), suggesting that the climate in this site is influenced by both southwest and northeast monsoons. Typically, 42.6% of the annual rainfall occurred during the northeast monsoon (November to March), 39.1% during the southwest monsoon (May to September), and the remaining 18.4% during the transitional months (April and October). The monthly variation in rainfall is similar to that found for the southwest regime in Peninsular Malaysia as described by Dale (1959).

Diurnal and seasonal variations in rainfall in 1996 and 1997 at Pasoh FR are shown in Fig. 3. Annual rainfall in 1996 and 1997 were 1,610 and 1,182 mm, respectively. The variation in monthly rainfall in 1996 was similar to that in average monthly rainfall at Pasoh Dua. Annual rainfall at Pasoh FR was normal in 1996 but much less than normal in 1997. The much smaller rainfall in 1997 was caused by the El Niño Southern-Oscillation (ENSO) event (Toma et al. 2000; Chap. 6). Monthly rainfall in 1996 and 1997 ranged from 2.2 to 206.7 mm with a mean of 115.6 mm. The variation in soil water storage in a tropical rain forest corresponds to the fluctuation in rainfall (Noguchi et al. 1997, 2000). The variation in monthly rainfall at Pasoh FR might also reflect the variation in soil water storage.

Toma et al. (2000) divided various 30-day rainfall totals into three categories: wet (more than 100 mm), moist (60–100 mm), and dry (less than 60 mm). The percentages of wet and dry days in 1996 were 65.6% and 10.9%, respectively. In

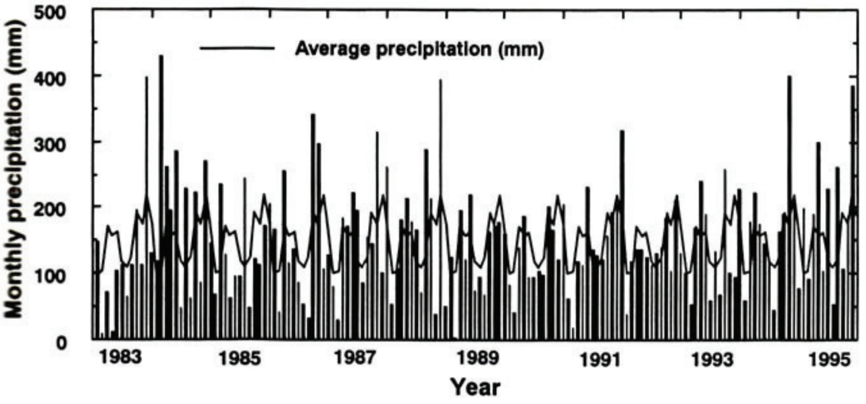

Fig. 2 Variation in monthly rainfall at Pasoh Dua based on 13-year records (1993-1995).

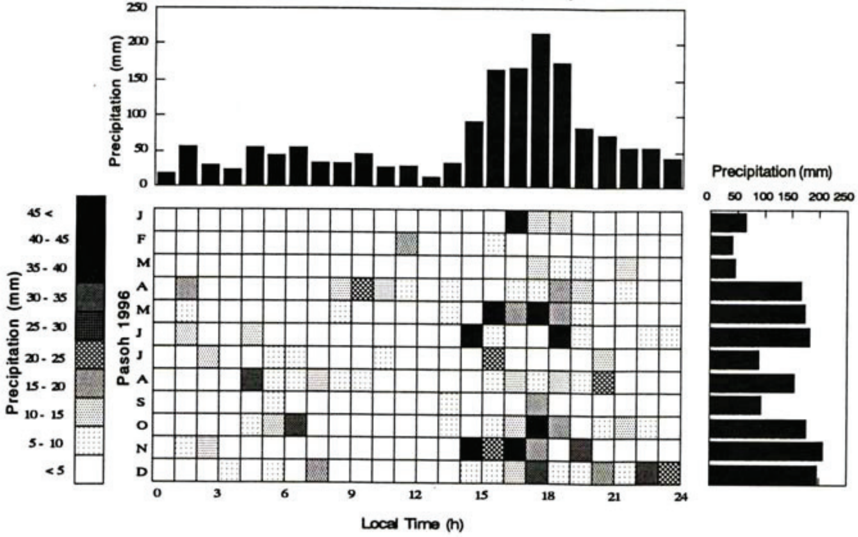

(a) Pasoh Forest Reserve (1996)

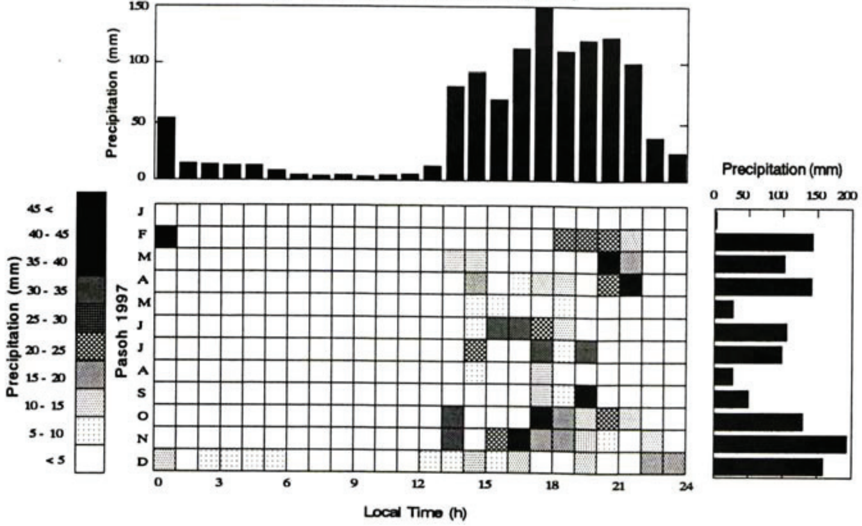

(b) Pasoh Forest Reserve (1997)

Fig. 3 Total rainfall at each time of day in each month at Pasoh FR in 1996 and 1997.

1997, the percentage of wet days (47.1%) decreased but the percentage of dry days (33.4%) increased because of the ENSO event. The longest period of dry days was 49 days, lasting from August 21 to October 8, 1997. On the other hand, annual rainfall at Bukit Soeharto Education Forest in East Kalimantan was more than 2000 mm, but the recorded period of dry days was longer (e.g. more than three months) than that at Pasoh FR. Toma et al. (2000) pointed out that high mortality rate of *Macaranga* spp. trees was observed during droughts. Thus, it is thought that dry periods have had a great effect on growth of vegetation.

Knowledge of the diurnal cycle of rainfall is important for evaluation of daily evapotranspiration because the rainfall time of a day and successive sunshine duration affect evapotranspiration (Oki & Musiake 1994). Fig. 3 shows the total rainfall at each time of day in each month at Pasoh FR. In 1996 and 1997, 63.6% and 55.4% of the total rainfall occurred during the daytime (07:00–19:00 h), respectively. A distinct diurnal cycle in rainfall, in which 52.7% and 52.1% of the rainfall occurred between 13:00 h and 19:00 h, is apparent. In 1996, 13.2% of the total rainfall occurred between 19:00 h and 22:00 h, whereas 29.1% of the total rainfall occurred between the same hours in 1997. Convectional storms are caused by differential solar heating of the ground and lower air layers, which typically occur during afternoons when warm moist air covers an area (Hewlett 1969). In this regard, most afternoon rainstorms at Pasoh Dua can be classified as convectional storms.

3.2 Characteristics of rainfall events

Noguchi et al. (1996) have already reported the rainfall characteristics in Bukit Tarek Experimental Watershed (BTEW). In the present study, we compared rainfall characteristics at Pasoh FR and BTEW over a period of 36 months.

The total numbers of rain events at Pasoh FR and BTEW were 366 and 555, respectively. The frequency of the amount of rainfall in each event at both Pasoh FR and BTEW showed an inverse J-shaped type distribution (Fig. 4), and the ranges of values were almost the same. However, the mean and median amounts of rain events at Pasoh FR were smaller than those at BTEW (Table 1).

Fig. 5 shows the percentages of rainfall in size classes at Pasoh FR and BTEW. Events of more than 25 and 50 mm of rainfall comprised 43.2% and 15.4% of the total rainfall at Pasoh FR and 57.9% and 17.8% of the total rainfall at BTEW,

Table 1 Statistical properties of amount, duration and intensity of rainfall.

	Pasoh FR			BTEW		
	Amount (mm)	Duration (h)	Intensity (mm h^{-1})	Amount (mm)	Duration (h)	Intensity (mm h^{-1})
Minimum	1.2	1.0	0.6	1.0	1.0	0.5
Maximum	93.1	22.0	63.8	96.0	18.0	76.5
Points	366	366	366	555	555	555
Mean	11.4	3.8	7.8	14.3	2.7	11.6
Median	5.6	2.0	3.8	8.0	1.0	6.5
RMS	17.7	5.20	12.1	21.3	3.87	17.5
Std. deviation	13.5	3.56	9.30	15.8	2.78	13.1
Std. Error	0.707	0.186	0.486	0.672	0.118	0.556
Skewness	2.36	2.34	2.36	1.79	2.30	1.82
Kurtosis	6.90	6.66	6.99	3.77	6.37	3.69

Pasoh FR: Pasoh Forest Reserve; BTEW: Bukit Tarek Experimental Watershed; Intensity: Maximum hourly rainfall intensity during a rain event.

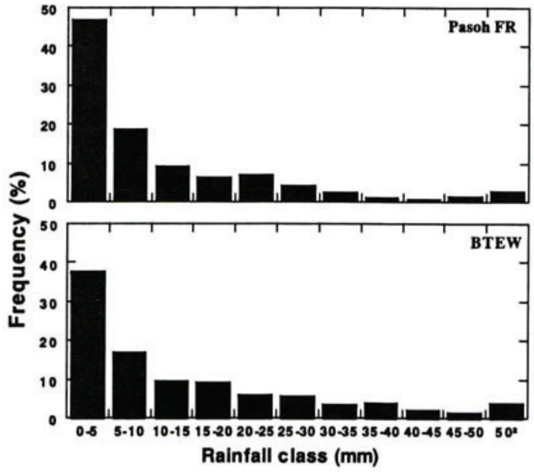

Fig. 4 Frequency distribution of the amounts of rainfall in each rain event at Pasoh FR and Bukit Tarek Experimmental Watershed (BTEW).

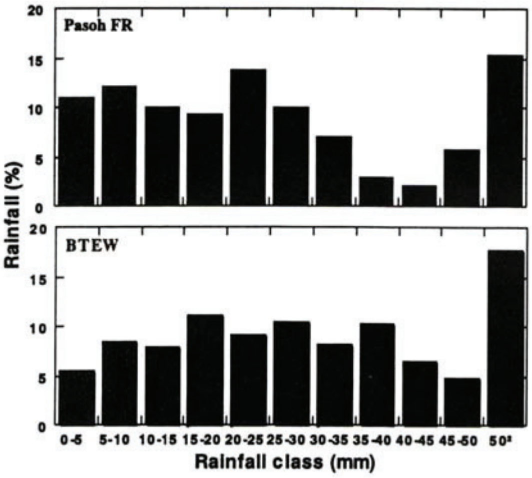

Fig. 5 Percentages of rainfall in certain-sized rain events in each rain event at Pasoh FR and BTEW.

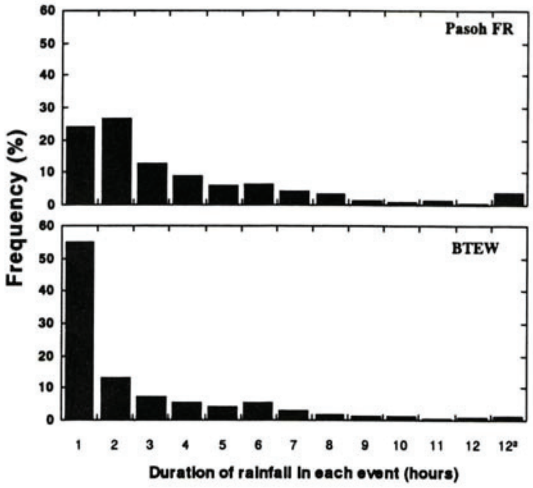

Fig. 6 Frequency distribution of duration of rainfall in each rain event at Pasoh FR and BTEW.

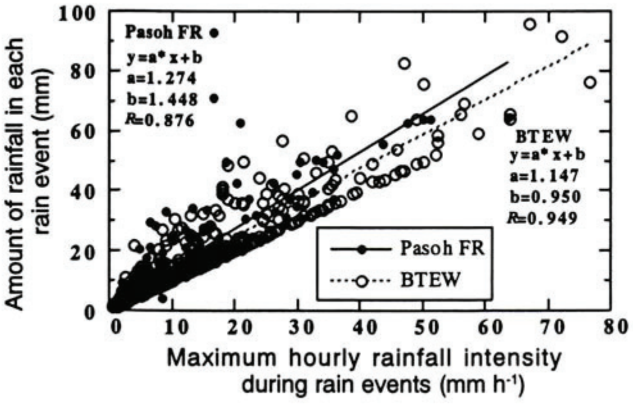

Fig. 7 Relationship between amount of rain and maximum rainfall per hour at Pasoh FR and BTEW.

respectively. Rain events of more than 25 and 50 mm constituted 12.3% and 2.7% of the total number of events at Pasoh FR and 20.7% and 4.0% of the total number of events at BTEW, respectively (Fig. 4). The smallest rain events (0–5 mm) constituted 46.7% and 37.8% of the total number of rain events at Pasoh FR and BTEW, respectively (Fig. 4). These small rain events (0–5 mm) produced 11% of the total rainfall at Pasoh FR, about two-times greater than that at BTEW (Fig. 5).

The frequency distributions of duration of rainfall in each rain event at Pasoh FR and BTEW are shown in Fig. 6. At Pasoh FR and BTEW, 50.8% and 68.2% of the total number of events occurred within 2-h periods. The duration of rainfall at Pasoh FR showed a wider range and a 1-h longer average than those at BTEW (Table 1). Figure 7 shows the relationship between total amount of rainfall in each rain event and maximum hourly rainfall intensity during the rain event. The amount of rainfall in each rain event was found to be proportional to the maximum hourly rainfall intensity at both sites. There was a higher positive correlation at BTEW ($R = 0.949$) than at Pasoh FR ($R = 0.876$). The mean and median values of maximum hourly rainfall intensity at Pasoh FR were smaller than those at BTEW (Table 1). However, the intensity of rainfall at Pasoh FR was also relatively high. The high intensity of rainfall has caused serious soil erosion on bare ground in this region.

4. CONCLUSION

Rainfall characteristics of tropical rainforest were investigated at the Pasoh FR in Negeri Sembilan, Peninsular Malaysia over a 3-year period. The rainfall was characterized by its short duration (mean: 3.8 h) and high intensity (mean: 7.8 mm h^{-1}). There was a distinct diurnal cycle in rainfall, in which 52% of the rainfall occurred between 13:00 and 19:00 h. Pasoh FR is located in the Southwest rainfall regime, in which the average annual rainfall (1,500–2,000 mm) is less than that of other regions of Peninsular Malaysia. The rainfall in 1997 (1,182 mm) was much lower than the norm due to El Niño Southern-Oscillation event. The longest period of dry days was 49 days. Soil moisture corresponds to the fluctuation of rainfall. Therefore, such dry periods as well as fluctuation in rainfall are major factors affecting the growth of vegetation.

ACKNOWLEDGEMENTS

We thank the Forestry Department of Negeri Sembilan and Director General of FRIM for giving us permission to work in the Pasoh FR. We also thank the staff of the Hydrology Unit of FRIM for collecting rainfall data. This study was carried out as a joint research project between NIES, FRIM and UPM (Global Environmental Research Program granted by the Japanese Environment Agency, Grant No. E-3).

REFERENCES

Abdul Rahim, N. (1983) Rainfall characteristics in forested catchments of Peninsular Malaysia. Malay. For. 46: 233-243.

Baharuddin, K. & Abdul Rahim, N. (1994) Suspended sediment yield resulting from selective logging practices in a small watershed in Peninsular Malaysia. J. Trop. For. Sci. 7: 286-295.

Dale, W. L. (1959) The rainfall of Malaysia, Part I. J. Trop. Geogr. 13: 23-37.

Hewlett, J. D. (1969) Principle of Forest Hydrology. The University of Georgia Press, 183pp.

Manokaran, N. & Swaine, M. D. (1994) Population dynamics of trees in dipterocarp forests of Peninsular Malaysia. Malayan Forest Records No. 40. Forest Research Institute Malaysia, Kuala Lumpur, 173pp.

Manokaran, N., LaFrankie, J. V., Kochummen, K. M., Quah, E. S., Klahn, J. E., Ashton, P. S. & Hubbell, S. P. (1992) Stand table distribution of species in the 50ha research plot at Pasoh Forest Reserve. FRIM Research Data No. 1. Forest Research Institute Malaysia, Kuala Lumpur.

Noguchi, S., Abdul Rahim, N., Sammori, T., Tani, M. & Tsuboyama, Y. (1996) Rainfall characteristics of tropical rain forest and temperate forest : Comparison between Bukit Tarek in Peninsular Malaysia and Hitachi Ohta in Japan. J. Trop. For. Sci. 9: 206-220.

Noguchi, S., Abdul Rahim, N., Zulkifli, Y., Tani, M. & Sammori, T. (1997) Rainfall-runoff responses and roles of soil moisture variations to the response in tropical rain forest, Bukit Tarek, Peninsular Malaysia. J. For. Res. 2: 125-132.

Noguchi, S., Zulkifli, Y., Baharuddin, K., Tani, M., Tsuboyama, Y. & Sammori, T. (2000) Seasonal soil water storage changes in a tropical rain forest in Peninsular Malaysia. J. Jpn. Soc. Hydrol. Water Resour. 13: 206-215.

Oki, T. & Musiake, K. (1994) Seasonal change of the diurnal cycle of rainfall over Japan and Malaysia. J. Appl. Meteorol. 33: 1445-1463.

Robiah bt. Bani, Leong, T. M., Yip, H. W. & Kelsom bt. Alias (1988) Mean monthly, mean seasonal and mean annual rainfall map for Peninsular Malaysia. Water Resour. Pub. 19: 16.

Toma, T., Marjenah & Hastaniah (2000) Climate in Bukit Soeharto, East Kalimantan. In Guhardja, E., Fatawi, M., Sutisna, M., Mori, T. & Ohta, S. (eds). Rainforest Ecosystems of East Kalimantan: El Niño, Drought, Fire and Human Impacts. Ecological Studies vol. 140. Springer-Verlag, Tokyo, pp.13-27.

Zulkifli, Y. (1996) Nutrient cycling in secondary rain forest catchments of Peninsular Malaysia. Ph.D. diss., Univ. Manchester, 380pp.

7 Soil and Belowground Characteristics of Pasoh Forest Reserve

Tamon Yamashita[1], Nobuhiko Kasuya[2], Wan Rasidah Kadir[3], Suhaimi Wan Chik[3], Quah Eng Seng[3] & Toshinori Okuda[4]

Abstract: We describe the soil and belowground characteristics of the Pasoh Forest Reserve (Pasoh FR), Peninsular Malaysia. Soil survey was conducted using the Malaysian classification system in primary and regenerating forests of Pasoh FR. The physical and chemical properties of various soil horizons were measured at the selected soil pits. Soil N dynamics as a soil biological process was also studied in a range of forest environments, including gap and closed forest. The fine root biomass in the topsoil was also quantified in primary forest. Pasoh FR has at least 18 soil types. The soils of Pasoh FR are whitish to yellowish in color rather than reddish. When compared to the other Southeast Asian tropical forest soils, the particle size distribution is characterized by lower sand and higher silt contents. Chemically, the Pasoh FR soil accumulates greater amounts of Al. Most CEC (cation exchange capacity) are occupied by Al. The high Al content leads to lower P availability. The pool of inorganic N at 0–10 cm soil depth ranges from 14.8 to 23.9 μg N g^{-1}. Net N mineralization rate in topsoil in the primary forest is estimated to be 100 kg N ha^{-1} yr^{-1}. Nitrification is pronounced at uppermost layer. The fine root biomass (FRB) less than 2, 3 and 5 mm in diameter (d) are 624, 751, 970 g m^{-2}, respectively. Within the top 20 cm, the FRB (< 1 mm in d) constitutes 73% of the total FRB (< 5 mm in d) from 0–4 cm and about 40% in subsequent layers. The Pasoh FR soil is supposed to be infertile. Net N mineralization is observed mainly in the topsoil. These facts suggest that the FRB (< 2 mm in d) constitutes a major part of the total, especially in the top soil to effectively absorb mineral nutrients released from decomposing organic matter.

Key words: chemical properties, fine root biomass, inorganic N pool, nitrification, N mineralization, physical properties.

1. INTRODUCTION

Soil is the fundamental resource for terrestrial ecosystems. Agricultural and forestry production are dependent upon soil fertility. Hence, soil supports not only plants and animals, but also human life. During recent decades, especially in the tropics, clearance and conversion of large areas of forest to more productive uses to support human life has proceeded at unprecedented rates (FAO 1995). Proper assessment and evaluation of soil are vital to rational and sustained use of forest resources.

Tropical soils are supposedly red, old, deeply weathered, leached, acidic, infertile, lateritic and unable to support intensive cultivation (e.g. Sibirtzev 1914 cited in Richter & Babbar 1991). In reality, the soils observed in humid tropics are

---

[1] Education and Research Centre for Biological Resources, Shimane University, Matsue 690-8504, Japan. Email: tamonyam@life.shimane-u.ac.jp

[2] Kyoto Prefectural University, Japan.

[3] Forest Research Institute Malaysia (FRIM), Malaysia.

[4] National Institute for Environmental Studies (NIES), Japan.

very diverse (Richter & Babbar 1991). Soils show diversity in both type and chemical, physical and biological properties and thus range from highly productive to almost totally infertile. Although diverse, most soils in humid tropics can be classified as highly weathered Oxisols, Ultisols or Alfisols. These groups account for about 80% of all soils in these regions (Sanchez 1976). Ultisols are the dominant soil group in the humid regions of Southeast Asia (Lal 1987) and are comparatively younger and have higher cation exchange capacity (CEC) than the inherently low fertility Oxisols. Characteristics of dominant soils in humid tropics were recently reviewed by Kauffman et al. (1998). They observed that a large portion of the humid tropics region was covered by soils of low fertility. They also referred to the importance of organic matter in such soils, as a nutrient source for plants. Nutrients in organic matter, especially N and P, are released through the processes of decomposition and mineralization.

Following the early work of Allbrook (1972), soil survey and soil analyses have been conducted intermittently in the Pasoh Forest Reserve (Pasoh FR). After permanent plots, such as the 50-ha Plot, were established, detailed soil maps have become available. In this chapter we review the soil characteristics of the Pasoh FR. We first use the distribution of soils in some permanent plots to demonstrate the diversity of Pasoh FR soils. Secondly, we describe the physico-chemical properties of several soil types and their interrelationships. Thirdly, we discuss biological properties, including N dynamics that are driven by microbial processes, and the distribution of fine roots, which are a hidden but active part of plants.

2. STUDY SITE

The Pasoh FR is 2,450 ha in area and is surrounded by oil palm plantations. The vegetation is classified as a lowland dipterocarp forest of Keruing (*Dipterocarpus*) -Meranti (*Shorea*) type. The Pasoh FR is located 70 km southeast of Kuala Lumpur, Peninsular Malaysia (2°59' N and 102°18' E).

Climatic conditions in the Pasoh FR are shown in Fig. 1. As no long-term climatic records are available, a recently published short-term record (Sulaiman et al. 1994) is used. The annual precipitation is about 1,600 mm and the mean

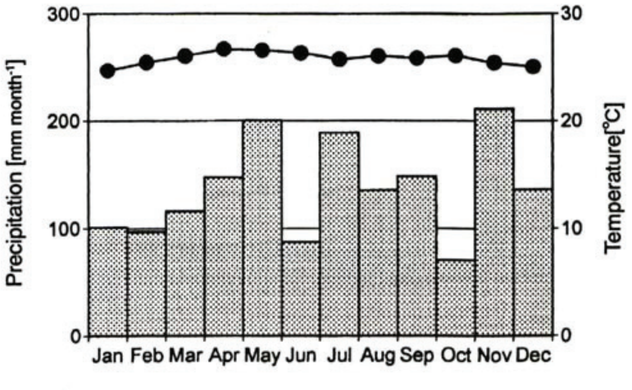

Fig. 1 Climatic condition of the Pasoh FR. Dots with line show the mean temperature and bars show the monthly precipitation during 1991 to 1993.

temperature is 26℃. During the dry season the precipitation is less than 100 mm per month and so the Pasoh FR seems to be drier than other tropical rain forests. The fluctuation of air temperature is limited within the narrow range and the deviation from the mean temperature is relatively small.

In this chapter we focus on three study sites, the 50-ha Plot, Plot 1 and Plot 2. These plots are shown as "primary forest plot", IBP plot and regenerating forest plot respectively in Chap. 2. The 50-ha Plot is covered by primary forest and is located in the center of the forest. Plot 1 is also covered by primary forest. By contrast, Plot 2 is characterized by regenerating forest and is located in the buffer zone of the Pasoh FR. In addition to these permanent plots, we used three more sites for physico-chemical analyses and root biomass measurement. Samples for physico-chemical analyses were taken also from a primary forest site other than the three permanent plots in the Pasoh FR that were mentioned above (the Plot 1, Plot 2 and 50-ha Plot). Mineral nitrogen pool was measured at the Plot 1, Plot 2 and a logged forest which was located in Serting area near Pasoh FR. In the logged forest in Serting, we also collected materials of termite mound for the measurement of the mineral nitrogen pool. Net nitrogen mineralization rate and fine root biomass were measured at another site in a primary forest which was established at the end of access-road to Pasoh FR and used in Yamashita & Takeda (1998).

3. DISTRIBUTION OF SOIL TYPES

En route to the 50-ha Plot, one of the permanent plots in the forest, one notices that the soil color is somewhat whiter than that commonly perceived to be associated with tropical soils. The "typical" soil color in tropical regions has often been considered, incorrectly, to be lateritic red (Richter & Babbar 1991). Of course, the Pasoh FR does have some areas where the soils are reddish in color. However, the range of reddish soils is restricted to a specific area.

There are several world wide soil classifications. The FAO/UNESCO system and Soil Taxonomy system are commonly used. Additionally, countries have their own local classification systems. In this section, we present the results of soil

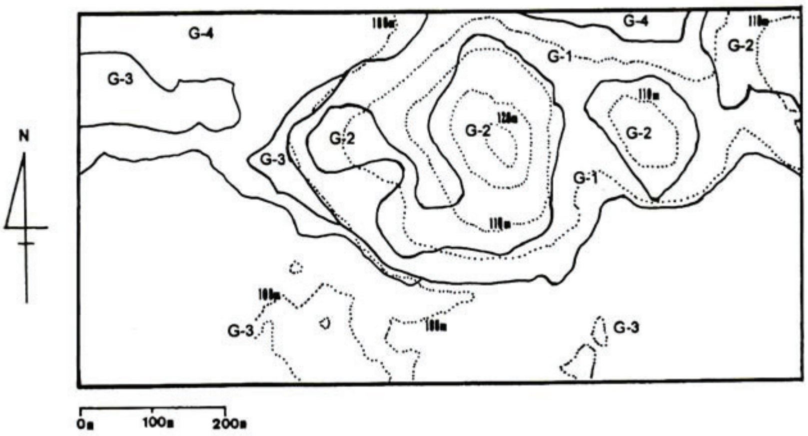

Fig. 2 Distribution of soil types within the 50-ha plot. The symbols 'G-1', 'G-2', 'G-3' and 'G-4' indicate group 1, group 2, group 3 and group 4, respectively. Dotted lines indicate the contour lines at 5 m intervals.

Table 1 Proportional areas of each soil type in the 50-ha Plot of Pasoh FR (The "na" indicates "not available").

Group	Soil type		Proportion to total area
	Malaysian method	Soil Taxonomy	
Group 1	Bungor	Typic Paleudults	20.8%
Group 2	Terap	na	10.8%
	Gajah Mati	Orthoxic Tropudults	5.7%
Group 3	Tebok	Typic Paleudults	8.6%
	Tebok (ms)	na	2.3%
	Tawar	Typic Kanhapludults	18.9%
	Tawar (p)	na	19.4%
Group 4	Awang	Aquic Paleudults	1.9%
	Alma	na	1.3%
	Kampong Pusu	Aeric Plinthic Kandiaquults	2.2%
	Kampong Pusu (cs)	na	8.1%

Table 2 Vertical distribution of soil color of each soil type in the 50-ha Plot. Soil color is described in the way of Munsell's soil color charts. Data of KPU (cs) is not available, but soil color is similar to KPU.

Group	Soil type	Top soil	Semi top soil	Deep soil
Group 1	BGR	10YR5/3	10YR5/8	10TR6/8
Group 2	TRP	7.5YR3/2	10YR5/4	10YR6/6
	GMI	10YR5/8	—	7.5YR6/8
Group 3	TBK	7.5YR4/3	7.5YR5/6	7.5YR6/8
	TBK(ms)	10YR5/4	10YR5/6	10YR6/8
	TWR	10YR3/3	10YR5/4	10YR6/8
	TWR(p)	10YR4/2	10YR5/3	10YR7/3
Group 4	AWG	10YR5/3	10YR6/4	10YR7/4
	AMA	10YR5/2	2.5Y7/2	2.5Y8/2
	KPU	5YR4/1	5YR7/1	5YR7/2
	KPU(cs)	—	—	—

surveys conducted at the 50-ha Plot in primary forest, Plot 1 in another area of primary forest and Plot 2 in regenerating forest, using the Malaysian classification method (Paramananthan 1983).

3.1 The 50-ha Plot

The 50-ha Plot is in a primary forest. A detailed soil map shows that four groups with 11 types of soil are contained within that plot (Fig. 2). Group 1 has only one soil type, Bungor (BGR), a well-drained soil developed from shale. Group 2 consists of Terap (TRP) and Gajah Mati (GMI) series, on lateritic materials. Group 3 which has four soil types, Tebok (TBK), Tebok medium sand variants (TBK (ms)), Tawar (TWR) and Tawar pale variants (TWR(p)) series, is a series of a moderately well or well drained soils. Group 4 has developed in alluvial or riverine areas and is divided into Awang (AWG), Alma (AMA), Kampong Pusu (KPU) and Kampong Pusu coarse sand variants (KPU (cs)) series.

Table 3 Description of soil profiles of Plot 1 and 2. Si, C and L in Texture indicates silty, clay and loam, respectively. Med, Cor, Gr, SA, A and Bl in Structure indicates medium, coarse, granular, subangular, angular and blocky, respectively. Root is shown by [size] / [frequency] and F, M and C in size indicate fine, medium and coarse, respectively.

Horizon	Depth [cm]	Texture	Soil Color	Mottle	Structure	Hardness	Root	Boundary
PLOT 1								
Malacca (Petroplinthic Haplorthox)								
A	0-5	C	10YR 4/2	-	Fine Gr	Friable	FM / few	clear
B11t	5-20	C	10YR 6/6	-	Med SA Bl	Friable	MC / few	gradual
B12	20-60	Si L	7.5YR 6/8	-	Med SA Bl	Friable	FM / common	diffuse
B13	60-80+	Si L	7.5YR 6/8	-	Med SA Bl	Friable	M / few	-
Bungor lateritic phase								
A	0-5	Si C L	10YR 5/3	-	Fine Gr	Friable	FM / frequent	clear
B11	5-25	Si L	2.5YR 7/6	-	Med SA Bl	Friable	MC / common	diffuse
B12	25-55	Si L	2.5YR 7/6	-	Med SA Bl	Friable	F / few	diffuse
B21	55-80	Si L	2.5YR 7/6	10YR 7/2	Med SA Bl	Slightly Firm	F / few	-
B22	80-90	Si L	2.5YR 7/6	10YR 7/2	Med SA Bl	Slightly Firm	F / few	gradual
B23	90-120+	Si L	2.5YR 7/6	10YR 7/2	-	Firm	F / few	-
PLOT 2								
Kuah (Typic Paleudults)								
A	0-10	L	10YR 4/3	-	Med SA Bl	Friable	FC / frequent	gradual
B	10-20	L	7.5YR 6/8	-	Med SA Bl	Friable	M / common	diffuse
BC1	20-70	Si L	7.5YR 6/8	-	Med SA Bl	Firm	M / few	diffuse
BC2	70-90+	Si L	7.5YR 6/8	-	Med SA Bl	Firm	M / very few	-
Kuala Brang								
A	0-10	C L	10YR 4/3	-	Med Gr	Friable	FC / frequent	gradual
B11	10-70	Si L	7.5YR 6/8	-	Med SA Bl	Friable	FM / common	diffuse
B12	70-90	Si L	7.5YR 6/8	-	Med SA Bl	Slightly Firm	M / few	diffuse
B21	90-110+	Si L	7.5YR 6/8	-	Med SA Bl	Firm	-	-
Bungor (Typic Paleudults)								
A	0-15	Si L	10YR 5/6	-	Med SA Bl	Friable	M / common	clear
B11	15-70	Si L	10YR 6/8	-	Med SA Bl	Friable	M / few	diffuse
B12	70++	Si L	10YR 6/8	-	Med SA Bl	Slightly Firm	M / few	-
Kampong Pusu (Aeric Plinthic Kandiaquults)								
Ap	0-10	Si L	10YR 5/3	-	Med SA Bl	Friable	M / common	clear
B11	10-60	Si L	10YR 7/1	10YR 6/8	Med SA Bl	Firm	MC / few	diffuse
B12	60-80	Si L	2.5Y 7/0	-	Cor A Bl	Firm	M / few	gradual
B13	80-100	Si C L	2.5Y 3/0	-	Cor A Bl	Firm	M / few	gradual
B14	100-120+	Si L	5Y 7/4	-	Cor A Bl	Firm	-	-

Unfortunately, not all soils classified under the Malaysian system are necessarily coordinated to the Soil Taxonomy (Soil Survey Staff 1998). Nevertheless, most soils of the 50-ha Plot are Ultisols (Table 1). Among the Ultisols, Udults are the dominant types in Groups 1, 2 and 3. The soils of Group 4 are influenced by water movement and KPU and AWG can be classified as Aquults and Aquic Paleudults, respectively (Jabatan Pertanian 1993).

Based on the detailed soil map, we estimated the areas of each soil type (Table 1) and described representative soil profiles and the vertical distribution of soil color (Table 2). The dominant soil group is Group 3, which occupies half of the plot. The soil color of this group is yellowish brown with the exception of TBK, which is bright brown or orange at deeper horizons. Soils from Group 4, which occur only along a narrow band, are periodically waterlogged during the rainy season. Soil color is gray except for AWG.

3.2 Plot 1

Plot 1, also in primary forest, is 6 ha in area and consists of only two soil types, the Malacca (MAL), and Bungor lateritic phase (BGR/l) series, belonging to Group 1 (Fig. 3). The plot is located on a gentle slope and MAL is distributed on the upper slopes and the BGR/l series on the lower slopes. MAL is the dominant soil type. The results of the soil survey are shown in Table 3. MAL is orange at deeper horizons and yellowish brown with clay texture in the upper horizons. BGR/l is a red colored soil with gray mottle at depth. Both soils have topsoil with a fine granular structure, and exhibit sub-angular blocky structures in deeper horizons.

3.3 Plot 2

Plot 2, in regenerating forest, is also 6 ha in area and consists of four soil types belonging to two groups (Fig. 4). Kuah (KUA), Kuala Brang (KBG), BGR and KPU series are recognized at this site. KUA is distributed on a broad ridge. The KBG series is found on upper slopes and BGR on lower slopes. KPU occurs in the poorly drained swampy area. KBG occupies the largest area of Plot 2, and KUA has the most limited distribution. The results of soil survey are shown in Table 3. As in the 50-ha Plot, KPU exhibits white or gray coloration reflecting poor drainage. BGR has silty loam texture at all horizons. Other soil series also show silty loam textures at deeper horizons. Other than the topsoil of KBG, which is granular, all horizons in this plot show subangular or angular structure.

4. SOIL PHYSICO-CHEMICAL PROPERTIES

Local variation in soil properties is at least as great in the tropics as elsewhere in the world (Richter & Babbar 1991). The physico-chemical properties of soils in the Pasoh FR can also be expected to exhibit diverse characteristics. Under similar climatic conditions, the study plots in the Pasoh FR have nevertheless developed not only various soil types but also differing soil properties depending upon differences in geology, biota, hydrology, and microclimate.

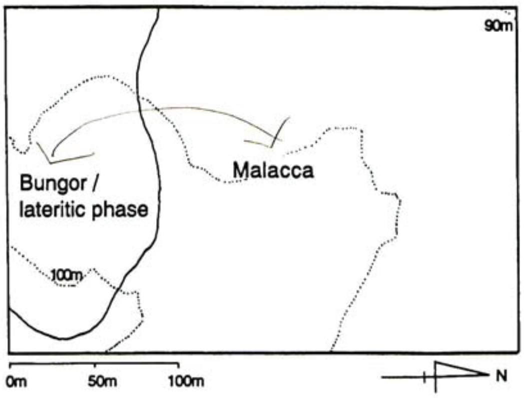

Fig. 3 Distribution of soil types within the Plot 1. Dotted lines indicate the contour lines at 5 m intervals.

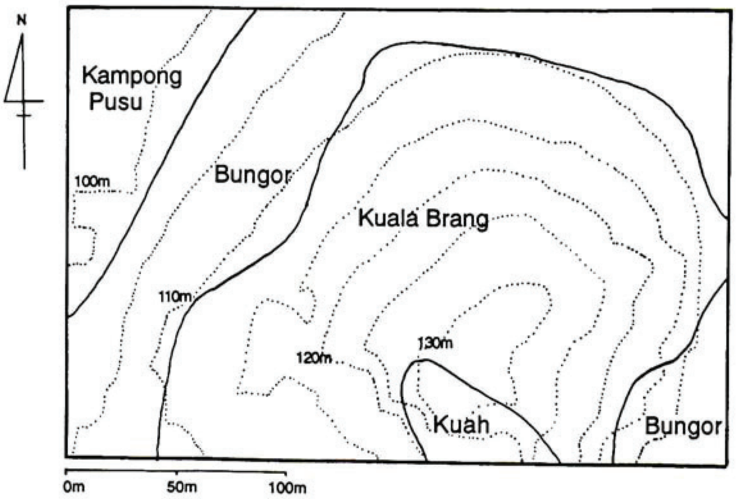

Fig. 4 Distribution of soil types within the Plot 2. Dotted lines indicate the contour lines at 5 m intervals.

4.1 Physical properties

An understanding of the physical properties of tropical soils is important both for sustaining high levels of production and for preserving the stability of ecological environments (Lal 1987). Physical properties can be divided into structural and functional properties. Particle size distribution, bulk density and other factors contribute to structural properties. In general, the higher potential for exchange sites on clay surfaces renders clay-rich soils more fertile than those dominated by coarser particles. The functional properties include water holding capacity and consistency.

We determined the vertical particle size distribution at Plots 1 and 2 and for several other soil types in the Pasoh FR (Fig. 5). MAL and BGR/l from Plot 1 and the deeper horizon of KPU from Plot 2 are low in sand (coarse + fine sand < 20%). The upper horizons of AWG series soils exhibit higher sand contents (> 60%). The other soil types show intermediate sand content. The clay content of the profiles ranges widely from 0 to 70%. Apart from MAL, the mean clay contents through the soil profiles in Plots 1 and 2 were around 20%. Silt contents of Padang Besar (PBR), Berserah (BER) and AWG are less than 20%.

Lal (1987) noted that 85% of the Ultisols and Alfisols in Northeast Brazil contained less than 20% silt and that 20% of soils had clay contents of between 0 to 20%. A recently developed Inceptisol in Venezuela contains greater amounts of silt (Pla Sentis 1977 cited in Lal 1987). The sedentary soils of West Africa are characterized by low silt content (Mbagwu et al. 1983), whereas loess soils from the sahel zone contain high amounts of silt and fine sand and are easily compacted. Soils from the Lambir Hills Forest in Sarawak have 62.4 to 87.1% sand, 5.2 to 15.9% silt and 7.5 to 21.6% clay (Ishizuka et al. 1998). Proportions of the three soil particle sizes in the Sakaerat Forest in Thailand range from 38.9 to 75.1% for sand, 5.5 to 16.6% for silt and 10.6 to 50.1% for clay (Sakurai et al. 1998). Ohta & Effendi (1992a) reported higher silt content in finer textured soils from East Kalimantan than from the Lambir or Sakaerat Forests. However, the East Kalimantan soil silt content is

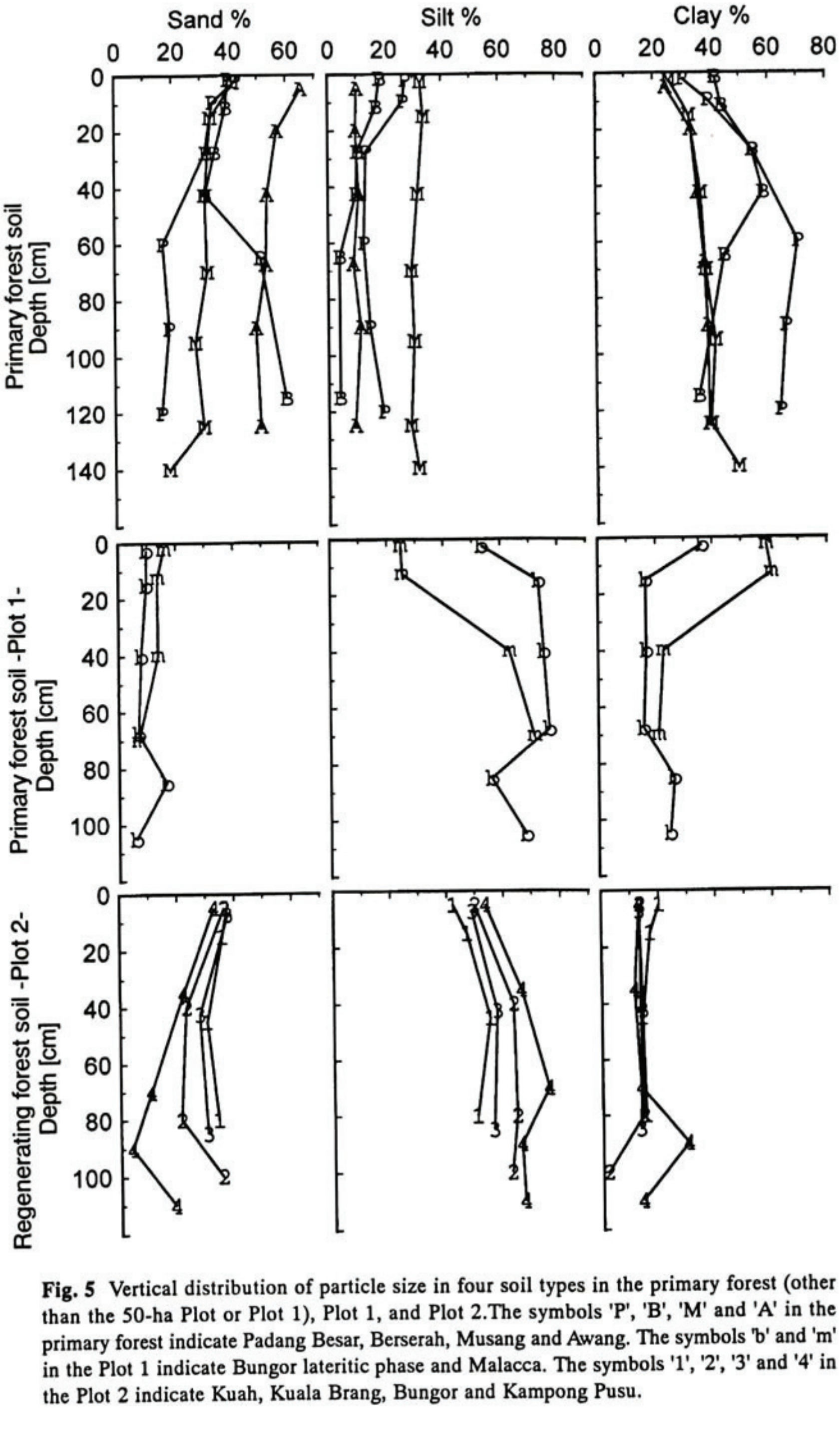

Fig. 5 Vertical distribution of particle size in four soil types in the primary forest (other than the 50-ha Plot or Plot 1), Plot 1, and Plot 2.The symbols 'P', 'B', 'M' and 'A' in the primary forest indicate Padang Besar, Berserah, Musang and Awang. The symbols 'b' and 'm' in the Plot 1 indicate Bungor lateritic phase and Malacca. The symbols '1', '2', '3' and '4' in the Plot 2 indicate Kuah, Kuala Brang, Bungor and Kampong Pusu.

still lower than that of the soils in Plots 1 and 2 of the Pasoh FR. Although the sand and silt content of BER and AWG are within the same range as those of soils from the Sakaerat Forest, the other soil series overall are characterized by lower sand content and higher silt content than those reported from Sakaerat or Lambir Hills Forests.

4.2 Chemical properties

The major cations are derived from weathering of parent materials. Weathering processes are physically, chemically and biologically driven. The exchange sites on the surface of clay minerals or organic materials adsorb cations, forming cation pools and these supply nutrients for most forest plants. The sizes of exchangeable cation pools in the soil are good indices for cation availability in forest ecosystems. In some types of soil, the capacity for soil nutrient retention originates primarily from organic matter (Kauffman et al. 1998). Organic matter is also an important

Table 4 Chemical properties of four soils in primary forest stands. 'av-P' indicates available P by Bray (II) method. BS indicates base saturation rate and is defined as (K+Na+Mg+Ca) × 100 × CEC^{-1}.

	Total [%]			mg kg^{-1}	cmol (+) kg^{-1}						[%]	
Horizon	**C**	**N**	**C/N**	**av-P**	**K**	**Na**	**Mg**	**Ca**	**Al**	**CEC**	**BS**	**pH**
Padang Besar (Orthoxic Tropudults)												
Ai	2.29	0.16	14.3	3.9	0.31	0.13	0.61	0.49	2.37	5.17	29.8	4.5
AB	0.83	0.07	11.9	1.4	0.08	0.09	0.23	0.05	3.21	7.67	5.9	4.4
B21t	0.42	0.06	7.0	0.9	0.14	0.18	0.10	0.08	3.58	5.34	9.4	4.7
B22t	0.42	0.04	10.5	0.5	0.10	0.12	0.07	0.05	3.59	5.94	5.7	4.7
B23t	0.31	0.04	7.8	0.3	0.09	0.09	0.06	0.03	3.28	6.45	4.2	4.6
BC	0.23	0.03	7.7	0.4	0.09	0.10	0.07	0.08	3.62	11.56	2.9	4.6
Berserah (Typic Kandiults)												
Ai	3.37	0.26	13.0	3.4	0.20	0.26	0.56	0.06	2.28	6.35	17.0	4.0
AB	1.56	0.14	11.1	1.5	0.12	0.14	0.39	0.06	1.84	3.77	18.8	4.2
B21t	0.60	0.06	10.0	0.5	0.05	0.06	0.10	0.08	1.62	3.50	8.3	4.4
B22t	0.66	0.06	11.0	0.3	0.04	0.04	0.05	0.05	2.10	3.78	4.8	4.3
B23(Qq)	0.47	0.04	11.8	0.9	0.06	0.07	0.03	0.04	1.77	2.39	8.4	4.5
BC	0.24	0.03	8.0	0.3	0.04	0.02	0.06	0.06	1.30	2.31	7.8	4.7
Musang (Plinthic Kandiudults)												
A	1.76	0.12	14.7	2.5	0.10	0.10	0.14	0.12	2.99	6.42	7.2	3.9
AB	1.03	0.08	12.9	1.6	0.03	0.03	0.03	0.02	3.42	8.01	1.4	4.1
B21	0.35	0.04	8.8	0.9	0.02	0.03	0.04	0.03	3.31	5.18	2.3	4.5
B22	0.24	0.03	8.0	0.3	0.03	0.02	0.00	0.08	3.46	5.08	2.6	4.5
B23	0.24	0.03	8.0	0.4	0.03	0.04	0.04	0.15	3.70	6.00	4.3	4.7
B24	0.16	0.03	5.3	0.3	0.02	0.04	0.01	0.04	4.38	10.38	1.1	4.7
BC	0.13	0.02	6.5	0.5	0.01	0.01	0.00	0.02	5.02	8.95	0.4	4.8
Awang (Aquic Paleudults)												
A	1.63	0.15	10.9	4.2	0.16	0.18	0.14	0.19	2.33	2.86	23.4	4.0
AB	0.91	0.09	10.1	2.2	0.12	0.13	0.09	0.10	2.15	2.94	15.0	4.5
B21	0.57	0.05	11.4	1.4	0.04	0.06	0.06	0.08	2.18	2.84	8.5	4.3
B22	0.43	0.05	8.6	1.2	0.02	0.02	0.06	0.12	2.84	2.73	8.1	4.5
B23	0.36	0.05	7.2	0.8	0.01	0.02	0.06	0.12	1.96	2.83	7.4	4.6
B24	0.28	0.04	7.0	1.1	0.02	0.03	0.04	0.09	1.86	2.61	6.9	4.5

source of soil nitrogen, phosphorus and sulfur. Organic matter content is evaluated from the total C and N.

Some chemical properties, including C, N and macro-nutrients, of four soil series from natural stands of primary forest, not from either the 50-ha Plot or Plot 1, are shown in Table 4. Unfortunately, no data is available from regenerating forest. Total C and N contents range from 0.13 to 3.37% and 0.02 to 0.26%, respectively. Available P is in the range 0.3 to 4.2 mg kg^{-1}. The sum of exchangeable cations (K + Na + Mg + Ca) varies between 0.11 to 1.54 cmol (+) kg^{-1} and CEC from 2.31 to 11.56 cmol (+) kg^{-1}. Exchangeable Al is 1.30 to 5.02 cmol(+) kg^{-1}. Base saturation results, between 0.4 and 29.8%, decrease abruptly from the upper to deeper horizons. The pH (H_2O), range 3.9 to 4.8, increased with depth. This last observation may reflect the increase in Fe and Al oxide contents and the decrease in organic matter content (Sanchez 1976).

Kauffman et al. (1998) reported a spread of organic C contents from 0.8 to 2.3% from a range of humid tropical forests. Yamashita et al. (1999) reported similar values in the Sakaerat Forest and much higher values in the Kog Ma Forest of Thailand. Some top soils in a dipterocarp forest in East Kalimantan (Ohta & Effendi 1992b) and a hill dipterocarp forest in Peninsular Malaysia (Tange et al. 1998) also have higher C content than those of the Pasoh FR. The trends for N content are similar to those of C.

In the Sakaerat Forest, available P in top soils ranges from 11.9 to 20.8 mg kg^{-1} (Sakurai et al. 1998). A broader variation (about 10 to 40 mg kg^{-1}) has been reported from the top horizons of a hill dipterocarp forest soil (Tange et al. 1998). Ultisols of East Kalimantan have an even wider range of available P, about 4 to 50 mg kg^{-1} (Ohta & Effendi 1992b). In the Pasoh FR, available P in topsoil was at most 4.2 mg kg^{-1}. A soil is usually deemed infertile if the available P falls to 3 mg kg^{-1} or less. By comparison with other tropical rain forest soils in Southeast Asia, the Pasoh FR seems to be deficient in available P.

In Ferralsols or other dominant soils in humid tropics, the ranges of total cations and CEC in topsoil are 1.0 to 2.2 cmol (+) kg^{-1} and 6.6 to 20.0 cmol (+) kg^{-1}, respectively. The exceptions are Luvisols and Cambisols (Kauffman et al. 1998). Values from Pasoh FR are within this range, but located at lower end. The base saturation rate is very low at deeper horizons reflecting low cation content. The soils of East Kalimantan (Ohta et al. 1993), Lambir (Ishizuka et al. 1998), Peninsular Malaysia (Tange et al. 1998), and Sakaerat (Sakurai et al. 1998) Forest show similar values to those presented in Table 4.

The average value of exchangeable Al for a range of tropical forest soils is reported to be less than 2 cmol (+) kg^{-1} (Kauffman et al. 1998). The highest value reported by Sakurai et al. (1998) in a deep horizon soil from the Sakaerat Forest was 2.15 cmol (+) kg^{-1}. Soils of the Pasoh FR contain greater amounts of exchangeable Al (maximum 5.02 cmol (+) kg^{-1} in Musang (MUS) series) than some previously reported values (Kauffman et al. 1998; Sakurai et al. 1998). However, Ohta et al. (1993) found much higher exchangeable Al contents ranging from 2 to 18 cmol (+) kg^{-1} in East Kalimantan. Aluminium or Al in soil fixes phosphorus to eventually form varicite or wavellite, which are unavailable to plants. Furthermore, Al *per se* is harmful to plant life.

4.3 Relationships between physical and chemical properties

Physical and chemical properties affect each other. CEC, available P and exchangeable Al are related to soil particle size (Fig. 6). The changes in CEC are

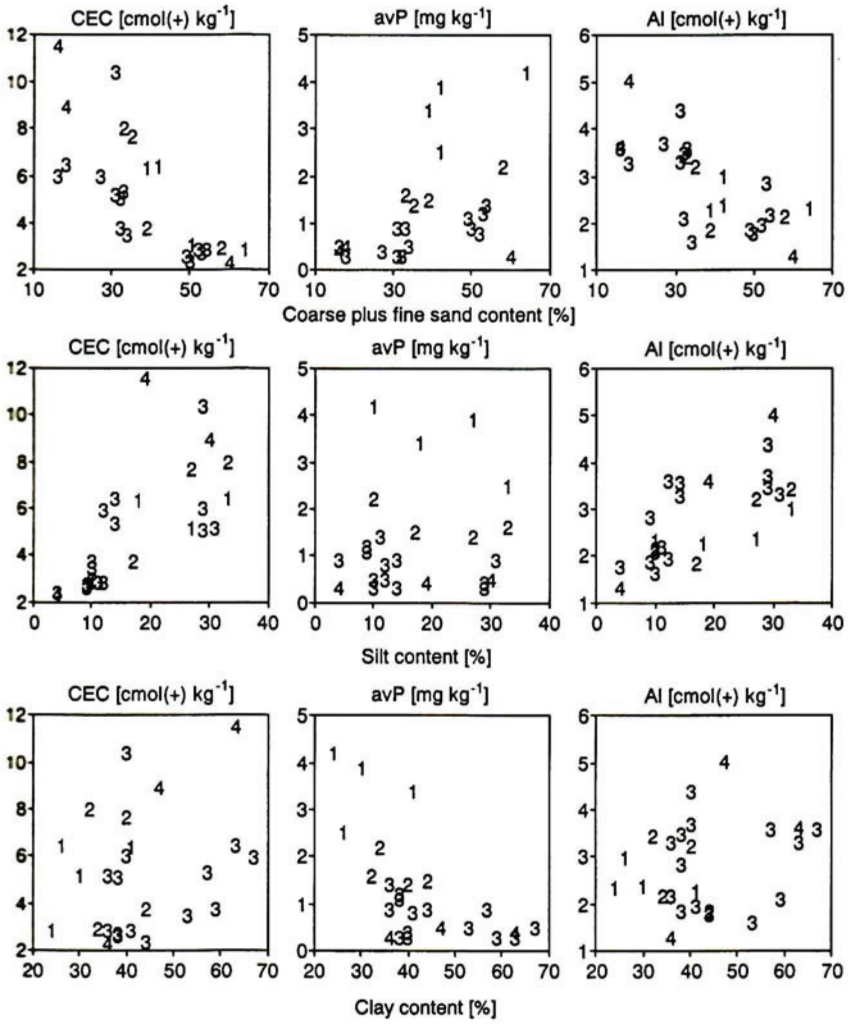

Fig. 6 Relationships between the soil particle sizes and three chemical properties. Upper, middle and bottom indicate the relationships of (coarse plus fine) sand fraction, silt and clay to chemical properties, respectively. The symbols '1', '2', '3' and '4' indicate A horizon, AB horizon, B horizon and BC horizon, respectively.

inversely related to coarse sand content and positively related to silt content. However, the clay fraction, which can function as an effective cation exchange site (Ohta et al. 1993), has no obvious effects on CEC in the Pasoh FR soil. Organic matter has potential for cation retention, but no significant correlations are observed between silt content and total C, nor between CEC and total C. Thus, there is a possibility that the silt fraction, or silt-related properties, might play important roles in cation retention in soils of the Pasoh FR.

Available P shows positive but weak correlation with sand content and negative correlation with clay content. This negative relationship between P availability and clay content is also observed in Ultisols at East Kalimantan (Ohta et al. 1993). A higher degree of P immobilization is observed in clayey Ultisols, than in sandy Ultisols (Woodruff & Kamprath 1965). Available P shows significant correlation with C and N. Sources of available P are weathered parent materials and organic matter. In weathered tropical soils, organic matter may be an important source of available P. Organic matter acts not only as a source of P but also tends to deactivate P-fixing agents (Ohta et al. 1993). Organic matter accumulates on the forest floor at the soil surface and gradually decreases with soil depth. Although the physical properties of soil could affect P availability, the amount of organic matter is the more dominant factor in determining P availability. Since the depth of a soil horizon indirectly determines the amount of organic matter, data points from the same horizon are plotted at approximate levels in a scatter diagram (Fig. 6).

Exchangeable Al indicates a negative relationship with sand content and a positive relationship with silt content. This trend for exchangeable Al is similar to that of CEC. There is a significant correlation between exchangeable Al and CEC. In the Pasoh soils exchangeable Al occupies at least 36% of the available CEC. The Awang series shows greatest Al occupancy at all horizons with more than 70% of CEC taken up by exchangeable Al. Al is widely distributed in the soils, the exchangeable Al content is dependent upon CEC, and Al affects the availability of P. Therefore the CEC and exchangeable Al are both inversely related to available P. The available P content is low in horizons with greater exchangeable Al. Comparatively high exchangeable Al content increases the possibility of P deficiency (Attiwill & Adams 1993).

5. SOIL BIOLOGICAL PROPERTIES

The constituents of soil biota include microbes, soil animals and plants. In this context, the soil N, an important resource for soil animals and plants, cycles between the abiotic and biotic components in soil system and is regulated by the microbial activity. Fine roots are the active interface between plants and the soil system. Both the soil N and fine root biomass are the critical biological factors for sustaining the forest productivity. To date however, they have been little studied in the Pasoh FR.

5.1 Soil N dynamics

Soil N is one of the critical nutrients for plant growth. The N availability limits net primary production in terrestrial ecosystems (Vitousek & Howarth 1991). Traditionally, N availability has been assessed by measuring net N mineralization rates in soils (Binkley & Hart 1989). Ordinarily, net N mineralization rate is defined as the increment in inorganic N during a certain period of incubation, i.e. [net N mineralization rate] = [inorganic N pool after incubation] - [inorganic N pool before incubation]. Reich et al. (1997) showed that the aboveground net primary production increased linearly with annual net N mineralization rate in temperate forest ecosystems.

Recently a new pathway to utilize organic N has been discovered in some ecosystems at higher latitudes where the N availability is low (Chapin et al. 1993; Northup et al. 1995; Read et al. 1989). The increased N content in wet and dry deposition has altered soil processes including soil N dynamics around industrialized areas in temperate zones (Aber et al. 1989; Dise & Wright 1995). The Pasoh FR received 9.6 kg N ha^{-1} yr^{-1} through precipitation in 1973 (estimated by authors using the data presented in Manokaran (1978)). N deposition ranged from 1.7 to 21 kg N ha^{-1} yr^{-1} in the tropics (Vitousek & Sanford 1986). The tropical forest in Monteverde received 7.5 kg N ha^{-1} yr^{-1} from 1991 to 1992 (Clark et al. 1998). Although the N deposition in tropical forest is still low by comparison with that in temperate zones, anthropogenic N deposition could possibly increase in tropical region for decades (Matson et al. 1999). Despite the importance of grasping of soil N dynamics in tropical forest ecosystems, the basic study on net N mineralization rates in soils was insufficient in tropical forests (Vitousek & Sanford 1986). Since then, net N mineralization rate has been measured mainly in the neotropics. Even now, studies on net N mineralization rates are limited for the tropical rain forests of Southeast Asia. We discuss the pool size of inorganic N and net N mineralization rate mainly in neotropics and then compare our results from the Pasoh FR.

5.2 Inorganic N pool

The pool size of inorganic N shows the balance between input to soil system (e.g. mineralization, deposition and fixation) and output (e.g. plant uptake, leaching and immobilization). In boreal coniferous forest, the pool of inorganic N decreases in summer and increases in winter (Bashkin & Kudeyarov 1977). At higher latitudes, the input of inorganic N seems to underperform the N output. Conversely, in a temperate coniferous plantation, the pool size increases in summer and decreases in winter (Yamashita et al. 1992). At this location the input exceeded the output even in summer. In the dry tropical forests of India (Roy & Singh 1995) and the Amazonian forests (Neil et al. 1995), the pool size decreases in the wet (summer) season and increases in the dry (winter) season. Soil systems appear to supply more N in the temperate zone and less in the boreal and tropical region, than plant requirements. Low input of inorganic N in the boreal regions is attributable to low mineralization rates due to low temperature. High output rate due to vigorous growth of plants is one of the causative factors for decrease in inorganic N pool during the summer season in the tropical savanna and forest.

Though the pool size oscillates with ambient environment, temporal variation is often ignored, because it is reported as an average. In the Amazonian forests, the pool of NH_4^+-N at 0 – 5 cm deep soil ranges from 1.83 to 17.59 μg N g^{-1} and that of NO_3^--N from 1.07 to 11.87 μg N g^{-1} (Neil et al. 1997). In the tropical savanna of India, the ranges in 0 – 10 cm deep soil for NH_4^+-N and NO_3^--N are 2.6 to 5.8 μg N g^{-1} and 0.2 to 1.2 μg N g^{-1}, respectively (Singh et al. 1991). The organic layer on the forest floor contains 7.8 to 94.4 μg N g^{-1} of NH_4^+-N and 0 to 2 μg N g^{-1} of NO_3^--N in the neotropics (Vitousek & Matson 1988). On an area basis, the inorganic N pool is <40 kg N ha^{-1} 15 cm^{-1} for NH_4^+-N and <5 kg N ha^{-1} 15 cm^{-1} for NO_3^--N in a secondary forest of Costa Rica (Matson et al. 1987), and 1.6 kg N ha^{-1} 10 cm^{-1} for NH_4^+-N and 6.7 kg N ha^{-1} 10 cm^{-1} for NO_3^--N in an old-growth forest of Costa Rica (Zou et al. 1992).

In the Pasoh FR, we determined the pool sizes of NH_4^+-N and NO_3^--N in 0 – 10 cm deep soil in the Plot 1, Plot 2, logged forest and material from termite mounds (Table 5). Differences in soil types may also affect the pool of inorganic N, but the current condition of the forest canopy could be a more effective determinant. Termite mounds accumulate organic matter and nutrient elements and are thought to be key contributors to nutrient dynamics in the Pasoh FR. Soil cores, 25 cm^2 in cross section and 10 cm long, were collected from the closed canopy site, gap center and gap peripherals of the primary (including Plot 1) and regenerating forests (Plot 2), and from another site in logged forest outside the Pasoh FR. The pool size ranged from 1.4 to 5.5 μg N g^{-1} for NH_4^+-N and from 12.2 to 19.3 μg N g^{-1} for NO_3^--N

Table 5 Pool size of inorganic N in soils of the Pasoh FR. Values are means ± 1SE. The word 'Sum' indicates the sum of NH_4^+-N plus NO_3^--N.

Site	condition	*N*	Concentration per dry weight [$\mu g\ g^{-1}$ DW]			Concentration per soil volume [$kg\ ha^{-1} 10cm^{-1}$]		
			NH_4^+-N	NO_3^--N	Sum	NH_4^+-N	NO_3^--N	Sum
Primary forest	closed forest	10	2.6 ± 0.2	12.2 ± 2.0	14.8 ± 1.9	1.8 ± 0.2	8.3 ± 1.3	10.1 ± 1.2
	gap center	8	1.4 ± 0.2	13.2 ± 1.1	14.6 ± 1.0	1.0 ± 0.2	9.7 ± 1.0	10.7 ± 0.9
	gap peripheral	8	1.8 ± 0.2	15.1 ± 3.7	16.9 ± 3.6	1.3 ± 0.1	11.2 ± 2.8	12.5 ± 2.7
Regenerating forest	closed forest	10	3.3 ± 0.7	16.9 ± 5.0	20.2 ± 5.3	2.5 ± 0.6	13.0 ± 4.2	15.6 ± 4.5
	gap center	8	2.8 ± 0.3	19.4 ± 3.4	22.3 ± 3.6	2.3 ± 0.2	15.9 ± 2.7	18.3 ± 2.9
	gap peripheral	8	6.1 ± 1.5	17.7 ± 3.6	23.9 ± 4.5	4.6 ± 1.1	13.5 ± 2.7	18.1 ± 3.3
Logged forest	not specified	10	4.7 ± 0.8	17.1 ± 1.9	21.8 ± 1.4	4.7 ± 0.9	17.0 ± 2.3	21.6 ± 2.2
Termites mounds	black coloured	1	65.8	67.7	134	–	–	–
	brown coloured	1	377	25.3	402	–	–	–

at the forest sites. Materials from termite mounds showed much higher contents of inorganic N reflecting higher biological activity. On an area basis, NH_4^+-N pool ranged from 1.0 to 4.7 kg N ha^{-1} 10 cm^{-1} and NO_3^--N ranged from 8.3 to 17.0 kg N ha^{-1} 10 cm^{-1}.

The NO_3^--N pool exceeded that of NH_4^+-N at all sites except one of the termite mounds (brown colored). But many of the published reports mentioned earlier, show the pool size of NH_4^+-N exceeding that of NO_3^--N. Negatively charged NO_3^--N tends to leach from the soil profile, due to the lack of anion exchange capacity (AEC) on soil particles under ordinary conditions. Positively charged NH_4^+-N is adsorbed onto soil particles that have substantial CEC. Upward transport or the accumulation of NO_3^--N is supposed to occur when the soil becomes drier (Sanchez 1976; Wild 1972). Where enough H^+ is produced in soil, the possibility of generating AEC dependent on zero point charge is suggested (Robertson 1986). AEC conditions (unlikely to occur in the Pasoh FR soils) or drier soil could lead to the NO_3^--N pool size being greater than that of NH_4^+-N in the Pasoh FR. In addition, Matson et al. (1999) pointed out the importance of electrostatic adsorption in controlling losses of excess NO_3^--N to aquatic ecosystems in the tropics.

Since the inherent properties on N dynamics were not described in each forest type before they had been disturbed, we can only compare the current status of N properties among the current forest types. With these restrictions, the effects of forest types and canopy conditions are tested by two-way ANOVA (Table 6). The NO_3^--N pool size shows no significant differences between forest type and conditions of canopy. The pool size of NH_4^+-N in the primary forest is significantly smaller than in other forest types ($P < 0.01$) and also differs between canopy conditions ($P < 0.05$). Soils in the gap peripherals contain more NH_4^+-N than under other canopy conditions. The sum of NH_4^+-N and NO_3^--N differs between the primary and regenerating forest ($P < 0.05$). As a result, the soils of the primary forests contain lesser amounts of inorganic N than in the disturbed forests. Vitousek & Denslow (1986) reported that the pool size of NO_3^--N in the Costa Rican forest showed no increase at the treefall gaps. Similarly, we found no increase in inorganic N pool size at the gap sites as a whole (gap center plus peripheral sites) by comparison with the closed canopy sites. However, in the regenerating forest, a significant increase was observed in the gap peripherals by comparison with the closed canopy sites ($P < 0.05$). Although Vitousek & Denslow (1986) concluded that an increase, not in nutrient, but in light availability seems to represent a more important shift in resources within the treefall gap, our results are not consistent with theirs at least for this specific forest type.

Table 6 Results of an analysis of variance to test for the effects of forest type (primary vs. regenerating) and canopy conditions (closed canopy vs. gap) on the inorganic N pool size at 0–10 cm depth in the soils of the Pasoh FR.

		NH_4-N		NO_3-N		Sum	
	df	*F*	*P*	*F*	*P*	*F*	*P*
Forest type (F)	1	9.715	0.003	2.857	0.097	4.875	0.032
Canopy condition (C)	1	0.021	0.887	0.462	0.500	0.440	0.510
F × C	1	3.294	0.076	0.002	0.965	0.103	0.750

5.3 Net N mineralization rate

The net N mineralization rate is strongly affected by ambient temperature and water regime. The rates are greatest in tropical forest soils and least in arctic or arid ecosystems (Attiwill & Adams 1993). In tropical rain forest, unlike temperate zones, however, seasonal variability in net N mineralization rate is relatively small (Matson et al. 1987; Vitousek & Denslow 1986). Although it is not satisfactory, one-off N mineralization measurements could be representative of annual patterns in the humid tropics (Vitousek & Matson 1988).

In Costa Rican forest, the net N mineralization rate is around 3 μg N g^{-1} day^{-1} and most of the mineralized N was nitrified with no time lag (Robertson 1984). Vitousek & Denslow (1986) reported the net N mineralization rate in intact forest and gaps ranged from 0.9 to 2.1 μg N g^{-1} day^{-1} in Costa Rican forest on volcanic soil. Two years later, Vitousek & Matson (1988) summarized the net N mineralization rate in a range of neotropical soils. They cited ranges from 0 (on Andept in Hawai'i) to 6.8 μg N g^{-1} day^{-1} (at a cleared site on Andept in Costa Rica) at a depth of 0 – 15 cm and from 0 to 8 μg N g^{-1} day^{-1} in organic layers. They also mentioned that these values were greater than in the temperate forest soils, except for forests on white sand or in upper montane areas. In the Amazonian forest, the N mineralization rate is also rapid and ranges from 0.93 to 5.47 μg N g^{-1} day^{-1} at 0 – 5 cm soil depth and 0.49 to 2.39 μg N g^{-1} day^{-1} at depths of 5 – 10 cm (Neil et al. 1997). Annual estimates of the net N mineralization rate in the Costa Rican forest are 588 to 1140 kg N ha^{-1} yr^{-1} (Matson et al. 1987). Nitrogen content in the aboveground fine litterfall is important for plant N requirements, and in various neotropical forests it has a range from 74 to 224 kg N ha^{-1} yr^{-1} (Vitousek & Sanford 1986). Annual estimates for the net N mineralization rate overwhelmingly exceed annual plant requirements. As the net nitrification rate was high at all the above sites, NO_3^--N is thought to be a major N source for plants in these tropical forests. In contrast, Ultisols in East Kalimantan produce NH_4^+-N but not NO_3^--N and the maximum N mineralization rate is 8.3 μg N g^{-1} day^{-1} in the A horizon (Ohta et al. 1992b). Even though the production rate of NH_4^+-N is relatively high, nitrification rates remain low in East Kalimantan.

We measured the net N mineralization rate of a primary forest soil from the Pasoh FR, at 25°C for 30 days using a laboratory incubation method. We collected organic layer, black topsoil and light yellow sub-soil. Results are shown in Table 7. The highest rate of 0.98 μg N g^{-1} day^{-1} is observed in the topsoil but this is still at the lower end of previously reported values. Assuming these values are representative of annual patterns, this extrapolates to an annual estimate on an area basis of 100 kg N ha^{-1} yr^{-1} in 0 – 10 cm deep soil. The annual litterfall of this site is 8.6 Mg ha^{-1} yr^{-1} and the N concentration of leaf litter is around 1.2% dry mass (Yamashita & Takeda 1998), the forest canopy needs about 90 kg N ha^{-1} yr^{-1}. The soil at 0 – 10 cm deep can produce inorganic N just equal to plant requirements in the Pasoh FR. Of the upper 10 cm of soil, the topsoil (0 – 2 cm) produces half of the N required by plants. As discussed above, more fertile sites produce more inorganic N than plant requirements. Excess N at such sites is lost to the aquatic system or denitrified to the atmosphere. Since inorganic N production is restricted to the topsoil and the mineralization rate is relatively low, N seems to cycle tightly within the terrestrial system in the Pasoh FR.

5.4 Fine root biomass

Fine roots play an important role not only in absorbing water and nutrients, but also in dry matter production by rapid turnover. Fine root biomass (FRB) measurement is the first step to clarifying the role of fine roots at ecosystem level.

In October 1991, fifteen soil cores (5.6 cm in diameter) were taken to the depth of 20 cm to measure the FRB in a primary forest of Pasoh FR. The soil cores were then cut horizontally at 4 cm intervals. The soil samples were sieved using tap water and the collected root samples separated according to diameter at root (d): d < 1 mm, 1 ≦ d < 2 mm, 2 ≦ d < 3 mm, 3 ≦ d < 5 mm and d ≧ 5 mm. The results show that the FRB for roots less than 2, 3 and 5 mm in diameter are respectively 624, 751, and 970 g m^{-2}. Vogt et al. (1996) compiled published FRB data for the tropics and showed that the average of 24 tropical broad-leaved evergreen forests was 1,020 (170) g m^{-2} (standard error in parenthesis). The average of six tropical broad-leaved evergreen forests growing on the same Ultisols as in the Pasoh FR was 638

Table 7 Net N mineralization rate at the various soil horizons in the natural forest of Pasoh.

	Concentration per dry weight [μg N g^{-1} DW day^{-1}]			Concentration per soil volume [kg N ha^{-1} cm^{-1} yr^{-1}]		
	NH_4^+-N	NO_3^--N	Sum	NH_4^+-N	NO_3^--N	Sum
Organic layer	0.46	0.00	0.46	0.8	0.0	0.8
Top soil	0.01	0.97	0.98	0.3	25.5	25.8
Sub soil	-0.02	0.25	0.23	-0.5	6.5	6.0

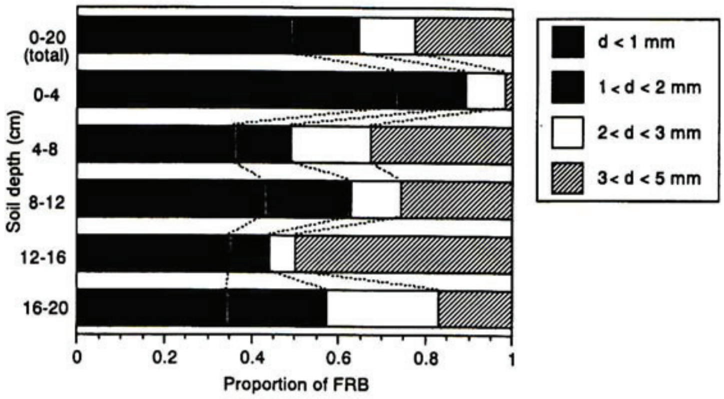

Fig. 7 Proportions of the fine root biomass (FRB) in different diameters at each soil layer. The symbol 'd' shows diameter of fine root.

(306) g m^{-2}. Yoda & Kira (1982) showed that the total FRB for d < 1 cm within 1 m depth was 2,050 g m^{-1} at the Pasoh FR and that the FRB decreased exponentially from surface to deeper horizons. Due to the different limits in the fine root diameters (2–6 mm), the data in Vogt et al. (1996) have been rearranged for comparison. The FRB in d < 2 mm and the FRB in d < 5 mm become 381 (131, N = 7) and 1,342 (263, N = 13) g m^{-2}, respectively. The former value is less than a third lower than the latter. In contrast, the FRB in d < 2 mm occupies 64% of the entire FRB in d < 5 mm in the Pasoh FR (Fig. 7).

Within the top 20 cm, the FRB in d < 1 mm constitutes 73% of total FRB in d < 5 mm at 0 – 4 cm layer and around 40% in all subsequent layers. The proportion of FRB in 3 ≦ d < 5 mm size range fluctuates widely; it is least in the 0 – 4 cm layer and highest at 12 – 16 cm. The vertical distribution differs between the root diameter classes (Fig. 8). The FRB in d < 1 mm peaks between 0 and 4 cm and decreases abruptly with increasing soil depth, by comparison with the gradual decrease in

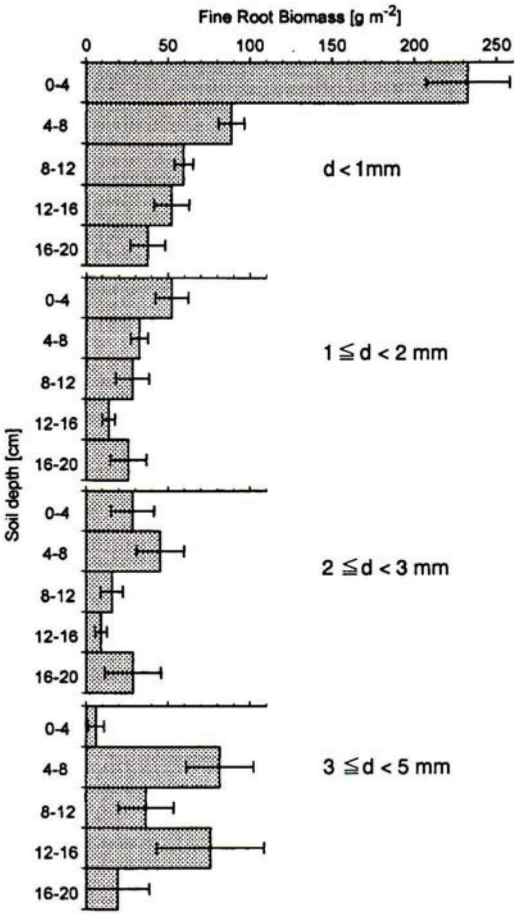

Fig. 8 Vertical distributions of the fine root biomass (FRB) in different diameters. 'd' shows fine diameter of root. Bars indicate one standard error of the mean.

FRB $1 \leqq d < 2$ mm. The size ranges $2 \leqq d < 3$ mm and $3 \leqq d < 5$ mm have peaks below 4 cm in depth. The two smaller classes of FRB are distributed most abundantly in the top layer indicating a lighter texture, while the larger diameter FRB is most abundant somewhere below 4cm depth in the clayey heavy soil in this forest. In the light of these observations, what factors control fine root distribution? From a large-scale perspective Vogt et al. (1996) reported that FRB was positively correlated with annual air temperature, and negatively with the P content of aboveground litterfall. At a more local level, they compared FRB of various diameters with the thickness of the organic layer and A_1, layer at each sampling point, and the organic content in the soil core. This showed that FRB ($d < 1$ mm) correlated with the thickness of A_1 layer, but not with the thickness of the organic layer. This suggests that it is not the accumulation of organic matter, but nutrient release in the A_1 layer that stimulates fine root proliferation.

The variability between the sampling points should be considered to examine the reliability of the data in this study. Bengough et al. (2000) showed that the coefficients of variance of the FRB in core samples from grassland were typically between 30 – 50%. The coefficients of variance in this study are 34, 43, 66 and 90% for $d < 1$ mm, $1 \leqq d < 2$ mm, $2 \leqq d < 3$ mm and $3 \leqq d < 5$ mm fine roots, respectively, indicating relatively sparse distribution of the larger diameter roots. Although the sampling depth (20 cm, in this study) is not enough to collect deep roots, variability of the FRB in $d < 2$ mm is easily detected as it is most abundant in the surface soil layer (just below the organic layer). The core diameter of the soil sampler (5.6 cm) and the number of replications (15) used in this study are within the range commonly adopted procedures (Oliveira et al. 2000). In the future, research on fine root turnover, detailed root distribution, and the interactions of roots of different species is needed, to address the role of roots of various species in the forest ecosystem.

6. CONCLUSION

The Pasoh FR is situated on relatively flat topography. However, there is a wide variation in soil types. Small differences in parent material or drainage cause different types of soils to develop. Although each soil type shows very unique properties, trends in physical properties as a whole can be categorized as low sand content and high silt content. We found that the silt fraction or silt related factors play a more important role than organic matter in cation retention. Critical chemical properties of Pasoh FR soils are extremely high content of Al and low P availability. These appear to act interactively. Where Al is high, P availability decreases, therefore control of Al is required to sustain land productivity in the Pasoh FR.

The inorganic N pool is characterized by a large NO_3^--N pool, which exceeds the NH_4^+-N pool. This might be attributed to the drier conditions or possibly to anion retention. The net N mineralization rate is quite low in comparison with other tropical rain forests. Not only P, but also N, seem to be critical factors for the plant growth.

The soils of the Pasoh FR should be categorized as infertile. The proportion of thinner fine root to total fine root is higher than reported values elsewhere. The proliferation of thinner roots enables the plants to absorb the scarce nutrients in the soil. However, the effective root zone is restricted to the top few cm of soil. N mineralization is also restricted to that zone. As disturbing this zone may cause irreversible damage to the terrestrial ecosystem, the conservation of this zone should be addressed especially in the Pasoh FR.

ACKNOWLEDGEMENT

The authors are grateful to Dr. Amir Husni bin Mohd Shariff for providing basic data on soil survey. They also thank to staff of Soil Chemical Laboratory of FRIM for rendering invaluable laboratory works, to Prof. Hiroshi Takeda for giving us the chance to join the NIES, FRIM and UPM joint research project, and to two anonymous reviewers for critical comments on the manuscript. This paper is partly supported by Japan Environment Agency (Grant No. E-2).

REFERENCES

Aber, J. D., Nadelhoffer, K. J., Streudler, P. & Melillo, J. M. (1989) Nitrogen saturation in northern forest ecosystems. Bioscience 39: 378-386.

Allbrook, R. F. (1972) The soils of Pasoh forest reserve Negeri Sembilan. Malay. For. 36: 22-33.

Attiwill, P. M. & Adams, M. A. (1993) Nutrient cycling in forests. New Phytol. 124: 561-582.

Bashkin, V. N. & Kudeyarov, V. N. (1977) Studying the year round dynamics of mineral nitrogen in a grey forest soil. Sov. Soil Sci. 8: 41-48 (in Russian with English summary).

Bengough, A. G, Castrignano, A., Pages, L. & van Noordwijk, M. (2000) Sampling strategies, scaling, and statistics. In Smit, A. L., Bengough, A. G, Engels, C. & Pellerin, van N. S. (eds). Root methods. Springer-Verlag, Berlin, pp.147-173.

Binkley, D. & Hart, S. C. (1989) The components of nitrogen availability assessments in forest soils. Adv. Soil Sci. 10: 57-112.

Chapin III, F. S., Molianen, L. & Kielland, K. (1993) Preferential use of organic nitrogen for growth by a non-mycorrhizal arctic sedge. Nature 361: 150-153.

Clark, K. L., Nadkarni, N. M., Schaefer, D. & Gholts, H. L. (1998) Atmospheric deposition and net retention of ions by the canopy in a tropical montane forest, Monteverde, Costa Rica. J. Trop. Ecol. 14: 27-45.

Dise, N. B. & Wright, R. F. (1995) Nitrogen leaching from European forests in relation to nitrogen deposition. For. Ecol. Manage. 71: 153-161.

FAO (1995) Forest Resources Assessment 1990, Global synthesis. Forestry Paper No. 124. FAO, Rome.

Ishizuka, S., Tanaka, S., Sakurai, K., Hirai, H., Hirotani, H., Ogino, K., Lee, H. S. & Kendawang, J. J. (1998) Characterization and distribution of soils at Lambir Hills National Park in Sarawak, Malaysia, with special reference to soil hardness and soil texture. Tropics 8: 31-44.

Jabatan Pertanian (1993) Panduan: Mengenali siri-siri tanah utama di Semenanjuang Malaysia. Jabatan Pertanian, Semananjung Malaysia, Kuala Lumpur. 118pp.

Kauffman, S., Sombroek, W. & Mantel, S. (1998) Soils of rainforests: characterization and major constraints of dominant forest soils in the humid tropics. In Schulte, A. & Ruhiyat, D. (eds). Soils of Tropical Forest Ecosystems. Springer, Berlinpp. pp.9-20.

Lal, R. (1987) Tropical Ecology and Physical Edaphology J. Wiley & Sons, New York, 732pp.

Manokaran, N. (1978) Nutrient concentration in precipitation, throughfall and stemflow in a lowland tropical rain forest in Peninsular Malaysia. Malay. Nat. J. 30: 423-432.

Matson, P. A., Vitousek, P. M., Ewel, J. J., Mazzarino, M. J. & Robertson, G. P. (1987) Nitrogen transformations following tropical forest felling and burning on a volcanic soil. Ecology 68: 491-502.

Matson, P. A., McDowell, W. H., Townsend, A. R. & Vitousek, P. M. (1999) The globalization of N deposition: ecosystem consequences in tropical environments. Biogeochemistry 46: 67-83.

Mbagwu, J. S. C., Lal, R. & Scott, T. W. (1983) Physical properties of three soils in southern Nigeria. Soil Sci. 136: 48-55.

Neil, C., Piccolo, M. C., Steudler, P. A., Melillo, J. M., Feigl, B. J. & Cerri, C. C. (1995) Nitrogen dynamics in soils of forests and active pastures in the western Brazilian Amazon basin. Soil Biol. Biochem. 27: 1167-1175.

Neil, C., Piccolo, M. C., Cerri, C. C., Steudler, P. A., Melillo, J. M. & Brito, M. (1997) Net nitrogen mineralization and net nitrification rates in soils following deforestation for pasture across the southwestern Brazilian Amazon Basin landscape. Oecologia 110: 243-252.

Northup, R. R., Yu, Z. S., Dahlgren, R. A. & Vogt, K. A. (1995) Polyphenol control of nitrogen release from pine litter. Nature 377: 227-229.

Ohta, S. & Effendi, S. (1992a) Ultisols of "lowland dipterocarp forest" in East Kalimantan, Indonesia. 1. Morphology and physical properties. Soil Sci. Plant Nut. 38: 197-206.

Ohta, S. & Effendi, S. (1992b) Ultisols of "lowland dipterocarp forest" in East Kalimantan, Indonesia. 2. Status of carbon, nitrogen, and phosphorus. Soil Sci. Plant Nut. 38: 207-216.

Ohta, S., Effendi, S., Tanaka, N. & Miura, S. (1993) Ultisols of "lowland dipterocarp forest" in East Kalimantan, Indonesia. 3. Clay minerals, free oxides, and exchangeable cations. Soil Sci. Plant Nut. 39: 1-12.

Oliveira, M. R. G, van Noordwijk, M., Gaze, S. R., Brouwer, G, Bona, S., Mosca, G & Hairiah, K. (2000) Auger sampling, ingrowth cores and pinboard methods. In Smit, A. L., Bengough, A. G, Engels, C. & Pellerin, van N. S. (eds). Root Methods. Springer-Verlag, Berlin, Heidelberg, Germany, pp.175-210.

Paramananthan, S. (1983) Field legend for soil surveys in Malaysia. UPM-PSTM, Kuala Lumpur, 80pp.

Read, D. J., Leake, J. R. & Langdale A. R. (1989) The nitrogen nutrition of mycorrhizal fungi and their host plants. In Boddy, L., Marchant, R. & Read, D. J. (eds). Nitrogen, phosphorus and sulphur utilization by fungi. Cambridge University Press, Cambridge, pp.181-204.

Reich, P. B., Grigal, D. F., Aber, J. D. & Gower, S. T. (1997) Nitrogen mineralization and productivity in 50 hardwood and conifer stands on diverse soils. Ecology 78: 335-347.

Richter, D. D. & Babbar, L. I. (1991) Soil diversity in the tropics. Adv. Ecol. Res. 21: 315-389.

Robertson, G P. (1984) Nitrification and nitrogen mineralization in a lowland rainforest succession in Costa Rica, Central America. Oecologia 61: 99-104.

Robertson, G P. (1986) Nitrification and denitrification in humid tropical ecosystems: potential controls on nitrogen retention. In Proctor, J. (ed). Mineral Nutrients in Tropical Forest and Savanna Ecosystems. Blackwell Scientific Publications, Oxford, pp.55-69.

Roy, S. & Singh, J. S. (1995) Seasonal and spatial dynamics of plant-available N and P pools and N-mineralization in relation to fine roots in a dry tropical forest habitat. Soil Biol. Biochem. 27: 33-40.

Sakurai, K., Tanaka, S., Ishizuka, S. & Kanzaki, M. (1998) Differences in soil properties of dry evergreen and dry deciduous forests in the Sakaerat Environmental Research Station. Tropics 8: 61-80.

Sanchez, P. A. (1976) Properties and management of soils in the tropics. J. Wiley & Sons, New York, 618pp.

Singh, R. S., Raghubanshi, A. S. & Singh, J. S. (1991) Nitrogen-mineralization in dry tropical savanna: effects of burning and grazing. Soil Biol. Biochem. 23: 269-273.

Sulaiman, S., Abdul Rahim, N. & LaFrankie, J. V. (1994) Pasoh Climatic Summary (1991-1993). FRIM Research Data No. 3. FRIM, Kepong.

Soil Survey Staff (1998) Keys to Soil Taxonomy. Eighth edition. USDA-NRCS, Washington D.C., 328pp.

Tange, K., Yagi, H., Sasaki, S., Niiyama, K. & Abd. Rahman, K. (1998) Relationship between topography and soil properties in a hill dipterocarp forest dominated by *Shorea curtsii* at Semangkok Forest Reserve, Peninsular Malaysia. J. Trop. For. Sci. 10: 398-409.

Vitousek, P. M. & Denslow, J. S. (1986) Nitrogen and phosphorus availability in treefall gaps of a lowland tropical rainforest. J. Ecol. 74: 1167-1178.

Vitousek, P. M. & Howarth, R. W. (1991) Nitrogen limitation on land and in the sea: How can it occur? Biogeochemistry 13: 87-115.

Vitousek, P. M. & Matson, P. A. (1988) Nitrogen transformations in a range of tropical forest soils. Soil Biol. Biochem. 20: 361-367.

Vitousek, P. M. & Sanford Jr, R. L. (1986) Nutrient cycling in moist tropical forest. Annu. Rev. Ecol. Syst. 17: 137-167.

Vogt, K. A., Vogt, D. J., Palmiotto, P. A., Boon, P., O'hara, J. & Asbjorsen, H. (1996) Reviews of root dynamics in forest ecosystems grouped by climate, climatic forest types and species. Plant Soil 187: 159-219.

Wild, A. (1972) Nitrate leaching under bare fallow at a site in northern Nigeria. J. Soil Sci. 23: 315-324.

Woodruff, J. R. & Kamprath, E. J. (1965) Phosphorus adsorption maximum as measured by the Langmuir isotherm and its relationship to phosphorus availability. Soil Sci. Soc. Am. Proc. 29: 148-150.

Yamashita, T. & Takeda, H. (1998) Decomposition and nutrient dynamics of leaf litter in litter bags of two mesh sizes set in two dipterocarp forest sites in Peninsular Malaysia. Pedobiologia 42: 11-21.

Yamashita, T., Takeda, H. & Watanabe, H. (1992) Spatio-temporal variations of mineral nitrogen in a *Chamaecyparis obstusa* plantation soil. Bull. Kyoto Univ. For. 64: 51-60 (in Japanese with English summary).

Yamashita, T., Nakanishi, A., Tokuchi, N. & Takeda, H. (1999) Chemical properties and nutrient accumulation in two Siamese forest soils. Appl. For. Sci., Kansai 8: 89-94 (in Japanese with English summary).

Yoda, K. & Kira, T. (1982) Accumulation of organic matter, carbon, nitrogen and other nutrient elements in the soils of a lowland rainforest at Pasoh, Peninsular Malaysia. Jpn. J. Ecol. 32: 275-291.

Zou, X., Valentine, D. W., Sanford Jr., R. L. & Binkley, D. (1992) Resin-core and buried bag estimates of nitrogen transformations in Costa Rican lowland rainforests. Plant Soil 139: 275-283.

ELSEVIER

Available online at www.sciencedirect.com
SCIENCE DIRECT

Forest Ecology and Management 224 (2006) 19–25

Forest Ecology and Management

www.elsevier.com/locate/foreco

Characteristics of spatial distribution of throughfall in a lowland tropical rainforest, Peninsular Malaysia

Shinji Konishi [a,1], Makoto Tani [b,*], Yoshiko Kosugi [b], Satoru Takanashi [b],
Mohd Md Sahat [c], Abdul Rahim Nik [c], Kaoru Niiyama [d], Toshinori Okuda [e]

[a] *Faculty of Agriculture, Kyoto University, Kyoto 606-8502, Japan*
[b] *Graduate School of Agriculture, Kyoto University, Kitashirakawa Sakyo, Kyoto 606-8502, Japan*
[c] *Forest Research Institute Malaysia, Kepong, 52109 Kuala Lumpur, Malaysia*
[d] *Forestry and Forest Products Research Institute, Tsukuba, Ibaraki 305-8687, Japan*
[e] *National Institute for Environmental Studies, Tsukuba, Ibaraki 305-8506, Japan*

Abstract

The spatial distribution of throughfall in a tropical rainforest in Peninsular Malaysia was evaluated using 100 bucket raingauges placed along a line as well as two large raingauges (collection areas of 9.58 and 7.08 m^2). Throughfall was clearly large in a treefall gap although it was not significantly different between a typical old-growth area with big trees and another area without big trees. A cyclic variation, the scale of which was 10–15 m, was detected in the entire forest through Fourier analysis, and this scale roughly corresponded to the index of canopy cover openness. The observations gave the spatial mean value of throughfall with enough accuracy considering that the distribution of throughfall in the forest was controlled by different scale effects consisting of the size of disturbance areas such as gaps as well as the size of individual canopies.

Keywords: Tropical rainforest; Throughfall; Malaysia; Spatial heterogeneity; Forest hydrology

1. Introduction

Tropical rainforests are considered the most complex terrestrial ecosystems and their environmental conditions exhibit high spatial variability. Such conditions pose difficulties for estimating water budgets due to highly heterogeneous processes of rainfall distribution through the canopy (e.g., Calder et al., 1986; Jetten, 1996). Lloyd and Marques (1988) showed that the spatial variability of throughfall estimated from many raingauges placed on the forest floor in an Amazonian rainforest was much larger than that in a temperate coniferous forest in United Kingdom. In this study, a probability distribution of throughfall was estimated by randomly locating the positions of the bottle gauges every week. This method is effective for estimating the spatial average of throughfall under heterogeneous canopies in tropical rainforests. However, this study did not consider the characteristics of spatial distribution or the causes that control throughfall at each position. The spatial distribution of throughfall is quite heterogeneous in such a tropical rainforest, but it is believed that the distribution is not perfectly random. It is quite natural to consider that the scale of fluctuations is probably derived from canopy structure. This information is important not only to estimate the spatial average of throughfall necessary for the interception-loss evaluation, but also to understand the basic physical environment in the forest understory controlling ecology of tree seedling regeneration (Bell and Lechowicz, 1994).

Recent studies of the spatial distribution of throughfall in tropical rainforests using so-called semi-variograms determined values for ‘range distance’, i.e. the distance between gauges beyond which their respective estimates could be considered spatially independent. Brouwer (1996) estimated a range distance of 7 m in Guyana and Loescher et al. (2002) obtained a much larger value (43 m) in a Costa Rican forest. Although the reason for these different distances was not clear, these studies demonstrated that clusters of similar throughfall values existed at scales ranging from several meters to several tens meters in tropical rainforests. Therefore, a net rainfall gauge comprised of a large (20 m^2) plastic sheet (used in Indonesia by Calder et al., 1986) may not be large enough for estimating mean throughfall in a tropical rainforest; such a

---

[*] Corresponding author. Tel.: +81 75 753 6086; fax: +81 75 753 6088.
E-mail address: tani@kais.kyoto-u.ac.jp (M. Tani).

[1] Present address: Tokyo Electric Power Company, Incorporated, Japan.

0378-1127/$ – see front matter © 2006 Elsevier B.V. All rights reserved.
doi:10.1016/j.foreco.2005.12.005

'large' gauge could unexpectedly be installed within a cluster with larger or smaller throughfall compared to the spatial mean (Roberts et al., 2004).

The present study provides information on the spatial distribution of throughfall in a tropical rainforest using 100 bucket raingauges placed along a line as well as two large raingauges installed on the forest floor. The effect of canopy scale processes on throughfall variability is a particular focus in this analysis.

This study was conducted in Pasoh Forest Reserve of Forest Research Institute Malaysia (FRIM), Peninsular Malaysia, as one of the hydro-meteorological themes under a collaborative research project on tropical rainforest ecosystem and biodiversity between Malaysian research institutions, such as FRIM and Universiti Putra Malaysia, and Japanese Research Institutions, such as the National Institute for Environmental Studies (NIES), Forestry and Forest Products Research Institute (FFPRI) and Universities (Okuda et al., 2003a). A long-term estimation of forest evapotranspiration has been already reported as part of this project (Tani et al., 2003a, 2003b) using meteorological data obtained at a 52-m observation tower (Tani et al., 2003c). However, an important unresolved topic related to this evapotranspiration estimation is reducing errors inherent in the estimated values of interception losses. The present study on spatial variability of throughfall is one strategy to achieve an accurate estimation of interception loss.

2. Site description

This study was conducted in the Pasoh Forest Reserve, located near Simpang Pertang in Negeri Sembilan, about 140 km southeast of Kuala Lumpur in Peninsular Malaysia (2°58′N, 102°18′E). This forest reserve has been a leading center for international field researches in the Asian tropical rainforest since 1970s, when the International Biological Programme (IBP) was carried out (Soepadmo, 1978; Okuda et al., 2003a). The core area (650 ha) of the reserve (2450 ha) is covered with a primary lowland mixed dipterocarp forest, which consists of various species of *Shorea* and *Dipterocarpus*. The continuous canopy height is about 35 m, although some emergent trees exceed 45 m. Based on the empirical equations obtained for the Pasoh forest by Kato et al. (1978), leaf area index (LAI) estimated from tree diameter observations (Niiyama, unpublished) is 6.52. The altitude of the core area ranges from 75 to 150 m above sea level.

A major rainy season in Pasoh is produced by the northeast monsoon from October to December while the generally weak southwest monsoon yields only a small peak of rainfall from March to May. The maximum and minimum monthly rainfall values in normal years are recorded in November and in January, respectively, and the annual rainfall is only 1804 mm, lower than that in other regions of Peninsular Malaysia (Tani et al., 2003a). Rainfall is characterized by its short duration (mean: 3.8 h) and relatively high intensity (mean storm intensity: 7.8 mm h^{-1}), and there is a distinct diurnal cycle in rainfall, 52% of which occurs between 13:00 and 19:00 (Noguchi et al., 2003).

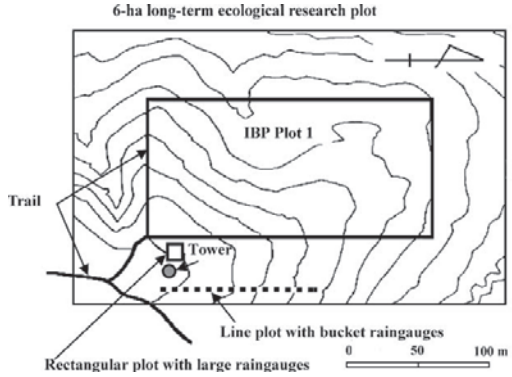

Fig. 1. Layout of throughfall observation plots in the Pasoh Forest Reserve, Peninsular Malaysia.

3. Methods

Our throughfall measurement plot was set near the 52-m tower and in a 6-ha long-term ecological research plot (Niiyama et al., 2003) in the core area of Pasoh Forest Reserve (Fig. 1). One hundred small plastic bucket raingauges were placed at 1-m intervals along a line starting from the near tower point and extending northwards (Fig. 2), i.e., the 'line plot'. The tower is located at the top of a gentle hill and surrounded by a typical old-growth lowland rainforest with both large and emergent trees. The observation line was on a gentle slope (3%) down to the north. Although the typical vegetation cover continued until 64 m from the near-tower point (0 m position), there was a gap caused by a fallen tree between 64 and 71 m; a markedly different vegetation cover appeared from 71 m to the north end of the transect (100 m position). Thus, the line plot was divided into subplots A, B, and C for 0–64 m, 64–71 m, and 71–100 m, respectively. The bucket raingauges were 22.75 cm in diameter and 28.0 cm

Fig. 2. A view of the line plot with bucket raingauges.

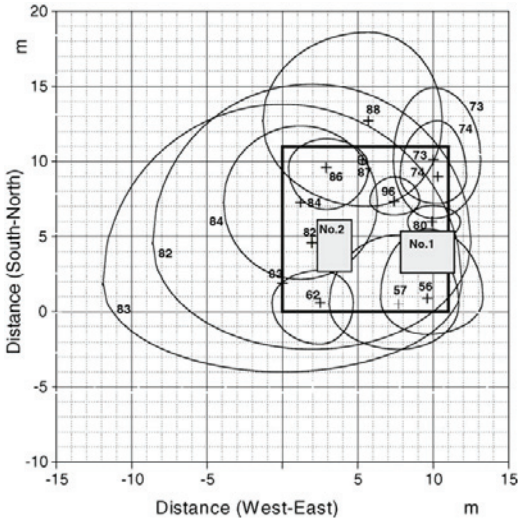

Fig. 3. Layout of the rectangular plot of large raingauges (No.1 and No.2) on a map of the canopy projection areas; (+) indicates the stem location of the tree (the number indicates tree identification number).

deep. A plate with small holes was suspended about 10 cm below the upper edge of the raingauge to protect against evaporation loss from stored water. The interval of rainwater volume measurement was about 10 days.

In addition, we installed two large rectangular raingauges near the line plot (Fig. 1): No.1 and No. 2, 9.58 m^2 (3.55 m × 2.70 m) and 7.08 m^2 (3.59 m × 1.97 m), respectively. These large gauges were located in an 11 m × 11 m plot; the layout is illustrated with canopy projection areas of the 13 individual trees in Fig. 3. A photograph of one large raingauge is shown in Fig. 4. The raingauge was composed of a water-sealed plywood plate and a PVC trough (the width of 14 cm), which was attached to the edge of the plate and supported about 0.5 m above the ground surface by timbers. The space under the plate was surrounded by wire netting to reduce risks by poisonous snakes (Roberts et al., 2004). Throughfall with stemflow from small trees within the plate was collected by the PVC trough and routed to a tipping bucket flow meter (bucket volume = 1 L; Ikeda TQX-1000, Japan) fixed under the trough. The tipping-bucket pulse was recorded by a data logger (Campbell CR10X, USA).

Gross rainfall was measured at the top of the 52-m tower by a tipping bucket raingauge (Ota Keiki 34-T, Japan) and recorded by a similar data logger. The rainfall data was compared with both data measured by storage-type and tipping bucket raingauges in an observatory located 430 m away from the tower. The rainfall measured on the tower may be influenced by strong wind, whereas, the rainfall in the observatory was often different from the tower site due to a large spatial variability of rainfall in tropics. Although these issues are generally involved for the estimation of gross rainfall, we have concluded from the careful comparison that the rainfall data measured on the tower can represent the gross rainfall at our throughfall study site.

Because all trees >5 cm in DBH were tagged, measured and identified in 20 m × 20 m sub-grids of the 6-ha long-term ecological research plot (Niiyama et al., 2003) (Fig. 1), we can show DBH distributions for the near-tower area (Subplot A) and the north-end area (Subplot C) in the line plot, as well as the distribution for the area including the two large raingauges (Fig. 5). Some big trees are distributed in Subplot A and the large raingauge site, whereas, only small trees with DBH <20 cm were included in Subplot C. Thus, vegetation cover in Subplot C contains no big trees compared to the typical old-growth forest cover near the tower. Subplot B was characterized by a gap composed of fallen trees and bush.

There is a possibility to detect variability in throughfall at the scale of individual tree canopies via our line plot system, but this system may fail to estimate the representative value of throughfall at smaller scales because large leaves often either shelter the gauges or concentrate throughfall into the gauges via so-called drip points (Roberts et al., 2004). On the other hand, the size of large raingauges is sufficient to negate the influence

Fig. 4. A view of large raingauge No. 1.

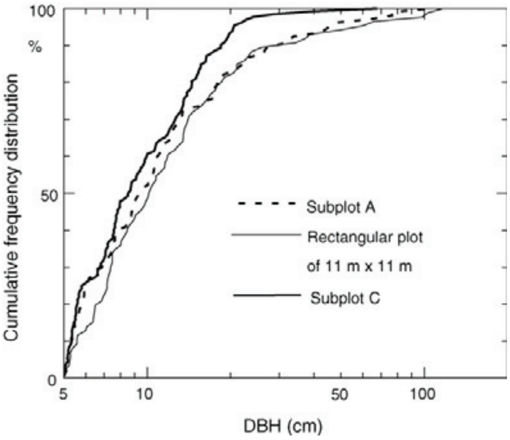

Fig. 5. DBH distributions in 20 m × 20 m sub-grids including throughfall plots within the 6-ha long-term ecological plot.

of micro-scale variability on throughfall. Nevertheless, we must recognize that our large raingauge may not cover all of the large-scale variability in throughfall over individual canopies (Roberts et al., 2004). Therefore, crosschecking data obtained from both systems (i.e., line plot and the two large raingauges) should give better insights into throughfall variability in tropical rainforests.

Because our research aims to detect effects of tree canopies on throughfall variability, additional measurements of canopy cover openness were made above each bucket raingauge using a digital camera with a fisheye lens. A Gap Light Analyzer developed by the Institute of Ecosystem Studies, Simon Fraser University was used for calculating canopy cover openness (see http://www.rem.sfu.ca/forestry/downloads/Files/GLAV2Users-Manual.pdf.). Because the tree height was generally very high, the vertex angle of the circular cone should be concentrated in a small area to investigate the relationship of the openness to throughfall distribution. We chose an angle of 9.47°, which yields a diameter of 5 m at the average canopy height of 30 m. The ratio of this canopy cover openness to the average openness of all the 100 raingauges is termed 'openness index' to represent its relative value.

Because a cyclic variation was found in the spatial distributions of throughfall and openness index (see Fig. 6), Fourier analysis was applied to detect the dominant spatial patterns. From the discrete data (x_n) of throughfall or openness index with the total number of N, the spectrum (P_k) for each wavelength (l_k) can be calculated as:

$$P_k = \left\{ \left(\frac{2}{N} \sum_{n=0}^{N-1} x_n \cos \frac{2\pi kn}{N} \right)^2 + \left(\frac{2}{N} \sum_{n=0}^{N-1} x_n \sin \frac{2\pi kn}{N} \right)^2 \right\}^{0.5}$$

$$l_k = \frac{kL}{N}, \quad k = 1, 2, 3, \ldots \frac{N}{2}$$

This analysis will specify dominant scales for the spatial distributions.

4. Results

The data from 26 August to 20 November 2003 were used for our analysis. The gross rainfall measured on the tower and the average throughfall of all 100 bucket gauges were 661.4 and 534.6 mm, respectively. This average throughfall, a ratio of 0.808 to the gross rainfall, is used for the standard value for our comparisons of throughfall values measured by bucket- and large raingauges. The ratio of throughfall at each bucket raingauge to the average throughfall is shown in Fig. 6. The average ratios and their standard deviations are listed with the ratios for large raingauges in Table 1. Considering the estimation accuracy, the average ratios for Subplots A, B, and C are also written with their standard errors as 0.981 ± 0.022, 1.174 ± 0.029, and 1.006 ± 0.027, respectively. The ratios of large gauges No. 1 and No. 2 are 1.031 and 1.036, respectively.

Throughfall in Subplot B is much larger than that in the other areas because Subplot B is located within a gap. The gap also influences on the small fluctuation for Subplot B (Fig. 6) as shown in the small standard deviation in Table 1. The openness index at each bucket raingauge position is also plotted in Fig. 6. The ratio of throughfall to the average (Tr) was weakly

Table 1
Ratio of throughfall to the average

	Original section				Modified section	
	Section (m)	Average	S.D.	Section (m)	Average	S.D.
Subplot A	0–64	0.981	0.175	0–43	1.002	0.152
Subplot B	64–70	1.174	0.071	61–74	1.181	0.073
Subplot C	70–100	1.006	0.147	80–100	1.037	0.113
Entire line plot	0–100	1.000	0.168	0–100	1.000	0.168
Large raingauge No. 1	–	1.031	–	–	1.031	–
Large raingauge No. 2	–	1.036	–	–	1.036	–

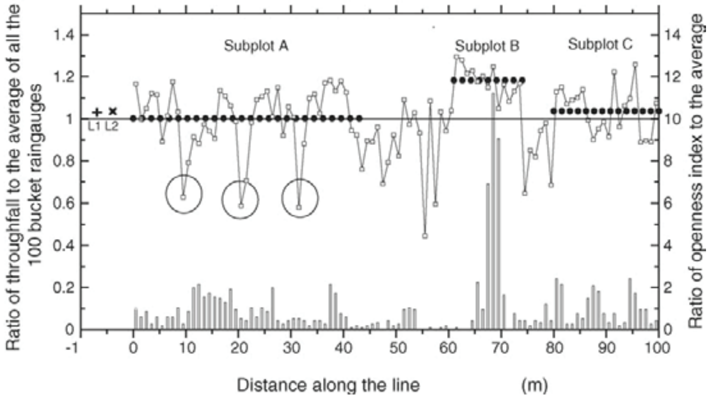

Fig. 6. Distribution of the ratio of measured throughfall (100 bucket gauges) to average throughfall (rectangular symbols) and openness index (bar graph). The horizontal solid line indicates unity (throughfall ratio is equal to that averaged over the entire line plot). The dotted lines show the average throughfall ratios for the modified sections of each subplot. The symbols (+) and (×) indicate the throughfall ratios measured at large raingauges No.1 (L1) and No.2 (L2), respectively. The large open circles highlight the very small throughfall ratios in Subplot A.

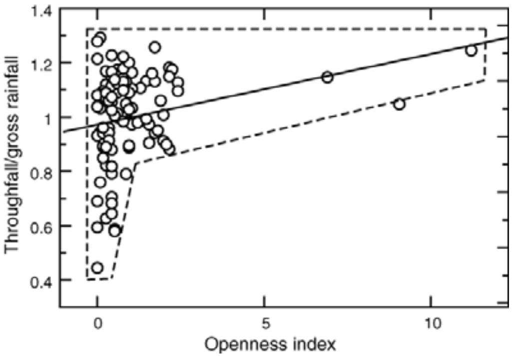

Fig. 7. Relationship between the openness index and the ratio of throughfall to the average of all 100 bucket raingauges. The solid line is the regression line and the area within the broken line polygon indicates the distribution range of the plots.

correlated with openness index (Op): (Tr = 0.026Op + 0.973, $r^2 = 0.245$) (Fig. 7). The fact that very large Op values coincide with large Tr values is quite natural because such positions were located under poorly developed canopy cover. However, widely scattered values of Tr were observed for relatively small Op values, suggesting that the openness index was not always the controlling factor of throughfall distribution.

A clear cyclic variation is detected in the spatial distributions of both throughfall and openness index in Fig. 6. Fig. 8 shows their spectra obtained through the Fourier analysis for all the data ($N = 100$). The spectra for scales of shorter than 10 m are relatively small both for the throughfall and openness index, while their first peaks are generated at 11 m and around 15 m, respectively. Although the relationship of throughfall to the openness index is not clear from Fig. 7, cyclic patterns at 10–15 m were common to both distributions. Tree canopies may roughly control the spatial variation of throughfall. At the range of longer scales, however, we can also find several dominant scales for the both in Fig. 8, suggesting that the mixing of various kinds of larger heterogeneities in our natural forest may influence on their spatial distributions.

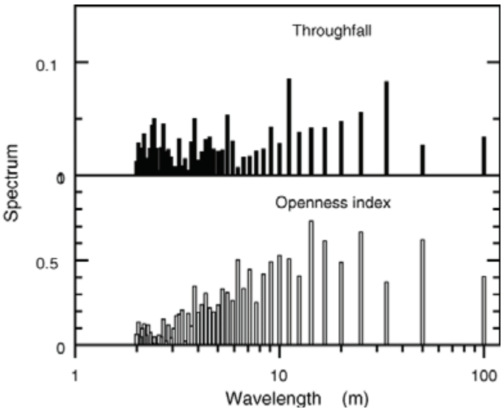

Fig. 8. Spectra for throughfall and the openness index obtained from the 100 bucket raingauges.

5. Discussion

At some places along the transect of Subplot A, throughfall has very small values (marked with circles in Fig. 6) and seems to be spatially punctuated. In these zones, the openness index is also small (<0.1) and most of the rainwater may be trapped by the dense canopy and diverted to surrounding areas. Except for these local small zones, throughfall is relatively even and larger than the mean value. Large openness indices are dominant in these major clusters. Our onsite observation showed that zones with large openness indices were located in the zone between two tree canopies. It may be plausible that throughfall is large in a canopy break, but the areas with large throughfall values are not limited to these narrow canopy zones. Instead, there are local areas with very small throughfall (marked with circles in Fig. 6) under individual canopies. This rough accordance between throughfall and openness index can explain the dominant cycle of 10–15 m that was observed in both indices (Fig. 8), although they were only weakly correlated (Fig. 7). In addition to this, the complex canopy structure would not be well represented by a canopy index based on light penetration; the physical analogues for canopy index and throughfall are quite different (Loescher et al., 2002). The inter-relationship between canopy scale and throughfall distribution will be discussed from other aspects.

Information on the canopy scale in our forest can be separately derived from the following two sources: (1) the canopy projection map covering the 11 m × 11 m that includes both large raingauges (Fig. 3), and (2) aerial photographs for the 6 ha area near our site (Okuda et al., 2003b). The canopy widths of trees reaching the top canopy layer (tree numbers 82, 83, 84, and 88) ranged from 10 to 20 m. The mean projected area of tree canopies visible from the air was 94.5 m^2, i.e., a diameter of 11 m. Of course, canopy areas are not equal, but this mean diameter is close to the range of values for the dominant cycle (10–15 m) for throughfall and thus suggests that this scale may generally control throughfall throughout this forest.

Focusing on differences in throughfall distribution at a larger scale, it is clear that near Subplot B the zone with large throughfall values extends to the neighboring areas in the gaps (Fig. 6). Although the canopy gap occupies only 7 m along our line plot, large throughfall values continued for about 3–4 m on both sides, and rather small values are found in the subsequent 5 m on each side. In contrast, the very large values of openness index are limited to the gap itself, and these values become small at distances of 10 m from the edges. The small values of openness index in the surrounding area of the gap may be caused by an edge effect. Actually, dense growth of small plants along a forest edge may cause low light exposure (Davies-Colley et al., 2000). Along this ‘fence line’, the lack of a high canopy may cause large amounts of throughfall even in the surrounding area regardless of the ‘dark conditions’ created by abundant small plants. Within Subplot C, throughfall values seem to be rather small in areas with large openness indices (Fig. 6). Although the reason is not clear, the lack of large trees (Fig. 5) may make the relationship between the openness index and throughfall weak.

Thus, the heterogeneity including different regeneration processes may cause complex relationships between throughfall and canopy openness different from those in typical old-growth areas (e.g., Subplot A). However, such a larger scale due to forest regeneration processes is also important for the spatial distribution of throughfall. As mentioned earlier, Loescher et al. (2002) found the range – i.e., the distance beyond which throughfall was statistically independent – to be 43 m for a tropical rainforest in Costa Rica using semi-variograms. Because this value was obtained from throughfall data with a span of 5 m, we can assume that it was difficult to detect a cyclic pattern at the canopy scale if it existed. This range (Loescher et al., 2002) more indicates the scale of clustering of large gaps in their study area. On the other hand, Brouwer (1996) estimated the range as a much smaller value (7 m) in Guyana, suggesting this value was derived from individual canopy effects. Of course, each of the study sites has different characteristics of canopy structure, but we can conclude that various scales control the spatial distribution of throughfall in such natural forests.

Finally, the spatial mean values of throughfall in each of our Subplots are assessed against the previous findings. Because zones in which gaps influenced throughfall extended beyond the gap margins, we can extend Subplot B to from 61 to 74 m (i.e., Subplot B′). Outside of Subplot B′, areas exist with small throughfall. It is natural that throughfall is large in Subplot B′ with a gap; this reflects small evaporation during and after rain events there. Such a local reduction in evaporation may cause an increase in evaporation from the surrounding zones due to small-scale advection smoothing the atmospheric heterogeneity, although the effect of advection has been discussed only for a forest edge (Giambelluca et al., 2003). This compensation of evaporation may account for the spatial distribution of throughfall around a gap.

When the boundary zones surrounding the gap are removed from the Subplots A and C, their respective areas can be narrowed: 0–43 m for Subplot A′ and 80–100 m for Subplot C′. These areas are considered to have typical forest conditions for throughfall, which are separated from gap influences. The ratios of averaged throughfall of the modified Subplots A′, B′, and C′ to the averaged throughfall of all the 100 bucket raingauges are 1.002 ± 0.023, 1.181 ± 0.020, and 1.037 ± 0.025, respectively (Table 1). Throughfall in Subplot B′ was significantly higher at the 1% level from values for both Subplots A′ and C′; however, no significant differences in throughfall were found (5% level) between Subplots A′ (with big trees) and C′ (without big trees). Thus, it is clear that this forest includes gaps with larger throughfall than the mean and surrounding areas with smaller throughfall. Although variations in throughfall are evident at both larger scales due to gap disturbances as well as at smaller scales caused by individual canopy influences, we can conclude that the spatially averaged throughfall in the Pasoh Forest Reserve may be similar to that in a typical old-growth forest with big trees. It is expected that the spatial heterogeneities of throughfall at local scales can be cancelled at larger scales.

The ratio of 1.031 and 1.036 for the large raingauges No.1 and No.2 are greater than that for the mean of bucket gauges from 0 to 43 m in Subplot A′ in this forest (Table 1). There is a possibility that the spatially averaged throughfall derived from 100 bucket raingauges may under- or overestimate the true value because large leaves shelter the gauges or concentrate throughfall into bucket gauges (Roberts et al., 2004). Indeed, we cannot exclude this possibility, but within Subplot A′, throughfall was relatively even or larger than the mean value except for the limited local zones with very small throughfall values (Fig. 6). Therefore, it is more plausible that both of the large raingauges were probably installed in the areas outside of the local zones, resulting in larger throughfall values than the true spatial mean value. Thus, we can conclude that the averaged throughfall of the 100 bucket raingauges was sufficiently accurate.

6. Conclusion

Based on throughfall samples collected in 100 bucket raingauges and two large raingauges, we have not only estimated the spatial mean value with sufficient accuracy, but also elucidated that the spatial distribution of throughfall was controlled by processes functioning at different scales consisting of the size of disturbance areas (e.g., treefall gaps) to the size of individual canopies. Considering estimation difficulties in the heterogeneous environment of a natural tropical forest, we can propose that our line plot system using bucket raingauges is a valid method for detecting the distribution scales of throughfall.

Acknowledgements

We thank the Forestry Department of Negeri Sembilan and Director General of FRIM for giving us permission to work in the Pasoh Forest Reserve. We also thank Dr. Shoji Noguchi of Japan International Research Center for Agricultural Sciences for his comprehensive support to our field study. Staffs of Hydrology Unit and Pasoh Station of FRIM are acknowledged for collecting data. They are Rajendran Pavadai, Ahmad Shahar Mohamad Yusof, Ibharim Hashim, Hashim Mohd, Abu Husin Harun, Hamidon Ahmad (Hydrology Unit) and Ahmad Awang (Pasoh Station). This study was conducted as a part of joint research project under Global Environment Research Program granted by Ministry of the Environment, Japan.

References

Bell, G., Lechowicz, M.J., 1994. Spatial heterogeneity at small scales and how plants respond to it. In: Caldwell, M.M., Pearcy, R.W. (Eds.), Exploitation of Environmental Heterogeneity by Plants: Ecological Processes Above- and Belowground. Academic Press, San Diego, pp. 391–414.

Brouwer, L.C., 1996. Nutrient Cycling in Pristine and Logged Tropical Rain Forest. Tropenbos-Guyana Series 1. Tropenbos-Guyana Programme. Guyana, Georgetown.

Calder, I.R., Wright, I.R., Murdiyarso, D., 1986. A study of evaporation from tropical rain forest – West Java. J. Hydrol. 89, 13–31.

Davies-Colley, R.J., Paynel, G.W., van Elswijk, M., 2000. Microclimate gradients across a forest edge. NZ J. Ecol. 24, 111–121.

Giambelluca, T.W., Ziegler, A.D., Nullet, M.A., Truong, D.M., Tran, L.T., 2003. Transpiration in a small tropical forest patch. Agric. Forest Meteorol. 117, 1–22.

Jetten, V.G., 1996. Interception of tropical rain forest—Performance of a canopy water balance model. Hydrol. Proc. 10, 671–685.

Kato, R., Tadaki, Y., Ogawa, H., 1978. Plant biomass and growth increment studies in Pasoh Forest. Malay. Nat. J. 30, 211–224.

Lloyd, C.R., de, O., Marques, A., de, O., 1988. Spatial variability of throughfall and stemflow measurements in Amazonian rainforest. Agric. For. Meteorol. 42, 63–73.

Loescher, H.W., Powers, J.S., Oberbauer, S.F., 2002. Spatial variation of throughfall volume in an old-growth tropical wet forest. Costa Rica J. Trop. Ecol. 18, 397–407.

Niiyama, K., Abdul Rahman, K., Iida, S., Kimura, K., Azizi, R., Appanah, S., 2003. Regeneration of a clear-cut plot in a lowland dipterocarp forest in Pasoh Forest Reserve Peninsular Malaysia. In: Okuda, T., Manokaran, N., Matsumoto, Y., Niiyama, K., Thomas, S.C., Ashton, P.S. (Eds.), Pasoh—Ecology of a Lowland Rain Forest in Southeast Asia. Springer, Tokyo, pp. 559–568.

Noguchi, S., Abdul Rahim, N., Tani, M., 2003. Rainfall characteristics of tropical rainforest at Pasoh Forest Reserve, Negeri Sembilan, Peninsular Malaysia. In: Okuda, T., Manokaran, N., Matsumoto, Y., Niiyama, K., Thomas, S.C., Ashton, P.S. (Eds.), Pasoh—Ecology of a Lowland Rain Forest in Southeast Asia. Springer, Tokyo, pp. 51–58.

Okuda, T., Manokaran, N., Matsumoto, Y., Niiyama, K., Thomas, S.C., Ashton, P.S., 2003a. Pasoh—Ecology of a Lowland Rain Forest in Southeast Asia. Springer, Tokyo.

Okuda, T., Suzuki, M., Adachi, N., Yoshida, K., Niiyama, K., Nur Supardi Md, N., Nor Azman, H., Manokaran, N., Mazlan, H., 2003b. Logging history and its impact on forest structure and species composition in the Pasoh Forest Reserve—Implications for the sustainable management of natural resources and landscapes. In: Okuda, T., Manokaran, N., Matsumoto, Y., Niiyama, K., Thomas, S.C., Ashton, P.S. (Eds.), Pasoh—Ecology of a Lowland Rain Forest in Southeast Asia. Springer, Tokyo, pp. 15–34.

Roberts, J.M., Gash, H.C., Tani, M., Bruijnzeel, L.A., 2004. Controls on evaporation in lowland tropical rainforest. In: Bonnell, M., Bruijnzeel, L.A. (Eds.), Forests, Water and People in the Humid Tropics. Cambridge University Press, Cambridge, pp. 287–313.

Soepadmo, E., 1978. Introduction to the Malaysian I.B.P. Synthesis Meetings. Malay. Nat. J. 30, 119–124.

Tani, M., Abdul Rahim, N., Ohtani, Y., Yasuda Mohd Md, S., Baharuddin, K., Takanashi, S., Noguchi, S., Zulkifli, Y., Watanabe, T., 2003a. Characteristics of energy exchange and surface conductance of a tropical rain forest in Peninsular Malaysia. In: Okuda, T., Manokaran, N., Matsumoto, Y., Niiyama, K., Thomas, S.C., Ashton, P.S (Eds.), Pasoh—Ecology of a Lowland Rain Forest in Southeast Asia. Springer, Tokyo, pp. 73–88.

Tani, M., Abdul Rahim, N., Yasuda, Y., Noguchi, S., Siti Aisah, S., Mohd Md, S., Takanashi, S., 2003b. Long-term estimation of evapotranspiration from a tropical rain forest in Peninsular Malaysia. In: Franks, S., Bloeschl, G., Kumagai, M., Musiake, K., Rosbjerg, D. (Eds.), Water Resources Systems—Water Availability and Global Change, IAHS Publ. No. 280. IAHS Press, Wallingford, pp. 267–274.

Tani, M., Abdul Rahim, N., Mohd Md, S., Noguchi, S., Ohtani, Y., 2003c. Five-year Meteorological Observation at Pasoh Forest Reserve, Negeri Sembilan, Peninsular Malaysia FRIM Report 78. Forest Research Institute Malaysia, Kuala Lumpur.